

AMMONIA EMISSIONS AND PATHOGEN INACTIVATION
DURING CONTROLLED COMPOSTING OF PIG MANURE

by

ANGELA LEIGH CRONJÉ

A thesis submitted to the Faculty of Engineering
The University of Birmingham
for the degree of
DOCTOR OF PHILOSOPHY

School of Chemical Engineering
Faculty of Engineering
The University of Birmingham
October 2003

UNIVERSITY OF
BIRMINGHAM

University of Birmingham Research Archive

e-theses repository

This unpublished thesis/dissertation is copyright of the author and/or third parties. The intellectual property rights of the author or third parties in respect of this work are as defined by The Copyright Designs and Patents Act 1988 or as modified by any successor legislation.

Any use made of information contained in this thesis/dissertation must be in accordance with that legislation and must be properly acknowledged. Further distribution or reproduction in any format is prohibited without the permission of the copyright holder.

ABSTRACT

The effects of adjusting the initial carbon to nitrogen (C:N) ratio and pH of pig manure and straw mixes on ammonia emissions and pathogen marker inactivation during composting were investigated by experimentation and modelling.

Three, 210-litre reactors were designed and built to control conditions, such as the maximum operating temperature, minimise temperature gradients and enable analysis of the off-gas for ammonia, water, oxygen and carbon dioxide.

Respirometry showed that the optimal temperature for composting pig manure was about 60 °C.

A simulation model suggested that ammonia emissions could be reduced by lowering the initial pH and increasing the initial C:N ratio of the organic material. Experimentally, lowering the initial pH significantly reduced ammonia emissions. The effect of the initial C:N ratio on ammonia emissions was not significant because of variations in the pig manure.

Pathogen markers were sometimes detected after composting from experiments with low ammonia emissions, so questioning the established criteria for pathogen inactivation.

Experimental data validated the model, which simulated organic material decomposition using first order reaction rate kinetics and predicted the temperature and ammonia emissions profiles from initial conditions.

DEDICATION

To my parents, grandparents and godparents,
and
to my maths teacher, Mrs Barnes.

ACKNOWLEDGEMENTS

My research was funded by The Engineering and Physical Sciences Research Council (EPSRC) and Silsoe Research Institute (SRI) with further support from the University of Birmingham.

I am most grateful to my supervisors, Dr Claire Turner and Dr Adrian Williams at SRI and Dr Andrew Barker and Dr Stuart Guy at the University of Birmingham for their guidance, support and encouragement throughout this project. I would also like to thank Dr Trevor Cumby and Dr Paul Hamer, who were part of my Thesis committee, for their expert advice.

I am indebted Christine, Colin, Katie and Paul in the central laboratory at SRI for their generous help with all the analytical work.

Further thanks go to all who helped with the construction the composting reactors and the electronic control systems:

Graham Pedrick in the workshop at SRI and Pete Hinton and his team in the School of Chemical Engineering workshop at the University of Birmingham.

Les Hartshorn and his team in Electronics at SRI and the John Sheard at the University of Birmingham.

The experimental work was carried out at SRI and I received much help from the support staff. John Tilcock for the carpentry work, John Pedder for the plumbing and Bob Watt, who often came into work out of hours to restart the air compressor after power cuts, which always seems to occur on Friday evenings and Sunday mornings. Special thanks go to Steve Watson and Rob Perkins for helping me collect the pig manure and being so good natured about it!

I would like to thank Rodger White for his help with the statistical analysis and Roger Cove and Tracey Fenn in Visual Media group for editing my photographs and producing of my presentation posters.

Thank you to my family and friends who have been wonderfully supportive during the past four years.

CONTENTS

CHAPTER 1. INTRODUCTION

1.1. The importance of composting	1-1
1.1.1. Composting as part of solid waste management	1-2
1.1.2. Composting in agriculture	1-3
1.2. Investigating composting	1-8
1.2.1. Aims and objectives	1-8
1.2.2. Project design	1-9
1.2.2.1. Experimentation	1-10
1.2.2.2. Modelling	1-10
1.3. Thesis layout	1-11

CHAPTER 2. LITERATURE REVIEW

2.1. Introduction.....	2-1
2.2. The composting process.....	2-2
2.2.1. Microbiology	2-3
2.2.1.1. Pathogens	2-4
2.2.2. Temperature	2-7
2.2.3. C:N ratio	2-8
2.2.3.1. The impact of ammonia emissions on the environment	2-10
2.2.4. pH	2-11
2.2.5. Moisture	2-12
2.2.6. Oxygen availability	2-13
2.2.6.1. Aeration	2-14
2.3. Composting systems	2-15
2.4. Modelling the composting process	2-16
2.4.1. Ammonia emissions models	2-18

CHAPTER 3. EQUIPMENT AND ANALYTICAL METHODS

3.1. Equipment.....	3-1
3.1.1. Respirometers	3-1
3.1.1.1. Constant pressure respirometer	3-2

3.1.1.2. Gas analyser respirometer	3-3
3.1.2. Composting unit	3-4
3.1.2.1. Composting reactor design	3-4
3.1.2.2. Control systems	3-6
3.1.2.2.1. Temperature and heat loss control	3-6
3.1.2.2.2. Aeration	3-7
3.1.2.2.3. Moisture	3-8
3.1.2.3. Monitoring systems	3-9
3.1.2.3.1. Temperature	3-9
3.1.2.3.2. Off-gas analysis	3-9
3.1.2.3.3. Mass loss	3-12
3.2. Analytical methods.	3-13
3.2.1. Preparation and sampling	3-13
3.2.2. Physical and chemical analyses	3-13
3.2.2.1. Total and volatile solids content.	3-13
3.2.2.2. Total organic carbon content	3-14
3.2.2.3. Nitrogen content	3-14
3.2.2.4. pH	3-15
3.2.2.5. Chemical oxygen demand	3-15
3.2.2.6. Bulk density and free airspace	3-16
3.2.2.7. Particle size distribution	3-17
3.2.3. Microbial analysis	3-18
3.2.4. Limitations of analytical tests	3-19
3.3. Characteristic of the organic material	3-20
3.3.1. Pig manure	3-20
3.3.2. Straw	3-23
3.3.3. Pig manure and straw mixes	3-25
3.3.3.1. Free air space	3-26
3.3.3.2. Thermodynamic properties	3-28
3.3.3.2.1. Specific heat capacity	3-30
3.3.3.2.2. Thermal diffusivity	3-30
3.3.3.2.3. Thermal conductivity	3-31

3.3.3.2.4. Results of thermal analyses	3-31
3.3.3.3. Composition of the pig manure and straw mixes	3-33
3.4. Summary	3-34

CHAPTER 4. RESPIROMETRY

4.1. Introduction.....	4-1
4.1.1. Theory and literature review	4-2
4.1.1.1. Process kinetics	4-2
4.1.1.2. Reaction rate coefficient	4-3
4.1.1.3. Specific oxygen uptake rate	4-3
4.1.1.4. Environmental factors	4-4
4.1.1.5. Respirometric techniques	4-6
4.1.1.6. Published results	4-6
4.1.1.6.1. Oxygen uptake rates	4-7
4.1.1.6.2. Reaction rate coefficient	4-8
4.2. Constant Pressure Respirometer	4-9
4.2.1. Introduction	4-9
4.2.1.1. Oxygen diffusion	4-10
4.2.2. Method	4-14
4.2.2.1. Sample preparation and analysis	4-14
4.2.2.2. Incubation	4-14
4.2.2.3. Oxygen uptake rate	4-15
4.2.3. Results	4-16
4.2.3.1. Specific oxygen uptake rate	4-16
4.2.3.2. Reaction rate coefficient	4-17
4.2.4. Discussion	4-18
4.3. Gas Analyser Respirometer	4-19
4.3.1. Introduction	4-19
4.3.2. Method	4-19
4.3.2.1. Sample preparation and analysis	4-19
4.3.2.2. Incubation	4-20
4.3.2.3. Oxygen uptake rate	4-21
4.3.2.4. Respiration quotient	4-22

4.3.3. Results and discussion	4-23
4.3.3.1. Specific oxygen uptake rate	4-23
4.3.3.2. Respiration quotients	4-25
4.3.3.3. Environmental factor effects	4-27
4.3.3.4. Reaction rate coefficient	4-30
4.3.3.5. Mass ratio	4-35
4.4. Conclusions.....	4-37

CHAPTER 5. MODELLING THE COMPOSTING PROCESS

5.1. Introduction.....	5-1
5.2. Model concept.....	5-2
5.2.1 The composting process	5-2
5.2.1.1. Process thermodynamics	5-2
5.2.1.2. Ammonia dynamics	5-3
5.2.2 The composting system	5-4
5.2.2.1. Ammonia turnover	5-5
5.2.2.1.1. pH	5-8
5.2.2.1.2. Interfacial surface area	5-10
5.2.2.2. Pathogen inactivation	5-11
5.2.3 Model outputs	5-12
5.3. Model equations.....	5-12
5.3.1 Mass model	5-13
5.3.1.1. Solids phase	5-13
5.3.1.1.1. pH	5-15
5.3.1.2. Liquid phase	5-15
5.3.1.2.1. Degree of off-gas saturation	5-16
5.3.1.3. Gas phase	5-17
5.3.2 Energy model	5-19
5.3.2.1. Heat generated by microbial activity	5-20
5.3.2.2. Heating the air	5-21
5.3.2.3. Heat of evaporation	5-22
5.3.3 Ammonia emissions model	5-23
5.3.3.1. Initial nitrogen content	5-23

5.3.3.2. Partition of ammonia	5-23
5.3.3.3. Ammonia in the gas phase	5-25
5.3.3.3.1. The mass transfer coefficient	5-26
5.3.3.4. Re-assimilation of nitrogen into biomass	5-28
5.3.4 Assumptions	5-28
5.4. Model simulations.....	5-30
5.4.1 Sensitivity analyses	5-33
5.4.1.1. Initial mixing ratio	5-33
5.4.1.2. Initial pH	5-38
5.4.1.3. Initial moisture content	5-41
5.4.1.4. Off-gas saturation	5-45
5.5. Discussion.....	5-49
5.5.1 Initial mixing ratio sensitivity analysis	5-49
5.5.2 pH sensitivity analyses	5-51
5.5.2.1. Initial pH of the organic material	5-51
5.5.2.2. Composting with a constant pH	5-53
5.5.3 Moisture content sensitivity analysis	5-55
5.5.3.1. Initial moisture content of the organic material	5-55
5.5.3.2. Off-gas saturation	5-57
5.6. Model sensitivity.....	5-59
5.7. Conclusions.....	5-61

CHAPTER 6. EXPERIMENTAL INVESTIGATION OF COMPOSTING FACTORS

6.1. Introduction.....	6-1
6.2. Experimental design.....	6-2
6.2.1. Ammonia emissions	6-4
6.2.2. Composting temperature	6-5
6.2.3. Experimental plan	6-6
6.3. Method	6-7
6.3.1. Preparation of the organic material.	6-7
6.3.2. Start-up of a composting trial	6-7
6.3.3. Statistical analysis	6-9
6.4. Results and discussion	6-10

6.4.1.	Temperature profiles	6-10
6.4.2.	Ammonia emissions profiles	6-12
6.4.3.	Pathogens	6-14
6.4.4.	Mass losses of the organic material	6-15
6.4.4.1.	Total solids	6-15
6.4.4.2.	Total mass	6-16
6.4.5.	Mass balances	6-17
6.4.5.1.	Nitrogen balances	6-17
6.4.5.2.	Water balance	6-19
6.4.5.3.	Carbon balance	6-21
6.4.6.	Statistical analysis	6-22
6.4.6.1.	Ammonia emissions	6-22
6.4.6.2.	Pathogen marker inactivation	6-24
6.4.6.3.	Total solids loss	6-25
6.5.	Conclusions.....	6-26

CHAPTER 7. VALIDATION, DISCUSSION AND CONCLUSIONS

7.1.	Model validation	7-1
7.1.1.	Biodegradability of straw	7-3
7.1.2.	R1-8-20	7-4
7.1.3.	R3-7-25	7-9
7.1.4.	R2-6-15	7-13
7.1.5.	Nitrogen balances	7-16
7.2.	Conclusions and future work	7-18

REFERENCES

APPENDIX

A1. Introduction.....	A1-1
A1.1. Ammonia emissions legislation	A1-1
A1.1.1. The National Emissions Ceiling Directive	A1-1
A1.1.1.1. Ammonia emissions and targets : 1990-2010	A1-2
A1.1.2. The Gothenburg Protocol	A1-2
A3. Equipment and analytical methods	A3-1
A3.1. The composting reactor	A3-1
A3.1.1. Radial heat loss simulations	A3-1
A3.1.2. Heat loss simulation programs	A3-9
A3.1.2.1. Reactor without insulation	A3-10
A3.1.2.2. Reactor with insulation	A3-14
A3.1.2.3. Reactor with insulation and heating cable	A3-18
A3.1.3. Heating cable geometry	A3-20
A3.2. The composting unit	A3-21
A3.2.1. Control of rig valves	A3-21
A4. Respirometry.....	A4-1
A4.1. Curve fitting	A4-2
A4.1.1. Double power equation	A4-2
A4.1.2. Enzyme activity equation	A4-4
A5. Modelling the composting process	A5-1
A5.1. Calculation of initial conditions	A5-1
A5.1.1. Interfacial surface area	A5-1
A5.1.2. Cross sectional area and airflow velocity	A5-3
A5.1.3. Gas partition coefficients	A5-4
A5.2. Model implementation in <i>ModelMaker</i>	A5-6
A5.2.1. <i>ModelMaker</i> features	A5-6
A5.2.2. Constructing and running a <i>ModelMaker</i> model	A5-7
A5.2.3. The composting model in <i>ModelMaker</i>	A5-10
A5.2.3.1. Mass model	A5-11
A5.2.3.2. Energy model	A5-17

A5.2.3.3. Ammonia emissions model	A5-18
A5.2.3.4. Main model view	A5-20
A5.2.3.5. Definition model view	A5-21
A5.2.4. Model logic	A5-28
A6. Experimental investigation of composting factors	A6-1
A6.1. A detailed analysis of the composting experiments	A6-1
A6.1.1. Trial 1 (C:N ratio 20)	A6-2
A6.1.1.1. Process analysis	A6-2
A6.1.1.2. Analysis of the organic material	A6-6
A6.1.2. Trial 2 (C:N ratio 25)	A6-10
A6.1.2.1. Process analysis	A6-10
A6.1.2.2. Analysis of the organic material	A6-14
A6.1.3. Trial 3 (C:N ratio 15)	A6-16
A6.1.3.1. Process analysis	A6-16
A6.1.3.2. Analysis of the organic material	A6-20
A6.1.4. Trial 4 (C:N ratio 20)	A6-22
A6.1.4.1. Process analysis	A6-22
A6.1.4.2. Analysis of the organic material	A6-26
A6.1.5. Trial 5 (C:N ratio 25)	A6-28
A6.1.5.1. Process analysis	A6-28
A6.1.5.2. Analysis of the organic material	A6-32
A6.1.6. Trial 6 (C:N ratio 15)	A6-33
A6.1.6.1. Process analysis	A6-33
A6.1.6.2. Analysis of the organic material	A6-38
A6.2. Summary of the organic material analyses	A6-41
A6.3. Nitrogen dynamics	A6-47
A6.4. <i>Genstat</i> (Version 6) statistical analyses	A6-49
A6.4.1. Input data	A6-49
A6.4.2. Output from statistical analysis	A6-51
A6.4.2.1. Ammonia emissions	A6-53
A6.4.2.2. Pathogen marker inactivation	A6-63
A6.4.2.3. Total solids loss	A6-66

PUBLICATIONS

Cronjé, A. L., Barker, A. J., Guy, S., Turner, C. and Williams, A. G., Oxygen uptake rate of composting pig manure (Poster Presentation). Abstract in: Proceedings of the International Symposium on Composting and Compost Utilization, May 2002, Columbus, Ohio, USA. JG Press Inc., Emmaus, USA. (2002).

Cronjé, A. L., Barker, A. J., Guy, S., Turner, C. and Williams, A. G., Ammonia emissions and pathogen inactivation during composting. In: Proceedings of the International Symposium on Composting and Compost Utilization, May 2002, Columbus, Ohio, USA. JG Press Inc., Emmaus, USA. (2002)

Cronjé, A. L., Barker, A. J., Guy, S., Turner, C. and Williams, A. G., The respiration rate of composting pig manure. Compost Science and Utilization (accepted Dec 2002)

Cronjé, A. L., Barker, A. J., Guy, S., Turner, C. and Williams, A. G., Composting under controlled conditions. Environmental Technology (accepted Apr 2003)

FIGURES

Figure 1.1. Waste management hierarchy: options for the treatment of solid organic waste.	1-2
Figure 1.2. Sources on composted organic material in 1999.	1-3
Figure 1.3. An unmanaged FYM field heap.	1-4
Figure 1.4. An outdoor FYM heap in winter on a concrete floor.	1-5
Figure 2.1. Composting stages as distinguished by the temperature and pH.	2-2
Figure 2.2. Food web pyramid that exists in traditional composting heaps.	2-3
Figure 3.1. Constant pressure respirometer.	3-2
Figure 3.2. Continuous gas analysis respirometer.	3-3
Figure 3.3. Composting reactor of the composting unit.	3-5
Figure 3.4. Control systems of the composting unit.	3-6
Figure 3.5. Condenser unit in which water is removed from the off-gas sample.	3-10
Figure 3.6. Gas analyser, control valve panel and PC-based data logger.	3-11
Figure 3.7. Ammonia acid trap.	3-11
Figure 3.8. Points of measurement on the rig of Reactor 1.	3-12
Figure 3.9. Measuring the pH of the organic material during composing.	3-15
Figure 3.10. Apparatus to measure bulk weight and free air space of a compost-type material.	3-16
Figure 3.11. Coliform colonies in pig manure extract for dilutions 10^{-1} to 10^{-6} grown on McConkey's agar.	3-22
Figure 3.12. Distribution of straw lengths from 1000 pieces measurements.	3-23
Figure 3.13. Fraction of added liquid absorbed by the straw (M_{abs} : M_{add}) for a range of mixing ratios of liquid and straw (M_{add} : M_{Straw}).	3-24
Figure 3.14. Pig manure and straw before and after mixing in the ratio of 4.	3-25
Figure 3.15. Schematic of the structure of the manure and straw mix.	3-26
Figure 3.16. Relationship between the bulk weight and FAS of the organic material calculated using equation (3 vii) (o) and equation (3 ix) (●).	3-28
Figure 4.1. Relationships between the effect functions and corresponding factors.	4-5
Figure 4.2. Diffusion of oxygen into the manure in the CPR.	4-11
Figure 4.3a. Stage 1: Oxygen concentration profiles in an air atmosphere	4-12
Figure 4.3b. Stage 1: Oxygen concentration profiles in an oxygen atmosphere	4-13
Figure 4.4a. Stage 2: Diffusion of oxygen from an air atmosphere	4-13

Figure 4.4b. Stage 2: Diffusion of oxygen from an oxygen atmosphere	4-13
Figure 4.5. Oxygen uptake profiles for manure incubated at 20 °C (×), 55 °C (●) and 70 °C (o).	4-16
Figure 4.6. Temperature effect on the reaction rate coefficient of pig manure.	4-18
Figure 4.7. Cumulative hourly emission rate of CO ₂ and uptake rate of O ₂ for the M:S ratio of 2:1 incubated in Reactor 1 at 30 °C (o) and 50 °C (●).	4-24
Figure 4.8. Average respiration quotients, Q_{resp} , in the fast and slow stages for the M:S ratios of 2:1 (●) and 4:1 (o).	4-25
Figure 4.9. Mean f_{OC} values for the M:S ratios of 2:1 (-) and 4:1 (o).	4-28
Figure 4.10. Mean f_{T2} and f_{T4} values for the M:S ratios of 2:1 (-) and 4:1 (o).	4-29
Figure 4.11a. Mass ratio for the organic material with the M:S ratio of 2:1.	4-36
Figure 4.11b. Mass ratio for the organic material with the M:S ratio of 4:1.	4-37
Figure 5.1. Composting system modelled.	5-5
Figure 5.2. Gas exchanges between the gas and liquid-solid phases during composting.	5-6
Figure 5.3. Mass of ammonia (NH ₃ + NH ₄ ⁺), M_{Amm} , as a percentage of the total nitrogen, M_{TN} , with respect to the total solids content (TS).	5-7
Figure 5.4. pH, temperature and solids content effect on the fraction of free ammonia, F.	5-9
Figure 5.5. Structure of the organic material used to estimate the interfacial area	5-10
Figure 5.6. The assumed pH profile during composting.	5-15
Figure 5.7. A hypothetical relationship between the degree of saturation of the off-gas and the airflow rate through the organic material.	5-17
Figure 5.8. Dissociation of ammonia in water.	5-25
Figure 5.9. K_L of ammonia as a function of composting temperature, T_C .	5-27
Figure 5.10. Mass profiles from the initial mixing ratio simulations.	5-34
Figure 5.11. Temperature profiles from the initial mixing ratio simulations.	5-35
Figure 5.12. Nitrogen profiles from the initial mixing ratio simulations.	5-36
Figure 5.13. Off-gas composition and aeration profile from the mixing ratio simulations.	5-37
Figure 5.14. Nitrogen profiles from initial pH simulations.	5-38
Figure 5.15. Off-gas composition and aeration profiles from the initial pH simulations.	5-39
Figure 5.16. Nitrogen profiles from constant pH simulations.	5-40
Figure 5.17. Mass profiles from initial moisture contents simulations.	5-41
Figure 5.18. Temperature profiles from initial moisture content simulations.	5-42

Figure 5.19. Nitrogen profiles from initial moisture content simulations.	5-43
Figure 5.20. Off-gas composition and aeration profiles from initial moisture content simulations	5-44
Figure 5.21. Mass profiles from ϕ simulations.	5-45
Figure 5.22. Temperature profiles from ϕ simulations.	5-46
Figure 5.23. Nitrogen profiles from ϕ simulations.	5-47
Figure 5.24. Off-gas composition and aeration profiles from ϕ simulations.	5-48
Figure 5.25. Moisture content and factor profiles from initial mixing ratio simulations.	5-50
Figure 5.26. Moisture content and process factor profiles from initial pH simulations.	5-52
Figure 5.27. Moisture content and process factors profiles from constant initial pH simulations.	5-54
Figure 5.28. Moisture content and process factor profiles from initial moisture content simulations.	5-56
Figure 5.29. Moisture content and process factor profiles from ϕ simulations.	5-58
Figure 6.1. The three composting reactors in the composting unit.	6-3
Figure 6.2. Dissociation curves of ammonia in aqueous (20 °C) and slurry solutions.	6-5
Figure 6.3. Approximately 47 kg of the organic material ready for loading into the reactors.	6-8
Figure 6.4. Centre composting temperature profile for each initial pH in a trial.	6-11
Figure 6.5. Cumulative ammonia emissions profiles for each initial pH in a trial.	6-13
Figure 6.6. Total percentage total solids (TS) loss in the organic material.	6-15
Figure 6.7. Total mass loss from the organic material in Reactor 1 during composting.	6-16
Figure 7.1. Straw biodegradability sensitivity analysis.	7-3
Figure 7.2. Total and evaporated water mass profiles of R1-8-20.	7-4
Figure 7.3. Measured and predicted temperature and total airflow profiles of R1-8-20.	7-6
Figure 7.4. Measured and predicted cumulative mass profiles of ammonia and carbon dioxide produced and oxygen consumed in R1-8-20.	7-7
Figure 7.5. Measured and predicted oxygen and carbon dioxide concentration profiles in the off-gas in R1-8-20.	7-8
Figure 7.6. Measured and predicted temperature and total airflow profiles of R3-7-25.	7-10

Figure 7.7. Measured and predicted cumulative mass profiles of ammonia and carbon dioxide produced and oxygen consumed in R3-7-25.	7-11
Figure 7.8. Measured and predicted temperature and total airflow profiles of R2-6-15.	7-13
Figure 7.9. Measured and predicted cumulative mass profiles of ammonia and carbon dioxide produced and oxygen consumed in R2-6-15.	7-14
Figure 7.10. Measured and predicted nitrogen balances a) R2-6-15, b) R1-8-20, c) R3-7-25	7-16
Figure A1.1. Ammonia emissions and targets:1990-2010.	A1-2
Figure A3.1. Section of reactor considered in heat loss simulations.	A3-1
Figure A3.2. Transfer mechanisms of heat loss from element 1.	A3-3
Figure A3.3. Radiative heat transfer coefficient change with temperature difference.	A3-4
Figure A3.4. Radial temperature profile for an initial temperature of 20°C.	A3-7
Figure A3.5. Radial temperature profile for an initial temperature of 40°C.	A3-8
Figure A3.6. Radial temperature profile for an initial temperature of 60°C.	A3-8
Figure A3.7. Equilibrating temperatures in an un-insulated reactor operating at 60 °C.	A3-14
Figure A3.8. Equilibrating temperatures in an insulated reactor operating at 60 °C.	A3-19
Figure A3.9. Equilibrating temperatures for a reactor in an insulated reactor with heating cable operating at 60 °C.	A3-19
Figure A3.10. Configuration of the heating cable on the reactor.	A3-20
Figure A3.11. Composting unit (three composting reactors and rig).	A3-22
Figure A3.12. Humidifying unit, temperature and aeration control boxes of Reactor 2 and 3.	A3-23
Figure A3.13. Ammonia acid trap.	A3-24
Figure A4.1. Reaction rate coefficients as a function of temperature for the fast (●) and slow (o) stages of M:S ratio of 2:1 based on equation (4 xvii).	A4-3
Figure A4.2. Reaction rate coefficients as a function of temperature for the fast (●) and slow (o) stages of M:S ratio of 4:1 based on equation (4 xvii).	A4-4
Figure A4.3. Reaction rate coefficients as a function of temperature for the fast (●) and slow (o) stages of M:S ratio of 2:1 based on the equation (4 xviii).	A4-5
Figure A4.4. Reaction rate coefficients as a function of temperature for the fast (●) and slow (o) stages of M:S ratio of 4:1 based on the equation (4 xviii).	A4-5

Figure A5.1. Interface display of the <i>ModelMaker</i> software.	A5-8
Figure A5.2. The window for setting the sensitivity analysis limits	A5-9
Figure A5.3. Results view of a graphical representation of the temperature profile.	A5-10
Figure A5.4. Decomposition of organic material at a constant reaction rate.	A5-11
Figure A5.5. Process kinetics as represented by model component.	A5-14
Figure A5.6. Water balance model as represented by model components.	A5-15
Figure A5.7. Gas phase of the mass model as represented by model components.	A5-16
Figure A5.8. Energy model as represented by model components.	A5-17
Figure A5.9. Ammonia emissions model as represented by model components.	A5-18
Figure A5.10. Diagram view of the model in <i>ModelMaker</i> .	A5-20
Figure A5.11. Model algorithm.	A5-29
Figure A6.1. Profiles of the process variables for the experiment R3-6-20.	A6-3
Figure A6.2. Profiles of process variables for experiment R2-7-20.	A6-4
Figure A6.3. Profiles of process variables for experiment R1-8-20.	A6-5
Figure A6.4. 40 day temperature profiles of R3-6-20 in Trial 1.	A6-8
Figure A6.5. 40 day temperature profile of T1-R2-7.	A6-9
Figure A6.6. Profiles of process variables for experiment R1-6-25.	A6-11
Figure A6.7. Profiles of process variables for experiment R3-7-25.	A6-12
Figure A6.8. Profiles of process variables for experiment R2-8-25.	A6-13
Figure A6.9. Profiles of process variables for experiment R2-6-15.	A6-17
Figure A6.10. Profiles of process variables for experiment R1-7-15.	A6-18
Figure A6.11. Profiles of process variables for experiment R3-8-15.	A6-29
Figure A6.12. Profiles of process variables for experiment R2-6-20.	A6-23
Figure A6.13. Profiles of process variables for experiment R1-7-20.	A6-24
Figure A6.14. Profiles of process variables for experiment R3-8-20.	A6-25
Figure A6.15. Profiles of process variables for experiment R3-6-25.	A6-29
Figure A6.16. Profiles of process variables for experiment R2-7-25.	A6-30
Figure A6.17. Profiles of process variables for experiment R1-8-25.	A6-31
Figure A6.18. Profiles of process variables for experiment R1-6-15.	A6-34
Figure A6.19. Profiles of process variables for experiment R3-7-15.	A6-35
Figure A6.20. Profiles of process variables for experiment R2-8-15.	A6-36
Figure A6.21. White fungal growth on the composted organic material in R3-7-15.	A6-39
Figure A6.22. Nitrogen inputs and outputs.	A6-48

Figure A6.23. Main view and statistical analysis window in <i>Genstat</i> (Version 6).	A6-50
Figure A6.24. Output view in <i>Genstat</i> (Version 6).	A6-52
Figure A6.25. Mean values of the ammonia emissions for the initial pH (a) and C:N ratio (b) of the organic material groups.	A6-54
Figure A6.26. The relationship between the ammonia emission rate and the mean airflow and temperature.	A6-57
Figure A6.27. Relationship between the ammonia emission rate and the mean airflow in initial pH groups: a) parallel lines b) separate lines.	A6-60
Figure A6.28. Relationship between the ammonia emissions and ammonia emission rate and the airflow rate within the initial pH groups.	A6-63
Figure A6.29. Ammonia emissions means for the initial pH (a) and C:N ratio (b) groups.	A6-67
Figure A6.30. Relationship between the TS loss and the measure initial pH.	A6-68

TABLES

Table 1.1. Agriculture sources of UK ammonia emissions (1996-97).	1-7
Table 2.1. Some pathogenic bacteria and viruses in biosolids and the diseases they cause.	2-5
Table 2.2. Degradability of compounds typically found in organic material.	2-7
Table 3.1. Analysis of the pig manure for each collection.	3-21
Table 3.2. Distribution of organic material and ash particles in pig manure.	3-21
Table 3.3. Analysis of the winter wheat straw from two harvests.	3-23
Table 3.4. Bulk weight (ω_{bulk}) and free air space (FAS) of test samples.	3-27
Table 3.5. Thermal properties of pig manure and straw mixes.	3-33
Table 3.6. Composition of the manure and straw mixes composted.	3-34
Table 4.1. Analysis of bulk pig manure.	4-16
Table 4.2. SOUR of manure at selected incubation temperatures.	4-17
Table 4.3. Physical and chemical characteristics of the pig manure and straw mix samples.	4-23
Table 4.4. SOUR and SCER between 10 °C and 70 °C for the fast and slow stages. (M:S ratio 2:1)	4-24
Table 4.5. SOUR and SCER between 10 °C and 70 °C for the fast and slow stages. (M:S ratio 4:1)	4-25
Table 4.6. Composition of the organic material and the Q_{resp} of the representative compounds.	4-26
Table 4.7. Values of the constants that describe the dependence of k_T on T.	4-33
Table 5.1. Values of constants used to determine the dissociation constant of the NH_3 in water.	5-24
Table 5.2. Parameter values of the manure and straw used for model simulations.	5-31
Table 5.3. Values of the organic material and process parameters.	5-32
Table 5.4. Cumulative masses of carbon dioxide produced and oxygen consumed.	5-59
Table 5.5. Factors and variables used to test the sensitivity of the model.	5-60
Table 5.6. Output values of the variables from the simulations of the sensitivity analyses.	5-60
Table 5.7. Sensitivity of process variables to incremental changes in the factor values.	5-61
Table 6.1. The design of experiment trials.	6-6

Table 6.2. Pathogen markers in the composted organic material and related process conditions.	6-14
Table 6.3. Nitrogen balances of the composting experiments	6-18
Table 6.4. Water balances of the composting experiments.	6-20
Table 6.5. Carbon balance of the experiments in Trials 1 and 6.	6-21
Table 6.6. Summary of the statistical analyses	6-23
Table 7.1. Parameter values for model validation simulations	7-3
Table 7.2. Initial and final experimental and model data for R1-8-20	7-9
Table 7.3. Initial and final experimental and model data for R3-6-25	7-12
Table 7.4. Initial and final experimental and model data for R2-7-15	7-15
Table A1.1. Emission ceilings for ammonia (thousands of tonnes of NH ₃ per year)	A1-13
Table A3.1. Values of thermodynamic and physical properties used in the model.	A3-6
Table A3.2. Valve combinations for off-gas analysis and automatic gas analyser calibration.	A3-21
Table A4.1. Diffusion coefficients and solubility of oxygen in water.	A4-1
Table A4.2. Total effect of the environmental factors in the GAR	A4-2
Table A5.1. Composition of organic material (14 kg TS) for the three M:S ratios and MC simulated in the model.	A5-1
Table A5.2. Estimations of the volumes and surface areas of 14 kgTS of organic material.	A5-3
Table A5.3. Estimation of the mean air velocity in the organic material for cooling aeration.	A5-4
Table A5.4. Calculated values of A, a, b, c, d and Mr _{VS} of the respective mixing ratios.	A5-5
Table A5.5. Main model components of <i>ModelMaker</i> software.	A5-6
Table A5.6. Default units of the model components.	A5-10
Table A5.7. Symbols used in <i>ModelMaker</i> to describe the composting model.	A5-12
Table A6.1. The complete experimental design required for blocked two-way ANOVA.	A6-1
Table A6.2. Mass changes in the organic material in Trial 1.	A6-7
Table A6.3. Mass changes in the organic material in Trial 2.	A6-14
Table A6.4. Mass changes in the organic material in Trial 3.	A6-21
Table A6.5. Mass changes in the organic material in Trial 4.	A6-27
Table A6.6. Mass changes in the organic material in Trial 5.	A6-32

Table A6.7. Mass changes in the organic material in Trial 6.	A6-38
Table A6.8. Analysis of the initial and final (composted) organic material in Trial 1 (C:N 20).	A6-41
Table A6.9. Analysis of the initial and final (composted) organic material in Trial 2 (C:N 25).	A6-42
Table A6.10. Analysis of the initial and final (composted) organic material in Trial 3 (C:N 15).	A6-43
Table A6.11. Analysis of the initial and final (composted) organic material in Trial 4 (C:N 20).	A6-44
Table A6.12. Analysis of the initial and final (composted) organic material in Trial 5 (C:N 25).	A6-45
Table A6.13. Analysis of the initial and final (composted) organic material in Trial 6 (C:N 15).	A6-46
Table A6.14. Ammonia emissions and associated process variables.	A6-47
Table A6.15. Input data for <i>Genstat</i> (Version 6) statistical analysis.	A6-49
Table A6.16. The meaning of the statistical terms used in the <i>Genstat</i> (Version 6) output.	A6-51

NOMENCLATURE

Units

Unit of measurement	Physical quantity	Unit symbol	Dimension
Atmosphere	Pressure	atm	$[M \cdot T^{-2} \cdot L^{-1}]$
Bar	Pressure	bar	$[M \cdot T^{-2} \cdot L^{-1}]$
Centimetre	Length	cm	$[L]$
Colony forming units	Amount	CFU	-
Degrees centigrade	Temperature	°C	$[\theta]$
Gram	Mass	g	$[M]$
Gram mole	Substance amount	g-mol	-
Hour	Time	h	$[T]$
Joule	Energy	J	$[M \cdot L^2 \cdot T^{-2}]$
Kelvin	Temperature	K	$[\theta]$
kilogram	Mass	kg	$[M]$
kilojoule	Energy	kJ	$[M \cdot L^2 \cdot T^{-2}]$
kilomole	Substance amount	kmol	-
kilowatt	Power	kW	$[M \cdot L^2 \cdot T^{-3}]$
Litre	Volume	l or dm ³	$[L^3]$
Metre	Length	m	$[L]$
Molarity or molar	Concentration	M or mol dm ⁻³	-
Milligram	Mass	mg	$[M]$
Minute	Time	min	$[T]$
Millilitre	Volume	ml	$[L^3]$
Millimetre	Length	mm	$[L]$
Mole	Substance amount	mol	-
Parts per billion	Concentration	ppb	$[M \cdot M^{-1}]$
Parts per millions	Concentration	ppm	$[M \cdot M^{-1}]$
Second	Time	s	$[T]$
Watts	Power	W	$[M \cdot L^2 \cdot T^{-3}]$

Abbreviations

		Units
Amm-N	Ammoniacal nitrogen content	% or g g ⁻¹ TS
AN	Ammoniacal nitrogen	g
ANOVA	Analysis of variance	-
ASH	Ash content	% or g g ⁻¹ TS
BOD	Biological oxygen demand	g O ₂ kg ⁻¹ TS
CCE	Cumulative carbon dioxide emissions	mg CO ₂ g ⁻¹ TS
COD	Chemical oxygen demand	g O ₂ kg ⁻¹ TS
COU	Cumulative oxygen uptake	mg O ₂ g ⁻¹ TS
C:N ratio	Carbon to nitrogen ratio	kg kg ⁻¹
CPR	Constant pressure respirometer	-
FAS	Free air space	% v v ⁻¹
FMD	Foot and mouth disease	-
F pr	Probability factor	-
FYM	Farm yard manure	-

GAR	Gas analyser respirometer	-
HCER	Hourly carbon dioxide emission rate	$\text{mg CO}_2 \text{ h}^{-1} \text{ g}^{-1}$
HOURL	Hourly oxygen uptake rate	$\text{mg O}_2 \text{ h}^{-1} \text{ g}^{-1}$
ISWM	Integrated solid waste management	-
Kj-N	Kjeldahl nitrogen content	% or g g^{-1} TS
LN	Leachate nitrogen	g
M	Manure	-
MC	Moisture content	% or g g^{-1}
M:S ratio	Manure to straw mixing ratio	kg kg^{-1}
NECD	National Emissions Ceiling Directive	
ON	Organic nitrogen	g
Org-N	Organic nitrogen content	% or g g^{-1} TS
OUR	Oxygen uptake rate	$\text{g O}_2 \text{ h}^{-1} \text{ kg}^{-1}$ TS
PID	Proportional-integral-differential response	-
S	Straw	-
SOUR	Specific oxygen uptake rate	$\text{g O}_2 \text{ h}^{-1} \text{ kg}^{-1}$ TS
SCER	Specific carbon dioxide emission rate	$\text{g CO}_2 \text{ h}^{-1} \text{ kg}^{-1}$ TS
TN	Total nitrogen	g
TOC	Total organic carbon	% g g^{-1} TS
TS	Total solids	g
VAF	Variance accounted for	%
VETC	Verocytotoxic	
VS	Volatile solids	g

Symbols

		Units
A	Acid equilibrium reaction constant	-
B	Acid equilibrium reaction constant	-
C	Acid equilibrium reaction constant	-
C_{HX}	Helix circumference	m
c_p	Specific heat capacity	$\text{kJ kg}^{-1} \text{ }^\circ\text{C}^{-1}$
CSA	Cross sectional area	m^2
D	Diffusion coefficient	$\text{cm}^2 \text{ s}^{-1}$
F	Fraction of AN as NH_3 or airflow rate	- or l min^{-1}
f_i	Function of environmental factor's effect	-
G	Specific gravity	$\text{cm}^3 \text{ cm}^{-3}$
h	Heat transfer coefficient	$\text{W m}^{-2} \text{ K}^{-1}$
H	Heat energy	J
H	Henry's coefficient	$(\text{kg m}^{-3})_l (\text{kg m}^{-3})_g^{-1}$
H_L	Latent heat	$\text{kJ kg}^{-1} \text{ H}_2\text{O}_{\text{evap}}$
k	Reaction rate coefficient	h^{-1}
k	Thermal conductivity	$\text{W m}^{-1} \text{ }^\circ\text{C}^{-1}$
K_a	Acid dissociation constant	$\text{mol l}^{-1} \text{ to } \text{kg m}^{-3}$
k_g	Gas phase mass transfer coefficient	$\text{kg m}^{-2} \text{ atm}^{-1} \text{ h}^{-1}$
K_G	Overall gas phase mass transfer coefficient	$\text{kg m}^{-2} \text{ atm}^{-1} \text{ h}^{-1}$
k_l	Liquid phase mass transfer coefficient	m h^{-1}
K_L	Overall liquid phase mass transfer coefficient	m h^{-1}
K_m	Mass transfer coefficient	m h^{-1}
L	Length	m

M or m	Mass	kg or g
M_r	Relative molecular mass,	$\text{g g}^{-1}\text{mol}^{-1}$
N or n	Number	-
\bar{n}	Average of normalised number of colonies	-
N_{cell}	Nitrogen content of cell	g g^{-1}
p	Pressure	bar or atm
Q	Heat energy	J
Q_{10}	Temperature coefficient	-
Q_{resp}	Respiration quotient	$\text{mol CO}_2 \text{ mol}^{-1} \text{ O}_2$
r	Radius	m
R	Universal gas constant (0.08314)	$\text{bar ml g}^{-1}\text{mol}^{-1} \text{ K}^{-1}$
R_m	Mass ratio	kg kg^{-1}
S	Degree of saturation of the off-gas	-
SA	Surface area of the phase boundary	m^2
T	Temperature	$^{\circ}\text{C}$ or K
TR	Reference temperature	$^{\circ}\text{C}$
v	Superficial velocity	ms^{-1}
V	Volume	l, dm^{-3} or m^3
VF	Volumetric flow rate	$\text{m}^3 \text{ h}^{-1}$
\bar{x}	Average number of colonies	-
Y_{cell}	Cell yield	$\text{g cell g}^{-1} \text{ TS loss}$
Z	Dilution	-
Greek		Units
α	Thermal diffusivity	$\text{m}^2 \text{ s}^{-1}$
β	Bio-degradability fraction	-
ε	Emissivity	-
φ	Saturation exponent	-
ρ	Density	kg m^{-3}
σ	Stefan-Boltzmann constant = 5.67×10^{-8} or standard deviation	$\text{W m}^{-2} \text{ K}^{-1}$ -
ω	Weight	kg
Chemical		
[...]	Concentration of substance	
$\text{C}_5\text{H}_7\text{O}_2\text{N}$	Cell chemical formula	
CO_2	Carbon dioxide	
$\text{CO}(\text{NH}_2)_2$	Urea	
H^+	Hydrogen ions or protons	
H_2O	Water	
NaOH	Anhydrous sodium hydroxide	
NH_3	Free or dissociated ammonia	
NH_4^+	Associated ammonium ion	
O_2	Oxygen gas	
OH^-	Hydroxide ion	

Subscripts

A	Air
abs	Absorbed
add	Added
air	Air entering the composting system
amb	Ambient
aq	Aqueous phase
atm	Atmospheric
Bath	Thermostatically controlled water bath
bulk	Bulk organic material
c + r	Combined (convective and radiative)
C	Composting
CO ₂ resp	Carbon dioxide produced during aerobic respiration
cond	Conductive heat transfer
conv	Convective heat transfer
d	Daily basis
e	Equilibrium
eff	Effective
emit	Emitted
evap	Evaporated
F	Final state
fast	Fast oxygen uptake rate stage
g or gas	Gas phase
gen	Generated
j	An organic material or element of organic material
I	Initial state
in	Initial gas concentrations
inf	Point of inflection
int	Interfacial
l or liq	Liquid phase
max	Maximum
min	Minimum
Mix	Manure and straw mix
O ₂ resp	Oxygen used during aerobic respiration
OC	Oxygen concentration
opt	Optimum conditions
out	Final gas concentrations
Reactor	Reactor vessel of the CPR respirometer
slow	Slow oxygen uptake rate stage
rad	Radiative heat transfer
ref	Reference
syn	Synthesised
t	Time
TR1	Reference temperature 1
TR2	Reference temperature 2
Tube	Tubes of the CPR respirometer
W	Water
WF	Free water

CHAPTER 1

INTRODUCTION

1.1. The importance of composting

Composting is a well-established means of recycling organic material and returning it to the land to replenish the soil nutrients and improve soil structure. It has been used for centuries throughout the world. In fact, it is documented that Chinese peasants farming in delta regions were composting 4000 years ago [Gray *et al* 1971c, Van Ginkel 2000] and by doing so, were able to support high population densities without exhausting the soil nutrients and breaking down its structure. Similarly, Himalayan farmers practised composting as part of the management of their terraced fields on the steep mountain sides, which were prone to erosion and leaching of nutrients from the soil, especially during the wet season. Their small-scale batch composting systems probably used the same basic management principals used today but increased knowledge of the fundamental processes, thanks to modern scientific methods, has enabled the advancement of composting to large-scale batch or continuous industrial operations for the treatment of organic waste. Composting, in effect, is a biological process carried out by a variety of bacteria and fungi, which, through a series of complex biochemical reactions, converts solid organic materials in predominantly aerobic conditions to a more stable product. The degree of decomposition and, therefore, stability of the composted organic material depends very much on the duration and the temperatures achieved during the process [Haug 1993]. Further understanding of the composting is achieved by modelling the process in conjunction with controlled composting experiments [Finsten *et al* 1986].

1.1.1. Composting as part of solid waste management

Over the past few years the composting industry in the United Kingdom (UK) has grown rapidly. The long-term sustainability of composting and the diversion of organic material from disposal, or at least a more controlled and hygienic method of disposal, have lead to its recognition as an essential part of an integrated solid waste management (ISWM) strategy. Figure 1.1 illustrates how composting can fit into an ISWM strategy [Biowise 2001] and shows the waste management hierarchy as defined in The Waste Strategy 2000 provided by the Department of the Environment Food and Rural Affairs (Defra) [Defra 2002].

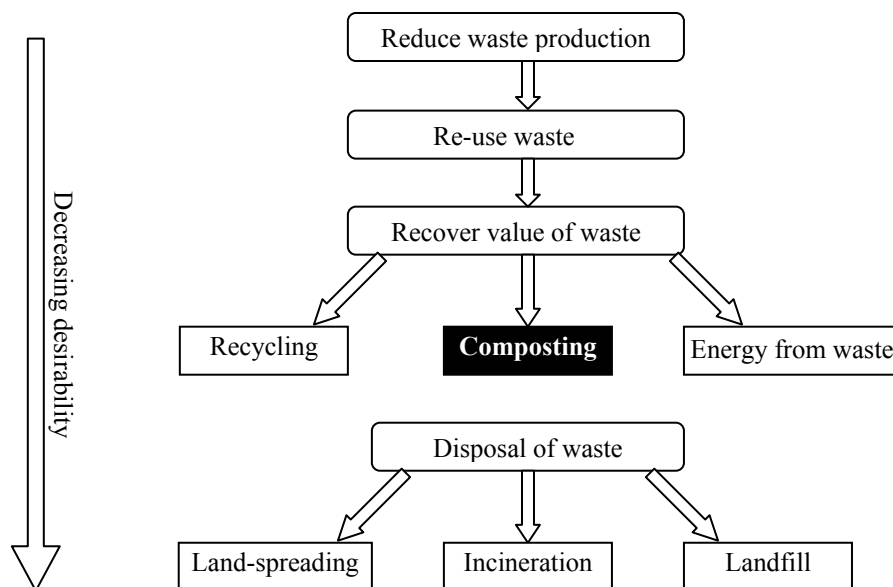


Figure 1.1. Waste management hierarchy: options for the treatment of solid organic waste.

Most biodegradable organic materials cannot be re-used but their value can be recovered easily and relatively cheaply by composting to give a product that can be used in agriculture, horticulture and other markets. Figure 1.2 shows the sources of the composted organic material as a percentage of the 833 044 tonnes of organic waste composted in the UK in 1999 [Slater *et al* 2001].

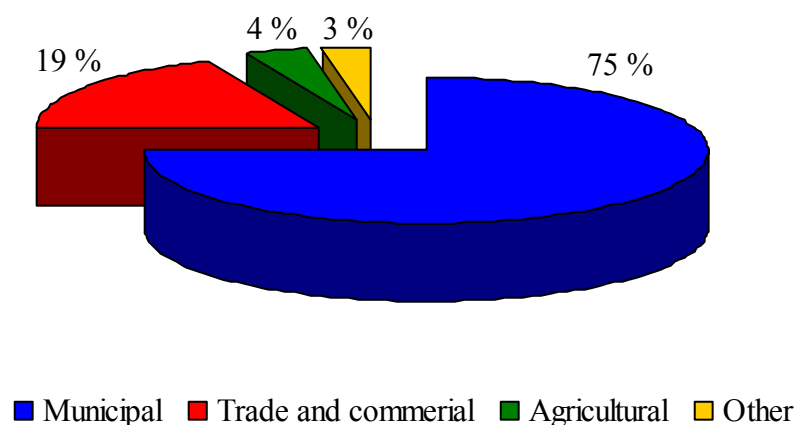


Figure 1.2. Sources on composted organic material in 1999.

1.1.2. Composting in agriculture

The amount of agricultural organic material composted in 1999 (Figure 1.2) constituted a mere 22 725 tonnes considering that 43 million tonnes of solid farmyard manure (FYM) alone was collected from UK farms in the same year. With the increase in size and intensity of animal-rearing farms, and use of animal bedding, this annual FYM quota continues to rise. A number of environmental and health problems are associated with the accumulation and disposal of agricultural wastes such as FYM [Swan *et al* 2003].

Handling FYM incurs considerable costs for farmers owing to the large mass and volume that has to be processed. Traditionally, FYM has been spread on the farmland after a few months' storage in field heaps. In the field heaps, spontaneous but unpredictable composting takes place because they are exposed to ambient conditions and their management tends to be limited to turning the heaps occasionally (Figure 1.3).

Disposal of nitrogen-rich manures has become even more of an issue for farmers as legislation restricting the amount, frequency and location of manure spreading is now in place. The European Community Nitrates Directive has designated nitrogen-vulnerable zones (NVZ) in catchments where nitrate from agricultural land is causing pollution of



Figure 1.3. An unmanaged field heap of FYM.

watercourses, which, since 2002, have increased from 8 % to 55 % of England's land area [Defra 2003a]. Seasonal spreading has been implemented, particularly on soils prone to leaching, which includes 'closed' periods during the autumn months when no manures can be applied to the farmland. Although the 'closed' periods do not apply to the spreading of FYM, defined by Defra as straw-based manures, storage is necessary when the ground is waterlogged, flooded, frozen or snow covered. Manures and FYM, therefore, now need to be stored for longer periods and usually during all the winter (Figure 1.4).



Figure 1.4. An outdoor FYM heap in winter on a concrete floor¹.

Another issue that has received much attention recently is the risks of pathogens being introduced into the human food chain from manures. FYM may contain significant levels of harmful faecal pathogens, such as *Salmonella* spp. and verocytotoxic (VTEC) *Escherichia coli* (*E. coli*) O157, although some are more prevalent in different manures [Suslow 2001]. The possibility of crop contamination following the spreading of the FYM on land has raised concerns [Maule 1998]. Scientific validation studies of pathogen reduction in manure are an imminent need [Suslow 2001].

¹ Photograph courtesy of Brian Chambers at ADAS, Gleanthorpe, Meden Vale, Mansfield, NG20 9PF, UK

If composting is managed well, high temperatures can be achieved within the FYM, which are believed to contribute to the inactivation of the pathogens and so render the FYM safe for handling. Solid manures offer the best opportunity for pathogen control via storage in field heaps [Chambers *et al* 2002] but pathogens have been detected after uncontrolled composting [Farrell 1992]. The onset of anaerobic activity is another undesirable consequence of poor management of the process and needs to be avoided.

The high nitrogen content of manures leads to the generation and release of ammonia gas in notable quantities during composting, which represents a loss of valuable ammoniacal nitrogen (c.196 kt p.a.) [Pain *et al* 2000] and lowers the agronomical value of composted FYM as an organic fertiliser [Gibbs *et al* 2000]. Furthermore, the release of ammonia is of environmental concern because it contributes to soil acidification and is the principal cause of eutrophication when it is deposited on land and in watercourses. This can occur locally or the gas can be carried considerable distances, crossing national boundaries. Agriculture is responsible for at least 80 % of the total ammonia emissions (340 kt annually) in the UK (Table 1.1). Storage and spreading of FYM has been identified as a significant source of ammonia emissions contributing almost 40 % to the annual total from agriculture [MAFF 1998]. Storage for FYM for an extended period may lead to emissions of ammonia but this loss would be more than offset by a reduction in the losses during subsequent spreading [Chambers *et al* 2002]. The resultant reduction in net ammonia losses stems from the fact that nitrogen is assimilated into a more stable biomass, which, when applied to the land, is released slowly under microbial activity.

The legislation governing ammonia emissions is internationally based under the European Union (EU) Integrated Pollution Prevention Control (IPPC) Directive (96/61/EC). Although the Directive affects large pig and poultry installations, it does not cover solid

manures and FYM. Neither has it, as yet, been implemented into UK law and until effective control measures for ammonia release have been established, a national target set out in the National Emissions Ceiling Directive (NECD) are used (Section A1.1.1) [Defra 2003b]. The target is the same as that set out by the UNECE Gothenburg Protocol (Section A1.1.2) to reduce annual emissions by about 17 % to 297 kt NH₃ by 2010 and agriculture is required to contribute to the reductions [UNECE 1999].

Table 1.1 Agriculture sources of UK ammonia emissions (1996-97) [Pain *et al* 2000]

Agricultural source	UK emissions, kt NH ₃ yr ⁻¹	% ¹
Cattle	143.2	52.3
Poultry	52.2	19.1
Pigs	32.8	12.0
Sheep	17.2	6.2
Fertilized tillage crops	14.9	5.4
Conserved fertilized grassland	13.5	4.9
Farmed deer	0.05	0.02
Total agricultural	273.9	80.8²
Total non-agricultural	65.3	19.2 ²
Total UK ammonia emissions	339.2	

¹ Percentage of the total agricultural ammonia emissions

² Percentage of the total ammonia emissions

Composting in well-managed heaps reduces the volume, mass (typically by about 40 %) and water content of FYM and produces a more stable organic material making subsequent land application more uniform, less costly and with lower impacts on air, land and water environments than unmanaged manures [Gibbs *et al* 2000]. Composting has the potential to give the farmer the flexibility and assurance needed for the safe disposal of FYM and the findings of this work could present new and effective procedures for handling the manures.

1.2. Investigating composting

Although composting has been used for many years to treat solid agricultural wastes, little account has been paid to its use as a method for inactivating pathogens or the conditions required to maximise inactivation. The presence of ammonia may enhance the inactivation of pathogens but its release is undesirable due to the negative agronomical and environmental consequences. The majority of descriptions of the complex processes involved in ammonia release during composting are qualitative. An investigation is required that links modelling ammonia emissions with other process factors and is backed up with experimental data. The findings of such an investigation and the potential of a working model could present the farming community with new and effective procedures for handling their FYM with the added benefit of knowing the product is safe to spread on the land.

1.2.1. Aims and objectives

The aim of the project was to investigate controlled composting of pig manure mixed with straw and so test the following hypothesis:

Ammonia emissions from a composting mix of pig manure and straw can be reduced by adjusting the initial pH and carbon to nitrogen (C:N) ratio of the organic material, whilst still achieving conditions in which inactivation of pathogen markers is complete.

To investigate the composting of FYM on a field scale would be costly and time consuming. Furthermore, outdoor conditions are notoriously difficult to control and essentially exclude quantification of some process factors [Finstain *et al* 1989] so that those factors, which control the composting process, would not necessarily be obvious. Another aspect to consider is the observed lack of homogeneity of microbial populations and activity

in outdoor composting [Viel *et al* 1987] due to the wide temperature range in the heap. In light of such evidence, the composting experiments were to be carried out indoors in vessels designed to control external factors. A major problem encountered with experiments carried out on a smaller scale is the disproportionately large heat losses from the surface due to the large outer surface area-to-volume ratio [Finstein *et al* 1989].

The project plan highlighted a number of objectives to achieve in order to realise the aim of the project. The principal objectives were as follows:

1. To design a composting unit with control and monitoring systems so that the process was optimised and conditions thermally resembled those experienced in the core of a large open composting heap.
2. To formulate a model that simulates the aspects of the composting process, in particular, the temperature and ammonia emissions profiles.
3. To test the composting unit and validate the model with experimental work by adjusting two selected process factors.

1.2.2. Project design

The project aimed to identify the conditions that lead to pathogen inactivation in the organic material while at the same time reducing ammonia emissions and to identify a possible relationship between these two processes. The development and use of the composting reactors in which the composting experiments were carried out under defined and controlled conditions facilitated the acquisition of experimental data and the validation of the model of the process.

1.2.2.1. Experimentation

Respirometry was used to evaluate the effect of temperature on microbial activity in the organic material, as indicated by the oxygen uptake rate (OUR), during the initial stage of composting. From these bench-scale experiments, the optimum temperature for microbial activity in a mix of pig manure and straw was determined.

Composting of the pig manure and straw mix was then investigated on a larger scale in reactors with a capacity of 200 litres. An experimental plan was designed so that the effect of the two selected process factors on composting could be evaluated using an analysis of variance (ANOVA). The composting unit consisted of three identical reactors, which enabled three levels of a process factor to be investigated within a single experiment trial. The factor, whose effect was less understood, or considered to be the more sensitive to change between the levels, the initial pH, was varied between the reactors within a trial. The other factor investigated, the initial C:N ratio, was changed between trials, which, in this investigation, were repeated. Volume, moisture content, ammonia content, gas flow and temperature were monitored and controlled. Emissions of ammonia, oxygen and carbon dioxide from the reactor were measured to enable mass balances to be determined and to develop the model.

1.2.2.2. Modelling

The decomposition of the organic material during composting was modelled on a macro-scale in a batch system without mixing, since this reflected the system used in the composting experiments, and to trace the movement of individual particles in the organic material due to mixing, would prove to be virtually impossible [Seki 2002]. Furthermore, the heterogeneity of organic material makes molecular and micro-scale models, typically used for soil systems, difficult to apply to a composting system [Seki 2002].

The model considered the composting process as a chemical reaction and the effect of process factors on microbial activity was addressed by empirically determined factor effect functions. The composting process was modelled as a first order rate reaction, which was ultimately driven by the degradable fraction of the organic material. From the degree of decomposition, mass and energy balances were simulated, resulting in profiles of the process factors. The loss of nitrogen as ammonia was dealt with in a sub-model, which ran concurrently with the mass and energy model. The model was developed and run using the modelling computer package, *ModelMaker*.

1.3. Thesis Layout

The thesis opens with a literature review, which includes a theoretical introduction to composting and the factors that play an important role in the process. The effect of ammonia emissions on the environment and pathogens inactivation during composting are further discussed. Published composting and ammonia emissions models are also reviewed and the background to the model basis is identified.

Chapter 3 looks at the analytical methods used to characterise the organic material and the equipment used to investigate the composting process. This includes details of the design of the equipment: two types of respirometer and a composting reactor.

Chapter 4 deals with respirometry experiments and some factors associated with respirometric activity, such as the respiratory quotient. This precedes the chapter on modelling as a number of empirical inputs to the model are evaluated by investigating the respirometric activity of the organic material in particular with respect to temperature.

Chapter 5 presents the model equations and results of sensitivity analysis simulations. The model is validated by comparing the results of the model simulations with the results of the composting experiments carried in the composting reactors.

Chapter 6 summarises the results of the composting experiments carried out to test the hypothesis. The composting process in each experiment is characterised by the temporal temperature, ammonia emissions and aeration profiles and the effect the selected process factors is statistically analysed.

Chapter 7 concludes the thesis with the validation of the composting model using the results of the composting experiments and a final discussion and conclusion, which includes some suggestions for future work. References, appendices and publications follow.

CHAPTER 2

LITERATURE REVIEW

2.1. Introduction

An exact, internationally used definition of composting does not exist. The numerous definitions [Golueke 1977, Thostrup 1988, Haug 1993, Biocycle 1994, U.S. EPA 2000, Burton and Turner 2003, The Composting Association 2003] do, however, describe the same process fundamentals, which the following encapsulates:

Composting is an autothermal process of controlled biological decomposition of solid, typically heterogeneous, organic material by successive microbial populations under predominantly aerobic conditions and elevated temperatures. The composted organic material is more stable and free of pathogens and its use has a lower impact on air, land and water environments than if it were untreated.

Composting is a complex and sometimes contradictory process, which, in order to use to its full potential in the ISWM strategy, requires a clear understanding of:

1. the influence of the nature of organic material
2. the physical and chemical requirements for optimum biological activity
3. the interrelationships between process factors and variables and the indicators of successful composting.

The chapter opens with an overview of the composting process and the factors that play an important role in its outcome, with attention paid to pathogen inactivation and ammonia emissions. A review of published composting models and areas of FYM composting, which require further research, conclude this chapter

2.2. The composting process

Microorganisms are key to composting. To maintain maximum microbial activity, process factors need to be optimal, which requires a degree of management and control of the process. Microorganisms are very sensitive to changes in process factors and physical or chemical properties; such as oxygen uptake, temperature, pH, volatile fatty acids and metabolites, can be used to indicate the state of the composting system and so form a basis for process control [Mohee 1998]. The temperature, pH, nutrient and oxygen availability and moisture strongly influence microbial activity [Das *et al* 1997]. Under optimal conditions, composting normally proceeds through three stages: active, cooling and maturing. The length of the maturing stage determines the stability of the composted organic material (Figure 2.1).

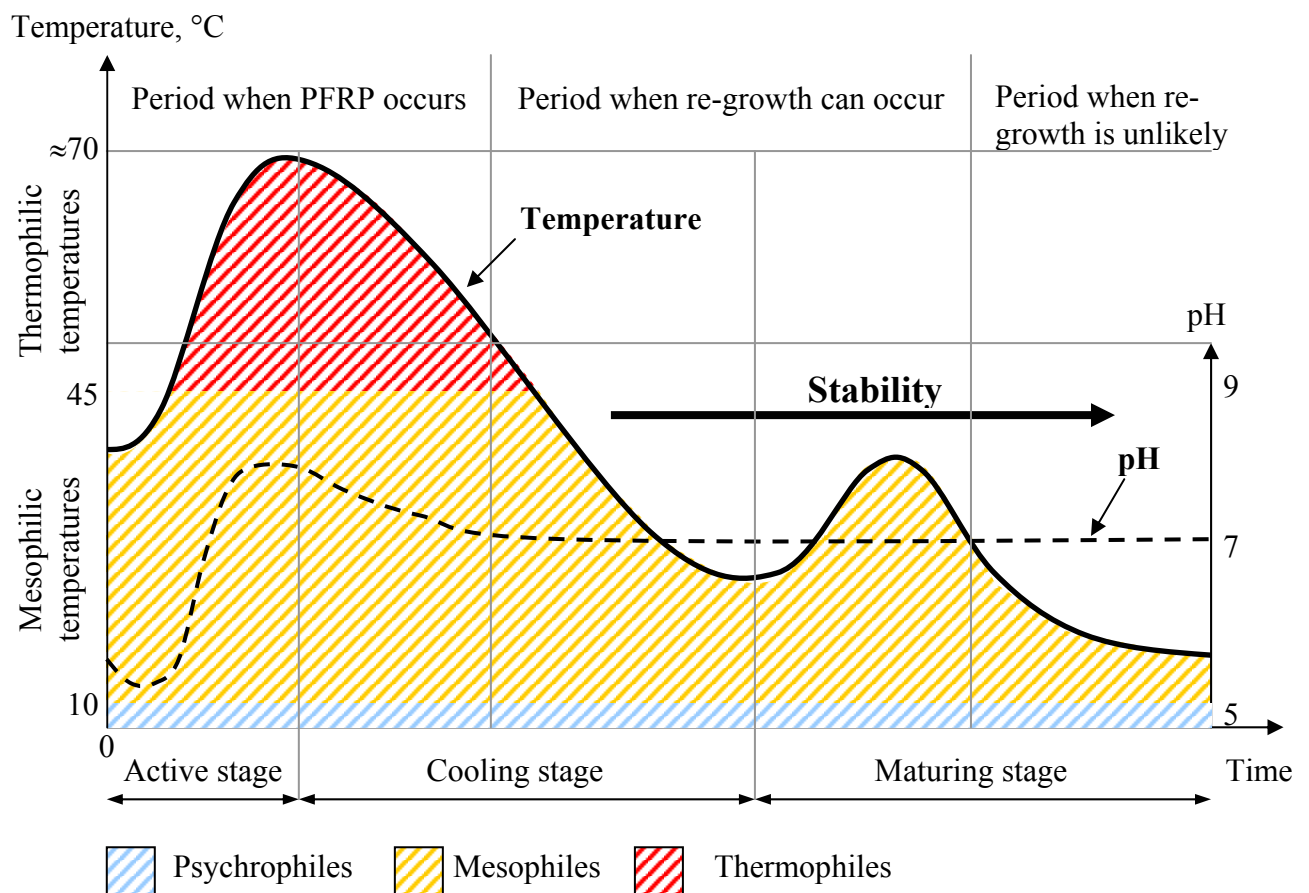


Figure 2.1. Composting stages as distinguished by the temperature and pH. PFRP – Process to further reduce pathogens [Farrell 1992]

2.2.1. Microbiology

A complex food web of microorganisms and invertebrates, categorised as primary, secondary, and tertiary consumers and supported by plant and animal residues (Figure 2.2), exists in a traditional composting heap [Trautmann and Olynciw 2002a].

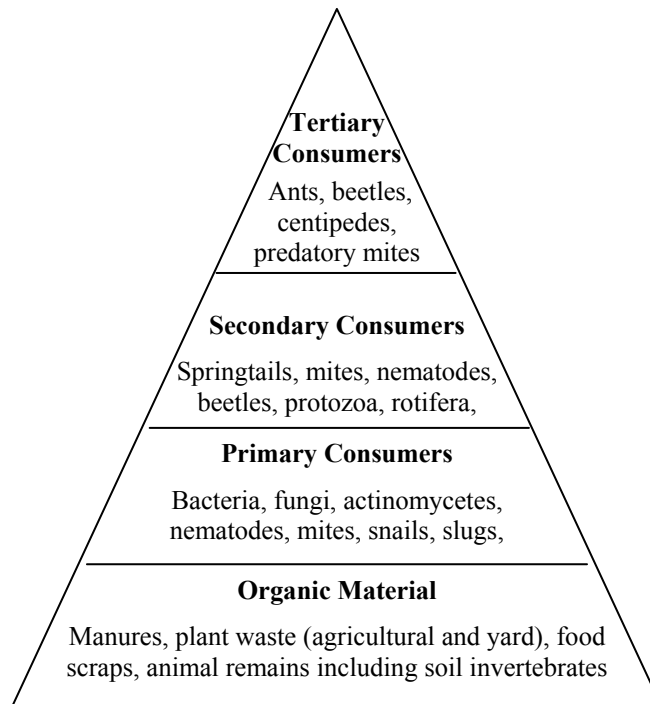


Figure 2.2. Food web pyramid that exists in traditional composting heaps.

Most of the microorganisms present during composting are bacteria, actinomycetes and fungi [Haug 1993, U.S. EPA 2000]. Bacteria make up 80 % to 90 % of the myriad of microorganisms and are responsible for most of the initial decomposition of the readily degradable organic material and heat generation during composting. Actinomycetes and fungi constitute most of the biomass, particularly in the later stages of composting when they are more prevalent. Fungi have a competitive advantage over bacteria and actinomycetes because they are able to operate in environments too dry, acidic, and low in nitrogen for bacteria [Trautmann and Olynciw 2002b] and are often found growing extensively on carbonaceous organic material [Mohee 1998]. Their enzymes enable them to decompose

complex organics such as cellulose, lignin, chitin, and proteins. As a consequence, bacterial activity continues even though the readily degradable organic material has been exhausted.

Ultimately, the type of organic material determines microbial population dynamics but, because the biochemical reactions during composting are catalysed by enzymes, temperature is the principal influence on microbial activity. Microbial populations operate within a specific temperature range. An increase above the maximum temperature in the range leads to the thermal destruction of the cell proteins and the death of the microorganisms, whilst temperatures below the minimum, affects the metabolism of the cell [Mohee 1998]. Psychrophiles favour temperatures below 10 °C, mesophiles thrive in temperature between about 20 °C and 45 °C and thermophiles grow well between about 50 °C to 70 °C (Figure 2.1) [Stainer *et al* 1980, U. S. EPA 2000]. The rapid changes and complexity of the microbiology during composting makes isolation of microbial populations difficult. Simple and more immediate and reliable physio-chemical process variables, such as temperature, are therefore used to follow the progress and to improve the efficiency of composting [Tiquia *et al* 2002].

2.2.1.1. Pathogens

The majority of microorganisms in organic material are beneficial to plant growth and soil fertility but others are pathogenic to plants, animals or humans. The level of pathogens and their reduction during composting is an important criterion to evaluate [Tiquia *et al* 2002]. Pathogens may be bacteria, viruses, fungi and parasites. The type and density of pathogens in the organic material depends on its source. Sewage sludge and animal manures often contain potential pathogens, which cause a variety of human diseases often of the gastrointestinal tract [Farrell 1992]. Table 2.1 lists the pathogenic bacteria and viruses found in biosolids and the diseases they cause [Epstein 1998].

Table 2.1. Some pathogenic bacteria and viruses in biosolids and the diseases they cause

Organism	Disease
<u>Bacteria</u>	
<i>Salmonellae</i>	Salmonellosis, Gastroenteritis, Typhoid fever (<i>S. typhi</i>)
<i>Shigellae</i>	Shigellosis, Gastroenteritis, Bacterial dysentery
<i>Campylobacter</i> spp.	Gastroenteritis,
<i>Mycobacterium</i> spp.	Tuberculosis
Pathogenic <i>Escherichia coli</i>	Gastroenteritis,
<i>Vibrio cholerae</i>	Cholera
<u>Viruses</u>	
Adenovirus	Conjunctivitis, Respiratory infections, Gastroenteritis
Poliovirus	Poliomyelitis
Echovirus	Aseptic meningitis
Reovirus	Respiratory infections, Gastroenteritis
Astroviruses	Epidemic gastroenteritis
Caliciviruses	Epidemic gastroenteritis
Hepatitis virus	Infectious hepatitis
Rotavirus	Gastroenteritis, Infant diarrhea
<u>Protozoa</u>	
<i>Giardia lamblia</i>	Giardiasis, diarrhea, weight loss
<i>Cryptosporidium</i>	Gastroenteritis

Unlike bacteria, viruses and helminth ova are unable to re-grow once inactivated and therefore are not usually checked for after composting. In pig slurry, African swine fever and swine vesicular disease virus were inactivated when exposed to temperatures between 55 °C and 60 °C [Turner *et al* 1999]. The densities of faecal coliforms and *Salmonellae* are related and either can be used as a suitable indicator of pathogen presence during composting [Farrell 1992]. Turner [2002] showed that inactivation of *E. coli* 11943 did not occur at mesophilic temperatures. At 50 °C, its inactivation depended on the moisture content and nature of the organic material but at 55 °C, inactivation was rapid.

Heat is the primary mechanism for pathogen inactivation but excessively high temperatures need to be avoided, as these are detrimental to the general microbial population

[Turner 2002]. For composting to be considered as a process to further reduce pathogens (PFRP) (Figure 2.1), the U. S. EPA specifies that all the organic material must be exposed to temperatures between 55 °C and 76 °C for a period between 3 and 15 consecutive days depending on the composting system used [Farrell 1992, Suslow 2001]. After composting, the density of *Samonellae* must be below 3 colony forming units (CFU) in 4 grams of dry organic material or faecal coliforms, below 1000 CFU g⁻¹ [Farrell 1992, Epstein 1998]. The Public Available Specification (PAS) developed by The Composting Association², however, specifies that *Salmonellae* must be absent in 25 g of dry organic material [PAS 100 2002]. The minimum dose of *E. coli* to cause human infections is about 10⁶ [Epstein 1998] but the newer VTEC *E. coli* O157-H7 strain, which has been the cause of an increasing number of infection cases, has a very low infective dose (< 10 cells). The specified faecal coliform density, therefore, seems arbitrary and high especially considering the ability of bacterial populations to re-grow.

The mechanism of pathogen inactivation is complex and, although temperature and time are the main factors, dryness, lack of nutrients, microbial antagonism and the production of antibiotics and parasitism also contribute to pathogen inactivation [U. S. EPA 2000, Suslow 2001]. Ammonia has biocidal properties and is toxic to many microorganisms, even at low concentrations [Burton and Turner 2003]. The presence of free ammonia in the organic material may, therefore, also enhance pathogen inactivation [Turner 2002]. Quantification of the effect of these other factors is needed [Stentiford 1993].

² The UK membership organisation promotes composting processes and compost products and encourages regulatory and economic framework suitable for long-term benefit and sustainability of the composting industry.

2.2.2. Temperature

The most important aspect of temperature is its impact on the microbial community. Temperature is a strong selective factor and microorganisms are only active within a species-specific temperature range [Mohee 1998]. Figure 2.1 shows the temperature profile typical of composting systems. The durations of each stage of composting depends on the composting system and characteristics of the organic material. The temperature at any point during composting depends on how much heat is generated, balanced by how much is lost from the system through evaporation, conduction, convection, and radiation [Trautmann 2002].

The spontaneous decomposition of the soluble, readily degradable fraction of the organic material at mesophilic temperatures during the active stage produces heat and the temperature rises rapidly to thermophilic temperatures and thermophilic bacteria predominate. The high temperatures accelerate the breakdown of proteins, fats, and complex carbohydrates like cellulose and hemicellulose (Table 2.2).

Table 2.2. Degradability of compounds typically found in organic material [Stentiford 1993]

Organic material Fraction	Stage of degradation		
	Active	Cooling	Maturing
Readily degradable fraction			
Sugars	Decreasing degradability ↑ ↓		
Starches, glycogen, fatty acids and glycerol			
Lipids, fats and phospholipids			
Amino and nucleic acids		↑ ↓	
Proteins			
Slowly degradable fraction			
Hemicellulose and cellulose		↑ ↓	
Chitin			↑ ↓
Simple aromatics and aliphatics			
Resistant fraction			
Lignocellulose			↑ ↓
Lignin			

The maximum temperature reached depends on the microbial populations but is typically $60^{\circ}\text{C} \pm 15^{\circ}\text{C}$ [Van Ginkel 1996, Mohee 1998]. Microbial activity slows as temperatures exceed the optimum and as the high-energy compounds become exhausted [Gray *et al* 1971a]. As the heat losses exceed heat generation, the temperature gradually returns to the mesophilic range (the cooling stage) and enters the maturation stage. The numbers and types of active mesophiles in these final stages of composting depend on which spores and microorganisms survived the high temperatures as well as on the immediate environment, but is characterised by the slow process of cellulose decomposition by fungi and actinomycetes making the remaining organic matter more stable and suitable for use as a compost.

2.2.3. C:N Ratio

The C:N ratio represents the mass proportion in which the microorganisms use the macronutrients carbon (C) and nitrogen (N) to build new cells (anabolism). Typically, the C:N ratio decreases during composting because about 70 % of C is lost in gaseous emissions [Barrington *et al* 2002a] whereas the majority of N is incorporated into biomass and is continuously recycled [U. S. EPA 2000].

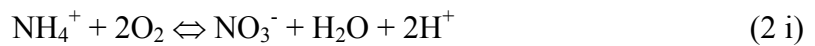
In general, anabolism requires 36 mol of C per mol of N [Haug 1993]. A C:N ratio of about 30 favours rapid composting with 15 being ideal for cell yields greater than $0.2 \text{ g cells g}^{-1} \text{ glucose}$ [Haug 1993]. The reported optimum C:N ratio ranges from 20 to 40 [Bishop *et al* 1983, Rynk 1992, Imbeah 1998, U. S. EPA 2000, Eckini *et al* 2002] as it depends on the organic material and the process criteria. Fungi favour C:N ratios as high as 200 [Mohee 1998]. Most of the N in organic material is readily available (85 % [Barrington *et al* 2002a]), which is not always the case with C. In plant material, a large proportion exists as resistant cellulose and lignin and is not readily available to

microorganisms. The optimum C:N ratio is therefore a function of the biodegradability of the carbon fraction [Richard 2000]. Often the same organic materials that are high in N are very wet, and those that are high in C are dry. Combining the different kinds of organic materials yields a mix that composts well.

If the C:N ratio is high, N is the limiting factor [U. S. EPA 2000] and the microorganisms undergo a number of life cycles to oxidise excess carbon until the C:N ratio is appropriate for their metabolic activities and composting is slow [Mohee 1998]. At lower C:N ratios, C is the limiting nutrient and N that is not incorporated into biomass is lost from the system through gaseous emissions (ammonia) primarily but also leaching and denitrification. With the loss of the excess N, the C:N ratio may therefore not necessarily decrease during the initial stages of composting. The chemistry of ammonia formation in FYM and the dynamics of its volatilisation are described in detail in Section 5.2.1.2 (Modelling chapter). Briefly, a basic environment and elevated temperatures favour the formation of ammonia and its low vapour pressure promotes its subsequent emission into the gas phase, which is exacerbated by high airflow and low moisture content. Experimental studies with pig manure amended with sawdust showed that ammonia emissions correlated well with the total airflow regardless of whether air was supplied continuously or intermittently [Keener *et al* 2002]. Barrington *et al* [2002a], however, found that ammonia emissions from composting pig manure and various bulking agents were, in fact, not related to the moisture content of the organic material nor aeration regime (active or passive) but to the loss of C. Hoeksma *et al* [1993] mixed acids into the liquid fraction of separated manure and found that ammonia emissions were reduced by 70 %. Zeolites (natural ion exchange minerals) can be added to the organic material to retain the excess nitrogen during composting by bonding with ammonium ions [Burton and Turner 2003].

2.2.3.1. The impact of ammonia emissions on the environment

Ammonia plays an important part in the long range transport of the acidic pollutants in the atmosphere. The basic ammonia (NH_3) reacts with water vapour and acid compounds, such as sulphur and nitrogen oxides, to form the ammonium salts and so contributes to the formation of acid rain [Burton and Turner 2003]. When deposited on land, nitrifying bacteria in the soil oxidise the ammonium ion (NH_4^+). The two hydrogen ions (H^+) released acidify the soil (equation 2 i), which has a profound effect on soils with low buffering capacity [Droon *et al* 2002].



Nitrogen is often the limiting factor in natural ecosystems. The additional nitrogen from the nitrate (NO_3^-) and NH_3 that has been deposited directly on the land, leads to eutrophication of surface water and soil. Furthermore, the uncharacteristically rapid growth in plants increases their susceptibility to insect and fungal attack and the stresses placed on the relatively small root system during drought and frost. The biodiversity of the plant species tends to decrease as invasive, nitrogen loving plants, such as grasses, nettles and brambles, replace the native species [Droon *et al* 2002]. Ammonia deposition on foliage can also inhibit the uptake of certain plant nutrients [Burton and Turner 2003].

Although the dynamics of and the process factors and variables involved in ammonia emission from FYM during composting are generally understood, there are insufficient data to quantify the processes in detail and insufficient statistical data to quantify all input variables. The model for emissions factors used to estimate emissions should reflect emission estimates because this will determine the type of model that should be developed or used to update inventories of ammonia emissions from agriculture [Droon *et al* 2002, Pain *et al* 2000].

2.2.4. pH

pH affects the nutrient availability to microorganisms and the overall metabolic activity of the biological cell [Mohee 1998]. Most bacteria operate best within a pH range of 6 to 7.5, whereas fungi can tolerate a wider pH range of 5.5 to 8.5 [McKinley *et al* 1986, Mohee 1998]. Most bacteria cannot survive at a pH of 3 and succumb at a pH above 10.5 with significant kills above about 11.5 [Haug 1993]. Composting organic material has a natural buffering capacity so that the initial pH usually need not be adjusted [U. S. EPA 2000] and a wider range of pH between 5 and 12 can be considered [Willson 1994].

The typical pH profile of composting is shown in Figure 2.1. Initially, pH falls to about 5 because of the accumulation of organic acid intermediates produced by microbial decomposition of the carbonaceous fraction of the organic material and dissolved carbon dioxide. Acid conditions are generally detrimental to aerobic bacteria and composting slows until populations, mostly fungi, which can metabolise the acids, develop. The pH then rises and stabilises between 7 and 8 regardless of the initial pH [Mohee 1998, U. S. EPA 2000]. The actual pH range depends on the nature of the organic material and anaerobicity in the initial stages leads to further acid accumulation and the pH drops to severely limiting levels.

The pH is of particular concern with high nitrogen content organic materials because the acidity of the organic material controls ammonia formation, which further increases the alkalinity [U. S. EPA 2000]. A high pH can slow microbial activity as well as promote ammonia emissions. A peak in pH may occur during the thermophilic stage when the ammonia content in the organic material and emissions peak.

2.2.5. Moisture

The thin liquid film on the particle surface of the organic material is the main site for microbial activity. The water is required for the solubilisation and transportation of nutrients, bacterial movement and gas exchange [Gray *et al* 1971b, Finstein and Hogan 1993, Miller 1993, Hamelers 2002, Richard *et al* 2002]. It is also the medium in which cellular reactions occur [U. S. EPA 2000]. The optimum moisture content for composting is not necessarily universal as the physical structure and water holding capacity of organic materials vary [Jeris and Regan 1973b, Finstein and Hogan 1993, Haug 1993, Jeppsson 1998]. On a wet basis, a moisture content between 55 % and 65 % is recommended [Bishop *et al* 1983, Imbeah 1998] but composting is feasible with higher moisture contents if there is enough oxygen to maintain aerobic activity [Liao *et al* 1993]. For example, lignified materials, such as straw and wood chips, retain their wet strength for a long time and can be composted with initial moisture contents as high as 85 % [Gray *et al* 1971b]. The maximum moisture content can be quantified by the free air space (FAS) of the organic material. The FAS represents the volumetric fraction of the void space in the organic material that is not filled with water and is occupied by air and other gases [Haug 1993]. An FAS above 30 % is recommended for composting [Haug 1993]. The FAS is of less importance in composting because the supply of oxygen does not only depend on the diffusion of air through the organic material. The relationship between moisture content and oxygen availability is discussed in Section 2.2.6.

The moisture content of the organic material also affects the temperature change during composting. Water has a higher specific heat capacity than organic material [Haug 1993] and a drier organic material will heat up and cool more quickly than a wetter one, if levels are suitable for microbial activity. The water in the organic material dampens the rapid changes in temperature as microbial activity fluctuates [Trautmann 2002]. Water

has a high latent heat of vaporization and cools the organic material while evaporating, particularly at higher temperatures [U. S. EPA 2000].

2.2.6. Oxygen availability

Aerobic reactions characterise composting, so oxygen availability is a key process factor. A lack of oxygen and the dominance of anaerobic conditions is a common reason for composting failures [Gray *et al* 1971b]. Oxygen availability is often the controlling factor especially during the initial active stage of composting. The transfer of oxygen from the air in the voids of the organic material to the sites of microbial activity is by diffusion and therefore depends on temperature, its concentration gradient, pore size and water film thickness.

To start, the oxygen concentration in the air spaces is about 15 to 20 %, which is optimal for microbial activity [De Bertoldi *et al* 1982]. As biological activity progresses, the concentration decreases. Aerobic microorganisms can survive low oxygen concentrations, but their activity is very much reduced [Haug 1993]. To avoid such limiting conditions, the oxygen concentrations should be at least 5 % in the voids [Schulze 1960, Richard 2000, U. S. EPA 2000]. Concentrations above 10 % are considered optimal for maintaining aerobic composting [Harper *et al* 1992, Haug 1993, Mohee 1998, Hamelers 2002, Trautmann 2002].

Microbial activity generally occurs on the surface of the organic particles. Therefore, decreasing particle size (increasing surface area to volume ratio) will encourage microbial activity [Trautmann 2002]. Small and compact particles can, however, impede air circulation through the pile. The porosity determines the extent to which the air can penetrate the organic material and is defined as the ratio of the void volume and the total volume of the organic material. The difference between the porosity and FAS is the space occupied by the water in the voids. Porosity indicates the amount of air and its potential movement in the organic

material [Mohee 1998]. Although the open structure in organic material improves the distribution of air, pockets of anaerobic activity may remain.

The amount of air supplied to the organic material may not reflect the actual amount reaching the microorganisms because the diffusion of oxygen is about 10^5 times slower in water than in air [Mohee 1998]. The thickness of the water film depends on the moisture content of the organic material and if it is too high, the diffusion of oxygen, and other gases, becomes restricted and metabolic demand may exceed supply. Some compost systems are able to maintain adequate oxygen passively, through natural convection and diffusion. Other systems require active aeration, using blowers (forced convection) or through turning or mixing the compost ingredients.

2.2.6.1. Aeration

Aeration is crucial to the composting temperature [Gray *et al* 1971, Johnson 1999]. Air supplied to support aerobic activity increases heat generation. Higher aeration is needed to dissipate heat, through sensible heating of the air and evaporation of water, and so keeps the temperature optimum for microbial activity. Too much air, however, will cause temperatures to fall below those required to inactivate pathogens in the organic material and may also dry it too much for microbial activity [Johnson 1999].

Passive aeration relies on natural convection driven by gas concentration, humidity and temperature differences to create an airflow through the organic material. Such aeration may not be adequate to meet peak oxygen demand during the initial stages of composting [Gray *et al* 1971b, Haug 1993] but can be assisted by mechanical mixing or turning, which replenishes the air, loosens the organic material and increases its porosity [Trautmann 2002].

Forced aeration is often used to accelerate composting [Gray *et al* 1971b]. This can be continuous or intermittent and in a positive or negative direction. An advantage of intermittent

or burst aeration is that it tends to avoid channelling of the air through the organic material, which can arise with continuous aeration. The merits of aeration methods are well documented [Finstein and Hogan 1993, Imbeah 1998, U. S. EPA 2000, Burton and Turner 2003].

2.3. Composting systems

A wide variety of systems are used for composting. These can be broadly classified as open and in-vessel. Open systems include turned piles such as windrows and static piles, either of which can be aerated by natural or forced convection [Finstein *et al* 1986, Fernandes *et al* 1994]. In-vessel systems can be vertical, such as tower composters, or horizontal, such as tunnel composters and rotating drums. The complexity of the container systems range from simple box containers, which rely on natural aeration, to chemical reactor-type vessels with elaborate control systems [Stentiford and De Bertoldi 1988, Thostrup 1988, Haug 1993, Stocks 2000, U. S. EPA 2000, Biowise 2001, Burton and Turner 2003]. Stentiford [1993] considers the merits of interventionary (mixed, agitated and stirred) and non-interventionary (static and silo) systems. Many factors determine which composting system is used, but the choice usually depends on:

- economics – capital, running costs and other sources of income such as gate fees, tax rebate or government incentives and sales
- type, availability and quantity of organic material to be composted
- location of the composting facility – a small or large foot print, proximity of communities and sources for organic materials
- objective – waste management, pathogen inactivation or designer compost production.

In windrow composting, turning is necessary to inactivate pathogens in the cooler outer layers. This ensures that they are exposed to higher temperatures at the core.

Temperatures above 55 °C need to be maintained for at least 15 consecutive days during which time the organic material must be turned 5 times. A minimum of 3 consecutive days is specified for in-vessels because heat distribution in the organic material is more consistent [Farrell 1992, Stentiford 1993].

2.4. Modelling the composting process

Simulation models are essential to improve the process design, analysis and management of composting facilities as they connect laboratory or pilot scale composting and industrial scale design [Haug 1993, Van Ginkel 1996]. Design strategies tend to be based on practical experience and a trial and error approach to optimise the process, which can prove costly [Hamelers 2001]. As composting facilities become more highly controlled systems, a much greater degree of process engineering is required [Marugg *et al* 1993].

Composting is a dynamic process governed by chemical and biochemical kinetic reactions [Haug 1993] and its outputs depend on current and initial inputs [Hamelers 2001]. Despite the many qualitative details, there is no standard mathematical model of the process and there are, therefore, many ways in which composting knowledge can be modelled [Kaiser 1996]. Also, there is no model that satisfactorily describes composting in local and broad detail because of its multicomponent, multiphase and heterogeneous nature [Seki 2002].

Composting models have been developed using analytical [Nakasaki *et al* 1987, Hamelers 1993, Haug 1993, Keener *et al* 1993, Marugg *et al* 1993] or numerical [Stombaugh and Nokes 1996, Das and Keener 1997] approaches, both of which help with understanding the dynamic relationship between some of the variables, the kinetics and the energy balances [Mohee 1998] and can be used interactively with system cost models [Keener *et al* 2002].

Two other distinct approaches to modelling composting are autoecological and synecological [Miller 1996, Mohee *et al* 1998]. Autoecological models are driven by microbial growth kinetics as described by a Monod-type equation adapted for the composting process [Hamelers 1993, Kaiser 1996, Stombaugh and Nokes 1996, Liang *et al* 1998, Seki 2002]. Both single component [Stombaugh and Nokes 1996] and multicomponent systems [Kaiser 1996, Liang *et al* 1998] have been considered. The model application is limited by the number of components that can be classified and treated as a homogeneous compound and microbial population. It can only give a rough representation of the chemical and biological changes occurring during composting [Kaiser 1996]. Also, although specific microorganisms are indicative of the composting conditions, with mixed populations the microbial interactions are complex and microbial presence does not necessarily correlate with activity [Mohee 1998].

Synecological models consider the interaction between the composting environment and the broad microbial populations with emphasis on kinetic and thermodynamic changes and the effect of process factors on the rate of microbial activity [Nakasaki *et al* 1987, Keener *et al* 1993, Haug 1993, Marugg *et al* 1993, Das and Keener 1997, Mohee *et al* 1998, Tollner *et al* 1998]. These models use first order reaction rate kinetics to describe the degradation of the organic material during the high-activity initial stages of composting, which are important in the design of composting equipment [Marugg *et al* 1993]. Microbial activity changes are usually expressed by empirically determined relationships with rate-limiting environmental factors [Jeris and Regan 1973a, 1973b, 1973c, Haug 1993, Nielsen and Berthelsen 2002, Richard *et al* 2002], which are assumed to act independently of each other so that a multiplicative structure can be used in the model. Richard *et al* [1998, 1999], however, showed that not only do some environmental factors influence each other but so does the changing composition of the organic material and this has received little attention.

The shortcomings of the integral approach used in most of the composting models are the omission of organic material subsistence and spatial variation and this precludes sound validation of the model [Van Ginkel 1996]. Van Ginkel [1996] introduced a model that described the temperature and gas concentration distributions in the organic material as determined by balances and transfer fluxes. Das and Keener [1997] developed and validated a numerical model, which simulated airflow patterns, heat and mass transfer and organic material degradation in a two-dimensional cross section of a deep-bed composting vessel and predicted spatial and temporal changes in the state variables. Seki [2002] developed a deterministic model of heat and mass transfer with microbial reaction kinetics in the organic material, which include volume changes, heat conduction and water transfer.

Hamelers [1993, 2001, 2002] presented a mechanistic model of composting, which simulated processes occurring in the organic material on a particle level. The model effectively calculated gradients of oxygen, biomass and soluble and polymeric compounds in the boundary layer surrounding a single particle. Hamelers [2002] argued that inductive empirical models are not generally applicable and have been developed to their practical limit and that a model, which includes process factors based on fundamental microbial kinetics would be more robust than the empirical relationships and would provide a more complete insight into the complexities of the process. As opposed to the common inductive approach, Hamelers [2002] used the deductive approach and formulated a model, which was characterised by a small number of combined, identifiable parameters, using existing theory.

2.4.1. Ammonia emission models

The majority of descriptions of the complex processes involved in ammonia release during composting are qualitative and require investigation and modelling to link emissions with process variables [Droon *et al* 2002]. Models tend to be mechanistic simulations of

ammonia losses from animal houses, slurry stores and land-applied manures and slurries [Zhang 1994, Cumby *et al* 1995, Boeker and Schulze Lammers 1996, Générmont and Cellier 1997, Monteny 1998, Ni 1999].

Few composting models consider the effect of process variables on ammonia emissions. Haug [1993], for example, estimated the concentration of ammonia in the off-gas directly from the decomposition of nitrogen in the organic material and only included the effect of cell synthesis on the dynamics of ammonia emissions. Liang *et al* [1998] included ammonia emissions in their autoecological model and considered the effect of pH and aeration flow rate on the emission rate. pH changes were based on a carbon dioxide–ammonia multi-solute aqueous system. Validation of the model, however, showed that predicted losses were higher than experimental results. This may reflect the uncertainty associated with the application of ammonia volatilisation constants that were determined from aqueous or slurry systems to solid state organic material systems [Arogo 1999, Ni 1999]. The model was also particularly sensitive to the parameters used in the microbial growth kinetics.

There is much scope for development of new and adaptation and refinement of present ammonia emission models for composting systems. A model based on first order reaction kinetics of organic material decomposition, which relates ammonia emissions to initial and current process conditions, would be a possible starting point in the investigation of ammonia emissions during composting. Although, the limit of the empirical approach is recognised, the use of an inductive model is relatively simple and can be used to gain insight into the overall effect of process variables when composting in the composting reactors.

CHAPTER 3

EQUIPMENT AND ANALYTICAL METHODS

3.1. Equipment

A composting unit was designed in which process factors were controlled so that the effect of selected factors could be evaluated. The unit consisted of three reactors, which were fitted with facilities for measuring the off-gas composition and temperature of the organic material. Before the composting experiments were done, the organic material was characterised to find the optimum temperature for microbial activity and the oxygen demand during initial stages of composting, when activity was expected to be most intense. This was investigated and quantified using respirometers, which measured the oxygen uptake rate of a known mass of organic material at constant temperature.

3.1.1. Respirometers

The constant pressure respirometer (CPR) (Figure 3.1.) was used to measure the oxygen uptake rate by separated solid pig manure incubated in a sealed oxygen atmosphere. The apparatus was essentially a modified version of the one designed by Haug [1991]. Advantages of the CPR were that it was mainly constructed of basic laboratory equipment and was simple to use. Also the 2-litre reactor flask could accommodate relatively large samples.

The gas analyser respirometer (GAR) (Figure 3.2.) measured the oxygen uptake rate and carbon dioxide production rate by a solid pig manure and straw mix incubated in an air atmosphere. A PC based program enabled the analysis and logging of the gas concentrations in each of the reactors and the calibration of the gas analyser to be done automatically.

3.1.1.1. Constant pressure respirometer

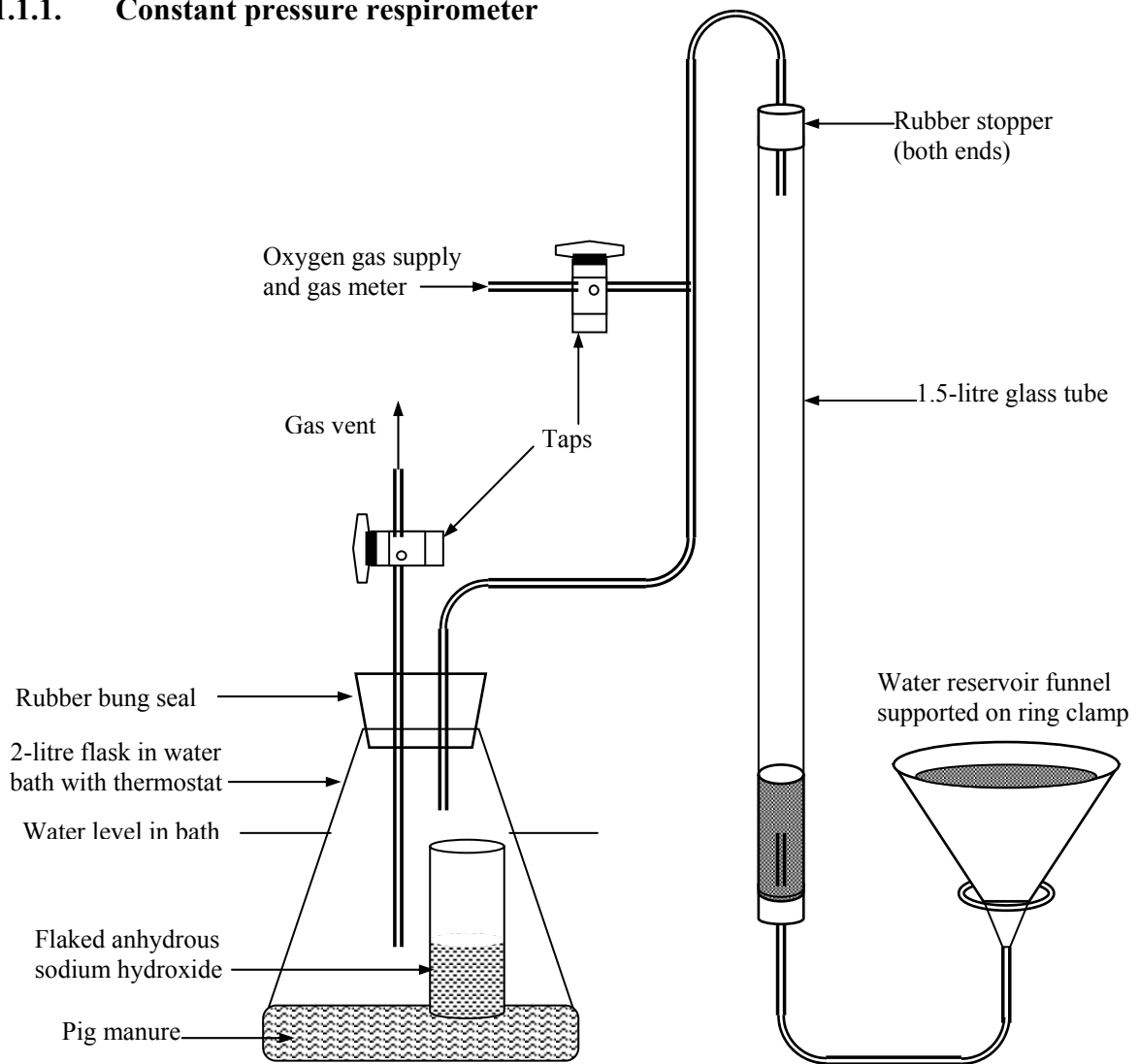


Figure 3.1. Constant pressure respirometer

The constant pressure respirometer was, in effect, a U tube manometer (Figure 3.1). The water reservoir was open to the atmosphere and the system operated under atmospheric pressure. The 2-litre flask was held at constant temperature in a thermostatically controlled water bath. The sodium hydroxide in the flask absorbed carbon dioxide produced during the decomposition of organic material. At constant pressure and temperature, the volume of gas in the system changed with the uptake of oxygen and the water level in the 1.5-litre glass tube rose. The gas meter measured the volume of oxygen admitted to return the water level to the initial position.

3.1.1.2. Gas analyser respirometer

Two 3-litre sealed glass reactor vessels were held at a constant temperature in a thermostatically controlled water bath (Figure 3.2).

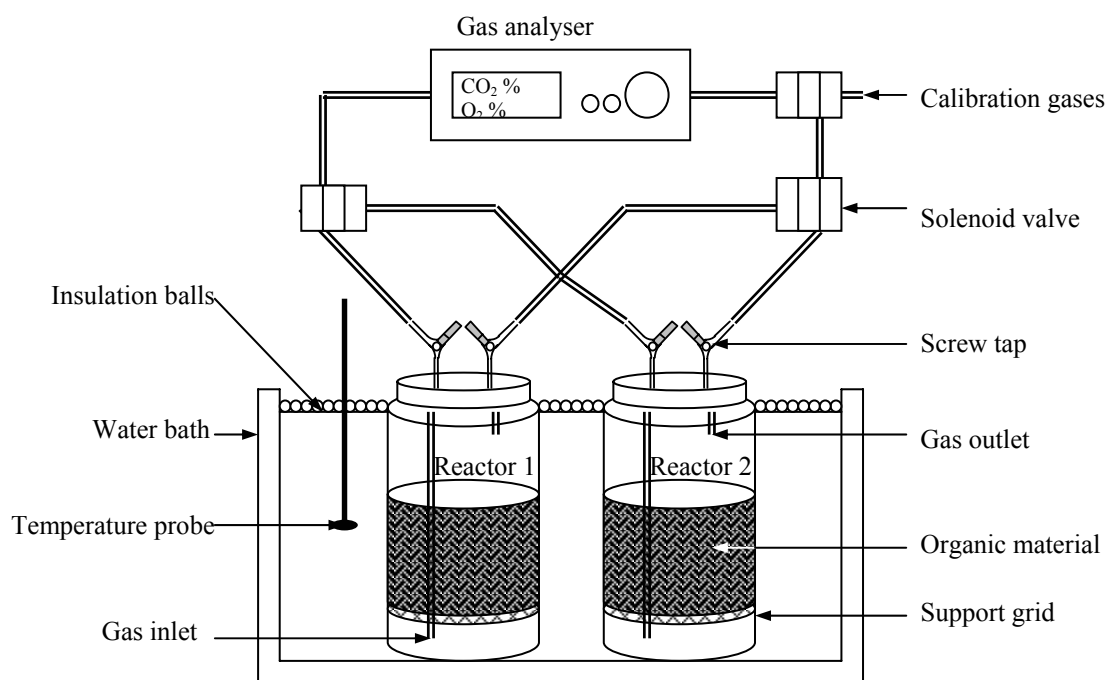


Figure 3.2. Continuous gas analysis respirometer

Gas entered and left each reactor through the screw tap ports in the lid. The stainless steel grids supported the organic material above the gas inlet in the reactors. A combined paramagnetic oxygen and infrared carbon dioxide gas analyser (Model 4102, Servomex Group Ltd, Crowborough, UK), with analogue outputs, measured the concentration of oxygen and carbon dioxide in the gas from one of the reactors for 45 minutes. The same reactor was then flushed with fresh air for a further 15 minutes and left an hour during which time the gas from the other reactor was similarly analysed. Standard gases of nitrogen, air and $9 \pm 0.12\%$ carbon dioxide in nitrogen were used to calibrate the measurements every 12 hours. A PC-based program logged the readings and controlled the solenoid valves on the gas lines through a digital interface.

3.1.2. The composting unit

The unit consisted of three identical vertical reactors equipped with control and monitoring systems, which measured and recorded process variables such as the temperature and off-gas composition. The rig design (Figure A3.1) enabled three composting experiments to be run and monitored simultaneously. The compost reactor was designed so that thermal conditions during composting represented those experienced at the core of a large compost heap, such as a commercial windrow.

3.1.2.1. Composting reactor design

The reactor body was made from a 10 millimetre-thick polypropylene sheet, rolled into a cylindrical vessel with an internal diameter of 600 mm, height of 1700 mm and total volume of 424 litres (Forbes Plastics Tanks and Environmental Technologies, Downham Market, UK). The organic material occupied about half of the volume (Figure 3.3). A stainless steel funnel for leachate collection, a perforated plenum and an aluminium lid were also included. Forced air entered between the funnel and plenum and exited through the main centre port in the lid. The impact plate (**IP**) on the gas outlet enhanced mixing of the off-gas in the headspace. Some off-gas was also drawn from a smaller side port in the lid for analysis of the ammonia content. Two spoked wheels held 400 mm apart on a stainless steel rod, served as internal supports for the organic material in the vertical reactor. Without this initial support, compaction in the lower layers when loading the reactor would restricted airflow through the organic material and so lead to channelling up the sides of the reactor instead of aerating the organic material sufficiently to meet oxygen demands. The external surface of the reactor between the lid and the funnel was covered with aluminium foil, which helped to distribute the heat, supplied by a heating cable, evenly over the surface. The whole reactor was covered with rock wool insulation panels for further insulation. The length of cable

required to cover the outside surface of the reactor was estimated by considering the geometry of a helix (Section A3.2.1). 20 metres of cable allowed for 10 loops of the helix, spaced 10 cm apart along the height of the reactor. This configuration appeared to cover enough of the reactor surface so that heating was even and hotter areas on the surface were avoided.

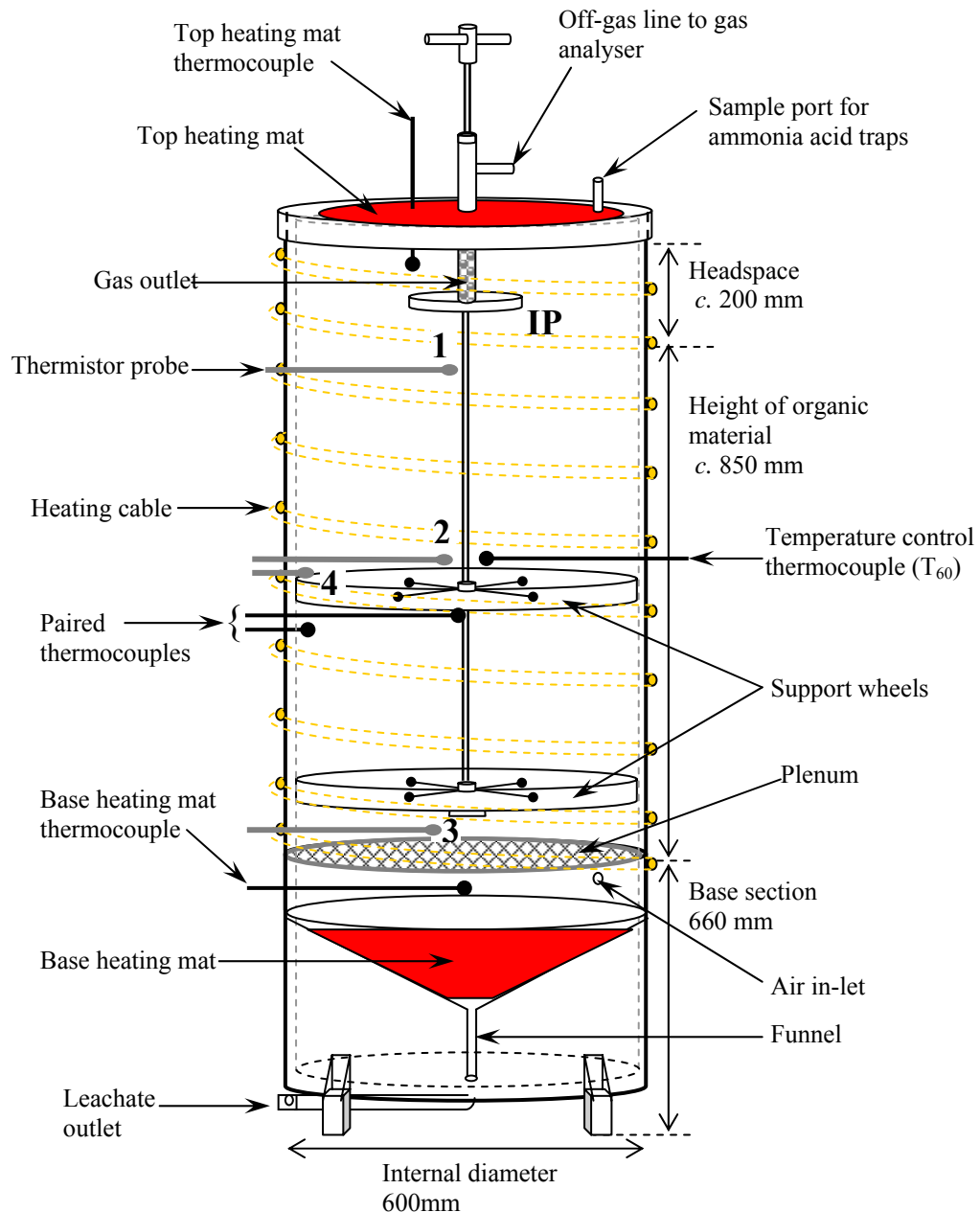


Figure 3.3. Composting reactor of the composting unit.

3.1.2.2. Control systems

3.1.2.2.1. Temperature and heat loss control

Four control loops on each reactor operated to limit the upper temperature and to reduce radial and vertical temperature gradients. The temperature controllers (Model 2208L, Eurotherm Controls Ltd, Worthing, UK) responded to input signals from K-type thermocouples encased in stainless steel. An on/off mode was used to control the temperature of the material (**A**) (Figure 3.4).

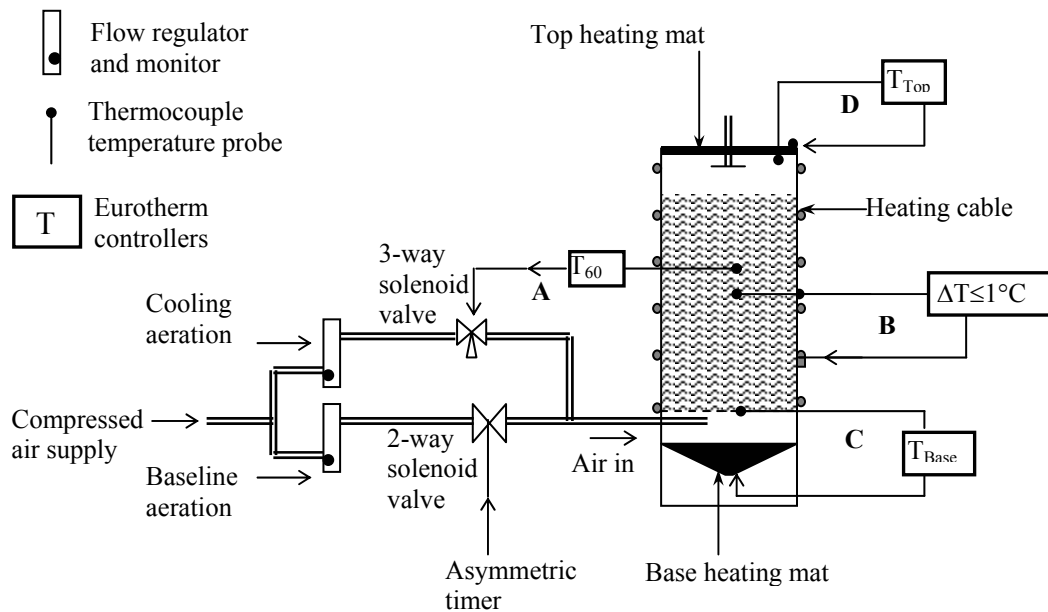


Figure 3.4. Control systems of the composting unit

The controller actuated a solenoid valve to supply a high airflow rate and dissipate the surplus heat when the central temperature exceeded $60^\circ C$. The upper limit of $60^\circ C$ was selected as this was found using respirometry to be the optimal temperature for microbial activity in the organic material tested [Cronjé *et al* 2002]. The controllers in loops (**B**), (**C**) and (**D**) dealt with the temperature gradients (Figure 3.4). They operated in proportional, integral and differential (PID) mode and were self-tuning.

The control loop (**B**) was configured to keep the temperature difference between the centre and side of the composting material to $\leq 1\text{ }^{\circ}\text{C}$ by a pair of thermocouples. When the temperature difference exceeded this set value, heat was supplied by the heating cable. The maximum power required from the heating cable was gauged by simulating the radial heat losses across a horizontal section of reactor (Section A3.2). The power of heating cable was found to be nearly three times the predicted amount required to compensate for the radial losses and the time for which it operated, therefore, needed to be controlled.

Vertical temperature gradients in the organic material develop as a consequence of evaporation, sensible heating of the air and heat losses from the top and base surfaces of the reactor. To reduce this temperature difference, silicon rubber heating mats (Holroyd Components Ltd, Saffron Walden, UK) were used to heat the funnel and lid. A PID controller (T_{Base}) regulated the base mat in response to the temperature measured by the thermocouple situated just above the plenum (**C**). The set-point temperature was manually adjusted to that at the centre of the bed so that the cooling effect of the baseline airflow was reduced. In the same way, PID control was used to regulate the top heating mat (T_{Top}). The controller acted in response to the temperature of the gas in the headspace just below the lid surface (**D**) with the set-point temperature manually altered to always be a few degrees above the temperature of the organic material to avoid condensation of water on the inside of the lid.

3.1.2.2.2. Aeration

A 2-stage aeration strategy was used. For metabolic requirements a baseline airflow aerated the organic material for 5 minutes every 10 minutes at 5 l min^{-1} . An on/off asymmetric timer actuated a 2-way solenoid valve on the airline and the controller automatically recorded the time for which the valve was open. The flow rate required was determined from the initial total solids (TS) content of the organic material using a factor of

0.28 l min⁻¹ kg_{TS}⁻¹ [Fraser and Lau 2002]. When air is supplied in bursts, as opposed to a continuous low flow rate, channelling along paths of least resistance in the material is less pronounced and air is forced into less accessible areas of the material. The ‘cooling’ airflow was delivered at 25 l min⁻¹ when the core temperature of the material was above 60 °C to dissipate the excess heat. The flow rate was determined using a factor of 1.40 l min⁻¹ kg_{TS}⁻¹ [Fraser and Lau 2002]. The time for which the three-way solenoid valve on the cooling aeration airline (Figure 3.4) was open was recorded every 10 minutes by a PC-based logger and was expressed as a percentage of the time. For example, 100 % implied that the valve had been open for the whole 10 minutes and 250 litres of air had flowed into the reactor.

Considerably more air was supplied to remove the excess heat generated by microbial activity than was needed to replace the oxygen consumed. About 9 times more dry air, in kg (kg_{TS} h)⁻¹, was required to dissipate excess heat from the organic material than to meet the stoichiometric oxygen demand for aerobic respiration at 60 °C.

3.1.2.2.3. Moisture

Controlling the water content of the organic material was essential in order to maintain conditions favourable for high microbial activity. As the temperature rose, more water evaporated, which was increased further with the higher airflow rate. In an attempt to achieve a uniform moisture distribution throughout the organic material and to delay the on-set of moisture limitation, the baseline air supply was humidified at 40 °C by bubbling the air through a closed water cylinder before passing into the reactor. A relative humidity probe (Hygroclip S3, Rotronic Instruments Ltd, Crawley, UK) continuously monitored the relative humidity and temperature of the air leaving the humidifier. The relative humidity was about 50 % and the mass of water in the humidified air (23.6 g kg⁻¹ dry air) was more than twice that

in ambient air (10.3 g kg^{-1} dry air). The baseline airflow therefore carried approximately 61 grams of water per day into the organic material.

3.1.2.3. Monitoring systems

3.1.2.3.1. Temperature

The temperature of the organic material during composting was measured by thermistors sealed in stainless steel probes and logged half-hourly by Squirrel data loggers (Series 1200, Grant Instruments Ltd, Cambridge, UK). The probes were positioned at three points along the central axis of the reactor, top (1), centre (2) and base (3), 400 mm apart (Figure 3.3). A fourth thermistor (4) was embedded 40 mm from the side into the composting material and was positioned vertically level with the thermistor at (2) so that the radial temperature gradient could be monitored.

3.1.2.3.2. Off-gas analysis

Analysis of oxygen, carbon dioxide and ammonia content in the off-gas from the reactors provided a valuable means of monitoring the process. A sample of gas, drawn from the off-gas leaving through the central gas outlet (Figure 3.3), passed through a condenser, a modified domestic refrigeration unit (Figure 3.5), to remove water vapour from the gas phase. The average saturation of the off-gas over about 24 hours was determined by the water collected in the condenser flasks from a measured volume of dry off-gas.

The gas then passed through a silica gel desiccator column and a $5 \mu\text{m}$ filter (P3D Parker Pneumatic Junior filter, RS components Ltd, Corby, Northamptonshire, UK) to dry the gas and remove any dirt particles before it entered the gas analyser. The oxygen and carbon dioxide concentrations in the off-gas were respectively measured by a combined paramagnetic oxygen and infrared carbon dioxide gas analyser with analogue outputs (Series 4102, Servomex Group Ltd, Crowborough, UK). A PC-based logger recorded the gas

concentrations in the off-gas from the reactors for 15 minutes every hour by controlling the solenoid valves on the gas lines through a digital interface (Figure 3.6). Nitrogen, air and 9 ± 0.12 % carbon dioxide in nitrogen standard gases were used to calibrate the gas readings every 12 hours.

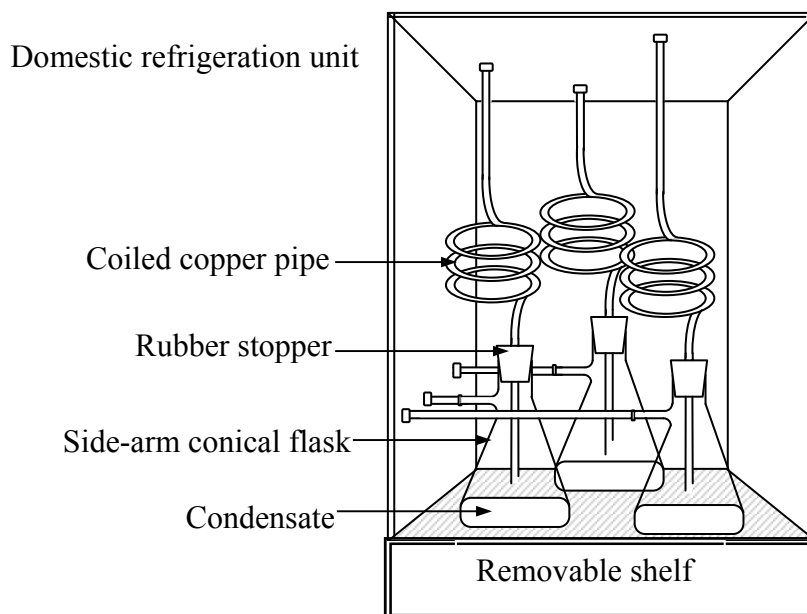


Figure 3.5. Condenser unit in which water is removed from the off-gas sample

Ammonia in the off-gas drawn from the headspace of each reactor was collected in sulphuric acid traps [Martinez *et al* 1997]. A trap consisted of two side-arm boiler tubes with glass sinters and contained 0.4 molar (M) sulphuric acid (H_2SO_4), a side-arm boiler tube to collect any liquid carried over, a 0.3 l min^{-1} pump (Model L12, Charles Austen Pumps Ltd., Byfleet, Surrey, UK) and an integrating gas meter (Remus 4 G1,6, Schlumberger Ltd) (Figure 3.7 and A3.10). Tubes were changed twice a day for the first 10 days and daily thereafter. The mass of ammonia collected was determined using steam distillation with back titration [APHA 1998], which had a 50 mg l^{-1} minimum detection limit.

The pipes carrying gas for analysis to the acid traps and to the condenser were heated with self-adhesive silicon heating tape (Clayborn Precision Heating Tape, Truckee, CA, USA) to prevent condensation inside. An on/off analogue temperature controller regulated the heating about the set point temperature of $60\text{ }^{\circ}\text{C} \pm 2\text{ }^{\circ}\text{C}$.

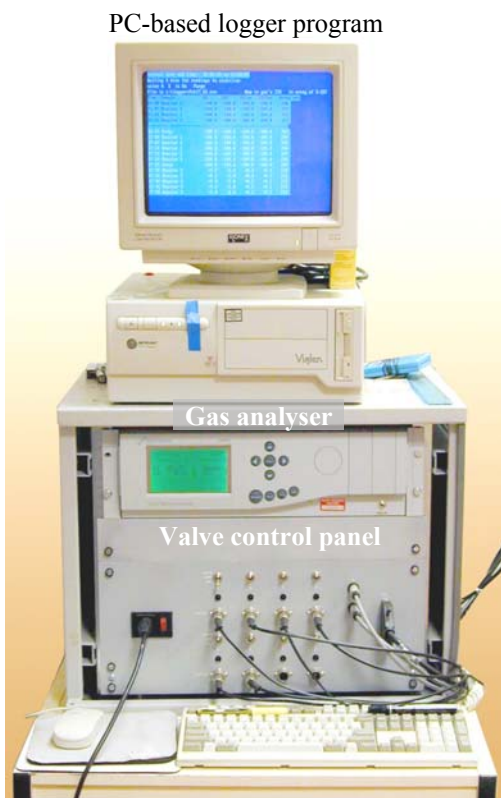


Figure 3.6. Gas analyser, control valve panel and PC-based data logger

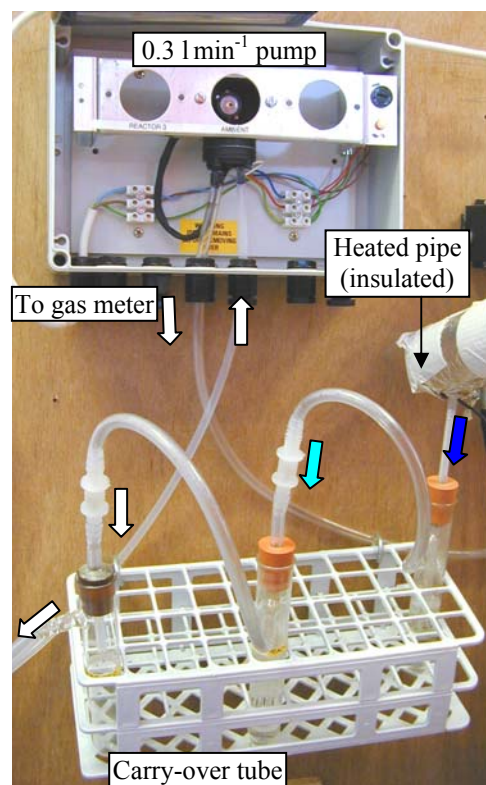
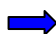
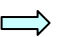
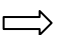


Figure 3.7. Ammonia acid trap




 Gas rich in NH_3 \longrightarrow Gas free of NH_3

The mass of oxygen consumed and carbon dioxide produced (ΔM_G) was the difference between the respective gas concentrations in the off-gas and the incoming air scaled up using the volume of air that entered the reactor and then converted to masses using equation (3 ii).

$$\Delta M_G = \frac{\Delta V_G \cdot M_{rG}}{22.4} \cdot \frac{273}{T_G} \quad (3 \text{ ii})$$

where ΔV_G = volume change of the gas (dm^3)

M_{IG} = relative molecular mass of the gas (32 g for oxygen and 44 g for carbon dioxide)

22.4 = volume of gas occupied by 1 mol of an ideal gas at 273 K (dm^3)

T_G = temperature of the gas which was at ambient temperature when analysed (K)

The total mass of ammonia and water leaving in the off-gas was determined by scaling up the mass of ammonia collected in the acid traps and water collected in the condenser using the volume ratio of the gas that passed through the respective measurement systems and the total dry air that entered the reactor, which was the sum of baseline and cooling aerations.

3.1.2.3.3. Mass loss

Reactor 1 was positioned on a 120 kg load cell (Sauter K120, August Sauter GmbH, Mettler-Toledo Ltd., Beaumont Leys, Leicestershire, UK) and the total mass of the reactor and composting organic material was recorded throughout the experiment. The loss in organic material was corrected for the loss of water in the gas stream and leachate. Figure 3.8 illustrates the points of measurement on the rig of Reactor 1.

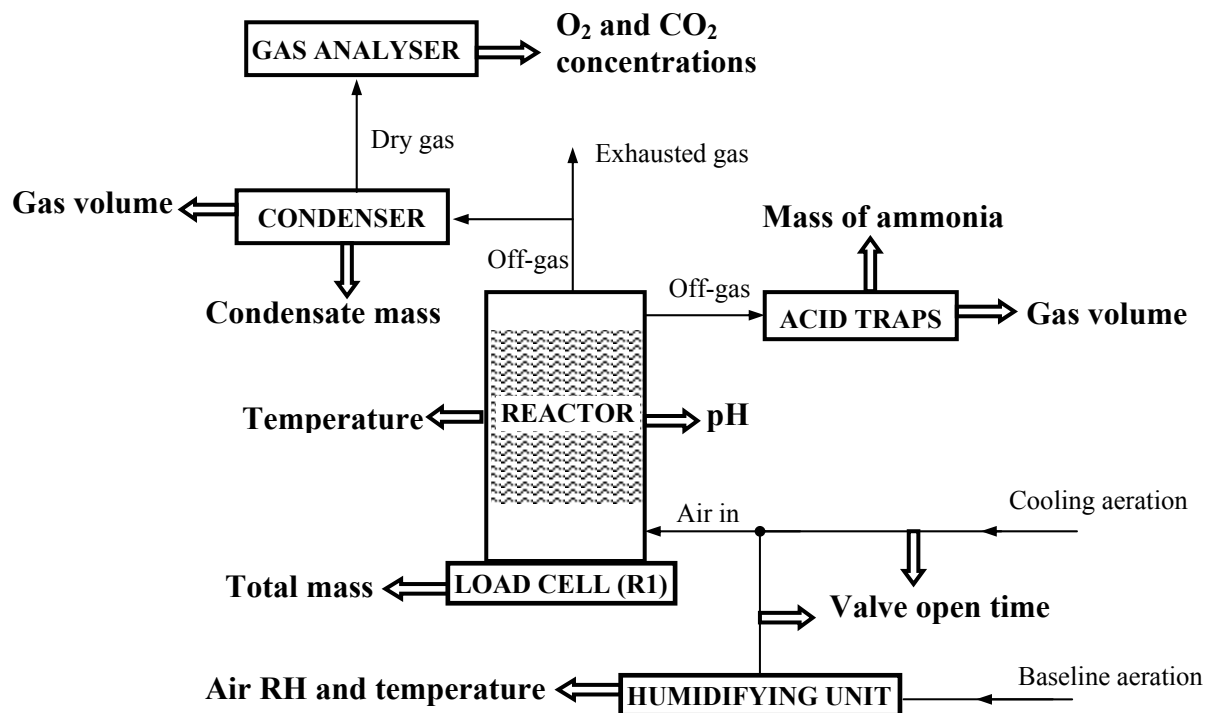


Figure 3.8. Points of measurement on the rig of Reactor 1.

3.2. Analytical Methods

3.2.1. Preparation and sampling

Thorough mixing of the pig manure and straw helped to reduce heterogeneity of the mix as a whole but representative samples are crucial for meaningful analytical results. All samples were analysed at least in duplicate.

Samples of at least 1 kg were used for the bulk density tests. The mass of the sample of organic material taken for analysis, therefore, tended to be more than the mass used in bench scale experiments and this needed to be taken into account when preparing the batches of organic material for each trial. In larger composting experiments, samples from sections of the organic material were collected as random grabs to make up samples of about 1 kg for chemical and physical analysis. Samples were kept at 2 °C in sealed plastic containers.

Microbial analysis was carried out on the organic material used in experiments carried out in the composting unit. Samples were collected in autoclaved containers that were designed for rapid collection and sealing so as to reduce contamination from external sources. The samples were then sub sampled immediately into sterile 100 ml Duran bottles in a Microflow biohazard class 2 cabinet and then stored at 2 °C.

3.2.2. Physical and chemical analyses

3.2.2.1. Total and volatile solids content

The total solids (TS) content of organic material is the ratio of the dry mass to wet mass of the sample. The dry mass of a wet sample was determined by drying a sample of at least 500 g in an oven at 105 °C for 16 hours. The moisture content (MC) equals mass fraction of the sample lost by drying based on its initial wet mass.

The volatile solids (VS) content was determined from a sub-sample of the dried organic material ashed at 550 °C. The residual mass represents the ash fraction and the VS content is the ratio of the mass lost with respect to the mass of dry sub-sample. APHA [1998] recommended 20 minutes at this temperature per 200 mg of residue. About 4 g of residue was typical for mixes of manure and straw and therefore ‘ashing’ time was approximately 7 hours.

3.2.2.2. Total organic carbon content

The total organic carbon (TOC) content was estimated from the following relationship, which is based on the typical lignin content of plant cell walls [Haug 1993].

$$\text{TOC} = \frac{\text{VS}}{1.8} \quad (3 \text{ vi})$$

3.2.2.3. Nitrogen content

The Kjeldahl nitrogen (Kj-N) and ammoniacal nitrogen (Amm-N) content of organic material with high nitrogen content (the equivalent mass of >50 mg kg⁻¹ or 50 ppm ammonia) was determined by steam distillation with back titration according to APHA standard methods. For Kj-N a weighed sample of approximately 5 g is pre-digested, which converts amino nitrogen, free ammonia and ammonium nitrogen to ammonium sulphate. For Amm-N the sample was distilled directly so that only the free ammonia and ammonium nitrogen is released from the organic material. The organic nitrogen (Org-N) content was the difference between the Kj-N and Amm-N. In FYM, the Kj-N content generally represents the total nitrogen (TN) content, as the nitrogen does not tend to exist in pig manure out of the tri-negative state, such as nitrates or nitrites [Kirchmann and Lundvall 1998, Petersen *et al* 1998, Sommer and Dahl 1999]. Colour spectrometry was used for the analysis of samples of low ammonia content of about 10 ppb to 20 ppm (undiluted) or 500 ppm (5:100 dilution).

3.2.2.4. pH

pH was measured using a standard 15 cm Ion Sensitive Field Effect Transistor (ISFET) probe with the Sentron 2001 pH system, which is temperature compensating. The probe can be used to take measurements directly from the organic material (Figure 3.9) or from samples diluted 1:10 (mass basis) with deionised water [MAFF/ADAS 1986].

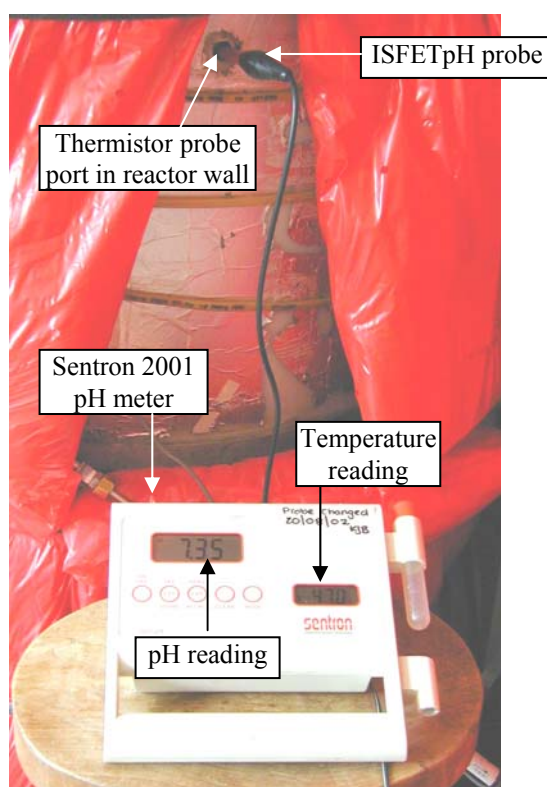


Figure 3.9. Taking the pH of the organic material during composting.

3.2.2.5. Chemical oxygen demand

The chemical oxygen demand (COD) is the measurement of equivalent oxygen used to oxidise the organic and inorganic fraction of the organic material. The standard method used was small-volume burette titration of a diluted sample after a closed-tube redox reaction under reflux conditions [APHA, AWWA, WEF 1998]. The test measured a COD in the range of 40 mg O₂ l⁻¹ to 400 mg O₂ l⁻¹, which could be extended by pre-dilution of the sample with water. The COD of Potassium hydrogen phthalate, 1.176 g O₂ g⁻¹, was used as a standard.

3.2.2.6. Bulk density and free air space

The bulk density (ρ_{bulk}) of organic material is the mass per unit volume of the material. It is a measure of the organic material and the air spaces in the sample and gives an indication of the ability of air to move through the material. Bulk weights above about 640 kg m^{-3} do not have enough air spaces for adequate airflow. ρ_{bulk} is calculated from the bulk weight (ω_{bulk}) and TS. ω_{bulk} is a function of the moisture content and compaction of the organic material and is determined according to the British Standard method developed for soil and soil improvers [BS EN 13040:2000] to measure the bulk weight of the organic material. The apparatus used is illustrated in Figure 3.10. The stainless steel test cylinder had a capacity of 0.1 m^3 and the plunger weighed 650 g. Compacting the organic material samples by the same amount is difficult to judge and to reduce the margin of error, the standard weight was applied for 3 minutes and at least three samples were used.

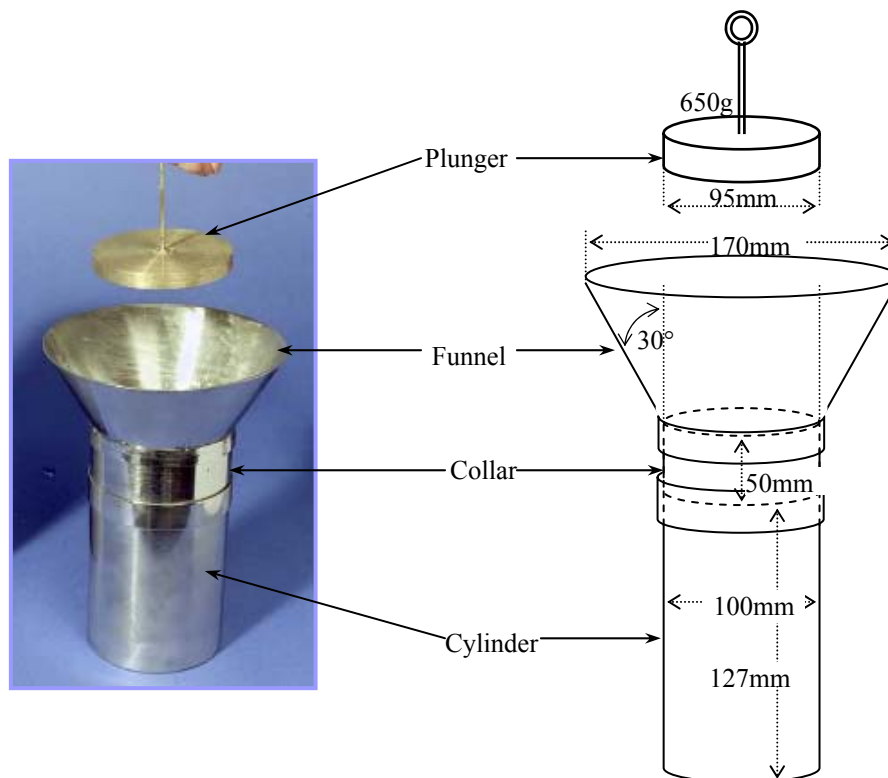


Figure 3.10. Apparatus to measure bulk weight and free air space of a compost-type material

The free air space (FAS) of the organic material is the ratio of gas volume to total volume. The FAS is related to ω_{bulk} by [Haug 1993]

$$\text{FAS} = 1 - \frac{\omega_{\text{bulk}} \cdot \text{TS}}{G \cdot \omega_{\text{W}}} - \frac{\omega_{\text{bulk}} (1 - \text{TS})}{\omega_{\text{W}}} \quad (3 \text{ vii})$$

Where G is the specific gravity of the solids fraction, as defined by equation (3 viii) and ω_{W} is the unit weight of water, which is assumed to be 1.

$$\frac{1}{G} = \frac{\text{VS}}{G_{\text{VS}}} + \frac{\text{ASH}}{G_{\text{ASH}}} \quad (3 \text{ viii})$$

G_{VS} is the specific gravity of the volatile solids fraction, VS and G_{ASH} is the specific gravity of the ash fraction, ASH. By definition $\text{TS} = \text{VS} + \text{ASH}$. On a TS basis, the ash fraction can then be described by $\text{ASH} = (1 - \text{VS})$. Haug [1993] states that the G_{VS} and G_{ASH} are normally equal to about 1 and 2.5, respectively.

For organic material with $\text{MC} < 80 \%$, the following simple linear relationship was empirically derived by Agnew and Leonard [2002] to describe the FAS fraction as a function of the bulk weight.

$$\text{FAS} = 100 - 0.09\omega_{\text{bulk}} \quad (3 \text{ ix})$$

3.2.2.7. Particle size distribution

A customised method for determining the size of particles in the pig manure was based on the wet sieving method described by [ISO 11277:1998 2002]. The series of graded sieves with hole sizes 4 mm, 2 mm, 1 mm, 500 μm and 250 μm were used. Four 200 g samples of pig manure were washed through the stack of sieves and an average was taken of the TS collected on each sieve and the wash water collected after drying according to Section 3.2.2.1. The distribution was expressed as a percentage of the total initial mass of TS.

3.2.3. Microbial analysis

The microbiology of the organic material was studied using agar plates. Bacto Nutrient agar is a general purpose medium. Bacto McConkey agar isolates and differentiates lactose-fermenting organisms from lactose non-fermenting gram-negative enteric bacteria.

The micro-organisms were extracted from a sample of known mass with 30 ml of 0.1 M sodium phosphate solution (pH 7). Successive ten fold serial dilutions of the extract with 0.7 % saline solutions were done for 5 levels. 0.1 ml of sample in diluent was added to each plate and spread uniformly over the surface of the growth medium using a sterile spreader. Duplicate plates of both growth media were made for each dilution. The total number of colonies was counted after 24 hours incubation at 37°C and a visual analysis considered the plate coverage and the colour and approximate size of individual colonies.

The density of general micro-organisms and specific coliforms in the original sample was calculated from the average of the number of colony forming units (N_{CFU}) on the respective growth media using the following equations:

$$N_{CFU} = \log_{10} \cdot \bar{n}_z \quad (3 \text{ ix})$$

\bar{n}_z is the average of the normalised number of colonies, n_z , in a sample extract of dilution z , from at least three dilutions. n_z is given as

$$n_z = \frac{\bar{x}_z}{v \cdot 10^z} \cdot \frac{V}{m_{TS}} \quad (3 \text{ x})$$

where \bar{x}_z is the average number of colonies counted on the pair of agar plates

v is the volume of diluted extract plated on the agar, ml

V is the volume of buffer solution used to extract the micro-organisms, ml

m_{TS} is the total solids mass of the sample, g

3.2.4. Limitations of analytical tests

Heating an organic material at 105 °C to determine the total solids (TS) content can result in a negative error due to the loss of some volatile material and temperature-induced chemical decomposition of ammonium carbonate [APHA 1998].

The volatile solids (VS) test is non-specific as it does not differentiate between the fraction of organic material that is readily biodegradable, slowly biodegradable and volatile but resistant to microbial attack during composting. Neither does the test relate exactly to the organic and inorganic fractions [Stocks 2002] or distinguish between the source of the VS, be they from the manure or the carbonaceous bulking agent [Finstein *et al* 1986]. The test is not very sensitive because a high percentage (usually about 80 %) of the TS is volatile and a reduction in the VS content could represent a more significant overall loss in one compost system than another [Stentiford 1993]. Keener *et al* [1993] state that using a VS basis introduces a superfluous parameter and should be discouraged. Decomposition and/or volatilisation of some mineral salts may take place on ignition of the organic material. There is also the slight loss of volatile solids during the initial drying of the sample. The total organic carbon content (TOC) test is more specific to the organic content of the material but, by association, it has similar disadvantages to the VS test.

The chemical oxygen demand (COD) test is also non-specific and measures the organic fraction of the material collectively [Finstein *et al* 1986]. Furthermore, the test does not necessarily oxidise all organic material and a relationship between the readily degradable fraction and the COD is unpredictable. Variation between sample duplicates tends to occur because of the heterogeneity of the organic material and is heightened by concentrated solutions [Stocks 2002].

The method of steam distillation and back titration for determining the nitrogen content of the organic material has a minimum detection limit of 50 mg kg^{-1} of sample. The method does not take into account nitrogen compounds in the tri-negative state, which includes nitrates and nitrites. Nitrate and nitrite tests using the Merckoquant test strips did not detect concentrations above 10 mg l^{-1} and 2 mg l^{-1} , respectively, in the samples.

The British standard method used to determine the bulk weight of the organic material requires disturbance of the organic material, which therefore alters the bulk weight of the material when *in situ*. This is not as much of an issue for the organic material to be composted as for the composted material and the use of disturbed and compacted samples can lead to erroneous values. The test does not take into account the compaction of the organic material and the bulk weight of disturbed samples only reflects that of the top layer of material. A linear relationship between the bulk weight and depth has been evaluated [Van Ginkel 1999] and can be used to correct for compaction.

3.3. Characteristics of the organic material

3.3.1. Pig manure

Solid pig manure was collected from the slatted floor on which weaner pigs were kept at a local farm. With the outbreak of foot and mouth disease (FMD), precautions were taken when moving manure between agricultural establishments so as not to be a vector, although there were no reported cases in Bedfordshire. The manure was collected and transported in airtight sealed 50 litre plastic containers. These were then stored at 2°C for between three and four weeks. Three weeks is the incubation period of the disease so that if there was no sign of FMD on the farm during this time then the manure was deemed to be safe to use. The manure in each container was analysed. The mean values for analyses are given in Table 3.1.

Table 3.1. Analysis of the pig manure for each collection.

Collection	MC %	TS %	VS %TS	ASH %TS	TOC %TS	Org-N %TS	Amm-N %TS	pH
Respirometry	74.9	25.1	80.4	19.6	44.6	3.21	1.67	
26-04-01	75.8	24.2	81.2	18.8	45.1	3.39	1.28	5.86
05-05-01	75.5	24.5	82.0	18.0	45.6	3.34	1.18	5.95
23-08-01	75.4	24.6	81.6	18.4	45.3	3.17	1.33	
10-09-01	76.6	23.4	83.3	16.7	46.3	3.64	0.89	6.33
12-02-02	75.6	24.4	80.2	19.8	44.5	3.46	1.08	6.30
21-06-02	71.6	28.4	78.1	21.9	43.4	3.38	1.18	

The total solids content of the manure from the last collection was higher because of the warmer summer conditions. The C:N ratio of pig manure, calculated from the TOC and TN, was about 10. The average bulk weight of pig manure was 1002 kg m⁻³ and, as explained in Section 3.2.1.5, air spaces were absent. The free airspace (FAS) was less than 3 %.

Table 3.2. Distribution of organic material and ash particles in pig manure

Particle size	TS content %	Ash content %TS	Mass, kg VS kg ⁻¹ TS
4 mm – 2 mm	1	14	0.01
2 mm – 1 mm	2	5	0.02
1 mm – 500 µm	21	6	0.20
500 µm – 250 µm	16	10	0.15
< 250 µm	60	30	0.42

The particle size distribution in the manure used in respirometry experiments is given in Table 3.2. The fraction of particles greater than 1mm were mainly of pieces of grains (spilt pig feed) and contributed only about 3 % to the TS. The TS of the particles between 250 µm and 1 mm were at least 90 % volatile whilst half of the particles smaller than 250 µm were non-volatile. Most of the VS however were still found to be in the smallest size range.

Extracts from a manure sample, diluted up to a factor of 10^{-6} in saline solution (Section 3.2.3), were plated onto Nutrient and McConkey's agar to determine the density of general and coliform colony forming units (CFU) in manure, respectively. The general microbial population numbered an average $10^{8.2}$ CFU g^{-1} TS and the coliforms, which were pink-red circles, averaged at $10^{5.9}$ CFU g^{-1} TS (Figure 3.11).

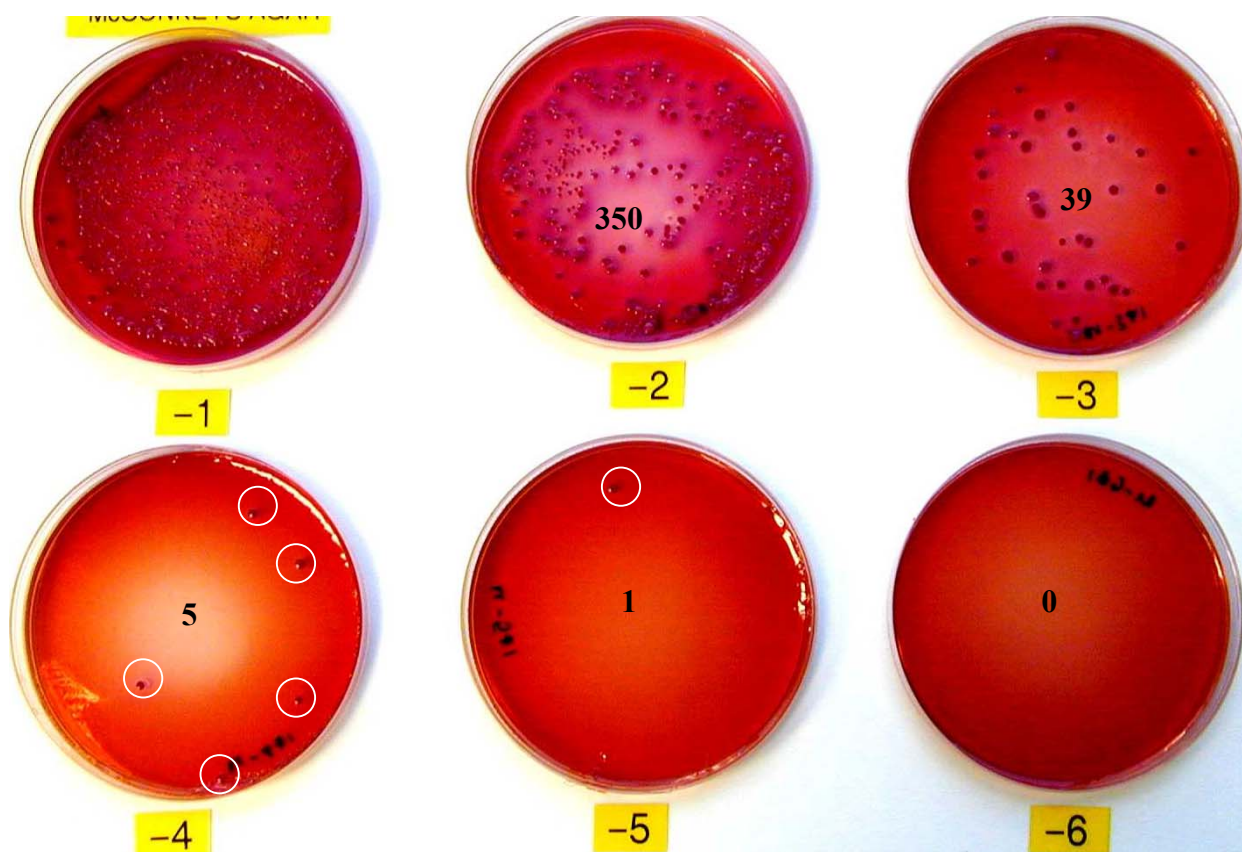


Figure 3.11. Coliform colonies in pig manure extract for dilutions 10^{-1} to 10^{-6} grown on McConkeys agar

3.3.2. Straw

Chopped dry winter wheat straw was used as the bulking agent and carbon source. The bulk weight was 45 kg m^{-3} , the FAS about 96 % and the C:N ratio was 96. The analysis of the winter wheat straw collected from two harvests are given in Table 3.3.

Table 3.3. Analysis of the winter wheat straw from each batch from the two harvests

Harvest	MC %	TS %	VS %TS	ASH %TS	TOC %TS	Org-N %TS	Amm-N %TS	pH
2000	13.4	86.6	92.4	7.6	51.3	0.58	0.04	7.9
2001	10.2	89.8	94.6	5.4	52.5	0.43	0.06	7.5

The mean length of the chopped straw was 7.3 cm with a standard deviation of 4.2. The median and mode averages were 6 cm and 5 cm, respectively. The length ranged from 1 cm to 31 cm and the distribution (Figure 3.12).

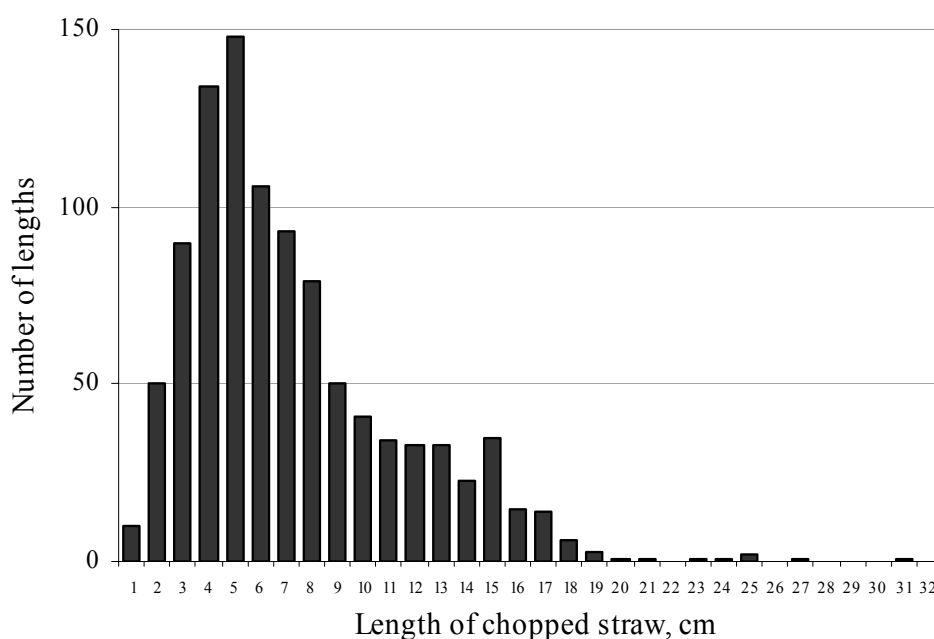


Figure 3.12. Distribution of straw lengths of the 1000 pieces measured

The physical structure and water absorption capacity of organic material affects oxygen transfer from the gas to the liquid and solid phases [Jeppsson 1998]. Water holding capacity of organic materials varies and the optimal initial and working moisture content is not necessarily universally applicable [Finstein and Hogan 1992]. The straw absorbs about 3.5 times its own dry mass in liquid. To estimate the mass of water that can be held by the chopped wheat straw, samples of equal mass were mixed in the mass ratios of 1.5 to 4 with water and 0.5 M and 1 M solutions of water and urea. The straw and liquid were mixed and

left for 24 hours in a sealed 5 litre container, which was also shaken every 2 hours (when possible) to distribute the liquid. The contents were then tipped into a container with a stainless steel grid fitted and the mass of liquid that drained out over 12 hours was collected and weighed (Figure 3.13). The results show the urea appears to enhance the ability of straw to absorb the liquid. The straw is able to hold twice its mass in liquid. The maximum moisture contents of the straw that were measured were 74 % for the water and 0.5 M solution and 76 % for the 1 M solution, as indicated on the data bars in Figure 3.13. The ‘safe’ working moisture content, in terms of avoiding any leaching, was about 66 %, which corresponded to the liquid to straw ratio of 2.

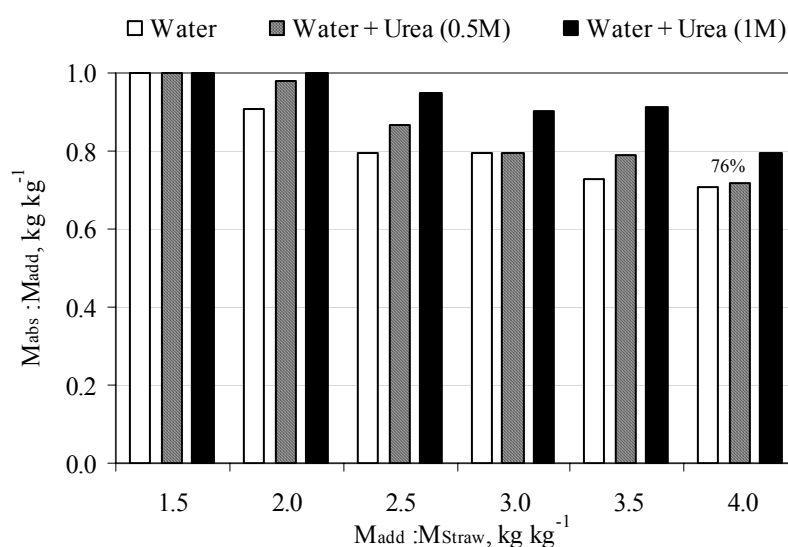


Figure 3.13. Fraction of added liquid absorbed by the straw ($M_{abs} : M_{add}$) for a range of mixing ratios of liquid and straw ($M_{add} : M_{straw}$)

The extracts of straw up to a dilution of 10^{-3} were plated onto Nutrient and McConkey’s agar. The average general microbial population density ($10^{4.2}$ CFU g^{-1} TS) was about 10^4 times less than in the pig manure. Coliforms in the straw averaged $10^{4.6}$ CFU g^{-1} TS, although the colonies were different in appearance compared with those in manure, being small pale pink circles with a darker centre.

3.3.3. Pig manure and straw mixes

Figure 3.14 shows the organic material when the pig manure is mixed with straw in the mass ratio of 4.



Figure 3.14. The pig manure and straw before and after mixing in the ratio of 4

The pig manure, with lack of structure and the low C:N ratio, did not promote optimum composting conditions. The straw was mixed with the manure to provide support, resulting in a bulky and open organic material, and carbon.

3.3.3.1. Free air space

The volume occupied by the air spaces is expressed as the free airspace of the matrix. The free air space (FAS) is a factor in the composting process, as it influences the availability of oxygen, the evaporation of water and the emissions of ammonia gas.

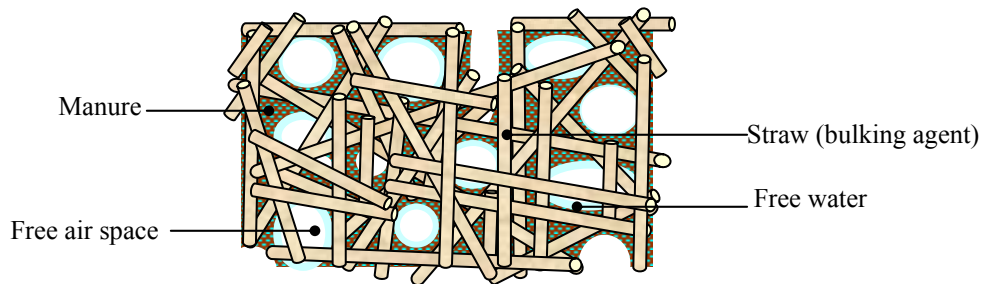


Figure 3.15. Schematic representation of the structure of the manure and straw mix.

The bulk weight, and consequently the FAS, depends on the moisture content of the organic material and mixing ratio of the manure to straw. The bulk weight is linearly related to the FAS because the particle density is reciprocally proportional to the moisture content. The minimum FAS is related to the optimum moisture content of the particular mix, which is a compromise between the moisture required for optimal microbial activity and the diffusion of oxygen. Bulking agents are fibrous materials and hold a certain amount of water whilst maintaining its structure and a minimum FAS.

The total volume of the mixed organic material is greater than the sum of the individual volumes occupied by the manure (of a specified total solids content) and straw because the manure supports the straw. Manure of a higher moisture content may only occupy the air space in the straw, and not increase the total volume of the organic material. Haug [1993] points out that more work is required to develop quantitative relationships between the increase in volume, as indicated by the increase in FAS, and the total solids content.

The bulk weight (ω_{bulk}) was determined for three mixing ratios of pig manure and straw (1, 2 and 4) with moisture contents up to 80 %. The corresponding FAS was calculated using equation (3 vii) and compared with those calculated with equation (3 ix). The moisture content of the manure and straw mixes was varied from the inherent moisture content of about 50 % by adding water to the organic material for higher moisture contents and by drying the samples at 60 °C for lower moisture contents. The approximate mass of organic material required to fill the composting reactor (212 litres) is given in the ‘Reactor’ column in Table 3.5. The reactor was expected to hold about 40 kg of organic material with an initial moisture content of 65 %. The FAS values of all the mixing ratios and moisture contents tested were well above 50 %.

Table 3.4. Bulk weight (ω_{bulk}) and free air space (FAS) of test samples

Mixing ratios on a wet mass basis (Manure : Straw)									
	1:1			2:1			4:1		
MC %	ω_{bulk} kg m ⁻³	FAS %	Reactor kg	ω_{bulk} kg m ⁻³	FAS %	Reactor Kg	ω_{bulk} kg m ⁻³	FAS %	Reactor kg
0	36	97	8	36	97	8	49	96	10
15	49	95	10						
40	72	93	15	68	93	15			
50	92	91	20	91	91	19			
60	110	89	23	155	85	33	172	83	36
70	145	86	31	211	79	45	243	76	51
80	265	74	56	275	73	58	390	62	83

The FAS, calculated by equation (3 vii), agreed with the values determined using equation (3 ix) at the lower bulk weights (Figure 3.16). As the bulk weight increased, so did the difference between the corresponding values in the two sets of data. The difference is probably because equation (3 viii) was derived from FAS values measured using an air

pycnometer. This measured the micro as well as the macro FAS of the organic material and therefore gave higher FAS values than those from equation (3 vii) that represents only the macro FAS [Agnew and Leonard 2002]. The micro FAS corresponds to the air spaces within a particle and does not contribute to the available oxygen content of the organic material. 95 % of the maximum oxygen uptake rate was maintained when the macro FAS was between 20-35 % [Haug 1993]. The open structure of the freshly mixed organic material was therefore unlikely to limit the movement and the uptake rate of gases because of the lack of FAS.

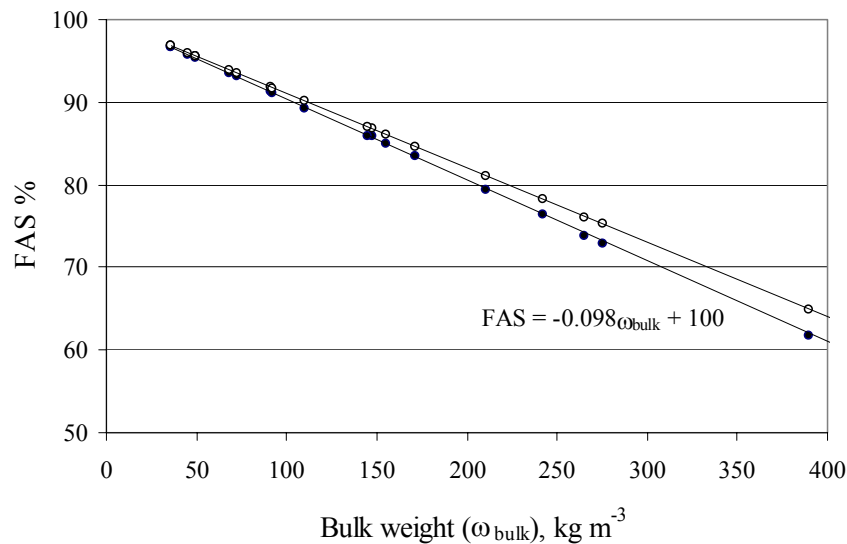


Figure 3.16. The relationship between the bulk weight and FAS of the organic material calculated using equation (3 vii) (o) and equation (3 ix) (●).

3.3.3.2. Thermodynamic properties

Heat removal is important in large volumes of composting organic material where the failure to remove excess heat can lead to temperature limiting situation. It is necessary to understand the heat transfer processes within the organic material when dealing with heat balances during the process. Specific heat capacity and thermal conductivity are important variables to determine as they tend to be specific to the organic material and depend on its moisture content. A relationship between moisture content, temperature and each of the

thermodynamic variables is necessary to enable the heat flows to be more accurately represented in a model of the process.

Mears *et al* [1975] investigated the thermodynamic properties of pig waste, which mainly consisted of faeces and uneaten feed, mixed with 5 % by weight straw. The thermal properties investigated were found to vary linearly with moisture content. The specific heat capacity, in $\text{kJ kg}^{-1} \text{ }^{\circ}\text{C}^{-1}$, was empirical related to the moisture content (MC) by

$$C_p = 0.032 \cdot \text{MC} + 0.650 \quad (3 \text{ xi})$$

The thermal conductivity (k), in $\text{W m}^{-1} \text{ }^{\circ}\text{C}^{-1}$, was calculated from the experimentally determined specific heat capacity, density (ρ) and thermal diffusivity (α) using the relationship

$$k = \alpha \cdot \rho \cdot C_p \quad (3 \text{ xii})$$

The k of the organic material was found to vary with moisture content according to the following relationship

$$k = 0.004 \cdot \text{MC} + 0.241 \quad (3 \text{ xiii})$$

They concluded that the material to be composted was of a low thermal conductivity and specific heat capacity, which were expected to decrease during the composting process due to the loss of water, even with the expected increase in the ash content, as ash tends to have a higher heat capacity than VS. The methods used were simple, repeatable and low cost.

In this work the specific heat capacity, thermal diffusivity and thermal conductivity were determined for mixes of manure and straw, in the wet mass mixing ratio of 2 and moisture contents of approximately 50 %, 65 % and 75 %. Six 200 g samples of each moisture content were used for the analysis of each thermal property.

3.3.3.2.1. Specific heat capacity

The calorimetric method of mixing was used to determine the specific heat capacity of the mix of manure and straw. The water and organic material of known mass and temperature were mixed in an insulated container and the temperature was monitored. The unknown specific heat capacity of the organic material was determined from the energy balance given by equation (3 xiv).

$$\left[c_p \cdot m \right]_W + c_p \cdot m \left[\right]_{\text{Mix}} \Big|_F \cdot T_F = \left[c_p \cdot m \cdot T \right]_W + c_p \cdot m \cdot T \left[\right]_{\text{Mix}} \Big|_I \quad (3 \text{ xiv})$$

c_p is the specific heat capacity, $\text{kJ kg}^{-1} \text{ }^\circ\text{C}^{-1}$, m is the mass, kg and T is the temperature of the material, $^\circ\text{C}$. The subscripts W, Mix, F and I represent the water, manure and straw mix, final and initial states, respectively. The test samples, cooled to 2°C , were mixed with 2 kg of water at 35°C . The temperature was logged until a steady value was reached.

To check whether heat was liberated on mixing water with the organic material, a sample and water at the same temperature were mixed. A rise in temperature was only measured when a dry sample was mixed into the water.

3.3.3.2.2. Thermal diffusivity

The thermal diffusivity (α) of organic material was determined by measuring the rate of temperature rise at the centre of a mass from a constant outside temperature. With a high α , the aluminium cylindrical container offered little thermal resistance to the transfer of heat from the heat source to the organic material and its effect was not considered. In order to ensure that the heat transfer is in the radial direction and not axially through the organic material, the ends were insulated. The expression used to determine α , is given as

$$\alpha = \frac{D}{t_1 - t_2} \quad (3 \text{ xv})$$

t is time in minutes and for a cylinder,
$$D = \frac{60 \cdot \ln T_1/T_2}{\left(\frac{5.783}{r^2} - \frac{\pi^2}{l^2} \right)}$$

where T is the temperature difference between the centre and heat source, °F

r is the cylinder radius, ft

l is length of the cylinder, ft

Subscripts 1 and 2 correspond to points on the curve of a natural log plot of the normalised temperature change in the organic material against time, through which a straight line can be drawn [CRD-C 36-37].

An aluminium test cylinder was sealed at both ends with expanded polystyrene and positioned vertically in a constant temperature water bath. The mass of organic material required to fill the cylinder, without being compressed, was noted. The temperature was recorded every minute by a centrally positioned temperature probe until a steady state was reached and no increase was apparent. The thermal diffusivity of the organic material was determined for six temperature differences from 10 °C to 60 °C (one sample was used for one temperature difference) and the average value of each moisture content was used to calculate the corresponding thermal conductivity.

3.3.3.2.3. Thermal conductivity

The thermal conductivity, k, was calculated from the α , c_p and density, ρ , of the organic material by using expression (3 xii). The density was taken as the mean bulk weight of the six samples for each moisture content.

3.3.3.2.4. Results of thermal analyses

The specific heat capacities and thermal diffusivities determined for the three moisture contents are given in Table 3.6. The thermal diffusivities measured at the six temperature differences from 10 °C to 60 °C and the corresponding calculated thermal conductivities are

given along with the mean values. The heat capacity of the organic manure was related to the moisture content as given by the following expression

$$c_p = 0.03 \cdot MC + 0.99 \quad (3 \text{ xvi})$$

Mears *et al* [1975] measured a specific heat capacity of approximately $2.4 \text{ J g}^{-1} \text{ }^{\circ}\text{C}^{-1}$ for pig waste and straw mix with a moisture content of 48 %. Likewise the mean thermal conductivity was related to the moisture content by

$$k = 0.005 \cdot MC + 0.165 \quad (3 \text{ xvii})$$

The measured thermal conductivity of compost-type material has ranged from about $0.23 \text{ W m}^{-1} \text{ }^{\circ}\text{C}^{-1}$ to $0.46 \text{ W m}^{-1} \text{ }^{\circ}\text{C}^{-1}$ [Haug 1993]. The average k measured in soil organic material and saturated soil organic material was about $0.25 \text{ W m}^{-1} \text{ }^{\circ}\text{C}^{-1}$ and $0.50 \text{ W m}^{-1} \text{ }^{\circ}\text{C}^{-1}$, respectively [De Vries and Peck 1958]. Mears *et al* [1973] measured values between $0.27 \text{ W m}^{-1} \text{ }^{\circ}\text{C}^{-1}$ and $0.44 \text{ W m}^{-1} \text{ }^{\circ}\text{C}^{-1}$ for moisture contents between 9 % and 48 %, respectively. Values were about four times greater than the calculated values given in Table 3.5. The organic material tested by Mears *et al* [1973] was a mix of pig waste and 5 % by mass of straw. The equivalent mixing ratio, in terms of the organic materials used here, would be 20, which equates to ten times as much pig manure. The manure and straw mixes tested in these experiments were highly porous with a bulk weight between 90 kg m^{-3} and 230 kg m^{-3} , and the relatively low thermal conductivity is feasible.

The thermal diffusivities, and therefore the thermal conductivities, increased with the temperature difference. The effects of convective heat transfer within a porous material, in which the differential temperatures cause a change in the density of the gas in the air spaces, are not entirely avoidable. The influence was more obvious in the organic material with the lowest moisture content of 48 % because it has a higher air content and the thermal diffusivity of air ($c. 2.5 \times 10^{-5} \text{ m}^2 \text{ s}^{-1}$) is two orders greater than that of water ($c. 1.5 \times 10^{-7} \text{ m}^2 \text{ s}^{-1}$).

Table 3.5. Thermal properties of pig manure and straw mixes

	MC = 48% $C_p = 2.57 \text{ J g}^{-1}\text{°C}^{-1}$ $\sigma = 0.05$		MC = 65% $C_p = 2.95 \text{ J g}^{-1}\text{°C}^{-1}$ $\sigma = 0.04$		MC = 73% $C_p = 3.41 \text{ J g}^{-1}\text{°C}^{-1}$ $\sigma = 0.06$	
T °C	$\alpha \times 10^{-7}, \text{ m}^2 \text{ s}^{-1}$	k, $\text{W m}^{-1}\text{°C}^{-1}$	$\alpha \times 10^{-7}, \text{ m}^2 \text{ s}^{-1}$	K, $\text{W m}^{-1}\text{°C}^{-1}$	$\alpha \times 10^{-7}, \text{ m}^2 \text{ s}^{-1}$	k, $\text{W m}^{-1}\text{°C}^{-1}$
10	1.70	0.038	2.01	0.109	2.03	0.159
20	2.42	0.054	2.19	0.118	1.81	0.142
30	2.42	0.054	2.40	0.130	2.04	0.160
40	3.35	0.074	2.51	0.136	2.61	0.205
50	3.92	0.087	2.77	0.150	3.05	0.239
60	4.65	0.103	3.05	0.165	3.14	0.246
Mean	3.08	0.068	2.49	0.134	2.45	0.192
σ		0.024		0.020		0.045

3.3.3.3. Composition of the pig manure and straw mixes

Composting pig manure mixed with straw was investigated on three levels of C:N ratio and pH. The mixing ratios of the manure and straw (M:S ratio), on a wet mass basis, which approximately gave the required C:N ratio of 15, 20 and 25, were 4, 3 and 2, respectively. For mixing ratios 3 and 4, some urea was need to further increase the nitrogen content and so reduce the C:N ratios to 20 and 15. The moisture content of the organic material was adjusted to 65 % by adding distilled water. The pH was adjusted by adding 1 M sulphuric acid (H_2SO_4) to the water that was added to the organic material (the water in the acid was taken into account in the water balance). The quantity of each constituent in the initial organic material is given in Table 3.6.

The pH of the pig manure was about 6. Once mixed with straw and left at ambient temperature for about one day the pH of the organic material increased to about 8. To achieve the three levels of pH investigated in the composting experiments, the freshly mixed manure and straw was kept in sealed black bin liners in cold storage for about a week until the pH had gradually increased to about 8. A predetermined amount of diluted sulphuric acid was then

added to the organic material on loading up the compost reactors. The amount of sulphuric acid required to reduce the pH from 8 to 7 and from 8 to 6 was estimated by gradually adding 0.1 M H₂SO₄ to samples of an M:S ratio 2:1 and 4:1 and an initial moisture content of 65 %, whilst monitoring the pH. These mixing ratios were assumed give the minimum and maximum amount of acid required, respectively. The respective average volumes of acid required to adjust the pH from 8 to 7 and 8 to 6 were 0.12 l kg⁻¹TS and 0.31 l kg⁻¹TS for a mixing ratio of 2 and 0.12 l kg⁻¹ TS and 0.43 l kg⁻¹ TS for a mixing ratio of 4.

Table 3.6. Composition of the manure and straw mixes composted.

M:S and C:N ratios	M:S ratio= 4:1 (C:N ratio = 15)			M:S ratio = 3:1 (C:N ratio = 20)			M:S ratio = 2:1 (C:N ratio= 25)		
	8	7	6	8	7	6	8	7	6
Theoretical pH									
Manure, kg	34.8	34.8	34.8	27.0	27.0	27.0	21.0	21.0	21.0
Straw, kg	8.7	8.7	8.7	9.0	9.0	9.0	10.5	10.5	10.5
Solid Urea, kg	0.4	0.4	0.4	0.1	0.1	0.1	0.0	0.0	0.0
1M H ₂ SO ₄ , l	0.0	0.5	2.0	0.0	0.5	1.9	0.0	0.5	1.8
Water, l	2.9	2.4	1.0	5.3	4.8	3.6	9.3	8.8	7.6
Total, kg	46.8	46.8	46.8	41.3	41.3	41.3	40.8	40.8	40.8

3.4. Summary

- A constant pressure respirometer was used to investigate the oxygen uptake by pig manure over a range of incubation temperatures, by measuring the change in gas volume.
- A continuous gas analysis respirometer was used to investigate the oxygen up take by straw amended pig manure over a range of incubation temperatures, by measuring the change in oxygen concentration in the reactor vessels' atmosphere with a gas analyser.
- The composting unit consisted of three identical composting reactors arranged in a rig with facilities for measuring and recording the temperature of the organic material, the

oxygen, carbon dioxide and ammonia content of the off-gas and the loss in wet mass during the composting time.

- Control systems on each composting reactor regulated the aeration, maintained the upper temperature in the organic material around 60 °C and compensated for heat losses from the reactor surface.
- Heat loss calculations showed that the external heating cable was capable of compensating for the radial heat losses at the highest expected temperature difference across the reactor.
- The pig manure had a moisture content of about 75 % and a C:N ratio of about 10 and practically no free airspace. The coliforms in the manure were characterised by circular red colonies, which averaged about $\log_{10} 5.9 \text{ CFU g}^{-1}\text{TS}$.
- The chopped straw had a moisture content between 10 % and 13 % with a C:N ratio of 96 and FAS above 95 %. The mode length of the straw pieces was 5 cm.
- The straw could hold about three times its own mass in liquid but to avoid leaching a liquid to straw ratio of 2 was recommended. Urea in solution enhanced the straw's absorbency.
- Coliforms were present in the straw but the colonies were relatively small and pale pink and averaged $4.6 \text{ CFU g}^{-1}\text{TS}$.
- A mix of pig manure and straw in the M:S ratio of 4:1 on a wet mass basis with a moisture content up to 80 % had a FAS well above recommended minimum of 35 %.
- The thermal properties of straw amended pig manure were functions of the moisture content. The specific heat capacity ranged from about $2.6 \text{ J g}^{-1} \text{ }^{\circ}\text{C}^{-1}$ to $3.4 \text{ J g}^{-1} \text{ }^{\circ}\text{C}^{-1}$ at moisture contents 48 % and 73 %, respectively. Similarly, the thermal conductivity ranged from about $0.07 \text{ W m}^{-1} \text{ }^{\circ}\text{C}^{-1}$ to $0.19 \text{ W m}^{-1} \text{ }^{\circ}\text{C}^{-1}$.
- Mixing ratios of the manure to straw of 2, 3 and 4 equated to C:N ratios of approximately 25, 20 and 15, respectively.

CHAPTER 4

RESPIROMETRY

4.1. Introduction

In the design of a composting system it would be imprudent not to have prior knowledge of the characteristics of the organic material and its behaviour under composting conditions [Haug and Ellsworth 1991]. The decomposition rate of the organic material is an overriding determinant of the system's performance. A measure of the decomposition rate contributes to optimal process design and control and avoids erratic performance [Finstein *et al* 1986]. A time-course test can be used to evaluate such a rate.

Respirometry involves the measurement of the oxygen consumed, and where possible, the carbon dioxide produced during aerobic microbial activity. The pattern of oxygen uptake with time determines the rate of decomposition [Haug and Ellsworth 1991]. The rate is related to the organic material's biodegradable volatile solids content and is an indication of its degree of decomposition. Respirometry can, therefore, be used to characterise the organic material to be composted and the composting process, and to evaluate the stability of the composted organic material. Microbial activity is affected by many environmental factors, in particular moisture content, since oxygen availability is proportional to water content and micro-organisms generally prefer higher water activities. High moisture contents however adversely affect the gaseous exchange by limiting gaseous movement and so restricting the oxygen diffusion to aerobic micro-organisms. This then leads to a decrease in activity.

There is limited data on the microbiological changes that determine the composting rate, produce most of the physical and chemical changes in the compost and affect the quality

of the composted organic material [Tiquia *et al* 1996]. This is highlighted by the fact that data tends to be specific to the compost system and material tested [Jeris and Regan 1973b, Keener *et al* 1993, Eckinci *et al* 2002]. The purpose of the series of respirometry tests was to find a simple and reliable indicator of microbial activity in mixes of pig manure and straw in order to improve the efficiency of the control systems on the composting unit (Section 3.1.2).

4.1.1. Theory and literature review

4.1.1.1. Process kinetics

Keener *et al* [1993] proposed that the rate of microbial activity, based on the unit mass of degradable organic material, follows first order reaction kinetics and is expressed as:

$$\frac{dm}{dt} = -k(x_1, x_2, \dots, x_n)(m_t - m_e) \quad (4 \text{ i})$$

k is known as the reaction rate coefficient and m_t is the mass of degradable organic material, m , at time t and m_e is the mass remaining when no further loss in m occurs. This state of equilibrium is reached after about 6 months to 1 year. x_i represents the effect of an environmental factor on activity. If all these factors remain constant, the solution to expression (4 i) is a dimensionless variable known as the compost mass ratio R_m . The standard solution to a first order differential rate equation takes the form of an exponential time expression, such that:

$$R_m = \frac{m_t - m_e}{m_0 - m_e} = e^{-k \cdot (x_1, x_2, \dots, x_n) t} \quad (4 \text{ ii})$$

R_m ranges from 1 at $t = 0$ to 0 at equilibrium. It is useful indicator of degree of decomposition and, therefore, the stability of the composting material [Hamelers 2002].

4.1.1.2. Reaction rate coefficient

The dependence of k on the numerous environmental factors (x_1 to x_n) is assumed to be multiplicative [Haug 1993, Richard 1997, Keener *et al* 2002] so that the exponent term can be written as:

$$k(x_1, x_2, \dots, x_n) = k^\ominus \cdot f_1(x_1) \cdot f_2(x_2) \cdot \dots \cdot f_n(x_n) \quad (4 \text{ iii})$$

k^\ominus is the value of the reaction rate coefficient under standard/optimal conditions and f_i , the function of each factor's effect. When the process is carried out under standard/optimal conditions the functions all equal 1 and $k \rightarrow k^\ominus$. The k value is also substrate specific and depends on the type of organic material composting [Keener *et al* 2002, Hamelers 2001] and has usually required empirical evaluation. Hamelers [2001, 2002] questioned the use of the multiplicative approach as it assumes that the environmental factors act independently of each other and that the organic material is homogeneous. The first order rate expression was shown to be applicable over a short time period of approximately 3 days [Keener *et al* 1993] during which the organic material is unlikely to show a loss of structure and free airspace due to compaction. Furthermore, for bench scale experiments, a well-prepared organic material can be considered to be relatively homogenous with little variation within and between the samples.

4.1.1.3. Specific oxygen uptake rate

The empirical value of k is calculated using the relationship between the specific oxygen uptake rate (SOUR) and the chemical oxygen demand (COD) of the material to be composted.

$$k = \frac{\text{SOUR}}{\text{COD}} \quad (4 \text{ iv})$$

The SOUR is derived from the gradient of the line on a plot of the cumulative mass of oxygen consumed against time. Keener *et al* [1993] expressed SOUR based on the TS content whilst others [Schulze 1960, Mohee 1998] used a VS basis. COD is expressed on the same basis such that k has the dimension $[T^{-1}]$ [Mohee 1998].

4.1.1.4. Environmental factors

The principal factors, which significantly affect the SOUR, and therefore k , are temperature, moisture content, free airspace and the oxygen concentration in the airspaces of the organic material [Haug 1993]. Another factor that has been considered is the C:N ratio [Mohee 1998, Ekinici *et al* 2002, Keener *et al* 2002]. The factor investigated here was temperature (T). The reaction rate coefficient was therefore specified as k_T . The other environmental factors were, where possible, kept constantly optimal in the experiments so that variation in their effects was minimised.

A number of expressions have been proposed, which describe the effect of moisture content (MC) on the decomposition rate for specific organic material [Haug 1993, Mohee 1998, Keener *et al* 2002, Richard *et al* 2002]. The S-shaped logistic curve proposed by Haug [1993], f_{MC} , was used to predict the effect of moisture contents and is given as:

$$f_{MC} = \frac{1}{e^{(-17.7 \cdot MC + 7.1)} + 1} \quad (4 \text{ v})$$

The experimental data on which equation (4 v) was based, shows that microbial activity gradually falls at moisture contents above 75 % [Haug 1993], which was also observed by Richard *et al* [2002].

Haug [1993] proposed a similar S-shaped logistic curve to describe the effect of the free airspace (FAS) on k and is given as:

$$f_{FAS} = \frac{1}{e^{(-23.7 \cdot FAS + 3.5)} + 1} \quad (4 \text{ vi})$$

The kinetics of oxygen transfer during composting are complex and depend on diffusion transport and particle size [Haug 1993, Hamelers 2001]. The oxygen concentration (OC) effect on microbial activity is minimal at concentrations above 5 % [Keener *et al* 2002], as was verified by experimental data [Schulze 1962]. The function, f_{OC} , was developed from experimental data of Schulze [1962] and was generalised and simplified to a Monod-type expression [Haug 1993].

$$f_{OC} = \frac{O_2 \%}{O_2 \% + 2} \quad (4 \text{ vii})$$

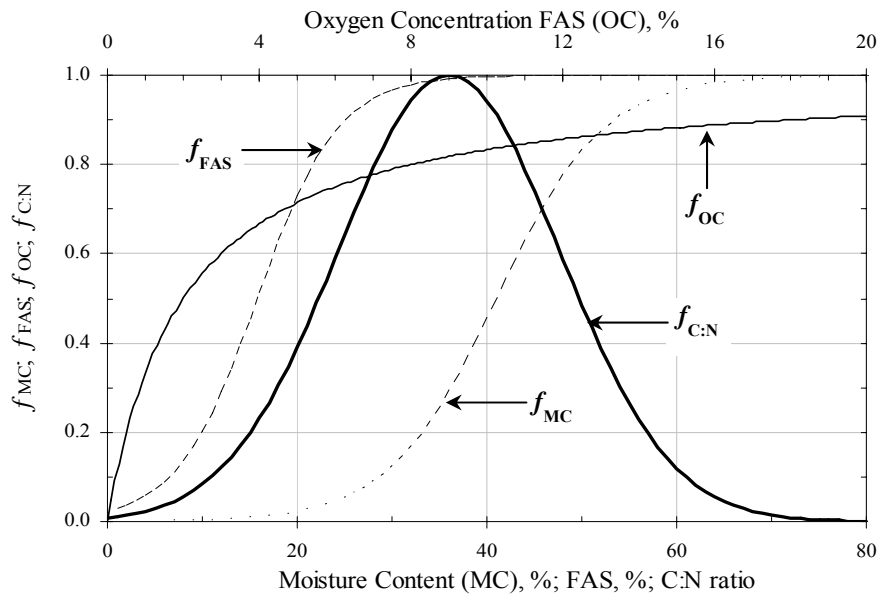


Figure 4.1. Relationships between the effect functions and corresponding factors.

The function that describes the effect of the C:N ratio on the reaction rate coefficient, $f_{C:N}$, was empirically evaluated [Ekinici *et al* 2002] and is given as:

$$f_{C:N} = e^{-0.5 \cdot \left(\frac{C:N + 35.9}{11.7} \right)^2} \quad (4 \text{ viii})$$

The equations (4 v) to (4 viii) are graphically illustrated in Figure 4.1.

4.1.1.5. Respirometric techniques

There is no one standard method of measuring respirometric activity of solid and semi-solid organic material, such as the straw and manure [Stentiford 1993]. Basic laboratory respirometry has generally centred on BOD and COD analyses, but these tests are designed primarily for small, liquid samples and are more suited to slurries than farmyard manure (FYM). Published respirometric techniques tend to be based on the BOD test but they do vary, depending on the nature of the sample and whether an atmosphere of oxygen or air is used. The equipment can be categorised as a constant volume, electrolytic or constant pressure respirometer.

The Warburg respirometer is a commonly used constant volume respirometer, which measures the uptake of oxygen as an incremental increase in pressure in the closed reactor vessel, but it too is restricted to small homogeneous samples by the amount of oxygen that can dissolve in the solution. The electrolytic respirometer operates at constant volume and a change in pressure activates an electric cell, which electrolyses the water to produce oxygen and maintain a constant pressure in the reactor vessel. The amount of oxygen is determined from the magnitude and duration of the current applied [Haug and Ellsworth 1991]. The method is suitable for solid organic material but is relatively expensive. Constant pressure respirometers work on the basis that at constant temperature and pressure, the uptake of oxygen is represented by a decrease in the gas volume in the system. The amount of oxygen consumed can be measured as a direct change in the volume of the system or as a change in the concentration of oxygen with a gas analyser.

4.1.1.6. Published results

Research on oxygen uptake and reaction rates of composting varies depending on organic material tested, the respirometer used and the experimental conditions and duration.

4.1.1.6.1. Oxygen uptake rates

Schulze [1960] measured the residual oxygen in the off-gas from composting ground garbage, 50 to 60 % moisture, in a 21 litre, rotating drum with an air atmosphere. The oxygen uptake rate (OUR) varied directly with the temperature (T), which ranged from 30 °C to about 63 °C, with values between 1 and 5 mg O₂ h⁻¹ g⁻¹ VS. His data fitted the relationship

$$\text{OUR} = 0.11 \times 1.066^T \quad (4 \text{ ix})$$

Hissett *et al* [1975] used a manometric respirometer to measure the aerobic degradability of pig and hen excreta. The OUR during batch aeration of liquid samples at 20 °C increased and decreased sharply with a peak at about 17 mg O₂ h⁻¹ g⁻¹ TS after 12 hours. The decrease was then gradual from about 8 mg O₂ h⁻¹ g⁻¹ TS at day 1 to 1 mg O₂ h⁻¹ g⁻¹ TS six days later.

Haug and Ellsworth [1991] used a constant pressure respirometer to measure the OUR in an oxygen atmosphere in order to determine the degradability of a sewage sludge and sawdust mix. The rate was highest during the first ten days, about 1.3 mg O₂ h⁻¹ g⁻¹ VS, and then decreased gradually until no further uptake was measured after 50 days. The total oxygen demand, as given by the COD of the organic material, was used to estimate the 46 % degradability of the volatile solids on a mass basis.

The OUR of bagasse and bagasse mixed with chicken manure at temperatures from 25 °C to 55 °C were investigated using an electronic respirometer [Mohee 1998]. In bagasse, the OUR rose with temperature to a maximum of about 2 mg O₂ h⁻¹ g⁻¹ VS at 40 °C and decreased sharply at higher temperatures. The effect of nitrogen on the OUR at 45 °C was investigated for mixes of bagasse and chicken manure with C:N ratios between 15 and 35. The highest OUR was measured in the mix with a C:N ratio of 25. The effect of temperature on the OUR for a mix of this C:N ratio followed a similar pattern as for the bagasse but the activity peaked at higher temperatures with maximum values about three times those bagasse.

Stocks [2000] used a constant pressure respirometer, similar to the one designed by Haug and Ellsworth [1991], to evaluate the activity in brewery waste and sludge mixed with straw and paper. Although an oxygen atmosphere was used, the OUR was markedly lower than that measured for other similarly bulky organic materials. The peak value was about 1.1 mg O₂ h⁻¹ g⁻¹ VS at 55 °C compared with the 6.3 mg O₂ h⁻¹ g⁻¹ VS measure for a chicken manure and bagasse mix at the same temperature [Mohee 1998]. It was suggested that the oxygen atmosphere might have in fact inhibited microbial growth, as oxygen is potentially toxic to growing organisms [Stocks 2000]. It should be noted that the organic material used in this case was porous and had a large surface area over which the oxygen could diffuse whereas Haug and Ellsworth [1991] used a liquid sample that had a small gas-liquid interface to which diffusion of oxygen was confined. As a rule of thumb, it may be that air should be used with bulky, porous organic materials and an oxygen atmosphere for sludge-like and liquid samples.

4.1.1.6.2. Reaction rate coefficient

Keener *et al* [1992] rewrote the equation (4 vii) to express the reaction rate coefficient, k , as a function of temperature, T , in the 'Q₁₀ effect' form, in which microbial activity doubles for a 10 °C rise, such that

$$k_T = k_{60} \times 1.9^{\frac{T-60}{10}} \quad (4 \text{ x})$$

k_{60} represents the maximum reaction rate coefficient, which was taken as 60 °C. Equations (4 ix) and (4 x) do not account for the decrease in microbial activity that occurs at high temperatures and are only valid for temperatures below the optimal for microbial activity.

Mohee [1998] used the relationship between the OUR and COD to calculate the reaction rate coefficient, k_d . The COD was a constant and k_d was, in effect, a factor of the OUR and was similarly related to temperature. Two exponential functions were derived from

multiple regression analysis, which applied to two specific temperature ranges; one that described an increase in activity and another, a decrease in activity with temperature. The optimal activity was 0.11 day^{-1} at 40°C in bagasse and 0.13 day^{-1} at 55°C in a broiler litter and bagasse mix.

4.2. Constant pressure respirometer

4.2.1. Introduction

The pig manure was semi-solid and sludge-like in nature, with no air spaces and unable to hold its shape when not contained. A constant pressure respirometer was used to measure the oxygen consumed by manure samples incubated at selected temperatures. The CPR (Figure 3.1) was essentially a version of the one designed by Haug and Ellsworth [1991] to evaluate the degradability of sewage sludge under optimum rate conditions. Advantages of the CPR were that it consisted essentially of basic laboratory equipment, it was simple to use and relatively large and heterogeneous samples could be accommodated in the 2-litre reactor flask. The largest reactor bottle that can be used with the Warburg respirometer is 500 ml. Haug and Ellsworth [1991] tested a suspension of the sewage sludge sample in an aqueous nutrient solution so that nutrient supply did not limit the rate. Solutions of a sample were found to have a respiration rate six times that of a solid sample [Lasaridi and Stentiford 1996]. In solution, the oxygen and degradable organic material were readily available to the microbes whereas activity in the solid organic material was limited by the solubilisation of oxygen and nutrients and subsequent diffusion to the zones of respiring micro-organisms. The solution provided an ideal environment for aerobic respiration but it did not necessarily represent the situation in actual composting systems and so a sample of just the semi-solid pig manure was used.

With a moisture content of about 75 % and little structure, the pig manure has few if any airspaces and the surface area between the manure and air is therefore small. The transfer rate of oxygen to aerobic micro-organisms is likely to be rate limiting, as Haug and Ellsworth [1991] found in his initial experiments. The oxygen concentration in the solutions was $>15 \text{ mg l}^{-1}$, which was deemed to be sufficient to maintain aerobic activity. The pig manure was therefore incubated in an oxygen atmosphere so that the large concentration gradient enhanced the diffusion of oxygen in, and the carbon dioxide out, of the manure.

4.2.1.1. Oxygen diffusion

Diffusion of a gas into a liquid medium takes place at the phase interface. Fick's Law of molecular diffusion expresses the mass diffusion rate in the gas (g) or liquid (l) phases as:

$$\frac{dm}{dt} = -A \left[D \frac{dS}{dx} \right]_l = -A \left[D \frac{dS}{dx} \right]_g \quad (4 \text{ xi})$$

A is the surface area at the interface, cm^2

$\frac{dS}{dx}$ is the phase concentration gradient perpendicular to the interface, $\text{g cm}^{-3} \text{ cm}^{-1}$

D is the diffusion coefficient, which is temperature dependent, $\text{cm}^2 \text{ s}^{-1}$.

In general, molecules diffuse about a thousand times faster in the gas phase than in the liquid phase [Haug 1993]. For molecules that are not highly soluble, transfer across the interface from the gas into the liquid phase limits the rate of diffusion and so the liquid phase term in equation (4 xi) needs to be considered. The manure was a continuous medium of liquid and solid phases with no air spaces and the assumption that oxygen diffuses through a 'water-organic material-micro-organism' system was reasonable [Haug 1993]. In the respirometer, oxygen transfer was modelled on the simplified situation illustrated in Figure 4.2. Diffusion of the oxygen to the sites of microbial activity was broken down into two stages.

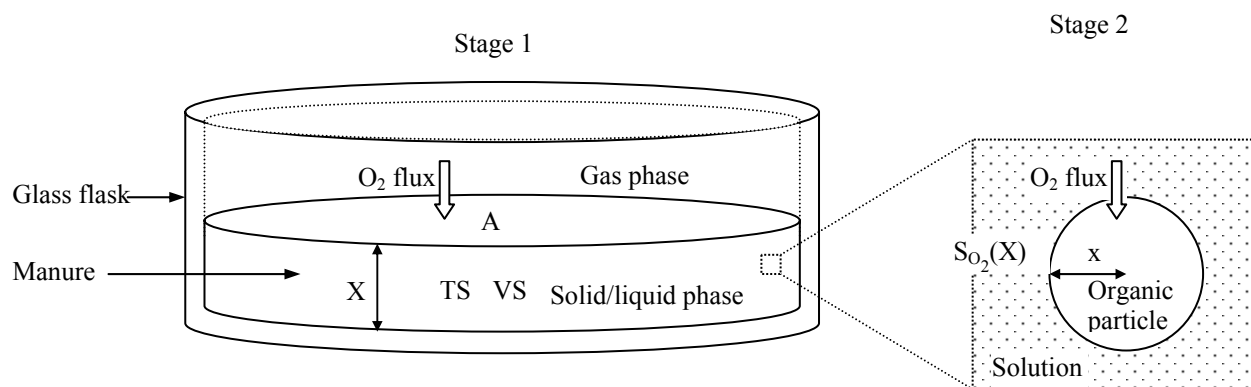


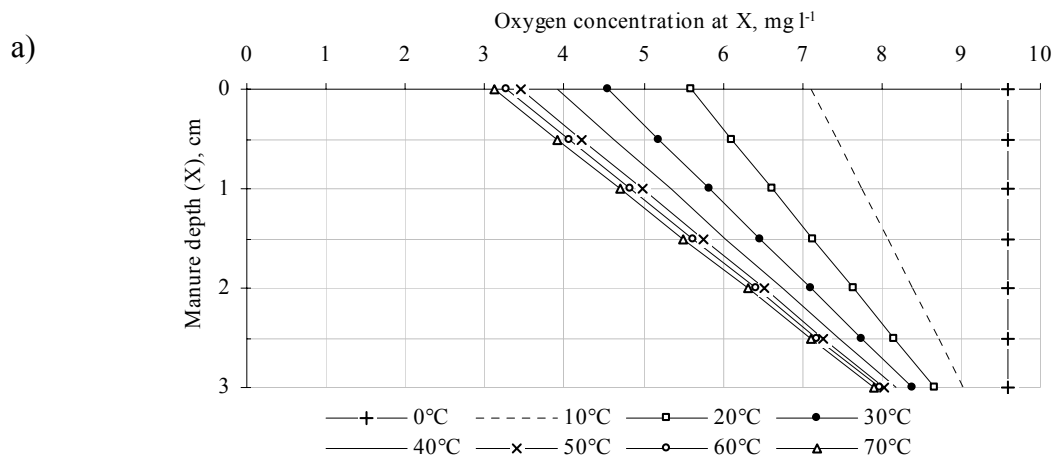
Figure 4.2. Diffusion of oxygen into the manure in the CPR.

The diffusion from the liquid side of the interface to the deeper layers of the manure was considered first. Then, the subsequent diffusion from the solution into the solid organic particles that are assumed to be the sites of microbial activity was calculated at depths through the manure. The diffusion into the particles was induced by the gradient that was established by the uptake of the oxygen by the actively respiring aerobic micro-organisms [Hamelers 2001]. The particles were assumed to be spherical with a 500 μm diameter - the approximate size of particles measured by the particle distribution analysis of manure. The concentration of oxygen in the gas phase side at the interface was assumed to be constant so that the concentration in the liquid phase at the interface, as determined from the solubility of oxygen in water, was constant at the incubation temperature. To simplify the model, the oxygen concentration was assumed to decrease linearly from the saturated surface at the interface to a minimum at the depth X (Figure 4.2). A more complex approach is unlikely to offer much improvement since numerous factors are empirically determined and imprecise [Haug 1993] and in a viscous wet material, oxygen diffusion takes more than 20 hours to diffuse just 1 cm [Nielsen and Berthelsen 2002]. The oxygen diffusion coefficients in water, D_{O_2} , are given in Table A4.1. The values calculated with the Wilke-Chang equation were used rather than those calculated with the Stokes-Einstein equation, which was only valid for the diffusion of molecules at least five times the size of the solvent molecules. The oxygen

and water molecules were comparable in size and the Stokes-Einstein equation gave low values for oxygen diffusion coefficients. The Wilke-Chang equation relates to the diffusion of oxygen in very dilute solutions with temperature. In manure the solid particles hindered diffusion and the distance travelled by the molecules was increased, and the effective diffusion coefficient, $D_{O_2\text{eff}}$, was calculated as a function of the initial volumetric total solids content, V_{TS} , using equation (4 xii). This was a simplification of the effect but is widely used in modelling sediments and soils [Hamelers 2001].

$$D_{O_2\text{eff}} = D_{O_2} \times (1 - V_{TS})^2 \quad (4 \text{ xii})$$

The diffusion of oxygen in manure, incubated at temperatures between 0 °C and 70 °C, was compared for air and oxygen atmospheres. The initial oxygen concentration in the manure was determined from the solubility of air in water at 0 °C, using the mass basis of 23.14 % oxygen in air. The oxygen concentration profiles are shown in Figures 4.3a) and b) for an air and oxygen atmosphere, respectively. The solubility of oxygen in water decreases with an increase in temperature. In the air atmosphere, oxygen diffused out of the manure at incubation temperatures higher than 0 °C, which led to a negative oxygen concentration gradient in the manure. In the oxygen atmosphere, the concentration of oxygen at the interface was high such that the concentration gradient was large and positive and the oxygen diffused into the manure.



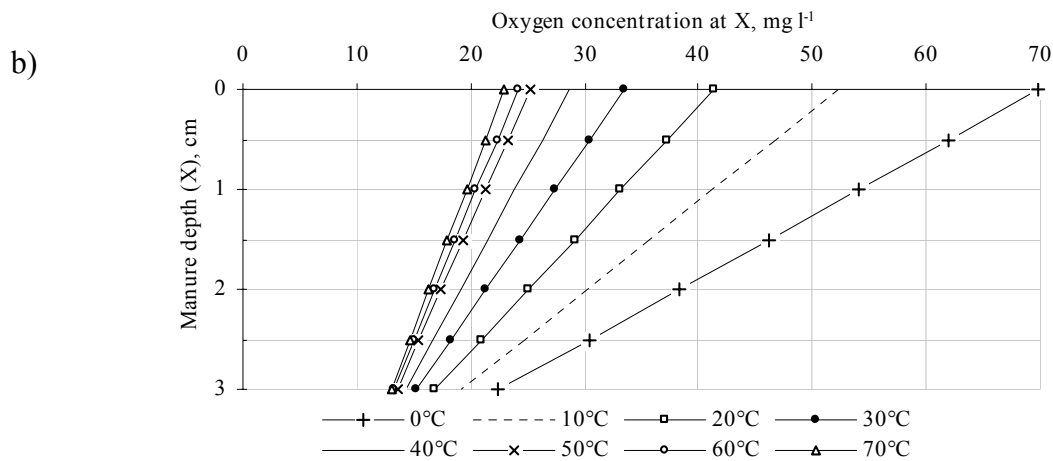


Figure 4.3. Stage 1: Oxygen concentration profiles in a) an air and b) oxygen atmosphere

The diffusion coefficients increased exponentially with temperature. As a consequence, the oxygen flux into the organic particles increased with temperatures and the rise became more pronounced at the higher incubation temperatures (Figure 4.4).

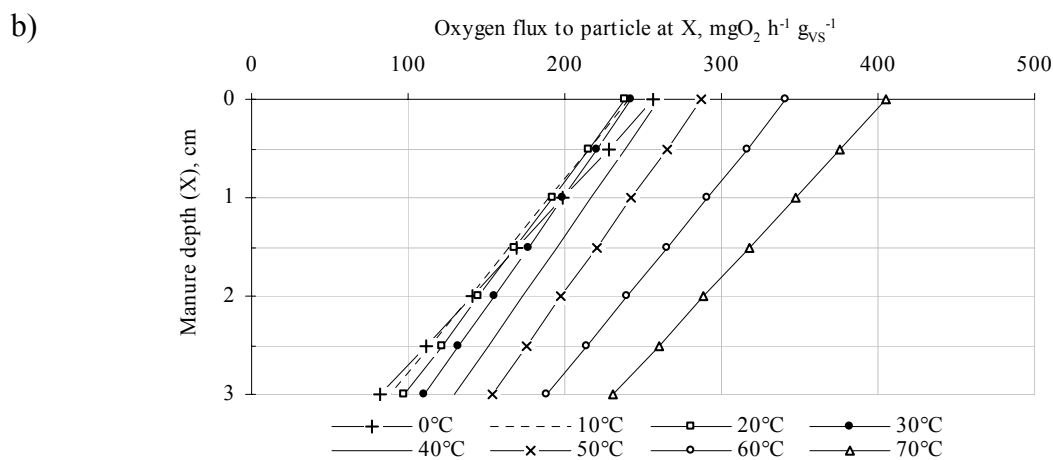
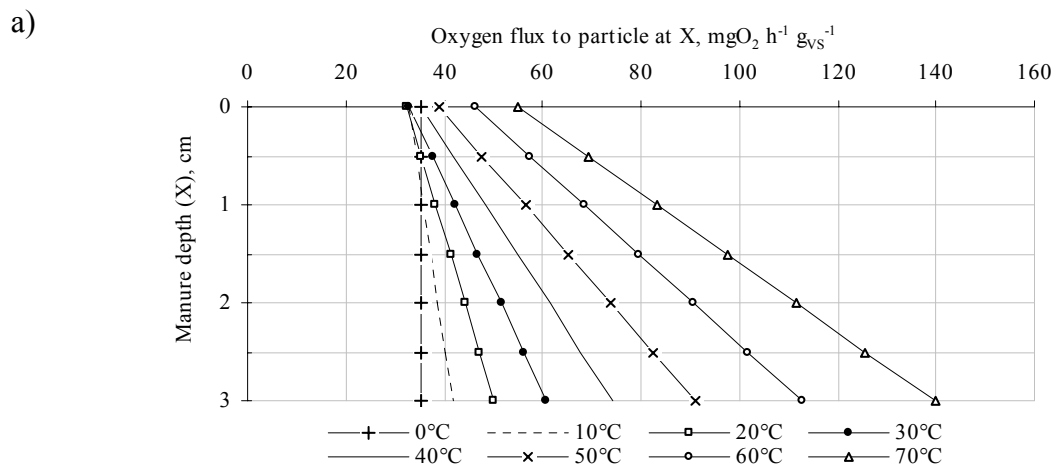


Figure 4.4. Stage 2: Diffusion of oxygen from a) an air and b) oxygen atmosphere

The concentration of the oxygen in the manure incubated in an oxygen atmosphere was an order higher than that incubated in an air. Temperature had a greater effect on the oxygen flux into the organic particles than the oxygen concentration gradient. With an oxygen atmosphere, the flux values in the manure were at least double those with an air atmosphere.

The OUR have tended to be between 1 and 10 mg O₂ h⁻¹ g⁻¹ VS but values up to about 20 mg O₂ h⁻¹ g⁻¹ VS were measured for liquid solutions of chicken and pig excreta [Hissett *et al* 1975]. Theoretically, an air atmosphere provides sufficient oxygen to meet the demand but an oxygen atmosphere avoids the possibility of the mass transfer of oxygen to the sites of microbial activity limiting the process kinetics.

4.2.2. Method

4.2.2.1. Sample preparation and analysis

The pig manure was mixed thoroughly and analysed for TS, VS, Kj-N and Amm-N content and COD in triplicate (Table 4.1). 500 g batches were frozen for at least three days and individually thawed at 2 °C two days before use.

4.2.2.2. Incubation

The selected incubation temperatures were 10 °C and between 20 °C and 70 °C in 5 °C intervals. A freshly thawed sample of organic material was incubated at one of the stated temperatures. The series of experiments was carried out in a randomised temperature order. To start, the system was flushed with pure oxygen and left to equilibrate at the water bath temperature. Sufficient time was allowed for the micro-organisms to develop their full potential at the incubation temperature [Stentiford 1993]. When gas had stopped expanding, the taps were closed and the timing started. The frequency of readings depended on the rate

of microbial activity. Readings were generally taken either every 12 hours or when the water level in the glass tube had risen to more than three-quarters of the height. At each reading, the ambient temperature, time and volume of oxygen fed into the system to return the water level in the glass tube to its initial position, were recorded. When the sodium hydroxide was renewed, the system was flushed with oxygen and left to equilibrate, as was done at the start. About 1.7 g of anhydrous sodium hydroxide (NaOH) was required per litre of oxygen consumed assuming that at 20 °C, 1 mole of O₂ occupied 24 litres and that for 1 mole of O₂ consumed 1 mole of CO₂ was produced, which was absorbed by 1 mole of NaOH. The water level in the bath was maintained at the initial level, which was especially important at the higher temperatures. The lag phase depended on the temperature to which the microbial population had to adapt and ranged from no time below 25 °C to about a week above 50 °C. The oxygen uptake was measured until the rate slowed when other factors, such as the organic material and moisture content, became rate limiting. The TS and VS of the manure was analysed after the experiment to account for the loss of water and organic material.

4.2.2.3. Oxygen uptake rate

The oxygen uptake was converted to an hourly rate (HOUR in g O₂ h⁻¹ kg⁻¹ VS) using equation (4 xiii)

$$\text{HOUR} = \frac{V_{\text{O}_2}}{\Delta t} \cdot \frac{M_r \cdot p_{\text{atm}}}{R \cdot T_{\text{amb}}} \cdot \frac{1}{m_{\text{VS}}} \quad (4 \text{ xiii})$$

V_{O₂} is the volume of oxygen required to return the water level to its initial position, ml

Δt is the time interval, h

p_{atm} is the atmospheric pressure, bars

T_{amb} is the ambient temperature, K

m_{VS} is the mass of volatile solids, kgVS

R is the gas constant, 0.08314 bar ml g-mol⁻¹ K⁻¹

M_r is the relative molecular mass of oxygen, 32 g g-mol⁻¹

4.2.3. Results

There was little variation between the basic characteristics of the samples of the pig manure and mean values were used to the calculations of the oxygen uptake rates and the reaction rate coefficients. Analysis of the manure before it was frozen in batches is given in Table 4.1.

Table 4.1. Analysis of bulk pig manure

Manure sample	TS %	VS %TS	TOC %TS	COD g O ₂ g ⁻¹ VS
1	26.8	81.6	45.3	1.49
2	24.9	81.4	45.2	1.53
3	25.3	81.8	45.4	1.50
Mean	25.7	81.6	45.3	1.51

4.2.3.1. Specific oxygen uptake rate

The cumulative oxygen uptake (COU), in g O₂ kg⁻¹VS, was plotted against time (Figure 4.5).

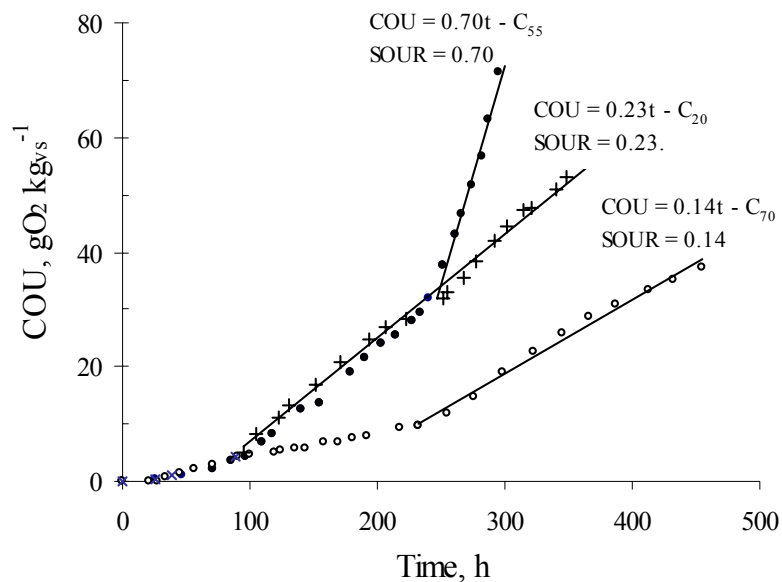


Figure 4.5. Cumulative oxygen uptake profiles for manure incubated at 20 °C (×), 55 °C (•) and 70 °C (○).

Figure 4.5 illustrates the method used to determine the SOUR from plots of COU against time for three incubation temperatures. The SOUR was equal to the gradient of the line fitted to the part of the plot, which corresponded to the period of highest microbial activity. The lines were fitted to the designated data (selected by eye) using the least square method with a 95 % confidence level. The regression line was fitted with *Microsoft Excel 97*. The mean of the determined SOUR values and the corresponding standard deviations are given in Table 4.2.

Table 4.2. Specific oxygen uptake rates of manure at selected incubation temperatures

Temperature °C	10	20	25	30	35	40	45	50	55	60	65	70
SOUR mg O ₂ h ⁻¹ kg ⁻¹ VS	195	181	699	633	702	521	547	844	860	246	226	152
σ (n)*	- (1)	- (1)	25 (2)	37 (4)	33 (4)	29 (3)	89 (4)	42 (5)	95 (3)	23 (3)	- (1)	- (1)

* n is the number of values considered for the incubation temperature

4.2.3.2. Reaction rate coefficient

The reaction rate coefficient, k_d , was calculated from the relationship between SOUR and COD, as given by equation (4 iv), and was expressed as per day. Figure 4.6 is a plot of k_d against temperature with the error bars indicating the maximum and minimum coefficient values. There are no error bars on the pairs of extreme temperatures and 58 °C as only a single measurement of the oxygen uptake rates was taken in each case.

To assess the biodegradability of the pig manure a sample was incubated at ambient temperature over a long period of time until no further oxygen uptake was measured. This took about 130 days and the loss in volatile solids was used to estimate the biodegradable fraction of the pig manure. 68 % of the initial mass of volatile solids remained, such that approximately a third of the volatile solids in the manure was degraded by the micro-organisms active at 20 °C.

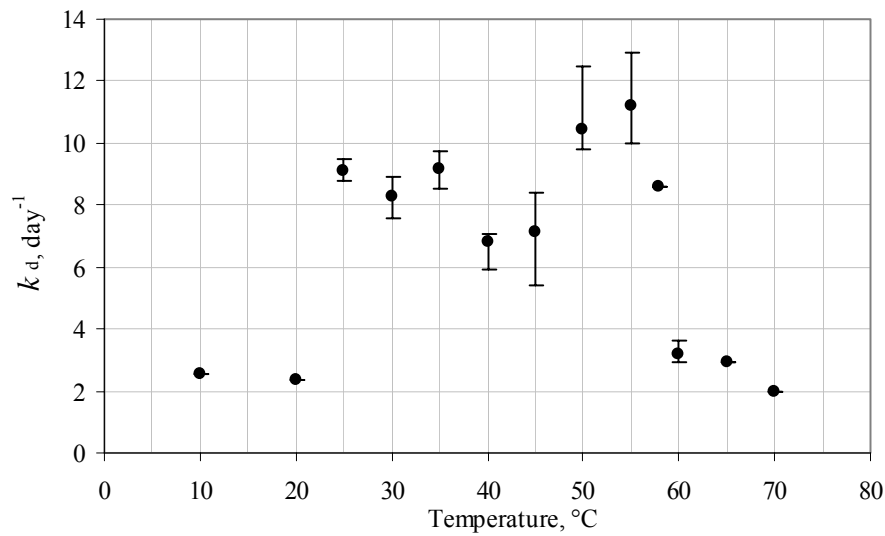


Figure 4.6. Temperature effect on the reaction rate coefficient of pig manure

4.2.4. Discussion

In pig manure the maximum rate of microbial activity occurred between 50 °C and 55 °C. Little activity took place at temperatures below 20 °C and above 60 °C. The activity decreased sharply at temperatures above the optimal whilst the increase in activity from 25 °C was more gradual. The pattern supports the theory regarding the activation and inactivation energies of micro-organisms. The relatively wide range of activity measured between 45 °C and 55 °C (Figure 4.6) may indicate that oxygen diffusion did not always meet the oxygen demand at these temperatures, which tended to correspond to conditions with high activity. Although this investigation gave a valuable initial assessment of the dependence of microbial activity in the pig manure on temperature, the data was not used to derive a functional relationship, as the conditions did not represent those that typically occur during composting. Further respirometric experiments were required to quantify the dependence of the activity on temperature with the organic material and under conditions to be investigated in the proposed compost unit.

4.3. Gas analyser respirometer

4.3.1. Introduction

In the design of the composting experiments, three mixing ratios were to be investigated. To gain foresight into the oxygen demand that could be expected at the start of the composting process, a series of controlled small scale respirometry experiments were carried out on mixes of pig manure and straw of the same mixing ratios using a gas analyser respirometer (Figure 3.2). As with the CPR, a sample of organic material was incubated at a selected constant temperature. The effect of the factor on microbial activity and the temperature, at which microbial respirometric activity was maximal, was evaluated. The manure and straw mixes were solid and bulky, with large air spaces. From the analysis of bulk density and FAS for various mixes of pig manure and straw, a mixing ratio of 4 with 80 % moisture content still theoretically provided sufficient air space to support aerobic activity. The organic material was incubated in an air atmosphere so that the concentration gradient was not artificially high, as was the case in the CPR. A gas analyser measured the oxygen and carbon dioxide concentration as volumetric percentages of the total gas. The respiration quotient was calculated and gave more insight into the nature of the reactions that dominate activity at a specific incubation temperature. The mixing ratio, and therefore C:N ratio, effect was noted and compared with the functional effect proposed by other authors.

4.3.2. Methods

4.3.2.1. Sample preparation and analysis

The pig manure and dry chopped straw were mixed in the wet mass ratios of 2 and 4 and respective moisture contents were 55 % and 63 %. To correct for the difference and to avoid moisture becoming a limiting factor for the microbial activity during the experiment,

distilled water was added to give an initial moisture content of 80 %, which is the upper limit in the optimal moisture content range for mixes of FYM and straw [Jeris and Regan 1973b]. Fifteen 2-litre storage bags were filled with the organic material for each mixing ratio and the batches were frozen for at least 3 days. Two days before an experiment, a batch was thawed at 2 °C. About two thirds of the organic material was used in the reactor vessels and the remainder was analysed for the COD, TS, VS Amm-N and Kj-N contents, pH and FAS.

4.3.2.2. Incubation

The selected incubation temperatures were 10 °C and between 20 °C and 70 °C in 5 °C intervals. A freshly thawed sample of organic material was incubated at one of the stated temperatures. The series of experiments were carried out in a randomised temperature order. The reactors were incubated in the thermostatically controlled water bath for about 4 days.

At the start of each experiment, whilst equilibrating, the apparatus was filled with nitrogen gas and run as a closed system to test for any gas leaks. If free of leaks, the apparatus was flushed and filled with air, which provided the oxygen. The gas in one of the reactors was analysed hourly. The oxygen and carbon dioxide concentrations were continuously measured for 45 minutes and the readings were logged every 5 minutes during this period. To ensure aerobic conditions, the reactor was flushed with fresh air for 15 minutes after the analysis of the gas. An hour therefore lapsed between consecutive analyses of gas from each reactor. The gas was pumped through the system at approximately two litres a minute. The water was kept at the same depth in the bath throughout the incubation period.

4.3.2.3. Oxygen uptake rate

The concentration of oxygen and carbon dioxide in the FAS was assumed to be the same as the content of the gas leaving the system. The oxygen and carbon dioxide concentrations were displayed as percentages of the total gas volume by the gas analyser. The

total gas volume was taken as that which occupied all the respirometer tubing and corresponding reactor vessel. The gas analyser was supplied with calibration gases (air, nitrogen and 8 % CO₂ in nitrogen) every 6 hours. The logged readings of the respirometer gases were converted for any drift by assuming it was linear between calibrations and adjustments were made accordingly. The gas leaving the reactors passed through a desiccation column and a gas filter, which removed water and any particles above 0.6µm in diameter. All gas entering the reaction chambers of the gas analyser was dry and close to room temperature. The volume of oxygen respired, ΔV_{O₂} ml, was converted to an hourly oxygen uptake rate (HOUR) in mg O₂ h⁻¹g⁻¹ TS with equation (4 xiv). The gas was assumed to behave ideally and the effect of the difference in temperature of the gas in the reactor, T_{Reactor}, and in the tubes, T_{Tube}, was accounted for.

$$\text{HOUR} = \frac{\Delta V_{O_2}}{\Delta t} \cdot \frac{M_r}{22.4} \cdot \frac{273}{V_{\text{Total}}} \left[\frac{V_{\text{Reactor}}}{T_{\text{Bath}}} + \frac{V_{\text{Tube}}}{T_{\text{Amb}}} \right] \cdot \frac{1}{m_{\text{TS}}} \quad (4 \text{ xiv})$$

Δt is the time interval between consecutive gas measurements (h)

M_r is the relative molecular mass of oxygen (32 g)

22.4 is the volume of gas occupied by 1 mg-mol of an ideal gas at 273 K (ml)

T_{Bath} is the incubation temperature (K) and T_{Amb} is the ambient temperature (K)

V_{Reactor} is the volume of the reactor occupied by gas (ml)

V_{Tube} is the volume of the tubing and the gas analyser occupied by gas (ml)

V_{Total} is the total volume of the respirometer occupied by gas (V_{Reactor} + V_{Tube}) (ml)

m_{TS} is the mass of total solids, TS, in the composting material (g).

Likewise, the hourly carbon dioxide emission rate (HCER), in mg CO₂ h⁻¹g⁻¹ TS, was calculated from the volume of carbon dioxide emitted ΔV_{CO₂} ml using equation (4 xiv) with the appropriate substitution for ΔV_{O₂} and M_r, which is 44 g for carbon dioxide.

The OUR varies during stages of composting as the temperature and organic composition change [Hamelers 2002]. The dependence of the rate on composition has received little attention [Hamelers 2002]. The readily available organic fraction is used first during the ‘fast’ stage. This is followed by the ‘slow’ stage, during which the decomposition of larger, more complex organic compounds, as well as the possible on set of rate-limiting environmental conditions, occurs [Keener *et al* 1993]. In larger scale composting operations, the distinction between the two stages of decomposition may not be obvious [Haug 1993].

4.3.2.4. Respiration quotient

The respiration quotient (Q_{resp}) is used in the study of biochemical systems. It is the molar ratio of the carbon dioxide produced to oxygen consumed and is expected to be close to 1 for aerobic respiration based on carbohydrates. %CO₂ and %O₂ are the respective measured percentage volume concentrations of the carbon dioxide and oxygen measured and subscript ‘in’ and ‘out’ correspond to the initial and final gas concentrations, respectively, of an incubation time interval in a microbial system.

$$Q_{\text{resp}} = \frac{\text{Volume of CO}_2 \text{ emitted}}{\text{Volume of O}_2 \text{ consumed}} = \frac{(\% \text{CO}_{2\text{out}} - \% \text{CO}_{2\text{in}})}{(\% \text{O}_{2\text{in}} - \% \text{O}_{2\text{out}})} \quad (4 \text{ xv})$$

The Q_{resp} of organic compounds do vary and can range from 0.5 to 3.3 [Van Ginkel 1996]. In anaerobic conditions, carbon dioxide is produced without the consumption of oxygen and so the Q_{resp} is greater than 1. As temperature increases, the carbon dioxide-producing anaerobic activity decreases. Q_{resp} can, therefore, reveal the type of organic material decomposing and the relative importance of aerobic and anaerobic reactions [Van Ginkel 1996].

4.3.3. Results and discussion

The mean values with standard deviations (σ) from the analysis of the samples of the pig manure and straw mix for the 14 experiments are given in Table 4.3. The measured COD, expressed in $\text{mg O}_2 \text{ g}^{-1} \text{ TS}$, did vary between some samples of the heterogeneous material. The average COD was used in equation (4 iv) to calculate k_T of the corresponding SOUR.

Table 4.3. Physical and chemical characteristics of the pig manure and straw mix samples.

M:S ratio		TS %	TS g	VS %TS	TOC %TS	Amm-N %TS	Org-N %TS	C:N	COD $\text{mgO}_2 \text{ g}^{-1} \text{ TS}$	pH	FAS
2:1	Mean	20.4	50.7	86.8	48.4	0.33	2.06	23.8	438	8.01	0.73
	σ	1.4	3.4	1.8	0.5	0.06	0.27	2.8	82	0.17	0.01
4:1	Mean	22.7	90.8	86.1	47.7	1.00	1.59	18.0	469	8.16	
	σ	0.8	1.4	1.4	0.9	0.22	0.43	1.3	82	0.34	

4.3.3.1. Specific oxygen uptake rate

The masses of the oxygen gas consumed and carbon dioxide emitted between consecutively logged gas readings were summed to give the respective cumulative oxygen uptake (COU), in $\text{mg O}_2 \text{ g}^{-1} \text{ TS}$, and cumulative carbon dioxide emitted (CCE), in $\text{mg CO}_2 \text{ g}^{-1} \text{ TS}$, over the total incubation period. The COU and CCE were plotted against time and the gradients of the plots were equal to the SOUR and specific carbon dioxide emission rate (SCER), respectively.

Haug [1993] considered a ‘fast’ and ‘slow’ fraction of the organic material, which during decomposition corresponded to a fast and slow oxygen uptake rate. These periods were termed the ‘fast’ and ‘slow’ stages respectively (Figure 4.7). Figure 4.7 shows the cumulative mass profile for oxygen and carbon dioxide for the organic material of an M:S ratio of 2:1 at incubation temperature of 30 °C and 50 °C. The clusters of points represent the readings, which were logged every 5 minutes during the 45-minute period when the gas in the

reactor was analysed. The fast stage lasted for about the first 10 hours after the lag time and the slow stage corresponded to the time thereafter, which was evident by a marked decrease, by about half, in the gradient of the lines. The lines were fitted to the data (selected by eye) using the least squares method with a 95 % confidence level.

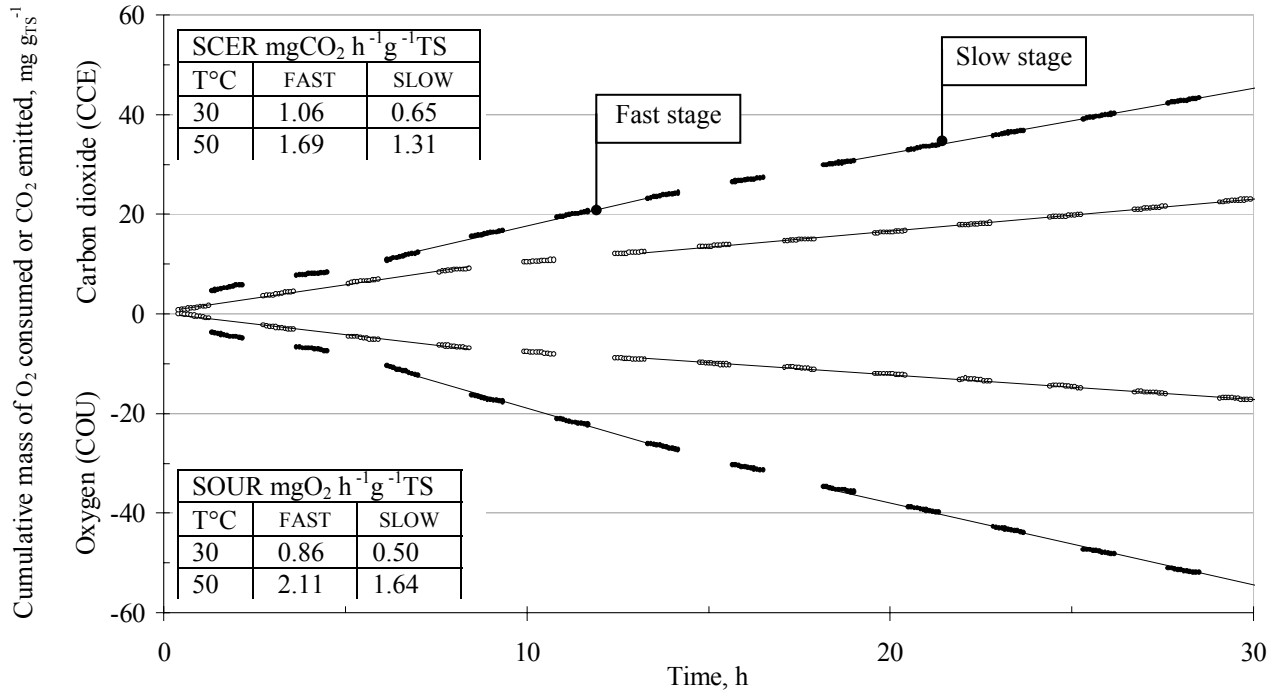


Figure 4.7. Cumulative hourly emission rate of CO₂ (HCER) and uptake rate of O₂ (HOUR) for M:S ratio of 2:1 incubated in Reactor 1 at 30 °C (o) and 50 °C (•).

Table 4.4. SOUR and SCER between 10 °C and 70 °C for fast and slow stages. (M:S ratio 2:1)

Temperature, °C	10*	20	25*	30	35	38	40	45	50	55	60*	65	70
SOUR fast stage, mg O ₂ kg ⁻¹ TS	243	500 ± 53	412	807 ± 56	1231 ± 2	1523 ± 20	1268 ± 99	1106 ± 162	2011 ± 59	3425 ± 23	4776	3371 ± 61	2562 ± 179
SOUR slow stage, mg O ₂ kg ⁻¹ TS	119	189 ± 11	195	547 ± 21	708 ± 32	722 ± 4	768 ± 21	955 ± 95	1694 ± 51	1522 ± 153	2160	1600 ± 180	1836 ± 113
SCER fast stage, mg CO ₂ kg ⁻¹ TS	143	562 ± 16	398	1027 ± 6	1055 ± 27	1007 ± 86	1200 ± 3	1448 ± 10	1635 ± 10	2905 ± 25	4007	2916 ± 25	2578 ± 105
SCER slow stage, mg CO ₂ kg ⁻¹ TS	67	225 ± 7	243	674 ± 53	538 ± 90	797 ± 22	690 ± 97	825 ± 7	1368 ± 62	1437 ± 102	1673	1606 ± 143	1776 ± 117

Table 4.5. SOUR and SCER between 10 °C and 70 °C for fast and slow stages (M:S ratio 4:1)

Temperature, °C	10	20	25	30	35	40	45	50	55	60	70*
SOUR fast stage, mg O ₂ kg ⁻¹ TS	1240 ± 17	2384 ± 90	2745 ± 83	2906 ± 1	2980 ± 50	2790 ± 62	3208 ± 3	3284 ± 5	3417 ± 25	3193 ± 26	2177
SOUR slow stage, mg O ₂ kg ⁻¹ TS	-	1158 ± 50	1270 ± 137	1214 ± 24	2008 ± 195	1904 ± 87	2868 ± 12	2297 ± 70	2396 ± 0	1595 ± 31	1506 ± 17
SCER fast stage, mg CO ₂ kg ⁻¹ TS	552 ± 25	1386 ± 40	1785 ± 14	1688 ± 16	1878 ± 36	1598 ± 45	2144 ± 50	2450 ± 14	2877 ± 46	2393 ± 50	1400
SCER slow stage, mg CO ₂ kg ⁻¹ TS	-	645 ± 9	771 ± 66	606 ± 20	1046 ± 81	1171 ± 72	1366 ± 128	1651 ± 60	1638 ± 22	1162 ± 17	1104 ± 11

The mean SOUR and SCER of the two reactors for the fast and slow stages are given in Tables 4.4 and 4.5 for the mixing ratios of 2 and 4, respectively. The ‘*’ indicates SOUR values that are based on the reading of just one of the reactors as the other leaked.

4.3.3.2. Respiration quotients

The respiration quotient, Q_{resp} , was determined using equation (4 xii). Where possible, as with the average SOUR and SCER values in Table 4.4 and 4.5, the average Q_{resp} of the two reactors was calculated and plotted against the incubation temperature (Figure 4.8).

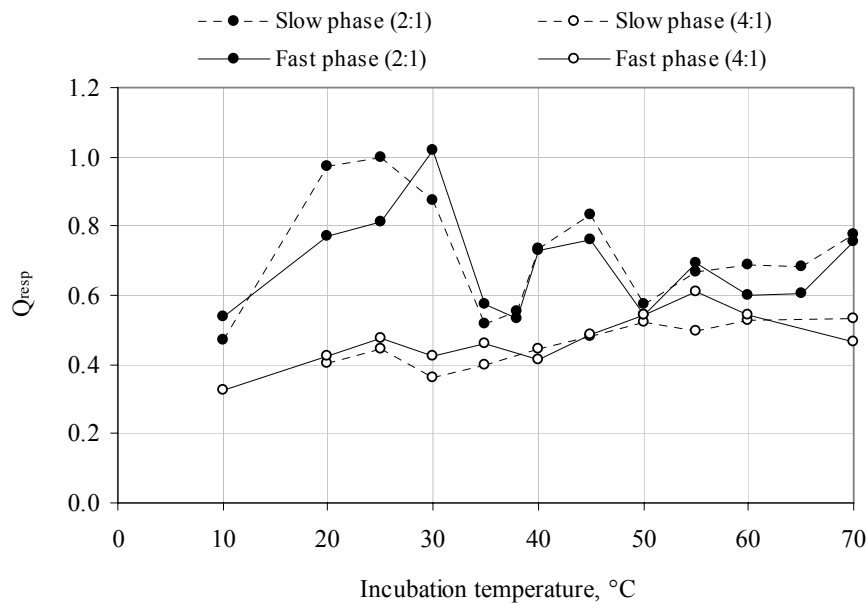


Figure 4.8. Average respiration quotients, Q_{resp} , in the fast and slow stages for M:S ratio of 2:1 (●) and 4:1 (○).

For M:S ratio of 2:1, the Q_{resp} increased from about 0.5 at 10 °C to about 1 at 30 °C and then decreased to between about 0.6 and 0.8 at the higher incubation temperatures. For M:S ratio of 4:1, the Q_{resp} of the increased from a minimum of about 0.3 at 10 °C to between 0.5 and 0.6 at temperatures above 50 °C. The fact that values were less than 1 indicated that aerobic activity prevailed during the incubation period.

Table 4.6 gives the approximate composition of pig manure, wheat straw and the pig manure and straw mixes. The values were either taken from literature or estimated from analysis of the organic material. The representative compounds and the corresponding Q_{resp} values are those used by Van Ginkel [1996] in his work with chicken manure and wheat straw. Two amino acids, glycine and glutamine, and uric acid were used to represent nitrogen-containing compounds in chicken manure [Van Ginkel 1996]. However, uric acid is not present in pig manure [Kirchmann *et al* 1998] and its respiration quotients, 0.5 or 3.3 depending on the reaction, are not considered.

Table 4.6. Composition of the organic material and the Q_{resp} of the representative compounds

Constituent	Representative Compounds	Q_{resp}	Units	Pig manure	Straw	Mixing ratios	
						2:1	4:1
Cellulose	Cellulose	1.0	% TS	12 ²	32 ³	25	22
Hemi-cellulose	Cellulose	1.0	% TS	20 ²	40 ³	33	29
Ligno-cellulose ¹	Cellulose	1.0	% TS		88 ⁴		
Lipids	Palmic acid	0.7	% TS	15 ²	2 ⁴	6	9
Ash			% TS	20 ⁵	10 ^{3,5}	14	15
Nitrogen *		0.5 - 3.3	%TS	5 ^{3,5}	<1 ^{3,5}	2	3
Water			%	75 ^d	10 ^d		

1. Ligno-cellulose covers lignin and the sugar polymer, which include cellulose, hemi-cellulose, starch and glycogen, 2. [Lannotti *et al* 1975], 3. [Lynch 1993], 4. [Van Ginkel 1996], 5. Experimental data from Sections 3.3.1 and 3.3.2, 6 Nitrogen containing compounds include proteins, such as glycine and glutamine [Van Ginkel 1996]

Ammonification and nitrification of nitrogen-containing compounds takes place at the lower temperatures of the mesophilic stage of composting (around 30 °C). The reactions have an average Q_{resp} of 1 and 0.9, respectively [Van Ginkel 1996]. This may have contributed to the rise in the average Q_{resp} values of about 1 between 20 °C and 30 °C but the overall effect would be small as nitrogen-containing compounds make up less than 5 % of the total solid in the organic material. Cellulose and hemicellulose are in abundance and their degradation is the likely reason for Q_{resp} being about 1. The low Q_{resp} obtained for organic material with M:S ratio of 4:1 suggests that cellulose degradation is less prevalent than in the organic material with M:S ratio of 2:1, and that degradation of lipids may be more significant. The Q_{resp} for the fast and slow stages were similar, which suggests that types of reactions did not vary much. The half-lives of carbonaceous compounds in soil are 3, 15 and 360 days for glucose, cellulose and lignin, respectively [Sylvia *et al* 1998]. It would be expected that, along with the readily degradable fraction of the pig manure, only the glucose and short-chain polysaccharides of straw were used during the 4 day incubation period.

During the composting of synthetic garbage, the Q_{resp} varied between 0.8 and 0.9 over the thermophilic temperature range (45 °C to 63 °C) [Schulze 1960]. The corresponding values for the composting pig manure and straw mix were lower and varied between 0.5 and 0.8. The difference may be due to the dissimilarity of the organic materials or that the excess of oxygen in the respirometer enabled reactions to take place that would have otherwise been suppressed if oxygen was not surplus.

4.3.3.3. Environmental factor effects

The reaction rate coefficients calculated from the SOUR were corrected by considering the multiplicative effect of the environmental factors; free airspace (FAS), oxygen concentration (OC) and moisture content (MC), on the microbial activity.

The effect of the C:N ratio given by equation (4 viii), was based on empirical data, for which the optimum C:N ratio was about 35. Mohee [1998], however, found that for a mix of chicken manure and bagasse, the oxygen uptake was highest for a C:N ratio of 25. The optimum C:N ratio depends on the organic material and it is clear from the C:N curve in Figure 4.1 that correcting for the C:N ratio, which was about 24 in this case, could give a deceptively low value for the factor. In the absence of a $f_{C:N}$ equation specific to mixes of pig manure and straw, C:N ratio was assumed to be close to optimum and was not corrected for.

The FAS was above 40 % in all the manure and straw mixes so that the value of f_{FAS} did not contribute an environmental effect to the reaction rate coefficient. The oxygen concentration, however, did vary with incubation time, temperature and mixing ratio. The mean f_{OC} values over the incubation period are shown in Figure 4.9.

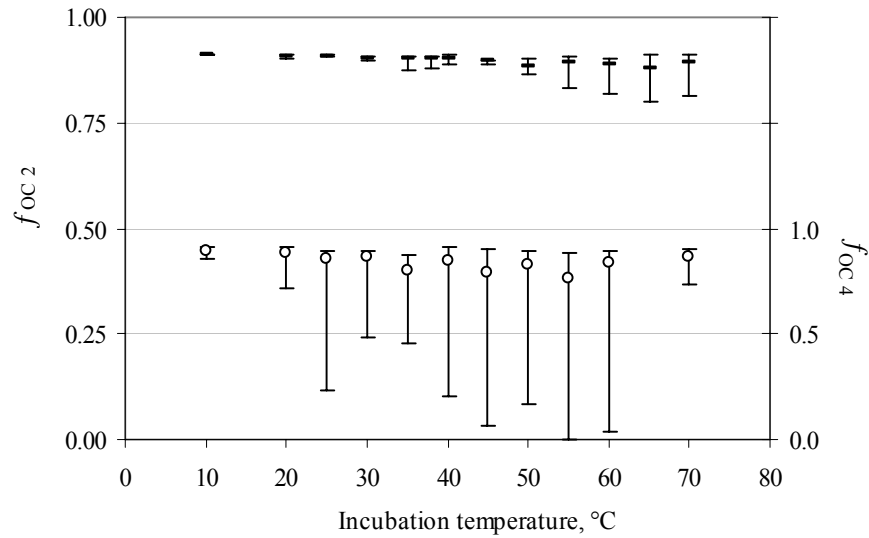


Figure 4.9. Mean f_{OC} values for the mixing ratios of 2 (-) and 4 (o).

The error bars represent the minimum and maximum values of f_{OC} . The oxygen concentration in the organic material with an M:S ratio of 2:1 did not drop below 8 % v v⁻¹ and all the mean values of the factors were about 0.9 and above. The oxygen in the organic material with a M:S ratio of 4:1 was exhausted on occasions and values lower than 2 % v v⁻¹

were recorded at incubation temperatures between 25 °C and 60 °C, inclusive. The lowest mean f_{OC} value was 0.76 at 55 °C for which the oxygen content was above 8 % v v⁻¹ ($f_{OC} = 0.8$) for only 50 % of the incubation period. The mean moisture content factor, f_{MC} , was above 0.95 for all the experiments. The respective total multiplicative factors, f_{T2} and f_{T4} for M:S ratios of 2:1 and 4:1 were, therefore, predominantly determined by the oxygen concentration and the variation with the incubation temperature (Figure 4.10) is similar to the pattern that is shown in Figure 4.9.

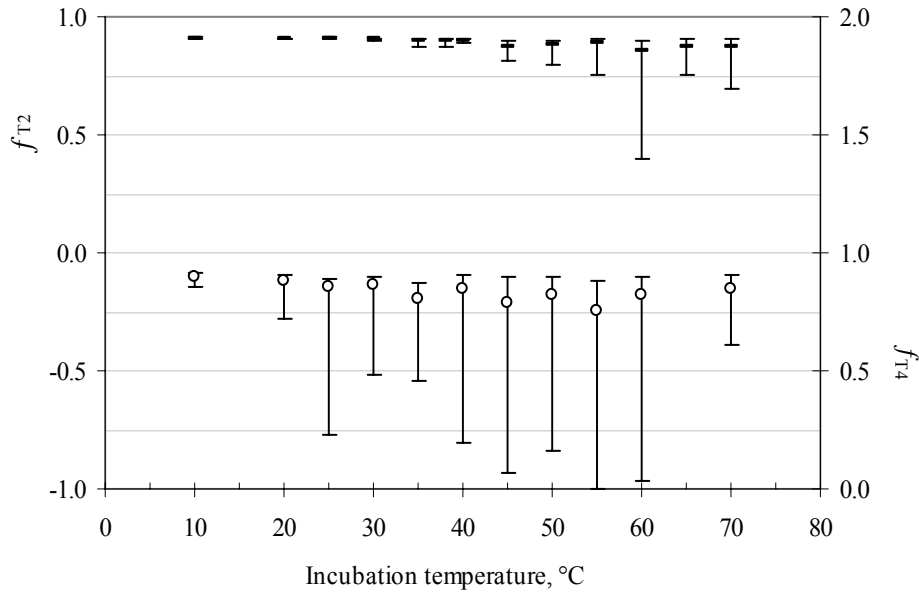


Figure 4.10. Mean total environmental factors, f_{T2} and f_{T4} , for M:S ratios 2:1 (-) and 4:1 (o).

The measured reaction rate coefficient, k_T , was corrected for the effect of the environmental factors using equation (4 iii) to give the reaction rate coefficient possible under optimum conditions, $k_{T\text{ opt}}$

$$k_{T\text{ opt}} = \frac{k_T}{f_{T-M:S}} \quad (4\text{ xvi})$$

The corrected reaction rate coefficients are graphically shown in Figures A4.1 and A4.2. The reaction rate coefficients of the slow stage were about half those of the fast stage. The error bars indicate the maximum and minimum recorded values.

4.3.3.4. Reaction rate coefficient

The growth and death rate constants vary exponentially with temperature according to the Arrhenius equation. A single modified Arrhenius-type expression, which accounts for the increase and decrease in microbial activity, was used to describe the dependence of k_T on temperature during aerobic digestion of liquid wastes (equation 4 xvii) [Andrews and Kambhu 1973, Haug 1993].

$$k_T = k_{TR1} (C_1^{T-TR1} - C_2^{T-TR2}) \quad (4 \text{ xvii})$$

k_{TR1} is the reaction rate coefficient at temperature TR1, day⁻¹

C_1, C_2 are temperature constants

TR1, TR2 are reference temperatures, °C

T is the experimental temperature

The temperature constants are specific to the organic material being tested, as they depend on the diffusion of oxygen and therefore the organic material's chemical and physical characteristics [Nielsen and Berthelsen 2002]. Initial attempts to determine the values of the equation parameters with a statistical program, *GenStat* (Version 6), failed due to the lack of data points at temperatures above 60 °C. The next approach taken was to estimate the values of the parameters from literature and by application of basic mathematical techniques for curve fitting, such as differentiation of equation (4 xvii) to determine the temperature, which corresponds to the turning point of the curve, T_{opt} (Section A4.2.1). Haug [1993] provided insight into the magnitude of the temperature constants and values of the reference temperatures. The reference temperatures TR1 and TR2 are typically taken from the mesophilic and thermophilic temperature range, respectively. TR2 was taken to be about 10 °C below T_{opt} and was designated as 50 °C. The temperature constants values were then iteratively adjusted with reference to 20 °C for TR1 and, correspondingly, k_{20} .

The best fit curve was determined by finding the highest percentage of variance accounted for. This value does not necessarily give actual criterion for the goodness of fit but is good for comparing the fit of different curves to the data points. The turning point on a plot of equation (4 xvii) equates to the temperature at which microbial activity is maximal, as shown in Figures A4.1 and A4.2 for the fast and slow stages, respectively. An increase in temperature above this optimum temperature leads to a rapid fall in the reaction rate coefficient to zero at a specific temperature determined by the temperature constant C_2 . The activity was predicted to cease around 73 °C. This upper temperature limit is realistic. At temperatures above 60 °C, the activity of enzymes, such as some cellulases, declines [Keener *et al* 1993] and temperatures between 70 °C and 75 °C are lethal to many micro-organisms [Van Ginkel 1996]. The concept that ‘the hotter the better’ during composting only applies when the temperature of the organic material is below 65 °C.

A further temperature rise gives negative k_T values. A negative reaction rate coefficient implies negative microbial activity, which is an unreal situation. Equation (4 xvii) is only valid within a specific temperature range. In practice, undesirably high temperatures may be encountered because of the accumulation of heat in large masses of composting organic material. When modelling such situations, it is preferable to use a relationship without a temperature range restriction and in which activity values remain positive.

Nielsen and Berthelsen [2002] improved equation (4 xvii) by application of enzyme activity theory and used the basis that,

$$\text{decomposition rate} = \text{reaction rate} \times \text{enzyme concentration}$$

The ‘reaction rate’ contained the Arrhenius-type temperature dependency, as was considered by equation (4 xvii). The second term, however, accounted for the additional effect of temperature on enzyme formation and decomposition and therefore concentration. With the

assumptions regarding enzyme catalysis and deactivation, the following equation relating the reaction rate and therefore the reaction rate coefficient to temperature was derived.

$$K = C \cdot e^{a \cdot (T - T_{\text{ref}})} \times \frac{1}{e^{b \cdot (T - T_{\text{inf}})} + 1} \quad (4 \text{ xviii})$$

K is the decomposition rate

C, a and b are empirically determined constants

T is the experimental temperature

T_{ref} is an arbitrary reference temperature

T_{inf} is the temperature at the point of inflection

T_{inf} is about 4 °C above the optimal temperature, as determined from the derivative of K (Section A4.2.1.2). On inspection of equation (4 xviii), the fraction term is approximately 1 at low temperatures and K is similar to equation (4 xvii). At high temperatures the denominator of the fraction term becomes large and K tends to 0. The rate of a reaction, as affected by temperature, is determined by the reaction rate coefficient, k_T . Equation (4 xviii) was, therefore, the form used to express k_T as a function of temperature and the constant A was designated as $k_{T_{\text{ref}}}$. The values of the constants, $k_{T_{\text{ref}}}$, a and b and temperatures T_{ref} and T_{inf} of the curves for the fast and slow stages of the mixing ratios 2 and 4 (Figures A4.3 to A4.4, respectively) are given in Table 4.7. In a similar way as previously described, the best fit curve was determined by the highest ‘percentage variance accounted for’ (VAF) value. The point of inflection at 66 °C suggests that the optimal operating temperature, T_{opt}, for a mix of pig manure and straw, as calculated from equation (A4 vii), is between about 57 °C and 62 °C and depends on the mixing ratio. For the M:S ratio of 4:1, the equation fitted to the data did not tally with the reaction rate coefficient at 10 °C of the fast stage and there was no

result for the slow stage to confirm the extrapolation of the curve below 20 °C. The equation for the M:S ratio of 4:1 is therefore only valid for temperatures above 20 °C.

Table 4.7. Values of the constants that describe the dependence of k_T on T

M:S ratio	Fast stage		Slow stage	
	2:1	4:1	2:1	4:1
T_{ref}	20	20	20	20
T_{inf}	66	66	66	66
C	0.020	0.139	0.014	0.067
A	0.070	0.018	0.062	0.028
B	0.360	0.180	0.250	0.210
T_{opt}	62.1	57.2	61.5	58.7
VAF %	91	75	75	40

Analysis of the curve fitting shows the percentage VAF by the curves fitted to the data for the fast and slow stages of the two mixing ratios ranged from 40 % to about 90 % (Table 4.7). The curves, however, described the pattern well for the rise in activity up to 60 °C, which was reflected by the higher percentages of 93 %, 75 %, 84 % and 84 %, for the respective stages and mixing ratios given in Table 4.7. The difference was most noticeable in mixing ratio 4 low stage with the VAF more than double if the rise in activity only is considered. More measurements of activity at temperatures above 60 °C are needed to verify the fit of the curve for the decrease in the reaction rate coefficient and therefore process kinetics. The equation describing the activity during the fast stage of the M:S ratio of 2:1 predicts that activity would cease at temperatures above 85 °C, whereas the equations for the slow stage and for the M:S ratio 4:1 suggest that activity would only cease altogether after about 95 °C. Mohee [1998] cited research by Miller [1993], which showed that the limit of microbial activity was 82 °C.

The effect of temperature on the rate of decomposition in biological systems can be expressed by a temperature coefficient Q_{10} , where an increase of 10 °C typically causes the reaction rate to double over a limited temperature range [Haug 1993, Johnson 1999] such that

$$Q_{10} = \frac{k_T}{k_{T-10}} = 2 \quad (4 \text{ xix})$$

During the fast and slow stages of the reaction up to 60 °C in the organic material with the M:S ratio of 2:1, the mean Q_{10} was 2.00 ($\sigma = 0.19$) and 1.77 ($\sigma = 0.14$), respectively. The Q_{10} values were similar to the values found with composting garbage of about 1.7 [Wiley 1958] and 1.9 [Schulze 1960]. Similarly, for the M:S ratio of 4:1, the Q_{10} was 1.26 ($\sigma = 0.12$) and 1.38 ($\sigma = 0.15$) for the respective stages up to 55 °C.

A Q_{10} less than 2 is indicative of diffusion controlled reactions because diffusion coefficients vary less with temperature [Haug 1993]. As the organic material with the M:S ratio of 2:1 was well aerated throughout the experiments, the diffusion of nutrients to the micro-organisms, after the exhaustion of the readily degradable organic material, may have been the controlling factor during the slow stage of the experiments that resulted in a decrease in Q_{10} . In solid organic material, microbial activity usually occurs in a thin layer of water surrounding the particles and it can be limited by the rate of nutrient solubilisation [Haug and Ellsworth 1991].

With the M:S ratio of 4:1, the oxygen in the organic material did fall to rate limiting concentrations at incubation temperatures between 25 °C and 60 °C, inclusive as discussed in ‘Environmental factor effects’ (Section 4.3.3.3). The Q_{10} for the increase from 10 °C to 20 °C in the fast stage was 1.95, which suggests that the oxygen present in the reactor vessels was sufficient to support aerobic activity at 10 °C and 20 °C. At the higher temperatures, the availability of oxygen probably limited microbial activity.

4.3.3.5. Mass ratio

The degree of decomposition of the pig manure and straw mix after incubation, as given by the mass ratio, R_m , indicates the stability of the organic material and is therefore an assessment of the performance of the microbial system at the incubation temperature. A lower R_m corresponds to a more stable material. As given in equation (4 ii), there are two methods of calculating the degree of decomposition. The first involves the direct measurement of the total solids content of organic material before and after incubation, and the second uses the reaction rate coefficient evaluated for the incubation temperature under consideration. Due to a small difference in the actual incubation time of each experiment, the second method was used to estimate the degree of decomposition after a set time period (3 days) so that a comparison of the performance of the microbial system could be made between the incubation temperatures. To verify this method, R_m was calculated by the first method and compared with values calculated by the second method for the actual duration of the experiment.

The three sets of calculations are presented in Figure 4.11a) and b) for the samples with the M:S ratios of 2:1 and 4:1, respectively, where

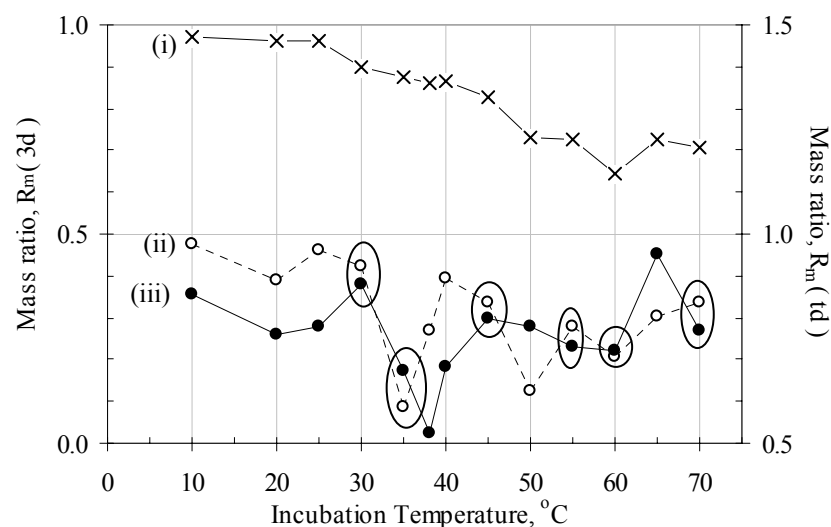
- (i) Gives the standardised mass ratio for a 3 days incubation period, $R_m(3d)$, using a weighted k_T value that accounts for the change from the fast to slow composting stages.
- (ii) Gives the mass ratio using weighted k_T values for the total incubation period, $R_m(td)$.
- (iii) Gives the mass ratio calculated using initial and final TS masses of the organic material and the corresponding equilibrium mass.

The results for (i) show that the degree of decomposition, and therefore the stability, of the organic material increased with the temperature up to 60 °C and 55 °C for the M:S ratios of 2:1 and 4:1, respectively. The trend reflects that of the corresponding reaction rate

coefficients. The plots for cases (ii) and (iii) follow similar patterns for each mixing ratio. For the M:S ratio of 2:1, the difference between the R_m values of the circled points was less than 10%. The largest difference was found between R_m values at 38 °C and 40 °C, about 40 % and 24 %, respectively. The differences between the rest of the corresponding values were less than 20 %. For the M:S ratio of 4:1, the difference between the corresponding R_m values of cases (ii) and (iii) was less than 10% except for the values at 45 °C, for which the difference was 11 %. The pattern shown in case (i) therefore gives a reasonably accurate indication of the change in stability of the incubated organic material with temperature. A temperature between 55 °C and 60 °C does indeed seem to be the optimal working temperature for mixes of pig manure and straw.

Both methods of calculating R_m are subject to analytical errors. With the first method errors arise in the determination of the total solids mass by sample drying. The second method requires the COD of the organic material to be determined, which can be a variable factor in heterogeneous solid organic material. This method also relies on the accurate determination of the k value and any errors are carried through to the R_m value, although to a lesser extent. The first method is independent of k and is a useful check of the results.

a)



b)

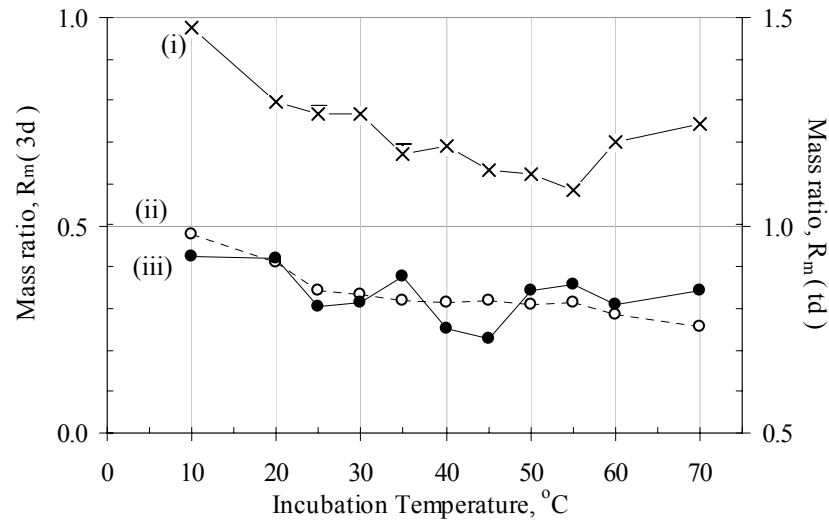


Figure 4.11. Mass ratio for the organic material with the M:S ratio of a) 2:1 and b) 4:1

(i) $R_m(3d)$ (—x—): mass ratio after a 3 day incubation period.

(ii) $R_m(td)$ (---- o ----): mass ratio after the total incubation period using k_T .

(iii) $R_m(td)$ (—●—): mass ratio after the total incubation using the mass values.

4.4. Conclusions

The oxygen uptake rate provides a clear indication of aerobic microbial activity during composting. In the samples of the pig manure and straw mixes, the respiration quotient was rarely greater than 1. The majority of reactions during composting can therefore be expected to be aerobic when sufficient oxygen is available. The reactions, however, may become diffusion-controlled in the samples with the M:S ratio of 2:1 as the microbial activity did not double with the 10°C increase in temperature during the slow stage as it did in the fast stage. The process kinetics in the samples of the M:S ratio of 4:1 did appear to be limited by the availability of oxygen, be it by the diffusion of the gas to the sites of activity or by the actual amount of gas that was present. Either a smaller sample mass or an enriched oxygen atmosphere may be sufficient measures to address this problem.

In the organic material with the M:S ratio of 2:1 the oxygen uptake rate and, consequently, the reaction rate coefficient, increased exponentially with temperature up to a maximal rate, which was followed by a rapid decrease at higher temperatures because of the inactivation of micro-organisms. The activity at thermophilic temperatures up to 70 °C was noticeably higher than at mesophilic temperatures. The highest rate of activity occurred around 60 °C, which also corresponded to the greatest stability. This is, therefore, the temperature at which a unit, composting a mix of pig manure and straw should aim to operate at. With the M:S of 4:1, the rise in the reaction rate coefficient with temperature was less marked, as was shown by the lower Q_{10} value, but the activity did also decrease rapidly at temperatures above the optimum, which was 55 °C in this mixing ratio.

Two distinct stages of the microbial activity were observed at all the temperatures and mixing ratios investigated. The activity during fast stage was about twice that of the slow stage. A clear change from the readily degradable fraction of the pig manure and straw to the fraction more resistant to microbial degradation did occur. The reaction rate coefficient for each stage can be described as a function of temperature by an empirically derived double power equation. Although perfectly valid over a specified temperature range, the theoretically derived equation proposed by Nielsen and Berthelsen [2002], which, not only accounted for the effect of temperature on enzyme activity, but also on enzyme concentration, was preferred because k values were positive for all temperatures. Microbial activity in the pig manure and straw mix was predicted to cease between 85 °C and 95 °C, which is higher than that stated in literature. More measurements of activity at temperatures between 60 °C and about 95 °C would be valuable. Practicality may limit the highest temperature that can be investigated.

This work has ultimately highlighted the importance of temperature control during the process in order to maintain a high rate of activity and good degree of decomposition usually synonymous with a more stable composted material. Further investigation of the effect of the C:N ratio on the oxygen uptake rate in a pig manure and straw mix would be beneficial.

This work on respirometry has been accepted for publication in *Compost Science and Utilisation*. The paper is given in Publications.

CHAPTER 5

MODELLING THE COMPOSTING PROCESS

5.1. Introduction

The solid state composting of organic material in the compost reactors (Section 3.1.2) was simulated in order to predict the performance of process variables, such as temperature, and the sensitivity of the system to changes in selected process factors. The process was described by a simulation, or mechanistic, model. The model consisted of three main interdependent simulations of mass, energy and ammonia changes with respect to time. The model was predominantly inductive and was based on the decomposition of organic material. Microbial activity drives composting but the process was simulated by modified chemical kinetics as expressed in a first order reaction rate equation proposed by Keener *et al* [1993]. An empirical sub-model was used to describe microbial activity as a function of temperature using data from the respirometry experiments (Section 4.3). The actual measurements of respiration rate enabled the simulated process to be self-limiting and to respond as real composting does. The process equations were implemented in *ModelMaker*, a software package that was developed primarily for implementing simulation models without the need for programming in computer code. The model predicted the temperature, total solids mass, off-gas content and aeration profiles during composting. Sensitivity analyses were performed to evaluate the effect of the initial carbon to nitrogen (C:N) ratio, as determined by the mixing ratio of manure to straw (M:S), moisture content and pH of the organic material on the process and on ammonia emissions in particular. The mixing ratio was investigated at three levels, 2, 3 and 4 which equated to a C:N ratio of approximately 25, 20 and 15 respectively.

Similarly, the moisture content and pH were investigated at three levels of, 60 %, 65 % and 70 % of the total mass, and 6, 7 and 8, respectively.

The development and performance of the model is presented in four parts in this chapter. The first deals with the model concept, the second and third deal with the equations and finally a sensitivity analysis.

5.2. Model concept

5.2.1. The composting process

Composting involves the decomposition of organic material by aerobic microbial activity. This activity consumes oxygen and produces carbon dioxide, water and heat. Maximising the rate of decomposition comes down to providing optimum conditions for microbial activity. A number of factors control the rate of decomposition and therefore the rate of heat production. Such factors include: the initial C:N ratio, pH, and moisture content of the organic material, the airflow rate and therefore oxygen supply, the relative humidity of the air and the temperature of the system.

5.2.1.1. Process thermodynamics

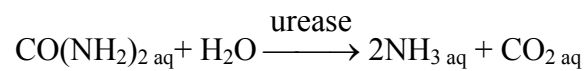
The temperature of the composting system is derived from the balance of heat generation and losses. Heat is generated by microbial activity. Microbial activity, as indicated by the respiration rate, increases rapidly with temperature to an optimum. Above this, increasing temperature decreases activity sharply (Figures A4.1 to A4.4). Heat is lost during composting by several paths: sensible heating of gas passing through the system, evaporation of water (latent heat) and conduction of heat to, and subsequent convection and radiation from, the reactor surface to the surroundings. If the total heat lost from the system is greater than that generated, the system will cool. It is therefore important to maintain a state

of equilibrium between heat losses and generation during maximum microbial activity so that the temperature remains optimal.

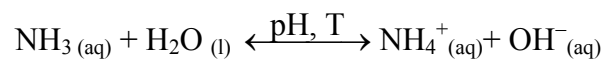
In the model, heat losses were restricted to sensible heating of the supplied air and latent heat of evaporation of water, whilst heat losses from the reactor surface were ignored since the experiments, used to validate the model, minimised such losses with the external heating cable (Section 3.1.2.2.1). Furthermore, the system was regarded as a single compartment without the spatial variation in temperature that may actually occur in real life.

5.2.1.2. Ammonia dynamics

Ammonia is initially generated in manure by enzymatic and microbial activities, mainly through the rapid hydrolysis of urea according to the following reaction.

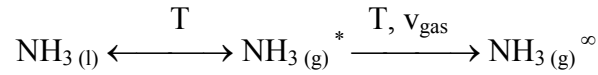


An excess of nitrogen promotes this activity and so increases the amount of ammonia in the organic material. Ammonia production from urease is assumed to have occurred before the simulations described here. In solution, ammonia exists as free ammonia (NH_3) and the dissociated (NH_4^+) ammonium ion. The equilibrium between NH_3 and NH_4^+ is influenced by temperature, T, and pH



An increase in ammonia concentration at the zone of generation drives the transfer of ammonia from the bulk organic material to the surface by mass diffusion. At the interface of the gas and liquid phases, ammonia in the two phases is in equilibrium, which predominantly depends on the temperature of the system. Ammonia gas is then released into the gas stream by convective mass transfer, unless there is almost no gas movement at the surface. Diffusive mass transfer of ammonia into the gas stream also occurs but this was assumed to be relatively small and was not considered in the model. Rapid removal of the ammonia from

the gas interface into the gas stream increases the concentration gradient across the phase boundary and therefore drives the release of ammonia from solution and promotes the ammonia emissions.



* indicates ammonia at the gas phase interface, ∞ the ammonia in the gas stream and v_{gas} is the velocity of the gas stream. The release of ammonia into the gas stream ($\text{NH}_{3\text{emit}}$) can be therefore be described by the following rate equation

$$\frac{d\text{NH}_{3\text{emit}}}{dt} = K_m \cdot A_{\text{in}} \cdot ([\text{NH}_3]_{\text{g}}^* - [\text{NH}_3]_{\text{g}}^\infty) \quad (5 \text{ i})$$

K_m is the overall convective mass transfer coefficient, which is a function of T and v_{gas} , A_{in} is the interfacial surface area at the phase boundary and $[\text{NH}_3]_{\text{g}}$ is the concentration of ammonia.

The main factors that drive ammonia emissions can therefore be summarised as: the ammoniacal nitrogen ($\text{NH}_{3\text{aq}} + \text{NH}_4^+_{\text{aq}}$) content of the organic material, pH, temperature, mass transfer coefficient, interfacial surface area and the airflow rate and humidity.

5.2.2. The composting system

The model considered composting as a contained batch process in which a known initial mass of organic material was left to compost until process factors became limiting and the process was perceived to stop. The organic material was considered to be in a vessel like the experimental reactors. The organic material was assumed to be pig manure thoroughly mixed with chopped straw so that it formed, on a macro-scale, a continuous packed bed of a relatively homogeneous open structure. Three physical phases existed in the compost system: intimately mixed solid and liquid phases with the remaining space being the gas phase.

Air entered the system at the base of the reactor, flowed up through the organic material, provided oxygen for aerobic microbial activity and removed waste gases, some heat

and water (Figure 5.1). The gas flow was assumed to be uniform over the cross section of the reactor. The off-gas was assumed to be at the same temperature as the organic material and initially saturated with water. The heated lid in the experimental apparatus prevented condensation inside the reactor lid and this was assumed in the model.

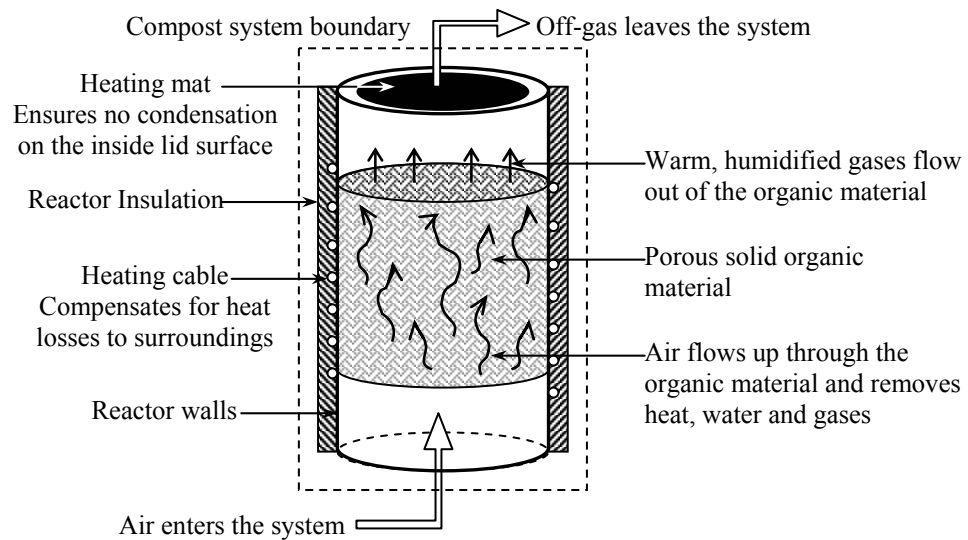


Figure 5.1. The composting system modelled

A two-stage aeration strategy was modelled. The organic material was aerated with a low airflow rate ‘baseline’ aeration that provided the oxygen to support aerobic microbial activity. This was supplemented by high rate ‘cooling’ aeration when the temperature exceeded 60°C. The cooling aeration removed excess heat so maintaining a temperature close to the optimum as deduced by the respirometry experiments (Section 4.3).

5.2.2.1. Ammonia turnover

Nitrogen exists in manure either as ammoniacal nitrogen (AN) or organic nitrogen, but not as nitrate [Lorimor 1998]. The percentage of nitrogen in the ammonia form is an important factor to consider for ammonia emissions as it is the main volatile form of nitrogen in manure. The production, loss and assimilation of ammonia (NH_3) in the organic material was considered in the model as four processes (Figure 5.2).

1. The microbial generation of ammonia in the organic material.
2. The ammonia-ammonium equilibrium chemistry in the organic material
3. The transfer of ammonia to the surface of the organic material and its release across the phase boundary into the air stream.
4. The assimilation of ammonia in the organic material by microbial activity into biomass.

The factors that affected each of the processes indicated in Figure 5.2 were as follows:

1. C:N ratio, moisture content and microbial activity
2. Temperature, pH and AN concentration
3. Temperature, moisture content, airflow rate and humidity, surface area of the organic material, mass transfer coefficient and ammonia concentration
4. Microbial activity and ammonia concentration

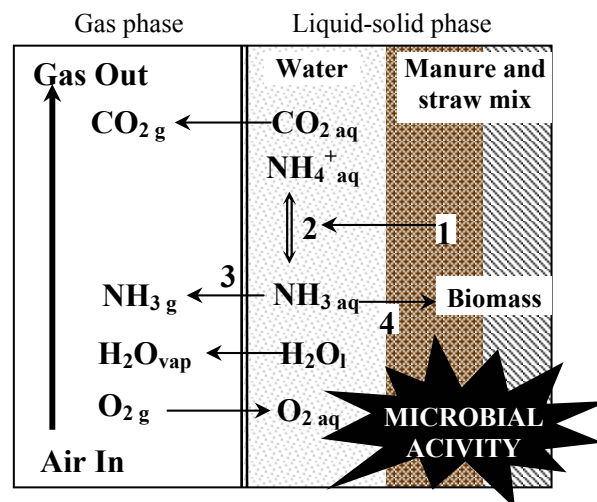


Figure 5.2. Gas exchanges between the gas and liquid-solid phases during composting.

Lorimor [1998] showed that the proportion of the total nitrogen (TN) that existed as AN was related to the total solids content of the manure (Figure 5.3). For manure with a moisture content 60 % and 70 %, about 32 % and 20 % of the total nitrogen, respectively, is in the ammonia form, and is maximum of amount of nitrogen that can be emitted ammonia.

Lorimor [1998] showed that the proportion of the total nitrogen (TN) that existed as AN was related to the total solids content of the manure (Figure 5.3). For manure with a moisture content 60 % and 70 %, about 32 % and 20 % of the total nitrogen, respectively, is in the ammonia form, and is maximum of amount of nitrogen that can be emitted as ammonia.

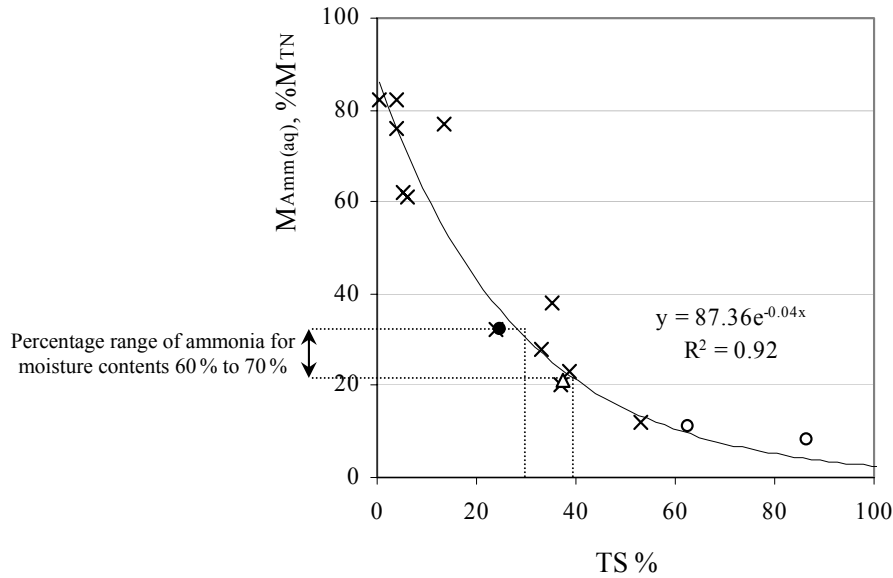


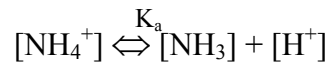
Figure 5.3. Mass of ammonia ($\text{NH}_3 + \text{NH}_4^+$), M_{Amm} , as a percentage of the total nitrogen, M_{TN} , with respect to the total solids content (TS). Sampling data (x) [Lorimor 1998], mean value for pig manure (•), straw (o) and pig manure and straw mixes (Δ) (Section 3.3).

The AN fraction of the organic material was assumed to have been formed before composting started. Furthermore, the degradation of any of the organic nitrogen (ON) during composting to the ammonia form (process 1) was not modelled as manure has a low C:N ratio (≈ 10) and is therefore rich in nitrogen. As Figure 5.3 shows, about a third of the TN in manure is typically as AN. For the 14 kg TS of organic material modelled, the manure contributed about 75 g, 95 g and 110 g of nitrogen of AN for mixing ratios of 2, 3 and 4, respectively and straw contributed about 1g. The initial AN content and the factors affecting the equilibrium (process 2) ultimately determine the total mass of ammonia emitted.

5.2.2.1.1. pH

pH is one of the most important factors governing ammonia emissions [Ni 1999] and was therefore was an input value in the model. The pH of the organic material determines the fraction of the AN that existed as free ammonia (NH_3) in solution. Scotford and Williams [2001] related the pH of organic material to ammonia emissions by assuming that the ammonia emissions were proportional to the concentration of NH_3 .

The acid-base dissociation reaction of ammonia is described as



K_a is the acid dissociation constant, which is described as

$$K_a = \frac{[\text{NH}_3][\text{H}^+]}{[\text{NH}_4^+]} \quad (5 \text{ ii})$$

The concentration of hydrogen ions, $[\text{H}^+]$, determines the pH of the solution as defined by

$$-\log_{10} [\text{H}^+] = \text{pH} \quad (5 \text{ iii})$$

The fraction of the total ammonia that exists as free ammonia, F , is given as

$$F = \frac{[\text{NH}_3]}{[\text{NH}_3] + [\text{NH}_4^+]} \quad (5 \text{ iv})$$

Substituting for $[\text{NH}_4^+]$ from equation (5 ii) and $[\text{H}^+]$ from equation (5 iii), equation (5 iv)

becomes

$$F = \frac{K_a}{K_a + 10^{-\text{pH}}} \quad (5 \text{ v})$$

Figure 5.4 shows the sharp increase in the fraction of free ammonia, F , with pH between a pH of 7 to 12. The increase is about ten fold up to pH 9 in water. An increase in solids reduces the fraction of free ammonia at a particular pH, but increasing temperature increases the fraction of free ammonia.

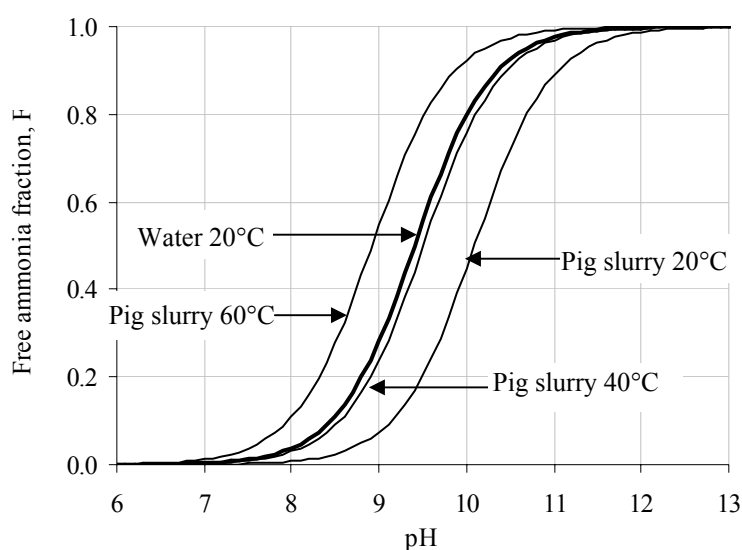


Figure 5.4. pH, temperature and solids content effect on the fraction of free ammonia, F.

The initial pH of the organic material, the degradation of organic acids and the loss of carbon dioxide and ammonia during composting determine the pH changes in the organic material. The organic material also exerts a buffering effect on the system because of the variety of compounds in the organic material such as the weak organic acids [Liang *et al* 1998]. The model did not simulate the changes in pH of the organic material, as this involved a complex and detailed approach to the process, which considered the stability of the multi-solute aqueous system formed between the ammonia and carbon dioxide in solution and the buffer effect of the organic material. The effect of the pH on ammonia-ammonium equilibrium (2) was considered by calculating a simple change in the pH of the organic material between an initial and final value, which was based on Gray *et al* [1971a]. Typically, the initial pH first decreases at the beginning of composting as acid-forming bacteria decompose carbonaceous material to simple organic acids [Mohee 1989]. The pH then increases rapidly at low temperatures up to about 9 at thermophilic temperatures as the organic acids are utilised and ammonia is formed [Schulze 1960, De Bertoldi *et al* 1982, McKinley *et al* 1986]. The pH then falls to around 7 ± 0.5 after ammonia is lost from the

organic material and the system starts to cool [Gray *et al* 1971a, De Bertoldi *et al* 1982, Haug 1993]. The initial fall in pH was not modelled as the pig manure already contained organic acids (pH<6) (Section 3.3) and it was assumed that the rapid rise in temperature allowed little time for any acid-forming bacterial activity.

5.2.2.1.2. Interfacial surface area

An important factor to consider with ammonia emissions is the interfacial surface area of the boundary between the liquid and gas phases. To estimate the possible interfacial surface area, the compost structure was assumed to consist of a series of cylindrical straw pieces, covered in manure and spherical air spaces (Figure 5.5). 14 kg total solids of the organic material occupied approximately 0.2 m³ in the reactor. The interfacial surface area at the phase boundary was calculated for the three levels of mixing ratio and moisture contents, which coincide with those used in the sensitivity analyses.

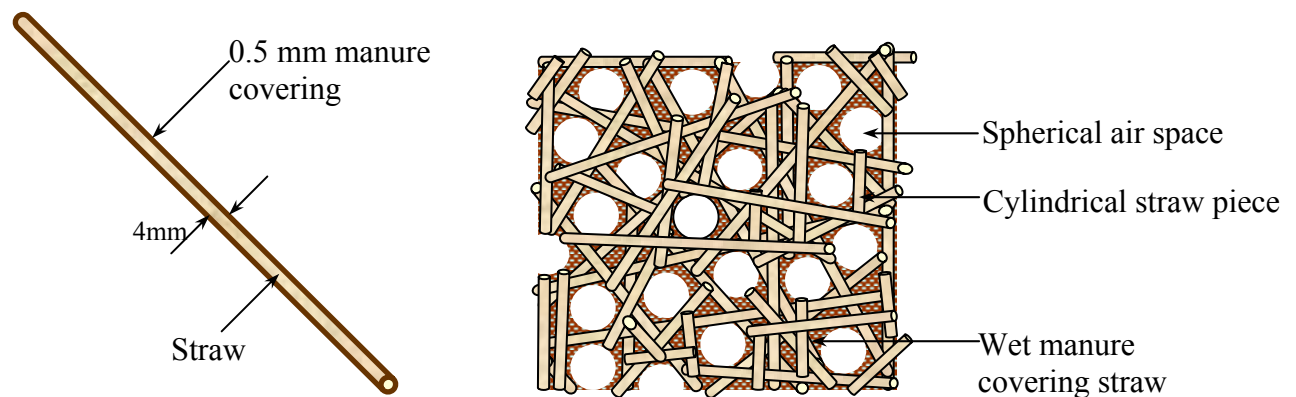


Figure 5.5. Structured of the organic material used to estimate the interfacial area.

The following assumptions about the structure of the organic material were made:

- The length of the piece of straw, L , was about 70 mm (Section 3.2.2) and the diameter was 3 mm. Straw absorbed 3 times its dry mass in water.
- The manure covered the straw with an even layer of about 0.5 mm. Excess manure occupied the corners of the voids in the organic material.

- The air space between the solids was spherical with a radius of 5 mm and were evenly distributed through out the organic material.
- Ammonia was only emitted from the manure.

Calculations of the surface areas are given in Section A5.1.1. If the surface area of straw covered by the manure, SA_M , was less than the total surface area of the air spaces, SA_A , then the interfacial surface area equalled SA_M (Table A5.2). Conversely, if, SA_M , was greater than, SA_A then the interfacial surface area equalled SA_A as some manure filled in part of the voids, with the bulk of it not exposed to the air. The results given in Table A5.2 show that the moisture content of the organic material did not alter the fact that the air space surface area in the organic material was greater than that of the manure. The straw was able to absorb the added water for all the moisture contents and so there was no free water in the void spaces. It was assumed that ammonia was only emitted from manure. Therefore the interfacial surface area equalled the surface area of the manure. For the mixing ratios of 2, 3 and 4, the interfacial surface area at the phase boundary was 34, 44, 50 m², respectively, regardless of the moisture content.

5.2.2.2. Pathogen inactivation

Rapid inactivation of pathogens during composting required the process factors such as temperature, water content, pH, oxygen content and the duration of composting to be set and maintained near optimum levels for microbial activity [Turner 2002]. Ammonia in high concentrations may be toxic to the micro-organisms and moisture content and pH of the organic material affect the thermo-sensitivity of micro-organisms but these have not been very well quantified. Consequently, temperature was the only criterion considered in pathogen inactivation in the model. If the temperature was above 55 °C for more than 3 consecutive days, then pathogen inactivation was assumed to have occurred.

5.2.3. Model outputs

The principal aim of the model was to simulate the ammonia emissions and temperature-time profiles during composting. Other important results of model simulations were:

- The mass of total solids and water in the organic material
- The composition of the off-gas (oxygen, carbon dioxide and ammonia concentrations)
- The cumulative mass of oxygen used and carbon dioxide and ammonia produced.
- The mass of total and organic nitrogen in the organic material
- The mass of ammonia at each step leading to the emission of ammonia from the organic material into the gas stream.
- The demand placed on the aeration to maintain the temperature at an optimum.
- The mass of water evaporated into the gas stream and carried out of the system.
- The factors limiting the process.
- The energy flows (sensible, evaporative and generated) that occur during composting, which ultimately determined the temperature of the organic material.
- The duration of the thermophilic stage of composting for pathogen inactivation.

5.3. Model equations

A simulation or mechanistic model is defined by a series of connected equations, which behave like the real system being modelled. The equations, which describe the model, are divided between three interdependent sub-models: the mass model, energy model and ammonia emission model.

5.3.1. Mass model

The mass model considered the mass balances of the solid, liquid and gas phases separately, although in real compost systems the liquid and solid phases were often not so distinguishable as the solids absorbed the liquid fraction.

5.3.1.1. Solid phase

The maximum decomposition rate of the organic material was simulated as a first order rate reaction, which described the rate of loss of total solids (M_{TS}) with time (t) according Keener *et al* [1993].

$$\frac{dM_{TS}}{dt} = -k_h (M_{TS} - M_e) \quad (5 \text{ vi})$$

The equilibrium mass, M_e , was the mass of organic material that was not decomposed by microbial activity and k_h was the hourly reaction rate coefficient. The negative sign indicates that the mass of the biodegradable fraction of the organic material decreased with time. M_e was estimated from the summation of equilibrium masses of the individual organic materials, j , in the mix, as calculated using the bio-degradability fraction, β .

$$M_e = \sum (M_j \cdot TS_j \cdot (1 - \beta_j)) \quad (5 \text{ vii})$$

M_j was the wet mass and TS_j was the fractional total solids content of an organic material j .

The reaction rate coefficient was not constant as it in effect described microbial activity and so depended on a number of process factors such as temperature, moisture content, oxygen availability and pH [Haug 1993]. The temperature effect, f_T , was evaluated experimentally using respirometry (Figure A4.3) and so formed an empirical sub-model and was given as

Temperature

$$f_T = \frac{e^{0.07 \cdot (T-20)}}{e^{0.36 \cdot (T-66)} + 1} \quad (5 \text{ viii})$$

T was the temperature of the organic material.

The effect of the oxygen, f_{OC} , and moisture content, f_{MC} , was also considered in the model and were described by the following functions, which are discussed in Section 4.1.1.4.

Oxygen concentration:
$$f_{OC} = \frac{[O_2]}{[O_2] + 2} \cdot \frac{20.96 + 2}{20.96} \quad (5 \text{ ix})$$

$[O_2]$ was the %v v⁻¹ concentration of oxygen in the off-gas, which was assumed to be the same as the concentration in the inter-particle spaces of the organic material. The second term on the right-hand side of equation (5 ix) was a correction factor so that in air the oxygen factor was unity (optimal). Therefore, a decrease in f_{OC} during composting was relative to that of air.

Moisture content:
$$f_{MC} = \frac{1}{e^{-17.7MC+7.1} + 1} \quad (5 \text{ x})$$

MC was the moisture content of the organic material.

As with the calculation of reaction rate coefficient in Section 4.3.3.3, the effects of the process factors were assumed to be multiplicative. Using the relationship between the specific oxygen uptake rate (SOUR) and the chemical oxygen demand (COD) to determine the reaction rate coefficient, k_h was given by

$$k_h = \frac{\text{SOUR (gO}_2\text{kg}_{TS}^{-1}\text{h}^{-1})}{\text{COD (gO}_2\text{kg}_{TS}^{-1})} \quad (5 \text{ xi})$$

The SOUR was corrected for the environmental effects and was defined as

$$\text{SOUR} = \text{SOUR}_{20^\circ\text{C}} \times f_{OC} \times f_{MC} \times f_T \quad (5 \text{ xii})$$

$\text{SOUR}_{20^\circ\text{C}}$ was the empirically estimated uptake rate at 20°C. Inclusion of the effects of process factors on the k_h meant that the assumptions free with optimum operating conditions did not have to be made, as sub-optimal conditions were simulated.

5.3.1.1.1. pH

A simple representation of the changes in pH of the organic material was used. The pH was assumed to rise from its initial value to between 8 and 9 in two days and then gradually decreased after eight days to around 7.5 (Figure 5.6). The microbial activity was assumed to be optimal in this pH range.

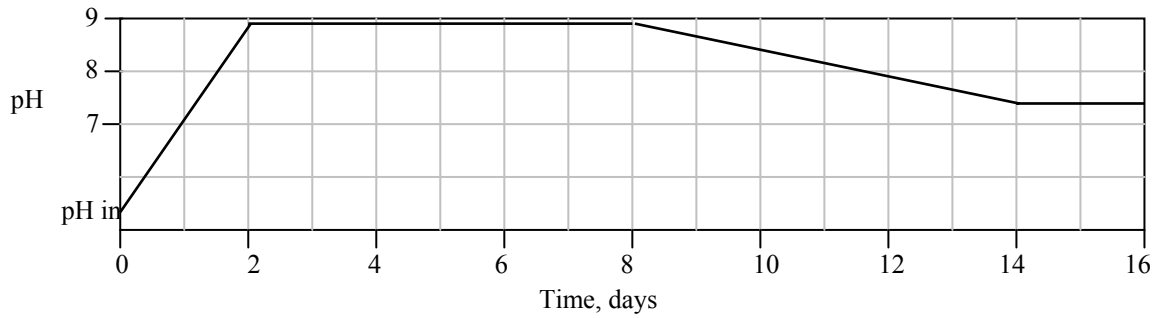


Figure 5.6. The assumed pH profile during composting.

The following expressions describe the pH change with time shown in Figure 5.6

$$\text{For } 0 \leq t \leq 2 \text{ days,} \quad \text{pH} = \frac{t}{48}(9 - \text{pH}_{\text{in}}) + \text{pH}_{\text{in}} \quad (5 \text{ xiii})$$

$$\text{For } 2 < t \leq 8 \text{ days,} \quad \text{pH} = 9 \quad (5 \text{ xiv})$$

$$\text{For } 8 < t \leq 14 \text{ days,} \quad \text{pH} = -\frac{t}{96} + 11 \quad (5 \text{ xv})$$

$$\text{For } t > 14 \text{ days,} \quad \text{pH} = 7.5 \quad (5 \text{ xvi})$$

5.3.1.2. Liquid phase

The liquid phase of the organic material was assumed to be just water. The ammonia and other solutes in the liquid phase formed a very small proportion and was therefore ignored. The mass of water in the organic material was a balance between the mass generated by microbial activity as a by-product of aerobic respiration and the water lost from the system in the gas phase and by leaching. It was assumed that water was lost by evaporation only and

that no leaching occurred. The change of moisture content of the organic material, MC, was therefore given as

$$MC \frac{dM_{\text{Total}}}{dt} = \frac{dM_{\text{H}_2\text{O}}|_{t=0} - dM_{\text{H}_2\text{O evap}} + dM_{\text{H}_2\text{O gen}}}{dt} \quad (5 \text{ xvii})$$

$M_{\text{H}_2\text{O}}|_{t=0}$ was the initial mass of water in the organic material, $M_{\text{H}_2\text{O evap}}$ was the mass of water lost through evaporation, $M_{\text{H}_2\text{O gen}}$ was the mass of microbially generated water and M_{Total} was the wet mass of the organic material.

The mass of water generated was taken as the stoichiometric amount produced by the oxidation of the organic material by considering the reaction partition constant (Section A5.3.1). The chemical formula of an ‘average’ molecule of the organic material was calculated by the considering the weighted contribution of the chemical formulae for molecules straw and of primary sludge, which was assumed to represent that of the pig manure, on a mass basis.

The loss of water to the gas phase by evaporation involved a change in state that influenced the energy balance of the system. Evaporation depended on the temperature and airflow rate through the organic material. During the thermophilic stage of composting, so much water may be lost that the moisture content becomes the limiting factor for microbial activity. It was initially assumed that the off-gas was saturated and at the temperature of the composting organic material. The mass of water evaporated was therefore the balance between water content of the saturated off-gas and that of the air entering.

5.3.1.2.1. Degree of off-gas saturation

With high air flow rates through the organic material, the assumption that the off-gas was always saturated with water could lead to an overestimation of the water loss. A semi-

mechanistic approach was used to predict the degree of off-gas saturation (S), which was assumed to fall exponentially with airflow rate (F) to a ‘reasonable’ minimum value (S_{\min}).

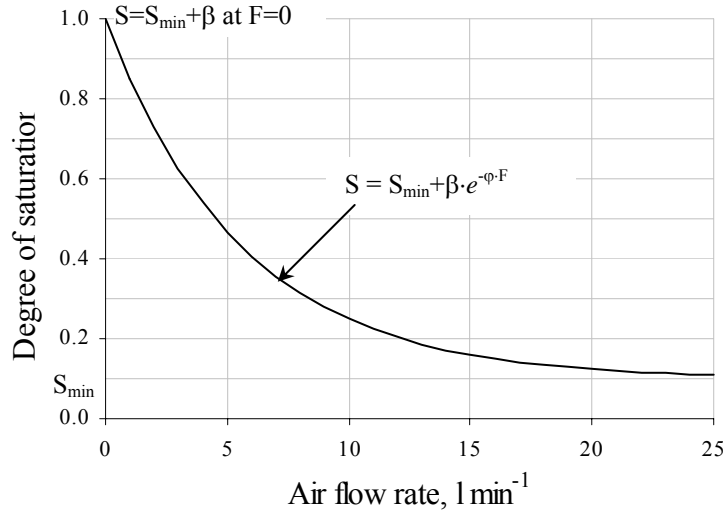


Figure 5.7. A hypothetical relationship between the degree of off-gas saturation and the airflow rate through the organic material.

To estimate the values of ϕ , the minimum degree of saturation, S_{\min} , was given the values of 0.1. By definition, $\beta = 0.9$ and

$$S = 0.1 + 0.9e^{(-\phi \cdot F)} \quad (5 \text{ xviii})$$

At the highest airflow rate through the system of 25 l min^{-1} , S was assumed to be close to the minimum value of S_{\min} , 0.11, say. Substituting in the values for $F = 25 \text{ l min}^{-1}$ gives

$$\phi = \frac{\ln \frac{0.11-0.1}{0.9}}{-25} = 0.18 \quad (5 \text{ xix})$$

The off-gas was initially assumed to be always saturated. In some later simulations, this degree of saturation factor was included in equation 5 xxxi.

5.3.1.3. Gas phase

Some oxygen was removed from the gas phase by aerobic activity. The carbon dioxide, produced by microbial activity, and the ammonia passed from the liquid phase into

the gas phase. The stoichiometric mass of oxygen consumed and of carbon dioxide produced during decomposition of the organic material was calculated using reaction partition constants. The oxygen and carbon dioxide content of the off-gas, expressed as a percentage, was determined by the respective mass balances given as

$$[\text{O}_2]_{\text{off-gas}} = \frac{M_{\text{O}_2 \text{ air}} - M_{\text{O}_2 \text{ resp}}}{M_{\text{off-gas}}} \times 100 \quad (5 \text{ xx})$$

$$[\text{CO}_2]_{\text{off-gas}} = \frac{M_{\text{CO}_2 \text{ air}} + M_{\text{CO}_2 \text{ resp}}}{M_{\text{off-gas}}} \times 100 \quad (5 \text{ xxi})$$

$M_{\text{O}_2 \text{ air}}$ and $M_{\text{CO}_2 \text{ air}}$ were the mass of oxygen and carbon dioxide in the dry air flowing into the organic material, $M_{\text{O}_2 \text{ resp}}$ and $M_{\text{CO}_2 \text{ resp}}$ were the mass of oxygen used and carbon dioxide produced during aerobic respiration and $M_{\text{off-gas}}$ was the total mass of the dry off-gas.

The total mass of off-gas included the mass of water evaporated from the organic material and was assumed to be saturated at the temperature at which it left the organic material. The gas percentages were converted from mass basis to a volume basis, which was equivalent to a molar basis according to the Gas Laws, by considering the respective relative molecular mass of the gases and the density of dry air. The volumetric oxygen content of the off-gas was used to calculate the f_{OC} of equation (5 ix). The mass balance of the gas phase was given by

$$\frac{dM_{\text{off-gas}}}{dt} = \frac{dM_{\text{dry air}}}{dt} - \frac{dM_{\text{O}_2 \text{ resp}}}{dt} + \frac{dM_{\text{CO}_2 \text{ resp}}}{dt} + \frac{dM_{\text{NH}_3 \text{ emit}}}{dt} \quad (5 \text{ xxii})$$

In this model, the mass of ammonia emitted, $M_{\text{NH}_3 \text{ emit}}$, was not calculated using reaction partition coefficients, but were dealt with in a separate model (Section 5.4)

5.3.2. Energy model

The first order rate equation was the root of the model, but the energy model was, in fact, the driving force of the process as it determined the temperature of the composting organic material, T_C , and therefore the decomposition rate. Although the organic material was contained during composting, in terms of thermodynamics it represented an open system because the gas phase crossed system boundaries. From the first law of thermodynamics, the net energy gain was a balance between the energy lost from the system and the energy coming into the system. During composting, heat was generated by microbial activity (H_{gen}) and was lost by evaporation (H_{evap}) and sensible heating of the air flowing through the organic material ($H_{\text{off-gas}} - H_{\text{air}}$) and through the reactor walls to the surroundings. Heat losses to the surrounding were not included in this model because the heat losses were compensated for with the heating cable on the reactor surface. The temperature of the organic material at anyone one instance was determined from the net heat in the organic material, the wet mass of organic material, M_{Total} , and the specific heat capacity of the wet organic material, C_p , and was defined by:

$$\frac{dT_C}{dt} = \frac{d}{dt} \left[\frac{H_{\text{gen}} + H_{\text{air}} - H_{\text{off-gas}} - H_{\text{evap}}}{M_{\text{Total}} \cdot C_p} \right] \quad (5 \text{ xxiii})$$

assuming that:

- No organic material entered or left the system
- No condensation of water vapour from the gas phase occurred inside the system boundaries
- All the organic material in the system was at the same temperature.

The specific heat capacity of the organic material varied according to its moisture content (MC) such that C_p was recalculated at each iteration using

$$C_P = C_{P_{TS}} \cdot (1 - MC) + C_{P_{H_2O}} \cdot MC \quad (5 \text{ xxiv})$$

$C_{P_{TS}}$ was the specific heat capacity of the total solids fraction and $C_{P_{H_2O}}$ was the specific heat capacity of the water fraction. Haug [1993] used a value of $1.05 \text{ kJ kg}^{-1} \text{ }^\circ\text{C}^{-1}$ for $C_{P_{TS}}$, which was close to the value of $0.99 \text{ kJ kg}^{-1} \text{ }^\circ\text{C}^{-1}$ obtained from equation (3 xvi) for $MC = 0$. The $C_{P_{H_2O}}$ was taken as $4.19 \text{ kJ kg}^{-1} \text{ }^\circ\text{C}^{-1}$ and $C_{P_{TS}}$ as $1.00 \text{ kJ kg}^{-1} \text{ }^\circ\text{C}^{-1}$.

5.3.2.1. Heat generated by microbial activity

The heat generated by microbial activity was based on the energy liberated per gram of oxygen gas consumed during respiration and was defined as

$$\frac{dH_{\text{gen}}}{dt} = H_{O_2} \cdot \text{SOUR} \cdot \frac{dM_{TS}}{dt} \quad (5 \text{ xxv})$$

H_{O_2} was the heat produced per gram of oxygen respired, $\text{kJ g}^{-1} \text{ O}_2$. The heat produced by respiration was less than the heat of combustion of the organic material since not all of the available energy in the organic material would be released by microbial activity. Also some of the organic material would be assimilated into microbial biomass. Published values of H_{O_2} range from about $14 \text{ kJ g}^{-1} \text{ O}_2$ for composting sewage sludge cakes [Bach 1987] to $16.2 \text{ kJ g}^{-1} \text{ O}_2$ for pure cultures grown on nutrient agar [Cooney *et al* 2002]. For composting of pig manure and straw, $14.8 \text{ kJ g}^{-1} \text{ O}_2$ was used, as suggested by Veeken [1999].

By using the oxygen uptake rate to determine the heat generated by microbial activity, possible limiting effects of process factors such as temperature, moisture and oxygen availability could be included in the model. The composting time was therefore not necessarily determined by the mass of organic material approaching equilibrium but by another condition such as the drying out of the organic material.

5.3.2.2. Heating the air

As the air flowed through the organic material it heated up and became humidified. The off-gas was initially assumed to be saturated and at the temperature of the organic material. The energy change free with the sensible heating of the air was the difference between that of the off-gas and the incoming air. The heat carried into the system by the moist air, H_{air} , was the product of the total mass of the air, M_{air} , including the water vapour content, its specific heat capacity, C_{Pair} and temperature T_{air} as described by equation (5 xxvi).

$$\frac{d H_{\text{air}}}{dt} = \frac{d M_{\text{air}}}{dt} \cdot C_{\text{Pair}} \cdot T_{\text{air}} \quad (5 \text{ xxvi})$$

As with the compost reactors, the mass of air flowing into the system depended on the aeration *i.e.* the low baseline aeration or the cooling aeration, which was determined by temperature. In addition, the temperature and therefore the relative humidity of the air varied because the baseline aeration air was heated and humidified whereas the cooling aeration air was at room temperature and humidity. The relative humidity of the baseline aeration air at 40°C was 50% and that of the cooling aeration air at 20°C was 70%. The mass of water carried by the air at the respective humidities, as given in steam tables [CIBS 1984], was 23.32 and 10.33 g kg⁻¹ dry air. The heat carried by the incoming air was therefore calculated by considering the dry air and the water fractions individually, such that equation (5 xxvi) was expressed as

$$\frac{d H_{\text{air}}}{dt} = \left[C_{\text{P dry air}} \frac{d M_{\text{dry air}}}{dt} + C_{\text{P H}_2\text{O VAP}} \frac{d M_{\text{H}_2\text{O VAP}}}{dt} \right] \cdot T_{\text{air}} \quad (5 \text{ xxvii})$$

In the same way as the heat carried by the air, the heat carried by the off-gas was a product of the off-gas mass, $M_{\text{off-gas}}$, specific heat capacity, $C_{\text{Poff-gas}}$, and temperature, $T_{\text{off-gas}}$.

$$\frac{d H_{\text{off-gas}}}{dt} = \frac{d (M_{\text{off-gas}} \cdot T_{\text{off-gas}} \cdot C_{\text{Poff-gas}})}{dt} \quad (5 \text{ xxviii})$$

With the data of the water content of the saturated off-gas from steam tables [CIBS 1984], equation (5 xxvii) was expressed as

$$\frac{d H_{\text{off-gas}}}{dt} = \frac{d (M_{\text{dry gas}} \cdot C_{P \text{ dry gas}} + M_{\text{sat}} \cdot C_{P \text{ H}_2\text{O}_{\text{VAP}}}) \times T_{\text{off-gas}}}{dt} \quad (5 \text{ xxix})$$

5.3.2.3. Heat of evaporation

The mass of water evaporated, M_{evap} , was related to the energy removed, H_{evap} , by the latent heat of evaporation, H_L , in $\text{kJ kg}^{-1} \text{H}_2\text{O}$ evaporated.

$$\frac{d H_{\text{evap}}}{dt} = M_{\text{dry air}} \cdot \frac{d(H_L \cdot M_{\text{evap}})}{dt} \quad (5 \text{ xxx})$$

The value of H_L depended on the temperature of the organic material and was recalculated throughout the model simulation using equation (5 xxxi) derived using data from Perry [1984]

$$H_L = -2.38 \cdot T_C + 2501 \quad (5 \text{ xxxi})$$

The off-gas was saturated and at the same temperature as the organic material such that the mass of water evaporated was therefore equal to the difference between mass of water in the off-gas and the mass in the air flowing into the system. The mass of water in the saturated off-gas, M_{sat} , expressed in $\text{g kg}^{-1} \text{dry air}$, was related to its temperature, T_{gas} , by

$$M_{\text{sat}} = S \cdot 0.0044 e^{(0.0594 \cdot T_{\text{gas}})} \quad (5 \text{ xxxii})$$

S was the degree of saturation of the gas as given by equation (xviii), which initially was assumed to be 1. With the change from baseline to cooling aeration, the heat of evaporation had a greater impact on the energy balance because more water was required to saturate the air, the volume of which flowing through the system, was about five times greater.

5.3.3. Ammonia emission model

5.3.3.1. Initial nitrogen content

The initial mass of AN and TN of the organic material was calculated using the mean values of the analytically determined nitrogen contents for the pig manure and straw (Tables 3.2 and 3.4, respectively), weighted by the mixing ratio. In lieu of actual analytical values, then the relationship between the mass percentage of the TN that existed as AN and the total solids (TS) content of the organic material (Figure 5.3) could be used. The relationship was described by an exponential regression equation (5 xxxiii) [Lorimor 1998].

$$M_{AN} = 87.4 \cdot e^{-0.04 \cdot TS} \cdot M_{TN} \quad (5 \text{ xxxiii})$$

where M_{AN} was the mass of AN and M_{TN} was the mass of total nitrogen in the organic material and TS was expressed as a percentage.

5.3.3.2. Partition of ammonia

The pH of the organic material controlled the equilibrium between the associated (NH_4^+) and dissociated or free (NH_3) ammonia, which corresponded to process 2 shown in Figure 5.2. The effect of pH on free ammonia formation in the organic manure was described by equation (5 v). The acid dissociation coefficient K_a was described by the reactions:



Such that
$$K_a = \frac{K_2}{K_1} \quad (5 \text{ xxxiv})$$

K_1 and K_2 were the dissociation constants of the respective equilibrium reactions and related the dissociated state to the free state, where

$$K_1 = \frac{[\text{NH}_4^+][\text{OH}^-]}{[\text{NH}_3][\text{H}_2\text{O}]}$$

and

$$K_2 = \frac{[H^+][OH^-]}{[H_2O]}$$

K1 and K2 depended on temperature as described by the relationship for the dissociation of ammonia in water as proposed by Edwards *et al* [1975]

$$\ln K = \frac{A}{T} + B \cdot \ln T + C \cdot T + D \quad (5 \text{ xxxv})$$

T was the absolute temperature in degrees Kelvin and the values of the constant terms, A, B, C and D for each equilibrium reaction are given in Table 5.1.

Table 5.1. Values of constants used to determine the dissociation constant of the NH₃ in water

	A	B	C	D
Equilibrium Reaction 1	-5914.08	-15.064	-0.0110	97.972
Equilibrium Reaction 2	-13445.9	-22.477	0	140.93

Ni [1999] used a semi-empirical relationship, equation (5 xxxvi), to calculate the dissociation constant in a model of ammonia emissions from pig manure.

$$K_a = 10^{-(0.0918 + \frac{2729.92}{T})} \quad (5 \text{ xxxvi})$$

The difference in the K_a calculated with equations (5 xxxv) and (5 xxxvi) was small (Figure 5.8). Equation (5 xxxvi) was therefore used in this model for simplicity and K_a was converted from mol l⁻¹ to kg m⁻³ by multiplying with the fraction $\frac{Mr_{NH_3}}{1000}$.

These K_a equations were derived from ammonia equilibrium systems in water. Research with concentrated chicken manure [Hashimoto and Ludington 1971] and pig slurry (1 % TS) [Zhang 1994] showed that the K_a value in these manure systems was in fact a sixth and a fifth of the K_a value for water system at about 20 °C, respectively, as illustrated by the F curve for pig slurry at 20 °C in Figure 5.4. To account for the effect of the pig manure, a sixth of the K_a value calculated with equation (5 xxxvi) was used to determine F.

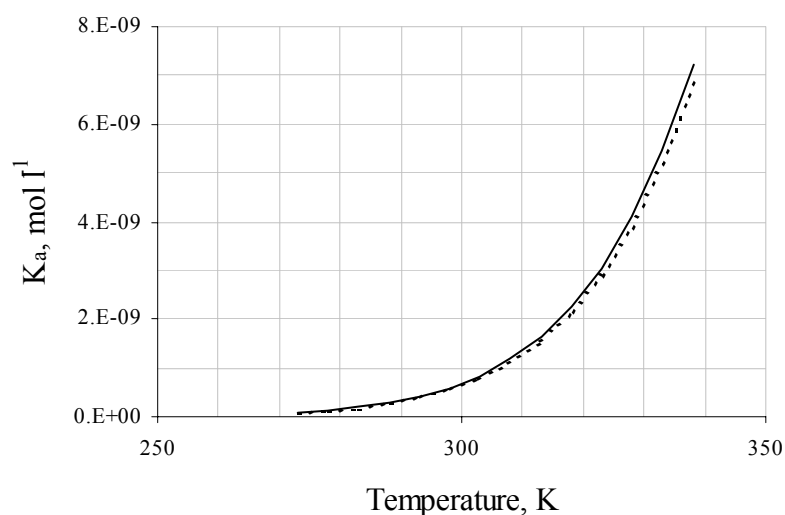


Figure 5.8. The dissociation of ammonia in water: eq. (5 xxxv) (—) and eq. (5 xxxvi) (-----)

The mass of free ammonia in the liquid phase at any one instance was the balance between the ammonia lost to the gas phase and the AN in the organic material (liquid phase) and was defined as

$$\frac{d M_{\text{NH}_3 \text{ aq}}}{dt} = \frac{d \left(\frac{17}{14} M_{\text{AN aq}} \cdot F \right)}{dt} - \frac{d M_{\text{NH}_3 \text{ gas}}}{dt} \quad (5 \text{ xxxvii})$$

$M_{\text{AN aq}}$ was mass of AN in the organic material and was the sum of the free and associated ammonia, $[\text{NH}_3 + \text{NH}_4^+]_{\text{aq}}$. $M_{\text{NH}_3 \text{ gas}}$ was the mass of ammonia lost to the gas phase and is defined in Section 5.3.3.3.

5.3.3.3. Ammonia in the gas phase

The mass of ammonia in the gas phase boundary was the balance between the mass of ammonia leaving the liquid phase and the mass being emitted into the gas stream, $M_{\text{NH}_3 \text{ emit}}$.

This depended on the airflow rate [Liang *et al* 1998] according to the following equation

$$\frac{d M_{\text{NH}_3 \text{ emit}}}{dt} = \frac{V F_{\text{air}}}{V_{\text{air}}} \cdot \frac{d M_{\text{NH}_3 \text{ gas}}}{dt} \quad (5 \text{ xxxviii})$$

$V F_{\text{air}}$ was the volumetric airflow rate in through the system ($\text{m}^3 \text{ h}^{-1}$). V_{air} was the volume of air in the organic material (m^3). The mass of ammonia at the phase boundary was defined as

$$\frac{d M_{\text{NH}_3\text{gas}}}{dt} = \frac{d M_{\text{NH}_3\text{aq}}}{dt} \cdot \frac{K_m \cdot SA}{H} - \frac{d M_{\text{NH}_3\text{emit}}}{dt} \cdot \frac{VF_{\text{air}}}{V_{\text{air}}} \quad (5 \text{ xxxix})$$

K_m was the mass transfer coefficient of ammonia (m h^{-1}). SA was the surface area of the phase boundary (m^2). H was Henry's constant, which described the partition of ammonia between the gas and liquid phase, and was strongly dependent on temperature as shown by equation (5 xL) [Monteny *et al* 1998]. In this case, the units of H were $(\text{kg m}^{-3})_l (\text{kg m}^{-3})_g^{-1}$.

$$H = 1384 \times 1.053^{(293-T)} \quad (5 \text{ xL})$$

5.3.3.3.1. Mass transfer coefficient

The mass transfer rate of ammonia from the liquid phase into the gas phase depends on its transfer rate in each of the phases as individual components. One of the transfer rates controls the overall mass transfer rate, K_m , in equation (5 i). If the ammonia diffuses from the liquid phase more rapidly than from the gas phase at the boundary, then the mass transfer rate in the gas phase determines the overall mass transfer rate and K_m corresponds to the overall mass transfer coefficient of ammonia in the gas phase, K_G . This situation largely depends on the gas flow rate and temperature in the system. If the resistance to mass transfer is greatest in the liquid phase then the mass transfer rate in the liquid phase and K_m corresponds to the overall mass transfer coefficient of ammonia in the liquid phase, K_L . The overall mass transfer coefficients in the gas and liquid phases were defined by Halsam *et al* [1924] as

$$K_G = k_g + \frac{1}{H \cdot k_l} \quad (5 \text{ xLi})$$

$$K_L = \frac{k_l \cdot k_g}{H \cdot k_l + k_g} \quad (5 \text{ xLii})$$

k_g and k_l are the mass transfer coefficients in the gas ($\text{kg m}^{-2} \text{atm}^{-1} \text{h}^{-1}$) and liquid phase (m h^{-1}), which were empirically related to temperature, T in Kelvin, and superficial gas velocity, v_{gas} ,

by [Haslam *et al* 1924] and adapted for ammonia release from pig manure [Anderson *et al* 1987].

$$k_g = 3.77 \times 10^{-4} \cdot v_{\text{gas}}^{0.8} \cdot T^{-1.4} \quad (5 \text{ xLiii})$$

$$k_l = 1.42 \times 10^{-12} \cdot T^4 \quad (5 \text{ xLiv})$$

For gases of low solubility, Henry's coefficient is small and $k_g \gg k_l \cdot H$ and $K_L \approx k_l$. The liquid phase offers the main resistance to gas transfer. For highly soluble gases, such as ammonia, Henry's coefficient is large and $k_g \ll k_l \cdot H$ and $K_L = \frac{k_g}{H}$. The main resistance to mass transfer was therefore in the gas phase. In the model, K_L was expressed as a function of temperature. The expression was derived graphically using regression analysis on K_L values calculated using equation (5 xxxxi) at temperatures between 10 °C and 60 °C (Figure 5.9). The mass transfer coefficient in the gas phase, k_g , was evaluated using the superficial gas velocity calculated by estimating the cross sectional area of the void spaces in the organic material (Section A5.1.2.). The calculation assumed a uniform airflow rate and cross sectional area in the organic material. A superficial gas velocity, v_{gas} , of $2.8 \times 10^{-3} \text{ m s}^{-1}$ was used in the model.

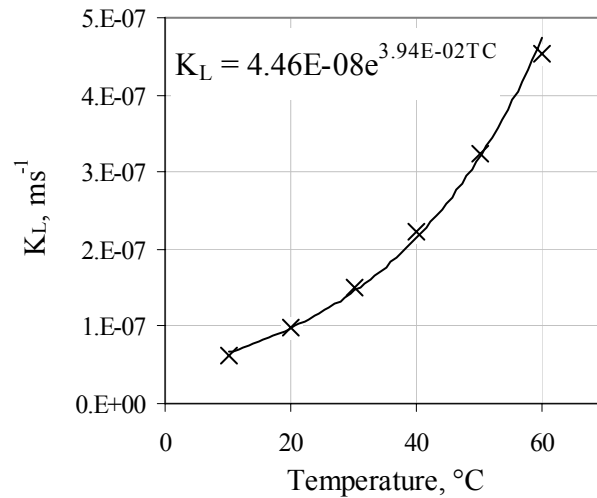


Figure 5.9. K_L of ammonia as a function of temperature, T_C .

Cumby *et al* [1995] found that the liquid mass transfer coefficient was smaller in pig slurry than in water whereas Arogo *et al* [1996] found that the solids content of liquid manure did not significantly effect the liquid mass transfer coefficient. A factor to account for the effect of the solids content of manure was therefore not included in equation (5 xLiv).

5.3.3.4. Re-assimilation of nitrogen into biomass

The ammonia in solution was assumed to be either emitted to the gas phase or re-assimilated by micro-organisms into biomass, which contributed to the organic nitrogen content. The mass of ammonia required for new cell synthesis, $M_{N_{syn}}$, was estimated from the relationship used by Haug [1993] as given by equation (5 xLv). The average cell was represented by the chemical formula $C_5H_7O_2N$, - a 12 % nitrogen content, such that N_{cell} equalled 0.12. The mass of cells produced, the cell yield, Y_{cell} , was approximately 0.2 kg kg^{-1} of total solids decomposed.

$$\frac{d M_{N_{syn}}}{dt} = \frac{d M_{TS}}{dt} \cdot N_{cell} \times Y_{cell} \quad (5 \text{ xLv})$$

The model assumed that the nitrogen used in cell synthesis was provided exclusively from the AN in solution such that the nitrogen balance in the organic material was

$$\frac{d M_{TN}}{dt} = \frac{d M_{N_{syn}}}{dt} - \frac{14}{17} \frac{d M_{NH_3, gas}}{dt} \quad (5 \text{ xLvi})$$

5.3.4. Assumptions

Simplifying assumptions were made about the composting process and the organic material and are summarised below.

- The organic material was relatively homogeneous, without large clumps of unmixed manure or straw and without excessively dry or wet areas.
- No organic material left or entered the system.

- The rate of decomposition was described by first order reaction rate kinetics.
- The process was described by chemical reactions rather than by microbially mediated biochemical reactions. Therefore, there was no lag stage during which the microbial population established itself.
- The effect of the environmental factors was multiplicative.
- The exponent constants of the temperature factor, f_T , (equation 5 viii) and the COD were the same for all mixing ratios.
- All phases of the organic material were at the same temperature.
- There was no pressure drop across the reactor in the direction of airflow.
- The air entering did not channel through the organic material but diffused evenly to all parts of the organic material.
- The air spaces were spheres of the same size, evenly distributed in the organic material.
- The off-gas was saturated and at the temperature of the organic material.
- The organic material was well mixed and gas concentration gradients did not exist. The concentration of a gas in the off-gas represented that in the air spaces.
- Heat transfer and mass transfer of oxygen and carbon dioxide between the liquid/solid and gas phase was instantaneous.
- No heat losses from the reactor surface to the surroundings occurred.
- Heat was lost from the system by convective sensible heat transfer and evaporation. No conduction or radiation from the organic material or the air in the base and headspace occurred.
- Condensation did not occur inside the system.
- The thermodynamic properties, such as the latent heat of evaporation and specific heat capacity, did not change with temperature.

- The pH of the organic material changed according to Figure 5.5.
- The ammonia emissions were controlled by the transfer of ammonia in the liquid phase.
- The micro-organisms only used ammoniacal nitrogen to assimilate new biomass.
- The nitrogen in biomass was stable and did not further contribute to ammonia emissions.
- Pathogens were inactivated by high temperatures only.

5.4. Model simulations

A model of the process equations was created with the software package *ModelMaker*. The solutions were found using Runge-Kutta integration, with a time step of one hour. Details of the implementation in *ModelMaker* are shown in Section A5.2.

Sensitivity analyses were performed on the process factors, which were determined by the initial characteristics of the organic material. The factors corresponded to those investigated in the composting experiments (Chapter 6). The factors analysed were:

1. The initial wet mass mixing ratio of manure to straw (M:S ratio) of 2, 3 and 4 for organic material with an initial moisture content of 65 % and pH of 8. The three mixing ratios corresponded to C:N ratios of about 25, 20 and 15, respectively.
2. The initial pH of 6, 7 and 8 for organic material with an initial M:S ratio of 3:1 and moisture content of 65 %.

During the composting process, the pH of the organic material is expected to change, initially as organic acids are decomposed and then as ammonia is produced. However, under some circumstances, such as when an acidic substrate with a low nitrogen content is composted, the pH may not change as much from the initial pH as Figure 5.6 suggests. A sensitivity analysis was therefore performed on pH for constant values of 6, 7 and 8 in an organic material with an initial M:S ratio of 3:1 and moisture content of 65 %.

Further sensitivity analyses were carried out to evaluate the effect of the moisture content of the organic material on the composting process. The moisture content was altered by either changing

- a) the initial moisture content of the organic material or
- b) the mass of water evaporated in the gas stream and lost from the system.

Initial moisture contents of 60 %, 65 % and 70 % were investigated for an organic material with an initial M:S ratio of 3:1 and pH of 8. The mass of water lost from the system in the off-gas was determined by the degree of off-gas saturation, S (Section 5.3.1.2.1). A sensitivity analysis was performed on S for an organic material with an initial M:S ratio of 3:1, pH of 8 and MC of 65 %.

The simulation results were presented as the mass, temperature and nitrogen profiles for each of the sensitivity analyses. The composition of the off-gas was also determined in the simulation. The profiles of the functional effects of the moisture content, f_{MC} , and oxygen content, f_{OC} , showed when each of the factors became limiting.

In *ModelMaker*, the Parameter view listed and quantified the initial and fixed value factors of the model that were referenced by the model components (Tables 5.2 and 5.3). The factors on which the sensitivity analyses were performed are indicated in the ‘condition’ column of Table 5.3. The default value is indicated by an asterisk.

Table 5.2. Parameter values of the manure and straw used for model simulations

Parameter	Symbol		Condition	Value		Units
	Pig manure	Straw		Pig manure	Straw	
Total solids (TS) content	TSM	TSS	None	0.25	0.90	kg kg ⁻¹
Volatile solids (VS) content	VSM	VSS	None	0.82	0.88	kg kg ⁻¹ TS
Biodegradability	BM	BS	None	0.73	0.55	kg kg ⁻¹ VS
Total nitrogen content	TNM	TNS	None	0.050	0.006	kg kg ⁻¹ TS
Amm. nitrogen content	ANM	ANS	None	0.014	0.0005	kg kg ⁻¹ TS

Table 5.3. The values of the organic material and process parameters

Parameter	Symbol	Conditions	Value	Units
	Organic material		Organic material	
Initial total solids mass	MTSin	None	14	kg
Initial moisture content	MCin	Sensitivity Analysis	0.60	kg kg ⁻¹
			0.65*	kg kg ⁻¹
			0.70	kg kg ⁻¹
Initial mixing ratio (M:S ratio)	Mix	Sensitivity Analysis	2	kg kg ⁻¹
			3*	kg kg ⁻¹
			4	kg kg ⁻¹
Initial pH	pHin	Sensitivity Analysis	6	-
			7	-
			8*	-
φ of equation 5 (xviii)	Phi	Sensitivity Analysis	0	-
			0.1	-
			0.2	-
Reference SOUR (20°C)	SOUR20	None	400	mg h ⁻¹ kg ⁻¹ TS
Chemical oxygen demand	COD	None	415	mg kg ⁻¹ TS
Initial temperature	TCin	None	20	°C
Air temperature	Tair	None	20	°C
Water heat capacity	CpW	None	4.186	kJ kg ⁻¹ °C ⁻¹
TS heat capacity	CpTS	None	1.27	kJ kg ⁻¹ TS °C ⁻¹
Dry air heat capacity	Cpair	None	1.10	kJ kg ⁻¹ °C ⁻¹
Heat of oxygen respiration	HO2	None	14.8	kJ g ⁻¹ O ₂
Latent heat of evaporation	HL	None	2454	kJ kg ⁻¹ H ₂ O
Water content of saturated air relative humidity 50%	WBA	None	23.32	g kg ⁻¹ dry air
Water content of saturated air relative humidity 70%	WCA	None	10.33	g kg ⁻¹ dry air
Volumetric airflow rate of baseline aeration	VFBA	Default	5	l min ⁻¹
Volumetric airflow rate of cooling aeration	VFCA	T > 60 °C	25	l min ⁻¹
Cell yield	Cell_Y	None	0.2	kg kg ⁻¹ TS
Cell nitrogen content	Cell_N	None	12	%TS

5.4.1. Sensitivity analyses

During a sensitivity analysis, the model systematically adjusted the value of the selected parameter to obtain an indication of how sensitive the calculated values of other model components were to the changes. The sensitivity analysis was defined in *ModelMaker* using the window displayed in Figure A5.2.

5.4.1.1. Initial mixing ratio (M:S ratio)

The initial total solids mass (14 kg) and wet mass (40 kg for an initial moisture content of 65 %) were set values but the equilibrium mass (MTSe) varied with the mixing ratio because of the different biodegradability of pig manure and straw. The biodegradability of the volatile solids was assumed to be about 73 % and 55 % for the manure and straw, respectively [Haug 1993]. These values were determined under anaerobic conditions at 35 °C. Data on the degradability of the straw and manure under aerobic conditions was limited and while significant degradation appears possible during aerobic composting, a number of factors affect the decomposition rate and there is some debate whether it is significantly higher than in anaerobic conditions [Richard 2000]. The initial pH of the organic material was always 8 for this sensitivity analysis.

The exponent constants of equation (5 viii), which described the temperature factor (f_T), depended on the mixing ratio of the organic material. In the model, it was assumed that the exponents were the same for all the mixing ratios and the values specific to organic material with a mixing ratio of 2, as determined empirically in the respirometry experiments, were used. The reaction rate coefficient was calculated from the SOUR and the corresponding COD of the organic material. Although the COD also depended on the mixing ratio, the COD for the mixing ratio of 2 was used for all the mixing ratios in order to be consistent in equation (5 xi).

Figures 5.10 to 5.12 respectively show the mass, temperature and nitrogen profiles that were generated from simulations with the three initial mixing ratios of 2, 3 and 4. Profiles of the mass of total solids (MTS) and water in the organic material (MW) and the cumulative mass of carbon dioxide produced (MCO2) represented the mass model. The rate of loss of total solids followed a first order decay curve after 1 day, which was reflected by the profiles of the cumulative mass of carbon dioxide produced and oxygen consumed (not shown) as their changes were related by the corresponding partition coefficients (Section A5.1.3). The rate of loss of water during the period when the cooling aeration was in use (25 to 100 hours) was constant as it largely depended on the rate of water evaporation into the gas stream, the flow rate and condition of which was predetermined.

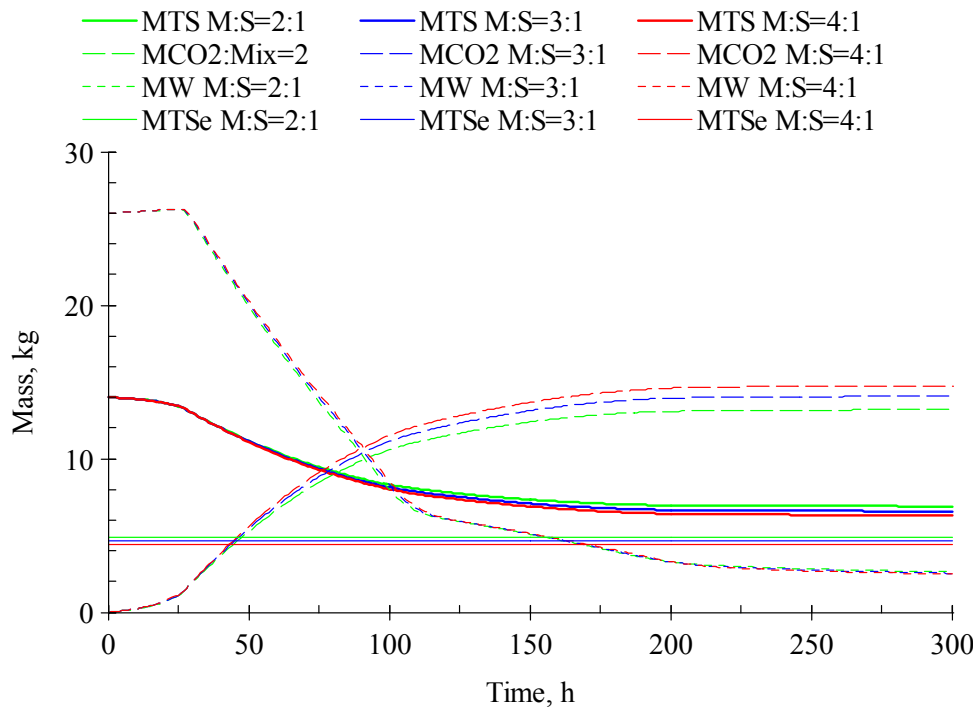


Figure 5.10. Mass profiles from the initial mixing ratio simulations (MTS – mass total solids, MW – mass organic material water, MCO2 – mass carbon dioxide and MTSe – equilibrium mass of total solids)

The temperature (TC) profile represented the energy model and reflected the balance between the energy flows into and out of the system as defined by equation (5 xxiii). With

only the baseline aeration in operation during the first day, the heat energy inputs to the system were greater than the outputs and so the temperature increased. On activation of the cooling aeration, the energy into and out of the system were in balance until the heat removed from the system became greater than that that was being produced by microbial activity. The temperature of the organic material then decreased, almost as rapidly as it had initially risen.

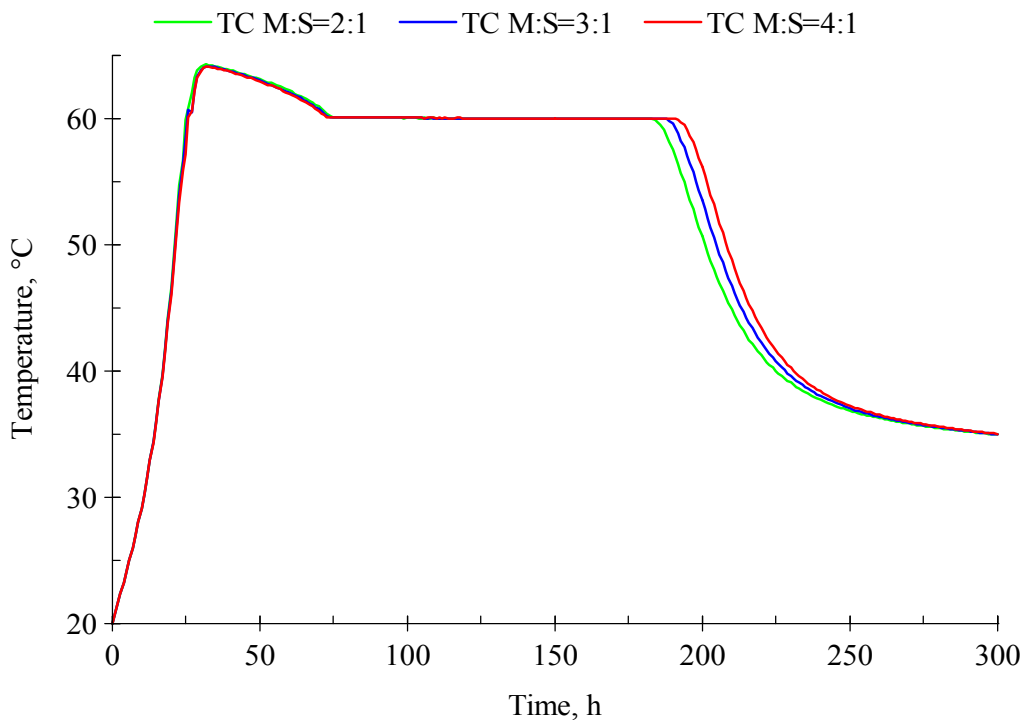


Figure 5.11. Temperature profiles from the initial mixing ratio simulations (TC- composting temperature of the organic material)

For the ammonia model, the change in the mass of the bulk ammoniacal nitrogen (MAN) from the initial value is shown along with the cumulative mass of ammonia emitted (MNH₃emit) and the mass of ammonia in the liquid phase at phase boundary (MNH₃aq) in Figure 5.22. The mass of ammonia at the phase boundary rose rapidly with the increase in pH of the organic material. As a result of ammonia emissions, which were encouraged by the high airflow rate of the cooling aeration and the high temperatures in the organic material, and the exhaustion of the ammoniacal nitrogen in the bulk of the organic material, the ammonia in

the liquid phase decreased after the first day until none remained after 6 days. The increase in the mass of ammonia emitted reflected the decrease of ammonia in the liquid phase and reached an asymptote after 6 days. The decrease in the mass of total nitrogen of the organic material (profile not shown) corresponded to the mass of nitrogen lost through ammonia emissions. The mass of organic nitrogen (profile not shown) increased as a result of the synthesis of new biomass until the ammoniacal nitrogen was exhausted after which the masses of total and organic nitrogen remained constant.

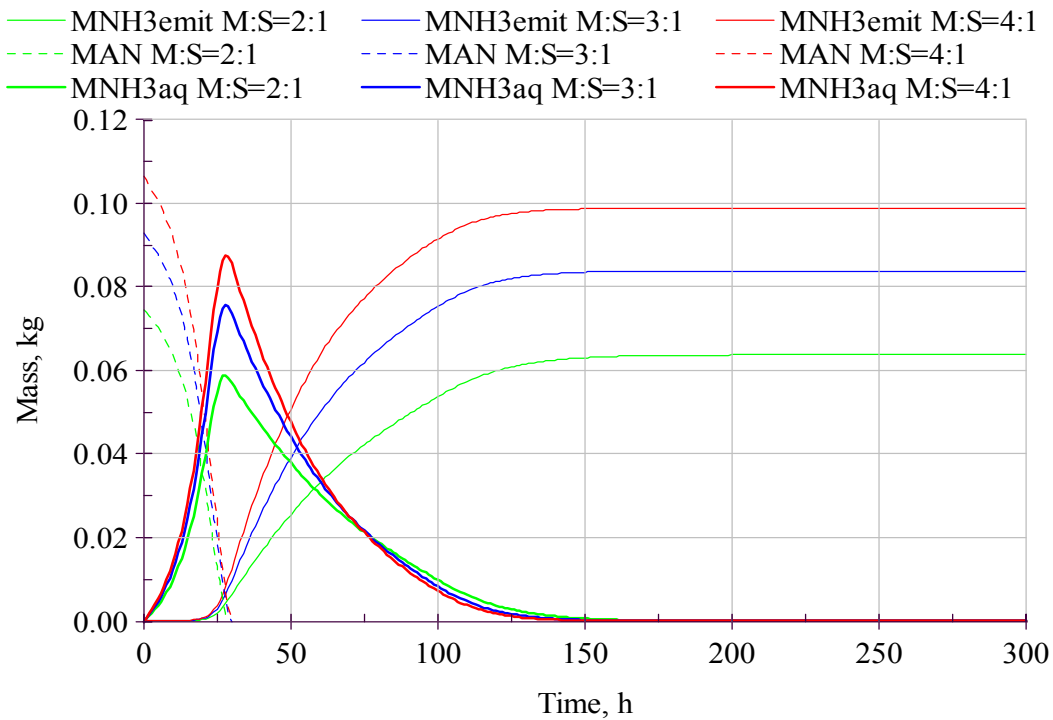
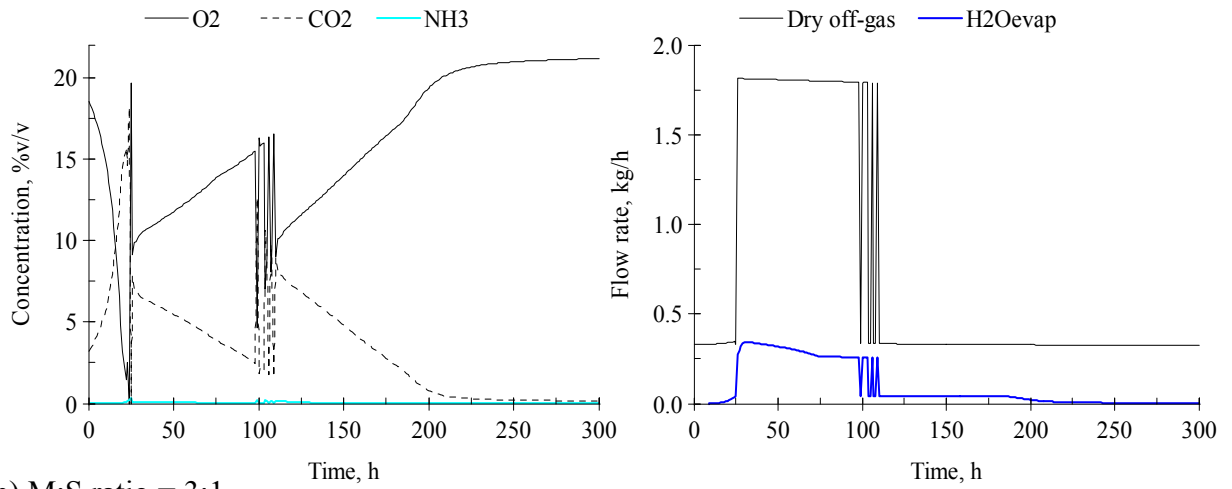


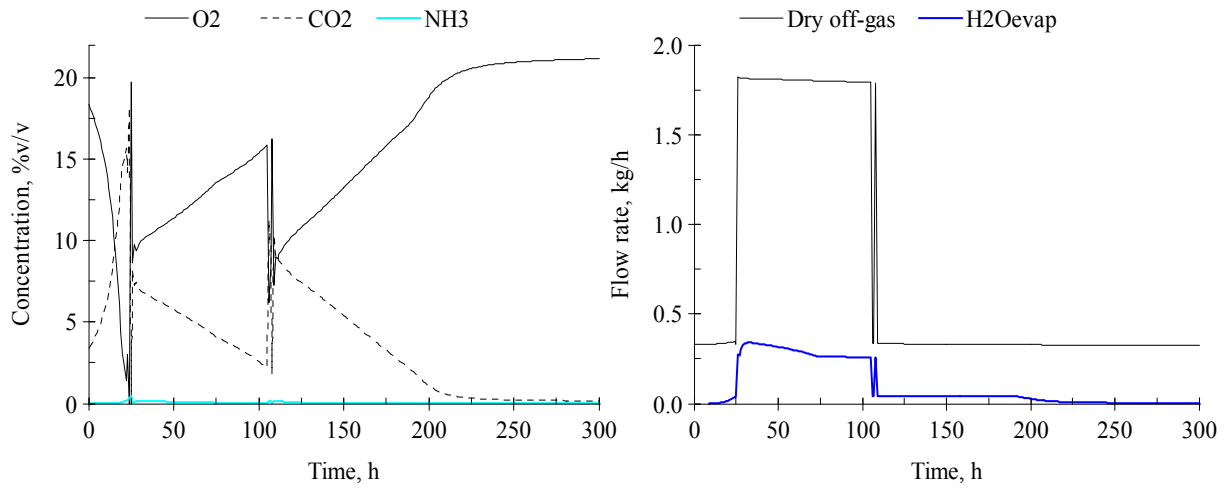
Figure 5.12. Nitrogen profiles from the initial mixing ratio simulations. (MNH3emit – total ammonia emitted, MAN – bulk ammoniacal nitrogen, MNH3aq – liquid phase ammonia)

Figures 5.13 a) to c) show the profiles of the oxygen, carbon dioxide and ammonia gas concentrations in the off-gas and the corresponding profiles of the dry gas flow and mass of water evaporated (H2Oevap) from the system for the mixing ratios 2 to 4, respectively. The ammonia concentration is shown on the same scale as the carbon dioxide and oxygen to illustrate the comparatively small volume ammonia that was in the off-gas.

a) M:S ratio = 2:1



b) M:S ratio = 3:1



c) M:S ratio = 4:1

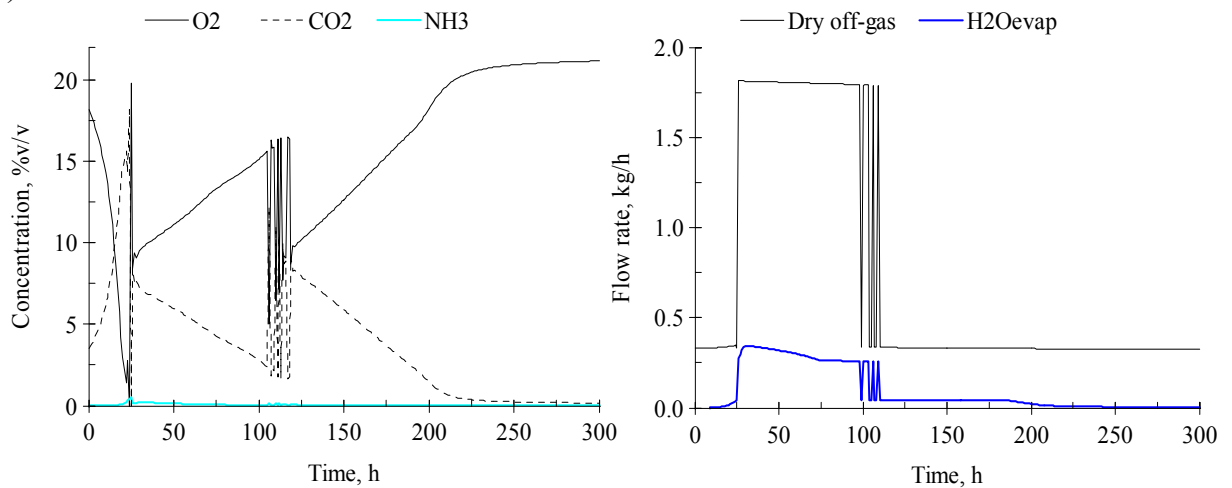


Figure 5.13. The off-gas composition and aeration profile from the mixing ratio simulations. (O2 –oxygen, CO2 -carbon dioxide and NH3 -ammonia gas concentrations and H2Oevap – mass of water evaporated)

5.4.1.2. Initial pH

The mass and temperature profiles from the sensitivity analysis performed on the initial pH of the organic material (pHin) for values of 6, 7 and 8 were virtually identical and the same as those from the runs with a mixing ratio of 3 in Section 5.5.1.2 and are not shown.

The profiles the bulk ammoniacal nitrogen, ammonia in solution at the phase boundary and the mass of ammonia emitted indicated the dynamics of the ammonia during the model simulation (Figure 5.2.4). The initial mass of ammoniacal the same for all three simulations (mixing ratio of 3) so that any difference in the ammonia profiles was in response to the different initial pH of the organic material.

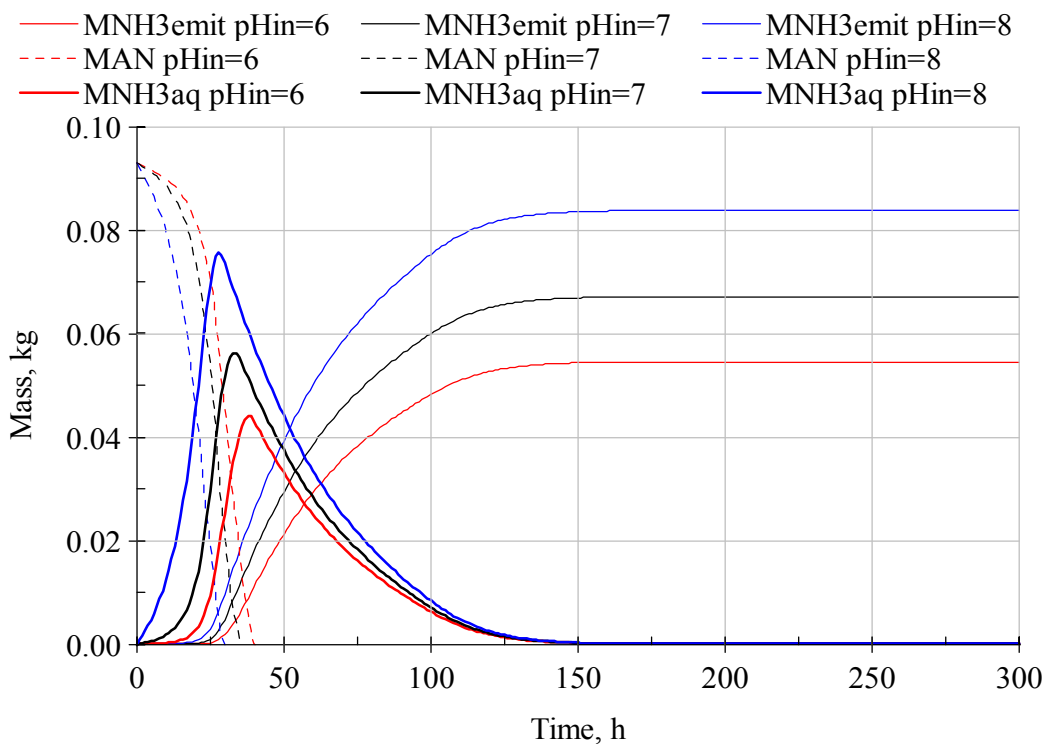
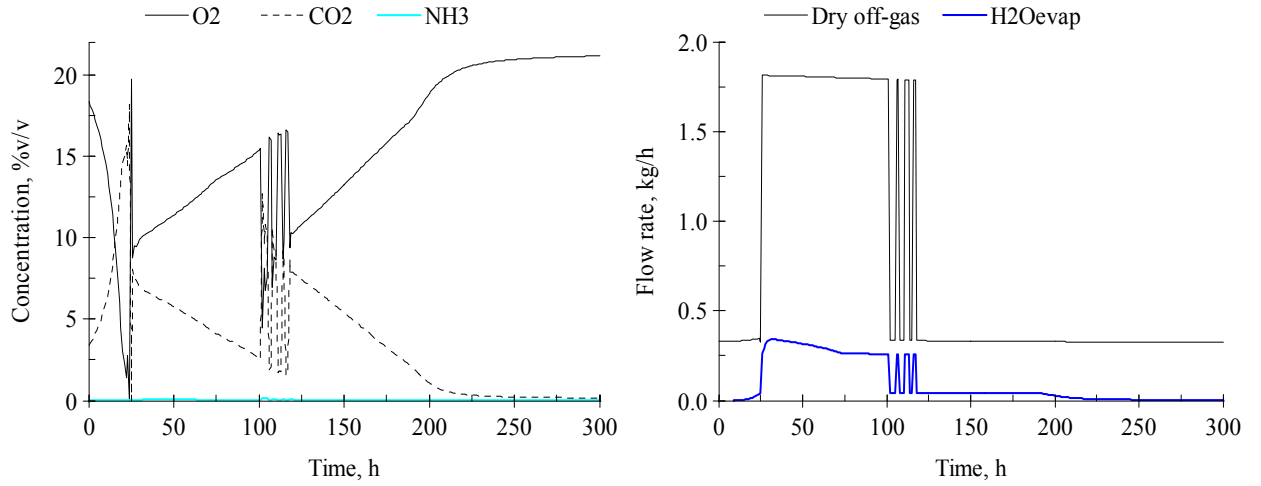


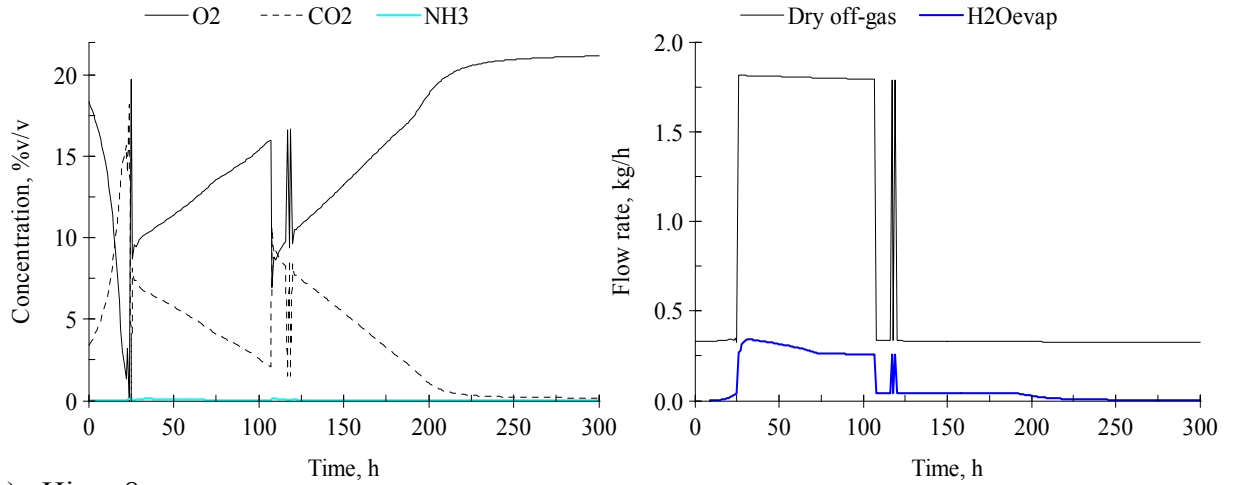
Figure 5.14. Nitrogen profiles from initial pH simulations. (MAN –ammoniacal nitrogen, MNH3emit -total ammonia emitted, MNH3aq – liquid phase ammonia mass)

Figures 5.15 a) to c) show the profiles of the oxygen, carbon dioxide and ammonia gas concentrations in the off-gas and the corresponding profiles of the dry gas flow and mass of water evaporated (H2Oevap) from the system for the initial pH values of 6 to 8, respectively.

a) pH_{in} = 6



b) pH_{in} = 7



c) pH_{in} = 8

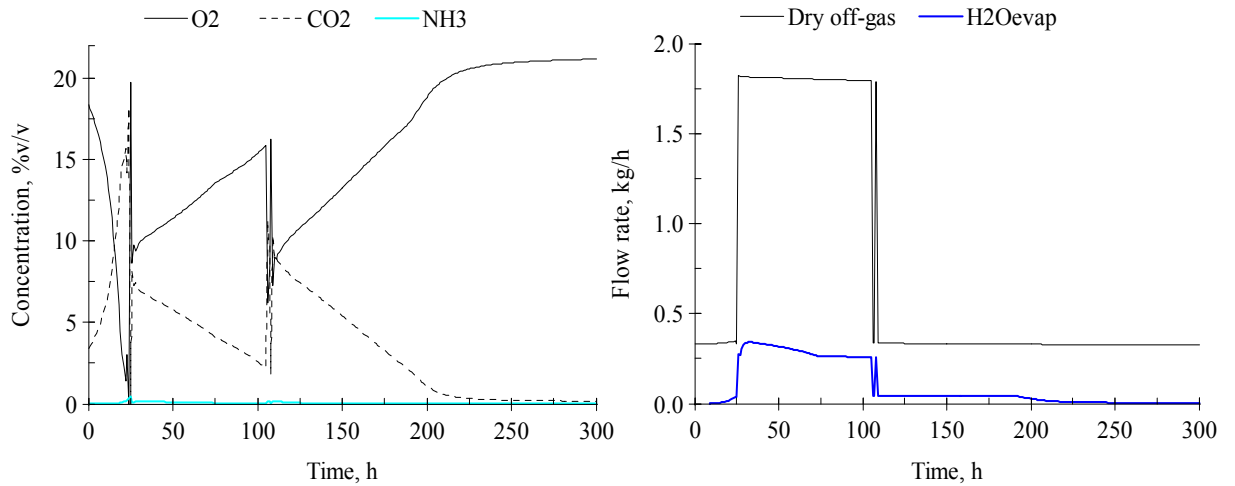


Figure 5.15. The off-gas composition and aeration profiles from the initial pH simulations. (O₂ - oxygen, CO₂ - carbon dioxide and NH₃ - ammonia gas concentrations and H₂Oevap – mass of water evaporated)

The oxygen concentration decreased sharply during the initial rise in temperature and increased to above 8 %v v⁻¹ after the cooling aeration was activated. The carbon dioxide concentration profile reflected that of the oxygen because the mass of oxygen consumed and carbon dioxide produced were related by partition coefficients (Section A5.1.3). The step change in the oxygen and carbon dioxide concentrations between 100 and 125 hours corresponded to the switch between the baseline and cooling aeration in response to temperature fluctuations about 60 °C. The ammonia concentration in the off-gas peaked at 25 hours when the cooling aeration was first activated.

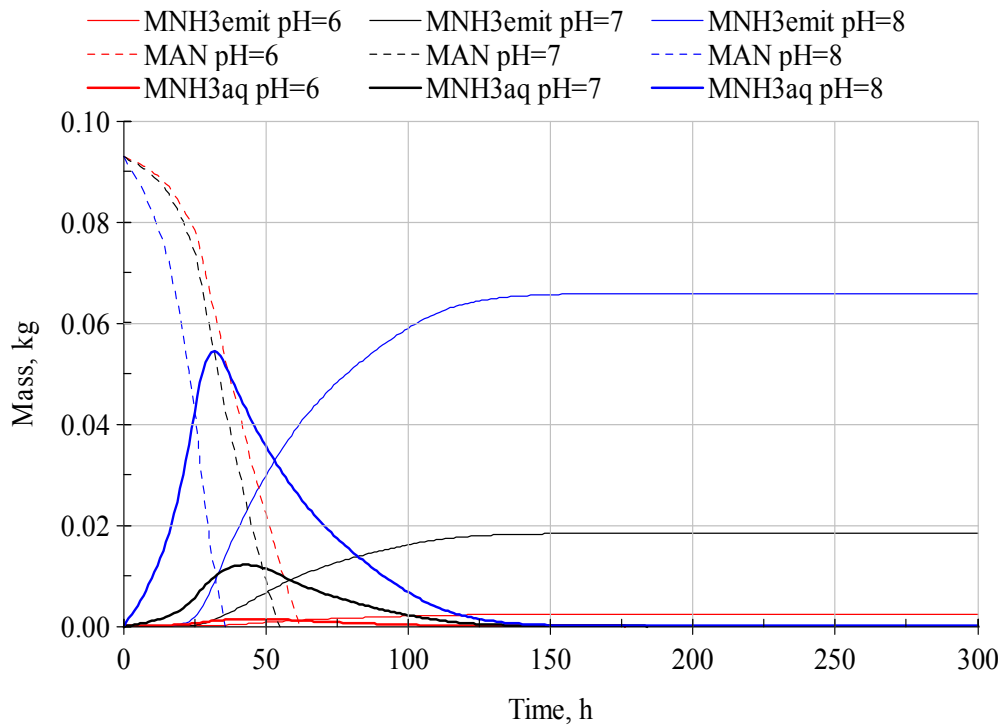


Figure 5.16. Nitrogen profiles from constant pH simulations. (MAN – ammoniacal nitrogen, MNH3emit – total ammonia emitted and MNH3aq –liquid phase ammonia mass)

To assess the effect of organic material pH further, the organic material pH was held constant at 6, 7 or 8. In this range, the pH was assumed to not affect microbial activity and so, as with the initial pH sensitivity analysis, the temperature profile and the total solids, carbon dioxide and water mass profiles did not vary between the three pH values. The ammonia profiles (Figure 5.16) were similar to those produced by the initial pH simulations.

However, the mass of ammoniacal nitrogen converted to ammonia and emitted was greatly reduced at pH values below 8.

5.4.1.3. Initial moisture content

The initial total solids mass (14 kg), equilibrium mass (4.6 kg) and the initial pH (8) were fixed. The wet mass varied according to the mass of water in the organic material i.e. about 35 kg, 40 kg and 47 kg for moisture content of 60 %, 65 % and 70 %, respectively. Although the optimum moisture content for composting farm yard manure with straw was reported to be as high as 80 % [Jeris and Regan 1973b], the values selected for initial moisture content sensitivity analysis were generally accepted as the optimum moisture contents for the composting [Gray *et al* 1971a, McKinley *et al* 1986]. Furthermore, straw was able to absorb at least three times its dry mass in water [Jeppsson 1998], which was equivalent to a moisture content of about 78% and therefore no leachate was expected.

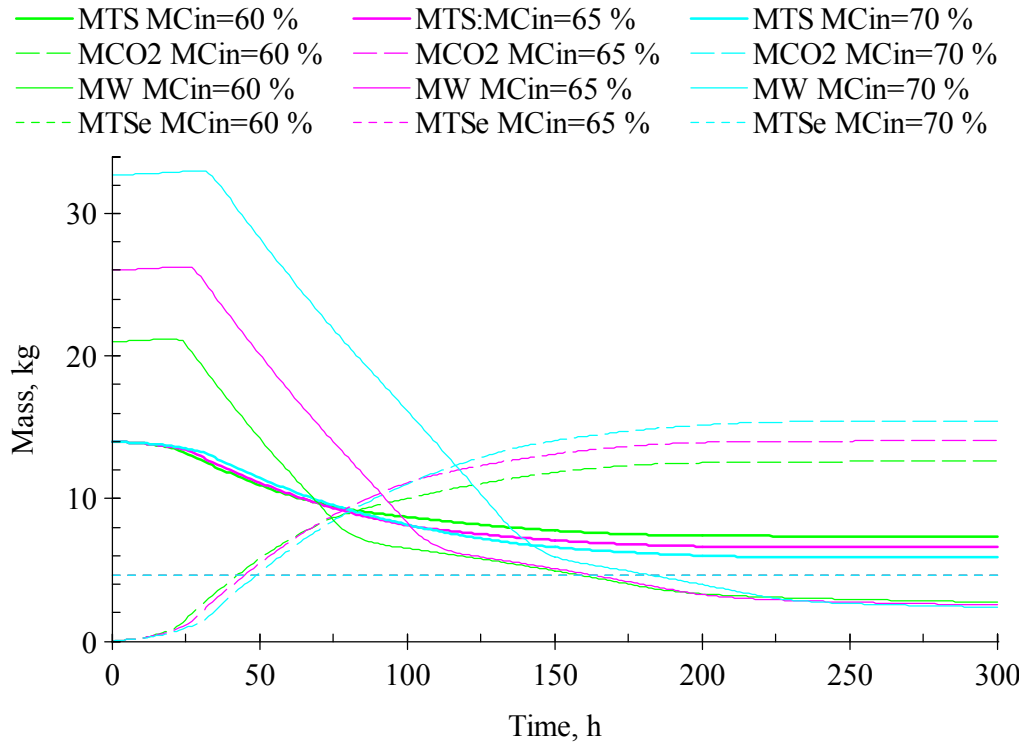


Figure 5.17. Mass profiles from initial moisture contents simulations. (MTS –total solids, MW – water and MCO2 – carbon dioxide mass)

Figures 5.17 to 5.19 respectively present the mass, temperature and nitrogen profiles generated from the simulations for the three initial moisture contents, 60 %, 65 % and 70 %. The initial mass of the water in the organic material obviously increased with the initial moisture content. The mass of water in the organic material during the simulation was a balance between the water generated as a result of the loss in total solids, as determined by its partition coefficient, and the water evaporated into the gas phase. The pattern of water loss was therefore the same because it was largely influenced by the flow rate and condition of the air. The moisture content of the organic material increased during the initial stages of composting when the rate of water generation was high and the rate of water evaporation was low. On activation of the cooling aeration, the mass of water lost by evaporation exceeded the mass generated by microbial activity, although this was still at its maximum rate. The profiles of process variables related to moisture content, such as the specific heat capacity of the wet organic material, reflected the difference in moisture content in the three simulations.

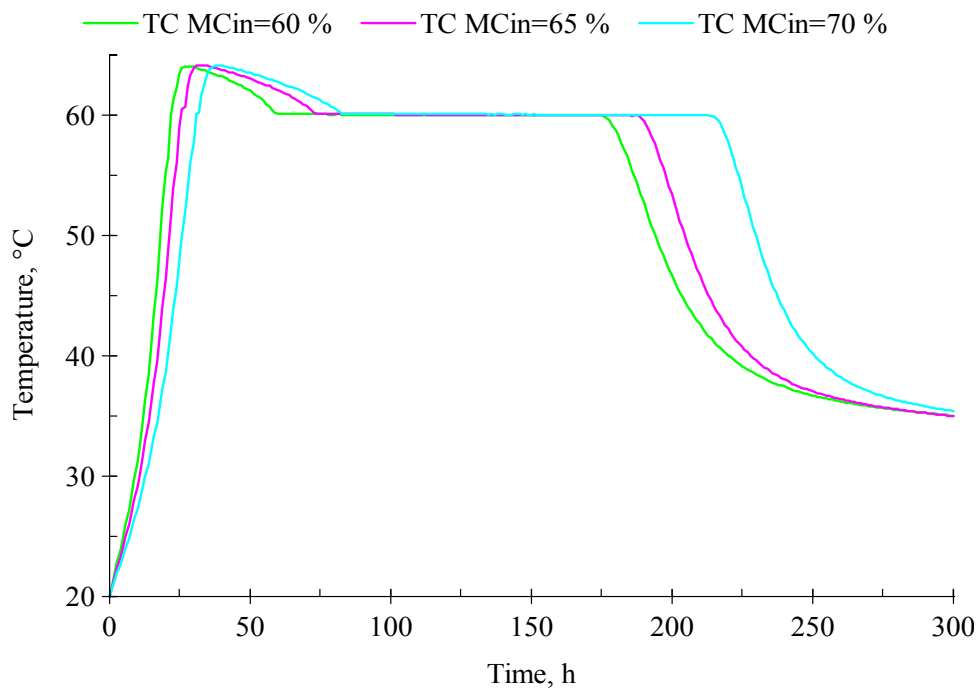


Figure 5.18. Temperature profiles from initial moisture content simulations. (TC – composting temperature)

The initially temperature rose more rapidly in the organic material with the lower initial moisture contents but the time for which the temperature was at 60 °C increased with the initial moisture content. The rate of ammonia emissions was therefore higher from the organic material with the lower initial moisture contents but the final mass of ammonia emitted increased with the initial moisture content.

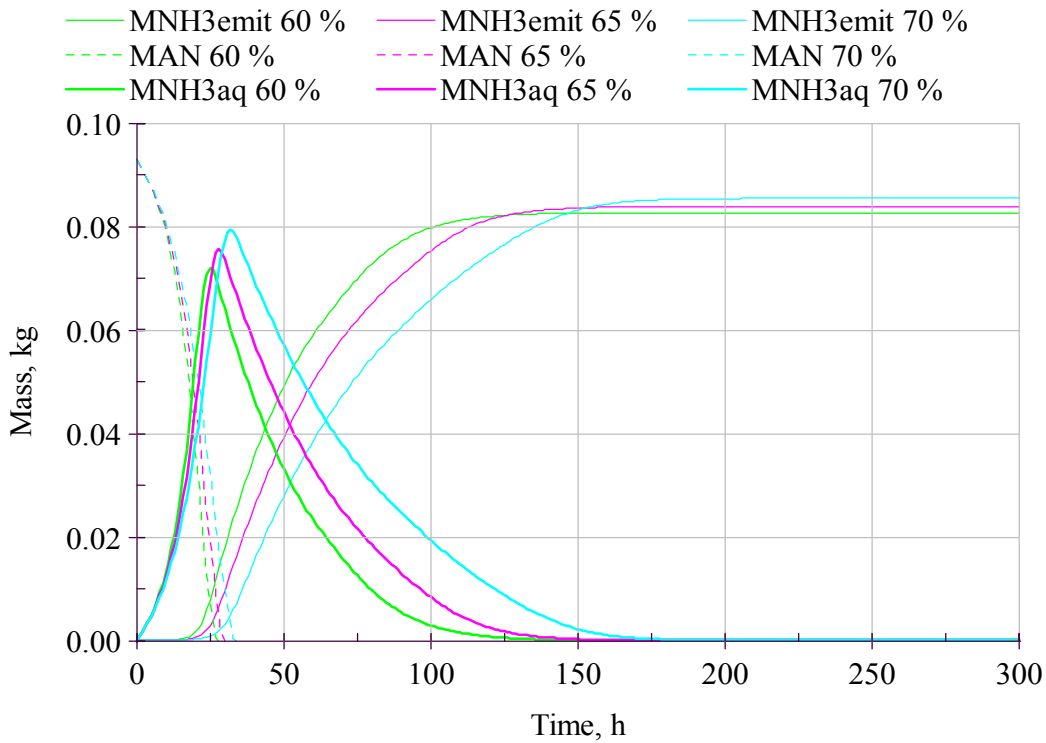
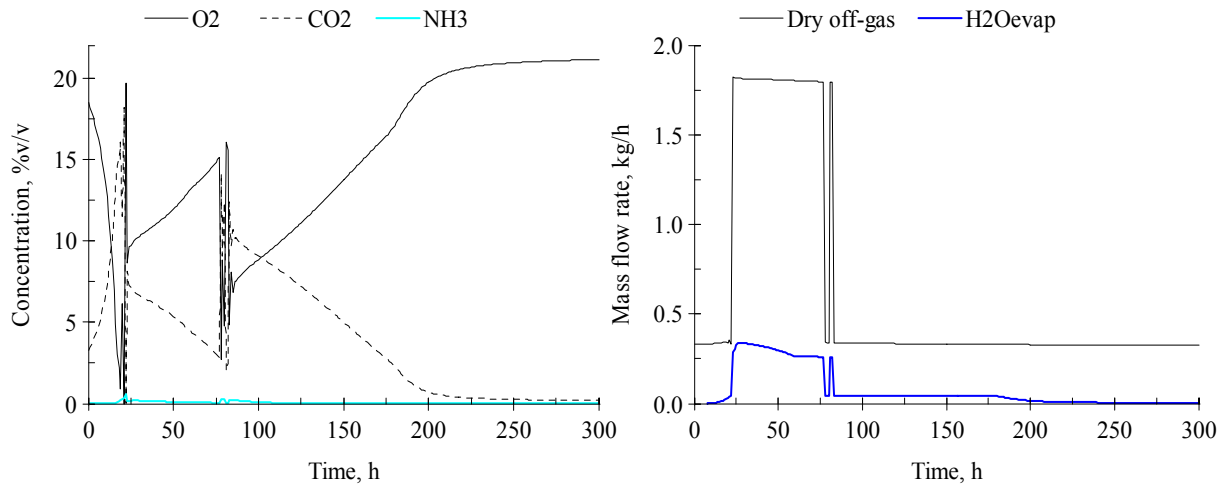


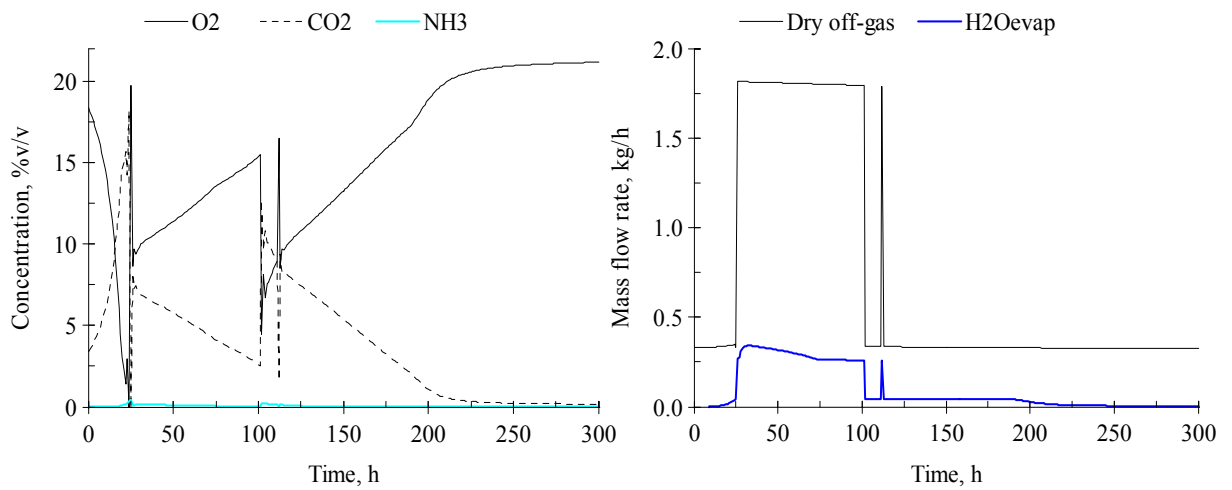
Figure 5.19. Nitrogen profiles from initial moisture content simulations. (MNH3emit – total ammonia emitted, MAN – ammoniacal nitrogen, MNH3aq – liquid phase ammonia mass)

Figures 5.20 a) to c) show the profiles of the oxygen, carbon dioxide and ammonia gas concentrations in the off-gas and the corresponding profiles of the dry off-gas flow and mass of water evaporated (H_2O_{evap}) for the initial moisture contents of 60% to 70%, respectively. The profiles were markedly different between the initial moisture content simulations, firstly with the onset and duration of fluctuations in the aeration and consequently in the off-gas concentrations, secondly with the concentrations to which the oxygen and carbon dioxide fell and finally with the duration for which evaporation of water occurred.

a) MCin = 60 %



b) MCin = 65 %



c) MCin = 70 %

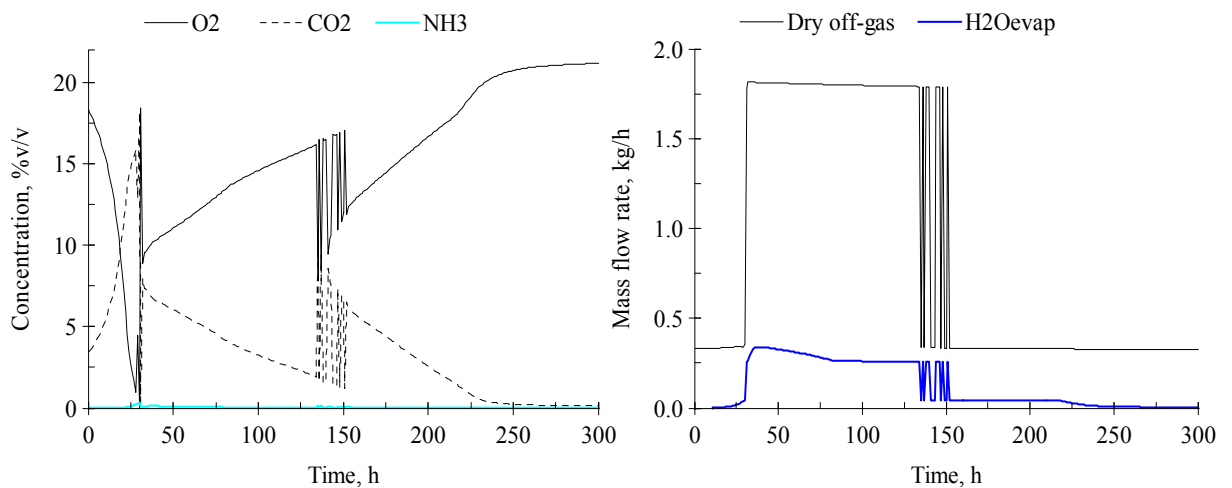


Figure 5.20. The off-gas composition and aeration profiles from initial moisture content simulations. (O2 - oxygen, CO2 - carbon dioxide, NH3 - ammonia gas concentrations and H2Oevap – mass of water evaporated)

5.4.1.4. Off-gas saturation

The mass of water evaporated into the gas stream, and therefore the degree of off-gas saturation (S), affected the amount of heat lost from the system. The temperature profile of the simulation was a good indicator the system's performance, and so showed the impact of S on the process. In the model, the sensitivity analysis was performed on ϕ (Equation 5 xviii) for values between 0 and 0.2. This exponent determined the value S, such that for $\phi=0$, $S=100\%$ and for $\phi=0.2$, $S\approx 11\%$ when the cooling aeration airflow rate was used ($F=25\text{ l min}^{-1}$). For values of ϕ above 0.02 ($S=65\%$ for $F=25\text{ l min}^{-1}$), the heat removed by evaporation was too low to control the temperature at 60°C using the specified airflow rate of the cooling aeration. A sensitivity analysis was therefore performed on ϕ for values of 0, 0.01 and 0.02 (Figures 5.21 to 5.23).

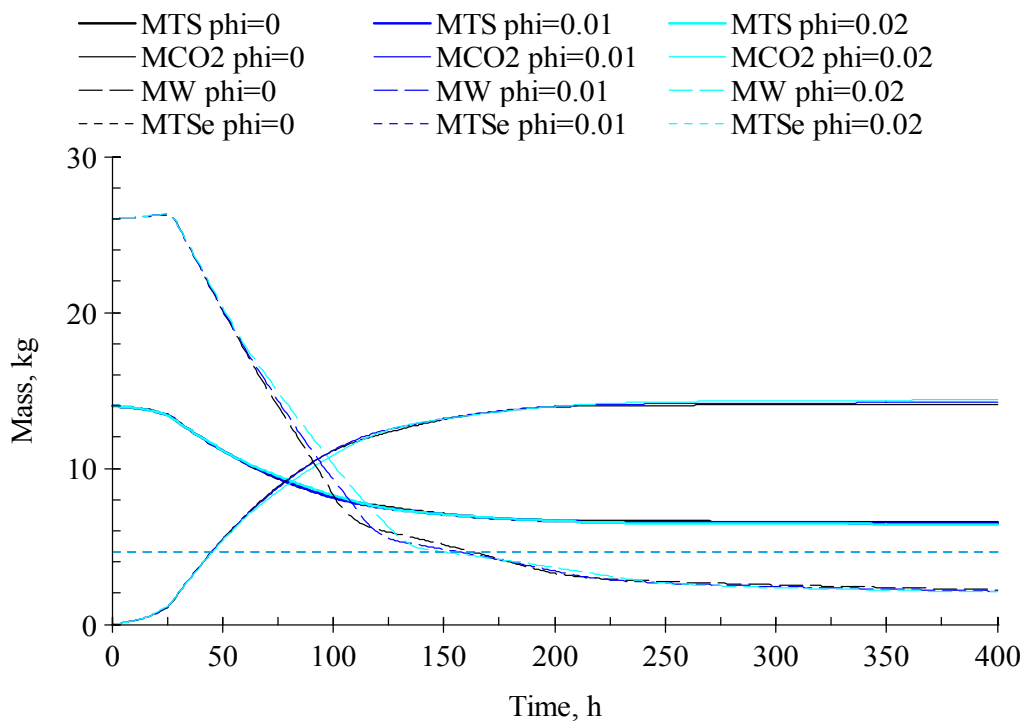


Figure 5.21. Mass profiles from ϕ simulations. $S = 65\%$ (—), 80% (—) and 100% (—). (MTS – total solids, MW – water and MCO2 – carbon dioxide mass)

After 50 hours the decrease in the mass of water in the organic material became less pronounced at the higher ϕ values but there was little difference between the final values reached after 250 hours (Figure 5.21). The small difference between the total solids and carbon dioxide mass profiles was due to the longer period at 60°C at the higher ϕ values (Figure 5.22). An increase in ϕ increased the mass of total solids lost and carbon dioxide produced but the asymptotes that the total solids profiles reached were least 1.8 kg above the equilibrium mass.

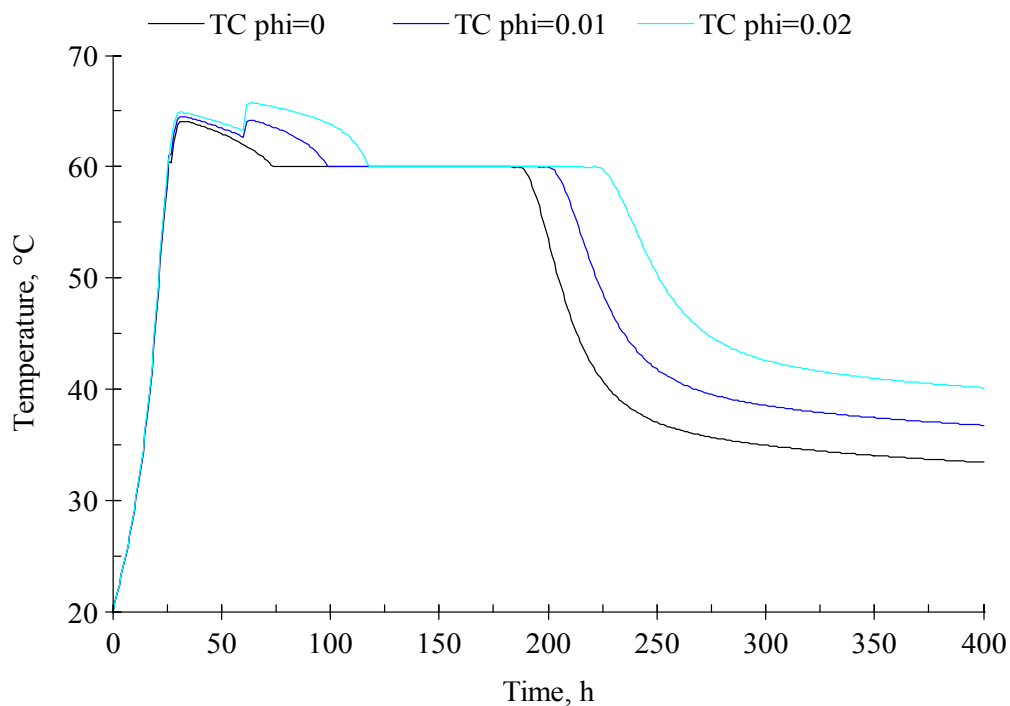


Figure 5.22. Temperature profiles from ϕ simulations. $S = 65\%$ (—), 80% (—) and 100% (—). (TC – composting temperature)

The temperature initially rose at the same rate regardless of the off-gas saturation (Figure 5.22). However, the temperature overshoot above 60°C after 25 hours, increased with the value of ϕ . Then at about 60 hours the temperature increased again in the systems with the unsaturated off-gas, which resulted in a second temperature rise before the cooling aeration was able to control the temperature around 60°C. The fall in the temperature at the end of the process was delayed and at a slower rate in the system with the unsaturated off-gas.

The effect of ϕ on the ammonia dynamics was only evident between 50 and 150 hours (Figure 5.23) when the rate of ammonia emission, and therefore the decrease in ammonia in solution at the phase boundary, increased with the value of ϕ . The total mass of ammonia emitted reached the same asymptote at the same time (150 hours) for all three ϕ values.

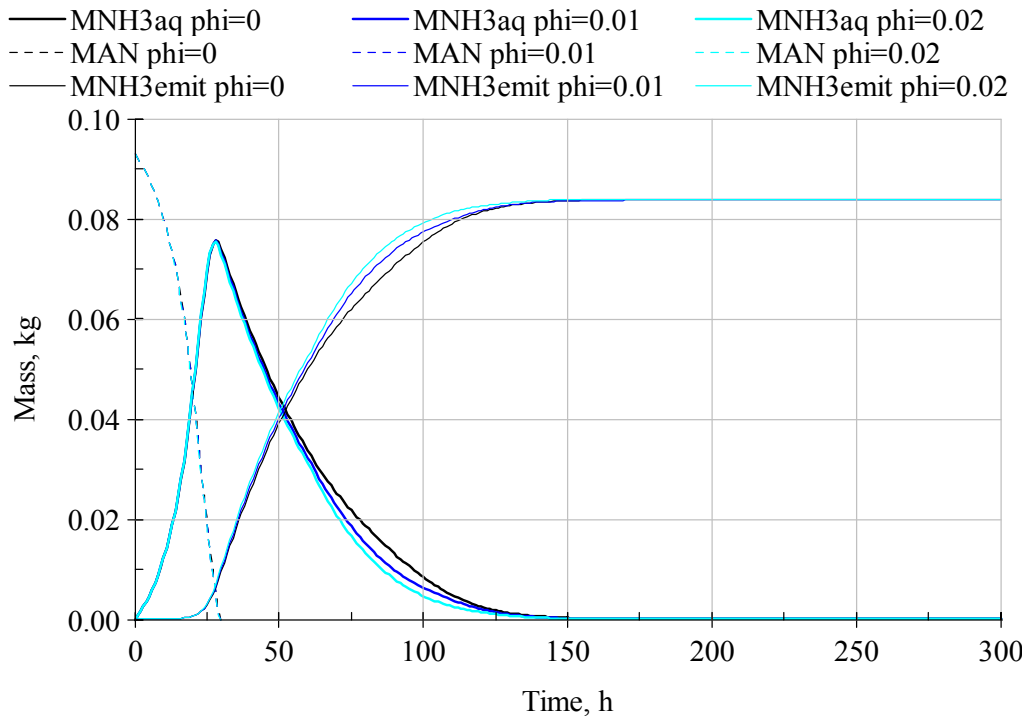


Figure 5.23. Nitrogen profiles from ϕ simulations. (MNH3emit – total ammonia emitted, MAN – ammoniacal nitrogen, MNH3aq – liquid phase ammonia mass)

Figures 5.24 a) to c) show the simulated profiles of the off-gas concentrations and the corresponding aeration profiles. The water evaporation profile (H_2O_{evap}) differed between simulations with the mass evaporated decreasing and the duration increasing with increasing ϕ values. The frequency and depth of the fluctuations in the oxygen and carbon dioxide concentrations decreased with increasing ϕ values, which reflected the pattern shown by the corresponding aeration profiles.

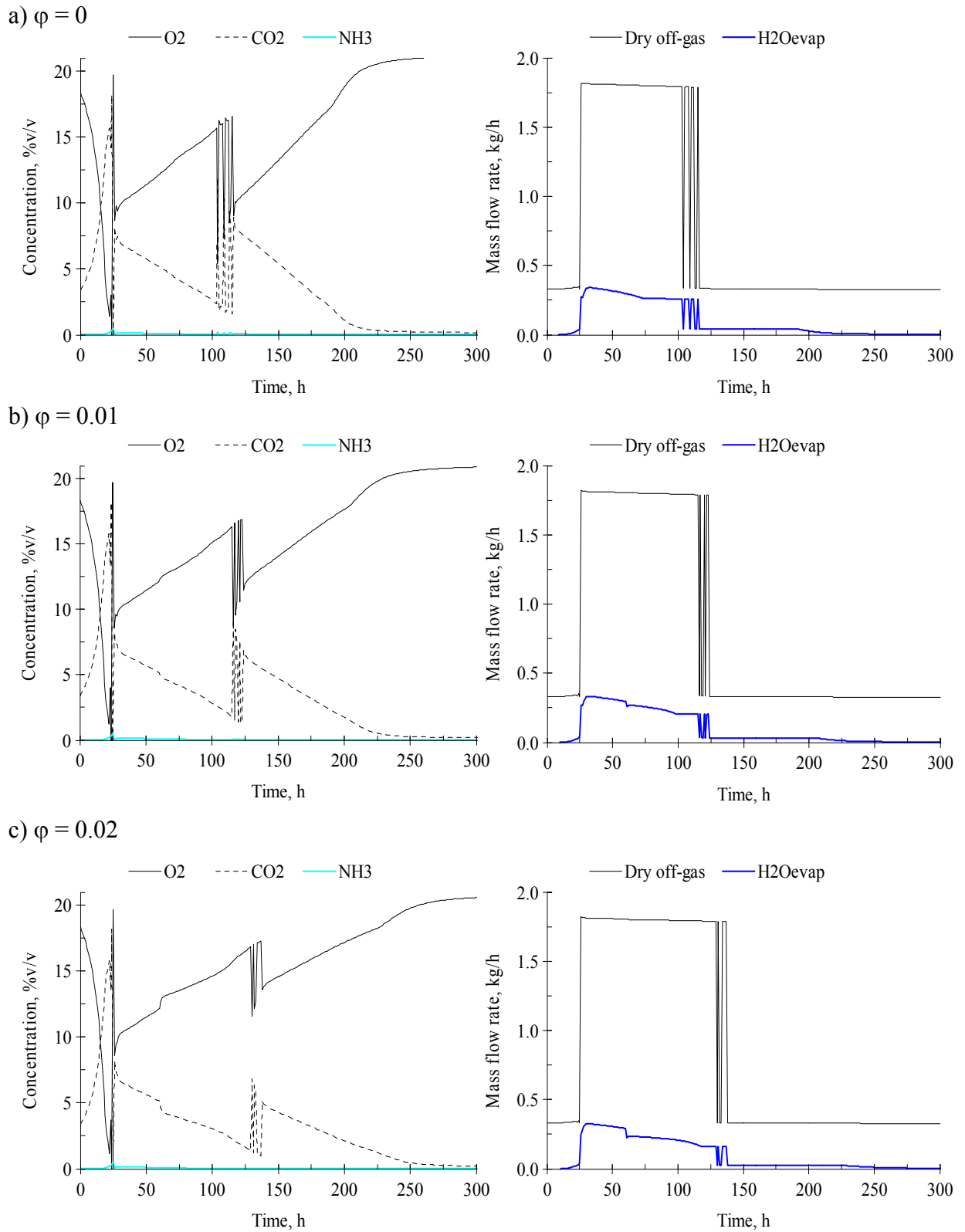


Figure 5.24. The off-gas composition and aeration profiles from ϕ simulations. (O₂ - oxygen, CO₂ - carbon dioxide and NH₃ - ammonia concentrations and H₂Oevap – mass of water evaporated)

5.5. Discussion

5.5.1. Initial mixing ratio sensitivity analysis

The effect of the mixing ratio on the decomposition rate was small because f_T , as defined by equation (5 viii), and the COD for initial mixing ratio of 2 was assumed to represent the activity for all the initial mixing ratios analysed. The difference between the decomposition rates was largely determined by equilibrium mass, MTSe, which were 4.9, 4.6 and 4.4 kg for the initial mixing ratios of 2 to 4, respectively. Equilibrium, however, was not reached in any of the mixing ratio simulations, as the moisture content in the organic material became a limiting process factor. The f_{MC} fell sharply after 100 hours (Figure 5.25). The mixing ratio had little effect on the mass profile of the water in the organic material and, therefore, the profiles of related process variables, such as the organic material specific heat capacity, were practically the same for the three levels simulated.

The temperature of the organic material rose at the same rate for the three initial mixing ratios (Figure 5.11) and the profiles were the same except that 60 °C was sustained for a little longer in the organic material with the initial mixing ratio of 4. The temperature was above 55 °C for more than 7 days in all the simulations, which was sufficient time to achieve thermal inactivation of pathogens.

The aeration strategy successfully controlled the upper temperature limit around 60 °C in all three simulations and provided sufficient oxygen to meet the microbial demand, except in the initial stage of composting when the temperature first approached 60 °C. Here, the rate of oxygen consumption, as determined by the SOUR defined in equation (5 xiii), was greater than that provided by the baseline airflow rate of 5 l min⁻¹ (0.34 kg h⁻¹). This led to a sharp fall in the f_{OC} and therefore the microbial activity (Figure 5.25). The high airflow rate of the

cooling aeration ($25 \text{ l min}^{-1} = 1.8 \text{ kg h}^{-1}$), resulted in a well aerated system during the period of maximum microbial activity. The f_{OC} fluctuated during the latter stages of the period of high microbial activity when the temperature began to rise and fall around the 60°C . The effect on the aeration demand, and therefore the amount of oxygen supplied to the organic material, was short lived and relatively small compared to the fall in f_{OC} on the first day. The oxygen concentration in the off-gas remained above the 8 \% v v^{-1} criterion for aerobic conditions for 96 % of the time (Figures 5.13 a) to c)).

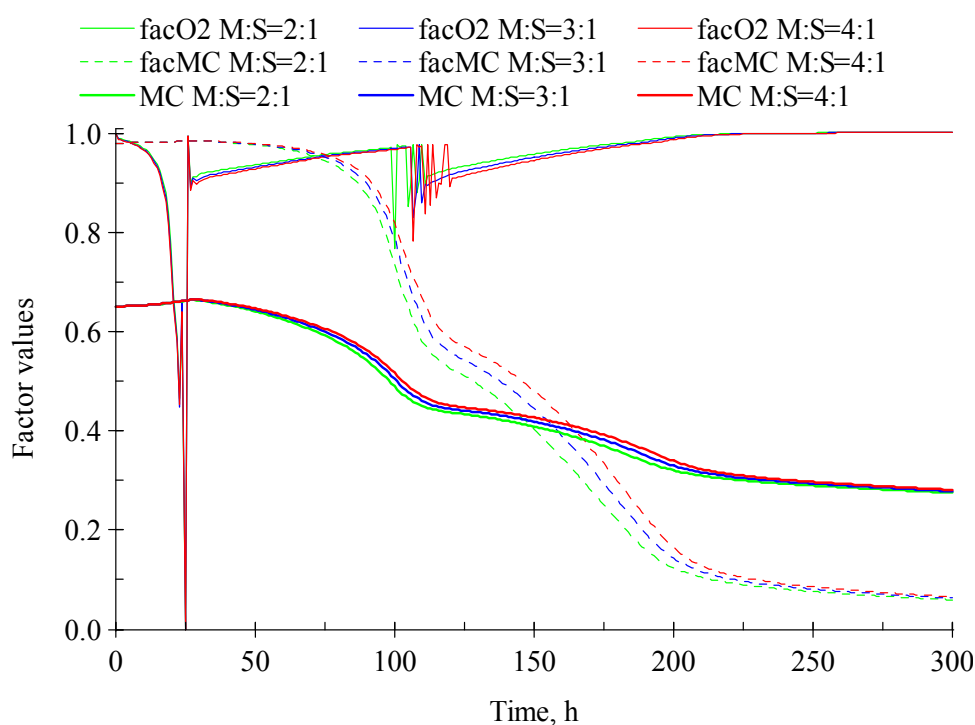


Figure 5.25. Moisture content and factor profiles from initial mixing ratio simulations (facO2 - oxygen content factor (f_{OC}) and facMC – moisture content factor (f_{MC}))

The initial mixing ratio affected the ammonia emissions, because of the greater nitrogen content in the organic material with the higher manure content. The bulk ammoniacal nitrogen profile (Figure 5.12) showed that the nitrogen was converted to ammonia within the first 30 hours. The mass of this ammonia that was emitted into the gas

stream depended on a number of process factors but the rate of emission was determined predominantly by the temperature and airflow rate. The ammonia emission rate was therefore relatively rapid when the temperature of the organic material reached 60 °C. The emission rate then slowed and all the ammonia in solution was lost from the organic material by 150 hours. The total mass of ammonia emitted was about 64 g, 84 g and 99 g for the initial mixing ratios 2, 3 and 4, respectively, which corresponded to 70 %, 74 % and 76 % of the initial ammoniacal nitrogen. The remaining nitrogen was assumed to have been assimilated into biomass. The mass of nitrogen incorporated into new biomass was therefore comparatively small and so the total nitrogen content fell as most of the ammoniacal nitrogen was emitted. The organic nitrogen content increased by about 9 % to 0.25 kg, 0.30 kg and 0.33 kg from 0.23 kg, 0.27 kg and 0.30 kg for the initial mixing ratios of 2 to 4, respectively.

The cumulative mass of carbon dioxide produced and the oxygen consumed for each initial mixing ratio is given in Table 5.4. The total mass of carbon dioxide produced and oxygen consumed increased with the initial mixing ratio, which agrees with the fact that the biodegradable fraction of the organic material increased with the mixing ratio.

5.5.2. pH sensitivity analyses

5.5.2.1. Initial pH of the organic material

The initial pH had no effect on the rate or degree of decomposition of the organic material as it had been assumed that, for the pH range covered in Figure 5.6, the pH did not limit microbial activity. The profiles of the mass of water in the organic material, the mass of carbon dioxide produced and the temperature of the organic material were the same for the three initial pH values. The total masses of carbon dioxide produced and oxygen consumed are given in Table 5.4.

The masses of ammonia emitted 55 g, 67 g and 84 g for the initial pH of 6, 7 and 8, were respectively (48 %, 60 % and 74 % of initial AN). Ammonia emissions were reduced by about 20 % when the initial pH was lowered from 8 to 7 and from 7 to 6. The reduction in a real composting system may not actually reflect the percentages given because the change in pH in the model was predetermined and was assumed to follow the course shown in Figure 5.4. However, reducing the initial pH did lead in a sizeable reduction in ammonia emissions and composting experiments may enable the actual reduction to be quantified. The comparison between the model and experimental values is made in Chapter 7 as part of the model validation. The lower mass of ammonia emitted corresponded to an increase in the mass of organic nitrogen in the organic material by 48 g and 38 g for the initial pH values of 6 and 7, respectively, compared with the 24 g for 8. The respective total nitrogen content of the organic material fell from 364 g at the start to 319 g, 309 g and 295 g at the end.

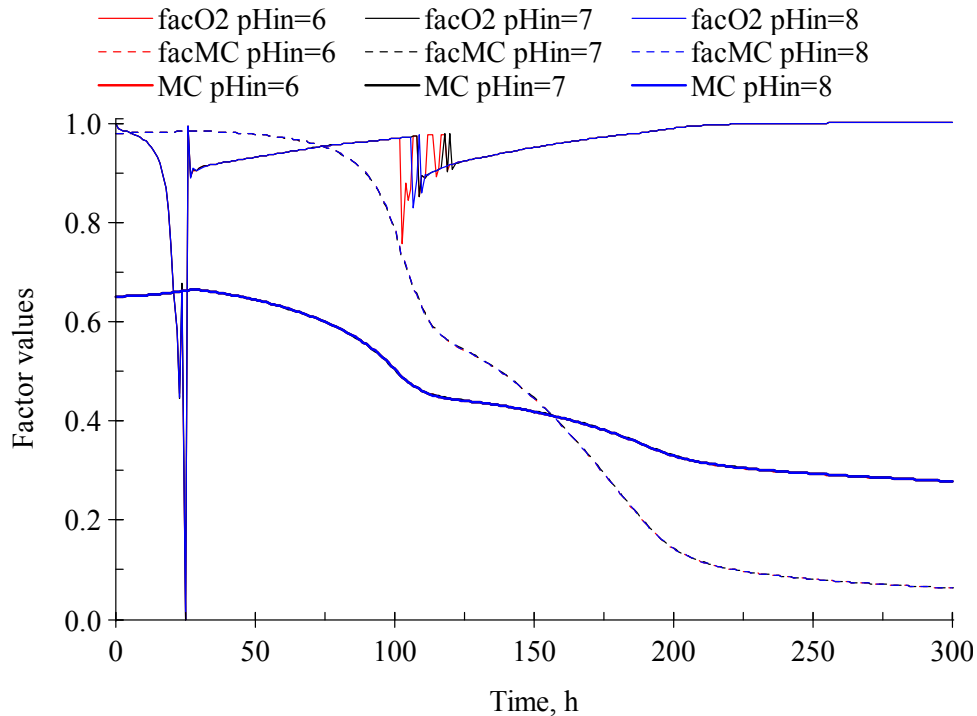


Figure 5.26. Moisture content and process factor profiles from initial pH simulations. (facO2 - oxygen content factor (f_{OC}) and facMC – moisture content factor (f_{MC}))

The profiles of the demand for cooling aeration were much the same except for when the composting process neared the end of the period at 60 °C. The cooling aeration fluctuations were reflected in the value of the oxygen factor. At all other times, the factor values were the same for all three initial pH values as was the moisture content of the organic material (Figure 5.26). After the initial sharp fall in the oxygen concentration of the off-gas as the temperature first approached 60 °C, the cooling aeration maintained the oxygen levels above 8 % v v⁻¹ of the dry gas in all three simulations. As with the simulations of the initial mixing ratio sensitivity analysis, the moisture content of the organic material, which was initially at 65 %, did become limiting at about 100 hours and the composting process stopped shortly thereafter, as moisture content factor (facMC) in Figure 5.25 reflected.

5.5.2.2. Composting with a constant pH

The pH of the organic material did not affect the rate or degree of its decomposition, with the mass of total solids decreasing by about 60 % to 5.5 kg for all the pH simulations. Correspondingly, the total mass of carbon dioxide produced and oxygen consumed was about 16 kg and 14 kg, respectively.

The mass of ammonia emitted from the organic material composting at a pH of 6, 7 and 8 was about 2 g, 18 g and 66 g, respectively (2 %, 16 % and 58 % of the initial AN). The pH of the organic material affected the ammonia emissions noticeably (Figure 5.4). Composting at the constantly maintained low pH was much more effective at reducing ammonia emissions than just starting with a low initial pH. The less nitrogen lost as ammonia corresponded to an increase in the mass of organic nitrogen in the organic material by 91 g and 78 g for pH 6 and 7, respectively, and only by the 39 g for pH 8. The respective total nitrogen content of the organic material fell from 364 g to 362 g, 349 g and 310 g.

As with the factor profile of the initial pH sensitivity analysis, there were no obvious differences between the factor values and the moisture content of the organic material apart from the oxygen factor values during the final stages of the period at 60 °C (Figure 5.27). These fluctuations between 100 and 150 hours reflected the fluctuations in the aeration (profiles not shown). After the initial sharp fall in the oxygen concentration of the off-gas as the temperature first approached 60 °C, the cooling aeration maintained the oxygen levels above 8 % v v⁻¹ of the dry gas in all of the simulations for this sensitivity analysis. The moisture content was the limiting factor after 150 hours and composting stop shortly thereafter, as shown by the moisture content factor (facMC) in Figure 5.27.

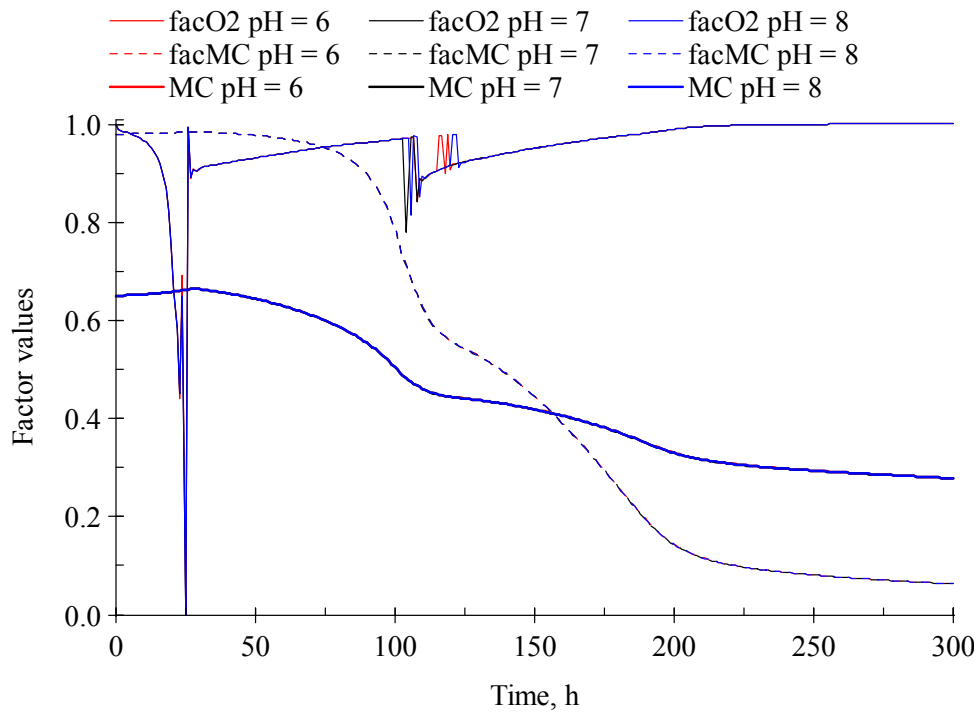


Figure 5.27. Moisture content and process factors profiles from constant initial pH simulations. (facO2 - oxygen content factor (f_{OC}) and facMC – moisture content factor (f_{MC}))

5.5.3. Moisture content sensitivity analyses

5.5.3.1. Initial moisture content of the organic material

The effect of the initial moisture content on the decomposition rate of the organic material was small but the degree of decomposition increased with the initial moisture content of the organic material due to the extended composting time. With the higher moisture content, the mass of the organic material therefore decreased to a value nearer to its equilibrium mass. The increase in the initial moisture content from 60 % to 65 % did, however, result in a comparatively greater loss in total solids than that for the increase from 65 % to 70 %. The moisture content of the organic material became limiting after about 60 hours for level 60 % whereas the moisture factor only started to drop sharply after about 90 and 130 hours at 60 % and 75 %, respectively (Figure 5.28).

The rise in temperature at the start of the simulation was faster in the organic material of the lower moisture content because of its lower specific heat capacity. The difference in the specific heat capacity was more pronounced between the moisture contents than the mixing ratios because the specific heat capacity of water is more than three times greater than that of the total solids fraction (Table 5.3). The extended composting time at the higher moisture contents was reflected in the temperature profiles. An increase from 60 % to 65 % and from 65 % to 70 % resulted in a 7 % and 14 % increase in the duration of the high microbial activity at 60 °C, respectively. The temperature was above 55 °C for between about 7 and 8 days and the criterion for thermal inactivation of pathogens during contained composting was therefore satisfied.

The cooling aeration of 25 l min⁻¹ controlled the upper temperature limit successfully around 60 °C for all the moisture content levels. The sharp drop in f_{OC} as the temperature first approached 60 °C happened sooner and was more pronounced in the organic material of the

lowest moisture content (Figure 5.28). Recovery was rapid on activation of the high airflow rate cooling aeration resulting in a well-aerated system, which was confirmed by the fact that the oxygen concentration in the off-gas remained above the 8 %v v⁻¹ for 95 % of the time in all three simulations.

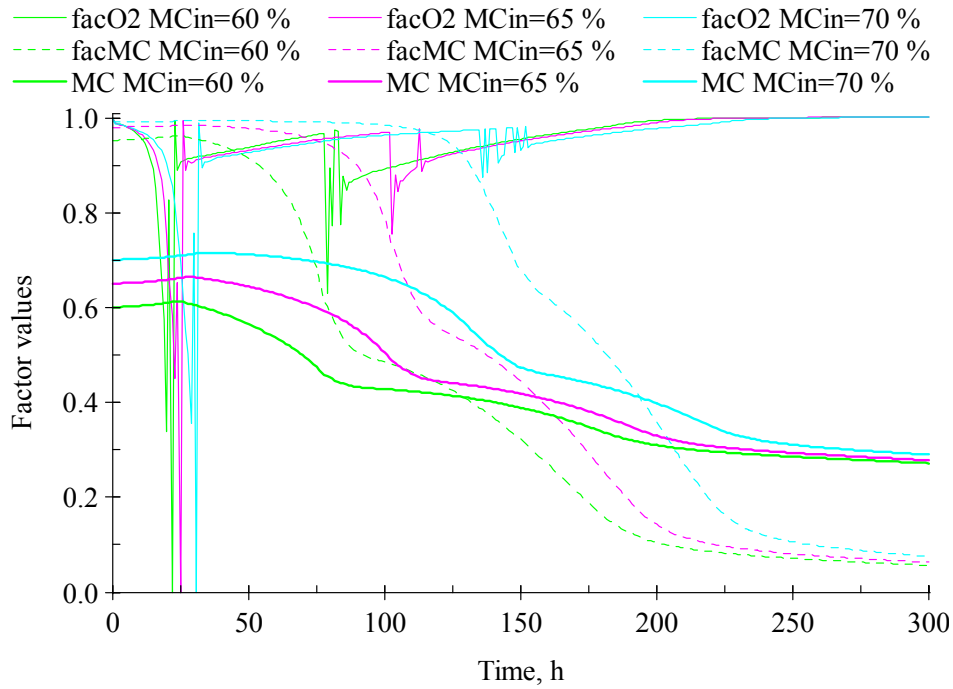


Figure 5.28. Moisture content and process factor profiles from initial moisture content simulations. (facO2 - oxygen content factor (f_{OC}), facMC – moisture content factor(f_{MC}))

The rate of ammonia emissions was inversely related to the volume of water in the organic material, as defined in equation (5 xxxix). An increase in moisture content therefore decreased the rate of ammonia emission but lead to a slight increase in the total mass of ammonia emitted. This occurred because, at lower moisture contents, the rise in temperature, and therefore decomposition rate, was more rapid. More ammoniacal nitrogen was therefore assimilated into biomass as the pH increased at a steady rate from the initial pH up to 9. All the ammonia in the liquid phase was emitted to the gas phase by about day 6. The assimilation of some of the ammoniacal nitrogen into biomass resulted in an increase in the mass of the organic nitrogen but the total nitrogen mass decreased because of the nitrogen lost

as ammonia. Ammonia emissions accounted for about 23 % of the initial total nitrogen and about 73 %, 74 % and 76 % of the initial ammoniacal nitrogen for the initial moisture contents of 60 %, 65 % and 70 %, respectively.

The cumulative mass of carbon dioxide produced and the oxygen consumed are given in Table 5.4. The total mass of carbon dioxide produced increased with the initial moisture content and the trend was the same for the total mass of oxygen consumed, as the degree of decomposition of the organic material increased because of the longer composting time.

5.5.3.2. Off-gas saturation

The effect of the exponent of the degree of off-gas saturation with water, ϕ , on the decomposition rate was small but the degree of decomposition increased with ϕ due to the extended composting time. The mass of the organic material therefore decreased to a value nearer to its equilibrium mass. The moisture content of the organic material became limiting after about 100 hours for the water saturated off-gas, and about 5 and 10 hours later in simulations with a ϕ value of 0.01 and 0.02, respectively, as shown by the moisture content factor (facMC) profiles of Figure 5.29. The initial mass of the water in the organic material was the same for each simulation but the pattern of water loss was different because the rate at which the water was evaporated from the organic material varied with ϕ . The moisture content of the organic material increased during the initial stages of composting before the mass of water lost by evaporation exceeded the mass generated by microbial activity.

The value of ϕ did not noticeably affected the rate of the initial temperature increase (Figure 5.22) because the moisture contents of the organic material were still much the same. However, when the cooling aeration was first activated at 25 hours, the off-gas, which did not become saturated, did not remove as much of the accumulated heat in the organic material as the saturated off-gas did. The temperature profiles of the systems with an unsaturated off-gas

therefore showed another sharp increase in the temperature at about 60 hours as the microbial activity increased almost to its maximum rate. This resulted in a second increase in the temperature, which took longer to return it to this upper temperature limit in the systems with the more unsaturated off-gas (higher ϕ value). The airflow rate of the cooling aeration (25 l min^{-1}) eventually controlled the upper temperature limit around 60°C for all the saturation levels. The decrease in the temperature at the end of the process was delayed in the systems with the unsaturated off-gas than in the system with the saturated off-gas. An increase in ϕ from 0 to 0.01 and from 0.01 to 0.02 resulted in a 9 % and 12 % increase in the duration of the high microbial activity at 60°C , respectively. The temperature was above 55°C for between about 7 and 9 days and the criterion for thermal inactivation of pathogens during contained composting was therefore satisfied.

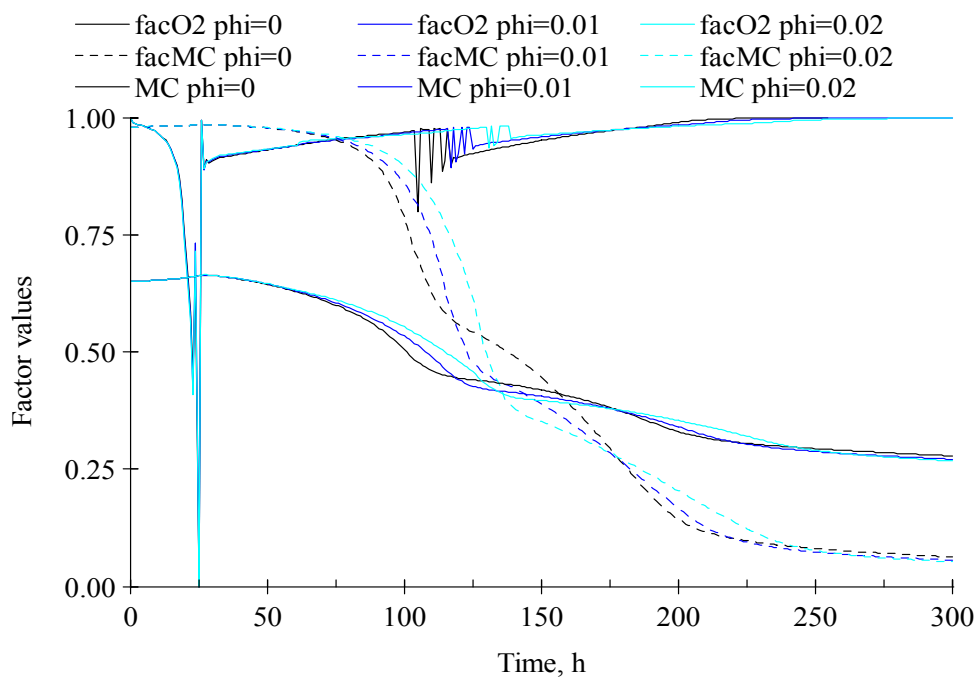


Figure 5.29. Moisture content and process factor profiles from ϕ simulations. (facO2 - oxygen content factor (f_{OC}), facMC – moisture content factor (f_{MC}))

The sharp drop in f_{OC} (Figure 5.29) as the temperature first approached 60 °C happened at the same time for all the ϕ values, as did the rapid recovery once the cooling aeration was activated. The system then became well-aerated as the aeration provided more oxygen than was consumed by the aerobic micro-organisms. The oxygen concentration did not fall below 8 % v v⁻¹ again and aerobic conditions prevailed for the rest of the simulation. The total mass of carbon dioxide produced and oxygen consumed are given in Table 5.4.

Table 5.4. The cumulative masses of carbon dioxide produced and oxygen consumed.

Gas mass, kg	Initial mixing ratio			Initial pH			Initial moisture content			Off-gas saturation exponent, ϕ		
	2	3	4	6	7	8	60%	65%	70%	0	0.01	0.02
CO ₂	13.3	14.1	14.8	14.1	14.1	14.1	12.7	14.1	15.5	14.1	14.2	14.4
O ₂	11.1	11.9	12.5	11.9	11.9	11.9	10.7	11.9	13.0	11.9	12.0	12.1

The simulation with an initial moisture content of 70 % produced the greatest total mass of carbon dioxide. This was closely followed by masses produced in the simulations with the initial mixing ratio of 4 and a ϕ value of 0.02. The mass of total solids would approach equilibrium mass closest in an organic material with an initial moisture content of 70 % because of the extended composting time.

5.6. Model sensitivity

The effect of the change a process factor, such as the initial pH of the organic material, on a process variable, such as the mass of ammonia emitted, was evaluated in order to assess the sensitivity of the model to incremental changes in its factor values. Table 5.5 lists the process factors and variables considered and the values of the incremental changes in the corresponding factors. The factors used were those on which the sensitivity analyses were performed by the model.

Table 5.5. The factors and variables used to test the sensitivity of the model

Factors	Symbol	Increment	Variables	Symbol	Units
Initial mixing ratio	M:S	1	Total ammonia emissions	A	g
Initial pH	pHin	1	Time of temperature above 55°C	T	h
Initial moisture content	MCin	5 %	Mass loss of total solids	M	kg
Off-gas saturation exponent	ϕ	0.01	Total volume of dry air into system	V	m ³

The sensitivities of the ammonia emissions, temperature, total solids mass and total mass of dry air (χ_A , χ_T , χ_M and χ_V , respectively) to a specific factor, f, were defined as

$$\chi_A|_f = \frac{A_f + \Delta A_f}{A_f}; \chi_T|_f = \frac{T_f + \Delta T_f}{T_f}; \chi_M|_f = \frac{M_f + \Delta M_f}{M_f} \text{ and } \chi_V|_f = \frac{V_f + \Delta V_f}{V_f} \quad (5 \text{ xLvii})$$

The output values of the variables from the simulations of the sensitivity analyses performed on the process factors listed in Table 5.5 were used to determine the values of the corresponding χ and are given in Table 5.6.

Table 5.6. Output values of the variables from the simulations of the sensitivity analyses.

Factor Variable	M:S ratio			pHin			MCin			ϕ		
	2	3	4	6	7	8	60%	65%	70%	0	0.01	0.02
A	64	84	99	55	67	84	83	84	86	84	84	84
T	171	174	178	174	174	174	167	174	195	174	190	215
M	7.1	7.5	7.7	7.5	7.5	7.5	6.7	7.5	8.2	7.5	7.5	7.6
V	215	217	248	220	220	217	189	213	256	222	231	248

The χ values of each process variable are given in Table 5.7 for the incremental changes in the factors specified in Table 5.5. Ammonia emissions depended on more than one process factor. Incremental changes in the initial mixing ratio and pH of the organic material led to between about a 20 % to 30 % increase in the total mass of ammonia emitted (A). The incremental changes in the initial moisture content and the off-gas saturation exponent (ϕ) had relatively little, if no effect on A. Increasing the mixing ratio from 2 to 3

had a 10 % greater effect on A than increasing the mixing ratio from 3 to 4. The difference was due to the initial ammoniacal nitrogen of the organic material, which did not increase uniformly with the mixing ratio. Changes in the initial pH of the organic material had no effect of the number of days for which the temperature was above 55 °C (T). An increase in M:S had a relatively small effect on T compared with increases in the initial moisture content and ϕ particularly for changes from 65 % to 70 % and 0.01 to 0.02, respectively.

The mass loss in total solids (M) was not affected by the initial pH of the organic material and was only slightly affected by changes in ϕ . An increase in the initial moisture content by 5 % had the greatest effect with M increasing by about 10 %; mainly because the composting time was extended. For the same reason an increase in the initial moisture content had a greatest effect on the volume of air that passed through the system (V), with an increase in ϕ having a smaller but appreciable effect on V.

Table 5.7. The sensitivity of process variables to incremental changes in the factor values

Factor, f Δf χ	M:S ratio		pH _{in}		MC _{in}		ϕ	
	2 to 3	3 to 4	6 to 7	7 to 8	60% to 65%	65% to 70%	0 to 0.01	0.01 to 0.02
(A- ΔA)/A	1.311	1.178	1.232	1.248	1.015	1.019	0.998	1.003
(T- ΔT)/T	1.018	1.023	1.000	1.000	1.042	1.121	1.092	1.132
(M- ΔM)/M	1.045	1.034	1.000	1.000	1.112	1.097	1.008	1.011
(V- ΔV)/V	1.011	1.033	1.000	0.989	1.127	1.203	1.040	1.075

5.7. Conclusions

The aeration strategy proposed for the composting system resulted in a well aerated organic material, in which the oxygen concentration was above 8 % v v⁻¹ of the dry off-gas for majority of the composting time. The exception occurred when the temperature of the organic

material initially approached 60 °C and oxygen uptake rate exceeded the oxygen that was provided solely by the baseline aeration. The cooling aeration successfully controlled upper temperature limit at 60 °C when the off-gas leaving the system was saturated with water vapour. The airflow rate of 25 l min⁻¹ for the cooling aeration was not as efficient at controlling the temperature of the organic material at the upper temperature limit when the off-gas saturation was less than 65 %.

The oxygen content was the limiting factor in the initial stages of composting whilst the moisture content became limiting in the later stages as the organic material dried. With an initial moisture content of 70 % and below, moisture content of the organic material limited the composting process before the mass of total solids reached its equilibrium mass.

Analysis of the sensitivity of the model showed that decreasing the initial mixing ratio or the pH were effective ways of reducing ammonia emissions. Maintaining the pH of the organic material below 8, was the most effective means of minimising the nitrogen lost as ammonia gas. The impact of the initial moisture content and the degree of off-gas saturation on ammonia emissions was minimal. The higher moisture contents reduced the ammonia emission rate but did not lead to an overall reduction in the mass of ammonia emitted. Delaying emissions could allow strategies for reducing ammonia emissions to be introduced to the composting system. The percentage of ammonia in the off-gas was small (less than 1 %) compared to the oxygen and carbon dioxide concentrations. The peak concentration at 25 hours coincided with the activation of the cooling aeration for the first time.

The period of composting at a maximum rate was appreciably extended in organic material with higher initial moisture contents up to 70 % or in system in which the off-gas was unsaturated. The duration of composting was not effected by the initial pH or mixing ratio of the organic material with an initial moisture content of 65 %. The model did not take

into account the effect of the free air space on the composting process and so would predict that the higher the moisture content, the longer the composting period at 60 °C and therefore the greater mass of total solids decomposed. This, however, may not occur practically if the voids in the organic material become filled with water. An empirical relationship between the free air space and the rate of microbial activity, as indicated by the SOUR, would need to be established. The temperatures were above 55 °C for more than 3 consecutive days in all the simulations and therefore pathogen inactivation should take place when composting organic material with an initial moisture content as low as 60 % and an initial mixing ratio of 2.

The model successfully simulated the composting process in a system, which did not experience heat losses from the reactor surface. The model allowed the effect of a number of process factors on various aspects of the composting process to be investigated and evaluated. Improvements to the model could be made following further investigation of process parameter values, such as the value of the exponents that determined the temperature factor so that the SOUR component (Figure 5.12) was conditional for the initial mixing ratio of the organic material. This could lead to a noticeable difference in the degree of decomposition of the organic material between the mixing ratios. The addition of a sub-model, which simulated the change in pH of the organic material by considering the buffering effect of the organic material and impact of ammonia and carbon dioxide produced and lost from the organic material, could make model predictions of ammonia emitted more accurate.

CHAPTER 6

EXPERIMENTAL INVESTIGATION OF COMPOSTING FACTORS

6.1. Introduction

Chapter 1 outlined reasons for composting on a laboratory scale in vessels in order to evaluate the effects of the process factors on the process variables. These were mainly to isolate the composting from ambient conditions and to regulate the process. The organic material (pig manure mixed with chopped straw - Section 3.3.3), was composted in the reactors described in Section 3.1.2. The reactors were designed to control the composting process using temperature feedback and so enable the effect of process factors on specific process variables to be measured.

The Experimental design (Section 6.2) details the plan followed in order to test the hypothesis stated in Chapter 1. The two principal objectives of the experiments were:

1. To evaluate the effect of the initial pH and carbon to nitrogen (C:N) ratio of the organic material on ammonia emissions from composting mixes of pig manure and straw.
2. To record the presence of pathogenic marker organisms in the organic material before and after composting and to assess the possible influence of composting conditions on pathogen inactivation.

The results of the trials are presented in Section 6.3 in order of increasing C:N ratio. Section A6.1 discusses the results of the composting process in the experiments of each trial in more detail as characterised by profiles of the temperature, cooling aeration, ammonia emissions and oxygen and carbon dioxide in the off-gas. General observations and analyses, including pathogen marker analysis, of the organic material are included.

6.2. Experimental design

The experiment was designed for an analysis of variance to be carried out to evaluate the effects of the initial pH and C:N ratio of the organic material on the temporal profiles of the temperature and cumulative ammonia emissions. Having three reactors in the composting unit, R1, R2 and R3 (Figure 6.1), enabled one of the selected factors to be investigated on three levels in a single trial. The following criteria were used to decide the levels on which to investigate the factor.

1. The range of values considered was typical of that experienced during composting
2. The microbial activity was not adversely affected within this range.
3. The incremental changes in each factor were relatively easy to achieve and were large enough to be measured.
4. The change in the factor affected the associated process variables appreciably so that the differences could be measured using the monitoring equipment available.

Conditioning the organic material to be composted was a simple and controllable means of influencing the composting process. Furthermore, the effect of the factor on a process variable could be referenced to a defined initial incremental change in the factor. The reactors operated as closed batch systems and that restricted control of the pH and C:N ratio of the organic material to their initial values. The levels of the initial pH and C:N ratio investigated and the theoretical impact of their incremental changes on ammonia emissions and the temperature of the organic material are discussed in Sections 6.2.1 and 6.2.2, respectively.

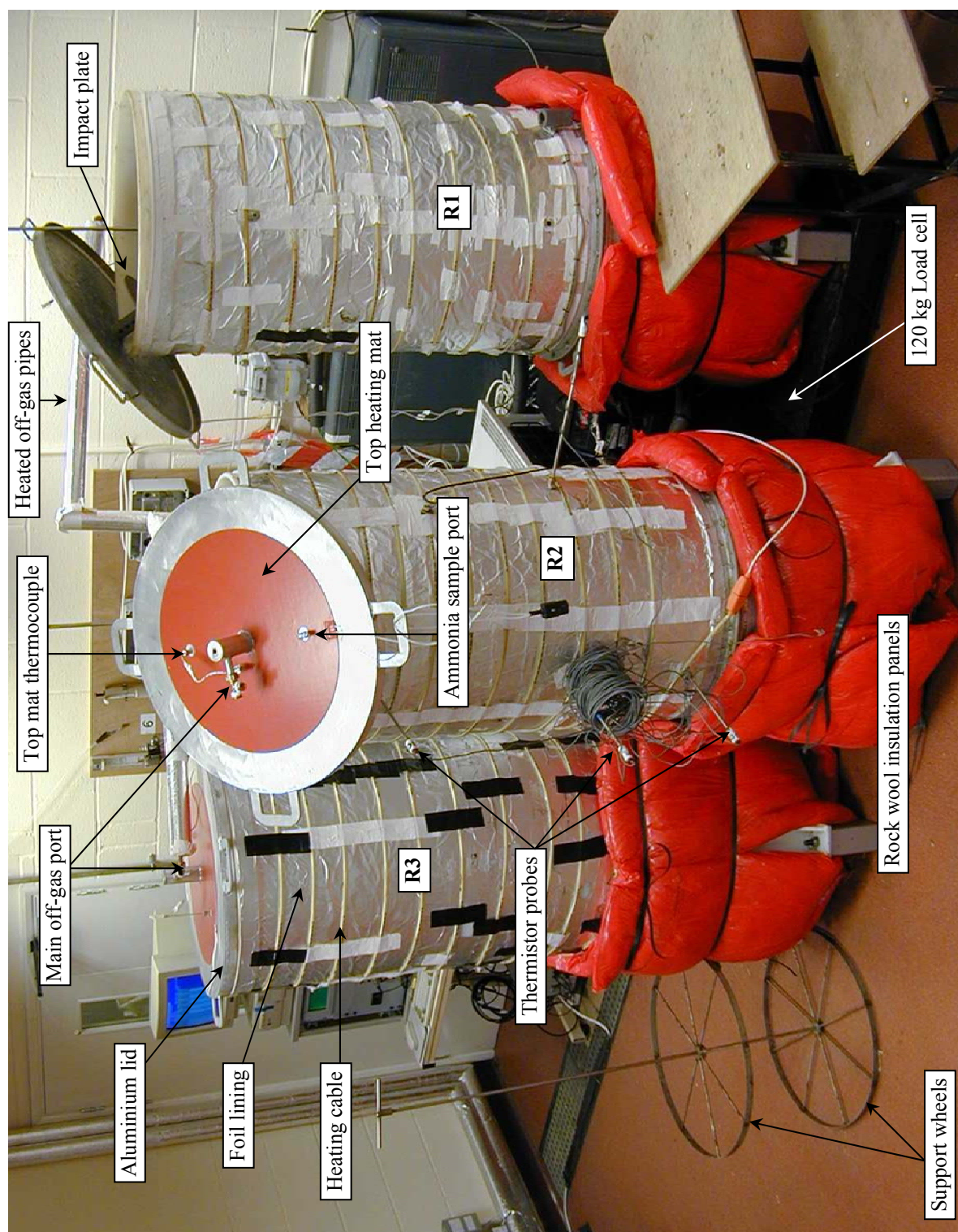


Figure 6.1. The three reactors of the composting unit

6.2.1. Ammonia emissions

The mass of ammonia emitted from the organic material depends on a number of process factors as highlighted in Chapter 2 and 5. The model concept (Sections 5.2.1.2 and 5.2.2.1) described how process factors, such as the ammoniacal nitrogen concentration, pH, water content, interfacial surface area and temperature of the organic material and the air flow rate, theoretically affect ammonia emissions.

The initial C:N ratio of the organic material determines the interfacial surface area and the initial mass of the manure, and therefore, the initial concentration of ammoniacal nitrogen. The C:N ratio also influences composting and if the amount of nitrogen is in excess of that required to build new cells, then ammonia emissions are exacerbated.

The pig manure and straw mixed in the mixing ratios of 2, 3 and 4 on a wet mass basis corresponded to C:N ratios of about 25, 20 and 15, respectively. Analysis of representative samples showed that the organic material of each of the three mixing ratios was suitable for composting (Section 3.3.3). The theoretical increase in the initial mass of ammoniacal nitrogen in the organic material was about 25 % and 15 % for the increase in the mixing ratios from 2 to 3 and 3 to 4, respectively. The initial mixing ratio model simulation showed that, for an initial 14 kg of total solids, these percentage increases in the initial ammoniacal nitrogen, led to 20 g and 15 g more ammonia emissions, respectively (Section 5.4.1.1).

The pH of the organic material affects the fraction of the ammoniacal nitrogen that exists as dissociated ammonia and the initial pH is likely to reduce subsequent ammonia emissions. Any delay in ammonia emissions during the early stages of composting leaves more ammoniacal nitrogen available for potential assimilation into biomass and so conserving nitrogen in a more stable form. Reducing the pH of the organic material from 8 to 7 and from 7 to 6 decreases the fraction of the total ammoniacal nitrogen that exists as ammonia in the

aqueous and slurry solutions 10 fold, regardless of the temperature (Figure 6.2). The theoretical effect of the initial pH of the organic material on ammonia emissions, as predicted by the model (Section 5.1.2.2), was appreciable, with about a 20 % reduction in the total mass emitted for each of the incremental decreases in the pH. The reduction in ammonia emissions was even more marked if the value of the initial pH were maintained for 4 days (Figure 5.18).

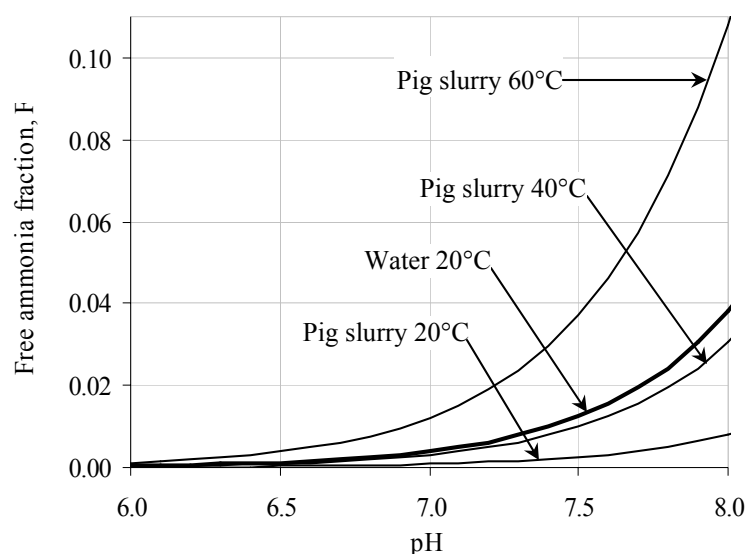


Figure 6.2. Dissociation curves of ammonia in water (20 °C) and slurry.

6.2.2. Composting temperature

Temperature is used as the main indicator of pathogen inactivation because it is a relatively easy process variable to monitor and control. The time for which the temperature was above 55 °C was therefore used to indicate the degree of pathogen inactivation. This was then checked by analysing the organic material for marker coliforms (Section 3.2.3) before and after composting. The initial pH and C:N ratio values selected for investigation do not directly affect pathogen inactivation and model simulations of the factors show little, if any effect on the temperature profile (Section 5.4.1.1 and 5.4.1.2).

The C:N ratio and pH of the organic material may indirectly affect pathogen inactivation through their effects on the ammonia emissions. High ammonia concentrations may facilitate the inactivation, not only of pathogens, which would be desirable, but also of the general microbial populations. The presence of active microbial populations in the organic material before and after composting was checked using nutrient agar (Section 3.2.3).

6.2.3. Experimental plan

The initial pH (6, 7 and 8) and C:N ratio (15, 20 and 25) values investigated met the four criteria (Section 6.2). Statistical analysis required that the factor to which the process variable was the more sensitive or whose effect on the process was less known was to be varied within the composting trial. Although the model gave some insight into the effect of pH on ammonia emissions and other composting variables, the pH profile used was predetermined. The three levels of initial pH were, therefore, investigated within a trial and the initial C:N ratios of the organic material were altered between trials (Table 6.1).

Table 6.1. The design of experiment trials

	Reactor 1	Reactor 2	Reactor 3
Trial 1	pH 8 <u>C:N 20</u>	pH 7 <u>C:N 20</u>	pH 6 <u>C:N 20</u>
Trial 2	pH 6 <u>C:N 25</u>	pH 8 <u>C:N 25</u>	pH 7 <u>C:N 25</u>
Trial 3	pH 7 <u>C:N 15</u>	pH 6 <u>C:N 15</u>	pH 8 <u>C:N 15</u>
Trial 4	pH 7 <u>C:N 20</u>	pH 6 <u>C:N 20</u>	pH 8 <u>C:N 20</u>
Trial 5	pH 8 <u>C:N 25</u>	pH 7 <u>C:N 25</u>	pH 6 <u>C:N 25</u>
Trial 6	pH 6 <u>C:N 15</u>	pH 8 <u>C:N 15</u>	pH 7 <u>C:N 15</u>

The experiments were repeated so that a total of six trials and eighteen composting experiments were done. Reactor variation was removed by not performing the repeated experiment in the same reactor.

6.3. Method

Each trial, including preparation, loading and unloading from the reactor and sampling of the organic material, lasted about one month, with the composting occupying about 14 days. Measurements of most process variables were automatically logged. The ammonia emissions were analysed and recorded manually as was the load cell reading for Reactor 1. After the 2 weeks of composting, the heat loss control and aeration systems were switched off, the lid was removed and the organic material was allowed to cool for a few hours. The composted organic material was sampled as the reactors were unloaded.

6.3.1. Preparation of the organic material

The pig manure, kept in cold storage at 1 -2°C, was hand mixed with the chopped straw in an unheated laboratory so that any windy and warm ambient conditions did not result in premature composting and release of ammonia from the freshly mixed organic material. During mixing, the organic material was continually put into 58 litre plastic bags, each holding between 8 and 10 kg of the organic material, which, when full, were immediately tightly closed and put into cold storage for about week. The masses of the organic material were not exactly the same as the masses given in Table 3.7 but the proportions of the constituents were maintained.

6.3.2. Start-up of a composting trial

Loading the organic material into the composting reactors was done at night when it was relatively cool. The mass of organic material required to fill one reactor was heaped onto the rubber mat and turned with a hay fork (Figure 6.3). The solution of deionised water, sulphuric acid and urea was then carefully added evenly over the organic material using a

watering can and the wetted organic material was then well turned to distribute the liquid, which was readily absorbed by the straw.



Figure 6.3. Approximately 47 kg of the organic material ready for loading into the reactors.

To avoid contamination with sulphuric acid, the organic material was loaded in the order of initial pH 8 (no acid added) first, then pH 7 and finally pH 6. After samples of the organic material were collected for microbial, physical and chemical analysis, the reactor was loaded in batches of about 5 kg. The organic material was spread evenly between the support wheels in the reactor after each batch was added. The reactor was filled to about 20 cm below the top. Immediately after loading, the reactor was closed and temperature logging started.

Aeration of the organic material and analysis of the off-gas was started after all the reactors were closed and the control systems initiated. Loading and setting-up each reactor took approximately 4 hours, and so the start times were different for each composting experiment in a trial. All process analyses were referenced to the time at which the temperature logging in each reactor started. Details of the process control and individual measurement systems are given in Section 3.1.2.2 and 3.1.2.3, respectively.

6.3.3. Statistical analysis

The results of the composting experiments were analysed using the statistical software, *Genstat* (Version 6). The relationships between the final value of the process variables (variates), such as the total ammonia emissions and loss in total solids, and the process factors and variables were assessed using general analyses of variance and simple linear regression. The simple one-way analysis of variance (ANOVA) was used. Further treatments, which deal with blocks in the analysis, were not possible because, in that sense, the investigation was not complete and a further 3 trials (9 more experiments) were required to complete the appropriate experimental design, as shown in Table A6.1. Relationships were tested for significance at the 0.05 probability level.

The effect of other process variables, such as the airflow rate and temperature of the organic material, on ammonia emissions and pathogen inactivation was statistically analysed using linear regression analysis. The amount of data available was relatively small for statistical analyses and so just simple linear regression models were considered, which were grouped according to the C:N ratio or pH in some cases, and an attempt to fit multiple variable regression models was not made.

6.4. Results and discussion

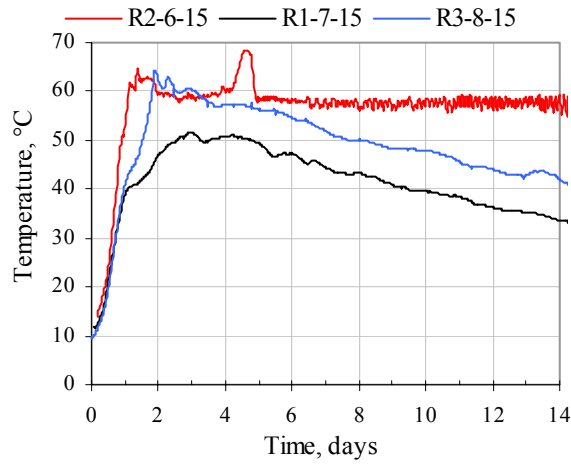
The results of the composting experiments are presented in order of increasing initial C:N ratio and pH within the trial. An experiment is identified by its reactor number and the initial pH and C:N ratio. For example, the experiment in Reactor 3 of Trial 1 is R3-6-20. Temperature, ammonia emissions and mass profiles are presented first followed by mass, water and nitrogen balances. The results are then statistically analysed (Section 6.4.4).

6.4.1. Temperature profiles

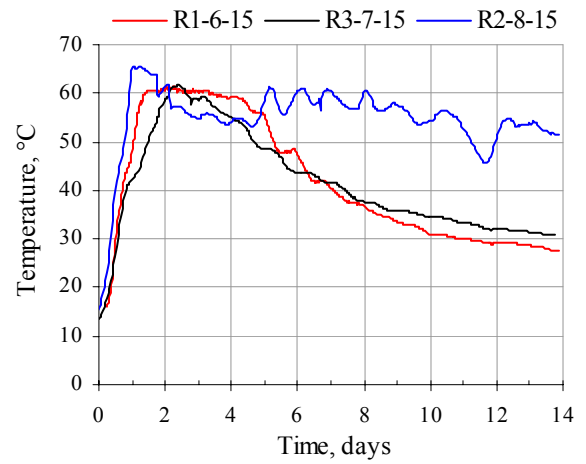
In Figure 6.4, the graphs show the centre temperature profiles of the three composting experiments in each trial. There was no apparent combination of the initial pH and C:N ratio that sustained rapid composting of the organic material. The most notable successes, in terms of high microbial activity were R2-6-15 (Figure 6.5a), R1-8-20 (Figure 6.5c) and R3-7-25 (Figure 6.5e). The demand for cooling aeration reflected the high activity (Figures A6.3, A6.7 and A6.9) but the high airflow rate through the organic material tended to bring composting to a premature end because the loss of water (R1-8-20 and R3-7-25). The repeated trials did not replicate the temperature profiles of the first three corresponding trials for example, in Trial 6 (Figure 6.5b), composting was notably better in R2-8-15.

Although the best composting took place in R3-8-20, overall, the experiments in Trial 4 (Figure 6.5d) were not very successful because thermophilic temperatures were not sustained. Conversely, those in Trial 5 (Figure 6.5f) all showed high activity resulting in similar temperature profiles. The lack of activity in all the experiments of Trial 4 may have occurred because the microbial populations in the particular batch of pig manure used were less active, perhaps inhibited by some external factor, such as disinfectant used on the farm. The lower initial general population densities (10^5 CFU g⁻¹ TS) (Table A6.10) reflect this.

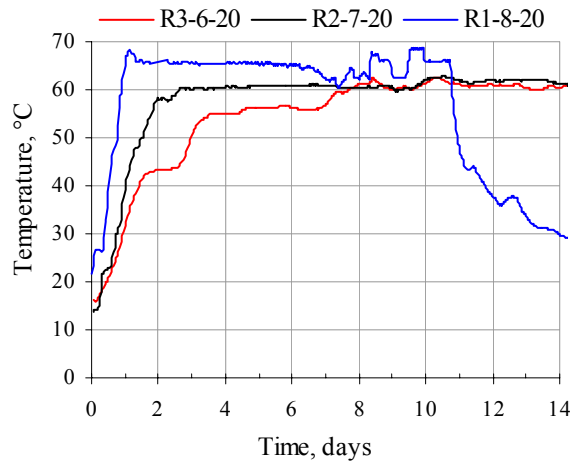
a) Initial C:N ratio 15 -Trial 3



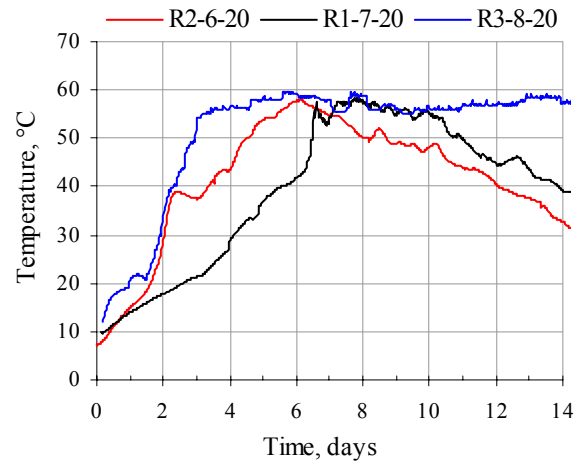
b) Initial C:N ratio 15 -Trial 6



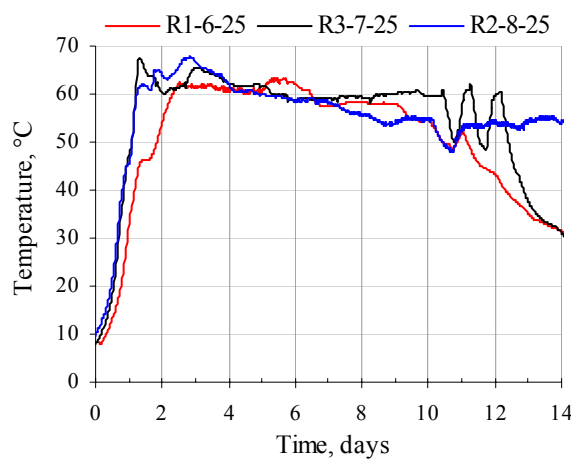
c) Initial C:N ratio 20 - Trial 1



d) Initial C:N ratio 20 -Trial 4



e) Initial C:N ratio 25 -Trial 2



f) Initial C:N ratio 15 -Trial 5

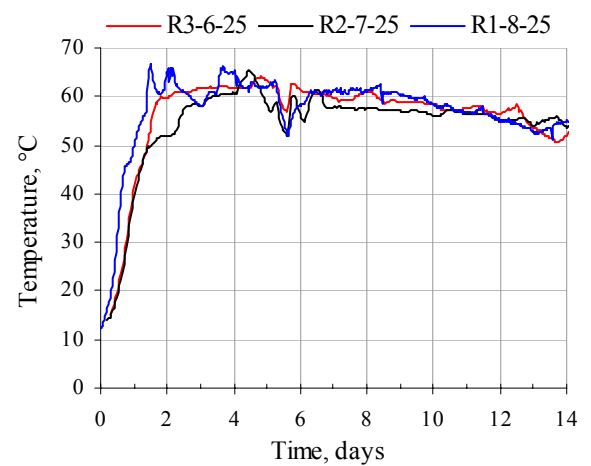


Figure 6.4. The centre temperature profiles of each initial pH of the organic material in Trials

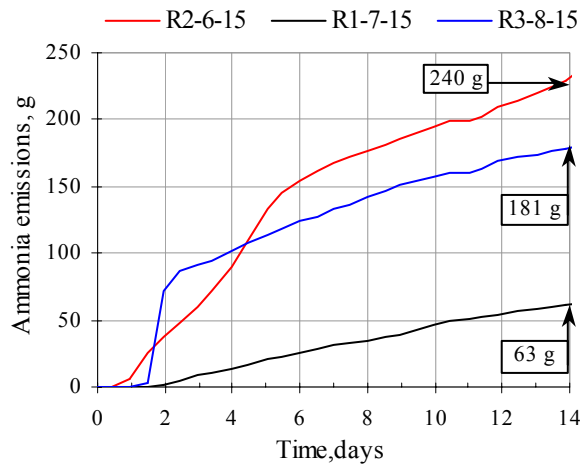
6.4.2. Ammonia emission profiles

The cumulative ammonia emissions profiles graphs of the composting experiments are shown in Figure 6.5. Ammonia emissions were highest from the organic material with the initial pH of 8 in all the trials except in Trial 3 (Figure 6.5a). Here, after day 4, the total ammonia emissions from R2-6-15 exceeded those from R3-8-15. Otherwise, ammonia emissions tended to be lowest from the organic material with an initial pH of 6.

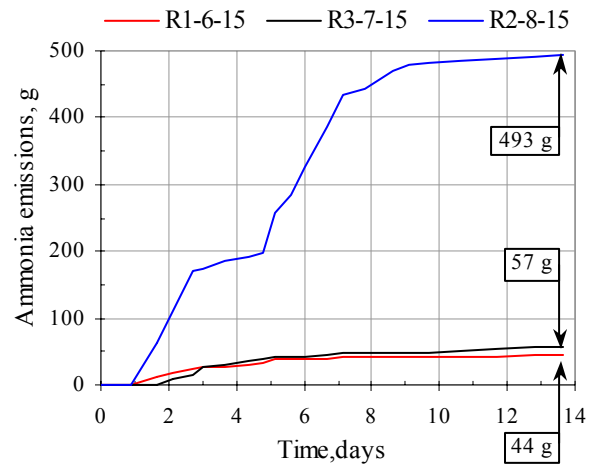
Microbial activity was higher in R2-6-15 than in R1-7-15 and R3-8-15 (Section A6.3.1), so that airflow rate and composting temperature were appreciably higher, which probably resulted in the higher ammonia emissions. If the rate of activity had been matched in R1-7-15 and R3-8-15, then the total ammonia emissions may well have exceeded that of R2-6-15. The significance of the effect of the airflow rate and composting temperature on ammonia emissions is evaluated in Section 6.5. As expected, the total masses of ammonia emitted were highest in the organic material with the lowest initial C:N ratio. The total mass from R2-8-15 is impossibly high and the overestimation may have occurred because the high airflow rate during the first 8 days may have magnified any errors in the measurement of ammonia in the off-gas and the total volume of air that flowed into the reactor. The nitrogen balance highlights the degree to which the ammonia emissions were exaggerated (Table 6.3).

Ammonia emissions from the organic material with an initial C:N ratio of 25 were markedly higher than those from the organic material with the initial C:N ratio of 20, even at the lower initial pH values. This unexpected outcome may have arisen because of the higher microbial activity, and therefore airflow rate, in the experiments with initial C:N ratio of 25. The mean airflow rate for C:N 25 was 377 l h^{-1} ($\sigma = 45$), about three times higher than the 133 l h^{-1} ($\sigma = 26$) for C:N 20 and the overall mean composting temperature during ammonia emissions was 4°C higher. The mean airflow rate for C:N 15 was 255 l h^{-1} ($\sigma = 84$).

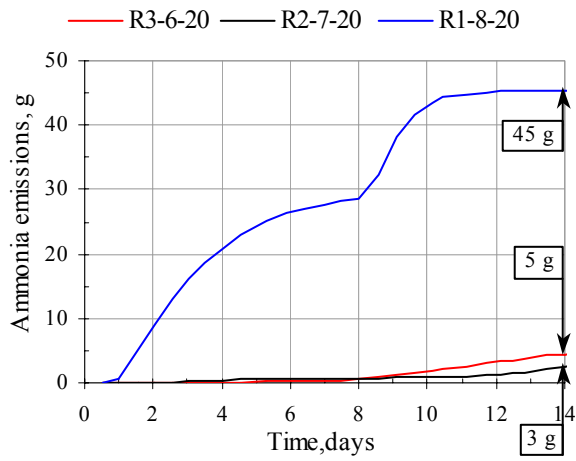
a) Initial C:N ratio 15 – Trial 3



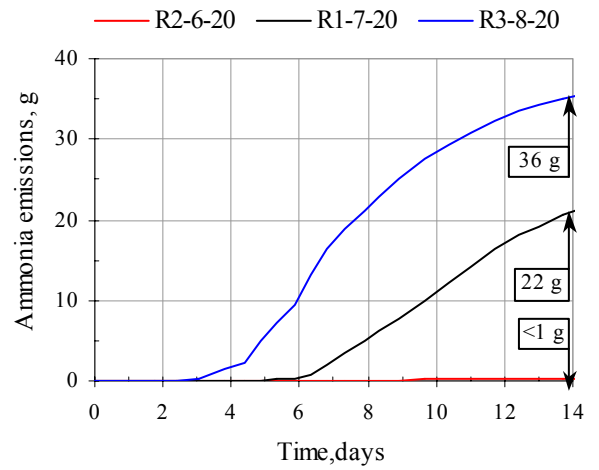
b) Initial C:N ratio 15 – Trial 6



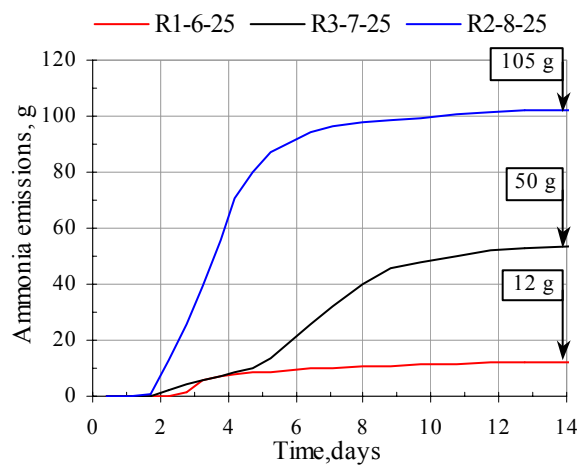
c) Initial C:N ratio 20 – Trial 1



d) Initial C:N ratio 15 – Trial 4



e) Initial C:N ratio 25 – Trial 2



f) Initial C:N ratio 25 – Trial 5

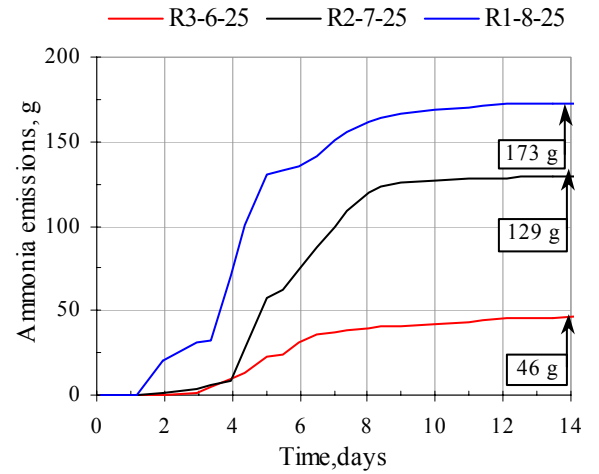


Figure 6.5. Profiles of cumulative ammonia emissions profiles in the Trials.

6.4.3. Pathogens

The ticks in Table 6.2 indicate the experiments in which pathogen markers were detected in the composted organic material. The coliform marker density in R2-7-15 was below 1×10^3 CFU g⁻¹ TS in the organic material but considering the ability of bacterial population to re-grow, their presence could not be disregarded. Although the organic material had been exposed to temperatures above 55 °C for at least 3 consecutive days, pathogen markers were still present. In these experiments, the ammonia emission rate (NH₃ rate) was relatively low. Perhaps this was not long enough and the temperature needs to be maintained for > 5 days when ammonia emissions are < 5 g day⁻¹. R3-15-8 was exposed to 55 °C for only 4 days but the ammonia emission rate was > 5 g day⁻¹. The ammonia emission rate was < 5 g day⁻¹ in R2-6-20, R3-8-20 and R1-6-25 but the temperature was above 55 °C for > 8 days and no pathogen markers were detected. R1-7-15 was the exception because, although the temperature did not reach 55 °C and the ammonia emissions rate were < 4 g day⁻¹, pathogen markers were not detected.

Table 6.2. Pathogen markers in the composted organic material and related process conditions.

C:N ratio	C:N 15 (T3)			C:N 15 (T6)			C:N 20 (T1)			C:N 20 (T4)			C:N 25 (T2)			C:N 25 (T5)		
pH	6	7	8	6	7	8	6	7	8	6	7	8	6	7	8	6	7	8
Reactor	R2	R1	R3	R1	R3	R2	R3	R2	R1	R2	R1	R3	R1	R3	R2	R3	R2	R1
T _{mean} , °C	54	40	49	41	41	52	52	51	53	48	38	42	46	50	53	55	53	54
σ	2.7	1.0	1.8	1.6	1.4	2.6	1.1	0.8	1.2	1.1	0.8	0.9	1.3	1.8	1.6	1.4	2.5	2.0
T>55°C days	14	0	4	5	3	12	8	10	7	12	5	8	14	15	10	11	12	11
NH ₃ rate g day ⁻¹	17	4	13	5	4	53	<1	<1	4	0	2	3	1	5	16	4	15	19
Pathogen	—	—	—	✓	✓*	—	✓	✓	—	—	✓	—	—	—	—	—	—	—

*Pathogen markers density <1000 CFU g⁻¹ TS

6.4.4. Mass losses of the organic material

6.4.4.1. Total solids

Figure 6.6 summarises the total solids (TS) mass losses given in Tables A6.6 to A6.12. In five of the six trials, the organic material with an initial pH 6 showed the greatest TS losses within the trials. The sulphuric acid used to reduce the initial pH could have enhanced the straw's susceptibility to microbial decomposition by partly hydrolysing its polysaccharide bonds. The acid conditions may have also favoured the growth of fungi on the straw [Trautmann and Olynciw 2002b]. In Trial 6, a high rate of composting was not maintained for more than three days in the organic material with an initial pH 6 and 7 compared with at least 7 days for pH 8, as shown by the temperature and cooling aeration profiles in Figures A6.18 to A6.20. Although pH 8 maintained the higher rate of activity, the TS mass loss was only marginally more than pH 6. The TS mass loss also tended to increase with the initial C:N ratio. The higher fraction of straw may have promoted rapid composting by giving the organic material a more open structure, to facilitate better gas distribution.

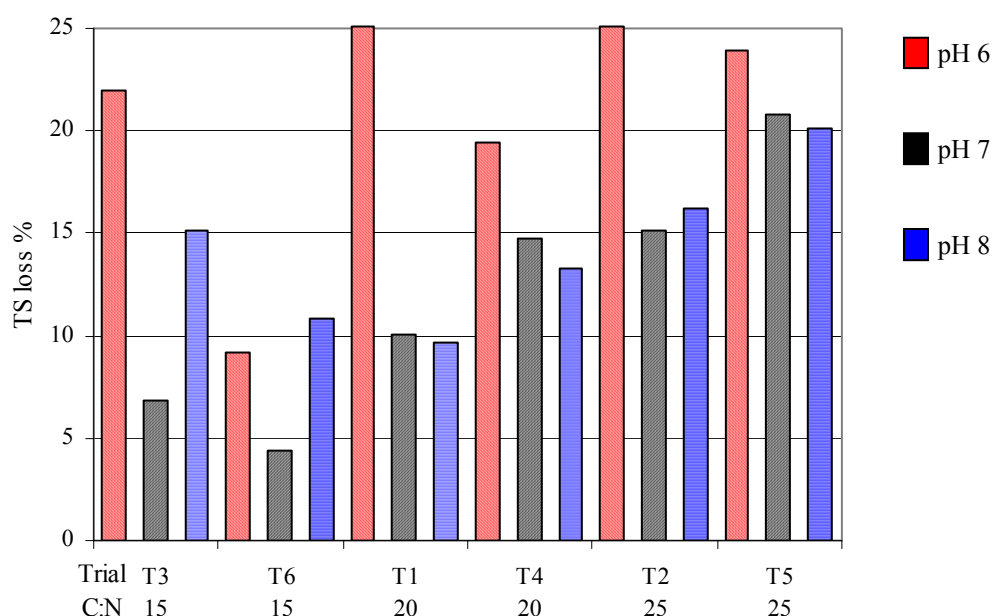


Figure 6.6. Percentage total solids (TS) mass loss in the organic material.

6.4.4.2. Total mass

The mass of the composted material unloaded from Reactor 1 agreed to within 90 % with the final readings on the load cell. Figure 6.7 shows the progressive loss in total mass of the organic material in Reactor 1. The total mass tended to show a large fall when the cooling aeration was activated and water was evaporated. The mean airflow rates ($l\ h^{-1}$) are shown in Figure 6.7 alongside the corresponding plots. The higher total mass losses tend to correspond to the higher airflow rates but the 25 % reduction of total solids in R1-6-25 (Figure 6.7) would have also contributed 3.5 kg to its total mass loss. Although R1-8-20 lost only 10 % loss of its total solids, the relatively high airflow rate and operating temperature (about $65^{\circ}C$) heightened the evaporation of the water resulting in a 66 % decrease in the water mass and therefore an appreciable drop in the total mass.

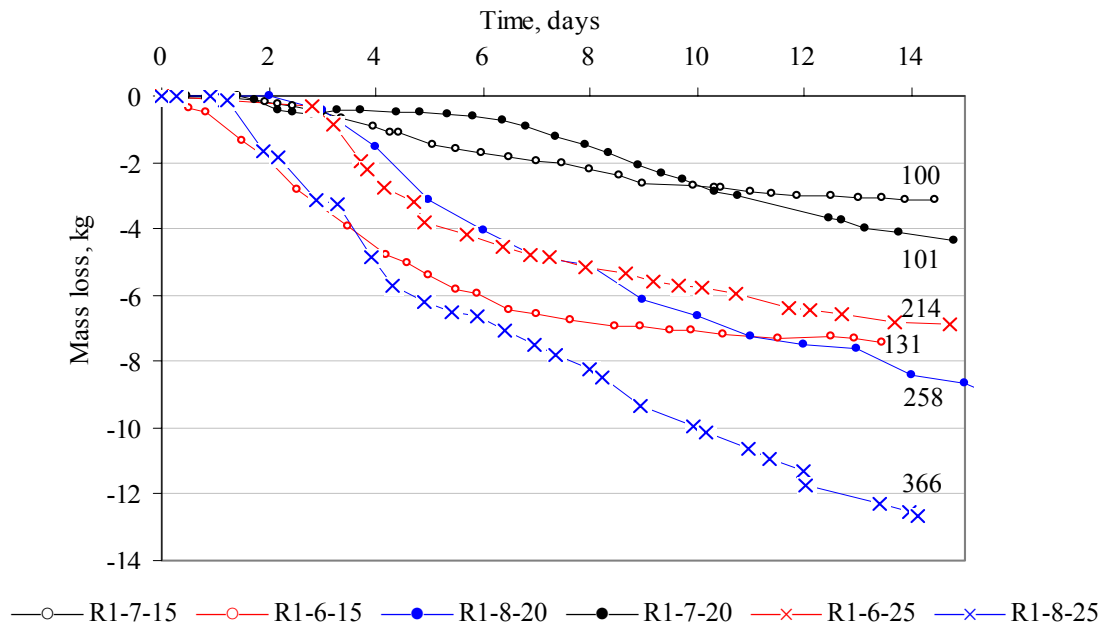


Figure 6.7. The total mass loss from the organic material in Reactor 1.

The lowest total mass losses occurred in R1-7-15 and R1-7-20. No cooling aeration was required and the water (8 % and 10 %) and TS (7 % and 14 %) losses were relatively low.

6.4.5. Mass balances

6.4.5.1. Nitrogen balance

The nitrogen balances are in Table 6.3. Nitrogen was predominantly lost from the organic material as ammonia in the off-gas. Some nitrogen left the system, almost exclusively as ammoniacal nitrogen (AN), in the leachate (LN). The initial and final mass of nitrogen in the organic material given in Table 6.3 corresponded to the total nitrogen (TN) content as determined by the TN concentration and the total solid content of the organic material given in Tables A6.7 to A6.12. The TN content was the sum of the AN and organic nitrogen (ON) contents of the organic material and the distribution for each trial is shown in Figures A6.22 a) to f). The error was the difference between the input and output nitrogen (nitrogen balance) expressed as a percentage of the input nitrogen. An error of 10 % or less is regarded as reasonable considering the inherent inaccuracies that may be incurred in the experimental measurements and the nitrogen analyses.

Variation between the small samples of organic material analysed occurred because of its heterogeneity. This affected the total TN content because the nitrogen content of the manure was high compared with that of the straw. The organic material for the experiments within a trial came from the same bulk mixture of pig manure and straw and so the initial TN concentration should be the same. The values in brackets in the 'nitrogen in' and error columns (Table 6.3) correspond to the nitrogen contents calculated using the mean initial TN concentrations of the three experiments in each trial, which are given in Tables A6.1 to A6.6. This approach reduced the mean errors in the balance from 18 % to 15 %.

The negative value in the balance column indicates a higher mass of nitrogen leaving the system than entering and so either, or both, the output TN mass and ammonia emissions were overestimated. This difference was large (error $\gg 10\%$) in four of the six C:N 15

experiments and in T5-7-25 and T5-8-20. In R2-8-15, the ammonia emissions were impossibly large and after analysis of the other results from the experiment, a new value (in brackets) was calculated using a lower air volume ratio for the scale-up. The TN content of the organic material increased in the experiments marked with the hash (#) in Table 6.3, which was not possible as there were no other nitrogen inputs during composting.

Table 6.3. The nitrogen balances of the composting experiments

C:N			Nitrogen in, g	Nitrogen out, g			Nitrogen balance, g	Error %
Trial	Reactor	pH	Organic material	Organic material	Ammonia emissions	Leachate		
15	R 2	6	569 (630)	511	198	0	-140 (-79)	25 (12)
T3	R 1 [#]	7	628 (584)	681	52	2	-107 (-151)	17 (26)
	R 3	8	626 (613)	605	150	0	-128 (-142)	21 (23)
15	R 1	6	580 (566)	556	35	10	-21 (-35)	4 (6)
T6	R 3	7	591 (573)	461	47	12	71 (41)	12 (7)
	R 2	8	540 (570)	486	393 (231)	7	-346 (-154)	64 (27)
20	R 3	6	389 (365)	342	15	9	24 (-1)	6 (<1)
T1	R 2	7	398 (398)	321	5	5	67 (67)	17 (17)
	R 1	8	328 (363)	257	38	0	33 (68)	10 (19)
20	R 2	6	434 (439)	348	0	4	81 (87)	19 (20)
T4	R 1 [#]	7	425 (429)	466	18	6	-65 (-61)	15 (14)
	R 3 [#]	8	420 (411)	422	30	7	-38 (-48)	9 (11)
25	R 1	6	317 (317)	303	10	4	0 (0)	0 (0)
T2	R 3	7	316 (315)	276	44	0	-3 (-4)	1 (1)
	R 2	8	299 (299)	264	85	0	-49 (-49)	16 (16)
25	R 3	6	317 (306)	271	38	0	8 (-3)	2 (<1)
T5	R 2 [#]	7	322 (323)	353	107	0	-137 (-137)	43 (43)
	R 1	8	300 (309)	271	142	4	-118 (-108)	39 (35)

In the experiments with positive balances, either the mass of ammonia collected in the acid traps or the volume of air that entered the reactors was low. Therefore, any error incurred when scaling up the estimated ammonia emissions was relatively small. The nitrogen deficit was probably due to a low measured TN concentration, which did not reflect the actual concentration in the whole composted organic material.

The AN content of the organic material increased in the majority of the experiments (Figures A6.22a to f). It was assumed in the model that the ON in the organic material was stable and therefore the AN could only decrease as a result of ammonia emission or assimilation into biomass. Such an assumption does not appear to have reflected the real composting system, which tended to show an appreciable conversion of ON to AN.

Also, because the AN and TN analyses used separate samples, any difference between the proportion of manure and straw in the samples affected the distribution of the AN and ON in the organic material.

6.4.5.2. Water balance

Water entered the system mainly in the organic material and the air of the baseline aeration and was generated by microbial activity (Table 6.4). Water left in the composted organic material, the off-gas (evaporated) and the leachate collected in the funnel. The mass of generated water was estimated using the theoretical mass produced per unit mass of VS decomposed (Section A5.1.3) and the corresponding VS mass losses calculated using the data in Tables A6.13 to A6.18. The mass of water evaporated was estimated by scaling up the mass of water collected in the condenser using the ratio of dry gas volumes of the gas that passed through the condenser and the air that entered the reactor. The mean error was 9 % and was about half that in the nitrogen balance.

A positive balance indicated a deficit in the output mass, which probably resulted from an underestimation of the total mass of water evaporated and not the water content of the organic material. Samples of the organic material used to determine the water content were at least 1 kg, and so, apart from the fact that some volatile organics may have been lost in the drying process, the masses of water entering and leaving the system were reasonably accurate.

Table 6.4. The water balances of the composting experiments.

C:N			Water in, kg			Water out, kg			Water balance, kg	Error %
Trial	Reactor	pH	Organic material	Aeration	Generated	Organic material	Evaporated	Leachate		
15	R 2	6	29.1	1.7	2.3	20.2	11.2	0	2	5
T3	R 1	7	28.9	1.0	0.6	26.4	1.9	0.4	2	6
	R 3	8	29.4	1.3	1.5	27.6	6.5	0	-2	6
15	R 1	6	30.1	1.1	0.9	23.8	2.9	1.9	5	17
T6	R 3	7	30.7	1.1	0.4	26.4	3.4	2.3	<1	0
	R 2	8	30.7	2.5	1.0	19.9	19.8 (12)	1.3	-7 (1)	20(0)
20	R 3	6	25.3	3.0	2.2	12.2	8.9	2.2	+7	23
T1	R 2	7	24.6	3.3	0.9	15.3	11.6	1.3	<1	1
	R 1	8	25.4	1.9	0.8	8.7	12.9	0.0	+7	23
20	R 2	6	22.5	1.1	1.8	17.7	3.8 ¹	1	3	11
T4	R 1	7	22.6	1.1	1.3	20.2	2.0 ¹	1.5	1	5
	R 3	8	23.0	1.1	1.2	18.4	3.4	1.7	2	7
25	R 1	6	23.5	1.4	2.0	18.8	4.1	1.4	3	10
T2	R 3	7	23.5	4.1	1.2	15.3	19.6	0	-6	21
	R 2	8	24.2	2.7	1.2	14.2	13.4	0	<1	2
25	R 3	6	24.2	2.4	1.9	15.1	14.2	0	<1	3
T5	R 2	7	23.5	1.6	1.7	15.2	14.8	0	-3	12
	R 1	8	23.9	1.9	1.6	12.6	12.2	1.4	1	4

¹ Values were calculated by assuming saturated off-gas

6.4.5.3. Carbon balance

The carbon balance considered the initial and final total organic carbon (TOC) mass in the organic material and the mass of carbon lost as carbon dioxide. The TOC content of the organic material was determined using the relationship with the VS content, as described by equation (3 vi). The concentration of carbon dioxide in the off-gas was only measured in Trial 1 and Trial 6 and therefore only these carbon balances are presented in Table 6.5.

Table 6.5. The carbon balance of the experiments in Trials 1 and 6

C:N			Carbon in, kg	Carbon out, kg			Carbon balance, kg	Error %	
Trial	Reactor	pH	Organic material	Organic material	Carbon dioxide	Leachate			
20	R 3	6	7.2	5.1	1.6	<0.1	+0.5	7	
	T1	R 2	7	7.8	6.7	0.9	<0.1	+0.2	2
		R 1	8	7.2	6.3	1.0	0.0	-0.1	1
15	R 1	6	7.8	6.9	1.4	<0.1	-0.5	7	
	T6	R 3	7	8.0	7.1	1.6	<0.1	-0.7	9
		R 2	8	7.9	6.8	4.8 (3.0)	0.0	-3.7 (-1.9)	47(23)

All the errors were below 10 % except in R2-8-15 in which the mass of carbon leaving the system as carbon dioxide was much higher. Again, this may have been caused by a large scale-up gas volume ratio error because of the high airflow. The average airflow rate was about 490 l h⁻¹ compared to 130 l h⁻¹ for R1-6-15 and R3-7-15. The higher mass of carbon dioxide produced does, however, reflect the off-gas concentration profile (Figure A6.20), which was almost always above 5 % v v⁻¹, and the high rate of microbial activity.

The total mass of ammonia emissions, mass of water evaporated and the carbon dioxide were all estimated using the airflow volume ratio, which was the likely cause of the notably high values in R2-8-15. For some reason, the total volume of air that passed through the reactor must have been lower than was recorded. Following analysis of the experimental

data, the total airflow through the reactor was probably closer to 85 m³ as opposed to the recorded 140 m³. The corrected ammonia emissions, evaporated water and carbon dioxide values for R2-8-15 are given in brackets in the respective balances. These corrected values were used in the statistical analysis because the anomalously high original values of R2-8-15 would have had a high leverage on the result of the significance tests.

6.4.6. Statistical analysis

The experimental design enabled ANOVA to be used to evaluate the significance of the relationship between the process factors (initial C:N ratio and pH) and final process variable values, such as the total ammonia emissions and the total solids loss (Section 6.2.3). The input data for statistical analysis by *Genstat* (Version 6) is given in Table A6.8 and the output of the analyses is given in full in Section A6.2.9. Table 6.6 gives a summary of the statistical analysis results, which includes the probability factor and variance accounted for. Table A6.16 is a glossary of the terms used in Table 6.6 and the output (Section A6.2.9).

6.4.6.1. Ammonia emissions

The full *Genstat* output of the analyses of the relationship between the ammonia emission rate (variate) and the process factors and variables (fitted terms) is given in Section A6.4.1.2. The ANOVA test shows a significant correlation with the initial pH but not with the initial C:N ratio. Although there were appreciable differences between the ammonia emissions of CN 20 compared with those of CN 15 and CN 25, there was not expected significant trend of increasing ammonia emissions with decreasing initial C:N ratio.

The *Table of means* shows the definite trend of increasing ammonia emissions with the initial pH except in the CN 15 group, where composting in R1-7-15 and R3-7-15 was relatively poor. The lower airflow and temperatures resulted in low ammonia emissions.

Table 6.6. Summary of the statistical analyses

Variates tested Fitted terms (type of analysis)	Mean ammonia emission rate	Pathogen markers	Total solids loss
CN pH CN and pH (ANOVA)	N.S. F pr < 0.05 N.S. (Figure A6.23)	—	N.S. F pr < 0.05 N.S. (Figure A6.27)
pH-measured (Simple linear regression)	F pr < 0.05 VAF = 25.7 %	—	F pr < 0.05 VAF = 23.5 % (Figure A6.28)
Airflow (Simple linear regression)	F pr < 0.05 VAF = 30.2 % (Figure A6.24a)	—	—
Temperature (Simple linear / Binomial proportions / Simple linear regression)	N.S. (Figure A6.24b)	N.S.	F pr < 0.05 VAF = 23.7 %
Residence time (Binomial proportions / Simple linear regression)	—	F pr < 0.05	N.S.
T>55°C (Binomial proportions regression)	—	N.S.	—
Mean ammonia emission rate (Binomial proportions regression)	—	F pr < 0.05	—
(Airflow).CN Airflow·CN15 Airflow·CN20 Airflow·CN25 (Simple linear regression with CN groups)	N.S. N.S. N.S. N.S. (Figure A6.25a)	—	—
(Airflow).pH Airflow·pH6 Airflow·pH7 Airflow·pH8 (Simple linear regression with pH groups)	F pr < 0.01 VAF = 47.4 % N.S. N.S. F pr < 0.05 (Figure A6.26a)	—	—

This situation therefore probably did not show the effect of the initial pH of C:N ratio but rather of the airflow and temperature on ammonia emissions. Simple linear regression

analysis showed a significant relationship with airflow but not with temperature. This situation therefore probably did not show the effect of the initial pH of C:N ratio but rather of the airflow and temperature on ammonia emissions. Simple linear regression analysis showed a significant relationship with airflow but not with temperature.

The significance of the relationship with the airflow and the measured initial pH of the organic material has to be interpreted with care, though, because the VAF is still low and some data points have large residuals and leverage on the fitted model. Ammonia emissions rise by about $0.08 \text{ mg g}^{-1} \text{ TN day}^{-1}$ (s.e = 0.03) per unit (one l h^{-1}) increase in airflow and by about $14.5 \text{ mg g}^{-1} \text{ TN day}^{-1}$ (s.e = 5.5) per unit increase in pH. The effect of the airflow on ammonia emissions within the initial pH and C:N ratio groups was analysed and the only improved fit was obtained when considering the initial pH group, where the F pr was about 0.001 and VAF was 50 %.

6.4.6.2. Pathogen marker inactivation

The *Genstat* output of the analyses concerned with pathogen inactivation is given in Section A6.3.2.2. The significance of the effect of process variables was analysed using logits. The 1 - 0 response (Table A6.15), where 1 indicated the presence of pathogen markers in the composted organic material, was modelled by binomial proportions. There was no significant relationship with either the mean composting temperature (Mean T) or the time for which the temperature was at least 55°C ($T \geq 55^{\circ}\text{C}$). As suggested in Section 6.4.3, ammonia may have contributed to pathogen inactivation and this was confirmed by the significance of the relationship between the presence of pathogen markers and mean ammonia emission rate (F pr = 0.014), where the positive responses clustered at the lower end of the range of ammonia emission rate.

The significance of the relationship with the residence time (res-time) is misleading. The *Genstat* output indicates that the positive responses of R3-6-20 and R2-7-20, the two experiments, which spent an appreciably longer time in the reactors, exerted a high leverage on the result of the analysis and there is in fact no trend (Section A6.4.2.2). Also, it would normally be expected that a longer composting time would lead to more complete pathogen inactivation, which is contrary to what the result of the statistical analysis shows. The reason for the presence of the pathogen markers in the composted organic material in these two experiments is discussed in Section A6.1.1.1.

6.4.6.3. Mass and water loss

The percentage loss in total solids was significantly affected by the initial pH ($F_{pr} = 0.012$) and not by the initial C:N ratio of the organic material. Simple linear regression analysis with the measured initial pH of the organic material confirmed the significance of the relationship ($F_{pr} = 0.024$) with the TS mass loss increasing by about 4.8 % (s.e = 1.9) per unit increase in the initial pH, for the pH range between 5 and 8.

The TS loss was not significantly affected by the residence time but the relationship with the mean composting temperature was significant ($F_{pr} = 0.23$) with an increase by about 0.6 % (kg) (s.e = 0.2) per unit °C increase in the mean composting temperature.

6.5. Conclusions

The composting reaction design enabled the process conditions to be controlled so that the change in process variables could be evaluated without ambient conditions affecting the outcome. The external heating cable reduced radial temperature differences to within 2°C for the majority of the composting time. The cooling aeration controlled the maximum centre

temperature about the optimum for composting of 60 °C. The vertical temperature difference was less than 10 °C when the cooling aeration was not operating.

In response to the hypothesis, the ammonia emissions can be reduced by adjusting the initial pH of the organic material. Adjusting the initial C:N ratio does appear to affect the ammonia emissions but further investigation is required to confirm any significant relationship. Pathogen inactivation cannot be guaranteed if ammonia emissions are low, even if the organic material is exposed to temperatures above 55°C for more than 3 days.

Even with the controlled conditions under which the organic material was prepared and composted, there was still a degree of unpredictability about the process. In order to draw absolute conclusions, more composting experiments need to be carried out and more data are needed for the statistical analyses. From this investigation, a number of trends were apparent:

1. Ammonia emissions decreased with the initial pH of the organic material.
2. Ammonia emissions increased with airflow through the organic material.
3. Higher ammonia emissions improved the chance of pathogen inactivation.
4. The loss of total solids increased with decreasing the initial pH of the organic material.

CHAPTER 7

VALIDATION, DISCUSSION AND CONCLUSIONS

7.1. Model validation

The model was validated using temperature, ammonia emissions, aeration and off-gas composition profiles and the total changes in such process variables as the mass of oxygen consumed and total solids (TS) lost. The following three composting experiments were selected to validate the model as each showed rapid microbial activity and together covered the three reactors and initial pH and C:N ratios considered in the experimental investigation.

- a) R1-8-20 from Trial 1
- b) R3-7-25 from Trial 2
- c) R2-6-15 from Trial 3.

A noticeable difference between the model simulations (Chapter 5) and the results from the composting experiments was the mass loss. A maximum of about 25 % of the initial TS was lost in the experiments whereas the model predicted a loss of at least 55 %. The following reasons may account for the discrepancy.

1. The equilibrium mass is determined by the biodegradability of the volatile solids (VS) of the organic material. In the model, the biodegradability values used had been determined under anaerobic conditions at 35 °C over months [Haug 1993]. The equilibrium mass of pig manure and straw under composting conditions may be higher than that predicted.
2. The temperature factor function used in the model only considered the fast stage of composting and did not account for slow stage, which is described in Section 4.3.3.1.

3. The reaction rate coefficient did not only depend on the oxygen concentration and the moisture content and temperature of the organic material. The model did not consider the effect of some process factors, such as the FAS, C:N ratio and pH, which may have limited the reaction rate.

Model simulations in Chapter 5 showed that the moisture content of the organic material became rate limiting after about six days. In the model, the baseline aeration was supplied at 5 l min^{-1} continuously except when the cooling aeration was operating. In the experiments, because there were three reactors in the rig, the baseline aeration supplied 5 l min^{-1} to each of the reactors for 5 minutes every 15 minutes. With less air passing through the reactor, less water was evaporated and any rate limiting effect of a low moisture content on the composting process was delayed. To make the process conditions between the model and experiments comparable, the intermittent baseline aeration used in the experiments was applied in the validation simulations.

Another variable that determined the loss of water from the organic material was the degree of off-gas saturation, S , which was a function of the airflow rate and depended on the value of the exponent constant, ϕ , of equation (5 xviii). Validation simulations were performed on ϕ values of 0, 0.01 and 0.02, which respectively corresponded to off-gas saturations of 100 %, 96 % and 91 % with the baseline aeration and to 100 %, 80 % and 64 % with the cooling aeration. By comparing the predicted and measured temperature profiles, the measured degree of off-gas saturation, which was estimated from the mass of water evaporated, could be verified.

The measure initial and process conditions of the composting experiments, such as the initial TS mass and pH and the operating upper temperature limit, were used in the model validation simulations and are listed in Table 7.1.

Table 7.1. Parameter values of the organic material used for model validation simulations

Parameter	R1-8-20	R3-7-25	R2-6-15	Units
Initial TS mass	14.6	13.8	17.5	kg
Initial moisture content	64	63	62	% TS
Initial VS content	88	87	88	% TS
Manure biodegradability	32	32	32	% VS
Straw biodegradability	Sensitivity analysis for values between 20 and 50%VS			
Initial total nitrogen content	2.3	2.3	3.3	% TS
Initial ammoniacal nitrogen content	0.5	0.9	1.0	% TS
Initial pH	7.6	6.6	6.2	-
Final or maximum pH	8.1	7.5	9.0	-
Upper temperature limit	65	60	60	°C
Mean off-gas saturation (σ)	93 (2)	80 (2)	91 (4)	%

7.1.1. Biodegradability of straw

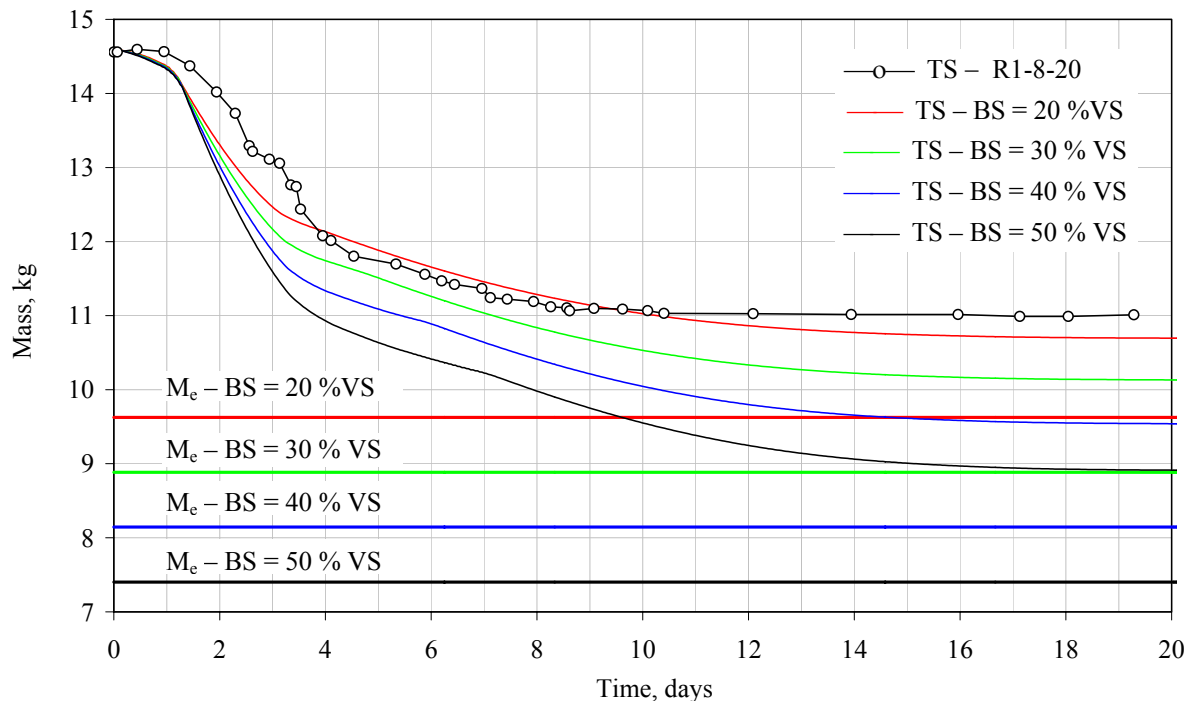


Figure 7.1. Straw biodegradability sensitivity analysis.

In Section 4.2, the biodegradability of the pig manure was estimated to be 32 % VS. The biodegradability of the straw and the equilibrium mass (M_e) were estimated by

performing a model sensitivity analysis on straw biodegradability values between 20 % VS and 50 % VS and comparing the TS mass profile with that of R1-8-20 (Figure 7.1). The empirical TS profile was estimated from the total mass of the organic material measured by the load cell, the mass of water evaporated and the water generated by the TS loss as calculated with the partition coefficients used in the model (Section A5.1.3). Out of the values analysed, the simulation for a straw biodegradability of 20 % VS fitted the empirical data best. The corresponding M_e mass was 9.63 kg.

7.1.2. R1-8-20

The profiles of the measured total and evaporated water mass are shown in Figure 7.2 with the corresponding predicted profiles for $\phi = 0, 0.01$ and 0.02 . The model calculated the mass of water evaporated hourly. The model data was, therefore, adjusted so that the mass evaporated could be compared with the measured mass evaporated (\blacktriangle) over the time intervals between the collections of the condensate from the off-gas.

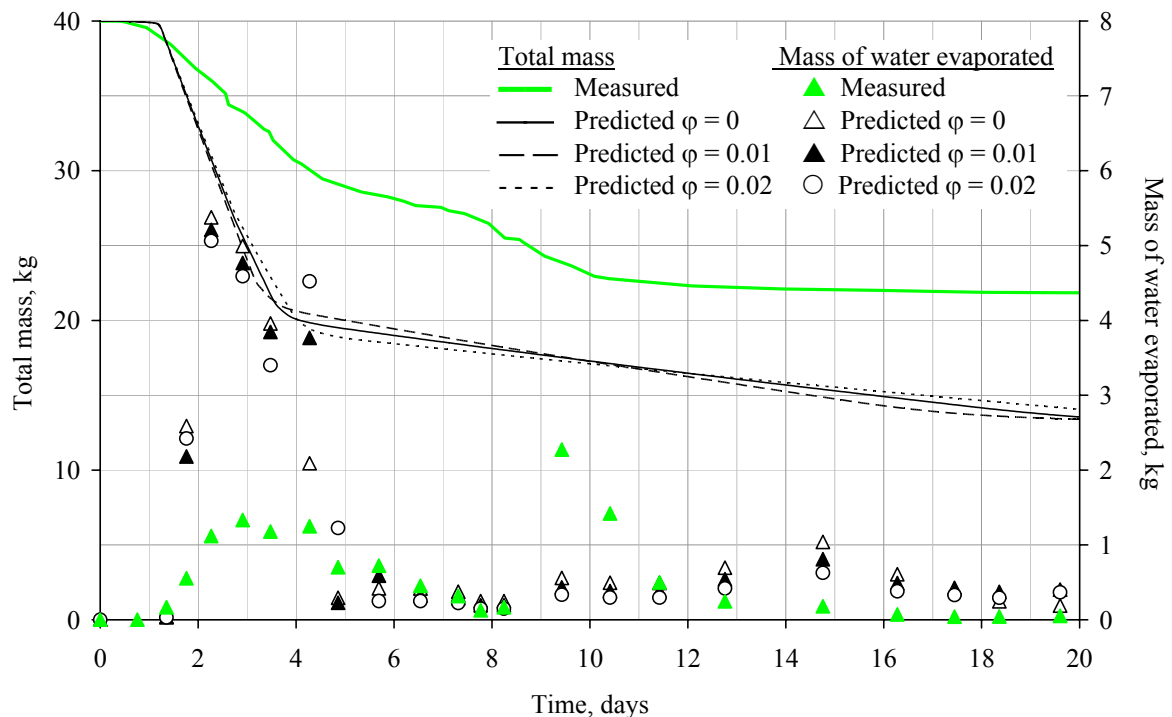


Figure 7.2. Total and evaporated water mass profiles of R1-8-20.

The predicted and measured mass of water evaporated followed similar patterns except that during the first 5 days the predicted mass was more than twice that measured, which was essentially due to the higher mass of air that flowed through the reactor. For example, for the $\phi = 0.01$ simulation, the total dry air mass that flowed into the reactor during the first 5 days was about 115 kg compared with the 41 kg in the experiment and after the 20 days, the respective total masses of dry air had increased to 158 kg and 98 kg. The overprediction of the mass of water evaporated was reflected in the higher drop in the predicted total mass of the organic material than was measured. The degree of off-gas saturation did not make a great difference to the overall predicted total mass profile.

In the experiment, composting proceeded at an upper temperature limit of 65 °C instead of the intended 60 °C and this was echoed in the validation simulations. Figure 7.3 shows the profiles of the measured temperature and cumulative mass of dry air that flowed into the reactor and the corresponding predicted profiles. The model predicted the rapid rise in temperature and the maintenance of the temperature about the upper limit. The model did not predict the rapid decrease in temperature on day 10 probably caused by the organic material becoming too dry to sustain microbial activity. The function used to describe the effect of moisture content (equation 5 x) needs to be addressed and the relationship suggested by Richard *et al* [2002] may be more appropriate for this system. Varying the degree of off-gas saturation did not improve the fit to the temperature profiles. The average measured off-gas saturation during the 14 days was 94 %, which was near to that given by $\phi=0.01$. Therefore all subsequent predictions shown for R1-8-20 are from the $\phi=0.01$ simulation.

The cumulative dry air mass profiles highlight the higher predict demand for cooling aeration between day 1 and 4 to maintain the upper temeprature limit about 65 °C than was measured.

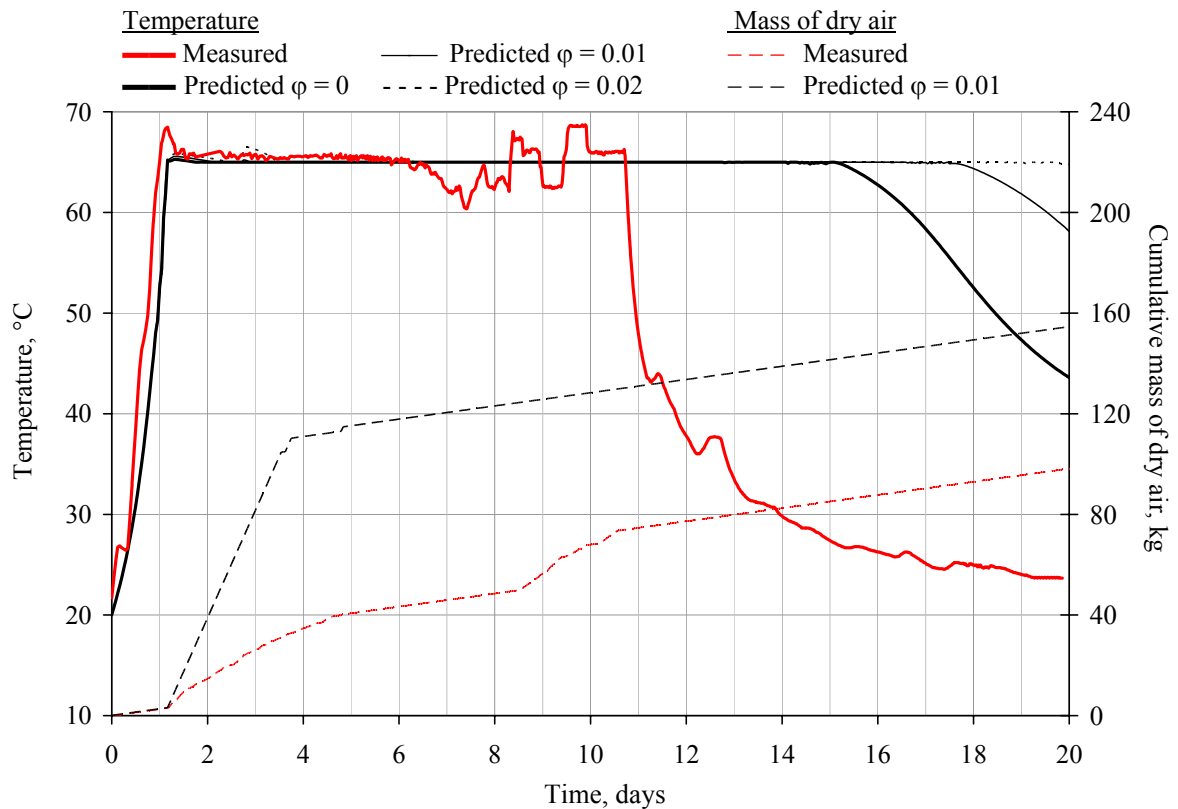


Figure 7.3. Measured and predicted temperature and total airflow profiles of R1-8-20.

Figure 7.4 shows the measured and predicted cumulative masses of ammonia and carbon dioxide produced and oxygen consumed. The model predicted that about 17 g more of ammonia was emitted than was measured. Again the discrepancy may be due to the higher airflow in the model because the ammonia emission rate depended on the airflow rate (equation 5 xxxviii). If the measured ammonia emissions were scaled up using the predicted volume of air, then about 80 g of ammonia was emitted. The airflow rate, therefore, did not solely determine the mass of ammonia emitted. In the model, the coefficients controlling ammonia dynamics (H , K_L and K_a) related to aqueous or pig slurry systems and may be appreciably different for composting FYM. Also, the fraction of the dissociated ammonia in the organic material is governed by the pH of the organic material (equation 5 v) and the pH profile followed in the model may not have reflected that in the experiment. This could not be checked as pH during composting was not measured in Trial 1. The model does not

account for possible spatial concentration variations in the organic material and the highly soluble ammonia gas emitted from the base section may have returned to the liquid phase as the gas flowed up through the organic material.

The predicted cumulative mass profiles of oxygen consumed and carbon dioxide produced were higher than the measured masses because of higher predicted airflow and the longer period of high microbial activity. The average predicted and measured respiration quotients, Q_{resp} , were 0.85 and 0.84, respectively, which are indicative of an aerobic systems [Van Ginkel 1996] and comparable with the 0.9 determined by Schulze [1962] for composting.

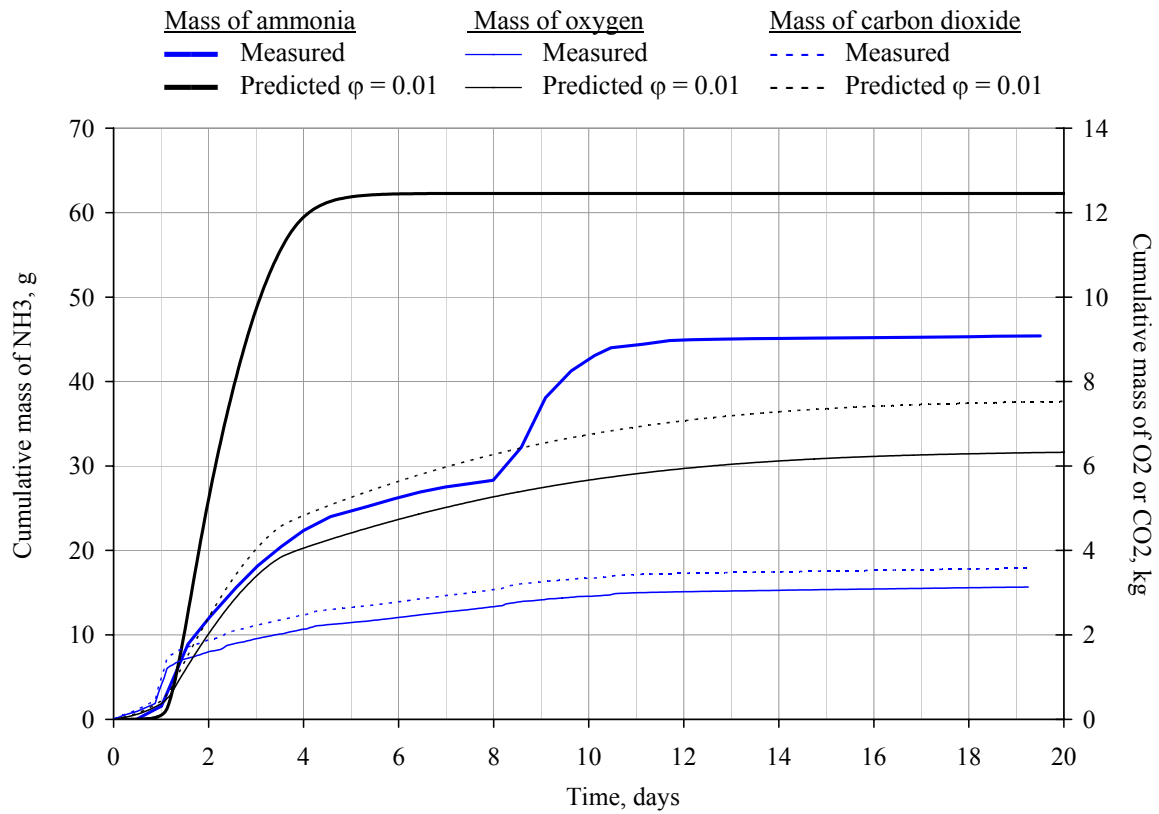


Figure 7.4. Measured and predicted cumulative mass profiles of ammonia and carbon dioxide produced and oxygen consumed in R1-8-20.

Figure 7.5 shows the measured and predicted concentration profiles of oxygen and carbon dioxide in the off-gas. In both cases the oxygen concentration decreased and carbon

dioxide concentration increased rapidly in within the first day of composting when the air was provided solely by the baseline aeration. The measured oxygen concentration quickly rose above 16 % v v⁻¹ on activation of the cooling aeration on day 1, with only minor fluctuations in the concentrations thereafter. The predicted gas concentrations in the off-gas were more sensitive to the step changes between the cooling and baseline aeration, which occurred on day 1 and between day 3 and 5. It also took notably longer for the gas concentrations in the off-gas to return their corresponding concentrations in the air, because of the longer period of high of microbial activity.

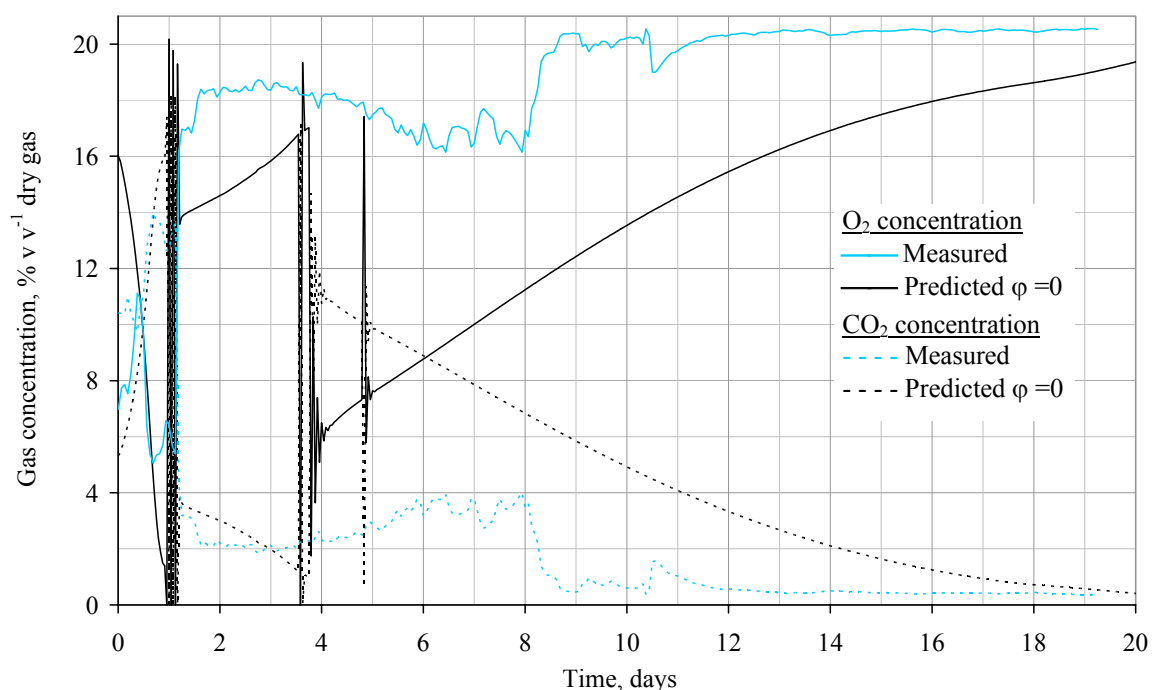


Figure 7.5. Measured and predicted oxygen and carbon dioxide concentration profiles in the off-gas in R1-8-20.

The measured gas concentrations were probably less sensitive to the switching between the two aerations because the off-gas could only analysed for 15 minutes every hour with the rig configuration. Also, there may have been some mixing of the off-gas in the headspace where as the model assumed pure plug flow of the gas leaving the reactor.

Table 7.2 gives the initial and final total, TS, water and total nitrogen (TN) masses of the organic material and the cumulative mass of water evaporated, oxygen consumed and carbon dioxide and ammonia produced. The change in each of these process variables (Δ) are given so that the measured and predicted results can be easily compared. The total mass of water generated was about 2 kg. TS loss given in Table A6.2 was calculated using the initial and final moisture contents of the organic material and was found to be only 1.4 kg.

Table 7.2. Measured and predicted initial and final values of process variables from R1-8-20

Measured	Total mass, kg	TS mass kg	Water mass, kg	TN mass, kg	Mass H ₂ O evaporated kg	Mass H ₂ O generated, kg	Mass O ₂ consumed, kg	Mass CO ₂ produced, kg	Mass NH ₃ , g
t = 0	40.0	14.6	25.4	0.33	0.0	0.0	0.0	0.0	0
t = 20 d	21.9	11.1	10.8	0.26	12.9	2.1	3.1	3.6	45
Δ	-18.1	-3.5	-14.6	-0.07	12.9	2.1	3.1	3.6	45
Predicted ($\phi = 0.01$)									
t = 0	40.0	14.6	25.4	0.33	0.0	0.0	0.0	0.0	0
t = 20 d	13.6	10.7	2.9	0.28	25.5	2.6	6.3	7.4	62
Δ	-26.4	-3.9	-22.5	-0.05	25.5	2.6	6.3	7.4	62

Apart from the TS, TN and water generated masses, predicted changes were much larger than those measured, which stemmed predominantly from the higher cooling aeration demand in the model. If the measured cooling aeration were used in the model, the airflow was not high or often enough to control the temperature at the upper limit in the initial stages.

7.1.3. R3-7-25

Figure 7.6 shows the profiles of the measured temperature and cumulative mass of dry air and the corresponding predicted profiles. During the first 10 day the model predicted the temperature profile well, most notably confirming the overshoot above the upper temperature

limit that was measured between day 1 and 5. Again, the model did not predict the sharp decrease in temperature on day 12. Varying the degree of off-gas saturation did not improve the fit to the temperature profiles.

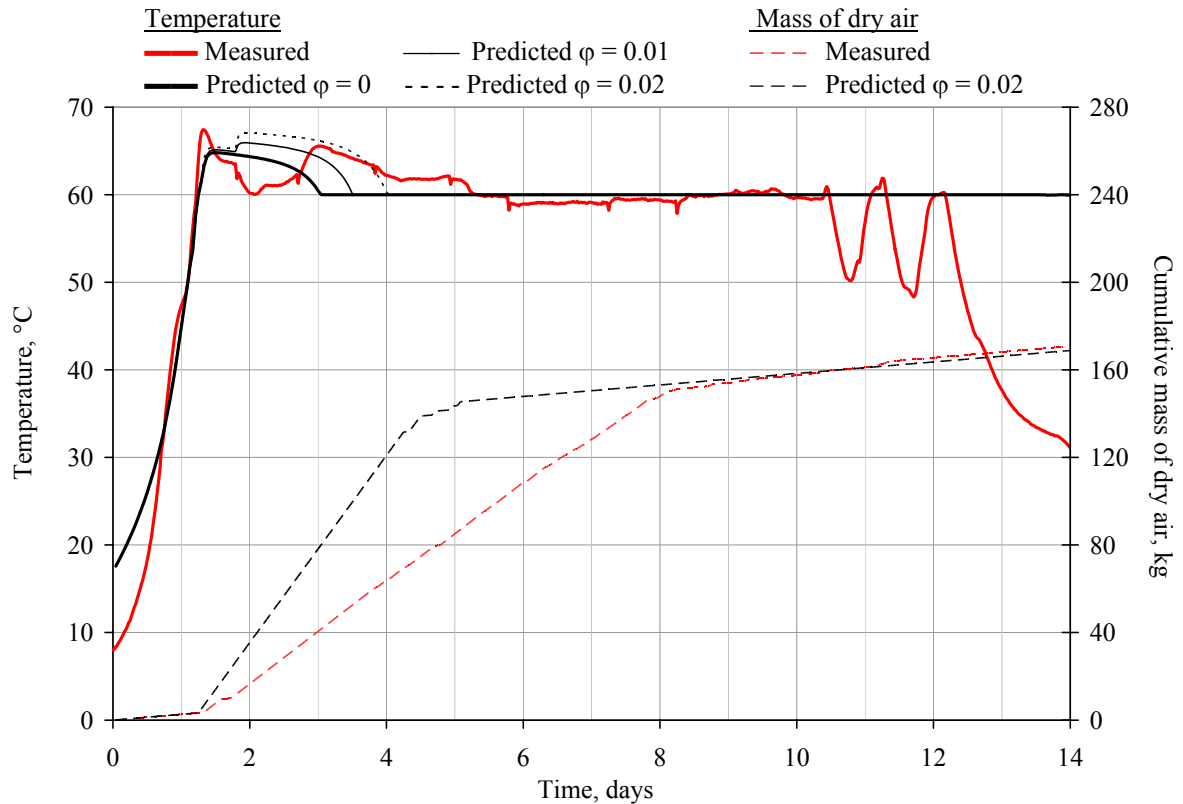


Figure 7.6. Measured and predicted temperature and total airflow profiles of R3-7-25.

The average measured off-gas saturation during the 14 days was 80 %, with values increasing after 5 days from 76 % to 90 % by the day 14. This suggested that $\phi = 0.02$ and subsequent predictions shown for R3-7-25 are from the $\phi = 0.02$ simulation. The predicted and measured total masses of dry air that flowed through the reactor (about 170 kg) were the same. The model predicted a more intense cooling aeration demand between day 1 and day 4 than was measured in the experiment.

The measured and model ammonia profiles are presented in Figure 7.7 with the pH profiles. In the model, the pH profile was based on that measured in the experiment ($\text{---}\Delta\text{---}$). The predicted total mass of ammonia emitted was 65 % higher than was measured. The

model predicted a rapid loss of ammonia, with no emissions after day 7, whereas the measured loss of ammonia was more gradual over the 14 days, which reflected the less intense cooling aeration demand. This notable difference between the emissions profile was probably due to the assumed plug flow of gases through the reactor.

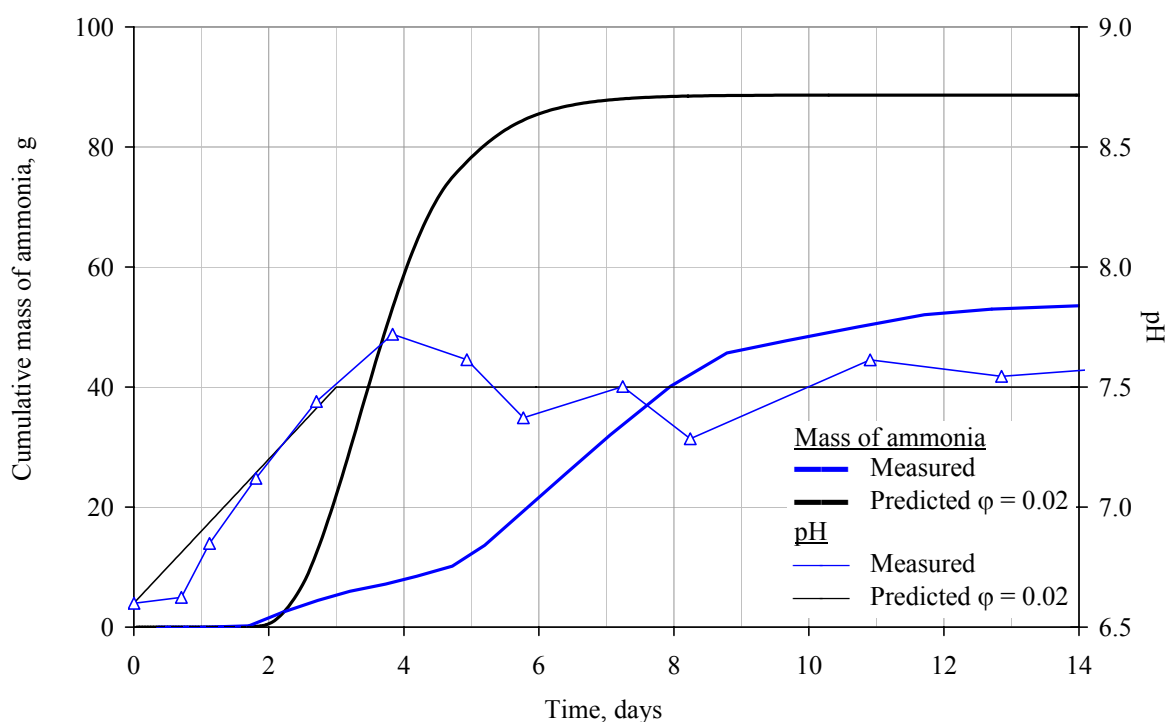


Figure 7.7. Measured and predicted cumulative mass profiles of ammonia and carbon dioxide produced and oxygen consumed in R3-7-25.

Table 7.3 gives the initial and final total, TS, water and TN masses of the organic material and the cumulative mass of water evaporated, oxygen consumed and carbon dioxide and ammonia produced. Reactor 2 was not positioned on the load cell and the measured total, TS and water masses were determined from analysis of the organic material before and after composting. The 2.1 kg loss of TS generated about 1.2 kg of water (Section A5.1.3). Also, the gas analyser was not available for this trial and the total mass of carbon dioxide produced and oxygen consumed were estimated from the VS loss using the gas partition coefficients. Both the predicted and measured respiration quotients, Q_{resp} , were, therefore, 0.88.

Table 7.3. Measured and predicted initial and final values of process variables from R3-7-25

Measured	Total mass, kg	TS mass, kg	Water mass, kg	TN mass, kg	Mass H ₂ O evaporated kg	Mass H ₂ O generated, kg	Mass O ₂ consumed, kg	Mass CO ₂ produced, kg	Mass NH ₃ , g
t = 0	37.3	13.8	23.5	0.32	0.0	0.0	0.0	0.0	0
t = 15 d	27.0	11.7	15.3	0.28	19.6	1.2	2.8	3.4	54
Δ	-10.3	-2.1	-8.2	-0.04	19.6	1.2	2.8	3.4	54
Predicted ($\phi = 0.02$)									
t = 0	37.3	13.8	23.5	0.32	0.0	0.0	0.0	0.0	0
t = 15 d	15.2	10.6	4.7	0.24	20.9	2.6	5.0	6.0	89
Δ	-22.1	-3.2	-18.8	-0.08	20.9	2.6	5.0	6.0	89

The predicted and measured masses of water evaporated were comparable. However, for the measured TS and water loss, the maximum mass of water that could have been evaporated was 13.5 kg. The scale up using the ratio of the air volumes may have overestimated the mass of water evaporated or more water may have been lost than analysis organic material implied. The discrepancy is shown in the water balance in Table 6.4.

The predicted total masses of oxygen consumed and carbon dioxide and water produced were higher because of the greater predicted TS mass loss. The analysis of the TS content of the organic material may have underestimated the loss, which was shown by the difference between the measured TS mass losses estimated from the total mass loss (3.5 kg) and determined analytically (1.4 kg) in R1-8-20. The higher predicted loss in TN reflected the higher predicted mass of ammonia emitted. The measured and predicted nitrogen balances are compared in Section 7.1.5.

7.1.4. R2-6-15

Figure 7.8 shows the measured centre and top temperature profiles. Although the centre temperature was below 60 °C, cooling aeration was still active. This probably occurred because the thermocouple controlling the cooling aeration was in contact with a slightly hotter part of the organic material. Unlike, R1-8-20 and R3-7-25, microbial activity continued at a high rate for the duration of the composting experiment. The sudden increase in the centre temperature on day 4 occurred because of a 12-hour power cut and no aeration was available to dissipate the excess heat.

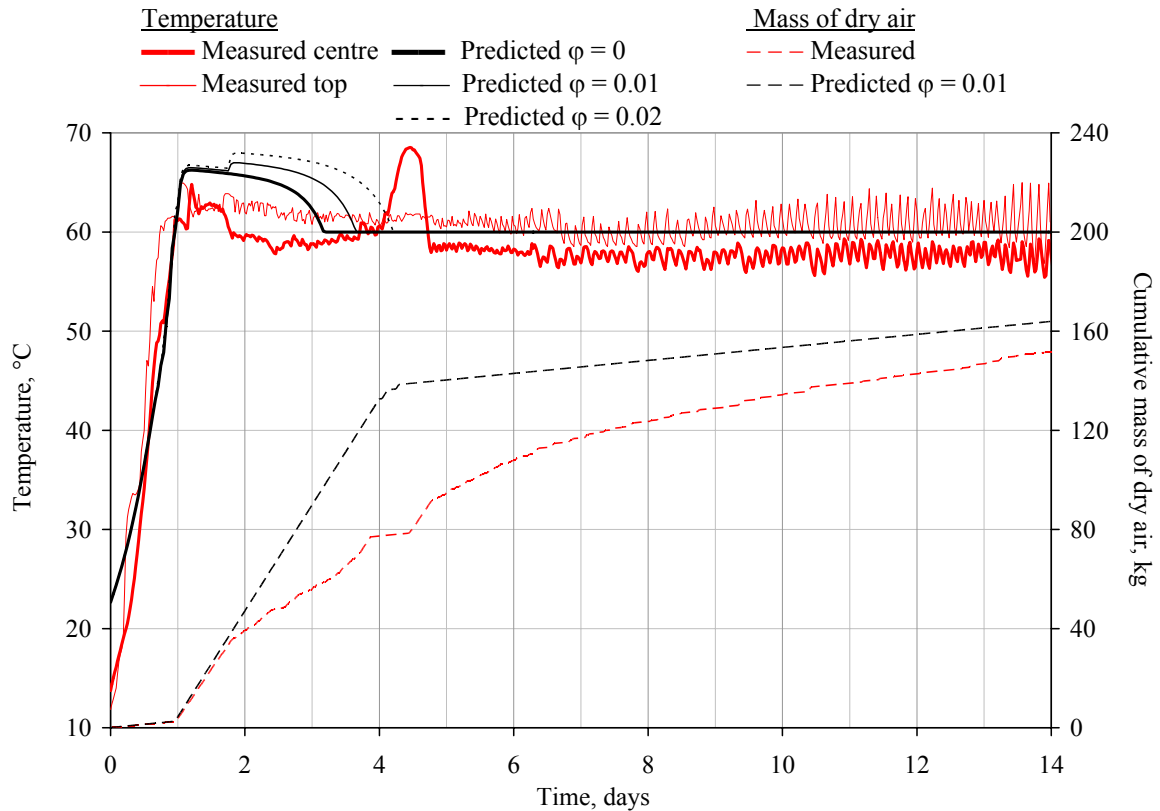


Figure 7.8. Measured and predicted temperature and total airflow profiles of R2-6-15.

All the temperature profiles of the three ϕ simulations closely follow measured profile. The average measured off-gas saturation was 90 %, which corresponds to $\phi=0.01$ and subsequent predictions shown for R2-6-15 are from the $\phi=0.01$ simulation.

The predicted and measured total masses of dry air that flowed into the reactor (164 kg and 152 kg, respectively) were comparable. The model required more cooling aeration in the initial stages to maintain the temperature about 60 °C. In the model, the effect of temperature on microbial activity was defined by the constants for a M:S ratio of 2:1 given in Table 4.7. Activity at 60 °C was lower for the M:S ratio of 4:1 (Figure A4.4) than 2:1 (Figure A4.3). The difference between the measured and predicted dry air mass profiles probably reflect the differences between these activity – temperature profiles.

The measured and predicted ammonia emissions and pH profiles are shown in Figure 7.9. In the model, the pH profile was based on the profile measured in the experiment (—△—). The total measured mass of ammonia emitted continued to rise up to 240 g over the 14 days while the model predicted no ammonia emissions after 6 day and a total mass of 170 g emitted. The nitrogen balance (Table 6.3) confirms that ammonia emitted were overestimated by between 80 g and 140 g and were probably closer to the predicted amount.

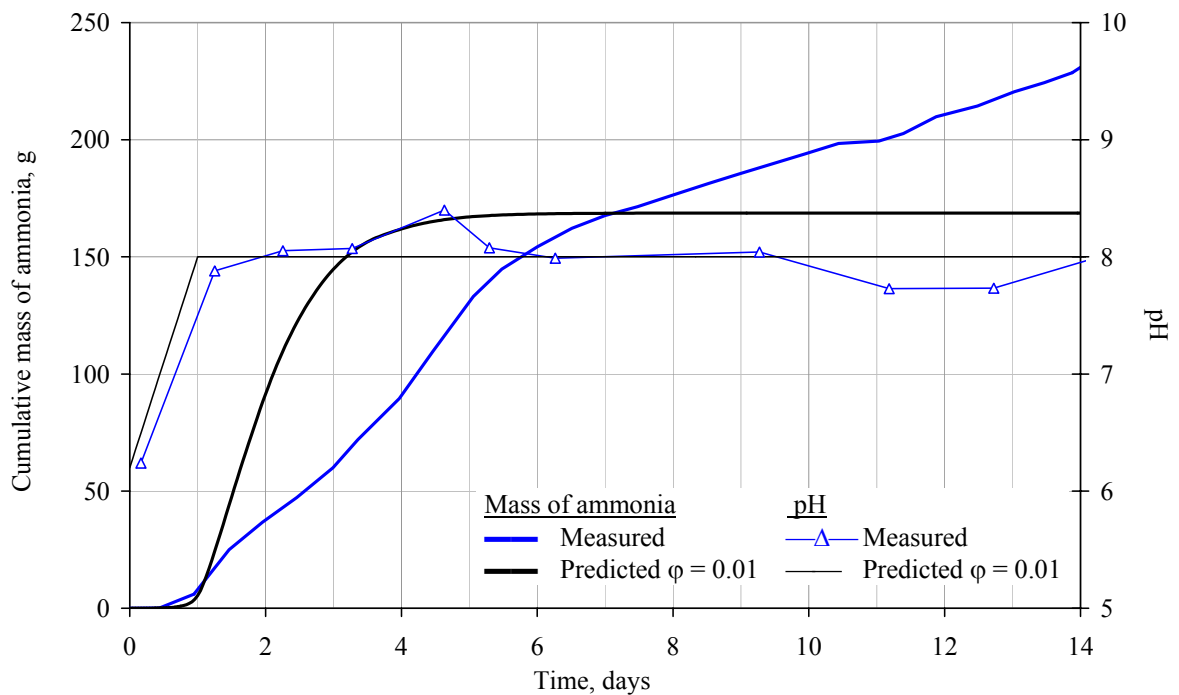


Figure 7.9. Measured and predicted cumulative mass profiles of ammonia and carbon dioxide produced and oxygen consumed in R2-6-15.

Table 7.4 gives the initial and final total, TS, water and TN masses of the organic material and the cumulative mass of water evaporated, oxygen consumed and carbon dioxide and ammonia produced. The measured total, TS and water masses were determined from analysis of the organic material before and after composting and the total mass of water and carbon dioxide produced and oxygen consumed were estimated from the VS loss using the gas partition coefficients (Section A5.1.3). The 3.8 kg TS loss generated 2.3 kg of water. The higher predicted mass of oxygen consumed and carbon dioxide and water produced measured reflected the slightly higher TS loss than was measured.

The predicted mass of water evaporated was more than twice that measured and, therefore, so was the water and total mass loss in the organic material. The TN loss was also predicted to be twice as much as was measured, which again implies that the measured mass of ammonia emitted was probably overestimated.

Table 7.4. Measured and predicted initial and final values of process variables from R2-6-15

Measured	Total mass, kg	TS mass, kg	Water mass, kg	TN mass, kg	Mass H ₂ O evaporated kg	Mass H ₂ O generated, kg	Mass O ₂ consumed, kg	Mass CO ₂ produced, kg	Mass NH ₃ , g
t = 0	46.6	17.5	29.1	0.57	0.0	0.0	0.0	0.0	0
t = 15 d	33.9	13.7	20.2	0.51	11.4	2.3	5.0	5.9	240
Δ	-12.7	-3.8	-8.9	-0.06	11.4	2.3	5.0	5.9	240
Predicted ($\phi = 0.01$)									
t = 0	46.1	17.5	28.6	0.58	0.0	0.0	0.0	0.0	0
t = 15 d	19.1	13.1	6.0	0.44	26.5	3.0	7.1	8.4	169
Δ	-27.0	-4.4	-22.6	-0.14	26.5	3.0	7.1	8.4	169

7.1.5. Nitrogen balances

Figures 7.10 a) to c) show the measure and predicted nitrogen balances with the initial and final TN mass in terms of the ammoniacal nitrogen (AN) and organic nitrogen (ON). There was no leachate from the reactors and any nitrogen losses were assumed to be as ammonia nitrogen ($\text{NH}_3\text{-N}$).

The most notable difference between the measured and predicted nitrogen balances was the presence of AN in the organic material after composting whereas in the model all the AN was either emitted or assimilated into biomass, which is why the predicted ON mass increased. The assumption that the ON was stable is not confirmed by the experimental data. There was a measured 12 % and 40 % loss in ON in R2-6-15 and R1-8-20, respectively. The measured 11 % increase in ON in R3-7-25 was also predicted in R2-6-15 and R1-8-20. The predicted ON increase in R3-7-25 was 26 %, probably because the composting pH was lower.

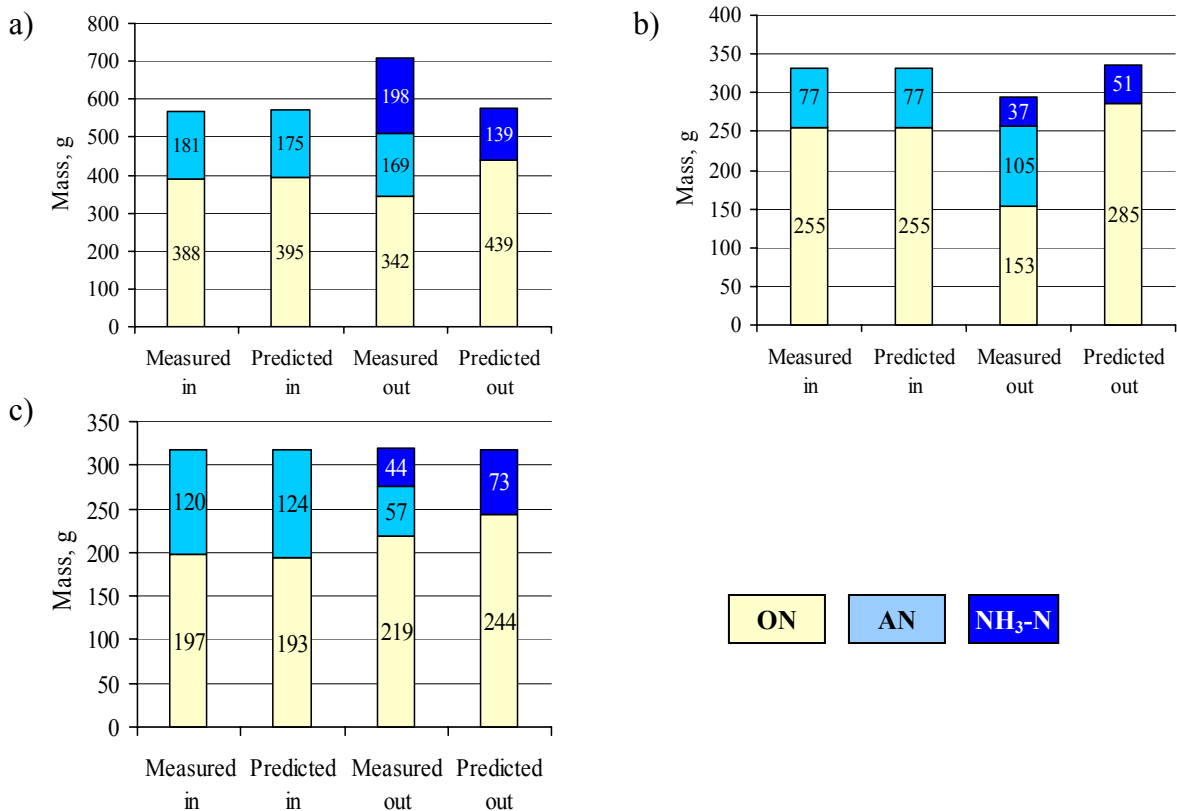


Figure 7.10. Measured and predicted nitrogen balances a) R2-6-15, b) R1-8-20, c) R3-7-25

7.2. Conclusions and future work

Respirometry:

1. The optimum temperature for microbial activity in pig manure is between 50 °C and 55 °C. Microbial activity decreases rapidly at higher temperatures.
2. Mixing the manure with straw increases the optimum temperature for microbial activity to around 60 °C and the oxygen uptake rate to about 7 times that of the pig manure alone.
3. The effect of temperature on microbial activity can be described by two Arrhenius-type equations: an empirically derived 'double power' equation or a theoretically derived equation based on enzyme activity theory. More kinetic data at temperatures above the optimum would increase the confidence of the fit of the equations. The coefficients of the equations are not absolute and are probably specific to the organic material used.
4. Two distinct rates of microbial activity were observed, which correspond to the decomposition of the readily degradable 'fast' fraction and less readily degradable 'slow' fraction of the organic material.
5. Microbial activity doubles with a 10 °C rise in temperature during the initial stages of composting ($Q_{10} = 2$) when there are no other rate limiting effects. Q_{10} can be used to assess whether the efficiency of the process is being compromised by the rate of oxygen or nutrient diffusion.
6. The stability of the composted organic material, as described by the mass ratio, can be reliably predicted from the reaction rate coefficient. The stability increases with the reaction rate coefficient and, therefore, the rate of microbial activity.

7. The effect of temperature on the microbial activity in various mixing ratios of pig manure and straw needs to be assessed so that an ideal mixing ratio, which can be equated to an optimum free air space or other related process factor, can be determined.
8. The respirometers offers a reliable and relatively cheap and simple means of measuring microbial activity under controlled conditions and can be further used to evaluate the effect of other environmental factors on microbial activity, such as the oxygen concentration.

The composting unit and reactor design

1. The composting unit allows composting conditions to be controlled so that the change in process variables, which would be expected to occur at the core of a large windrow, can be evaluated without ambient conditions affecting the outcome.
2. An external heat input of 58 W m^{-2} is required to compensate for heat losses from the surface of the insulated reactor and to keep the radial temperature difference across the organic material to within 1°C .
3. The external heating cable is an effective, compact and relatively cheap way to compensate for the heat losses from the reactor surface.
4. A cooling aeration air flow rate of 25 l min^{-1} acting in response to temperature feedback is able to control the temperature at the optimum for microbial activity.
5. For the intermittent baseline aeration used, an airflow rate above 5 l min^{-1} is recommended in the initial stage of high microbial activity to meet oxygen demand, particularly for organic material with a high manure content, and avoid oxygen became a limiting factor.

6. The inclusion of an overriding response to oxygen concentration feedback operating in parallel with the temperature feedback in the cooling aeration control loop would help to ensure an adequate supply of oxygen to sustain rapid aerobic activity.
7. Along with temperature, the cooling aeration demand provides rapid, online means of tracking microbial activity during composting.
8. Moisture control needs more attention. Re-circulation of the off-gas back to the reactor could be considered in order to reduce both moisture loss and the vertical moisture and the temperature gradient arising during cooling aeration.

The composting process

1. Well managed composting is generally an effective method of dealing with pathogen-infected organic material.
2. The established criteria for composting so that it can be considered as a process to further reduce pathogen (PFRP) are brought into question following the detection of high concentrations (10^6 CFU g⁻¹ TS) pathogen markers in the composted organic material that been exposed to the temperatures above 55 °C for more than 3 days in 5 of the 17 composting experiments (the temperature one of the experiments did not reach 55 °C).
3. Higher ammonia emissions improve the chance of pathogen marker inactivation but further evaluation of an ammonia threshold is required. This is another investigation that could be done under controlled conditions using the gas analyser respirometer.
4. Ammonia emissions decrease with the initial pH of the organic material and increase with airflow through the organic material.

5. The C:N ratio did influence the ammonia emissions but there was no significant trend in the experiments performed. More experimental data is needed to evaluate statistically the effect of the C:N ratio on ammonia emissions.
6. The addition of sulphuric acid, which was used to lower the initial pH of the organic material, enhances the total solids loss, probably through partial hydrolysis of the carbonaceous fraction of the organic material.
7. The heterogeneity of the organic material causes uncertainty in its analysis, especially for nitrogen analysis, which uses small samples. A method of preparing more consistent samples for analysis needs to be used.

Modelling the composting process

1. The simulation model is based on first order reaction kinetics and uses a multiplicative approach to describe the effect of environmental factors. The model simulates changes in the following process variables:
 - Temperature
 - Aeration demand and oxygen uptake rate
 - Total, TS, nitrogen and water mass of the organic material
 - Composition of the off-gas in terms of water content and oxygen, carbon dioxide and ammonia concentrations
 - Total mass of ammonia and carbon dioxide produced and oxygen consumed
 - Individual effects of environmental factors on process kinetics
 - Nitrogen dynamics in the organic material
 - Heat flows in the system
2. The model behaves intuitively and was of great use in aiding experimental design.

3. The model predicts that the ammonia emissions would be greater from composting pig manure and straw mixes with higher initial pH values and mixing ratios (lower C:N ratios) and this was seen in the experiments.
4. The model predicts that the loss of water from the organic material through evaporation prematurely limits microbial activity, which was observed in some of the composting experiments.
5. The model responds to the control functions, such as the upper temperature limit in a similar way to the experiments
6. The model does not accurately predict the final stages of composting because the initial empirical data corresponds to the fast stage of decomposition and because the reaction is based on the presence of biodegradable organic material and oxygen and not on the transport of the nutrients and oxygen to the sites of microbial activity. However, it is the initial stages of high microbial activity that is of most interest for pathogen inactivation, ammonia emissions and in the design of the composting systems.
7. The model considers the effects of oxygen concentration, temperature and moisture content on composting kinetics. The use of a single factor, such as oxygen availability, which combines the effect of the oxygen concentration, FAS and moisture content on microbial activity, is a possible means of improving the model kinetics without having to consider the individual effects of a large number of factors.
8. The model does not consider changes in volume of organic material due to compaction and the subsequent effect on the FAS and oxygen availability. A decrease in volume was observed in the composting reactors even with the support wheels in place. Including a volume reduction factor would complicate a relatively simple model and may not

necessarily improve model predictions for the processes occurring in the initial stages as compaction tends to occur during the later stages of composting.

9. Including a sub-model to predict pH changes in the organic material would be an important addition to the ammonia model. Values of coefficients involved in the emission of ammonia need to be evaluated for a solid, bulky organic material. The dynamics between the organic nitrogen and ammoniacal nitrogen content of the organic material requires further investigation as experimental analysis shows that the organic nitrogen is not necessarily stable during composting.

REFERENCES

- Agnew, J. M. and Leonard, J. J., Using a modified pycnometer to determine free air space and bulk density of compost mixtures while simulating compressive loading. In: Proceedings of the 2002 International Symposium: Composting and Compost Utilization, May 2002, Columbus, Ohio, USA. JG Press Inc. (eds.), Emmaus, USA. (2002).
- Anderson, G. A., Smith, R. J., Bundy, D. S. and Hammond, E. G., Model to predict gaseous contaminants in swine confinement building. *Journal of Agricultural Engineering Research*, 37, 235-253, (1987).
- Andrews, J. F. and Kambhu, K., Thermophilic aerobic digestion of organic solid wastes. EPA – 670/2-73-061, PB 222 396. NTIS, Springfield, VA, USA. (1973)
- APHA, AWWA, WEF, Standard methods for water and wastewater examination, 20th Edition. Clesceri, S. C., Greenberg, A. E., and Eaton, A. D. (eds.), Public Health Association, New York, USA. (1998).
- Arogo, J., Day, D. L., Christianson, L. L., Riskowski, G. L. and Zhang, R., Evaluation of mass transfer coefficient of ammonia from liquid swine manure. First International Conference on Air Pollution from Agricultural Operations. Kansas City, Missouri, USA, 111-118, (1996).
- Bach, P. D., Nakasaki, K., Shoda, M. and Kubota, H., Thermal balance in composting operations. *Journal of Fermentation Technology*, 65 (2), 199-209, (1987).
- Barrington, S., Choiniere, D., Trigui, M. and Knight, W., Effect of carbon source on compost nitrogen and carbon losses. *Bioresource Technology*, 83, 189-194, (2002a).
- Barrington, S., Choiniere, D., Trigui, M. and Knight, W., Compost convective airflow under passive aeration. *Bioresource Technology*, 86, 259-266, (2002b).
- Biocycle, Composting source separated organics. The J G Press, Inc. Emmaus, Pennsylvania, USA. (1994).

Biowise, Industrial solid waste treatment: A review of composting technology. Department of trade and industry. (2001).

Bishop, P. L. and Godfrey, C., Nitrogen transformation during sludge composting. *Biocycle: Journal of Waste Recycling*, 24, 34-39, (1983).

Boeker, P. and Schulze Lammers, P., Modelling of ammonia emissions in animal husbandry. In: *The Proceedings of the International Conference on Agricultural Engineering*, 23rd-26th September 1996, Madrid, Spain. 743-744, (1996).

Braithwaite, R. L., A study of garbage composting in controlled insulated barrels. Master's Thesis, Michigan state University, East Lansing, Michigan, USA. (1956).

British Standard BS EN 13040:2000, Soil improvers and growing media sample preparation for chemical and physical determination of dry matter content, moisture content and laboratory compacted bulk density. (2000).

Burton, C. H. and Turner, C., Manure management: Treatment strategies for sustainable agriculture, 2nd edition. Beck, J. A. F., Martinez, J., Martens, W., Pahl, O., Piccinni, S. and Svoboda, I. (eds), Silsoe Research Institutes, Wrest Park, Silsoe, Bedfordshire, UK. (2003).

CRD-C 36-37: Method of test for thermal diffusivity of concrete. In: *Handbook for Concrete and Cement* (Out of print). U. S. Army Corps of Engineers. Vicksburg, Missouri: U.S. Army Engineer Waterways Experiment Station. (1949-).

[On line] Available at: www.wes.army.mil/SL/MTC/handbook/handbook.htm (August 2003).

Chambers, B. J., Nicholson, N. and Chadwick, D., Environmental implications of controlling manure borne pathogens. In: *Agriculture and the Environment*. R & D Newsletter, October 2002, volume 10. Michael Rose (ed) LMID, Defra, Ergon House, Horseferry Road, London. (2002).

[Online] Available at: www.defra.gov.uk/enviro/research/agennews10.pdf (2002).

CIBS guide, C1 and 2. Properties of humid air, water and steam, 1975. The Chartered Institute of Building Services, London. (1984).

Composting Association (The), Information Sheet 1: What is composting? The Composting Association (eds), Avon House, Tithe Barn Road, Wellingborough, UK. (2003).

Cooney, C. L., Wang, D.I.C. and Mateles, R.I., Measurement of heat evolution and correlation with oxygen consumption during microbial growth. *Biotechnology and Bioengineering*, 9, 269-281, (1968).

Cronjé, A. L., Turner, C., Williams, A. G., Barker, A. J. and Guy, S., Ammonia emissions and pathogen inactivation during composting. In: *Proceedings of the 2002 International Symposium: Composting and Compost Utilization*, May 2002, Columbus, Ohio, USA. JG Press Inc. (eds.), Emmaus, USA. (2002a).

Cronjé, A. L., Barker, A. J., Guy, S., Turner, C. and Williams, A. G., Oxygen Up-take Rate of Composting Pig Manure. In: *Proceedings of the 2002 International Symposium: Composting and Compost Utilization*, May 2002, Columbus, Ohio, USA. JG Press Inc. (eds.), Emmaus, USA. (2002b).

Cumby, T. R., Moses, B. S. O. and Nigro, E., Gases from livestock slurries: emission kinetics. In: *Proceedings of the 7th International Symposium on Agricultural and Food Processing Wastes*. Ross, C. C. (ed), Hyatt Regency Chicago, Chicago, IL. 230-240, (1995).

Das, K. and Keener, H. M., Numerical model for the dynamic simulation of a large scale composting system. *Transactions of the American Society of Agricultural Engineers*, 40 (4), 1179-1189, (1997).

De Bertoldi, M., Citemesi, U. and Griselli, M., Microbial populations in compost process. *Composting*. JG Press Inc. (eds.), Emmaus, USA. 26-33, (1982).

De Vries, D. A. and Peck, A. J., On the cylindrical probe method of measuring thermal conductivity with special reference to soils I. *Australian Journal of Physics*, 11, 255–271, (1958).

Defra, Waste no want not: A strategy for tackling the waste problem in England. *Strategy Unit Waste Study*, Department for Environment Food and Rural Affairs, Nobel House, 17 Smith Square, London, UK. (2002).

Defra, Agriculture and the Environment R& D Newsletter. Volume 11, June 2003 Department for Environment Food and Rural Affairs, Nobel House, 17 Smith Square, London, UK. (2003a).

Defra, Key facts about: Air quality - Ammonia emission targets 1990-2010 in the UK. (2003b)

[Online] Available at: www.defra.gov.uk/environment/statistics/airquality/aqkf07.htm. (Web page created in 10 September 2003 and updated 16 September 2003).

Dewes, T., Ammonia emissions during the initial phase of microbial degradation of solid and liquid cattle manure. *Bioresource Technology*, 70, 245-248, (1999).

Doorn, M. R. J., Natschke, D. F. and Meeuwissen, P. C., Review of emission factors and methodologies to estimate ammonia emissions from animal waste handling. U. S. EPA Report No. EPA-600/R-02-017. Arcadis Geraghty and Miller Inc., Research Triangle Park, NC, USA. (2002).

Edwards, T. J., Newman, J. and Prausnitz, J. M., Thermodynamics of aqueous solutions containing volatile weak electrolytes. *AIChE Journal*, 21, 248-259, (1975).

Ekinci, K., Keener, H. M. and Elwell, D. L., Composting short paper fibre with broiler litter and additives II: Evaluation and optimization of decomposition rate versus mixing ratio. *Composting Science and Utilization*, 10 (1), 16-28, (2002).

Elwell, D. L., Keener, H. M. and Hansen, R. C., Controlled, high rate composting of mixtures of food residuals, yard trimmings and chicken manure. *Compost Science and Utilization*, 4(1), 6-15, (1996).

Epstein, E., Pathogenic health aspects of land application. *Biocycle*, September issue, 62-67, (1998)

Farrell, J. B., Faecal pathogen control during composting. *Science and Engineering of Composting*, Renaissance Publications, Ohio, USA. 282-300, (1992).

Fernandes, L., Zhan, W., Patni, N. K. and Jui, P. Y., Temperature distribution and variation in passively aerated static compost piles. *Bioresource Technology*, 48, 257-263, (1994).

Finstein, M. S. and Hogan, J. A., Integration of composting process microbiology, facility structure and decision-making. In: Science and Engineering of Composting. Renaissance Publications (eds.), Worthing, Ohio, USA. 1-23, (1993).

Finstein, M. S., Miller, F. C. and Strom, P. F., Monitoring and evaluating composting process performance. Journal of Water Pollution Control Federation, 58, 272-278, (1986).

Finstein, M. S., Hogan, J. A. and Miller, F. C., Physical modelling of the composting Ecosystem. Applied and Environmental Microbiology, 55, 1082-1092, (1989).

Fraser, B. S. and Lau, A. K., The effects of process control strategies on composting rate and odour emission. Compost Science and Utilisation, 8, 274–292, (2000).

Gendebien, A. H., Ferguson, R., Brink, J., Horth, H., Sullivan, M., Davis, R., Brunet, H., Dalimier, F., Landrea, B., Krack, D., Perot, J. and Orsi, C., Survey of wastes spread on land. European Commission Directive General for Environment. (2001).

[Online] Available at <http://europa.eu.int/comm/environment/waste/studies/compost/landspreading.pdf>

Générmon, S. and Cellier, P., Mechanistic model of estimating ammonia volatilization from slurry applied to bare soil. Agricultural and Forest Meteorology, 88, 145-167, (1997).

Gibbs, P., Parkinson, R. J., Burchett, S. and Misselbrook, T., Effective use of animal manures on farm through compost technology. In: Proceedings of the Microbiology of Composting and Other Biodegradation Processes Conference (eds.), 17th-20th October 2000, Innsbruck, Austria. (2000).

Golueke, C. G., Biological reclamation of solid wastes. Rodale Press, Emmaus, PA, USA. (1977)

Gray, K. R., Sherman, K. and Biddlestone, A. J., A review of composting – Part 1. Process Biochemistry. Morgan-Grampian Limited (eds), 28 Essex Street, Strand, London. 1-7, (1971a).

Gray, K. R., Sherman, K. and Biddlestone, A. J., Review of composting - Part 2: The practical process. Process Biochemistry. Morgan-Grampian Limited (eds), 28 Essex Street, Strand, London. 1-7, (1971b).

Gray, K. R., Sherman, K. and Clark, R., Review of composting - Part 3: Processes and products. *Process Biochemistry*. Morgan-Grampian Limited (eds), 28 Essex Street, Strand, London. 1-7, (1971c).

Halsam, R. T., Hershey, R. L. and Keen, R. H., Effect of gas velocity and temperature on rate of absorption. *Industrial and Engineering Chemistry*, 16 (12), 1224-1230, (1924).

Hamelers, H. V. M., A theoretical model of composting kinetics. In: *Science and engineering of composting*. The Ohio State University, 37-58, (1993).

Hamelers, H. V. M., A mathematical model for composting kinetics. Ph.D Thesis. Agricultural University Wageningen, Wageningen, The Netherlands. (2001).

Hamelers, H. V. M., Modelling composting kinetics: A deductive approach. In: *Proceedings of the 2002 International Symposium: Composting and Compost Utilization*, May 2002, Columbus, Ohio, USA. JG Press Inc. (eds.), Emmaus, USA. (2002).

Hansen, R. C., Keener, H. M. and Hoitink, H. A. J., Poultry manure composting: design guidelines for ammonia. *American Society of agricultural Engineers* (eds.), Paper No.89-4075, St Joseph, MI, USA. (1989).

Harper E. R., Miller F. C. and Macauley, B. J., Physical management and interpretation of an environmentally controlled composting ecosystem. *Australian Journal of Experimental Agriculture*, 32, 657-667, (1992).

Haug, R. T. and Ellsworth, W. F., Measuring compost substrate degradability. *Biocycle*, January 1991, 56-62, (1991).

Haug, R. T., *The Practical Handbook of Compost Engineering*. Lewis Publishers (eds.), Boca Raton, Florida, USA. (1993).

Hissett, R., Evans, M. R. and Baines, S., The use of respirometric methods for assessing the biodegradability of different components of agricultural wastes. *Progress in Water technology*, 7 (2), 13-21, (1975).

Hoeksma, P., Verdoes, N. and Monteny, G. J., Two options for manure treatment to reduce ammonia emission from pig housing. In: Proceedings of the First International Symposium on Nitrogen Flow in Pig Production and Environmental Consequences, Wageningen. EAAP, 69, 301-306, (1993).

Hogan, J. A., Miller, F. C. and Finstein, M. S., Physical modelling of the composting ecosystem. Applied and Environmental Microbiology, 1082-1092, (1989).

Imbeah, M., Composting piggery waste: A review. Bioresource Technology, 63, 197-203, (1998).

International Standard ISO 11277:1998, Soil quality - Determination of particle size distribution in mineral soil material - Method by sieving and sedimentation. International Organisation for Standardization, Technical Committee ISO/TC 190, Soil Quality, Subcommittee SC 5, Physical Methods. (2002).

Jeppsson, K. H., Ammonia emissions from different deep litter materials for growing finishing pigs. Swedish Journal of Agriculture, 28, 197-206, (1998).

Jeris, J. S. and Regan, R. W., Controlling environmental parameters for optimum composting I: experimental procedures and temperature. Compost Science, 14 (1), 10-15, (1973a).

Jeris, J. S. and Regan, R. W., Controlling environmental parameters for optimum composting II: moisture, free air space and recycle. Compost Science, 14 (2), 8-15, (1973b).

Jeris, J. S. and Regan, R. W., Controlling environmental parameters for optimum composting III. Compost Science, 14 (3), 8-15, (1973c).

Johnson, A. T., Biological process engineering. John Wiley and Sons, Inc. (eds.), New York, USA. (1999).

Kaiser, J., Modelling composting as a microbial ecosystem: a simulation approach, Ecological modelling, 91, 25-37, (1996).

Keener, H. M., Marugg, C., Hansen, R. C. and Hoitink, A. A. J., Optimizing the efficiency of the composting process. Science and Engineering of Composting: Design, Environmental,

Microbiological, and Utilization Aspects. Renaissance Publications (eds.), Worthing, Ohio, USA. 54-94, (1993).

Keener, H. M., Ekinci, K., Elwell, D. L., Michel Jr, F. C., Principles of composting process optimization. In: Proceedings of the 2002 International Symposium: Composting and Compost Utilization, May 2002, Columbus Ohio, USA. JG Press Inc. (eds.), Emmaus, USA. (2002).

Kirchmann, H. and Lundvall, A., Treatment of Solid Animal Manures: Identification of Low NH_3 Emission Practices. Nutrient Cycle Agroecosystems, 51, 65-71, (1998).

Lasaridi, K. E. and Stentiford, E. I., Respirometric techniques in the contest of compost stability assessment: principles and practice. In: The science of composting. Part 1. De Bertoldi, M., Sequi, P., Lemmes, B. and Papi, T. (eds), Chapman and Hall, Glasgow. 274-285, (1996).

Liang, Y., Leonard, J. J., Feddes, J.J., McGill, W. B. and Juma, N.G., Simulation of substrate decomposition and nitrogen loss in composting. 1998 CSAE/SCGR Conference, Vancouver, BC, Canada, July 1998. CSAE/SCGR, (1998).

Liao, P. H., Vizcarra, A. T., Chen, A. and Lo, K. V., Composting separated solid swine manure. Journal of Environmental Science and Health, 9, 1889-1901, (1993).

Lo, K. V., Lau, A. K. and Liao, P. H., Composting of separated solid swine wastes. Journal of Agricultural Engineering Resources, 54, 307-317, (1993).

Lorimor, J., 1998 ISU Swine Research Report, Extension Publication AS-640, January 1999, 175-177, (1999).

Ludwig, G. W., Effects of various temperatures upon the aerobic digestion of garbage. Master's Thesis, Georgia Institute of Technology, Atlanta, Georgia, USA. (1954).

Lynch, J. M., Substrate availability in the production of composts. In: Science and Engineering of Composting. Renaissance Publications (eds.), Ohio, USA. 24-35, (1993).

MAFF/ADAS, The analysis of agricultural materials. Ref. Book 427, 3rd Edition. Her Majesty's Stationery Office (eds.), London. (1986).

MAFF, Code of good agricultural practice for the protection of air. HMSO (eds.), London. (1998).

Martinez, J., Jolivet, J., Guiziou, F. and Langeoire, G., Ammonia emissions from pig slurries: evaluation of acidification and the use of additives in reducing losses. In: Proceedings of the International Symposium: Ammonia and Odour Control from Animal Production Facilities, October 1997, Vinkeloord, The Netherlands. Voermans, J. A. M. and Monteny G. J. (eds.), Rosmalen, The Netherlands: NVTL. 421-428, (1997).

Marugg, C., M. Grebus, Hansen, R. C., Keener, H. M. and Hoitnik, H. A. J., A kinetic model of the yard waste composting process. Compost Science and Utilization, Premier issue, 38-51, (1993).

Maule, A., Environmental survival of *E. coli* (O157): Implications for spread of disease. International Food Hygiene Conference: *E. coli* (O157), October 1998, Paris. (1998).

McKinley, V. L., Vestal, J. R. and Eralp, A. E., Microbial activity in composting. The Biocycle Guide to In-vessel Composting. The JG Press Inc (eds), Emmaus, USA. (1986).

Mears, D. R., Singley, M. E., Ghulam, A. and Rupp III, F., Thermal and physical properties of compost. In: Energy, Agriculture and Waste Management. Proceedings of the 1975 Cornell Agricultural Waste Management Conference. Jewell, J. (ed), AnnArborn Publishers Inc., Ann Arbor, MI, USA. 515-527, (1975).

Miller F. C., Composting as a process based on the control of ecologically selective factors. In: Soil Microbial Ecology - Applications in Agricultural and Environmental Management. Metting Jr., F. B. (ed.), Marcel Dekker Inc., New York, USA. 515-544, (1993).

Miller, F. C., Composting of municipal solids waste and its components. In: Microbiology of solid waste. CRC press. 116-145, (1996).

- Mohee, R., Composting potential of bagasse and broiler litter and process simulation using a dynamic model. A dissertation presented for the degree of doctor in philosophy, University of Mauritius. (1998).
- Mohee, R., White, R. K. and Das, K. C., Simulation model for composting cellulosic (bagasse) substrates. *Compost Science and Utilization*, 6 (2), 82-92, (1998).
- Monteny, G. J., Schulte, D. D., Elzing, A. and Lamaker, E. J. J., A conceptual mechanistic model for the ammonia emissions from free stall cubicle dairy cow houses. *Transactions of the ASAE*, 41 (1), 193-201, (1998).
- Nakasaki, K., Kato, J., Akiyama, T. and Kubota, H., A new composting model and assessment of optimum operating for effective drying of composting materials. *Journal of Fermentation Technology*, 65(4), 441-447, (1987).
- Ni, J., Mechanistic models of ammonia release from liquid swine manure: a review. *Journal of Agricultural Engineering Resource*, 72, 1-17, (1999).
- Nielsen, H. and Berthelsen, L., A model for temperature dependency of thermophilic composting process rate. *Compost Science and Utilization*, 10 (3), 249-257, (2002).
- Pain, B. F., Misselbrook, T. H., Jarvis, S. C., Chambers, B. J., Smith, K. A., Webb, J., Philips, V. R. and Sneath, R. W., Inventory of ammonia emissions from UK agriculture 1998. Ministry of Agriculture, Fisheries and Food. Contract Report WA0630. HMSO (eds.), London. (2000).
- Perry, R. H. and Green, D. W., *Perry's Chemical Engineers' Handbook*, 6th Edition. McGraw-Hill Book Company (eds.), New York, USA. (1984).
- PAS 100: Specification for composted materials. The Composting Association (eds), Avon House, Tithe Barn Road, Wellingborough, UK. (2002).
- Persson, J. A., *Handbook for Kjeldahl Digestion*, 2nd Edition. Person, J. A. (ed), Tecator AB, Höganäs, Sweden. (1996).

Petersen, S. O., Lind, A-M. and Sommer, S. G., Nitrogen and organic matter losses during storage of cattle and pig manure. *Journal of Agricultural Science Cambridge*, 130, 69-79, (1998).

Richard, T. L., *Municipal Solid Waste Composting: Physical and Biological Processing*. *Biomass and Bioenergy* 3 (3-4), 163-180, (1992).

Richard, T. L., *The kinetics of solid-state aerobic biodegradation*. Ph. D. Thesis. Cornell University. Ithaca, NY. (1997).

Richard, T. L. and Walker, L. P., Temperature kinetics of anaerobic solid-state biodegradation. In: *Proceedings of the 1998 IBE*, 1, A10-A30, (1998).

Richard, T. L., Walker, L. P. and Gosset, J. M., The effects of oxygen on solids-state biodegradation kinetics. In: *Proceedings of the 1999 IBE*, 2, A22-A39, (1999).

Richard, T. L., *The science and engineering of composting: Effect of Lignin on Biodegradability*. (2002).

[Online] Available at. <http://compost.css.cornell.edu/calc/lignin.html> (web page created in April 1996 and up-dated in October 2000).

Richard, T. L., Hamelers, H. V. M., Veeken, A. and Silva, T., Moisture relationships in composting processes. *Compost Science and Utilization*, 10 (4), 286-302, (2002).

Sawyer, C. N. and McCarty, P. L., *Chemistry for Environmental Engineering*, 3rd Edition. McGraw-Hill Book Company (eds.), NY. (1978).

Schulze, K. L., Rate of oxygen consumption and respiratory quotients during the aerobic decomposition of a synthetic garbage. *Compost Science*, Spring, 36-40, (1960).

Schulze, K. L., Continuous thermophilic composting. *Compost Science*, Spring, 22-34, (1962).

Scotford, I. M. and Williams, A. G., Practicalities, costs and effectiveness of floating plastic cover to reduce ammonia emissions from a pig slurry lagoon. *Journal of Agricultural Engineering*, 80 (3), 273-281, (2001).

- Seki, H., a new deterministic model for force-aeration composting processes with batch operation. Transactions of the ASAE, 45 (4), 1239-1250, (2002).
- Slater, R. A., Frederickson, J. and Gilbert, J. E., The state of composting 1999: Results of The Composting Association's survey of UK composting facilities and collection systems in 1999. The Composting Association, Avon House, Tithe Barn Road, Wellingborough, UK. (2001).
- Smårs, S., Beck-Friis, B., Jönsson, H. and Kirchmann, H., An advanced experimental composting reactor for systematic simulation studies. Journal of Agricultural Engineering Resource, 78, 415–422, (2001).
- Smits, J. P., Rinzema, A., Tramper, J., Schlosser, E. E. and Knol, W., Accurate determination of process variables in a solid-state fermentation system. Process Biochemistry, 31 (7), 669-678, (1996).
- Sommer, S. G. and Dahl, P., Nutrient and carbon balance during the composting of deep litter. Journal of Agricultural Engineering Resource, 74, 145-153, (1999).
- Stainer, R. Y., Adelberg, E. A. and Ingraham, J. L., General Microbiology, 4th Edition. The MacMillan Press Ltd., London, UK. (1980).
- Stentiford, E. I., Diversity of composting systems. In: Science and Engineering of Composting. Renaissance Publications (eds.), Ohio, USA. 95-110, (1993).
- Stentiford, E. I. and De Bertoldi, M., Composting – Process technical aspects. In: Compost processes in waste management, Proceedings of a European Communities workshop, September 1988, Neresheim, Germany. Bidlingmaier, W. and L'Hermite, P (eds). E. Guyot SA, 25 rue Ransfort, Brussels, Belgium. (1988).
- Stocks, C., The stabilisation of brewery waste by composting. PhD Thesis. School of Chemical Engineering, The University of Birmingham, UK. (2000).
- Stombaugh, D. P. and Nokes, S. E, Development of a biologically based aerobic composting simulation model. Transactions of the ASAE, 39 (1), 239-250, (1996).

Suslow, T., Oria, M., Beuchat, L., Garret, E., Parish, M., Harris, L., Farber, J. and Busta, F., Chapter II: Production practices as risk factors in microbial food safety of fresh and fresh cut produce. In: Analysis and evaluation of preventive control measure for the control and reduction/elimination of microbial hazards on fresh and fresh cut produce. U. S. Food and Drug Administration, Centre for Food Safety and Applied Nutrition. (2001).

[Online] Available at: <http://www.cfsan.fda.gov/~comm/ift3-2a.html>. (web page updated December 2001).

Swan, J. R. M., Kelsey, A., Crook, B. and Gilbert, E. J., Occupational and environmental exposure to bioaerosols from composts and potential health effects – A critical review of published data. Prepared by The Composting Association and the Health and Safety Laboratory for the Health and Safety Executive 2003. HMSO (eds.), London. (2003).

Sylvia, D. M., Fuhrmann, J. J., Hartel, P. G. and Zuberer, D. A., Principles and applications of soil microbiology. Prentice-Hall (eds.), Upper Saddle River, NJ, USA. (1998).

Thostrup, P., Evaluation of composting system – Concerning engineering, environment and economy. In: Compost processes in waste management -Proceedings of a European Communities workshop, September 1988, Neresheim, Germany. Bidlingmaier, W. and L'Hermite, P (eds). E. Guyot SA, 25 rue Ransfort, Brussels, Belgium. (1988).

Tiquia, S. M., Tam, N. F. Y and Hodgkiss, I. J., Microbial activities during composting of spent pig manure-sawdust litter at different moisture contents. Bioresource Technology, 55, 201-206, (1996).

Tiquia, S. M., Wan, J. H. C. and Tam, N. F. Y., Microbial population dynamics and enzymatic activity during composting. Compost Science and Utilization, 10 (2), 150-161, (2002).

Tollner, E. W., Smith, J. and Das, K. C., Development and preliminary validation of a compost process simulation model. In: Proceedings of the 1998 Conference – Composting in the Southeast, 9th – 11th September 1998, Athens, Georgia. Das, K. C. (ed), University of Georgia, Atlanta, USA. (1998).

Trautmann, N., The science and engineering of composting: Compost Physics. (2002).

[Online] Available at: <http://compost.css.cornell.edu/physics.html> (web page created in August 1995 and up-dated in January 2002).

Trautmann, N. and Olynciw, E., The science and engineering of composting: Invertebrates of the compost pile. (2002a).

[Online] Available at: <http://compost.css.cornell.edu/invertebrates.html> (web page created in August 1995 and up-dated in January 2002).

Trautmann, N. and Olynciw, E., The science and engineering of composting: Compost microorganisms. (2002b).

[Online] Available at: <http://compost.css.cornell.edu/microorg.html> (web page created in August 1995 and up-dated in January 2002).

Turner, C., Williams, S. M., Burton, C. H., Farrent, J. W., Wilkinson, P. J. and Cumby, T.R., Pilot scale thermal treatment of pig slurry for the inactivation of animal virus pathogens. *Journal of Environmental Science. Health Part B, Pesticides, Food Contaminants and Agricultural Wastes*, B34 (6), 989-1007, (1999).

Turner, C., The thermal inactivation of *E. coli* in straw and pig manure. *Bioresource Technology*, 84, 57-61, (2002).

UNECE, Protocol to the 1979 Convention on Long-range Transboundary Air Pollution to Abate Acidification, Eutrophication and Ground-level Ozone (ECE/EB.AIR/72 – E/F/R). Information Service, United Nations Economic Commission for Europe, Palais des Nations, Office 356, CH - 1211 Geneva 10, Switzerland. (1999).

[Online] Available at: www.unece.org/env/lrtap/protocol/99multi.htm .

U. S. EPA, Environmental Regulations and Technology, Control of Pathogens and Vector Attraction in Sewage Sludge, EPA/625/R-92/013. United States Environmental Protection Agency, Office of research and Development, National Risk Management Research Laboratory, and Centre for Environmental Information, Cincinnati, OH. (1999).

U. S. EPA, Composting - Part 637 Environmental Engineering. In: *National Engineering Handbook*. United States Environmental Protection Agency, Cincinnati, OH. (2000).

- Van Ginkel, J. T., Physical and biochemical processes in composting material. Ph. D Thesis. Agricultural University Wageningen, Wageningen, The Netherlands. (1996).
- Veeken, A. H. M., de Wilde, V. and Hamelers, H. V. M., Reduction of ammonia emissions during composting by uncoupling of oxygen demand and heat removal. In: Proceedings of International Conference Orbit 99: Biological Treatment of Waste and the Environment, September 1999, Weimar, Germany. Bidlingmaier, W., De Bertolli, M., Diaz, L. and Papadimitriou, E. (eds.). 111-119, (1999).
- Viel, M., Sayag, D., Peyre, A. and André, L., Optimization of in-vessel co-composting through heat recovery. *Biological Wastes*, 20, 167–185, (1987).
- Wiley, J. S., II Progress report on high-rate composting studies. In: Proceedings of the 12th Industrial Waste Conference, Purdue University. 596-603, (1957).
- Willson, G. B., Combining raw material for composting. In: *Composting Source Separated Organics*. Biocycle (eds). The J G Press, Inc. Emmaus, Pennsylvania, USA. 195-198, (1994).
- Zhang R. H., Day, D. L., Christianson, L. L. and Jepson, W. P., A computer model for predicting ammonia release rate from swine manure pits. *Journal of Agricultural Engineering resource*, 58, 223-229, (1994).

APPENDIX

A1. Introduction

A1.1. Ammonia emissions legislation

A1.1.1. The National Emissions Ceiling Directive

Statutory Instrument 2002 No. 3118 The National Emission Ceilings Regulations 2002

© Crown Copyright 2002

Statutory Instruments printed from this website are printed under the superintendence and authority of the Controller of HMSO being the Queen's Printer of Acts of Parliament.

STATUTORY INSTRUMENTS

2002 No. 3118

ENVIRONMENTAL PROTECTION

The National Emission Ceilings Regulations 2002

<i>Made</i>	<i>16th December 2002</i>
<i>Laid before Parliament</i>	<i>17th December 2002</i>
<i>Coming into force</i>	<i>10th January 2003</i>

National Emission Ceilings for SO₂, NO_x, VOC and NH₃

The amount specified for the purpose of regulation 3 is the relevant figure shown in the Table below less the emissions of that pollutant from Gibraltar in the relevant year.

<i>SO₂ kilotonnes</i>	<i>NO_x kilotonnes</i>	<i>VOC kilotonnes</i>	<i>NH₃ kilotonnes</i>
585	1167	1200	297

A1.1.1.1. Ammonia emissions and targets: 1990-2010

Ammonia emissions (excluding natural emissions from wild animals, pets and humans) fell by 15 % between 1990 and 2001 to 290 thousand tonnes. This compares with the target for 2010 of 297 thousand tonnes under the UNECE Gothenburg Protocol and the EU National Emissions Ceiling Directive. However, other possible sources of emissions are being researched which may be added to the inventory in future. Agriculture accounts for 83 per cent of total ammonia emissions [Defra 2003].

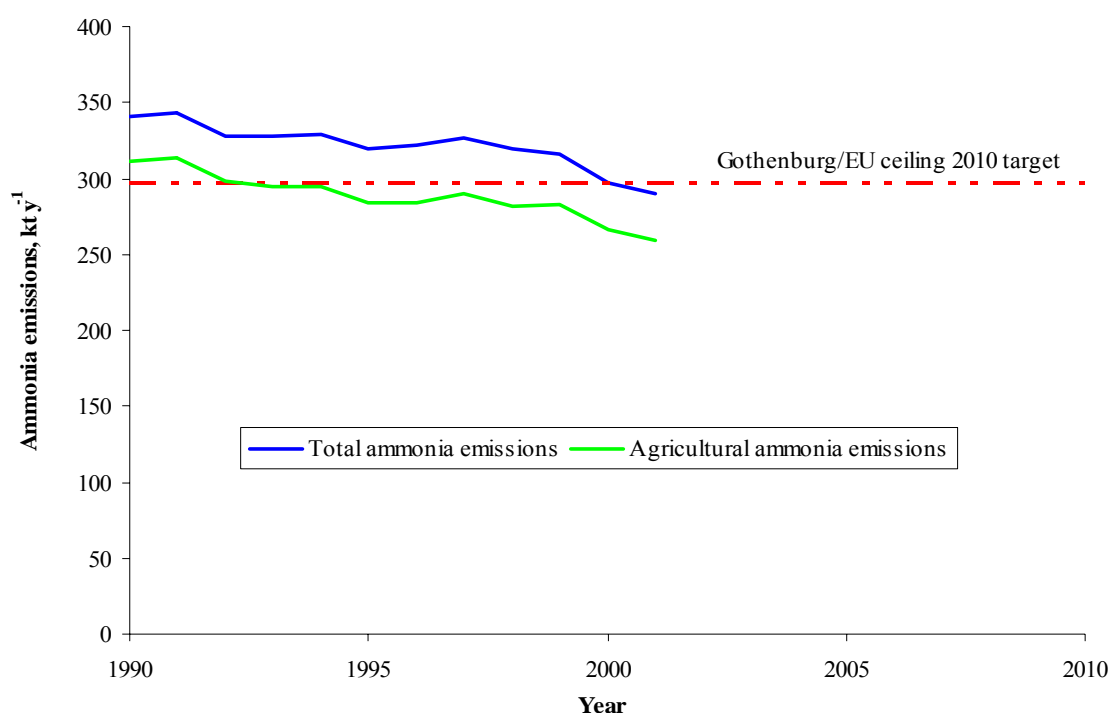


Figure A1.1. Ammonia emissions and targets: 1990 – 2010 [Defra 2003].

A1.1.2. The Gothenburg Protocol

The UNECE Gothenburg Protocol commits Parties to meet emission ceiling targets for four polluting gases (sulphur dioxide, oxides of nitrogen, volatile organic compounds and ammonia) that cause acidification, eutrophication and ozone formulation. The sections of The Gothenburg Protocol [UNECE 1999] relevant to ammonia emissions from agriculture, and FYM specifically, are given below.

Convention on Long-range Transboundary Air Pollution



1999 GOTHENBURG PROTOCOL TO THE 1979 CONVENTION ON LONG-RANGE TRANSBOUNDARY AIR POLLUTION TO ABATE ACIDIFICATION, EUTROPHICATION AND GROUND-LEVEL OZONE

The Executive Body adopted the Protocol to Abate Acidification, Eutrophication and Ground-level Ozone in Gothenburg (Sweden) on 30 November 1999.

The Protocol sets emission ceilings for 2010 for four pollutants: sulphur, NO_x, VOCs and ammonia. These ceilings were negotiated on the basis of scientific assessments of pollution effects and abatement options. Parties whose emissions have a more severe environmental or health impact and whose emissions are relatively cheap to reduce will have to make the biggest cuts. Once the Protocol is fully implemented, Europe's sulphur emissions should be cut by at least 63%, its NO_x emissions by 41%, its VOC emissions by 40% and its **ammonia emissions by 17% compared to 1990**.

The Protocol also sets tight limit values for specific emission sources (e.g. combustion plant, electricity production, dry cleaning, cars and lorries) and requires best available techniques to be used to keep emissions down. VOC emissions from such products as paints or aerosols will also have to be cut. Finally, farmers will have to take specific measures to control ammonia emissions. Guidance documents adopted together with the Protocol provide a wide range of abatement techniques and economic instruments for the reduction of emissions in the relevant sectors, including transport.

It has been estimated that once the Protocol is implemented, the area in Europe with excessive levels of acidification will shrink from 93 million hectares in 1990 to 15 million hectares. That with excessive levels of eutrophication will fall from 165 million hectares in 1990 to 108 million hectares. The number of days with excessive ozone levels will be halved. Consequently, it is estimated that life-years lost as a result of the chronic effects of ozone exposure will be about 2,300,000 lower in 2010 than in 1990, and there will be approximately 47,500 fewer premature deaths resulting from ozone and particulate matter in the air. The exposure of vegetation to excessive ozone levels will be 44% down on 1990.

Article 3
BASIC OBLIGATIONS

1. Each Party having an emission ceiling in any table (Table A1.1) shall reduce and maintain the reduction in its annual emissions in accordance with that ceiling and the timescales specified. Each Party shall, as a minimum, control its annual emissions of polluting compounds in accordance with the obligations.
6. Each Party should apply best available techniques to mobile sources and to each new or existing stationary source, taking into account guidance document (Section A1....) adopted by the Executive Body at its 17th session (decision 1999/1) and any amendments thereto.
7. Each Party shall:
 - (a) Apply, as a minimum, the ammonia control measures specified (Table A1.2);
 - (b) Apply, where it considers it appropriate, best available techniques for preventing and reducing ammonia emissions, as listed in guidance document adopted by the Executive Body at its 17th session (decision 1999/1) and any amendments thereto.
8. Paragraph 10 shall apply to any Party:
 - (a) Whose total land area is greater than 2 million square kilometres;
 - (b) Whose annual emissions of sulphur, nitrogen oxides, ammonia and/or volatile organic compounds contributing to acidification, eutrophication or ozone formation in areas under the jurisdiction of one or more other Parties originate predominantly from within an area under its jurisdiction that is listed as a Pollutant emissions management area (PEMA), and which has presented documentation in accordance with subparagraph (c) to this effect;
 - (c) Which has submitted upon signature, ratification, acceptance or approval of, or accession to, the present Protocol a description of the geographical scope of one or more PEMAs for one or more pollutants, with supporting documentation, and
 - (d) Which has specified upon signature, ratification, acceptance or approval of, or accession to, the present Protocol its intention to act in accordance with this paragraph.
9. A Party to which this paragraph applies shall:
 - (a) If within the geographical scope of EMEP (The Cooperative Programme for Monitoring and Evaluation of Long-range Transmission of Air Pollutants in Europe),

be required to comply with the provisions of this article and Table 1.1 only within the relevant PEMA for each pollutant or

- (b) If not within the geographical scope of EMEP, be required to comply with the provisions of paragraphs 1 to 7 and Table 1.1, only within the relevant PEMA for each pollutant (nitrogen oxides, sulphur and/or volatile organic compounds) and shall not be required to comply with paragraph 8 anywhere within its jurisdiction.

11. The Parties shall, subject to the outcome of the first review provided for under article 10 (b), and no later than one year after completion of that review, commence negotiations on further obligations to reduce emissions.

Article 8

RESEARCH, DEVELOPMENT AND MONITORING

The Parties shall encourage research, development, monitoring and cooperation related to:

- a. The international harmonization of methods for the calculation and assessment of the adverse effects associated with the substances addressed by the present Protocol for use in establishing critical loads and critical levels and, as appropriate, the elaboration of procedures for such harmonization;
- b. The improvement of emission databases, in particular those on ammonia and volatile organic compounds;
- c. The improvement of monitoring techniques and systems and of the modelling of transport, concentrations and depositions of sulphur, nitrogen compounds and volatile organic compounds, as well as of the formation of ozone and secondary particulate matter;
- d. The improvement of the scientific understanding of the long-term fate of emissions and their impact on the hemispheric background concentrations of sulphur, nitrogen, volatile organic compounds, ozone and particulate matter, focusing, in particular, on the chemistry of the free troposphere and the potential for intercontinental flow of pollutants;
- e. The further elaboration of an overall strategy to reduce the adverse effects of acidification, eutrophication and photochemical pollution, including synergisms and combined effects;
- f. Strategies for the further reduction of emissions of sulphur, nitrogen oxides, ammonia and volatile organic compounds based on critical loads and critical levels as well as on technical developments, and the improvement of integrated assessment modelling to

calculate internationally optimized allocations of emission reductions taking into account the need to avoid excessive costs for any Party. Special emphasis should be given to emissions from agriculture and transport;

- g. The identification of trends over time and the scientific understanding of the wider effects of sulphur, nitrogen and volatile organic compounds and photochemical pollution on human health, including their contribution to concentrations of particulate matter, the environment, in particular acidification and eutrophication, and materials, especially historic and cultural monuments, taking into account the relationship between sulphur oxides, nitrogen oxides, ammonia, volatile organic compounds and tropospheric ozone;
- h. Emission abatement technologies, and technologies and techniques to improve energy efficiency, energy conservation and the use of renewable energy;
- i. **The efficacy of ammonia control techniques for farms and their impact on local and regional deposition;**
- j. The management of transport demand and the development and promotion of less polluting modes of transport;
- k. The quantification and, where possible, economic evaluation of benefits for the environment and human health resulting from the reduction of emissions of sulphur, nitrogen oxides, ammonia and volatile organic compounds; and
- l. The development of tools for making the methods and results of this work widely applicable and available.

GUIDANCE DOCUMENT ON CONTROL TECHNIQUES FOR PREVENTING AND ABATING EMISSIONS OF AMMONIA

Introduction

1. The purpose of this document is to provide guidance to the Parties to the Convention in identifying ammonia control options and techniques for reducing emissions from agricultural and other stationary sources in the implementation of their obligations under the Protocol.
2. It is based on information on options and techniques for ammonia emission reduction and their performance and costs contained in official documentation of the Executive Body and its subsidiary bodies.

3. The document addresses the control of ammonia emissions produced by agriculture and other stationary sources. **Agriculture is the major source of ammonia, chiefly from livestock excreta, in livestock housing, during manure storage, processing and application to land and from excreta from animals at pasture.** Emissions also occur from inorganic nitrogen (N) fertilizers when these are applied to land. Emissions could be reduced through abatement measures in all the above areas as well as by adjustments to livestock diets that result in less nitrogen in excreta available for ammonia formation. This guidance document addresses the known potential abatement measures under the headings: slurry and manure application techniques; slurry storage techniques; livestock housing; feeding strategies and other measures; and non-agricultural stationary sources.
4. Abatement of ammonia emissions from agriculture differs fundamentally from the abatement of any industrial emissions because of the intrinsic difficulties entailed in regulating biological as opposed to engineering processes. Ammonia emissions depend largely on livestock type and management, soils and climate and these factors differ widely across the region of the United Nations Economic Commission for Europe (UNECE). While some of the techniques listed in this document are in commercial operation in some countries, their effectiveness has, for the most part, not been fully evaluated on working farms. Consequently, the efficiency of each of the abatement techniques for ammonia carry with them a degree of uncertainty and variability. The values used in this guidance document should be regarded as indicative only.
5. It is possible to categorize many of the potential abatement techniques on the basis of the level of current knowledge and practicality. Techniques in this document are grouped into three categories:
 - (a) Category 1 techniques: they are well researched, considered to be practical, and there are quantitative data on their abatement efficiency, at least on the experimental scale;
 - (b) Category 2 techniques: they are promising, but research on them is at present inadequate, or it will always be difficult to quantify their abatement efficiency;
 - (c) Category 3 techniques: they have been shown to be ineffective or are likely to be excluded on practical grounds.
6. Options for ammonia reduction at the various stages of livestock manure production and handling are interdependent, and combinations of measures are not simply additive in terms of their combined emission reduction. Controlling emissions from applications of

manures to land is particularly important, because these are generally a large component of total manure emissions and because land application is the last stage of manure handling. Without abatement at this stage, much of the benefit of abating during housing and storage may be lost.

7. Because of this interdependency, Parties will need to rely on additional modelling work before they can use the techniques listed here to develop an ammonia abatement strategy to meet their national emission targets.
8. The costs of the techniques will vary from country to country. A thorough knowledge of current husbandry practices is required to calculate the costs associated with any particular abatement technique. This calculation will involve an assessment of all the costs and financial benefits of each measure. Capital costs will need to be amortized at the standard UNECE rate of 4% and calculated separately from annual operating costs. Many measures may incur both capital and annual costs. For example, new livestock housing will incur the capital cost of the building itself plus potential annual costs of extra maintenance and/or energy. Costs in this guidance document are shown for the Netherlands or the United Kingdom and are given as examples only. A fuller explanation of the means of calculating costs is provided in section G.
9. Wherever possible, techniques listed in this document are clearly defined and assessed against a 'reference' or unabated situation. The 'reference' situation, against which the percentage emission reduction is calculated, is defined at the beginning of each section. In most cases the 'reference' is the practice or design that gives rise to the highest ammonia emission: in many countries the 'reference' will be the most commonly practised technique, at present.
10. The document reflects the state of knowledge and experience of ammonia control measures which had been achieved by 1998. It will need to be updated and amended regularly, as this knowledge and this experience continuously expand, for example with new low-emission housing systems for pigs and cattle, as well as with feeding strategies for all livestock types.

A. Good agricultural practice

11. The concept of "good agricultural practice" aims to identify those measures to control ammonia emissions that protect the environment in the most cost-effective way. The set

may comprise simple and highly cost-effective measures such as simple means of matching the protein in livestock diets as closely as possible to the animals' requirements; regular cleaning of livestock collecting areas and the timing of applications of manures to land so as to maximize crop uptake of nutrients. It could also include more demanding measures such as techniques for slurry and manure application, slurry storage, livestock housing and other techniques, as listed below.

12. While some of the measures may provide highly cost-effective means of abating ammonia, they may be difficult to quantify and cost because there is often a wide range of implementation already within the farming community and they cannot therefore easily be judged against a 'worst case' or 'most commonly practised' reference.
13. Good agricultural practice aims to achieve a compromise between economic farming and environmental protection. This compromise will differ from country to country depending on economic, environmental and farm structural conditions. Any statutory requirements to adhere to such advice will therefore necessarily vary from country to country.

C. Slurry storage techniques

14. **At present, there are no proven techniques for reducing ammonia emissions from stored solid manures.** This section relates only to techniques for slurry storage. After removal from animal houses, slurry is stored either in concrete or steel tanks or silos or in lagoons, often with earth walls.

Manure treatment

75. Various options for reducing emissions by manure treatment are investigated or discussed. Some potentially promising options are:
 - (a) **Composting of solid manure or slurry with added solids.** Experimental results are very variable and sometimes even show increased emissions;
76. **The efficiency of manure treatment options should generally be investigated under country- or farm-specific conditions.** Apart from ammonia emissions, other emissions, nutrient fluxes and the applicability of the system under farm conditions should be assessed. Due to the mentioned uncertainties, these measures generally have to be regarded as category 2 or 3 techniques.

Feed or manure additives

78. A wide variety of feed and manure additives have been suggested to reduce ammonia emissions. **They mostly aim at reducing the ammonia content or the pH by chemical or physical processes. Their efficiency in reducing ammonia emissions depends on how well they achieve these aims and on where in the manure management process they are introduced.** As most of the products available on the market have not been independently tested or the test results were not statistically significant and reproducible, they have to be regarded as category 3 measures.

Annex II

EMISSION CEILINGS

The emission ceilings listed in the table A1.1 relate to the provisions of article 3, paragraphs 1 and 10, of the present Protocol. The 1980 and 1990 emission levels and the percentage emission reductions listed are given for information purposes only.

Annex IX

MEASURES FOR THE CONTROL OF EMISSIONS OF AMMONIA FROM AGRICULTURAL SOURCES

1. The Parties that are subject to obligations in article 3, paragraph 8 (a), shall take the measures set out in this annex.
2. Each Party shall take due account of the need to reduce losses from the whole nitrogen cycle.

A. Advisory code of good agricultural practice

3. Within one year from the date of entry into force of the present Protocol for it, a Party shall establish, publish and disseminate an advisory code of good agricultural practice to control ammonia emissions. The code shall take into account the specific conditions within the territory of the Party and shall include provisions on:
 - Nitrogen management, taking account of the whole nitrogen cycle;
 - Livestock feeding strategies;
 - Low-emission manure spreading techniques;

- Low-emission manure storage systems;
- Low-emission animal housing systems; and
- Possibilities for limiting ammonia emissions from the use of mineral fertilizers.

Parties should give a title to the code with a view to avoiding confusion with other codes of guidance.

B. Urea and ammonium carbonate fertilizers

4. Within one year from the date of entry into force of the present Protocol for it, a Party shall take such steps as are feasible to limit ammonia emissions from the use of solid fertilizers based on urea.
5. Within one year from the date of entry into force of the present Protocol for it, a Party shall prohibit the use of ammonium carbonate fertilizers.

C. Manure application

6. Each Party shall ensure that low-emission slurry application techniques (as listed in guidance document V adopted by the Executive Body at its seventeenth session (decision 1999/1) and any amendments thereto) that have been shown to reduce emissions by at least 30% compared to the reference specified in that guidance document are used as far as the Party in question considers them applicable, taking account of local soil and geomorphological conditions, slurry type and farm structure. The timescales for the application of these measures shall be: 31 December 2009 for Parties with economies in transition and 31 December 2007 for other Parties. 1/
7. Within one year from the date of entry into force of the present Protocol for it, a Party shall ensure that solid manure applied to land to be ploughed shall be incorporated within at least 24 hours of spreading as far as it considers this measure applicable, taking account of local soil and geomorphological conditions and farm structure.

D. Manure storage

8. Within one year from the date of entry into force of the present Protocol for it, a Party shall use for new slurry stores on large pig and poultry farms of 2,000 fattening pigs or 750 sows or 40,000 poultry, low-emission storage systems or techniques that have been shown to reduce emissions by 40% or more compared to the reference (as listed in the guidance document referred to in paragraph 6), or other systems or techniques with a demonstrably equivalent efficiency. 2/

9. For existing slurry stores on large pig and poultry farms of 2,000 fattening pigs or 750 sows or 40,000 poultry, a Party shall achieve emission reductions of 40% insofar as the Party considers the necessary techniques to be technically and economically feasible. 2/ The timescales for the application of these measures shall be: 31 December 2009 for Parties with economies in transition and 31 December 2007 for all other Parties. 1/

E. Animal housing

10. Within one year from the date of entry into force of the present Protocol for it, a Party shall use, for new animal housing on large pig and poultry farms of 2,000 fattening pigs or 750 sows or 40,000 poultry, housing systems which have been shown to reduce emissions by 20% or more compared to the reference (as listed in the guidance document referred to in paragraph 6), or other systems or techniques with a demonstrably equivalent efficiency. 2/ Applicability may be limited for animal welfare reasons, for instance in straw-based systems for pigs and aviary and free-range systems for poultry.

Notes

1/ For the purpose of the present annex, "a country with an economy in transition" means a Party that has made with its instrument of ratification, acceptance, approval or accession a declaration that it wishes to be treated as a country with an economy in transition for the purposes of paragraphs 6 and/or 9 of this annex.

2/ Where a Party judges that other systems or techniques with a demonstrably equivalent efficiency can be used for manure storage and animal housing in order to comply with paragraphs 8 and 10, or where a Party judges the reduction of emissions from manure storage required under paragraph 9 not to be technically or economically feasible, documentation to this effect shall be reported in accordance with article 7, paragraph 1 (a).

Table A1.1. Emission ceilings for ammonia (thousands of tonnes of NH₃ per year)

Party	Emission levels 1990 (base year 1990)	Emission ceilings for 2010	Percentage emission reductions for 2010
Armenia	25	25	0%
Austria	81	66	-19%
Belarus	219	158	-28%
Belgium	107	74	-31%
Bulgaria	144	108	-25%
Croatia	37	30	-19%
Czech Republic	156	101	-35%
Denmark	122	69	-43%
Finland	35	31	-11%
France	814	780	-4%
Germany	764	550	-28%
Greece	80	73	-9%
Hungary	124	90	-27%
Ireland	126	116	-8%
Italy	466	419	-10%
Latvia	44	44	0%
Liechtenstein	0.15	0.15	0%
Lithuania	84	84	0%
Luxembourg	7	7	0%
Netherlands	226	128	-43%
Norway	23	23	0%
Poland	508	468	-8%
Portugal	98	108	10%
Republic of Moldova	49	42	-14%
Romania	300	210	-30%
Russian Fed.	1191		
R. F. PEMA ¹	61	49	-20%
Slovakia	62	39	-37%
Slovenia	24	20	-17%
Spain	351	353	1%
Sweden	61	57	-7%
Switzerland	72	63	-13%
Ukraine	729	592	-19%
UK	333	297	-11%
EC	3671	3129	-15%

¹ Russian Federation PEMA: the area of Murmansk oblast, the Republic of Karelia, Leningrad oblast (including St. Petersburg), Pskov oblast, Novgorod oblast and Kaliningrad oblast. The boundary of the PEMA coincides with the State and administrative boundaries of these constituent entities of the Russian Federation.

A3. Equipment and analytical methods

A3.1. The composting reactor

A3.1.1. Radial heat loss simulations

Three situations were considered: a) the reactor without insulation, b) the reactor insulated with rock wool panels, and c) the reactor insulated with rock wool panels and the heating cable. The program, written in Quick Basic and performed using the macro functions of Microsoft Excel, is given in Section A3.3.

The organic material in the section was divided into nine elements of equal mass. The wall was one and the rock wool insulation, when present, was divided into two elements of equal mass. The heating cable was coiled around the outside reactor surface. The radius of an element, r , corresponded to that of outer vertical surface and the temperature, T , was taken as that at the mean radius. The ambient air was nominated as 0, the outermost element, as 1 and the central element, as 'n', where n was the number of elements in the section (Figure A3.1). 'S' denoted the outside reactor surface. The centre was assumed to be hottest so that heat flowed radially through the material from n to the ambient air.

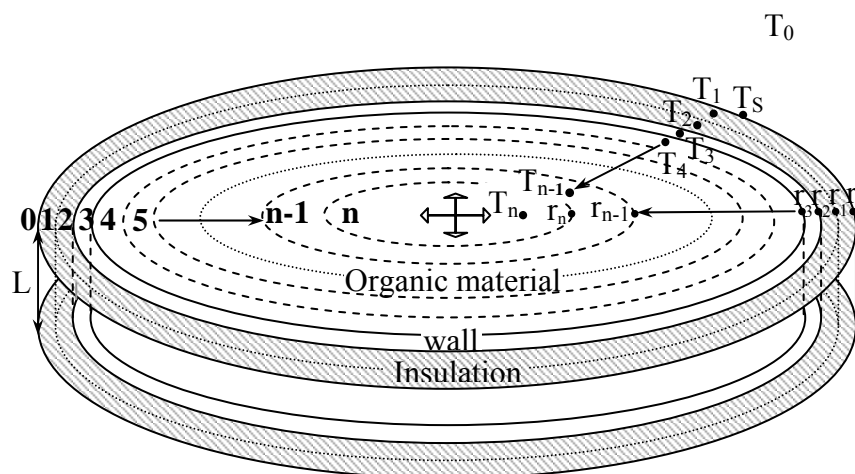


Figure A3.1. Section of reactor considered in radial conductive heat loss simulations.

The mass in each element was assumed to be constant during a simulation. The heat balance across an element, j , was therefore given as:

$$\frac{dQ_j}{dt} = M_j \cdot Cp_j \frac{dT_j}{dt} = \frac{dQ_{gen}}{dt} + \frac{dQ_{in}}{dt} - \frac{dQ_{out}}{dt} \quad (A3 \text{ i})$$

where Q_j = heat content of element j , J

M_j = mass of element j , kg

Cp_j = specific capacity of element j , J (kg K)⁻¹

T_j = temperature of element j , K

Q_{gen} = heat generated by microbial activity in element j , J

Q_{in} = heat flowing radially into element j from element $j+1$, J

Q_{out} = heat flowing radially from element j to element $j-1$, J

Q_{gen} only applied to the organic material elements and was determined from the heat released as a result of electron transfer per gram of oxygen consumed during aerobic respiration, 13.6 kJ g⁻¹O₂ [Haug 1993]. The oxygen uptake rate (OUR) was based on the volatile solids (VS), at temperature, T , in degrees centigrade and was expressed in gO₂(kg_{VS} h)⁻¹ [Schulze 1960, Haug 1993] by,

$$OUR = 0.11 \times 1.066^{-T} \quad (A3 \text{ ii})$$

The temperature of the outmost element depended on the heat loss from the element to the ambient air. The process involved conduction of heat across the element, q_{conv} , and subsequent loss of from the reactor surface by convection, q_{conv} , and radiation, q_{rad} , which operated in parallel (Figure A3.2). Conduction through element 1 was driven by the temperature difference between the element and outside surface and therefore considers the log mean area of the element. Convection and radiation were surface effects driven by the

temperature difference between the reactor surface and the surrounding air and were therefore concerned with the outside surface area.

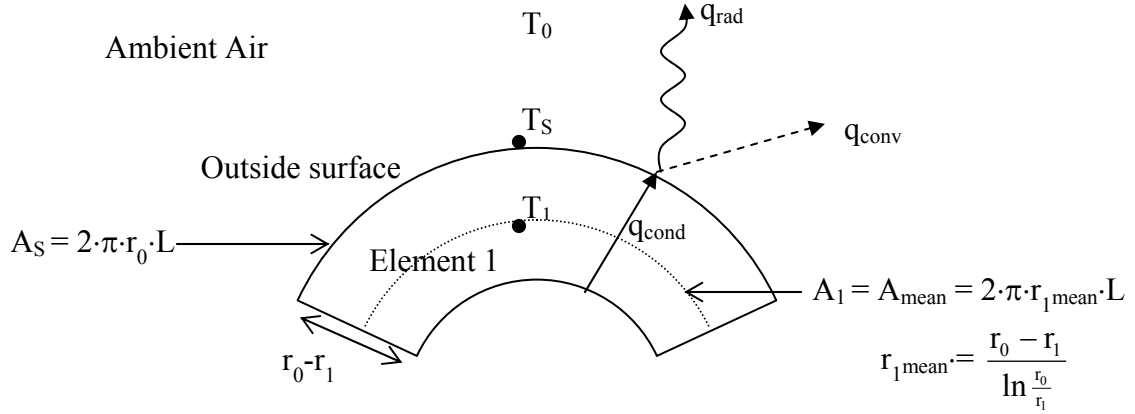


Figure A3.2. Transfer mechanisms of heat loss from element 1.

The respective heat flows by conduction, convection and radiation, q_{cond} , q_{conv} and q_{rad} were described by equations (A3 iii) to (A3 v).

$$q_{\text{cond}} = (T_1 - T_S) \cdot \frac{2 \cdot \pi \cdot L \cdot k_1}{\ln \frac{r_0}{r_1}} \quad (\text{A3 iii})$$

k_1 was the thermal conductivity of the material of element 1 ($\text{W m}^{-1} \text{K}^{-1}$).

$$q_{\text{conv}} = A \cdot h_{\text{conv}} \cdot (T_S - T_0) \quad (\text{A3 iv})$$

A was the outside surface area of the reactor (m^2) and h_{conv} was the convective heat transfer coefficient ($\text{W m}^{-2} \text{K}^{-1}$)

$$q_{\text{rad}} = A \cdot h_{\text{rad}} \cdot (T_S - T_0) \quad (\text{A3 v})$$

h_{rad} was the radiative heat transfer coefficient ($\text{W m}^{-2} \text{K}^{-1}$). The Stefan-Boltzmann Law [Perry 1984] defines h_{rad} as

$$h_{\text{rad}} = \sigma \cdot \epsilon \cdot \frac{T_S^4 - T_0^4}{T_S - T_0} \quad (\text{A3 vi})$$

ε was the emissivity of the surface, which, for a matt surface was about 0.9. The Stefan-Boltzmann constant, σ , was $5.67 \times 10^{-8} \text{ W m}^{-2} \text{ K}^{-1}$ and T_s and T_0 were in Kelvins.

Figure A3.3 shows that h_{rad} is linearly related to $(T_s - T_0)$ in the range considered such that

$$h_{\text{rad}} = 0.028 \cdot (T_s - T_0) - 4.34 \quad (\text{A3 vii})$$

The relationship however requires the surface temperature of the reactor to be known. T_s not equal to T_1 and to calculate it would require further iterations. A 5°C change in the temperature difference results in about a 2.5 % change in the value of h_{rad} . The coefficient was therefore assumed to be a constant value for the purpose of evaluating the potential of the heating cable to minimise radial heat losses.

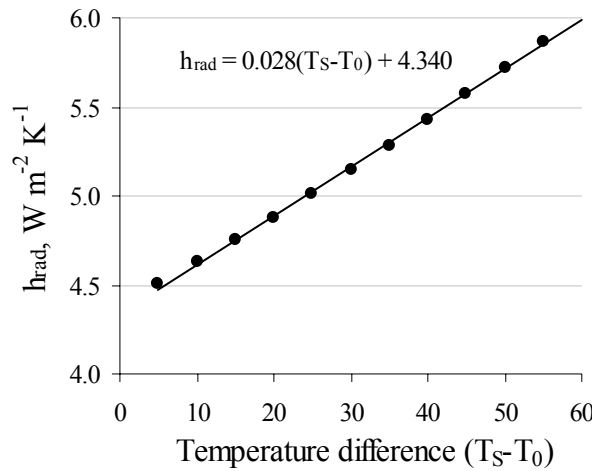


Figure A3.3. Radiative heat transfer coefficient as a function of temperature difference.

The total heat loss from the outside surface was the sum of the convective and radiative heat loss such that

$$q_{\text{conv+rad}} = (T_s - T_0) \cdot 2 \cdot \pi \cdot r_0 \cdot L \cdot h_c \quad (\text{A3 viii})$$

h_c was the combined heat transfer coefficient of convection and radiation ($\text{W m}^{-2} \text{ K}^{-1}$).

A combined heat transfer coefficient was used because heat loss by convection and radiation from the outside surface happens independently of each other and their effect on heat loss was therefore additive. For surfaces around 40°C the convective and radiative heat transfer

coefficients were both about $5 \text{ W m}^{-2} \text{ K}^{-1}$. The combined heat transfer coefficient was therefore assumed to be $10 \text{ W m}^{-2} \text{ K}^{-1}$ for all the simulations.

Convection and radiation operated in series with conduction. The heat loss was therefore dependent on the mechanism which was limiting, be it the transfer through the element or from the outside surface. At steady state, the flow of heat by conduction therefore equalled the flow heat by convection plus radiation. Substituting for the surface temperature, an unknown in equations (3 iii) and (3 iv), gave equation (A3 ix), which described the heat flow from the element 1 to the ambient air.

$$\frac{dQ_{(1,0)}}{dt} = \frac{T_1 - T_0}{\frac{1}{2\pi L} \left[\frac{\log_e \frac{r_0}{r_1}}{k_1} + \frac{1}{h_c \cdot r_0} \right]} \quad (\text{A3 ix})$$

The heat transfer through the reactor was assumed to be by conduction only such that heat of the element for n to 2 was given by:

$$\frac{dQ_{(n,n-1)}}{dt} = \frac{2 \cdot \pi \cdot L \cdot k_n \cdot [T_n - T_{n-1}]}{\log_e \frac{r_{n-1}}{r_n}} \quad (\text{A3 x})$$

For case c, the heat supplied by the heating cable (Q_{cable}) to the wall ($n=3$), was included in the heat balance when the wall temperature was updated, as described by equation (3 vii).

$$\frac{dT_3}{dt} = \frac{Q_4 - Q_3 + Q_{\text{cable}}}{M_3 \cdot C_{p3}} \quad (\text{A3 xi})$$

A constant vertical airflow was included in the heat balance to remove excess heat from each element of the organic material so that the centre temperature equilibrated at the initial temperature. Values of the physical properties of the materials in the section of the reactor are given in Table A3.1.

Table A3.1. The values of thermodynamic and physical properties used in the model

Quantity	Symbol	Units		Rock wool (insulation)	Polypropylene (wall)	Organic material
Specific heat capacity	c_p	$J (kg K)^{-1}$		1090 ¹	1800	=0.032 MC + 0.986
Thermal conductivity	K	$W (m K)^{-1}$		0.052 ¹	0.330	=0.005 MC - 0.165
Combined heat transfer coefficient	h_{c+r}	$W (m^2 K)^{-1}$		10 ¹	10 ²	-
Heat generation	H_{gen}	$W kg_{VS}^{-1}$	20°C	-	-	1.50
			40°C	-	-	5.37
			60°C	-	-	19.28
Mass (per element)	M	Kg		0.520	1.028	0.591
Section length	L	M		0.100	0.100	0.100
Outer radius	R	M		0.356	0.306	0.300
Density	ρ	$kg m^{-3}$	50 %			92
			65 %	100 ¹	900	165
			80 %			303
Total solids	TS	%		-	-	35
Volatile solids	VS	% _{TS}		-	-	88

¹. [Perry 1984]² value is applied to case a where the reactor element is not insulated

The specific heat capacity, thermal conductivity, bulk density of the organic material were experimentally determined for a mix manure and straw with a M:S ratio of 2:1. The thermal properties varied linearly with the moisture content, as given by the respective equations in Table A3.1. They are also reported to vary with the ash content of the solids fraction, as the inorganic solids have a higher heat capacity than the organic solids [Haug 1993]. However, the correlation is less pronounced than with the moisture content because, for example, the specific heat capacity of water is about four times greater than that of the solids [Haug 1993]. Furthermore, for an increase in the mixing ratio from 2 to 4, the ash content of the total solids increases by less than 2 % and the corresponding increase in the

specific heat capacity of the organic material is small. The physical properties of the polypropylene reactor wall were provided by the manufactures of the reactor body.

Simulations of the radial heat loss were carried out for three initial temperatures, 20 °C, 40 °C and 60 °C, and three moisture contents of the organic material, 50 %, 65 % and 80 %. As with the mass of the organic material, the moisture content was assumed to be constant during a simulation. The ambient air temperature was a constant 5 °C. One iteration lasted one second. Temperatures equilibrated after about 55 000 iterations (Figures A3.7 to A3.9) and a simulation was therefore equivalent to 14 hours. For the organic material with a moisture content of 65 %, the final temperature reached in each unit was plotted against the reactor radius to give a temperature profile across the reactor for 20 °C, 40 °C and 60 °C. The minimum and maximum error bars on the points represent the equilibrium temperatures obtained for simulations with the organic material at a moisture content of 50 % and 80 %, respectively (Figure A3.4, A3.5 and A3.6, respectively).

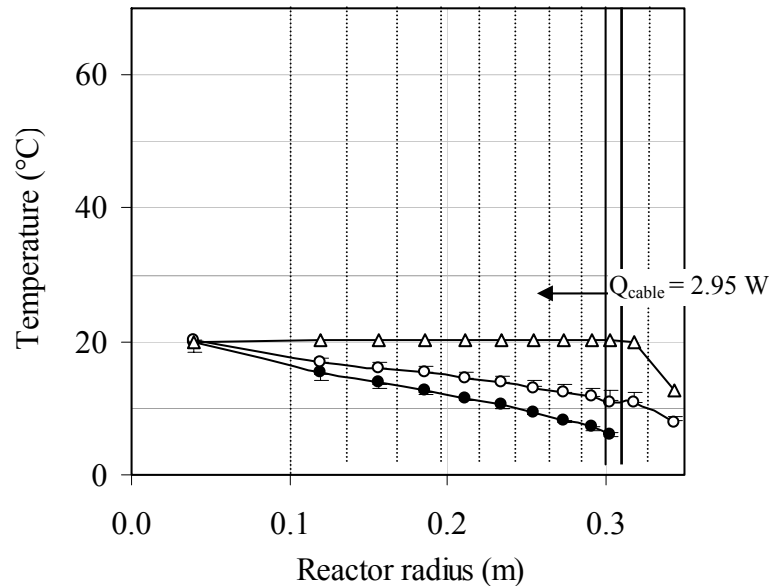


Figure A3.4. Radial temperature profile for an initial temperature of 20 °C [un-insulated reactor (—●—), insulated reactor (—○—) and insulated reactor with heating cable operating at 2.95 W (—△—)]

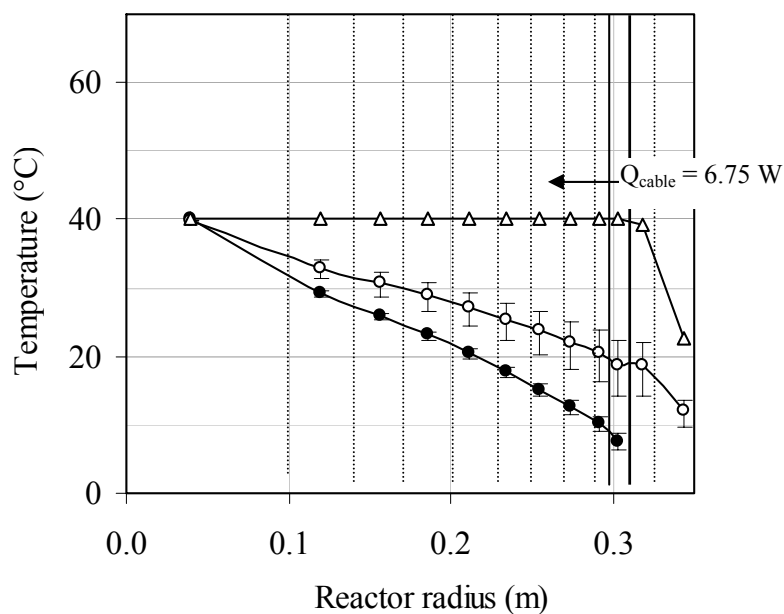


Figure A3.5. Radial temperature profile for an initial temperature of 40°C. [Un-insulated reactor (—●—), insulated reactor (—○—) and insulated reactor with heating cable (—△—) operating at 6.75 W]

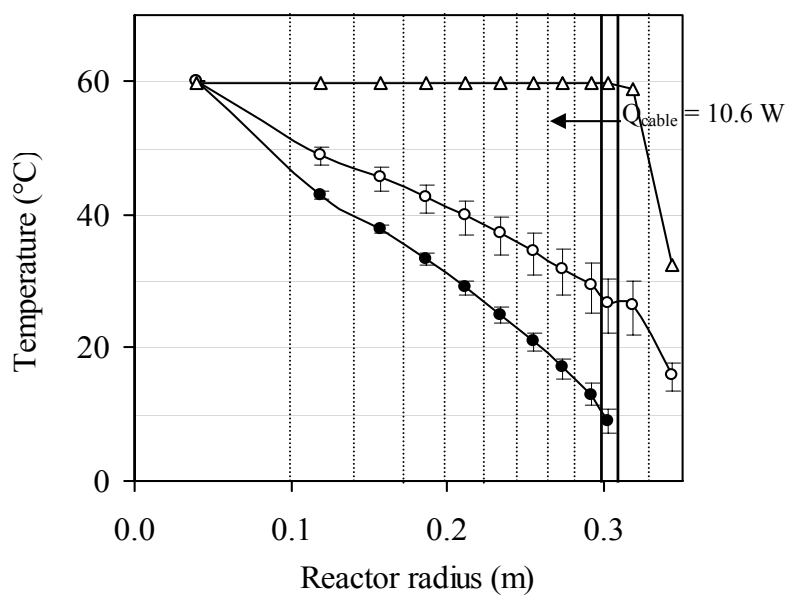


Figure A3.6. Radial temperature profile for an initial temperature of 60°C. un-insulated reactor (—●—), insulated reactor (—○—) and insulated reactor with heating cable (—△—) operating at 10.6 W]

The error bars indicate that effect of the moisture content on radial heat losses was not linear between 50 % and 80 % and the difference between the equilibrium temperatures of these moisture contents in each unit was greater for the insulated than the un-insulated reactor. Also, the moisture content did not affect the amount of heat supplied by the heating cable to reduce the radial temperature difference to within a degree.

The insulation reduced the radial temperature difference by about 35 % but the temperature of the outer element of the organic material was still about half that in the centre element. In order to keep the temperature difference in the section to within a degree, a maximum of approximately 11 W was required from the heating cable, which equated to a power flux of 58 W m^{-2} . This value did not depend on the moisture content of the organic material. For the whole outside surface of the reactor, cable needed to supply 116 W. The heating cable supplied a maximum 15 W m^{-1} length of cable, and so 8 metres of cable was able to meet the power demand. This length allowed 4 loops of cable around the outside of the reactor, positioned 26 cm vertically apart. The configuration may have resulted in uneven heating over the surface of the reactor. For the 20 m of cable used to cover the outside of the reactor (Section 3.1.1), the power input from the cable was 300 W and the flux was:

$$= 15 \times \frac{\text{cable length } (\approx 20 \text{ m})}{\text{covered area of reactor } (\approx 2 \text{ m}^2)} = 150 \text{ W m}^{-2} \quad (\text{A3 xii})$$

A3.1.2. Heat loss simulation programs

The Macros facility of the Microsoft Excel computer program was used to simulate the radial heat losses from the reactors. The Macros were written in the Visual Basic language and calculated the temperature at each radius across the reactor at steady state. On a graph steady state was reached when the temperature-time profile was constant after about 60 000 iterations. The emboldened values in the Sections A3.1.2.1 to A3.1.2.2 were those which

were changed for the each simulation depending on the temperature at the core of the system and the moisture content of the organic material.

A3.1.2.1. Reactor with no insulation

'Declare thermal conductivity of organic material (kc) and reactor wall (kw), specific heat capacity of the organic material (Cp), the combined heat transfer coefficient (hcr), and the length (L) and thickness of element (x) and wall (xw)

Dim kc, kw, kair, Cp, hcr, L, x, xw,

'Declare temperature (T), radii (r), rate of heat change (dQ_dt), of temperature change (dT_dt) and of heat generation (dQgen_dt), conductivity (k) in arrays

Dim T(100), r(100), dQ_dt(100, 100), dT_dt(100), k(100)

'Declare some integers

Dim A&, e&, b&

' Define the number of elements in simulation

e& = 10

'Declare and calculate π

Dim PI

PI = Atn(1) * 4

'Define vertical length of section

L = 0.1

'Declare moisture content (50%, 65% or 80%)

Dim MC

MC = **65** '%

'Define densities of organic material and reactor wall

Dim RHO, RHOw

If MC = 50 Then

RHO = 92

End If

If MC = 65 Then

RHO = 160

End If

If MC = 80 Then

$$\text{RHO} = 303$$

End If

$$\text{RHO}_w = 900$$

'Define initial ambient temperature and initial temperatures of all elements (293, 313 or 333K)

$$T_{\text{air}} = 278$$

For A& = 1 To e&

$$T(0) = T_{\text{air}}$$

$$T(\text{A\&}) = 333$$

Next

'Define outer radius and thickness of reactor wall (element 1)

$$r(0) = 0.306$$

$$x_w = 0.006$$

'Calculate the total mass of the organic material (Mu)

Dim Mu

$$\text{Mu} = \text{PI} * (r(0) - x_w)^2 * L * \text{RHO}$$

'There are (e& - 1) elements of organic material

'Declare and define the element masses – organic material (m) and wall (mw)

Dim m, mw

$$m = \text{Mu} / (\text{e\&} - 1)$$

$$\text{mw} = 1.028$$

'Calculate radii of organic material elements assuming equal masses and volumes

Dim V

$$V = m / \text{RHO}$$

$$r(\text{e\&}) = 0.01$$

$$r(\text{e\&-1}) = (V / (\text{PI} * L))^{\wedge} 0.5$$

For A& = e&-2 To 1

$$r(\text{A\&}) = (V / (\text{PI} * L) + r(\text{A\&+1})^2)^{\wedge} 0.5$$

Next

'Define the thermal conductivities of organic material and wall

```

kw = 0.33
k(1) = kw
For A& = 2 To e&
    k(A&) = (0.005 * MC) - 0.165
Next
'Define convective heat transfer coefficient from outside surface to surroundings – laminar
hcr = 10
'Define specific heat capacities and densities
Cp = (0.03 * MC) + 0.99
Cpw = 1.8
If T=293 Then
    Cpa = 1.023 'J/(g K) saturated air @ 293K
    RHOa = 1.2 'g/l saturated air @ 293K
End If
If T = 313 Then
    Cpa = 1.051 'J/(g K) saturated air @ 313K
    RHOa = 1.102 'g/l saturated air @ 313K
End If
If T = 333 Then
    Cpa = 1.126 'J/(g K) saturated air @ 333K
    RHOa = 0.985 'g/l saturated air @ 333K
End If
'Calculate heat generation (1.5 for 293K, 5.37 for 313K or 19.28 for 333K)
hgen = 19.28 'J/kg
dQgen_dt = hgen * m * (1 - MC / 100) * 0.88 'J
'Define vertical airflow rate (Vaf), vertical temperature difference (dT_V)
Vaf = 121.4 'l/min
dT_V = 1 '°C
'Calculate vertical heat loss
dQoutV_dt = Vaf / 60 * RHOa * Cpa * dT_V 'J
iters& = Cells(9, 2)
For b& = 1 To 10

```

For del_t& = 1 To iters&

'Calculate conductive and convective plus radiative heat loss from wall to the surroundings

$$dQ_dt(1, 0) = 2 * PI * L * (T(1) - T(0)) / (1 / (hcr * r(0)) + (\log(r(0) / r(1))) / k(1))$$

'Calculate heat flows in direction of increasing radius and decreasing element number

For n = 2 To e&

$$dQ_dt(n, n - 1) = 2 * PI * L * k(n) * (T(n) - T(n - 1)) / \text{Log}(r(n - 1) / r(n))$$

Next

'Calculate temperature change in wall

$$dT_dt(1) = (dQ_dt(2, 1) - dQ_dt(1, 0)) / (1000 * mw * Cp_w)$$

'Calculate temperature change in organic material elements

For n = 2 To e& - 1

$$dT_dt(n) = (dQ_dt(n + 1, n) - dQ_dt(n, n - 1) + dQ_{gen_dt} - dQ_{outV_dt}) / (1000 * m * Cp)$$

Next

$$dT_dt(e\&) = (dQ_{gen_dt} - dQ_dt(e\&, e\& - 1) - dQ_{outV_dt}) / (1000 * m * Cp)$$

'Update unit temperatures

For n = 1 To e&

$$T(n) = T(n) + dT_dt(n)$$

Next

Next

'Transfer data to Excel spread sheet

$$\text{Cells}(b\& + 11, 1) = b\&$$

$$\text{Cells}(b\& + 11, 2) = T(1) \quad \text{' element 1 wall temperature}$$

$$\text{Cells}(b\& + 11, 3) = T(2) \quad \text{' element 2 temperature}$$

$$\text{Cells}(b\& + 11, 4) = T(3) \quad \text{' element 3 temperature}$$

$$\text{Cells}(b\& + 11, 5) = T(4) \quad \text{' element 4 temperature}$$

$$\text{Cells}(b\& + 11, 6) = T(5) \quad \text{' element 5 temperature}$$

$$\text{Cells}(b\& + 11, 7) = T(6) \quad \text{' element 6 temperature}$$

$$\text{Cells}(b\& + 11, 8) = T(7) \quad \text{' element 7 temperature}$$

$$\text{Cells}(b\& + 11, 9) = T(8) \quad \text{' element 8 temperature}$$

$$\text{Cells}(b\& + 11, 10) = T(9) \quad \text{' element 9 temperature}$$

$$\text{Cells}(b\& + 11, 11) = T(10) \quad \text{'element 10 centre temperature}$$

End Sub ' grad_array

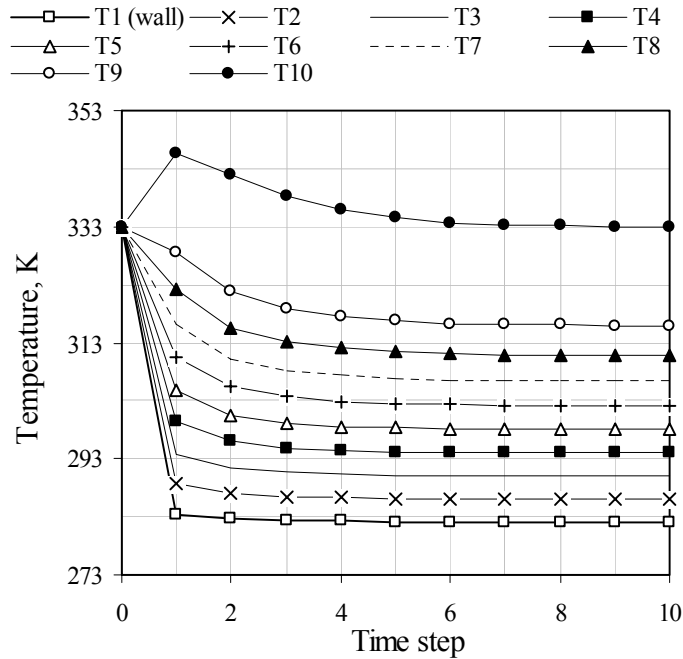


Figure A3.7. Temperature changes in an un-insulated reactor operating at 60 °C

A3.1.2.2. Reactor with insulation

'Declare thermal conductivity of composting organic material (kc), reactor wall (kw) and insulation (kins), the specific heat capacity of the organic material (Cp), and the length (L) and thickness of element (x) and wall (xw)

Dim kc, kw, kair, kins, Cp, hcr, L, x, xw,

'Declare temperature (T), radii (r), rate of heat change (dQ_dt), of temperature change (dT_dt) and of heat generation (dQgen_dt), conductivity (k) in arrays

Dim T(100), r(100), dQ_dt(100, 100), dT_dt(100), k(100)

'Declare some integers

Dim A&, e&, b&

' Define the number of elements in simulation

e& = 12

'Declare and calculate π

Dim PI

PI = Atn(1) * 4

'Define vertical length of the section

L = 0.1

'Declare moisture content (50%, 65% or 80%)

Dim MC

MC = **65** '% moisture

'Define densities of organic material and reactor wall

Dim RHO, RHOw

If MC = 50 Then

RHO = 92

End If

If MC = 65 Then

RHO = 160

End If

If MC = 80 Then

RHO = 303

End If

RHOw = 900

'Define initial ambient temperature

Tair = 278

'Define initial temperatures of all elements

For A& = 1 To e&

T(0) = Tair

T(A&) = **333**

Next

'Declare radii of external layers

r(0) = 0.356 'outside of insulation (assume 50 mm thickness)

r(2) = 0.306 'outside of wall

xw = 0.006 'thickness of reactor wall

r(1) = ((r(0) ^ 2 + r(2) ^ 2) / 2) ^ 0.5 '=0.332

Dim m

m_ins = 1.04

m_ins1 = m_ins / 2

m_ins2 = m_ins / 2

mw = 1.028

'Calculate the total mass of organic material in the section (Mu) and mass of each element - e&-3 elements of organic material

Dim Mu

$$\text{Mu} = \text{PI} * (\text{r}(2) - \text{xw})^2 * \text{L} * \text{RHO}$$

$$\text{m} = \text{Mu} / (\text{e\&} - 3)$$

'Calculate radii of elements - assume equal masses and volumes (V) organic material

Dim V

$$\text{V} = \text{m} / \text{RHO}$$

$$(\text{e\&}) = 0.01$$

$$\text{r}(\text{e\&-1}) = (\text{V} / (\text{PI} * \text{L}))^{0.5}$$

For A&=e&-2 To 3

$$\text{r}(\text{A\&}) = (\text{V} / (\text{PI} * \text{L}) + \text{r}(\text{A\&+1})^2)^{0.5}$$

Next

'Define thermal conductivities – organic material, wall, air and insulation

$$\text{kw} = 0.33$$

$$\text{kins} = 0.052$$

$$\text{kair} = 0.033$$

$$\text{k}(1) = \text{kins}$$

$$\text{k}(2) = \text{kins}$$

$$\text{k}(3) = \text{kw}$$

For A& = 4 To e&

$$\text{k}(\text{A\&}) = (0.005 * \text{MC}) - 0.165$$

Next

'Define combined heat transfer coefficient from outside surface, hcr

$$\text{hcr} = 10$$

'Define specific heat capacities and densities of saturated air

$$\text{Cp} = (0.03 * \text{MC}) + 0.99$$

$$\text{Cpw} = 1.8$$

If T=293 Then

$$\text{Cpa} = 1.023 \text{ 'J / (g K) saturated air @ 293K}$$

$$\text{RHOa} = 1.2 \text{ 'g/l saturated air @ 293K}$$

End If

If T = 313 Then

Cpa = 1.051 'J/(g K) saturated air @ 313K

RHOa = 1.102 'g/l saturated air @ 313K

End If

If T = 333 Then

Cpa = 1.126 'J/(g K) saturated air @ 333K

RHOa = 0.985 'g/l saturated air @ 333K

End If

'Calculate heat generation

hgen = 19.28 'W/kg

dQgen_dt = hgen * m * (1 - MC / 100) * 0.88 ' W

'Calculate vertical heat loss

Vaf = **143** 'l/min vertical airflow rate

dT_V = 1 '°C vertical temperature difference

dQoutV_dt = Vaf / 60 * RHOa * Cpa * dT_V

'Define heat input from cable over the area of the element considered

dQin_dt = 0

iters& = Cells(9, 2)

For b& = 1 To 10

For del_t& = 1 To iters&

'Calculate conductive and convective plus radiative heat loss from outer element of insulation to surroundings

dQ_dt(1, 0) = * 2 * PI * L * (T(1) - T(0)) / (1 / (hc * r(0)) + (log(r(0) / r(1))) / k(1))

'Calculate heat flows in direction of increasing radius and decreasing element number

For n = 2 To e&

dQ_dt(n, n - 1) = 2 * PI * L * k(n) * (T(n) - T(n - 1)) / Log(r(n - 1) / r(n))

Next

'Calculate temperature change in insulation and wall

dT_dt(1) = (dQ_dt(2, 1) - dQ_dt(1, 0)) / (1000 * m_ins1 * Cpins)

dT_dt(2) = (dQ_dt(3, 2) - dQ_dt(2, 1)) / (1000 * m_ins2 * Cpins)

dT_dt(3) = (dQ_dt(4, 3) - dQ_dt(3, 2) + dQin_dt) / (1000 * mw * Cpw)

'Calculate temperature change in composting organic material elements

For n = 4 To e& - 1

$$dT_dt(n) = (dQ_dt(n + 1, n) - dQ_dt(n, n - 1) + dQgen_dt - dQoutV_dt)/(1000 * m * Cp)$$

Next

$$dT_dt(e\&) = (dQgen_dt - dQ_dt(e\&, e\& - 1) - dQoutV_dt) / (1000 * m * Cp)$$

'Update temperatures

For n = 1 To e&

$$T(n) = T(n) + dT_dt(n)$$

Next

Next

'Transfer data to Excel worksheet

$$\text{Cells}(b\& + 11, 1) = b\&$$

$$\text{Cells}(b\& + 11, 2) = T(1) \text{ 'element 1 insulation outer temperature}$$

$$\text{Cells}(b\& + 11, 3) = T(2) \text{ 'element 2 insulation inner temperature}$$

$$\text{Cells}(b\& + 11, 4) = T(3) \text{ 'element 3 wall temperature}$$

$$\text{Cells}(b\& + 11, 5) = T(4) \text{ 'element 4 temperature}$$

$$\text{Cells}(b\& + 11, 6) = T(5) \text{ 'element 5 temperature}$$

$$\text{Cells}(b\& + 11, 7) = T(6) \text{ 'element 6 temperature}$$

$$\text{Cells}(b\& + 11, 8) = T(7) \text{ 'element 7 temperature}$$

$$\text{Cells}(b\& + 11, 9) = T(8) \text{ 'element 8 temperature}$$

$$\text{Cells}(b\& + 11, 10) = T(9) \text{ 'element 9 temperature}$$

$$\text{Cells}(b\& + 11, 11) = T(10) \text{ 'element 10 temperature}$$

$$\text{Cells}(b\& + 11, 12) = T(11) \text{ 'element 11 temperature}$$

$$\text{Cells}(b\& + 11, 13) = T(12) \text{ 'element 12 temperature-centre}$$

End Sub ' grad_array

A3.1.2.3. Reactor with insulation and heating cable

The program was the same as for the reactor with rock wool insulation except 'the heat input from cable over the area of the element considered' was given a value such that

$$dQin_dt = 2.95 \text{ for an initial temperature of } 20^{\circ}\text{C}$$

$$dQin_dt = 6.75 \text{ for an initial temperature of } 40^{\circ}\text{C}$$

$$dQin_dt = 10.6 \text{ for an initial temperature of } 60^{\circ}\text{C}$$

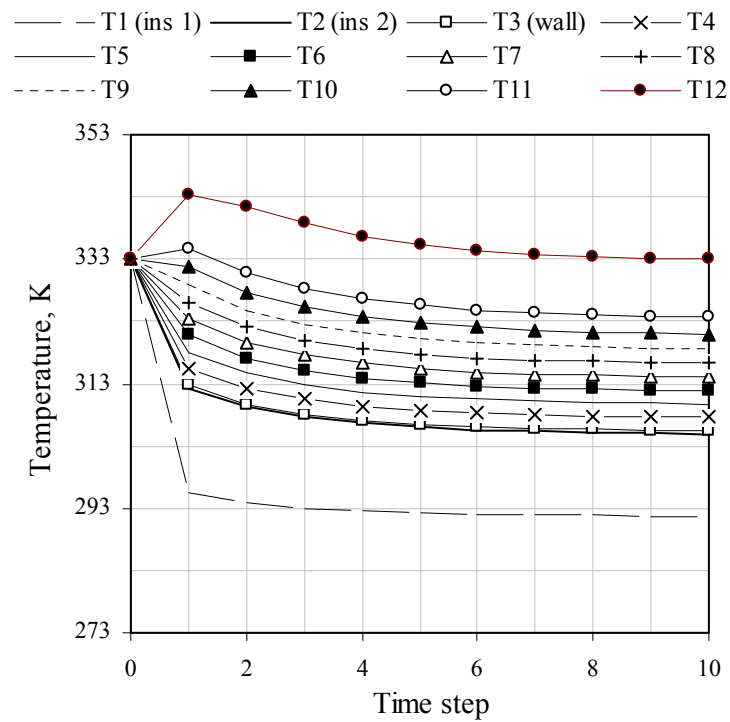


Figure A3.8. Temperature changes in an insulated reactor operating at 60 °C

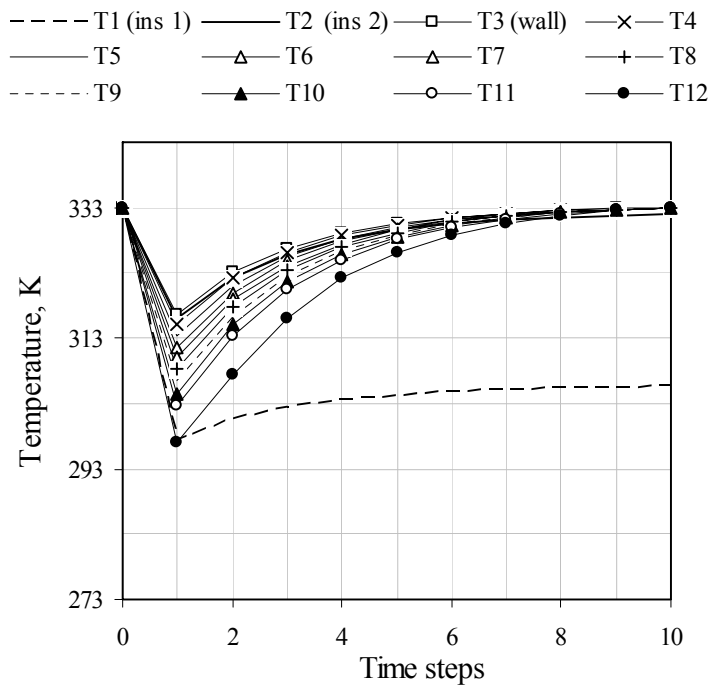


Figure A3.9. Temperature changes in an insulated reactor with heating operating at 60 °C

A3.1.3. Heating cable geometry

The height of the reactor covered but the heating cable was around 1.05 m and the surface area was about 2 m². To determine the length of the heating cable required to achieve and even distribution of heat across the reactor surface, the geometry of the cable coiled around the reactor in a helix configuration was considered. The reactor cylinder was opened out to a rectangle, so that the helix became a series of diagonal lines (Figure A3.10). A single loop of the helix formed the hypotenuse of a right angle triangle with the circumference of the helix, C , along the x axis and the height between loops, l , along the y axis.

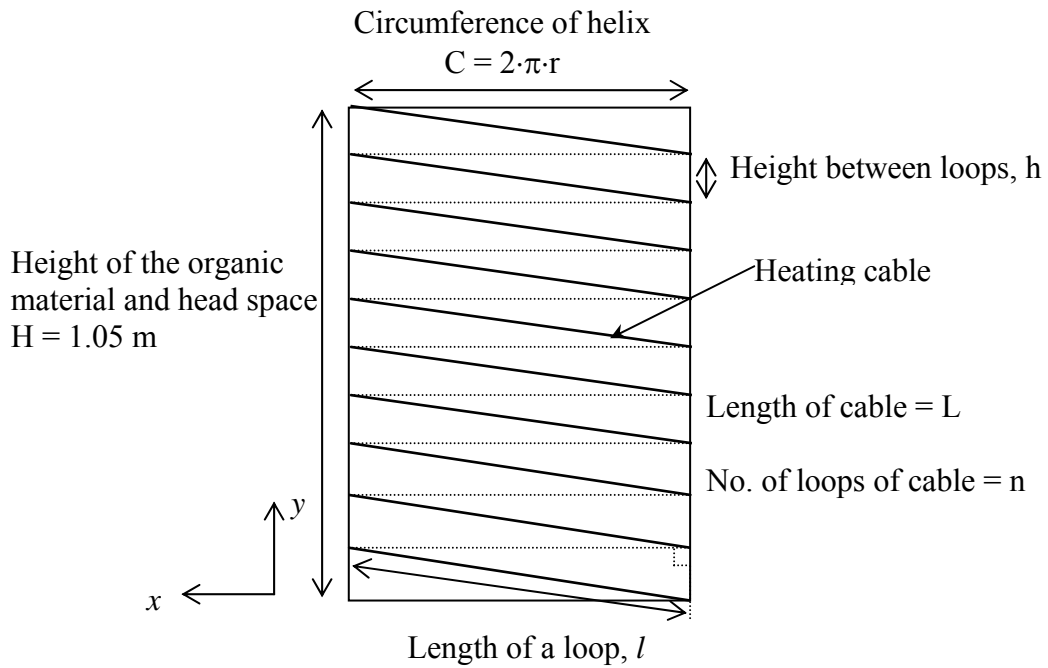


Figure A3.10. Configuration of the heating cable on the reactor.

For 10 loops of cable, the height between the loops was given by

$$h = \frac{H}{n} = \frac{1.05}{10} = 0.105 \text{ m} \quad (\text{A3 xii})$$

The outside radius of the reactor, $r_o = 0.310 \text{ m}$, and the thickness of the cable was 5 mm, such that the radius of the helix, r , equalled the mean radius of r_o and $(r_o + 0.005)$, therefore

$$r = \frac{0.005}{\ln\left(\frac{r_o + 0.005}{r_o}\right)} \approx 0.312 \text{ m} \quad (\text{A3 xiii})$$

and $C = 1.96 \text{ m}$

Applying the Pythagoras theorem to the right angle triangle gave

$$l = \sqrt{C^2 + h^2} \approx 1.97 \text{ m} \quad (\text{A3 xiv})$$

The length of cable, L , required for 10 loops around the reactor was therefore 19.66m

A3.2. The composting unit

A3.2.1. Control of rig valves

The Macros facility available in the Microsoft Excel computer package, programmed in Visual Basic language, was used to run the valve switch combinations and the logging of the data for the analysis of oxygen and carbon dioxide in the off-gas. The program allowed only two separate valve entries to be used per data log. It was possible to couple valves so that a single entry affected two valves. Here, valves 3 and 4 and valves 5 and 6 were coupled, as their actuation was always required at the same instance. The valve actuation combinations for the analysis of the off-gas from each reactor and for the automatic calibration on the gas analyser are given in Table A3.2. The valves correspond to those indicated in Figure A3.11.

Table A3.2. Valve combinations for off-gas analysis and automatic gas analyser calibration.

Gas line	V1	V2	V3	V4	V5	V6	
Reactor R1	N/C	N/O	N/O	N/O	N/O	C/O	One valve switch V1
Reactor R2	N/O	N/O	N/O	N/O	N/O	C/O	No valve switch
Reactor R3	N/O	N/C	N/O	N/O	N/O	C/O	One valve switch V2
N ₂	N/O	N/O	<u>N/C</u>	<u>N/C</u>	N/C	N/O	One valve V5 and one coupled valve switch V3-V4
9% CO ₂ in N ₂	N/O	N/O	<u>N/C</u>	<u>N/C</u>	<u>N/C</u>	<u>N/C</u>	Two coupled valve switch V3-V4 & V5-V6
Air and Purge	N/O	N/O	N/C	N/O	N/O	C/O	One valve switch V3

N/C - the valve is 'normally closed' when not actuated
 N/O - the valve is 'normally open' when not actuated
 C/O - the valve can be 'open or closed'

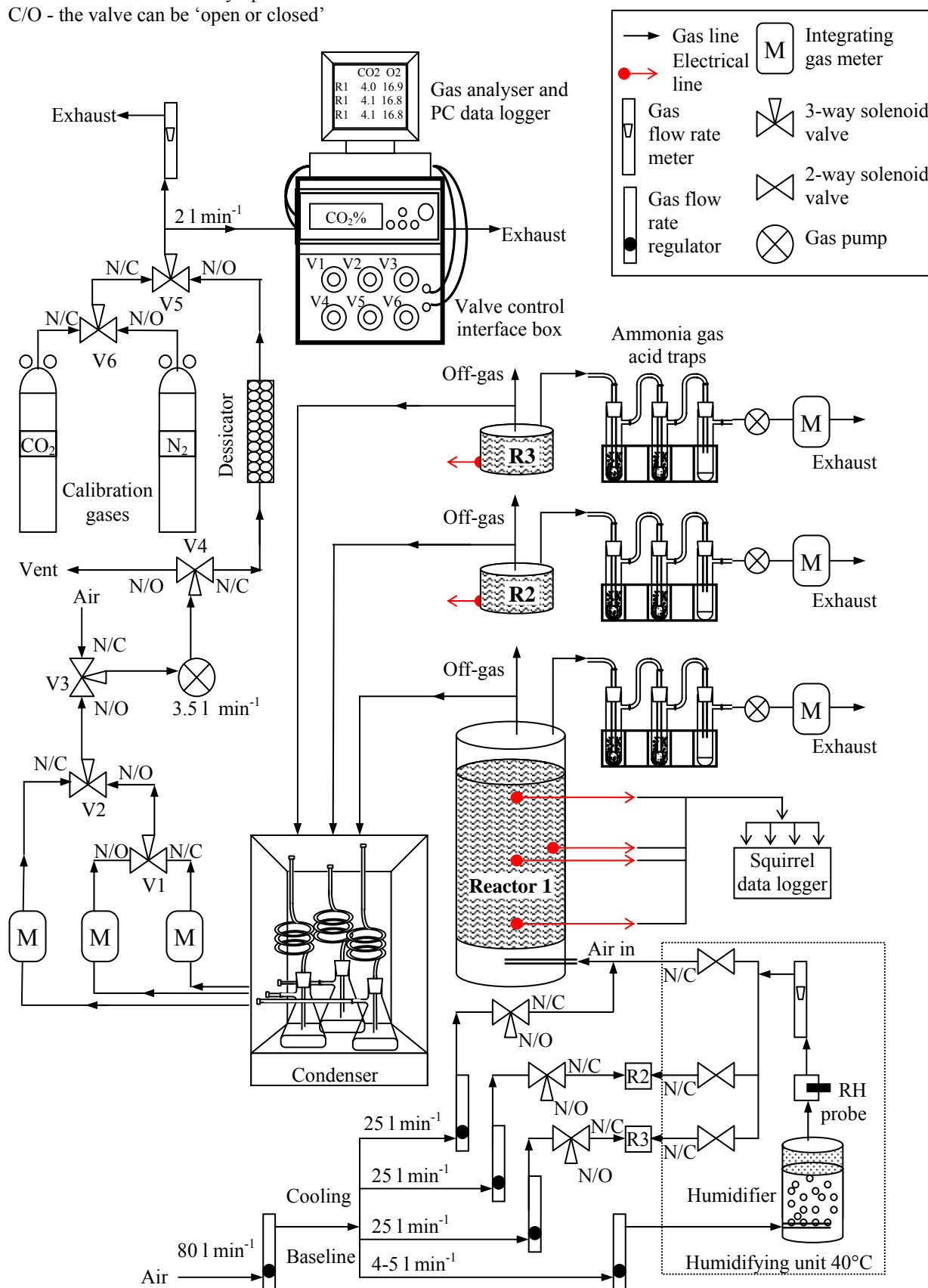


Figure A3.11. The composting unit (three composting reactors and rig).

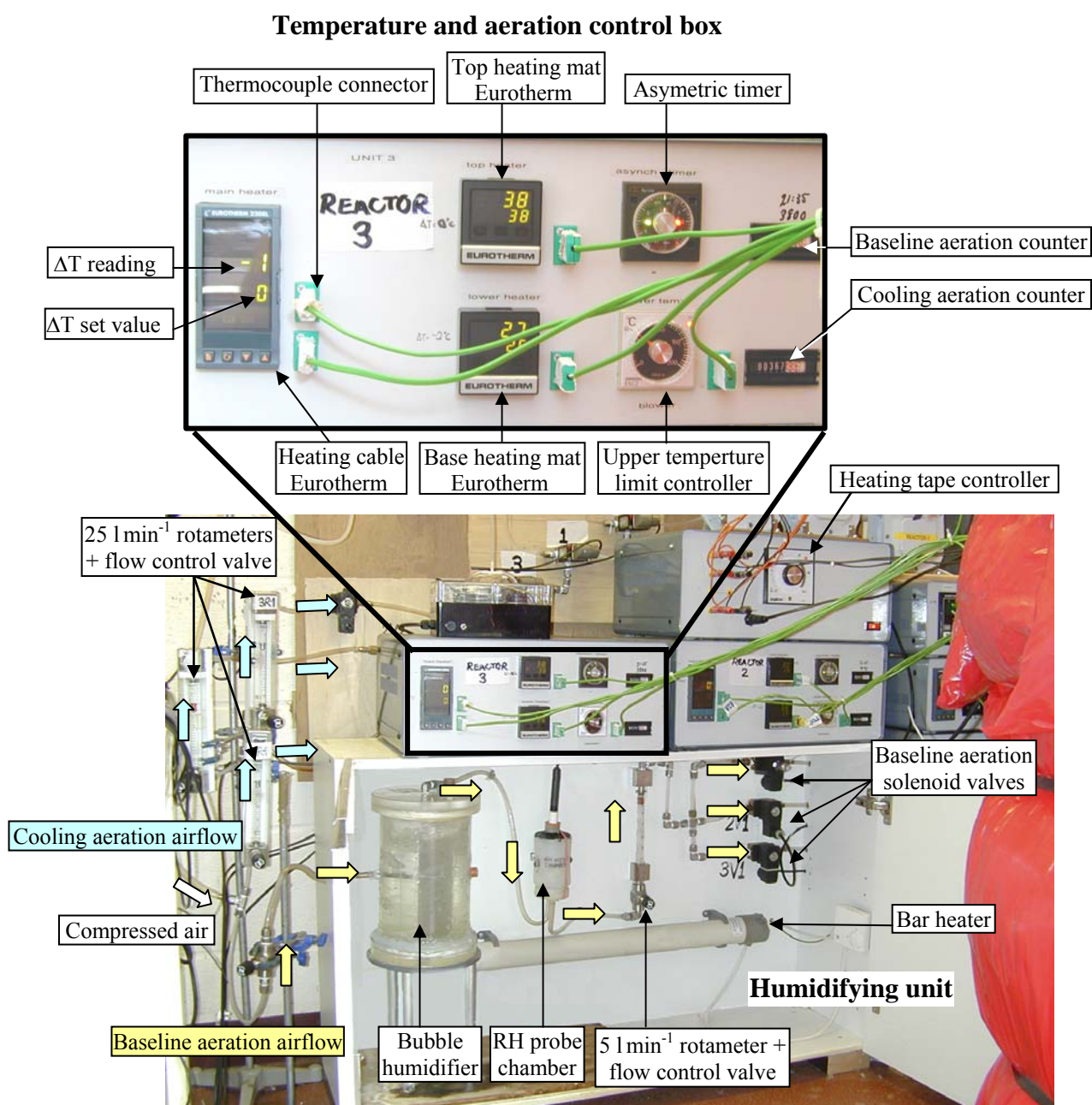


Figure A3.12. Humidifying unit and temperature and aeration control boxes of Reactor 2 and 3.

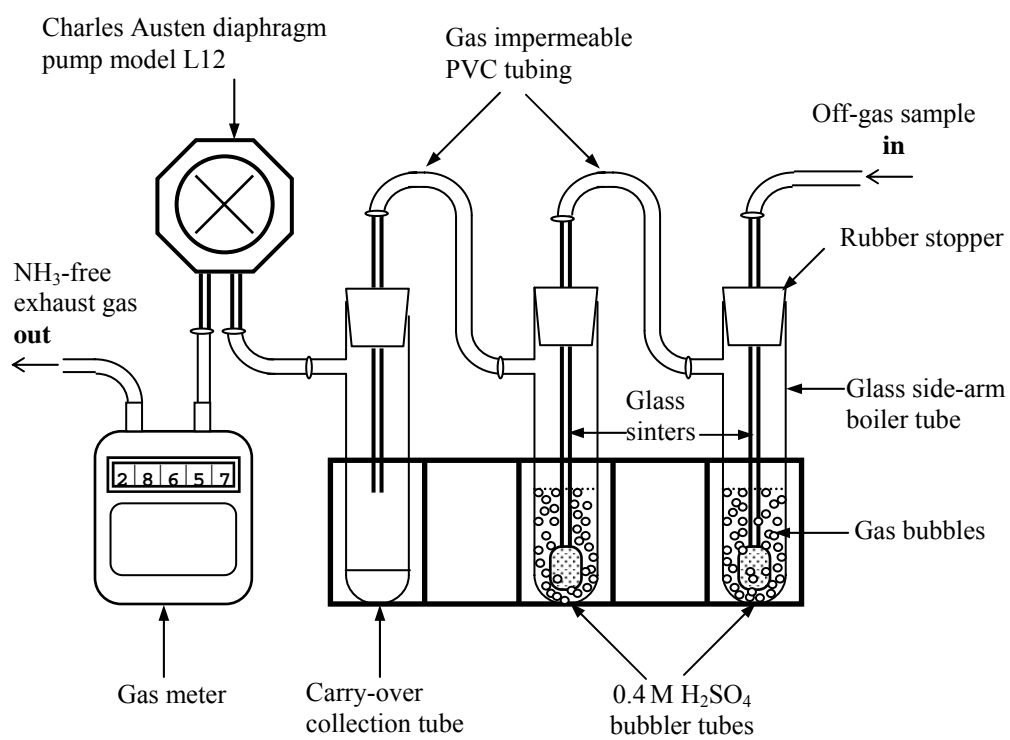


Figure A3.13. An ammonia acid trap

A4. Respirometry

Table A4.1. The diffusion coefficients and solubility of oxygen in water

Temperature °C	Diffusion coefficient ¹ $\times 10^{-5} \text{ cm}^2 \text{ s}^{-1}$	Diffusion coefficient ² $\times 10^{-5} \text{ cm}^2 \text{ s}^{-1}$	Solubility air in H_2O ² $\times 10^{-5} \text{ g cm}^{-3}$	Solubility O_2 in H_2O ² $\times 10^{-5} \text{ g cm}^{-3}$
0	1.27	1.00	4.14	6.99
5	1.43	1.11	3.55	6.03
10	1.60	1.24	3.08	5.23
15	1.79	1.38	2.71	4.60
20	2.00	1.54	2.42	4.13
25	2.24	1.72	2.15	3.66
30	2.51	1.91	1.96	3.34
35	2.81	2.13	1.78	3.03
40	3.14	2.37	1.69	2.87
45	3.51	2.64	1.59	2.70
50	3.93	2.94	1.49	2.53
55	4.39	3.28	1.45	2.47
60	4.91	3.65	1.42	2.41
65	5.48	4.07	1.38	2.35
70	6.13	4.54	1.35	2.29

¹ Calculated from the Wilke-Chance equation

² Calculated from the Stoke-Epstein equation [Johnson 1999].

Table A4.2. The total effect of the environmental factors in the gas analyser respirometer

Temperature, °C	M:S = 2:1 (C:N = 25)		M:S = 4:1 (C:N = 15)	
	$f(M:S)$	$f(M:S)^*$	$f(M:S)$	$f(M:S)^*$
10	0.911	0.810	0.895	0.306
20	0.908	0.514	0.880	0.301
25	0.908	0.600	0.859	0.294
30	0.903	0.673	0.867	0.296
35	0.900	0.389	0.802	0.274
38	0.898	0.564		
40	0.901	0.476	0.844	0.289
45	0.874	0.346	0.790	0.270
50	0.878	0.380	0.821	0.281
55	0.888	0.590	0.756	0.259
60	0.855	0.460	0.823	0.281
65	0.871	0.392		
70	0.874	0.601	0.851	0.291
Mean	0.890	0.523	0.835	0.286
σ	0.005	0.037	0.013	0.004

$$f(M:S) = f_{MC} \cdot f_{OC} \cdot f_{FAS}(M:S) \text{ and } f(M:S)^* = f_{MC} \cdot f_{OC} \cdot f_{FAS} \cdot f_{C:N}(M:S)$$

A4.1. Curve fitting

A4.1.1. Double power equation

Equation (4 xvii) is differentiated with respect to temperature, T , with reference to 20°C , such that $TR1$ and k_{TR1} are equal to 20 and k_{20} , respectively. The optimal operating temperature for microbial activity, T_{opt} occurred around 60°C and therefore $TR2 \approx 60-10 = 50$. k_{20} is a constant term and equation (4 xvii) can re-written for K , as

$$K = \frac{k_T}{k_{20}} = (C_1^{T-20} - C_2^{T-50}) \quad (\text{A4 i})$$

Assuming that microbial activity ceases at about 75°C, then $K = 0$ at $T = 75$. Substituting into equation (A4 i) and rearranging to express the temperature constant C_1 relative to C_2 gives

$$\frac{T_0 - 50}{T_0 - 20} = \frac{\ln C_1}{\ln C_2} \approx 0.455 \quad (\text{A4 ii})$$

The derivative of equation (A4 i) is zero at T_{opt} so that

$$\frac{dK}{dT} = \frac{dC_1^{T_{\text{opt}}-20}}{dT} - \frac{dC_2^{T_{\text{opt}}-50}}{dT} = C_1^{T_{\text{opt}}-20} \cdot \ln C_1 - C_2^{T_{\text{opt}}-50} \cdot \ln C_2 = 0 \quad (\text{A4 iii})$$

Substituting for T_{opt} and equation (A4 ii) into equation (A4 iii) and rearranging gives

$$\frac{C_1^{60-20}}{C_2^{60-50}} = \frac{\ln C_2}{\ln C_1} \approx 0.455 \quad (\text{A4 iv})$$

Taking natural logs and rearranging equation (A4 iv), with further substitution of equation (A4 ii) gives an estimate of the temperature constants as

$$C_1 \approx 1.045 \text{ and } C_2 \approx 1.101$$

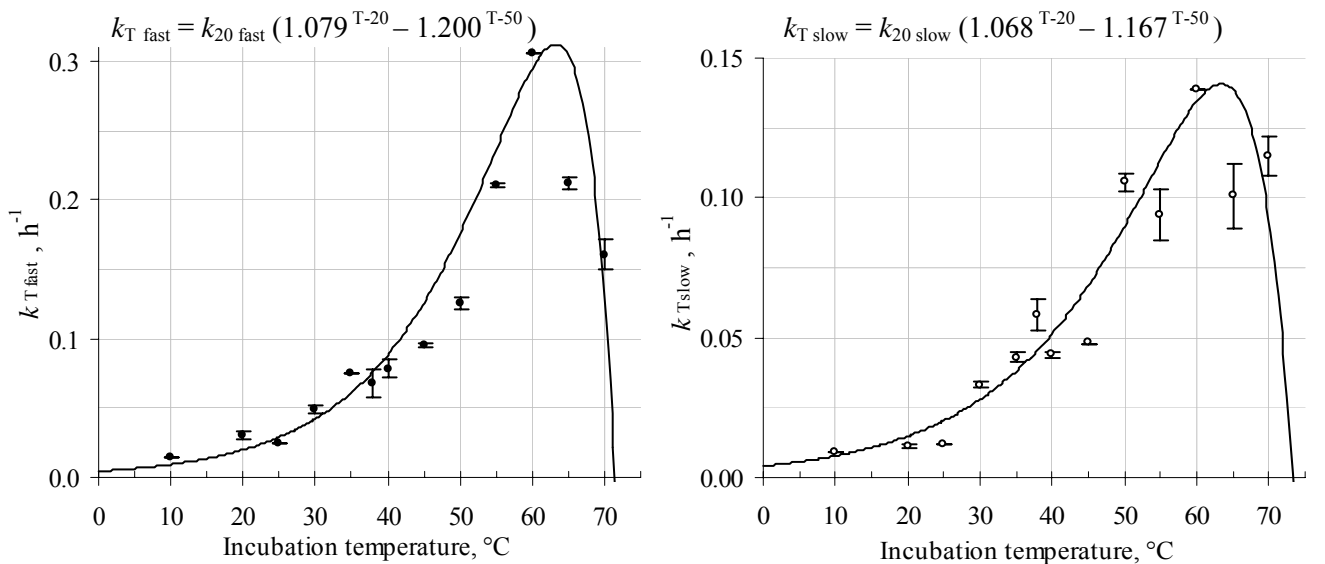


Figure A4.1. The reaction rate coefficients as a function of temperature for the fast (●) and slow (○) stages of M:S ratio of 2:1 based on equation (4 xvii).

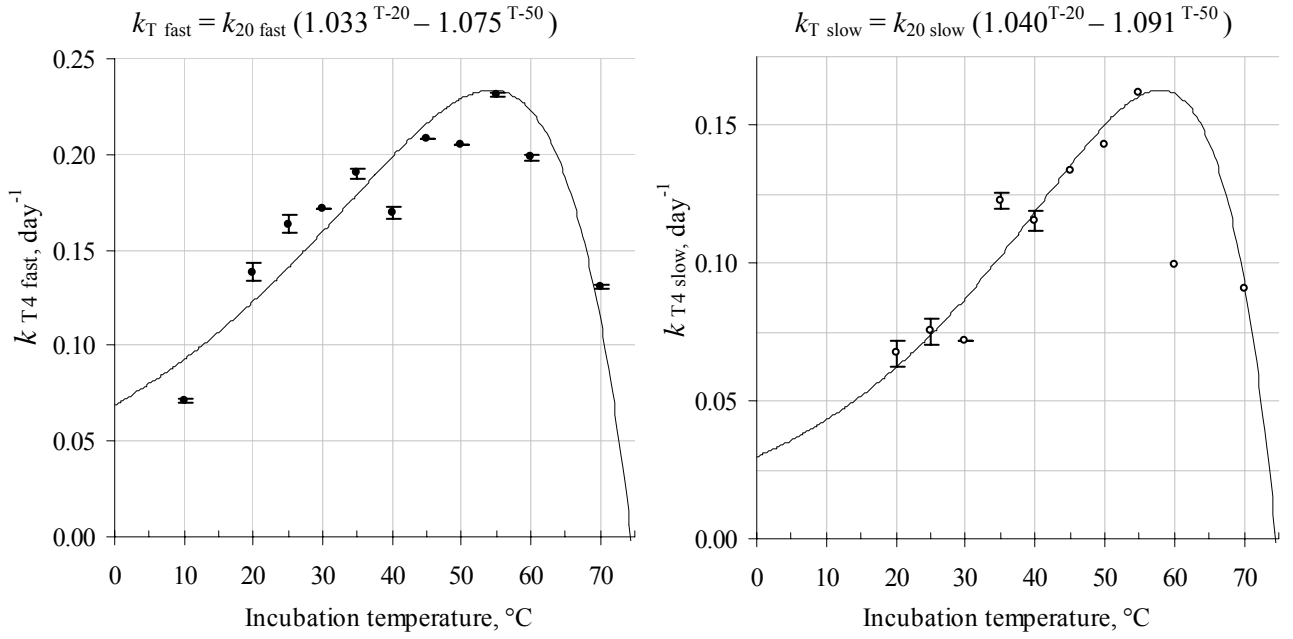


Figure A4.2. The reaction rate coefficients as a function of temperature for the fast (●) and slow (○) stages of M:S ratio of 4:1 based on equation (4 xvii).

A4.1.2. Enzyme activity equation

The optimal operating temperature, T_{opt} , was determined by differentiating equation (4 xviii) with respect to temperature, T , which requires the use of the quotient rule given as

$$\frac{d}{dx} \cdot \frac{f(x)}{g(x)} = \frac{f'(x) \cdot g(x) - g'(x) \cdot f(x)}{(g(x))^2} \quad (\text{A4 v})$$

For equation (4 xviii), $f(x) = e^{a(T-T_{\text{ref}})}$ and $g(x) = e^{b(T-T_{\text{inf}})} + 1$ and the respective derivatives of the terms are

$$f'(x) = a \cdot e^{a(T-T_{\text{ref}})} \text{ and } g'(x) = b \cdot e^{b(T-T_{\text{inf}})}.$$

When $T = T_{\text{opt}}$ the derivative of k_T with respect to T , $\frac{dk_T}{dT}$, equals 0 and equation (A4 v)

$$\text{becomes} \quad a \cdot e^{a(T_{\text{opt}}-T_{\text{ref}})} \cdot (e^{b(T_{\text{opt}}-T_{\text{inf}})} + 1) - b \cdot e^{b(T_{\text{opt}}-T_{\text{inf}})} \cdot e^{a(T_{\text{opt}}-T_{\text{ref}})} = 0 \quad (\text{A4 vi})$$

Rearrangement of equation (A4 v) to express T_{opt} explicitly gives

$$T_{\text{opt}} = T_{\text{inf}} - \frac{1}{b} \ln\left(\frac{b}{a} - 1\right) \quad (\text{A4 vii})$$

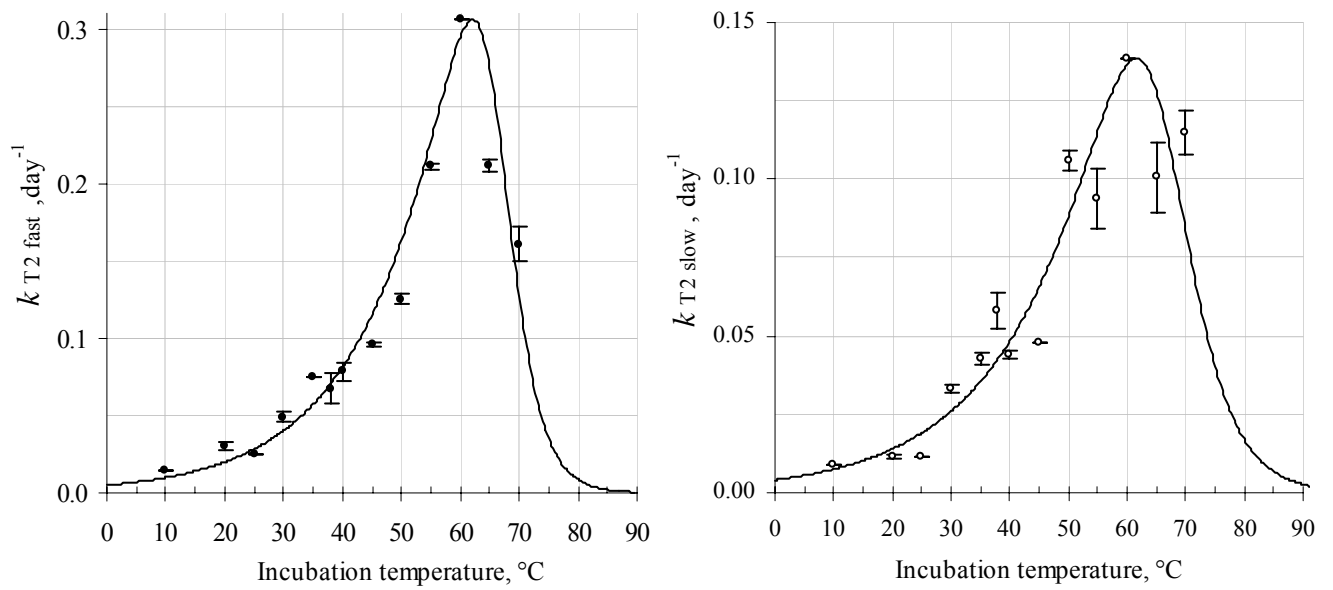


Figure A4.3. The reaction rate coefficients as a function of temperature for the fast (●) and slow (○) stages of M:S ratio of 2:1 based on the equation (4 xviii).

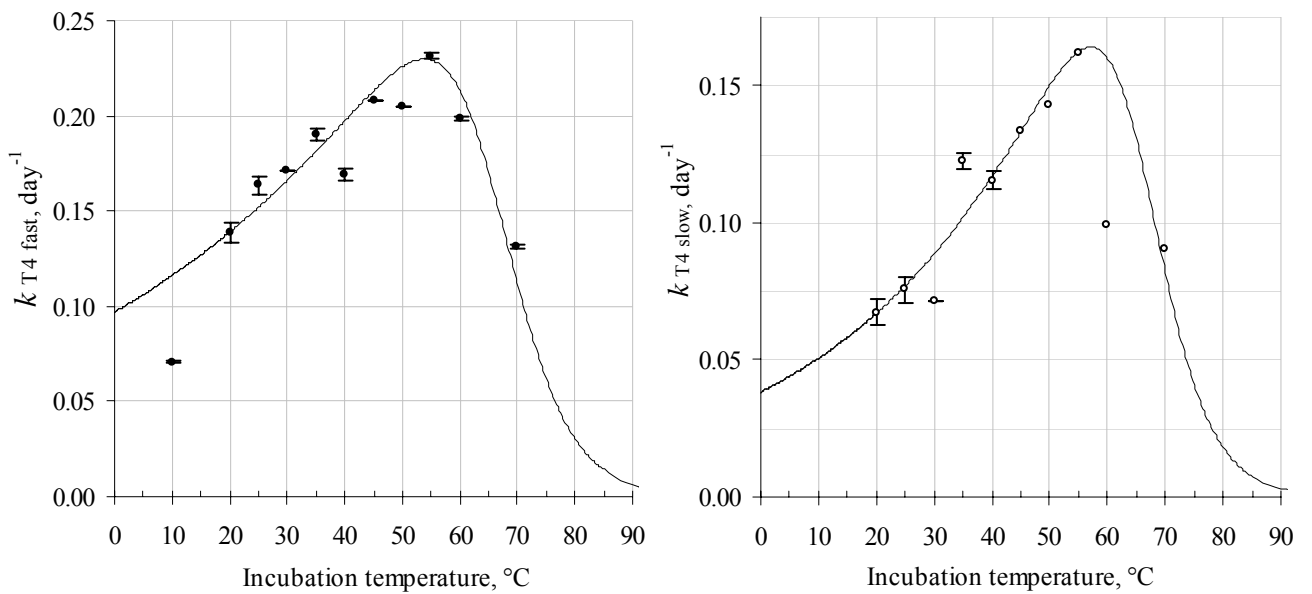


Figure A4.4. The reaction rate coefficients as a function of temperature for the fast (●) and slow (○) stages of M:S ratio of 4:1 based on the equation (4 xviii).

A5. Modelling the composting process

A5.1. Calculation of initial conditions

A5.1.1. Interfacial surface area

The interfacial surface area at the phase boundary was calculated for the three levels of moisture content (MC) and mixing (M:S) ratios, which were simulated in the model's sensitivity analyses. The total solids content of the straw, manure and organic material was 0.9, 0.25 and 0.35, respectively. Table A5.1 gives the total mass of the organic material and the mass of the straw, manure and added water in the 14 kg of dry organic material. The bulk density of the organic material was estimated from values in Table 3.5. The mass of a representative sample of 450 pieces of straw weighed 34 g. The total number of straw pieces in S kg of straw, N, was calculated for each lot of organic material.

Table A5.1. Composition of organic material (14 kg TS) for the three M:S ratios and MC simulated in the model.

MC %	M:S ratio	Bulk weight ω_{bulk} , kg m ⁻³	Total mass M_{TOT} , kg	Straw mass S, kg	Straw pieces N	Manure mass M, kg	Water add W, kg
60	2	155	35	8.8	115 810	17.5	5.0
	3	165	35	7.4	98 260	22.3	1.1
	4	170	35	6.4	85 330	25.8	-1.8
65	2	195	40	10.0	129 040	20.0	10.0
	3	210	40	8.5	117 910	25.5	6.1
	4	220	40	7.4	107 280	29.5	3.2
70	2	210	47	11.7	154 410	23.3	16.7
	3	230	47	9.9	131 020	29.7	12.7
	4	245	47	8.6	113 780	34.4	9.8

A piece of straw had a volume of $4.95 \times 10^{-7} \text{ m}^3$ and a curve surface area of $6.6 \times 10^{-4} \text{ m}^2$, such that the total volume and surface area of the straw were given by:

$$V_S = N \times 4.95 \times 10^{-7} \text{ m}^3 \quad (\text{A5 i})$$

and
$$SA_S = N \times 6.6 \times 10^{-4} \text{ m}^2 \quad (\text{A5 ii})$$

The volume of manure was
$$V_M = \frac{M}{\rho_M} \quad (\text{A5 iii})$$

where ρ_M was the density of manure given in Section 3.3.1. as 1002 kg m^{-3} .

The surface area of the straw that was cover with 0.5mm of manure, SA_M , was given as

$$SA_M = \frac{V_M}{\pi \cdot L(0.002^2 - 0.0015^2)} \cdot 6.6 \times 10^{-4} \text{ m}^2 \quad (\text{A5 iv})$$

The volume of water free in the airspaces was estimated as:

$$V_{WF} = \frac{W(S \times 3 \times 0.9 - S \times 0.1)}{\rho_W} \quad (\text{A5 v})$$

where where ρ_W was the density of water (1000 kg m^{-3}).

The remaining volume was assumed to be air space and was given as:

$$V_A = V_{TOT} - V_M - V_S - V_{WF}. \quad (\text{A5 vi})$$

The number of spherical air spaces (radius, $r_A = 0.005$), N_A , was therefore equal to

$$N_A = \frac{V_A}{\frac{4}{3} \pi \cdot r_A^3} \quad (\text{A5 vii})$$

Assuming that no air spaces touched then total surface area of the air spaces, SA_A , was

$$SA_A = N_A \cdot 4\pi \cdot r_A^2 \quad (\text{A5 viii})$$

The results of the above calculations are given in Table A5.2 for each of the mixing ratios. The negative value for the volume of free water shows that straw was able to absorb more water than was added. There was therefore no free water in the voids of the organic material and air occupied the void space not filled by the manure. The embolded values were the those used as the interfacial surface areas at the phase boundary.

Table A5.2. Estimations of the volumes and surface areas of 14 kgTS of organic material.

MC%	M:S	V _{Tot} , m ³	V _S , m ³	V _M , m ³	V _W , m ³	V _{FW} , m ³	SA _S , m ²	SA _M , m ²	SA _A , m ²
60	2	0.23	0.065	0.020	0.005	-0.021	87	34	72
	3	0.21	0.056	0.025	0.001	-0.021	74	44	65
	4	0.21	0.048	0.029	-0.002	-0.021	64	50	61
65	2	0.21	0.065	0.020	0.010	-0.016	87	34	68
	3	0.19	0.056	0.025	0.006	-0.016	74	44	61
	4	0.18	0.048	0.029	0.003	-0.016	64	50	57
70	2	0.22	0.065	0.020	0.017	-0.009	87	34	72
	3	0.20	0.056	0.025	0.013	-0.009	74	44	65
	4	0.19	0.048	0.029	0.010	-0.009	64	50	60

A5.1.2. Cross sectional area and airflow velocity

It was assumed that the spherical air spaces (voids) were distributed evenly through the organic material such that the maximum number of possible voids in a 1cm length of organic material was determined for the three mixing ratios and moisture contents. The volume of the layer was therefore given as

$$V_{\text{layer}} = \pi \cdot r_{\text{reactor}}^2 \cdot 0.01 \quad (\text{A5 ix})$$

The number of spheres in the layer was a fraction of the total number spheres in the organic material N_s such that

$$n_s = \frac{V_{\text{layer}}}{V_{\text{total}}} \times N_s \quad (\text{A5 x})$$

The corresponding cross sectional area, CSA, was calculated by considering the voids as cylinders of the same volume and height as the sphere. The total cross section area was therefore given as

$$\text{CSA} = \frac{2}{3} \pi \cdot r^2 = 5.24 \times 10^{-5} \text{ m}^2 \quad (\text{A5 xi})$$

where r was the radius of the sphere (0.005m).

The air flow velocity, v_{air} , was calculated by considering the volumetric flow rate of the cooling aeration, 25 l min^{-1} .

$$v_{\text{air}} = \frac{25}{1000 \cdot 60} \times \frac{1}{\text{CSA}} \quad (\text{A5 xii})$$

Table A5.3. Estimation of the mean air velocity in the organic material for cooling aeration.

MC%	M:S	$V_{\text{Tot}}, \text{m}^3$	N_s	n_s	CSA, m^2	$v_{\text{air}} (10^{-3}), \text{m s}^{-1}$
60	2	0.23	228 787	2 862	0.150	2.78
	3	0.21	207 294	2 791	0.144	2.89
	4	0.21	194 840	2 741	0.144	2.89
65	2	0.21	217 320	2 858	0.150	2.78
	3	0.19	194 655	2 766	0.145	2.87
	4	0.18	182 002	2 723	0.143	2.91
70	2	0.22	229 737	3 021	0.158	2.64
	3	0.20	205 241	2 931	0.154	2.71
	4	0.19	191 836	2 901	0.152	2.74

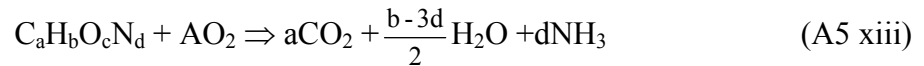
A5.1.3. Gas partition constants

The gas partition constants for the three mixing ratio were calculated by assuming a standard chemical formula for the pig manure and straw.

Chemical formula of manure was based on that for primary sludge: $\text{C}_{22}\text{H}_{39}\text{O}_{10}\text{N}$ (Mr 477)

Chemical formula of straw was based on that for long chain glucose units: $\text{C}_6\text{H}_{10}\text{O}_5$ (Mr 164)

The elemental make up of the mix was represented by $\text{C}_a\text{H}_b\text{O}_c\text{N}_d$ the stoichiometric oxygen demand for aerobic respiration was equal to A in the reaction equation:



For a mix of manure (M) and straw (S) in the wet mass ratio, M:S, the relative molecular mass of the volatile solids fraction of the organic material was given by:

$$\text{Mr}_{\text{VS}} = \frac{\text{M} \cdot \text{TS}_\text{M} \cdot \text{VS}_\text{M}}{\text{M} \cdot \text{TS}_\text{M} \cdot \text{VS}_\text{M} + \text{S} \cdot \text{TS}_\text{S} \cdot \text{VS}_\text{S}} 477 + \frac{\text{S} \cdot \text{TS}_\text{S} \cdot \text{VS}_\text{S}}{\text{M} \cdot \text{TS}_\text{M} \cdot \text{VS}_\text{M} + \text{S} \cdot \text{TS}_\text{S} \cdot \text{VS}_\text{S}} 164 \quad (\text{A5 xiv})$$

The elemental composition of the mix is given by

$$\begin{aligned}
 a &= \frac{22 \cdot M \cdot TS_M \cdot VS_M + 6 \cdot S \cdot TS_S \cdot VS_S}{M \cdot TS_M \cdot VS_M + S \cdot TS_S \cdot VS_S} \\
 b &= \frac{39 \cdot M \cdot TS_M \cdot VS_M + 10 \cdot S \cdot TS_S \cdot VS_S}{M \cdot TS_M \cdot VS_M + S \cdot TS_S \cdot VS_S} \\
 c &= \frac{10 \cdot M \cdot TS_M \cdot VS_M + 5 \cdot S \cdot TS_S \cdot VS_S}{M \cdot TS_M \cdot VS_M + S \cdot TS_S \cdot VS_S} \\
 d &= \frac{1 \cdot M \cdot TS_M \cdot VS_M}{M \cdot TS_M \cdot VS_M + S \cdot TS_S \cdot VS_S}
 \end{aligned}
 \tag{A5 xv}$$

A balance of oxygen molecules gives

$$A = \frac{4a + b - 3d - 2c}{4} \tag{A5 xvi}$$

The decomposition of 1 mol of mix therefore produces of a mol CO₂, $\frac{b-3d}{2}$ mol of water and d mol of ammonia and consumes of A mol of oxygen.

For manure with TS_M = 0.25 and VS_M = 0.82 and for straw with TS_S = 0.90 and VS_S = 0.88, the values from the of a, b, c, d and A and Mr_{MIX} are given in Table A5.4

Table A5.4. Calculated values of A, a, b, c, d and Mr_{VS} of the respective mixing ratios

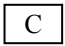

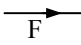



M:S	M kg	S kg	A	a	b	c	D	Mr VS
2:1	20.0	10.0	12.98	11.32	20.97	6.66	0.34	268
3:1	25.5	8.5	14.83	12.84	23.54	7.14	0.43	298
4:1	29.5	7.4	16.23	13.98	25.47	7.49	0.50	320

A5.2. Model implementation in *ModelMaker*

A5.2.1. *ModelMaker* features

The first step of implementing a model in *ModelMaker* was to construct a diagram that was composed of a series of components, each of which represented a particular mathematical function. The basic components of the *ModelMaker* were Compartments, Variables, Parameters and Definitions, Influences and Flows. The symbols and the corresponding functions that described the components are given in Table A5.5.

Table A5.5. The main model components of *ModelMaker* software

Symbol	Component	Equation
	Compartment	$\frac{dC}{dt} = f(y)$
	Initial value	$C_{t=0} = g(D, P)$
	Variable	$V = f(y)$
	Flow	$F = f(y)$
	Influence	None
	Defined value	$D = g(D, P)$
	Parameter	$P = \text{constant}$

$f(y)$ was a function of the component values defined in the model
 $g(D, P)$ was a function of defined values and model parameters

Compartments acted as integrators. The value assigned to the Compartment was calculated by a differential equation and therefore represented a rate of change. Influences and Flows linked components. The Influence represented the transfer of a quantity between Compartments. The Flow was a special model component, which was defined by an equation and the value of which was automatically subtracted from the source Compartment and added to the destination Compartment. Compartment, Flow and Variable components were characterised as conditional or unconditional.

A5.2.2. Constructing and running a *ModelMaker* model

The main window interface of the model software was divided into two panels, the Model explorer and the Model view (Figure A5.1). A number of views were activated in the model using the Main toolbar. The model was created and defined in the Diagram view using the component buttons in the Diagram toolbar. A component could be given 'universal' status, which was indicated by green hatching in the component box. The component symbol could then be referenced by another component in the model without a direct flow or influence connection. The Definition view displayed all of the equations that defined each component. The Parameter view was used to enter and define parameter values of the model equations using the Parameter toolbar, which was displayed only when the Parameter view was active.

The circled GO button on the main toolbar activated the 'Run' window with which the model simulation was started. The duration of the simulation was specified in the 'Stop Value'. The 'Repeated Run' box was activated if a sensitivity analysis was to be carried out on a selected factor. The Advanced button allowed further simulation specifications to be made as well as facilities to configure a sensitivity analysis.

Figure A5.2 shows the 'Run Options' window in which a process factor was selected and the limits defined for the sensitivity analysis. For the three selected initial moisture content (0.60, 0.65, and 0.70) simulations, the number of repeated runs, found under the Repeated Run tab, was specified as 2. The same was done for the initial pH of 6, 7 and 8 and mixing ratios of 2, 3 and 4.

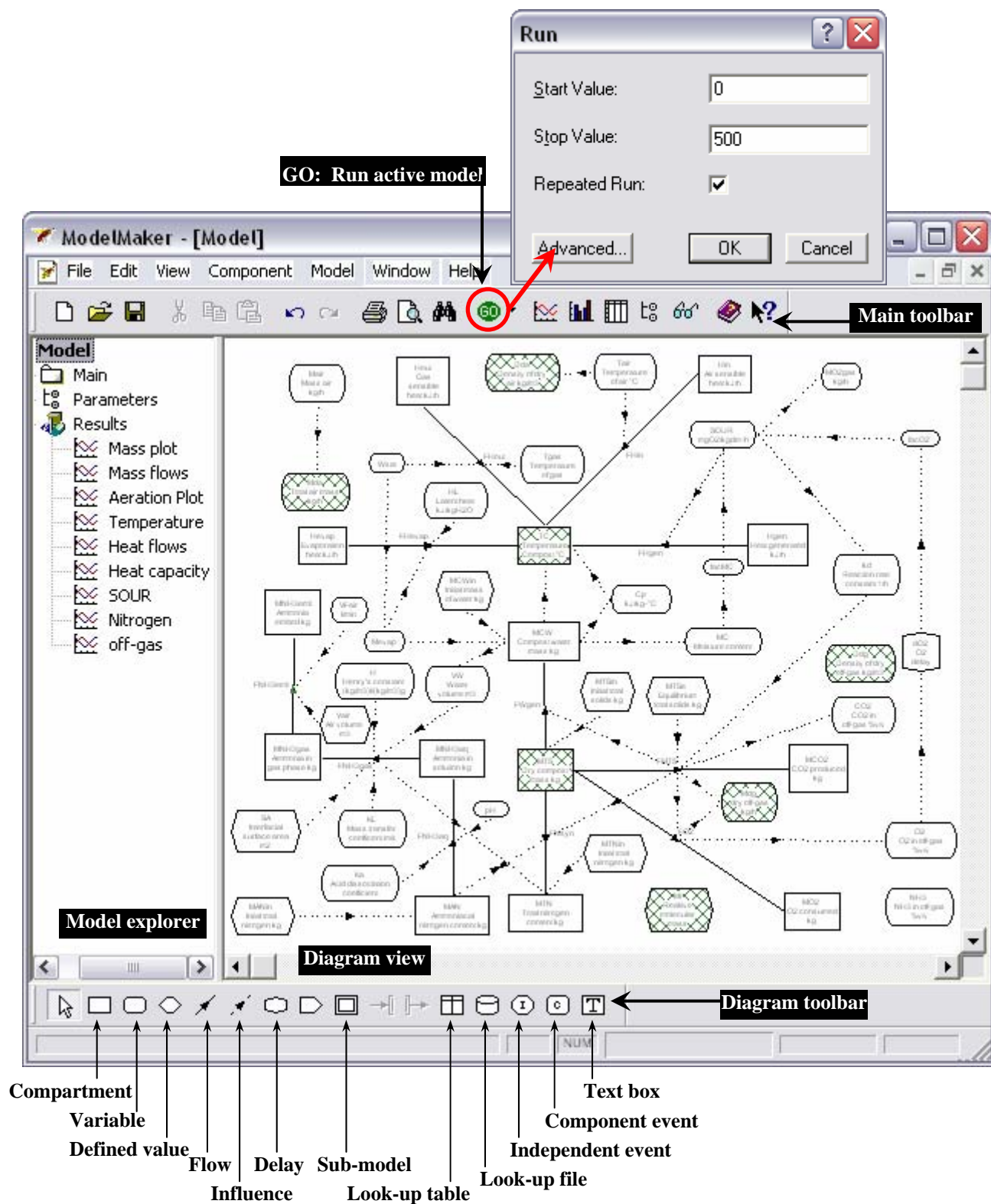


Figure A5.1. Interface display of the *ModelMaker* software

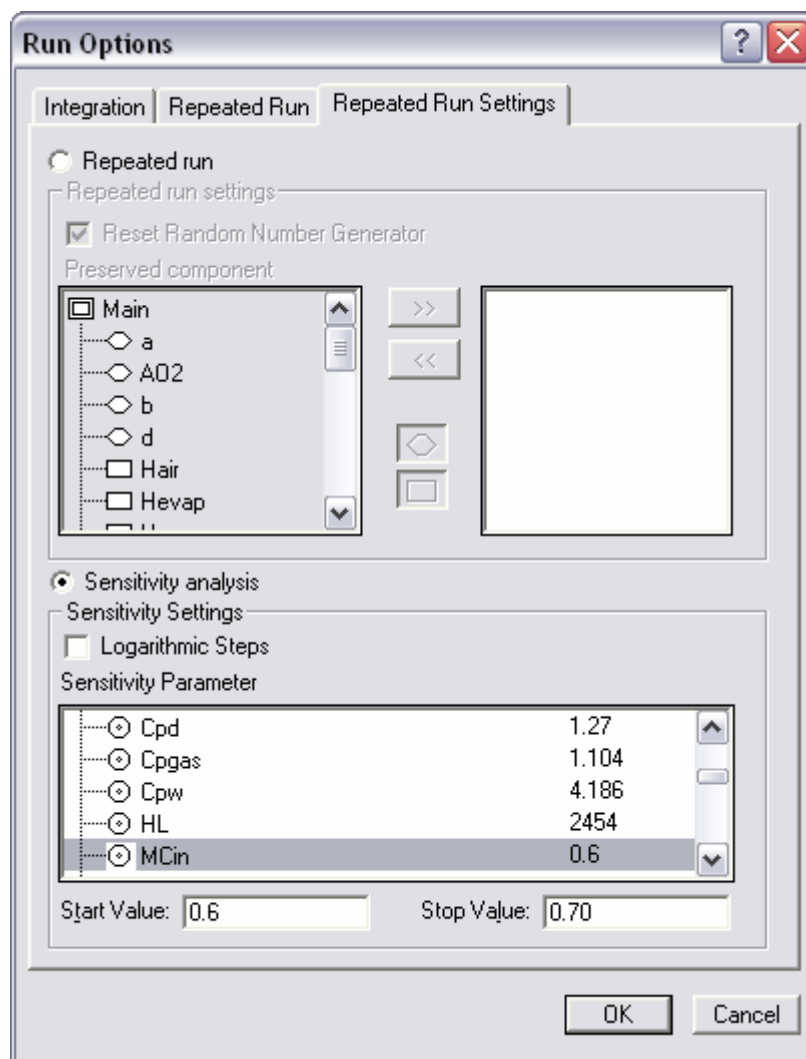


Figure A5.2. Window for setting the sensitivity analysis limits

The results of a model simulation were presented graphically or as a table, which was created using the corresponding buttons on the main toolbar and was displayed in the Results view (Figure A5.3). The outputs of the model were displayed after each time step so that the change in process variables was followed as the simulation proceeded. For a sensitivity analysis, the graphical displays of the result of each simulation were shown on the same view so that the effects of the process factors could be compared directly. The Archive view stored results, so that they were not updated after a subsequent simulation.

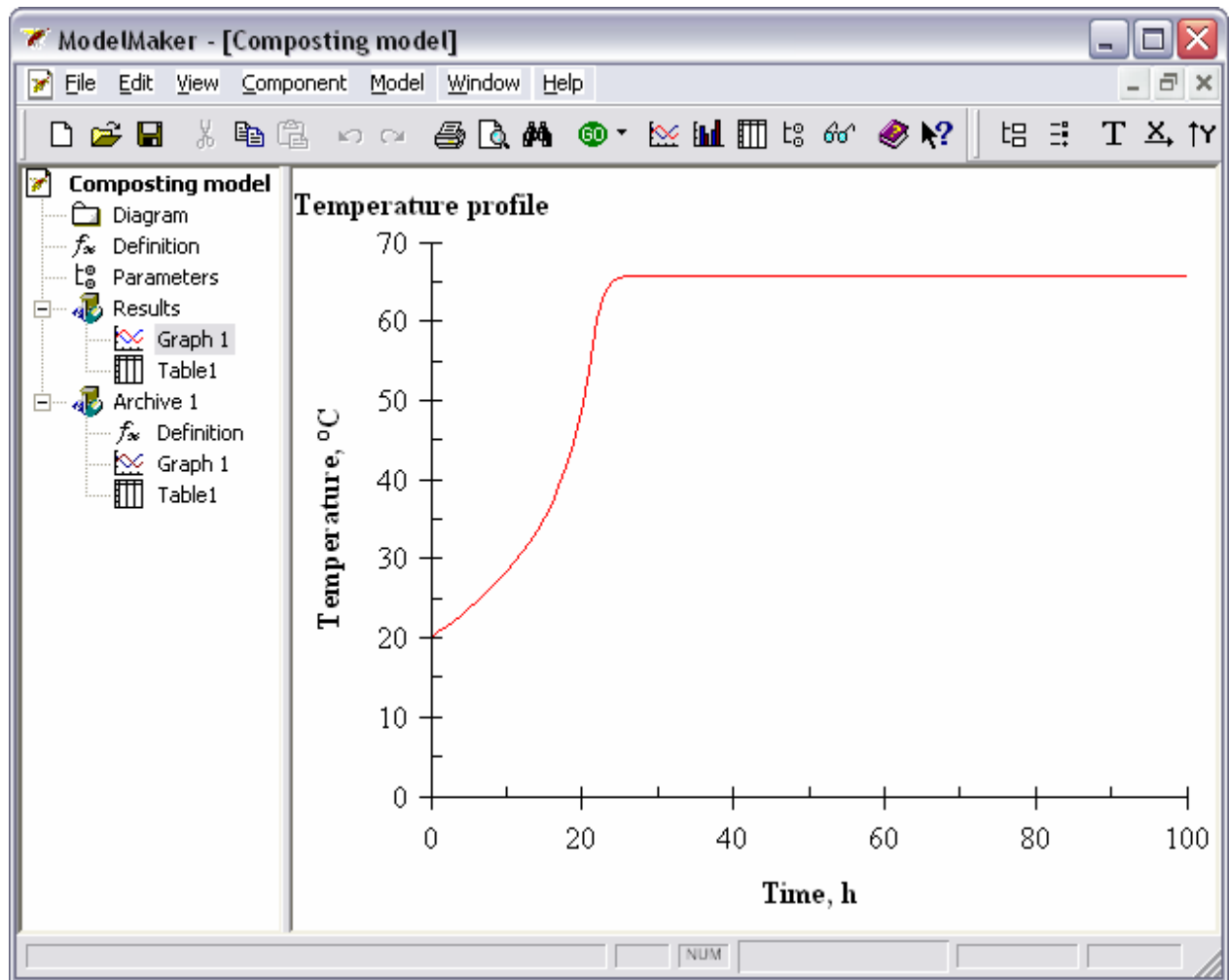


Figure A5.3. Results view of a graphical representation of the temperature profile.

A5.2.3. The composting model in *ModelMaker*

Table A5.6. The default units of the model components

Dimension	Unit	Symbol
Length	Metre	M
Time	Hour	H
Mass	kilogram	kg
Energy	kilojoule	kJ
Pressure	Atmosphere	Atm
Temperature	degrees Celsius	°C

The units used by default for the model components, unless otherwise specified are given in Table A5.6. The time period was in hours and all rate terms were therefore expressed on an hourly basis. The output points of the model simulations were recorded every hour, as was done for the temperature of the organic material in the composting experiments. This allowed for relatively easy comparison between the model and experimental data. Table A5.7 lists the symbols that are used to implement the composting model in *ModelMaker*.

A5.2.3.1. Mass model

The Compartment component of *ModelMaker* is a powerful tool. The decomposition of organic material could be simulated in a single Compartment with reference to the necessary parameter inputs. The equation (5 vi) was defined in the model by the compartment MTS.

MTS

The outcome of the simulation of the decomposition of M kg wet organic material with a total solids content TS run at a constant hourly reaction rate for time, t_e , which was the period needed to reach equilibrium, was typical of a decay curve (Figure A5.4).

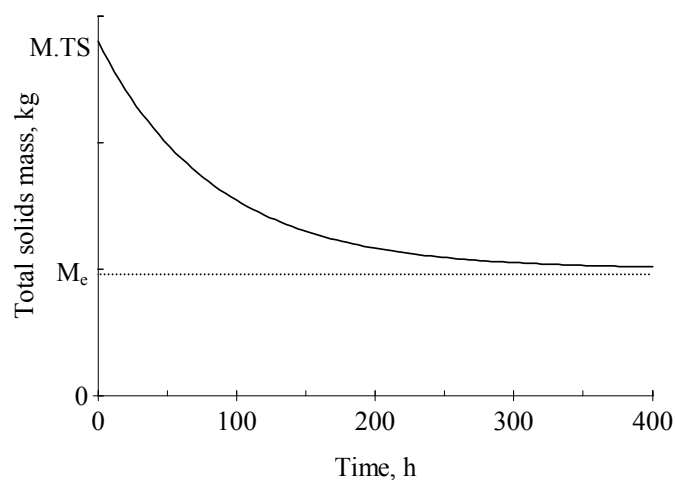


Figure A5.4. Decomposition of organic material at a constant reaction rate.

Table A5.7. Symbols used in *ModelMaker* to describe the composting model

Symbol	Description	Units
AO2	Stoichiometric oxygen coefficient	$\text{kg kg}_{\text{VS}}^{-1}$
a, b, c and d	Stoichiometric partition coefficients	$\text{kg kg}_{\text{VS}}^{-1}$
CO2	Carbon dioxide in off-gas	$\% \text{ v v}^{-1}$
Cp	Specific heat capacity of the organic material	$\text{kJ kg}^{-1} \text{ }^{\circ}\text{C}^{-1}$
Cpda	Specific heat capacity of dry air	$\text{kJ kg}^{-1} \text{ }^{\circ}\text{C}^{-1}$
CpTS	Specific heat capacity of the dry organic material	$\text{kJ kg}^{-1} \text{ }^{\circ}\text{C}^{-1}$
Cpw	Specific heat capacity of water	$\text{kJ kg}^{-1} \text{ }^{\circ}\text{C}^{-1}$
Cpwvap	Specific heat capacity of water vapour	$\text{kJ kg}^{-1} \text{ }^{\circ}\text{C}^{-1}$
Dda	Density of dry air	kg m^{-3}
Ddg	Density of dry off-gas	kg m^{-3}
Dwvap	Density of water vapour	kg m^{-3}
facMC	Moisture content factor	-
facO2	Oxygen factor	-
FHgen	Flow of heat generated	kJ h^{-1}
FHgas	Flow of sensible heat in the off-gas	kJ h^{-1}
FHair	Flow of sensible heat in the air	kJ h^{-1}
FHevap	Flow of heat due to evaporation of water	kJ h^{-1}
FMTS	Flow of total solids	kg h^{-1}
FNH3emit	Flow of ammonia gas emissions	kg h^{-1}
FNH3aq	Flow of total solids	kg h^{-1}
FNH3gas	Flow of ammonia into the gas phase	kg h^{-1}
FNsyn	Flow of nitrogen synthesis into biomass	kg h^{-1}
FO2	Flow of oxygen	kg h^{-1}
FWgen	Flow of water generated	kg h^{-1}
H	Henry's coefficient	$\frac{(\text{kg m}^{-3})_{\text{liq}}}{(\text{kg m}^{-3})_{\text{gas}}}$
Hair	Heat content of the air	kJ
Hevap	Heat used to evaporate water	kJ
Hgas	Heat content of the gas	kJ
Hgen	Heat generated	kJ
HL	Latent heat of evaporation of water	$\text{kJ kg}^{-1} \text{H}_2\text{O}_{\text{evap}}$
Ka	Acid dissociation coefficient	kg m^{-3}
kh	Reaction rate coefficient	h^{-1}
KL	Overall mass transfer coefficient	m s^{-1}

Table A5.7. *continued*

Symbol	Description	Units
Mair	Mass of air	kg
MAN	Mass of ammoniacal nitrogen in the organic material	kg
MANin	Initial mass of ammoniacal nitrogen	kg
MC	Moisture content of the organic material	kg kg ⁻¹
MCO2	Mass of carbon dioxide (cumulative)	kg
Mda	Mass of dry air	kg
Mdg	Mass of dry off-gas	kg
Mevap	Mass of water evaporated	kg
MNH3aq	Mass of ammonia at the phase boundary in the liquid phase	kg
MNH3emit	Mass of ammonia emitted (cumulative)	kg
MNH3gas	Mass of ammonia at the phase boundary in the gas phase	kg
MO2	Mass of oxygen (cumulative)	kg
MON	Mass of organic nitrogen in the organic material	kg
Mr	Relative molecular mass of organic material	kg kg-mol ⁻¹
MTN	Mass of total nitrogen in the organic material	kg
MTS	Mass of total solids	kg
MTSin	Initial mass of total solids	kg
MTSe	Equilibrium mass of total solids	kg
MW	Mass of water in the organic material	kg
MWin	Initial mass of water in the organic material	kg
NH3	Ammonia in the off-gas	% v v ⁻¹
O2	Oxygen in off-gas	% v v ⁻¹
pH	pH of the organic material	-
S	Degree of saturation	-
SA	Interfacial surface area of the organic material	m ²
SOUR	Specific oxygen uptake rate	gO ₂ kg _{TS} ⁻¹ h ⁻¹
SOUR20	Specific oxygen uptake rate at 20°C	gO ₂ kg _{TS} ⁻¹ h ⁻¹
t	Time	h
TC	Composting temperature	°C
VFCA	Volumetric flow rate of baseline aeration	l min ⁻¹
VFBA	Volumetric flow rate of cooling aeration	l min ⁻¹
VW	Volume of water in the organic material	m ³
Vair	Volume of air in the voids of the organic material	m ³
VFair	Volumetric flow rate of air through the organic material	m ³ h ⁻¹
WBA	Water content of baseline aeration	kg kg ⁻¹ dry air
WCA	Water content cooling aeration	kg kg ⁻¹ dry air
Wsat	Water content of saturated air	kg kg ⁻¹ dry air

The reaction rate coefficient, k_h , in equation (5 vi) was represented in the model as the Variable component ‘kh’ and was calculated from the quotient of the SOUR, also a variable, and the COD. The COD was a Parameter value and was therefore not shown in the model layout, part of which is depicted by Figure A5.5. The SOUR was described as:

$$\text{SOUR} = \text{facMC} \cdot \text{facO2} \cdot \text{facpH} \cdot \text{SOUR}_{20} \frac{e^{0.07(\text{TC}-20)}}{e^{0.36(\text{TC}-66)} + 1} \quad (\text{A5 xvii})$$

SOUR_{20} was the empirically determined value of the SOUR at 20 °C and TC was the temperature of the composting organic material. The Variable components facMC and facO2 were defined by equation (5 ix) and (5 x), respectively.

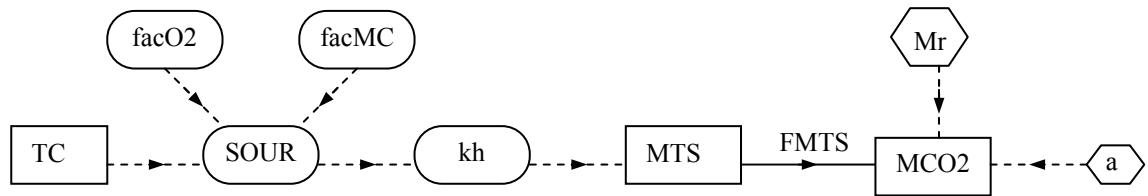


Figure A5.5. Process kinetics as represented by the model component.

The Defined value component, Mr, was the relative molecular mass of the degradable fraction of organic material and ‘a’ was the partition coefficient particular to carbon dioxide, which related the stoichiometric mass produce to the decomposition of the organic material (Section A5.1.2). The cumulative mass of the carbon dioxide produced was evaluated in the Compartment MCO2. The Flow, FMTS, was defined by the term on the right side of equation (5 vi) and the MTS Compartment was defined as

$$\text{MTS} = -\text{FMTS} \quad (\text{A5 xviii})$$

For the water balance, the mass of water in the organic material (MW) was calculated from the initial mass of water (MWin), the mass generated by microbial activity as a by-product of aerobic respiration and the water lost from the system in the gas phase, Mevap.

The stoichiometric mass of water generated was related to the decomposition of organic material by the partition coefficients, 'b' and 'd', the values of which are given in Table A5.1.

The Flow describing the mass of water generated, FWgen, was defined as

$$FW_{gen} = \frac{FMTS}{Mr} \cdot \frac{1}{2}(b - 3d) \cdot Mr_{H_2O} \quad (A5 \text{ xix})$$

Mr_{H_2O} was the relative molecular mass of water (18).

Figure A5.6 shows the water balance as represented in the model. The water balance centred on the MW Compartment, defined by equation (A5 xx), and was integrated with respect to time, t. The MWin, as calculated from the initial moisture content.

$$\frac{dMW}{dt} = FW_{gen} - \frac{dMevap}{dt} \quad (A5 \text{ xx})$$

The mass of water evaporated was the balance between the mass of water to saturate the off-gas, Wsat, and the mass of water in the air entering the system.

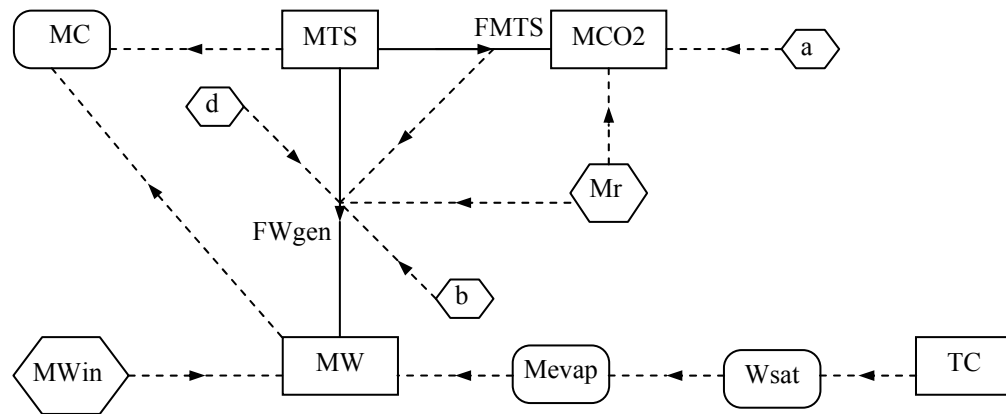


Figure A5.6. Water balance model as represented by the model components.

The cumulative mass of carbon dioxide produced and oxygen consumed during the decomposition of the organic material was evaluated in the Compartment components MCO2 and MO2, respectively (Figure A5.6). The stoichiometric mass of oxygen consumed, as calculated by the Flow FO2, was related to FMTS by the partition coefficient A, the

calculation and value of which is given Section A5.1.2. In Figure A5.6, the Variables CO2 and O2 represent the percentage of the gas in the off-gas at one iteration on a dry volume basis. The mass of dry off-gas, MDG, was defined by equation (5 xxii), which, in the model, was represented as

$$MDG = MDA - FO_2 + a \frac{FMTS}{Mr} + FNH_3emit \quad (A5 \text{ xxi})$$

MDA was the mass of dry air flowing into the system, $kg \text{ h}^{-1}$, which was determine by the aeration strategy. FNH_3emit was the mass flow of ammonia leaving the system in the off-gas and is defined in Section A5.2.2.3.

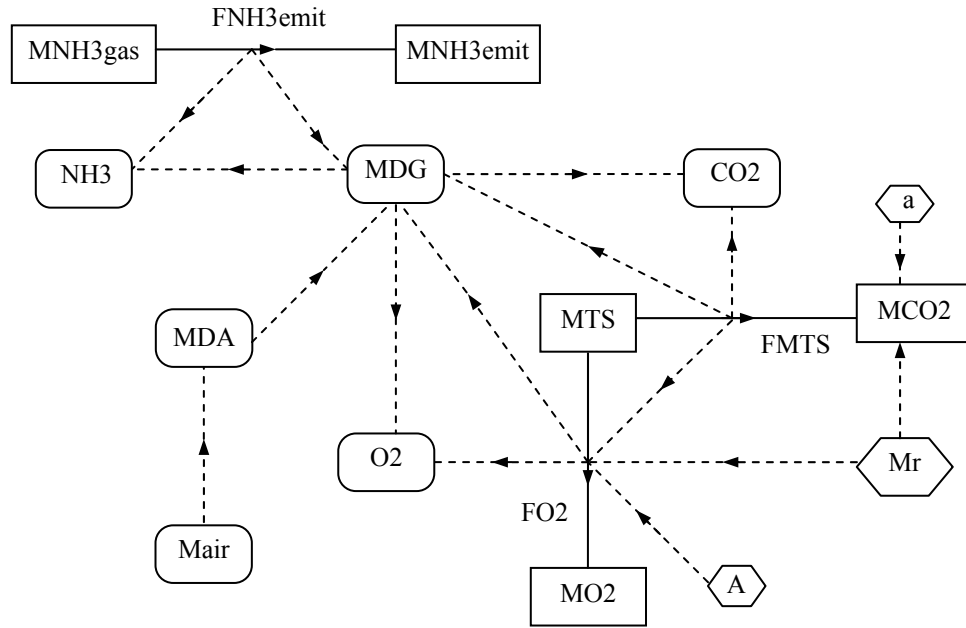


Figure A5.7. Gas phase calculation of the mass model as represented in the model.

The mass of air, M_{air} , and MDA was represented in the model by a conditional Variable component because the aeration used depended on the temperature of the organic material. The conditions of the airflows therefore read

$$\text{For } T \leq 60 \quad M_{air} = VFBA \frac{60}{1000} \cdot \frac{D_{da} + WBA \cdot D_{wvap}}{1 + WBA} \quad \text{and} \quad MDA = \frac{M_{air}}{(1 + WBA)} \quad (A5 \text{ xxii})$$

$$\text{For } T > 60 \quad \text{Mair} = \text{VFCA} \cdot \frac{60}{1000} \cdot \frac{\text{Dda} + \text{WCA} \cdot \text{Cwvap}}{1 + \text{WCA}} \quad \text{and} \quad \text{MDA} = \frac{\text{Mair}}{(1 + \text{WCA})} \quad (\text{A5 xxiii})$$

VFBA and VFCA were the volumetric flow rates of the baseline and cooling aeration, respectively (l min^{-1}). Dda was the density of dry air and Dwvap the density of water vapour (kg m^{-3}). WBA and WCA were the water contents of the baseline and cooling aeration (kg kg^{-1} dry air), respectively. The values were defined in Table A5.4 and, in the model, in the Parameter view of *ModelMaker*. The other terms in the equation (A5 xxii) and (A5 xxiii) converted the volumetric flow rates from l min^{-1} to mass flow rates in kg h^{-1} .

A5.2.3.2. Energy model

The net energy gain in the system was a balance between the heat generated by microbial activity (Hgen) and that removed by evaporation (Hevap) and sensible heating of the air (Hgas – Hair) flowing through the organic material. The temperature of the organic material was calculated from the net heat gain and evaluated in the Compartment TC, where

$$\text{TC} = \frac{\text{FHgen} + \text{FHair} - \text{FHgas} - \text{FHevap}}{(\text{MW} + \text{MTS}) \cdot \text{Cp}} \quad (\text{A5 xxiv})$$

The Flows were defined by equations (5 xxv), (5 xxvii), (5 xxviii) and (5 xxxix), respectively.

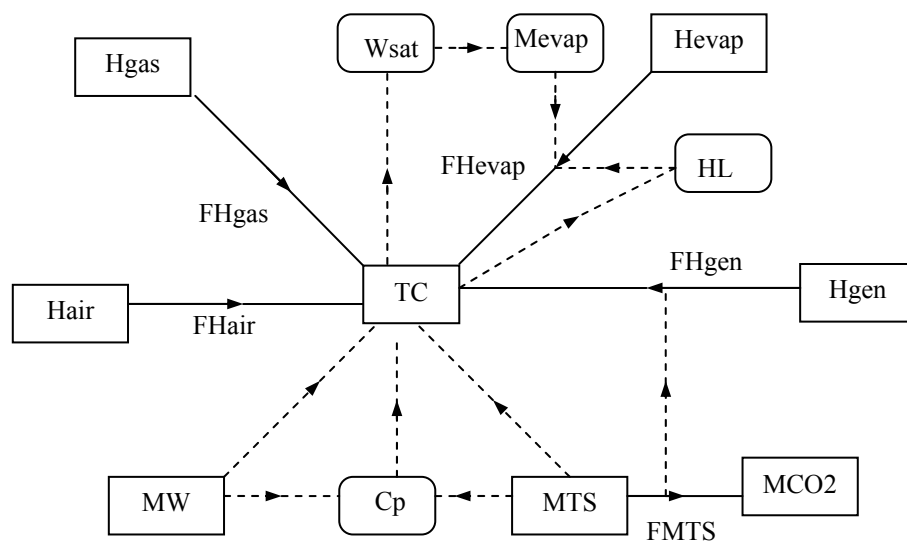


Figure A5.8. Energy model as represented by model components.

The specific heat capacity of the wet organic material, C_p , was calculated at each iteration and was determined from the mass of water and total solids in the organic material and the respective heat capacities and was therefore represented in the model by a Variable component (Figure A5.8). The latent heat variable, HL , was described by equation (5 xxx) and depended on the temperature of the organic material.

A5.2.3.3. Ammonia emission model

The ammonia model was represented in the main model as shown in Figure A5.9.

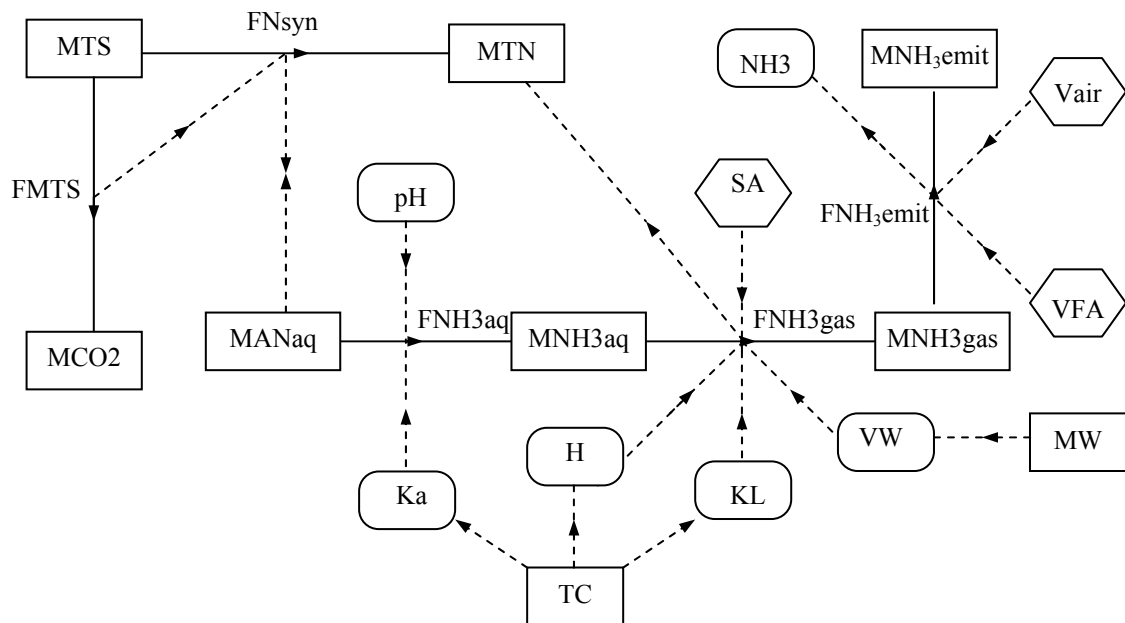


Figure A5.9. Ammonia emissions model as represented by model components

As the organic material decomposed, biomass was synthesised, as equation (5 xLvi) described. This consumed some of the ammoniacal nitrogen in the organic material, MAN_{aq} , and was represented by the Flow, FN_{syn} . The Flow had conditional status, which stated that when the ammoniacal nitrogen in the organic material was exhausted, then biomass synthesis ceased even though the decomposition of organic material continued. The nitrogen assimilated into biomass was assumed to be stable and unavailable for further conversion back into ammoniacal nitrogen. The mass of organic nitrogen therefore increased whilst the

ammoniacal nitrogen decreased with time, be that due to ammonia emissions or the formation of new biomass. The nitrogen in the new biomass contributed to the total nitrogen content of the organic material, MTN, and the MTN compartment was defined as

$$MTN = FN_{syn} - \frac{14}{17} FNH3_{gas} \quad (A5 \text{ xxv})$$

and the MANaq compartment was defined as

$$MAN_{aq} = -FN_{syn} - \frac{14}{17} FNH3_{aq} \quad (A5 \text{ xxvi})$$

FNH3aq represented the equilibrium reaction between the associated and free ammonia in the manure as described by the first term on the right hand side of equation (5 xxxvii) and therefore depended on the pH and ammonia acid dissociation constant, Ka, of the system. FNH3gas was the flow of ammonia across the liquid-gas phase boundary, which was determined by the Henry's constant, H, the liquid phase mass transfer coefficient, KL, the interfacial surface area, SA and the volume of water in the liquid phase, VW. VW was calculated from the mass of water in the organic material, MW. Ka, H and KL were represented by Variable components as all depended on the temperature of the organic material, TC and were update at each iteration.

The MNH3aq compartment evaluated the mass of ammonia in the liquid phase as a balance between that formed (FNH3aq) and that lost to the gas phase (FNH3gas). MNH3gas was the mass of gas at the boundary in the gas phase and was given by equation (5 xxxix). This was represented in the model as a Compartment by

$$MNH3_{gas} = FNH3_{gas} - FNH3_{emit} \quad (A5 \text{ xxvii})$$

MNH3emit compartment calculated the cumulative mass of ammonia emitted and was equal to FNH3emit, which was defined by equation (5 xxxviii). VFA represented the volumetric flow rate of air (m³ h⁻¹). The volume of air in the organic material, Vair, was defined by the

A5.2.3.5. Definition model view

The definitions of the model components were expressed in *ModelMaker* as follows:

Define value: a Unconditional

$$a = 12.84$$

Define value: AO2 Unconditional

$$AO2 = 14.83$$

Define value: b Unconditional

$$b = 23.54$$

Define value: COD Unconditional

$$COD = 415 \text{ g O}_2 \text{ kg}^{-1} \text{ TS}$$

Define value: d Unconditional

$$d = 0.43$$

Define value: Kain Unconditional

Initial acid dissociation coefficient kg/m3

$$Kain = 17/1000 * (10^{-(0.0918 + 2730/(TCin + 273))})/6$$

Define value: MANin Unconditional

Initial mass of ammoniacal nitrogen kg

$$MANin =$$

$$ANM^{17/14} * MTSin * TSM * mix / (mix * TSM + TSS) + ANS^{17/14} * MTSin * TSS / (mix * TSM + TSS)$$

Define value: Mr Conditional Universal

Relative molecular mass of volatile solids

$$Mr = 320 \text{ for } mix=4$$

$$= 298 \text{ for } mix=3$$

$$= 268 \text{ for } mix=2 \text{ by default}$$

Define value: MTSe Unconditional

Equilibrium mass kg

$$MTSe = MTSin * TSS / (mix * TSM + TSS) * VSS * (1 - BS) \\ + MTSin * mix * TSM / (mix * TSM + TSS) * VSM * (1 - BM)$$

Define value: MTNin Unconditional

Initial total nitrogen kg

$$MTN_{in} = TNM \cdot TSM \cdot MTS_{in} \cdot Mix / (Mix \cdot TSM + TSS) + TNS \cdot MTS_{in} \cdot TSS / (Mix \cdot TSM + TSS)$$

Define value: MWin Unconditional

Initial mass of water kg

$$MWin = MC_{in} \cdot MTS_0 / (1 - MC_{in})$$

Define value: SA Conditional

Phase boundary surface area m²

$$SA = 50 \text{ for } mix = 4$$

$$= 44 \text{ for } mix = 3$$

$$= 34 \text{ for } mix = 2$$

Variable: CO2 Conditional

CO2 in the off-gas % v/v

$$CO2 = 18.15 \text{ for } 0.04/100 \cdot Mda/Dda + FMTS \cdot a/Mr \cdot 22.4 \cdot (273 + TC)/273 > 18.15$$

$$CO2 = (0.04/100 \cdot Mda/Dda + FMTS \cdot a/Mr \cdot 22.4 \cdot (273 + TC)/273) / Mda \cdot Ddg \cdot 100 \text{ default}$$

Variable: Cp Unconditional

Specific heat capacity kJ/kg-°C

$$Cp = ((Cpd \cdot MTS) + (Cpw \cdot MW)) / (MTS + MW)$$

Variable: Dda Unconditional

Density of dry air, kg/m³

$$Dda = 101.3 / (0.287 \cdot (T_{air} + 273))$$

Variable: Ddg Unconditional

Density of dry gas, kg/m³

$$Ddg = 101.3 / (0.287 \cdot (TC + 273))$$

Variable: facMC Unconditional

$$facMC = 1 / (\exp(-17.684 \cdot MC + 7.622) + 1)$$

Variable: facO2 Conditional

$$facO2 = 0 \text{ for } dO2 < 0$$

$$= dO2 / (dO2 + 2) \cdot (20.96 + 2) / 20.96 \text{ by default}$$

Variable: H Unconditional

Henry's constant for NH₃ (kg/m³)_{aq}/(kg/m³)_{gas}

$$H = 1384 * 1.053^{(-TC)}$$

Variable: HL Unconditional

Latent heat of evaporation kJ/kgH₂O

$$HL = -2.38 * TC + 2501$$

Variable: Ka Unconditional

Acid dissociation coefficient kg/m³

$$Ka = 17/1000 * (10^{-(0.0918 + 2730/(TC + 273))})/6$$

Variable: kh Unconditional

Reaction rate constant 1/h

$$kh = (SOUR/(1000 * COD))$$

Variable: KL Unconditional

Mass transfer coefficient liquid phase m/h

$$KL = 2.79 * 10^{-8} * \exp(3.94/100 * TC)$$

Variable: Mair Conditional

Total air mass kg/h

$$\begin{aligned} Mair &= VFCA * (Dda + WCA * Dwvap) * 60/1000 / (1 + WCA) \text{ for } TC > 60 \\ &= VFBA * (Dda + WBA * Dwvap) * 60/1000 / (1 + WBA) \text{ by default} \end{aligned}$$

Variable: MC Unconditional

Moisture content

$$MC = MCW / (MCW + MTS)$$

Variable: Mda Conditional Universal

Dry air mass kg/h

$$\begin{aligned} Mda &= Mair / (1 + WCA) \text{ for } TC > 60 \\ &= Mair / (1 + WBA) \text{ by default} \end{aligned}$$

Variable: Mdg Unconditional

Dry off-gas mass, kg/h

$$Mdg = Mda + FTS * 44 / Mr * a - FO_2 + F_{NH_3 \text{emit}}$$

Variable: Mevap Conditional

Mass of water evaporated to saturate the incoming air, kg kg⁻¹ dry air

Mevap = Wsat*Mdg-WCA*Mda for TC>60
= Wsat*Mdg-WBA*Mda by default

Variable: MTN Unconditional

Total nitrogen content kg

MTN = MON+MAN

Variable: NH3 Unconditional

NH3 in off-gas %v/v

NH3 = FNH3gas/17*22.4*(273+TC)/273/Mda*Dda*100

Variable: O2 Conditional

O2 in off-gas %v/v

O2=0 for 20.96/100*Mda/Dda<FO2/32*(22.4*(273+TC)/273)

O2 = (20.96/100*Mda/Dda-FO2/32*22.4*(273+TC)/273)/(Mdg/Ddg)*100 default

Variable: pH Conditional

pH of the organic material

pH = 7.5 for t > 336

= -t/96+11 for t > 192

= 9 for t > 48

= t/48*(9-pHin)+pHin by default

Variable: S Conditional

Degree of saturation

S = 0.1+0.9*exp(-Psi*VFCA) for TC>60

= 0.1+0.9*exp(-Psi*VFBA) by default

Variable: SOUR Unconditional

mgO2/kgdm-h

SOUR = facO2*facMC*(SOUR20*(exp(0.07*(TC-20)))/(exp(0.36*(TC-66))+1))

Variable: Tair Conditional

Temperature of air °C

Tair = 20°C for TC>60°C

= 40°C by default

Variable: Tgas Unconditional

Temperature of gas °C

$T_{\text{gas}} = TC$

Variable: Vair Unconditional

Volume of air in organic material m³

$V_{\text{air}} = (SA/3)*4*10^{-3}$

Variable: VFair Conditional

Volumetric airflow rate m³/h

$V_{\text{Fair}} = VFCA*60/1000$ for $TC > 60$
 $= VFBA*60/1000$ by default

Variable: VW Unconditional

Volume of water m³

$VW = MCW/980$

Variable: Wsat Unconditional

Water content of saturated gas, kg kg⁻¹ dry air

$W_{\text{sat}} = 0.0044*\exp(0.0594*TC)$

Delay: dO2

Oxygen factor delay

Delay = 1

Initial Value = 20.96

Maximum Delay = 1

Flow: FHair Conditional

Flow from Hair to TC

$F_{\text{Hair}} = M_{\text{da}}*(C_{\text{pda}}+W70*C_{\text{pwvap}})*T_{\text{air}}$ for $TC > 60^{\circ}\text{C}$
 $= M_{\text{da}}*(C_{\text{pda}}+W50*C_{\text{pwvap}})*T_{\text{air}}$ by default

Flow: FHevap Unconditional

Flow from Hevap to TC

$F_{\text{Hevap}} = M_{\text{evap}}*HL$

Flow: FHgas Conditional

Flow from Hgas to TC

$$\begin{aligned} \text{FHgas} &= \text{Mdg} * (\text{Cpdg} + \text{Wsat} * \text{Cpwwap}) * \text{Tgas} \text{ for TC} > 60^{\circ}\text{C} \\ &= \text{Mdg} * (\text{Cpdg} + \text{Wsat} * \text{Cpwwap}) * \text{Tgas} \text{ by default} \end{aligned}$$

Flow: FHgen Unconditional

Flow from Hgen to TC

$$\text{FHgen} = 14.5 * \text{SOUR} / 1000 * \text{MTS}$$

Flow: FMTS Unconditional Universal

Flow from MTS to MCO2

$$\text{FMTS} = \text{kh} * (\text{MTS} - \text{MTS_E})$$

Flow: FNH3aq Unconditional

Flow from MANaq to MNH3aq

$$\text{FNH3aq} = 17/14 * \text{MANaq} * \text{Ka} / (\text{Ka} + 10^{-\text{dpH}})$$

Flow: FNH3emit Unconditional

Flow from MNH3gas to MNH3emit

$$\text{FNH3emit} = \text{MNH3gas} / \text{Vair} * \text{VFair}$$

Flow: FNH3gas Unconditional

Flow from MNH3aq to MNH3gas

$$\text{FNH3gas} = \text{MNH3aq} / \text{VW} * 1 / \text{H} * \text{KL} * \text{SA}$$

Flow: FNsyl Unconditional

Flow from MTS to MTN

$$\text{FNsyl} = \text{Cell_Y} * \text{FMTS} * \text{Cell_N}$$

Flow: FO2 Unconditional

Flow from MTS to MO2

$$\text{FO2} = \text{FMTS} / \text{Mr} * \text{AO2} * 32$$

Flow: FWgen Unconditional

Flow from MTS to MW

$$\text{FWgen} = \text{FMTS} / \text{Mr} * (\text{b} - 3 * \text{d}) / 2 * 18$$

Compartment: Hair Unconditional

Air heat kJ/h

$$\text{dHair}/\text{dt} = -\text{FHair}$$

Initial Value = 0.0

Compartment: Hevap Unconditional

Evaporation heat kJ/h

$$d\text{Hevap}/dt = -F\text{Hevap}$$

Initial Value = 0.0

Compartment: Hgas Unconditional

Off-gas heat kJ/h

$$d\text{Hgas}/dt = -F\text{Hgas}$$

Initial Value = 0.0

Compartment: Hgen Unconditional

Heat generated kJ/h

$$d\text{Hgen}/dt = -F\text{Hgen}$$

Initial Value = 0.0

Compartment: MAN Unconditional

Mass ammonia in solution kg

$$d\text{MAN}/dt = -14/17 * F\text{NH3aq} - F\text{Nsyn}$$

Initial Value = MANin

Compartment: MCO2 Unconditional

Total mass CO2 produced, kg

$$d\text{MCO2}/dt = +F\text{MTS}/M_r * 44 * a$$

Initial Value = 0.0

Compartment: MNH3aq Unconditional

Mass ammonia in liquid phase at the phase boundary kg

$$d\text{MNH3aq}/dt = +F\text{NH3aq} - F\text{NH3gas}$$

Initial Value = 0.0

Compartment: MNH3emit Unconditional

Mass of ammonia emitted kg

$$d\text{MNH3emit}/dt = +F\text{NH3emit}$$

Initial Value = 0.0

Compartment: MNH3gas Unconditional

Mass of ammonia at the gas phase at the phase boundary kg

$$d\text{MNH}_3\text{gas}/dt = \text{FNH}_3\text{gas} - \text{FNH}_3\text{emit}$$

Initial Value = 0.0

Compartment: MO2 Unconditional

Total Mass O2 consumed, kg

$$d\text{MO}_2/dt = +\text{FO}_2$$

Initial Value = 0.0

Compartment: MON Unconditional

Total nitrogen content kg

$$d\text{MON}/dt = +\text{FN}_{\text{syn}}$$

Initial Value = $\text{MTN}_{\text{in}} - \text{MAN}_{\text{in}}$

Compartment: MTS Conditional Universal

Dry compost mass kg

$$d\text{MTS}/dt = -\text{FMTS} \text{ by default}$$

Initial Value = MTS_{in}

Compartment: MW Unconditional

Water Mass, kg

$$d\text{MW}/dt = +\text{FW}_{\text{gen}} - \text{Mevap}$$

Initial Value = MWin

Compartment: TC Unconditional Universal

Temperature of composting organic material, °C

$$d\text{TC}/dt = (-\text{FHevap} + \text{FH}_{\text{gen}} + \text{FH}_{\text{in}} - \text{FH}_{\text{out}}) / (\text{Cp} * (\text{MCW} + \text{MTS}))$$

Initial Value = TC_{in}

A5.2.4. Model logic

The model algorithm is depicted by the flow chart of Figure A5.10. To begin with, the model calculated the initial conditions of the system, in the Define value components, from the model parameters. The model proceeded by time steps, which were calculated from the set total run time of the simulation and number of output points. In this implementation of the model, an output was given every hour.

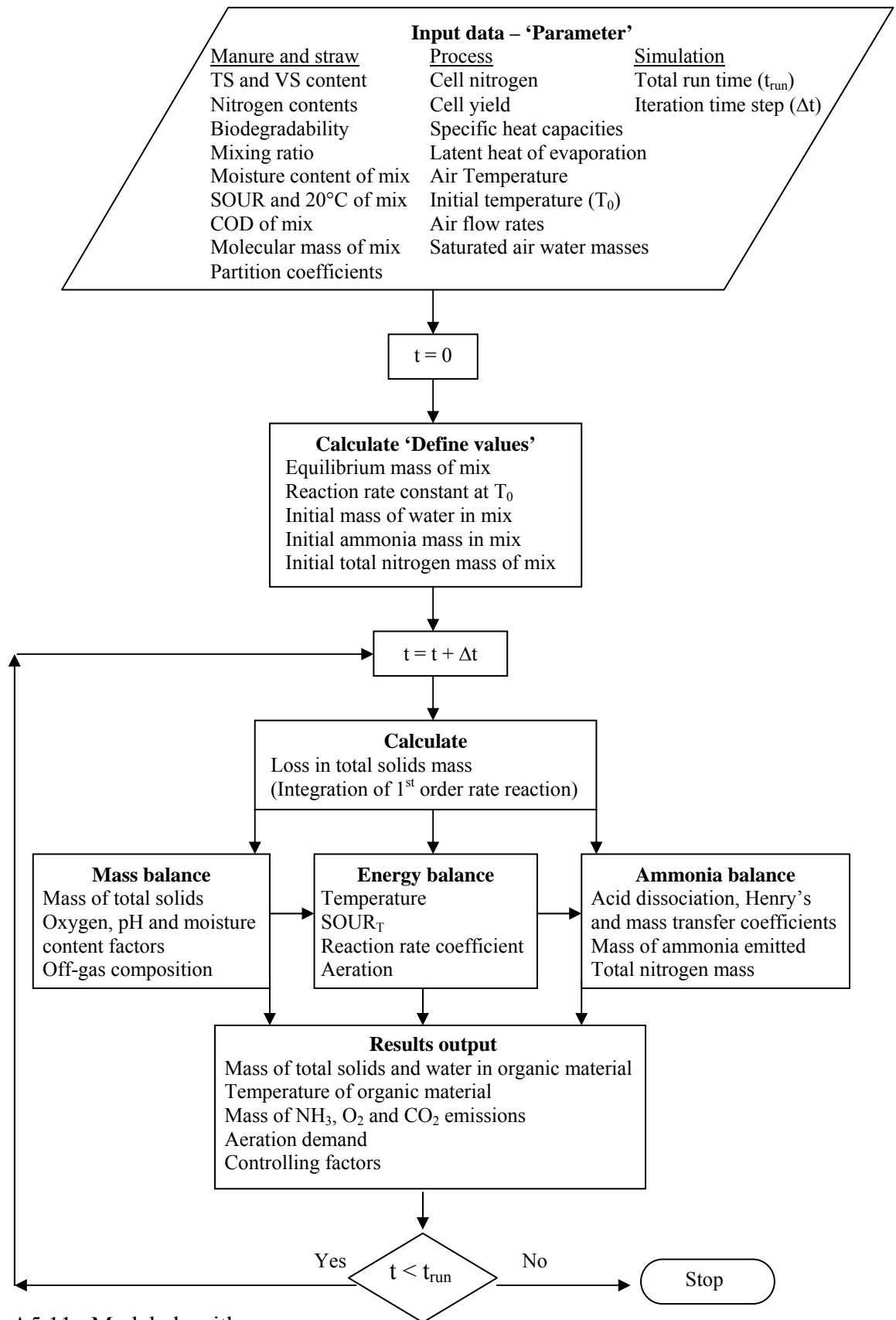


Figure A5.11. Model algorithm.

The first step of the simulation involved the integration of the first order reaction rate equation, which described the loss of total solids in the organic material. From the loss in total solids, the mass and energy balances were carried out. The new reaction rate coefficient was computed using the new specific oxygen uptake rate (SOUR), oxygen and moisture content factors and temperature. The new value of k_h was then used in the next time step to calculate the loss in total solids mass. The SOUR connected the mass model and the energy model by controlling the heat generated at each iteration, which in turn partly determined of the temperature of the organic material for the next iteration.

The ammonia model used temperature, loss in total solids and the moisture content in the calculation of ammonia emissions and total nitrogen content and was carried out concurrently with the energy and mass models. The recalculation of process variables continued until the time reached the set simulation run time at which point the simulation stopped.

A6. Experimental investigation of composting factors

Table A6.1. The complete experimental design required for blocked two-way ANOVA

	Reactor 1	Reactor 2	Reactor 3
Trial 1	pH 8 <u>C:N 20</u>	pH 7 <u>C:N 20</u>	pH 6 <u>C:N 20</u>
Trial 2	pH 6 <u>C:N 25</u>	pH 8 <u>C:N 25</u>	pH 7 <u>C:N 25</u>
Trial 3	pH 7 <u>C:N 15</u>	pH 6 <u>C:N 15</u>	pH 8 <u>C:N 15</u>
Trial 4	pH 7 <u>C:N 20</u>	pH 6 <u>C:N 20</u>	pH 8 <u>C:N 20</u>
Trial 5	pH 8 <u>C:N 25</u>	pH 7 <u>C:N 25</u>	pH 6 <u>C:N 25</u>
Trial 6	pH 6 <u>C:N 15</u>	pH 8 <u>C:N 15</u>	pH 7 <u>C:N 15</u>
Trial 7	pH 6 <u>C:N 20</u>	pH 8 <u>C:N 20</u>	pH 7 <u>C:N 20</u>
Trial 8	pH 7 <u>C:N 25</u>	pH 6 <u>C:N 25</u>	pH 8 <u>C:N 25</u>
Trial 9	pH 8 <u>C:N 15</u>	pH 7 <u>C:N 15</u>	pH 6 <u>C:N 15</u>

A6.1. A detailed analysis of the composting experiments

The results of the composting experiments are presented by Trial in Section A6.1 to Section A6.6. Each section is in two parts. In the first, the composting process is described by the temporal changes of the process variables. The ambient and composting temperature, which was measured at points 1 (Top), 2 (Centre), 3 (Base) and 4 (Side) in the organic material (Figure 3.1), are plotted along side the total ammonia emissions and the cooling aeration profiles. Where possible, the profiles of the total mass of carbon dioxide produced and oxygen consumed, the concentrations of the gases in the off-gas and the corresponding respiratory quotient, the off-gas saturation and the pH of the organic material are included. The second part considers the results from the microbial, chemical and physical analysis of the organic material before and after composting. In both parts, the results are presented in order of increasing initial pH.

A6.1.1. Trial 1 (C:N ratio 20)

In Trial 1 the initial mixing ratio of the organic material was 3, which corresponded to an initial C:N ratio of 20. The organic material with an initial pH of 6, 7 and 8 was composted in Reactor 3, 2 and 1, respectively.

A6.1.1.1. Process analysis

Figures A6.1 to A6.3 show the profiles of the process variables of R3-6-20, R2-7-20 and R1-8-20, respectively. The pH of the organic material during composting was not measured.

Initially, the temperature of organic material rose rapidly, reaching 60 °C on day 2 and 1 in R2-7-20 and R1-8-20, respectively. In R3-6-20, the increase in temperature slowed after day 1 and it only reached 60 °C on day 8. The organic material was held about 60 °C in R3-6-20 and R2-7-20 almost without the need for cooling aeration. In R1-8-20 composting proceeded at about 65 °C instead of the intended 60 °C. The fact that the cooling aeration was not in constant demand suggests that the thermocouple, which measured the centre temperature of the organic material for the aeration control system, was in a cooler part of the organic material than the thermistors, which measured the temperature of the organic material for the data logger.

The side temperatures closely followed the centre temperature. The slight increase in the radial temperature difference after day 9 in the R3-6-20 and R2-7-20 occurred because the organic material between the support wheels slumped a little and the side thermistors were exposed. The respective radial temperature differences in R3-6-20, R2-7-20 and R1-8-20 were ≤ 1 °C for only 21 %, 42 % and 42 % but ≤ 3 °C for 100 %, 92 % and 98 % of the hourly recorded temperatures. The vertical temperature difference across the organic material was less than 10 °C except when the cooling aeration was operating, which lead to a notable drop in the base temperature.

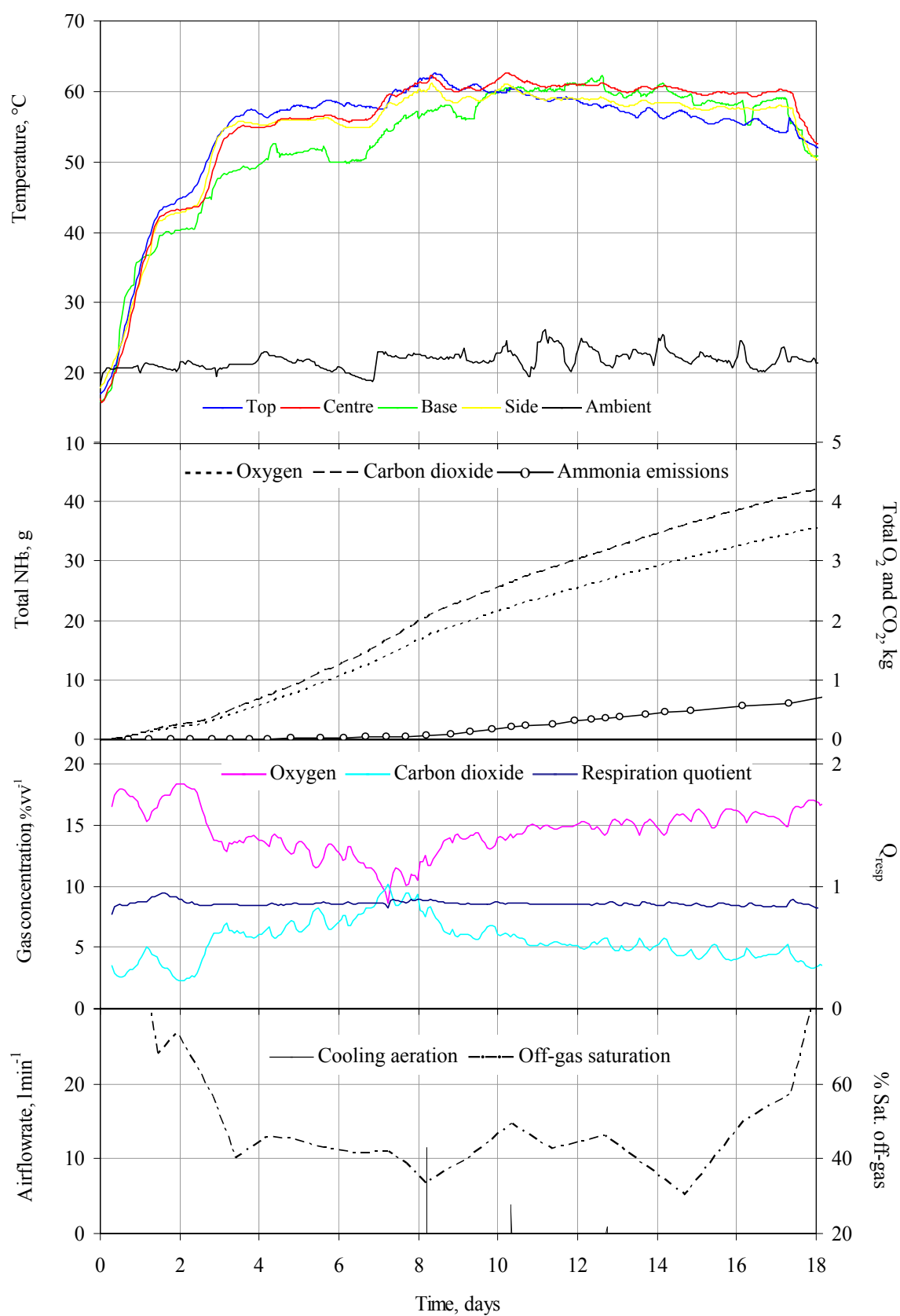


Figure A6.1. Profiles of the process variables for the experiment R3-6-20.

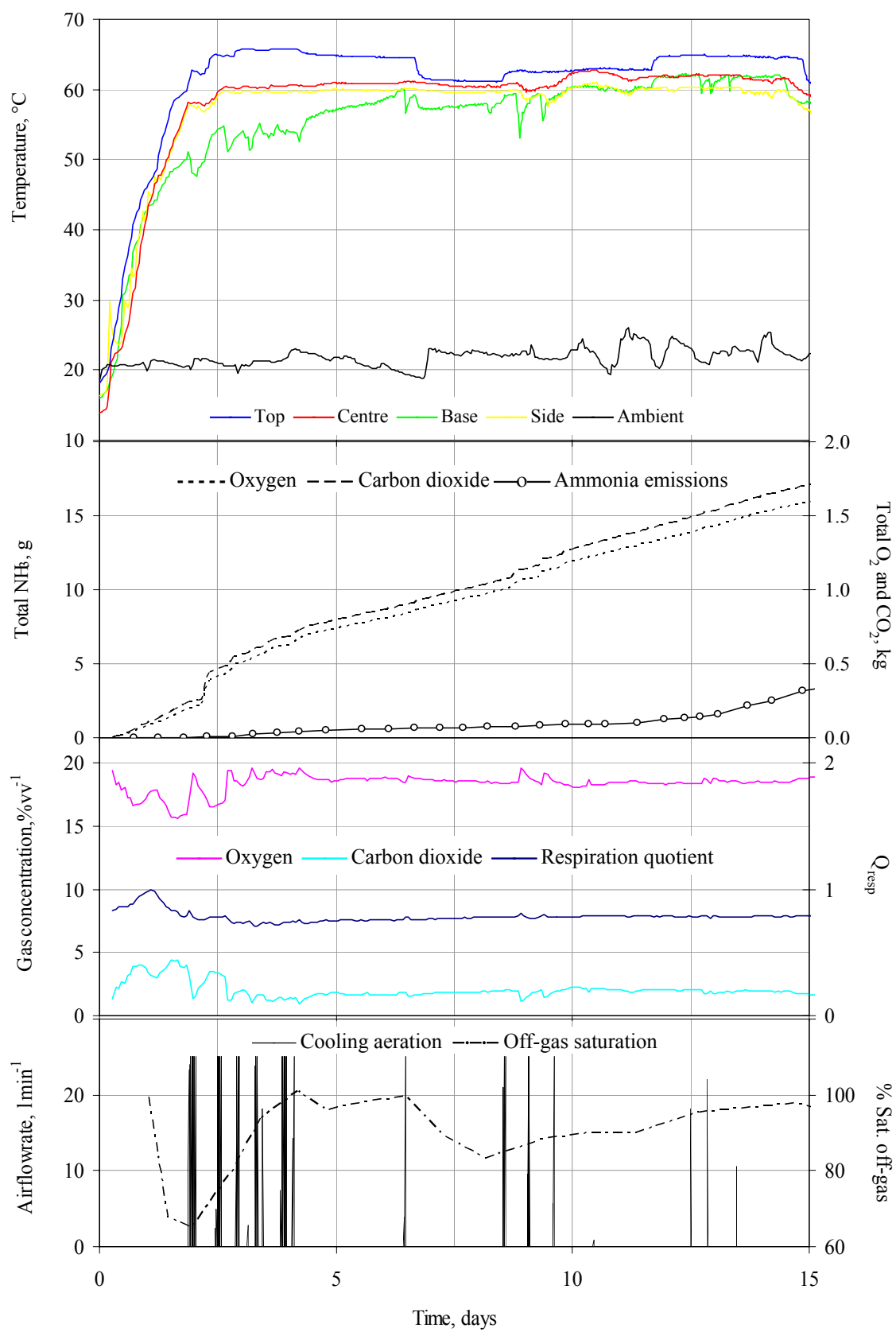


Figure A6.2. Profiles of process variables for experiment R2-7-20

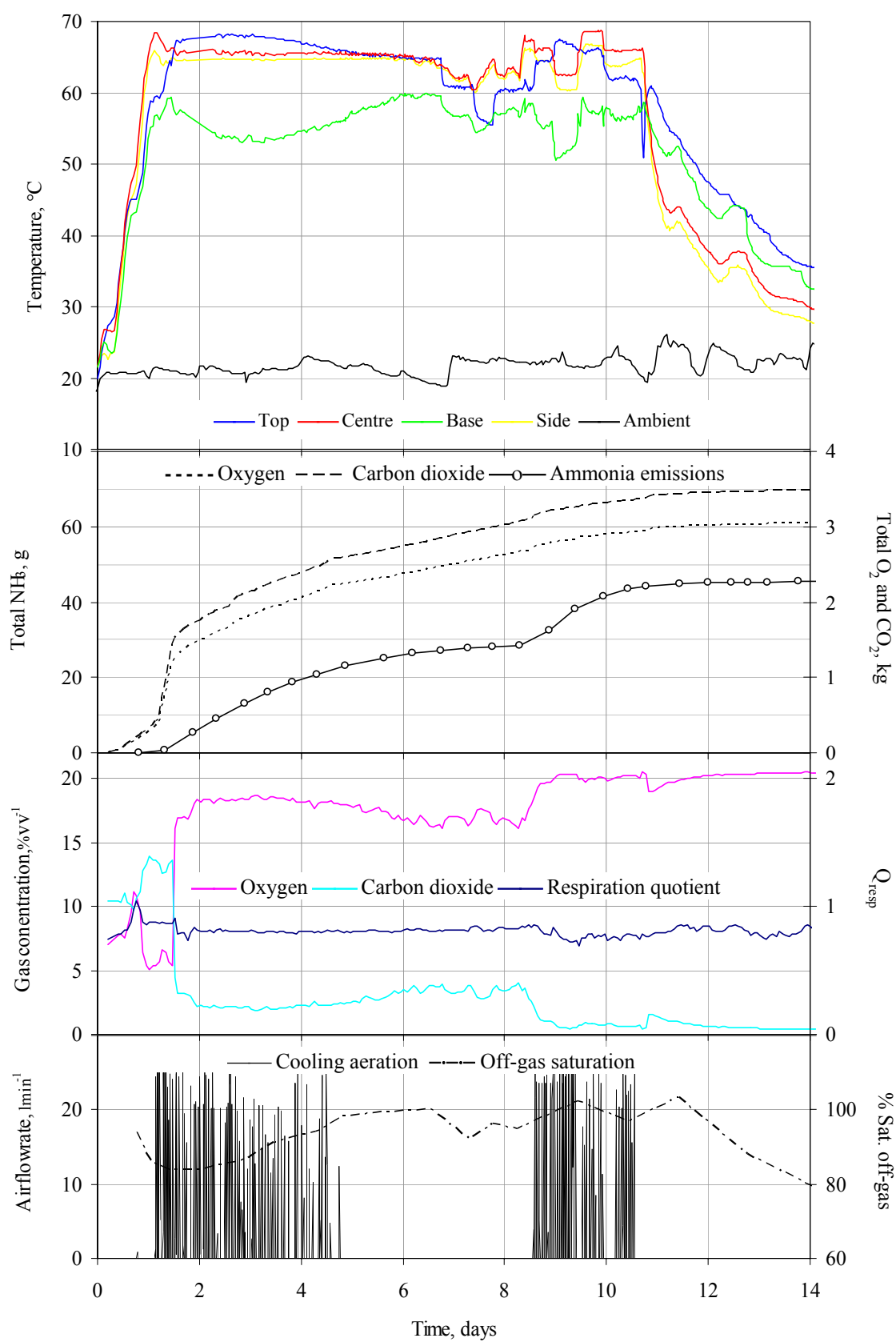


Figure A6.3. Profiles of process variables for experiment R1-8-20.

The sudden and sharp fall in temperature around day 11 in R1-8-20 was probably caused by the organic material drying out, after the second period of cooling aeration, to such an extent that microbial activity was limited.

The gas concentration profiles of R3-6-20 and R1-8-20 in particular were characteristic of the temperature feedback aeration control strategy used [Fraser and Lau 2000]. During the initial rise in temperature when microbial activity was rapid and only the baseline aeration was operating, the oxygen concentration in the off-gas decreased to a minimum. On reaching the upper temperature limit, the cooling aeration was activated and the oxygen replenished.

Ammonia emissions were very low (<1 g) in R3-6-20 and R2-7-20 compared with those from R1-8-20, which were appreciable after day 1, rising rapidly again after day 9 during the second burst of cooling aeration. The airflow may have significantly affected the ammonia emissions.

A6.1.1.2. Analysis of organic material

Initially, the intention was to stop the composting experiments when the organic material cooled to a temperature close to ambient, as occurred in R1-8-20, and to unload the reactors at the same time. However, after the initial appreciable but short-lived drop in temperature on day 17 and 14 in R3-6-20 and R2-7-20, respectively, composting actively continued for longer than the time shown in Figures A6.3 and A6.4. The organic material was only unloaded from R3-6-20 and R2-7-20 after 40 days, although the temperatures were still appreciable higher than ambient, because of the uncertainty of how long composting would continue for and the limited time available for carrying out all the composting experiments. The intense stage of composting, which lasted for about the first two weeks, was of most interest in these composting experiments because ammonia emissions and pathogen

inactivation usually took place within this time. The first 14 days or so are therefore shown in the graphs but the analysis of the organic material before and after composting takes into account its full residence time in the reactor.

Table A6.8 summarises the microbial, physical and chemical analysis of the organic material in each reactor before and after composting. The Top, Mid and Base indicate the areas in the organic material from which samples were collected when unloading i.e. top, middle and base sections, respectively. The percentage losses in the total, total solids (TS), volatile solids (VS) and water mass in the organic material are given in Table A6.2. The organic material from R3-6-20 had lost more than twice the TS and VS mass than that from R2-7-20 and R1-8-20. In R3-6-20 and R2-7-20, composting continued under similar thermal conditions for the same length of time (40 days), so that the obvious difference in the TS loss points to the addition of the acid to lower the initial pH of the organic material. The 66 % loss of water from R1-8-20 confirms that composting ended prematurely because the moisture content (40 %) drop too low to sustain microbial activity.

Table A6.2. Mass changes in the organic material with a C:N ratio of 20 in Trial 1

T1 C:N =20		Total mass, kg		TS mass, kg		VS mass, kg		Total	TS loss	Water	VS loss
Reactor	pH	Initial	Final	Initial	Final	Initial	Final	loss %	%TS	loss %	%TS
R 3	6	40.0	23.2	14.7	11.0	12.9	8.9	42	25	52	31
R 2	7	40.1	29.3	15.5	13.9	13.8	12.0	27	10	37	13
R 1	8	40.0	21.9	14.6	13.2	12.8	11.4	45	10	66	11

The infinity symbols in the general microbial analysis (Table A6.8) indicate that the colonies were too numerous and indistinguishable to count, even at the higher dilutions. The temperature of the organic material in all three reactors was held above 55 °C for more than the three consecutive days. No pathogen markers colonies were detected in the composted organic material from R1-8-20. However, colonies were detected in the composted organic

material from R3-6-20 and R2-7-20. The coliform count was 3×10^6 CFU g⁻¹ TS in the top section of the composting organic material from R3-6-20 and above 4×10^6 CFU g⁻¹ TS and 1×10^6 CFU g⁻¹ TS, respectively, in the top and middle sections of the composted organic material from R2-7-20, values which were much higher than the acceptable concentration of 1×10^3 CFU g⁻¹ TS for coliforms in composted material [PAS 100 2002]. It was not possible to say whether pathogen inactivation did not take place during the first 14 days or whether re-growth of pathogenic populations occurred when the temperature dropped below 55 °C. The temperature profiles of R3-6-20 and R2-7-20 over the 40 days are shown in Figure A6.4 and A6.5, respectively. The conditions after day 30 and 25 in R3-6-20 and R2-7-20, respectively, correspond to the stage of composting when re-growth of bacterial pathogenic population can occur (Figure 2.1).

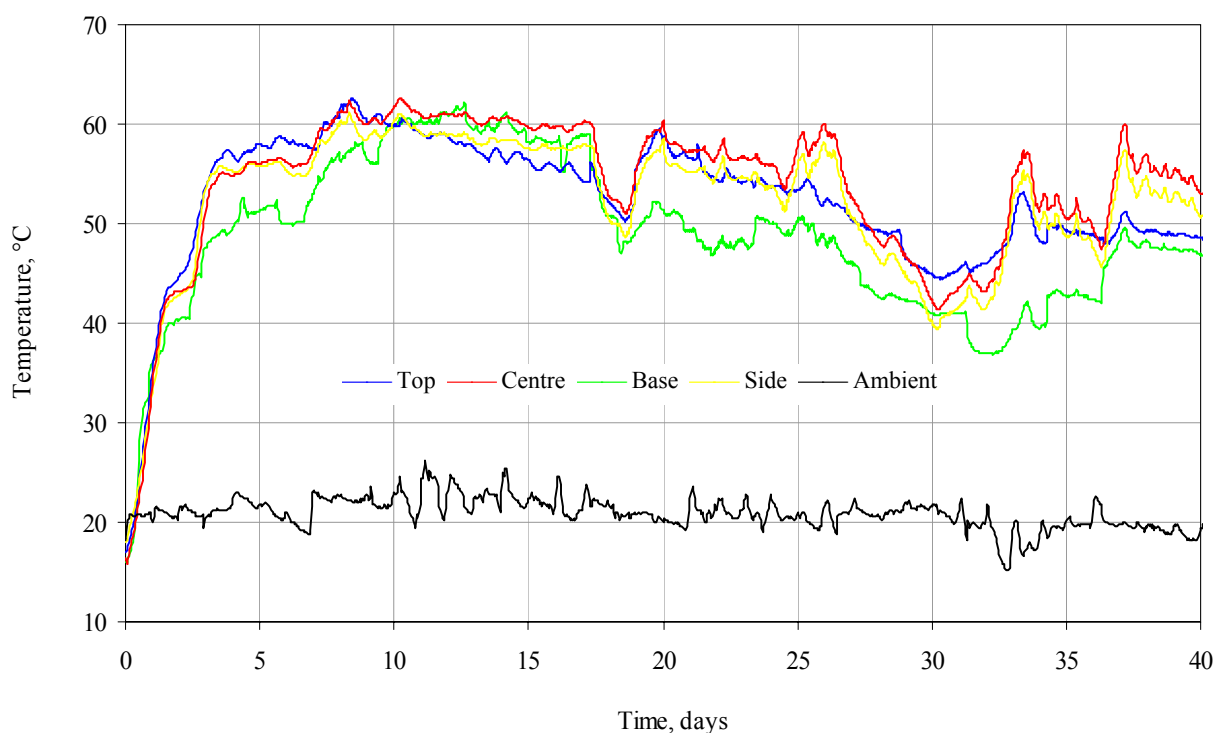


Figure A6.4. The 40 day temperature profiles of R3-6-20 in Trial 1

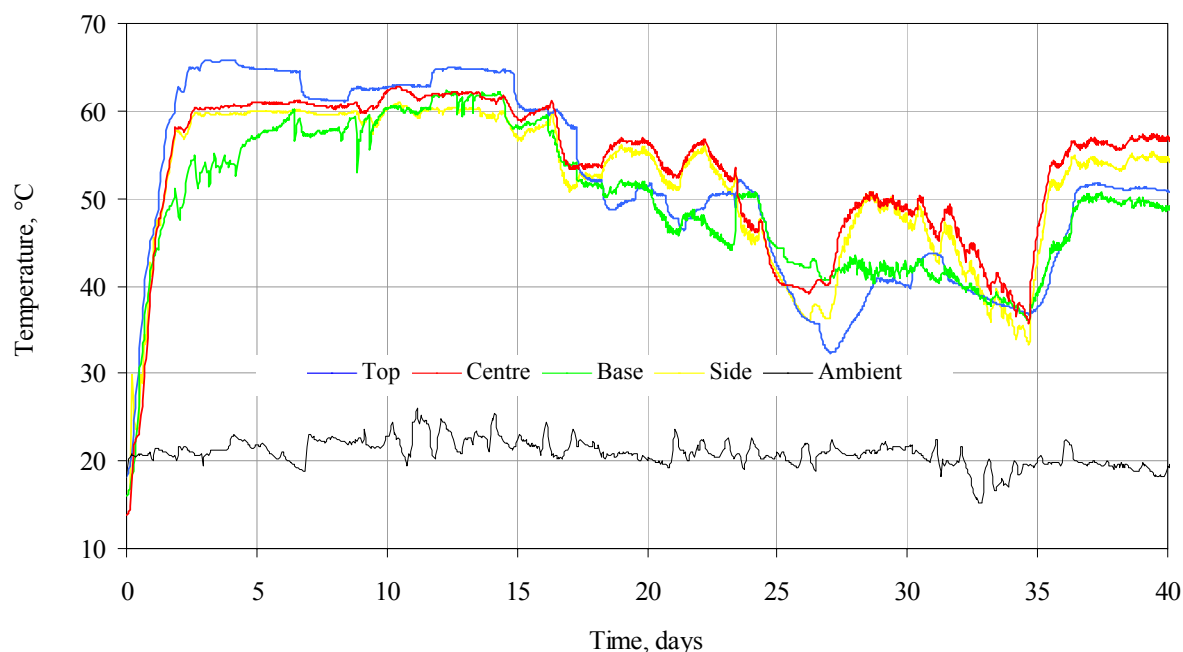


Figure A6.5. The 40 day temperature profile of T1-R2-7

Figure A6.21 shows the typical appearance of the composted organic material in the reactor just before unloading. The white matter was fungal growth, which if the organic material dried out, became dusty and sporiferous and was unpleasant to handle. The top surface of the composted organic material unloaded from R3-6-20 was damp and covered with white fungal growth. Otherwise, the top section and the core through the organic material were drier, a light reddish brown colour, relatively soft texture and sweet smelling (no noxious odours or ammonia gas). The base section and sides of the organic material were relatively wet and dark brown with some white fungal growth. The composted organic material unloaded from R2-7-20 was damp, light brown, soft in texture, and also sweet smelling. The lower layers of the base section were dry and sporiferous. The composted organic material unloaded from R1-8-20 was a uniformly dry and dark brown. The top surface was covered in white growth. The lower layer of the base section was very dry and sporiferous. There was a smell of ammonia gas as the composted organic material was unloaded.

The percentage water loss in the organic material (Table A6.2) reflected the dryness observed in the composted organic material. The top surface and sides of the organic material in R3-6-20 and R2-7-20 were wetter than the core because, when the experiments were stopped and the heating mats were turned off, the organic material was still relatively warm and the water vapour in the head space condensed on the inside surface of the lid before the lid was cool enough to remove. The difference in the appearance and texture of the composted organic material of R1-8-20 from that of R3-6-20 and R2-7-20 may have been due to the acid added or the longer composting time.

Almost 90 % of the initial mass of total nitrogen (TN) in the organic material was retained in R3-6-20 and about 80 % in R2-7-20 and R1-8-20. The mass of ammoniacal nitrogen (AN) in organic material increased, more than doubling in that from R1-8-20.

The measured initial pH of the organic material was lower than was intended in all three experiments (Table A6.8). The initial dry pH measurement of R3-6-20 was a low 4.4. The pH increased, irrespective of the initial pH, to final values mostly falling between 7 and 8, with the higher end of the range being most recurrent.

A6.1.2. Trial 2 (C:N ratio 25)

In Trial 2, the initial mixing ratio of the organic material was 2, which corresponded to an initial C:N ratio of 25. The organic material with an initial pH of 6, 7 and 8 was composted in Reactor 1, 3 and 2, respectively.

A6.1.2.1. Process analysis

Figures A6.6 to A6.8 show the profiles of the process variables of R1-6-25, R3-7-25 and R2-8-25, respectively. The gas analyser was not available to measure the concentration of oxygen and carbon dioxide in the off-gas in this trial. The temperature of organic material rose rapidly reaching 60 °C on day 2 in R1-6-25 and on day 1 in R3-7-25 and R2-8-25.

Although cooling aeration was activated, the rapid microbial activity led to an overshoot in temperature, which was most notably in R3-7-25 and R2-8-25, before it was controlled about 60 °C. The cooling in R2-8-25 appears to have been excessive and the temperature gradually fell to about 55 °C.

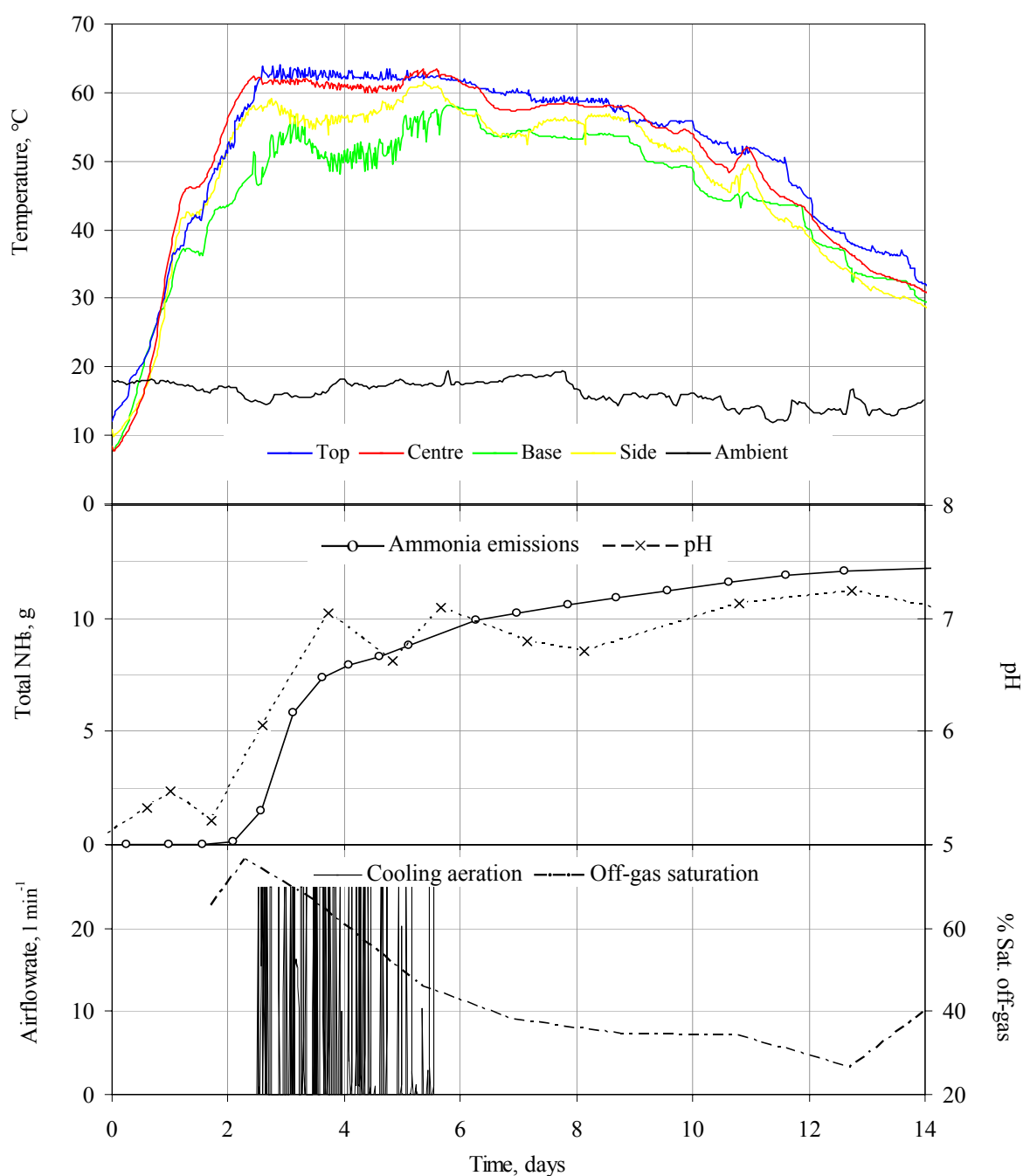


Figure A6.6. Profiles of process variables for experiment R1-6-25.

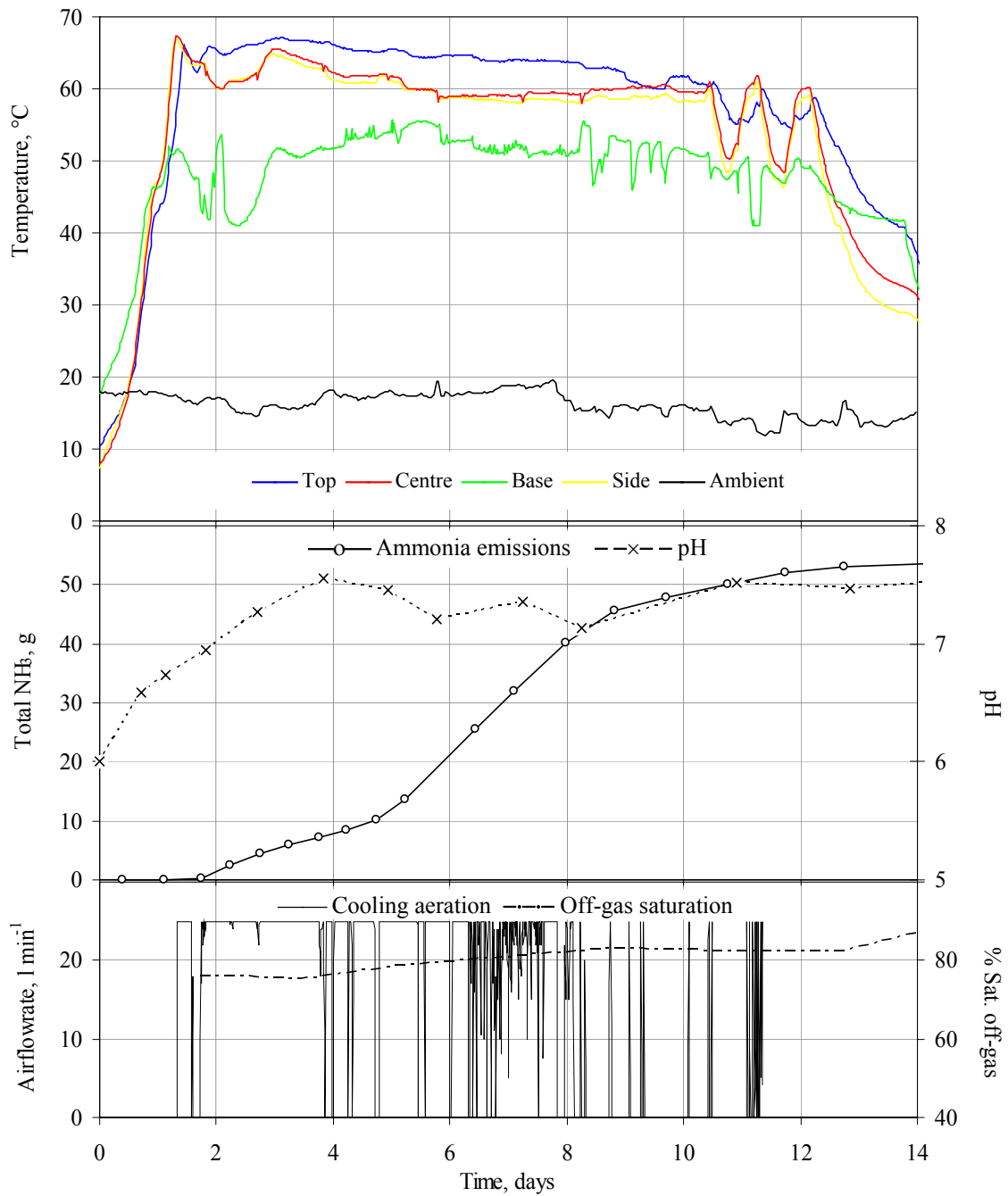


Figure A6.7. Profiles of process variables for experiment R3-7-25.

The side temperatures closely followed the centre temperature in R3-7-25 and R2-8-25 with the respective temperature differences being $\leq |2|^\circ\text{C}$ for 77 % and 82 % the temperatures recorded hourly. In R1-6-25, the centre and top temperature profiles were more similar than the side temperature profile, with the radial temperature difference being $\leq |3|^\circ\text{C}$

for less than half the composting time. Continual use of the side thermistor's port in the reactor wall for measuring the pH organic material with the pH probe (Figure 3.10) made a gap in the organic material where the side thermistor probe was normally positioned and the temperature of the air and not the organic material was measured.

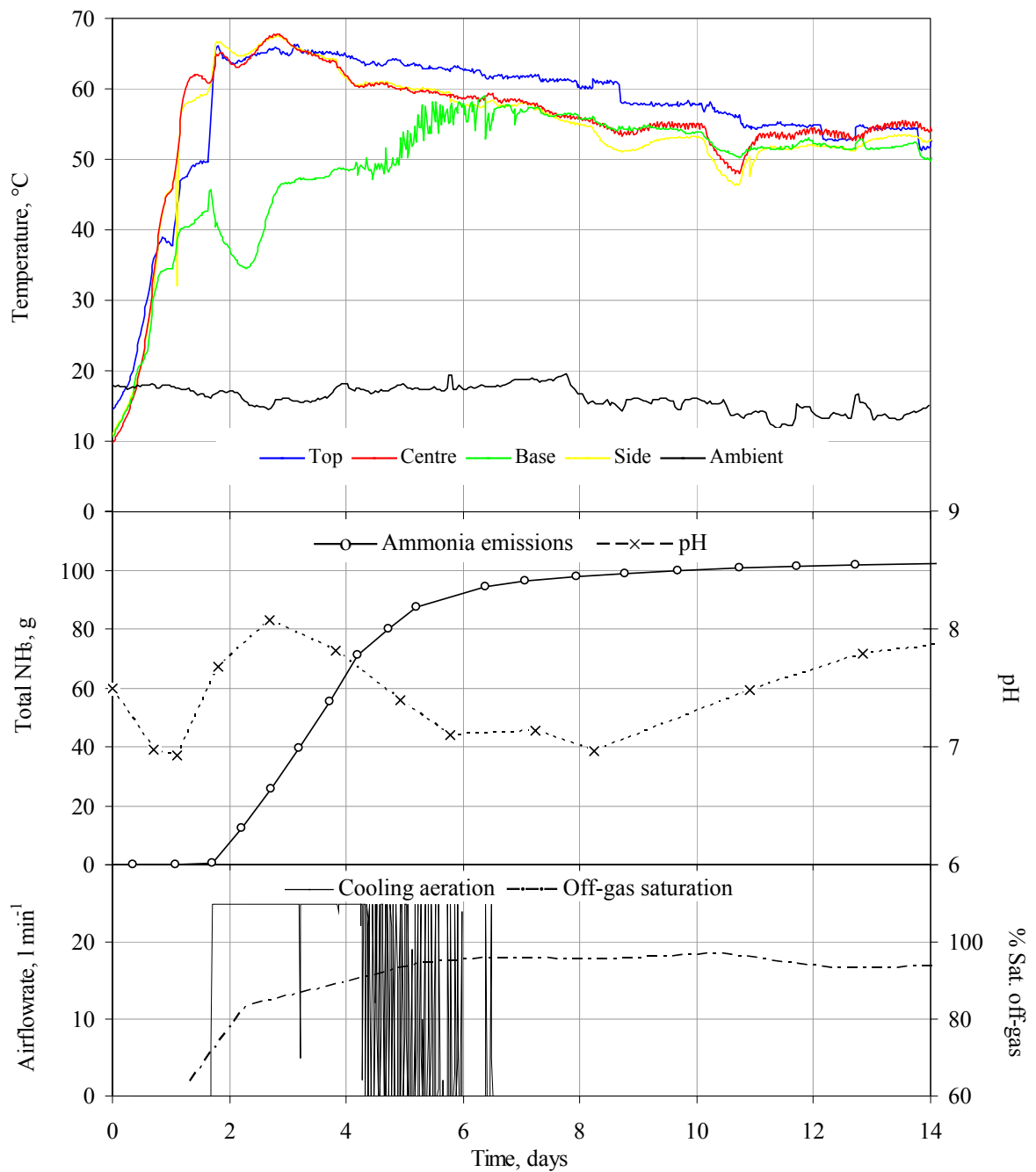


Figure A6.8. Profiles of process variables for experiment R2-8-25.

The vertical temperature difference depended on the aeration in use. The almost continual use of the cooling aeration in R3-7-25 kept the base sections at least 10 °C below the centre temperature for about 12 of the 14 days. As in R1-8-20 of Trial 1, the sharp temperature drop after day 12 in R3-7-25 may have been due to the drying out of the organic material or the exhaustion of the readily degradable organic material.

The pH of the organic material increased from its initial value to around its final value within 4 days. This final pH of the organic material was approximately 7, 7.5 and 8 in R1-6-25, R3-7-25 and R2-8-25, respectively.

A6.1.2.2. Analysis of organic material

Tables A6.9 summarises the microbial, physical and chemical analysis of the organic material in each reactor of Trial 2 before and after composting. The temperature of the organic material was above the 55 °C for more than the three consecutive days required for pathogen inactivation in all three reactors. The microbial analysis showed healthy general microbial populations in composted organic material, particularly so in R2-8-25 whose numbers throughout the composted organic material were similar to those in the composted organic material in Trial 1. The high numbers of general colony counts in the composted organic material appear to coincide with relatively longer composting periods around 60 °C. No pathogen markers were detected in any of the samples of the composted organic material.

Table A6.3. Mass changes in the organic material with a C:N ratio of 25 in Trial 2

T2 C:N =25		Total mass, kg		TS mass, kg		VS mass, kg		Total	TS loss	Water	VS loss
Reactor	PH	Initial	Final	Initial	Final	Initial	Final	loss %	% _{TS}	loss %	% _{TS}
R 1	6	37.4	29.2	13.9	10.4	12.2	8.8	22	25	20	28
R 3	7	37.3	27.0	13.8	11.7	12.1	10.2	28	15	37	16
R 2	8	37.3	25.2	13.1	11.0	11.5	9.4	32	16	41	18

The overall percentage losses in total, TS, VS and water mass are given in Table A6.3. R1-6-25 showed the highest loss in TS, which was unexpected as the temperature profiles suggested that microbial activity and, therefore, organic material decomposition was greatest in R2-8-25.

The very top layer of the composted material in R1-6-25 was wet with a thin layer of white fungus. Below the surface the organic material remained wet on the sides and the core was drier with white spores throughout. The base section was very dry and sporiferous except for very bottom layer, which was as wet as the top surface. There was a slight smell of ammonia from the middle section. In R3-7-25 the top layer of the composted organic material was dry and sporiferous. Below, the organic material was moist with a wetter sides and some white fungal growth. The core became drier and more sporiferous towards the base. The lower layers of the base section were dry but free of any fungal growth or spores and was reddish brown like the composted organic material from R2-7-20 and R3-6-20 of Trial 1. The top layer of the composted organic material in R2-8-25 was very wet (as a result of condensation on the inside surface of the lid when the reactors were shut down). Below, it was uniformly dry and reddish brown and there was little fungal growth or spores. The core of the middle section was also dry but darker brown and sporiferous with wet sides. The base section was very dry and dusty but the lower base layers were wetter, had few spores and was reddish brown.

The data in Table A6.3, suggests that the overall moisture content of the composted organic material in all three reactor was at least 56 %, which should not have limited microbial activity. However, according to the above description of the composted organic material, the moisture was not uniformly distributed and the core of the organic material was

in fact too dry to support microbial activity. A low moisture content in R2-8-25 was, therefore, the likely cause of the rapid decrease temperature on day 12.

96 % of the initial mass of TN in the organic material was retained in R1-6-25 and about 88 % in R3-7-25 and R2-8-25. The mass of AN in organic material increased by about 40 % and 20 % in R1-6-25 and R2-8-25, respectively, but fell to about half the initial mass in the organic material in R3-7-25.

A6.1.3. Trial 3 (C:N ratio 15)

In Trial 3, the initial mixing ratio of the organic material was 4, which corresponded to an initial C:N ratio of 15. The organic material with an initial pH of 6, 7 and 8 was composted in Reactor 2, 1 and 3, respectively.

A6.1.3.1. Process analysis

Figures A6.9 to A6.11 show the profiles of the process variables of R2-6-15, R1-7-15 and R3-8-15, respectively. The gas analyser was not available to measure the oxygen and carbon dioxide concentrations in the off-gas in this trial.

The centre temperature of organic material in R2-6-15 rose rapidly to 60 °C on day 1 and this temperature was maintained for the 14 days. R3-7-15 reached a maximum temperature of about 50 °C between day 2 and 5 and then decreased to 35 °C by day 14. In R3-8-15, the temperature did reach 60 °C on day 2 but then gradually fell to 40 °C.

A power cut on the day 4 stopped the heating cable, heating mats and forced aeration from operating for about 12 hours and the radial temperature difference increased with no heat to compensate for the loss from the reactor wall. The impact of the power cut was most notable in R2-6-15 (Figure A6.9) where the centre, side and base temperatures rose rapidly with no cooling aeration to remove the excess heat. The vertical temperature difference in the organic material was regularly within 10 °C when only the baseline aeration was operating.

Figure A6.9 clearly shows the excessive cooling of the base section of the organic material by the cooling aeration. The demand for the cooling aeration was noticeably lower after day 6 in R2-6-15 as microbial activity and, therefore, the generation of heat, slowed and the base temperature rose to within 10 °C of the centre temperature.

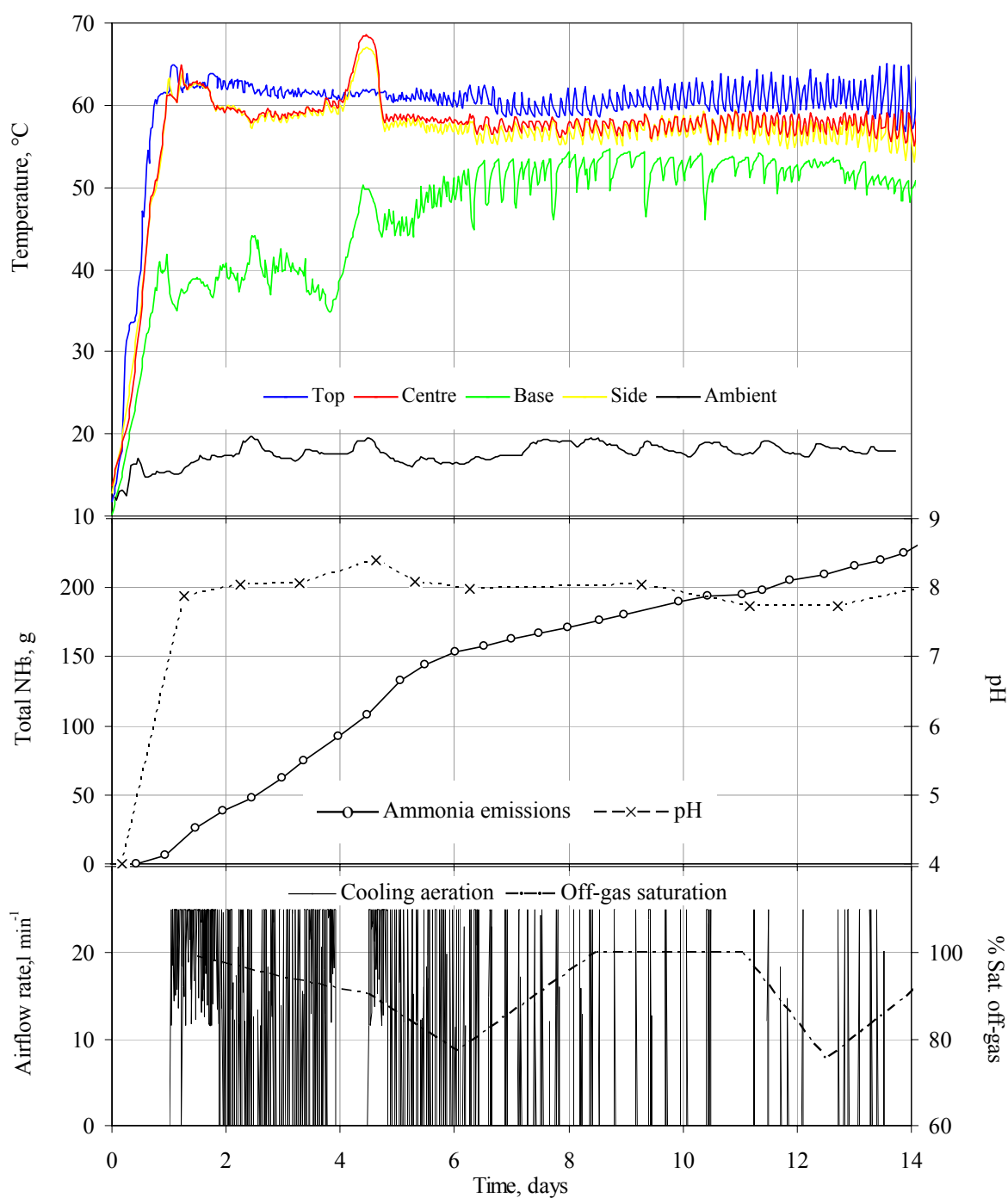


Figure A6.9. Profiles of process variables for experiment R2-6-15.

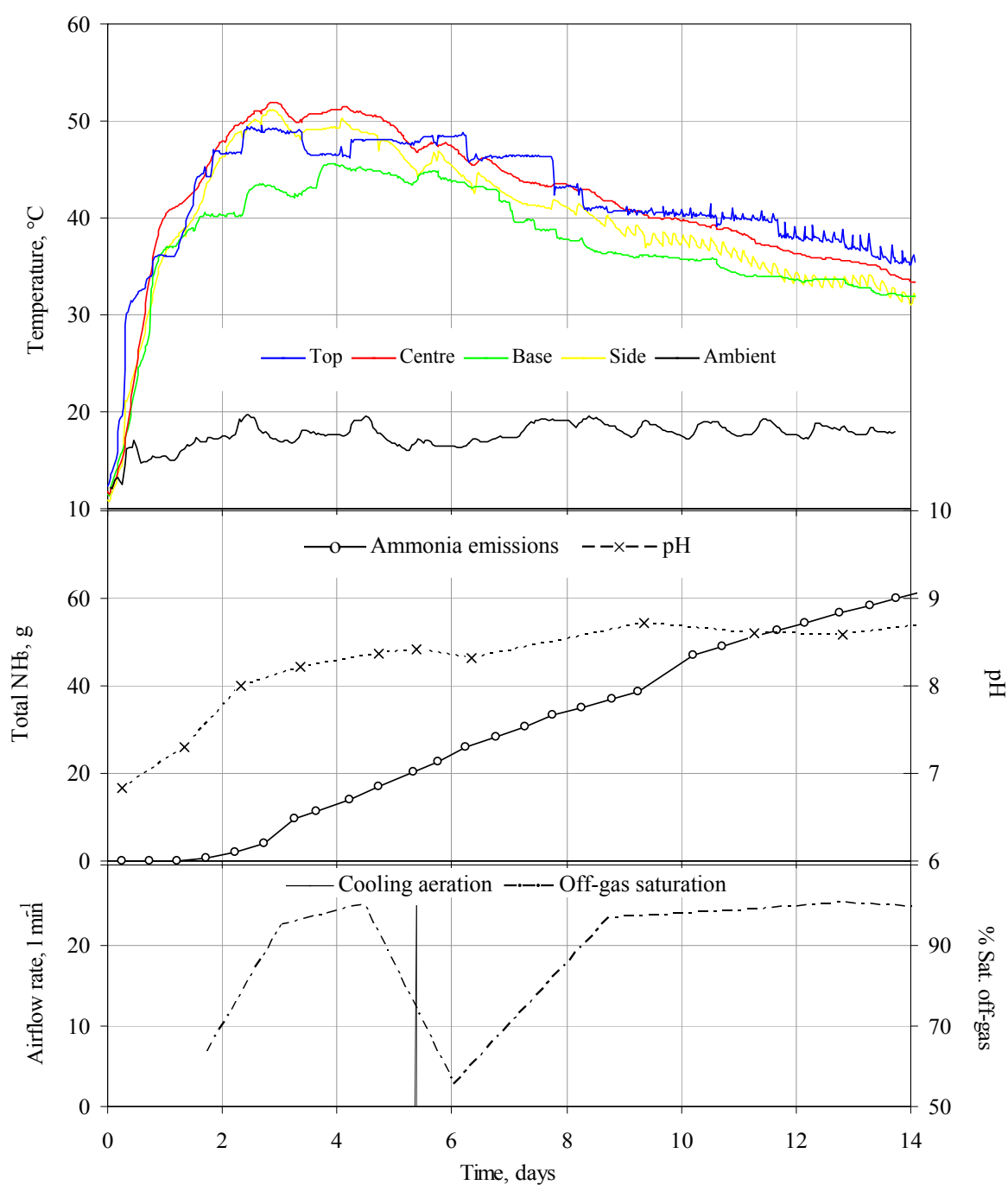


Figure A6.10. Profiles of process variables for experiment R1-7-15.

The respective radial temperature differences across the organic material in R2-6-15, R1-7-15 and R3-8-15 were $\leq |2|$ °C for 98 %, 50 % and 100 % of the hourly recorded temperatures. In R1-7-15 was the difference was $\leq |3|$ °C for 95 % of the time. The discrepancy may have occurred because the heating cable acted in response to the temperature

difference measured by the centre and side thermocouples, which were on the opposite side of the reactor to the thermistor and may well have measured a slightly difference temperature to the thermistor.

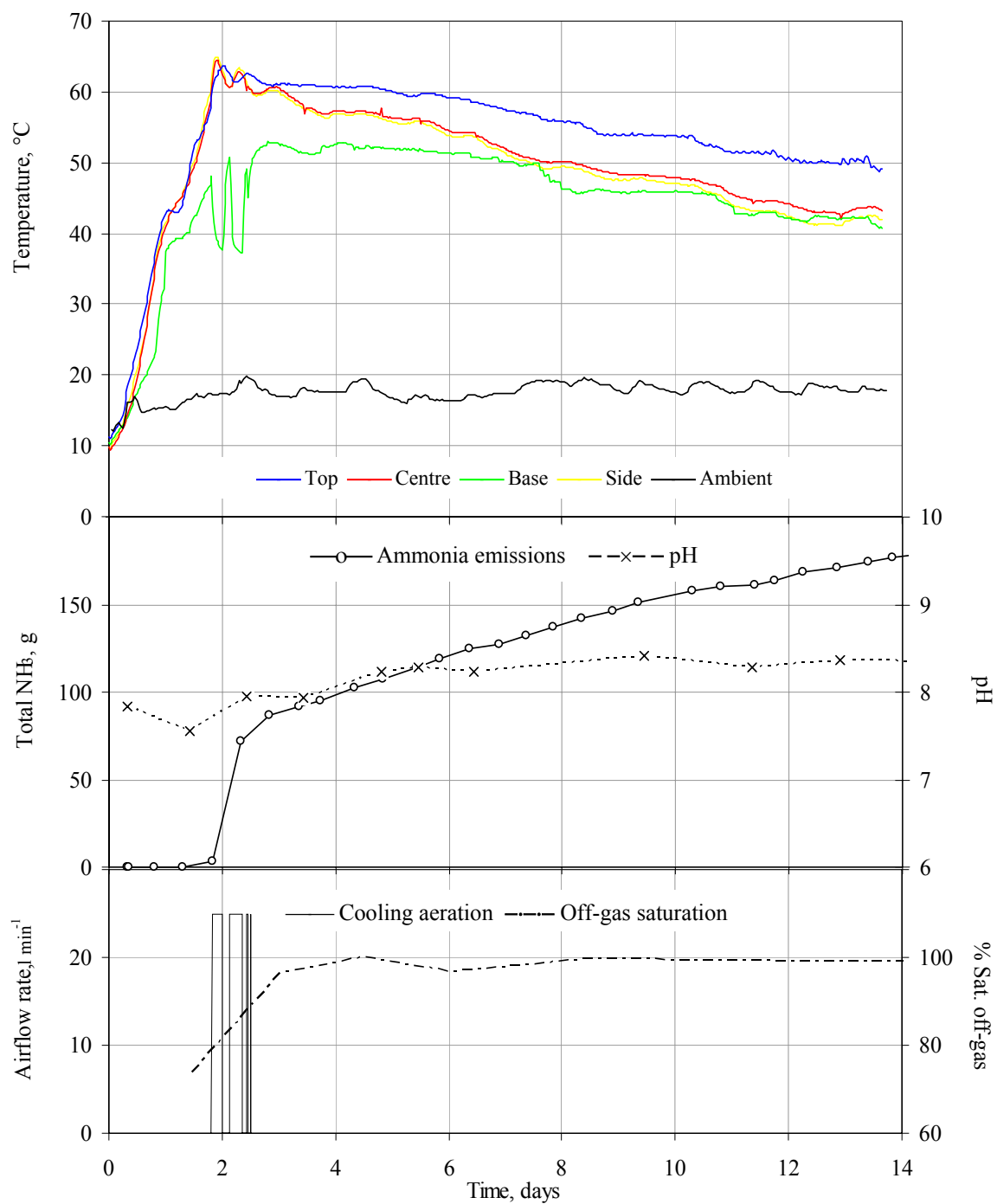


Figure A6.11. Profiles of process variables for experiment R3-8-15

The profiles of the pH of the organic material are from dry measurements with the pH probe. The rise in pH from the initial value to around its final value reflected the corresponding temperature profiles in R2-6-15 and R1-7-15. The pH of R3-8-15 gradually increased from just less than 8 to about 8.5 after a slight drop in value on day 1.

Unlike the profiles in Trial 1 and 2, the total mass of ammonia gradually increased, almost at a constant rate during the 14 days. This suggests that the organic material was rich in AN, which was not exhausted after 14 days. The total mass of ammonia emitted from R2-6-15 was over 200 g where as about 60 g and 180 g were emitted from R2-7-15 and R3-8-15, respectively. If composting R1-7-15 and R3-8-15 had proceeded as actively as in R2-6-15, so that a similar volume of air had flowed through the reactor, then the mass of ammonia emitted may well have equalled, if not surpassed, the 200 g from R2-6-15.

A6.1.3.2. Analysis of organic material

Tables A6.10 summarises the microbial, physical and chemical analysis of the organic material in Trial 3. The general microbial colony counts in the composted organic material samples from all three reactors were relatively low compared with the previous trials. No pathogen markers were detected, even though the temperature was not above 55 °C for more than three consecutive days in two of the three reactors. Ammonia is toxic to most microorganisms, and the much higher concentrations in the organic material composted in this trial (C:N 15) may have contributed to the inactivation of pathogens and the general microbial populations.

R2-6-15 and R3-8-15 retained 90 % and 97 % of the initial TN mass, respectively. However, the mass of TN in the composted organic material from R1-7-15 was apparently about 60 g higher than the initial mass. This reflected the heterogeneous nature of the organic material and the consequent experimental errors that result. The mass of AN decreased in

R2-6-15 but increased by about 35 % in R3-8-15 and more than doubled in R1-7-15, which reflected by the increase in AN concentration (≈ 2 %TS) measured in the composted organic material from R1-7-15. The measured dry pH values above 9 were indicative of the high concentration ammonia in the composted organic material, which was still relatively wet and so retained the ammonia in the liquid phase.

The overall percentage losses in total, TS, VS and water mass are given in Table A6.4. The percentage loss from of TS coincides with the extent of composting that took place, as indicated by the temperature profiles, with the greatest loss being in R2-6-15 and the least in R1-7-15. A similar pattern was shown by the loss in VS mass with almost a third of the mass being lost from the organic material in R2-6-15.

Table A6.4. Mass changes in organic material with a C:N ratio of 15 in Trial 3

T3 C:N =15		Total mass, kg		TS mass, kg		VS mass, kg		Total	TS loss	Water	VS loss
Reactor	PH	Initial	Final	Initial	Final	Initial	Final	loss %	%TS	loss %	%TS
R 2	6	46.6	33.9	17.5	13.7	15.3	11.1	27	22	31	28
R 1	7	45.1	41.6	16.2	15.1	14.2	12.2	8	7	8	14
R 3	8	46.4	42.0	17.0	14.5	14.9	12.2	10	15	5	18

The smell of ammonia was quite strong when the composted organic material was unloaded from R2-6-15. The top and middle sections were moist in the core and wet at the sides and there was little fungal growth. The organic material became drier towards the base, which was dry and sporiferous. Similarly, the composted organic material in R1-7-15 was moist with wetter sides. There was no white fungal growth and the smell of ammonia was stronger than in R2-6-15. The core of the base section became drier towards the bottom and there was some white fungal growth and spores. The very top layer and sides of the composted organic material in R3-8-15 were wet. The core was moist with middle section

being more so than the top and base sections. The lower layers of the base section were quite dry. The smell of ammonia was not as strong as the other 2 reactors and there was no white fungal growth.

The stability of the composted material can be gauged from the organic content, as indicated by the COD and C:N ratio [Haug 1993] (Table A6.10). The C:N ratios decreased, mainly as a result of an increase in the concentration of TN in the organic material, but also because of the small loss in total organic carbon (TOC). The COD decreased by about a third. However, the COD of the composted organic material was still relatively high, being similar in value to that of the organic material in Trial 1 and 2 before composting. The composted organic material was more stable but it was not necessarily stable and would need more time to stabilise.

A6.1.4. Trial 4 (C:N ratio 20)

As in Trial 1, the initial mixing ratio of the organic material was 3 and therefore the initial C:N ratio was 20. The organic material with the initial pH of 6, 7 and 8 was composted in Reactor 2, 1 and 3, respectively.

A6.1.4.1. Process analysis

Figures A6.12 to A6.14 show the profiles of the process variables for R2-6-20, R1-7-20 and R3-8-20, respectively. The combined oxygen and carbon dioxide gas analyser was not available in this trial. Furthermore, holes had formed in the copper pipes carrying the off-gas from Reactors 1 and 2 to the condenser and the off-gas saturation of R2-6-20 and R1-7-20 was not determined. The temperature of organic material in all three reactors rose relatively slowly and none reached 60 °C. Unfortunately, without the gas analyser, it was not possible to gauge whether the aerobic microbial activity was limited by low oxygen concentrations or by another process factor. Composting was relatively poor in all the experiments, which

suggests that microbial populations in the pig manure used may have been less active. The temperature peaked at about 58 °C on day 6 in R2-6-20 and R3-8-20 and then gradually fell to below 40 °C. The centre temperature in R1-7-20 was around 55 °C from day 3 and, so, met the criterion for pathogen inactivation

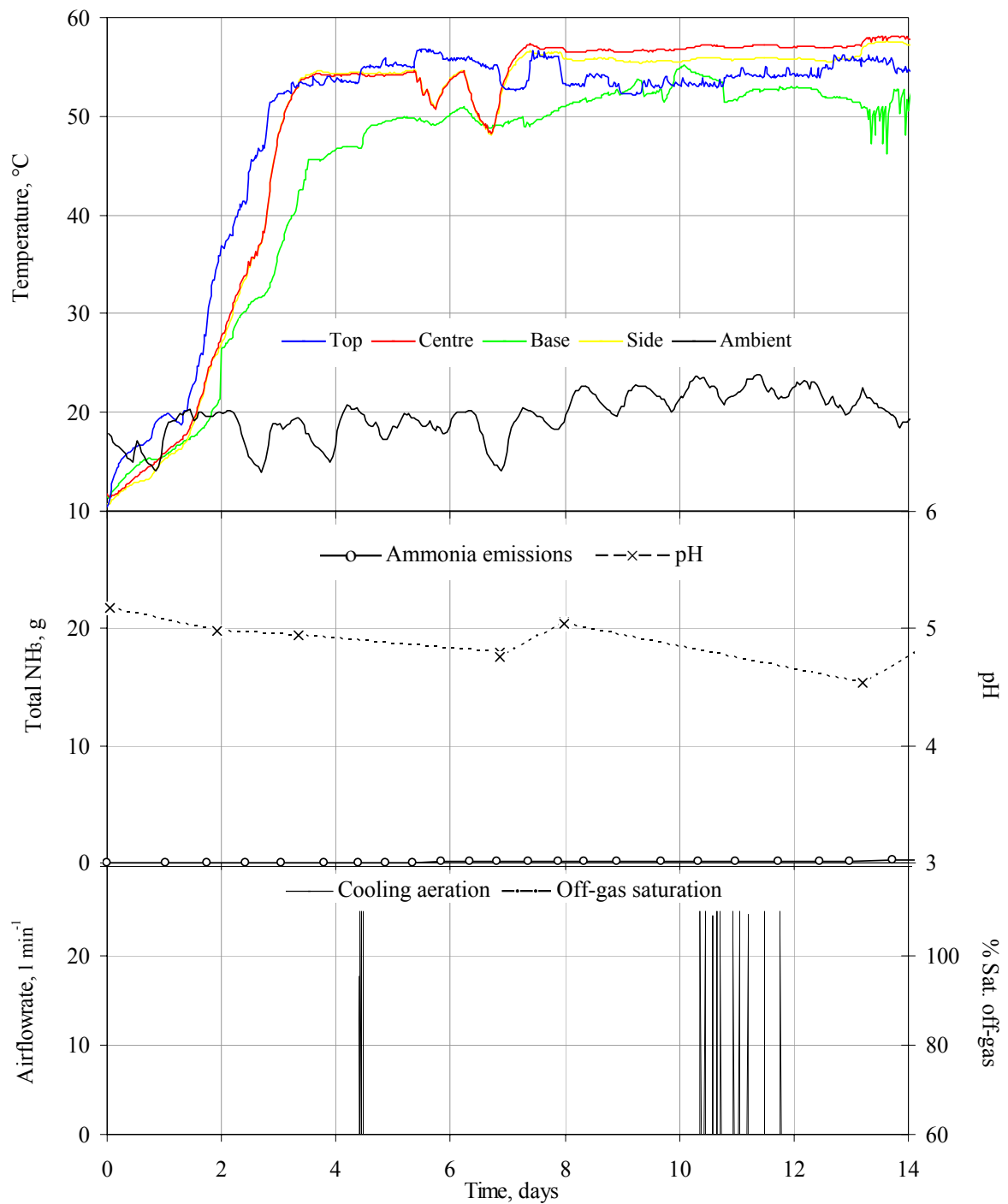


Figure A6.12. Profiles of process variables for experiment R2-6-20.

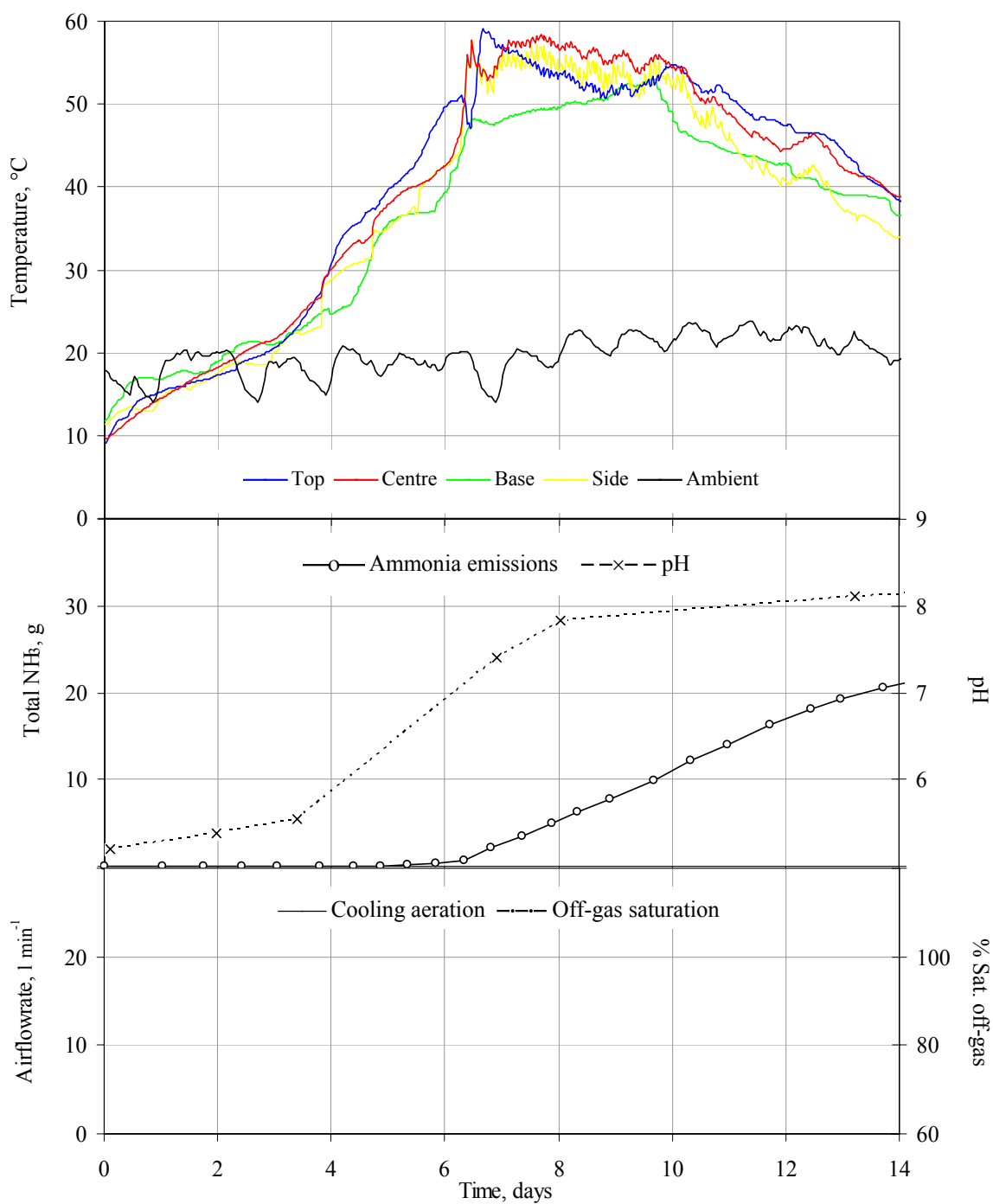


Figure A6.13. Profiles of process variables for experiment R1-7-20

No demand was automatically placed on the cooling aeration. On day 4, the cooling aeration to R2-6-20 was manually activated to aerate the organic material and so check whether the fact that 60 °C had not been reached was due to the lack of oxygen. For the same reason, the set point temperature on the cooling aeration controller was lowered to 55 °C

between days 10 and 12. Neither incident affected the centre temperature, which suggests that the oxygen concentration was not the limiting factor.

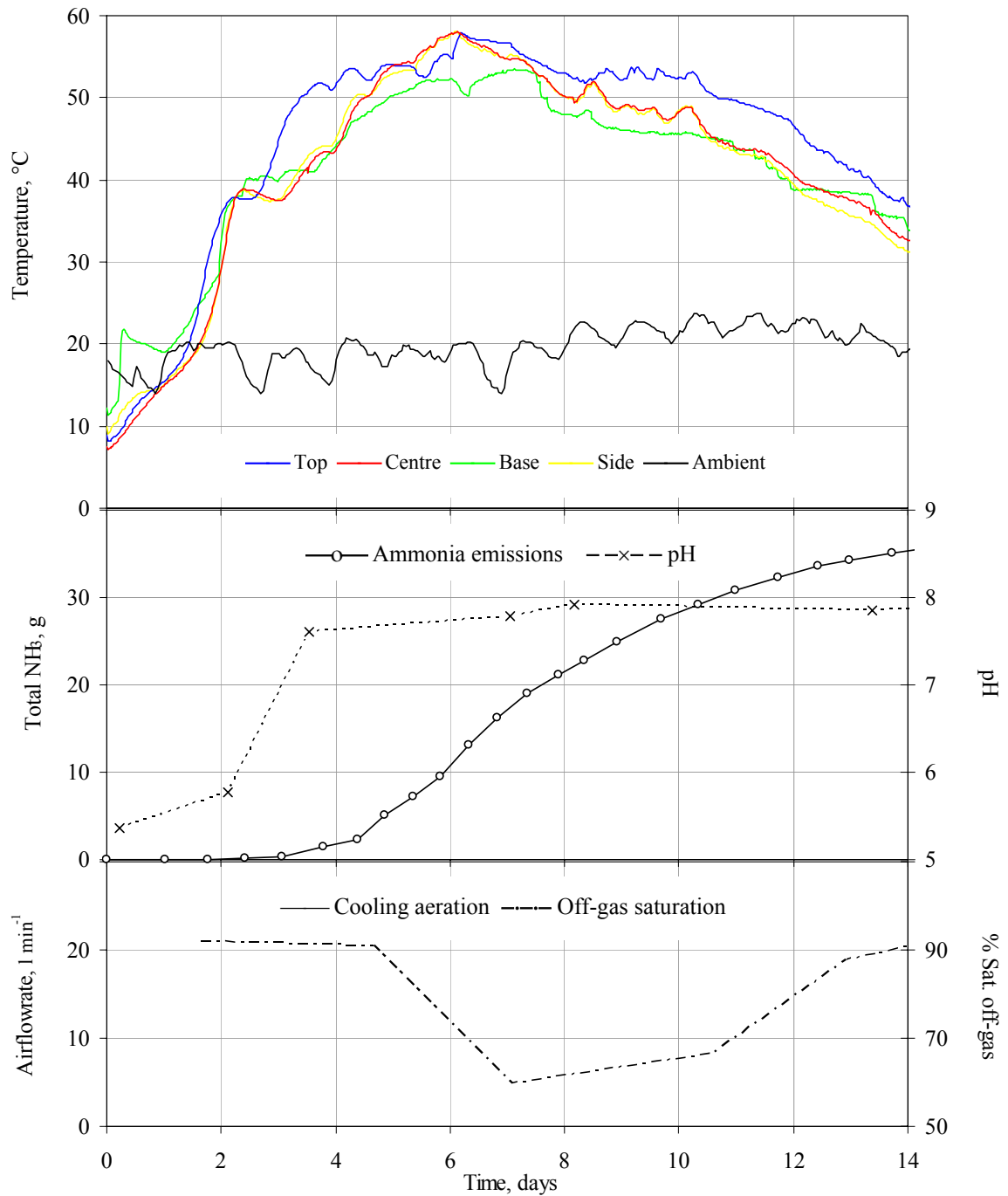


Figure A6.14. Profiles of process variables for experiment R3-8-20.

The respective radial temperature differences in R2-6-20, R1-7-20 and R3-8-20 were $\leq |1|^\circ\text{C}$ for only 71 %, 24% and 72 % and $\leq |2|^\circ\text{C}$ for 100 %, 45 % and 95 % of the hourly

recorded temperatures. Again, because the side temperature port was used for measuring the pH of the organic material, the radial temperature difference in R1-7-20 was within than 3 °C for only 75 % of the composting time.

All the initial pH values were relatively low, with the dry pH measurements being about 5.2. The pH of the organic material increased to around 8 after day 2 in R3-8-20 and day 8 in R1-7-20 but remained low around 5 in R2-6-20 throughout the 14 days. The ammonia emissions profiles reflected the pH profiles, with the total emissions being less than 1 g in R2-6-20 and rising to about 20 g from day 6 in R2-7-20 and to 35 g from day 2 in R3-8-20. The addition of the acid to lower the pH of the organic material does appear to have reduced the total mass and delayed the onset of ammonia emissions. As the cooling aeration was not really used in the experiments, this trial may prove to be the best for comparing the effect of the initial pH of the organic material, as the high airflow rate of the cooling aeration appears to have significantly affected on the ammonia emissions in previous trials.

A6.1.4.2. Analysis of organic material

Tables A6.11 summarises the microbial, physical and chemical analysis of the organic material in each reactor before and after composting. As in R1-7-15 and R3-8-15 of Trail 3, the initial general microbial colony counts in the organic material of all the experiments in the trial were less than 1×10^6 CFU g⁻¹ TS, which seems to be indicative of a relatively slow composting rate. The coliform counts were also low to begin with and after composting no pathogen markers were detected in R2-6-20, which was expected as the temperature was above 55 °C for more than 3 consecutive days, and R3-8-20, although the temperature was above 55 °C for only 40 hours. Pathogen markers were detected in the composted organic material of R2-7-20 with the density increasing from about 2×10^3 CFU g⁻¹ TS to 13×10^3 CFU g⁻¹ TS. The temperature was above 55 °C for less than 3 consecutive days.

The overall percentage losses in total, TS, VS, and water mass are given in Table A6.5. As in Trial 3, the percentage loss in TS coincides with the extent of composting that took place with the greatest loss being in R2-6-20, although the difference between the three experiments was not as great as seen in the previous trials. In fact, the loss in VS was the same for R2-6-20 and R1-7-20.

Table A6.5. Mass changes in the organic material with a C:N ratio of 20 in Trial 4

T4 C:N =20		Total mass, kg		TS mass, kg		VS mass, kg		Total	TS loss	Water	VS loss
Reactor	PH	Initial	Final	Initial	Final	Initial	Final	loss %	%TS	loss %	%TS
R 2	6	38.1	30.3	15.6	12.6	13.6	10.8	20	19	21	21
R 1	7	37.8	33.2	15.2	13.0	13.4	10.7	12	14	11	21
R 3	8	37.6	31.1	14.6	12.7	12.8	10.7	17	13	20	16

The TN concentration in the composted organic material of R2-6-20 was the same as the initial concentration but with the loss in TS, only 80 % of the initial mass of TN remained. However, no leachate was collected from the reactors and ammonia emissions were practically zero, which leaves 86 g of nitrogen unaccounted for. Conversely, the TN concentration in the composted organic material of R1-7-20 and R3-8-20 was higher than the initial value resulting in an increase in the TN, which, as explained in Trial 3, was not possible. The under and overestimated TN mass probably arose from the difficulty associated with analysing heterogeneous organic material. The mass of AN (AN) in the composted organic material increased by more than 80 % in all the experiments.

The composted organic material unloaded from R2-6-20 was light brown and relatively dry in the top section becoming moist in the middle section. There was no smell of ammonia or fungal growth and spores. The base section had dense fungal growth and was moist becoming very wet at the bottom. The top surface and sides of the composted organic

material unloaded from R1-7-20 were very wet. There was fungal growth in the rest of the uniformly moist organic material, which was slightly wetter in the base section. The smell of ammonia was quite strong. Similarly, the top layer and sides of the composted organic material unloaded from R3-8-20 were very wet. There was fungal growth in the moist top section but the middle and base sections were relatively dry, becoming drier and sporiferous towards the very base.

There was little change in the COD except in R3-8-20, which suggests that the composted organic material from this reactor was more stable than that from R2-6-20 and R1-7-20. There was little change in the TOC so that any decrease in C:N ratio was a due to the an increase in the TN content. The results of the analyses on the composted organic material do not always appear to reflect the observed composting conditions in the reactors.

A6.1.5. Trial 5 (C:N ratio 25)

As in Trial 2, the initial mixing ratio of the organic material was 2 and the initial C:N ratio was therefore 25. The organic material with the initial pH of 6, 7 and 8 was composted in Reactor 3, 2 and 1, respectively.

A6.1.5.1. Process analysis

Figures A6.15 to A6.17 show the profiles of the process variables for R3-6-25, R2-7-25 and R1-8-25, respectively. The oxygen, carbon dioxide and condensate measurements could not be taken because the pump on the off-gas sample line started to leak.

The temperature of organic material in all three reactors increased from about 15 °C to 60 °C within two day of composting, except in R2-7-25 where the temperature increased slowed after 55 °C and only reaching 60 °C after day 3. In R3-6-25 and R1-8-25, 60 °C was maintained for 6 and 7 days, respectively, whereas after one and a half days after first reaching 60°C, the temperature in R2-7-25 decreased but stayed at temperatures above 50 °C.

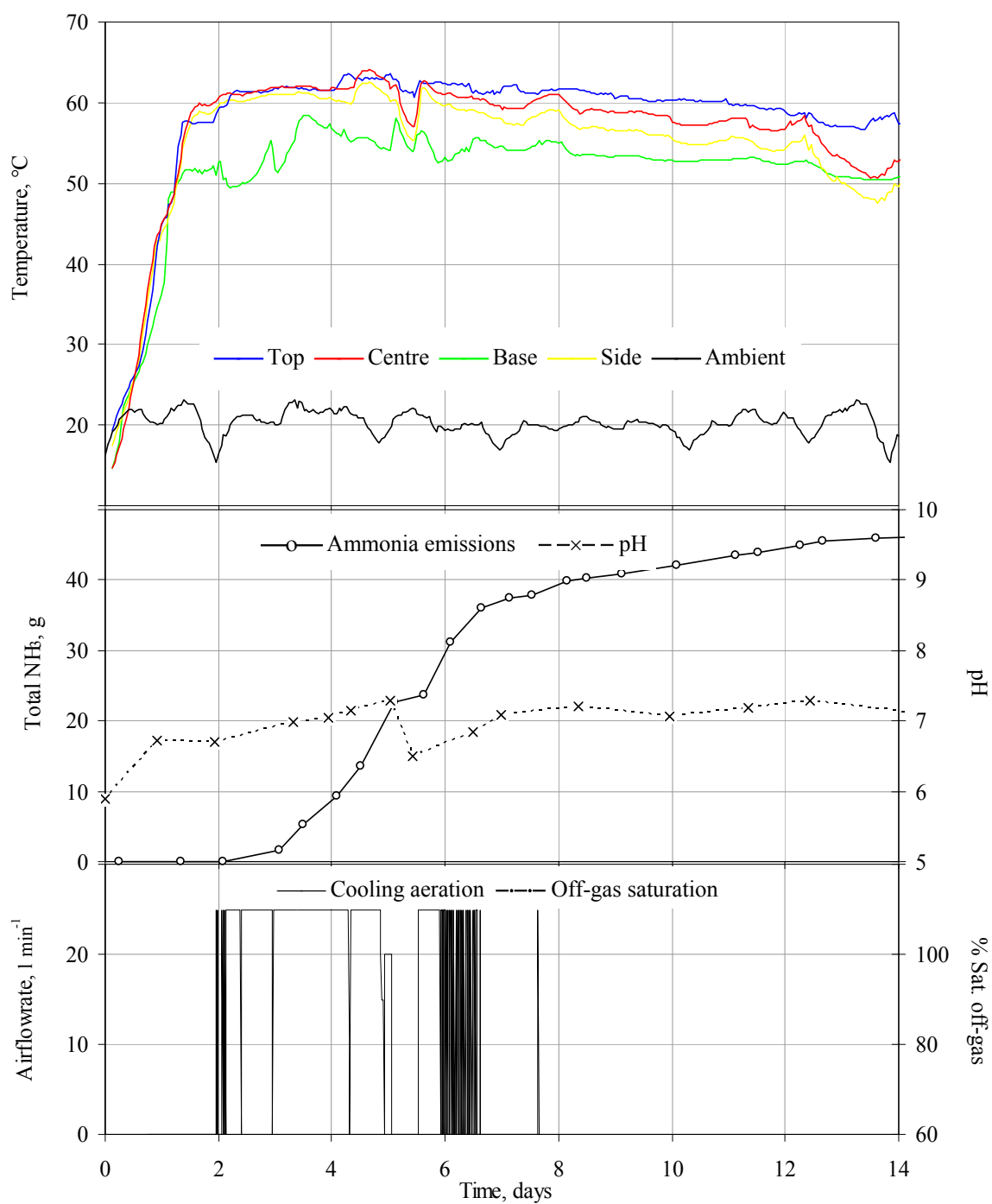


Figure A6.15. Profiles of process variables for experiment R3-6-25

The radial temperature difference across the organic material in R2-7-25 was $\leq |2|^\circ\text{C}$ the whole time whereas after 7 days in R3-6-25, the centre temperature was more than 2°C higher than the side temperature. This was probably caused by organic material falling away from the side temperature probe. Although the side temperature profile shadowed that of the

centre temperature in R1-8-25, the difference was between 2 °C and 4 °C for 85 % of the time. The organic material was exposed to temperatures above 55 °C for more than 3 consecutive days in all the reactors except for in the base of R2-7-25 and R3-8-25, where temperatures fluctuated about 50 °C.

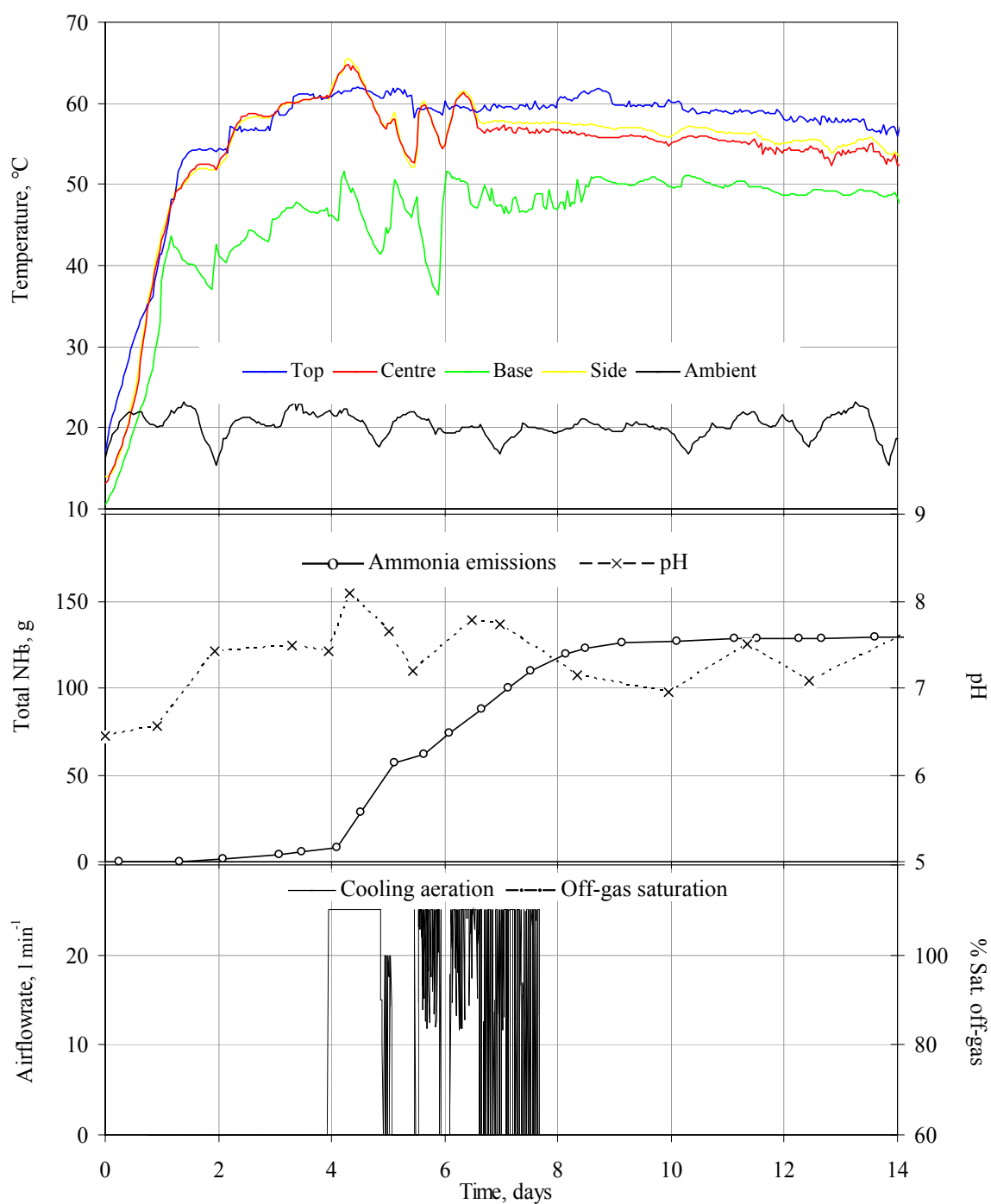


Figure A6.16. Profiles of process variables for experiment R2-7-25

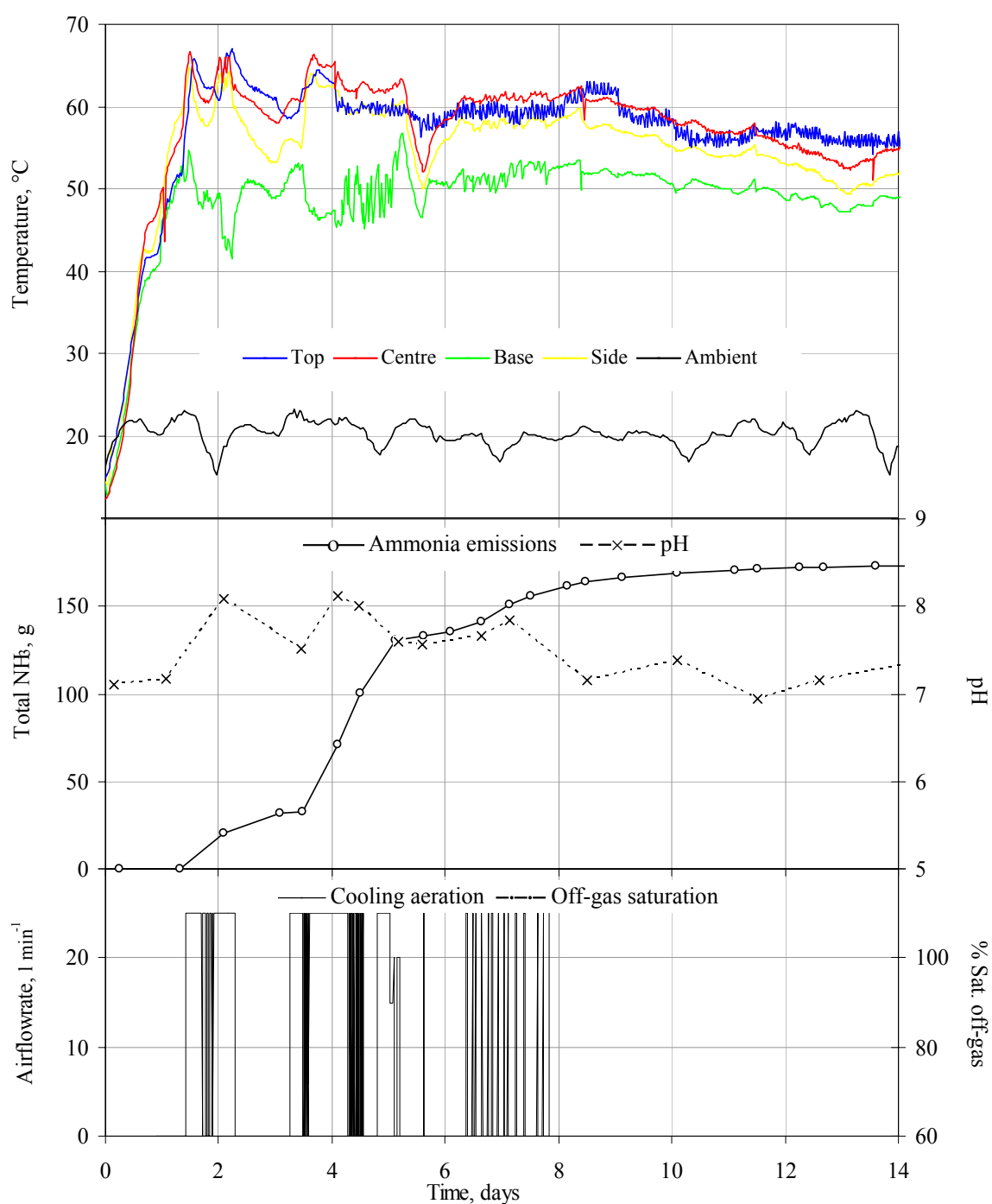


Figure A6.17. Profiles of process variables for experiment R1-8-25

The initial pH of the organic material was more acidic than intended but the pH rose quickly to between about 7 and 8, with R3-6-25 being at the lower end of the range and R1-8-25 at the higher end. About 30 % and 40 % less cooling aeration passed through than R2-7-25 and R3-8-25 than R3-6-25, but the respective total ammonia emissions were a quarter and

a third more. Also, there was a delay in ammonia emissions from R3-6-25 and R2-7-25 compared with R1-8-25, from which ammonia was emitted in notable quantities after day 1.

A6.1.5.2. Analysis of organic material

Tables A6.12 summarises the microbial, physical and chemical analysis of the organic material in each reactor before and after composting. The relatively low initial general microbial population density in the organic material ($<1 \times 10^6$ CFU g⁻¹TS) did not appear to affect the composting rate as it seemed to in Trial 3 and 4. No pathogen markers were detected in any of the samples of the compost organic material and a reduction by as much as three orders was measured in the general microbial population density in samples from the top sections of R1-8-25 and R2-7-25.

The overall percentage losses in total, TS, VS and water mass of the organic material are given in Table A6.6. Again, the percentage loss in TS coincides with the extent of composting with the greatest loss being in R3-6-25, although the loss in R2-7-25 and R1-8-25 were also high. The loss in VS was correspondingly greatest in R3-6-25.

Table A6.6. Mass changes in the organic material with a C:N ratio of 25 in Trial 5

T5 C:N =25		Total mass, kg		TS mass, kg		VS mass, kg		Total loss %	TS loss %TS	Water loss %	VS loss %TS
Reactor	pH	Initial	Final	Initial	Final	Initial	Final				
R 3	6	37.7	25.4	13.5	10.3	12.0	8.9	33	24	39	26
R 2	7	37.7	26.5	14.2	11.3	12.6	9.7	30	20	35	23
R 1	8	37.5	23.5	13.6	10.7	12.2	9.4	37	21	46	23

The very top layer of the composted organic material unloaded from R3-6-25 was dry with a little white fungal growth, which became denser in the moist organic material below. Again, the middle section was dry and sporiferous, with damp patches. The base section was very dry except for the very base, which was wet. There was no smell of ammonia gas. The

top section of the composted organic material unloaded from R2-7-25 was moist becoming drier towards the base section, which was very dry except for the wet bottom layer. All dry areas were sporiferous and ammonia gas was not evident. The top layer and the sides of the composted organic material unloaded from R1-8-25 were wet. The top section was generally moist and showed some fungal growth throughout. The core of the middle section down to the base was dry and saporiferous. Ammonia gas was not evident.

The composted organic material from R3-6-25 and R1-8-25 retained 86 % and 90 % of its initial TN. The TN mass in the composted organic material from R2-7-25 was overestimated (10 % above the initial mass) because of the relatively high TN concentration measured in samples from the middle and base sections (Table A6.5). The mass of AN in the composted organic material increased by 26 % in R3-6-25 and decreased by 14 % and 40 % in R2-7-25 and R1-8-25, respectively, which corresponds to the fact that the highest mass of ammonia was emitted from R1-8-25 relative to its initial AN mass.

A6.1.6. Trial 6 (C:N ratio 15)

As in Trial 3, the initial mixing ratio of the organic material was 4 and the initial C:N ratio was 15. The organic material with the initial pH of 6, 7 and 8 was composted in Reactor 1, 3 and 2, respectively.

A6.1.6.1. Process analysis

Figures A6.18 to A6.20 show the profiles of the process variables of R1-6-15, R3-7-15 and R2-8-15, respectively. The pH meter was not available for this trial. The concentration of oxygen and carbon dioxide in the off-gas was measured. The temperature in R1-6-15 and R2-8-15 rose rapidly to 60 °C in one day, while it took 2 days in R3-7-15. The initial increase in the temperature coincided with a sharp decrease in the oxygen concentration in the off-gas to below 5 % in R1-6-15 and R3-7-15 and about 6 % in R2-8-15.

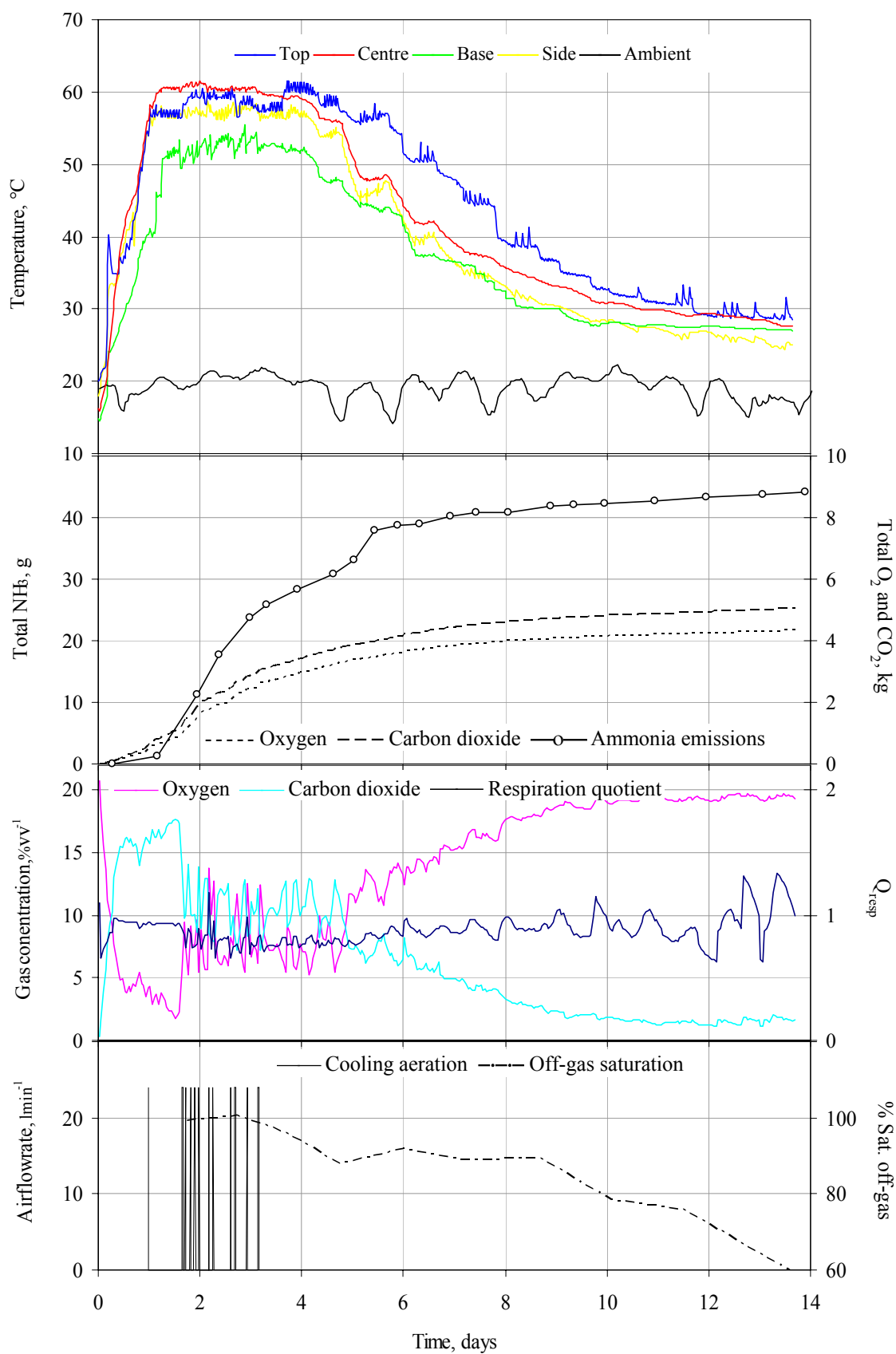


Figure A6.18. Profiles of process variables for experiment R1-6-15.

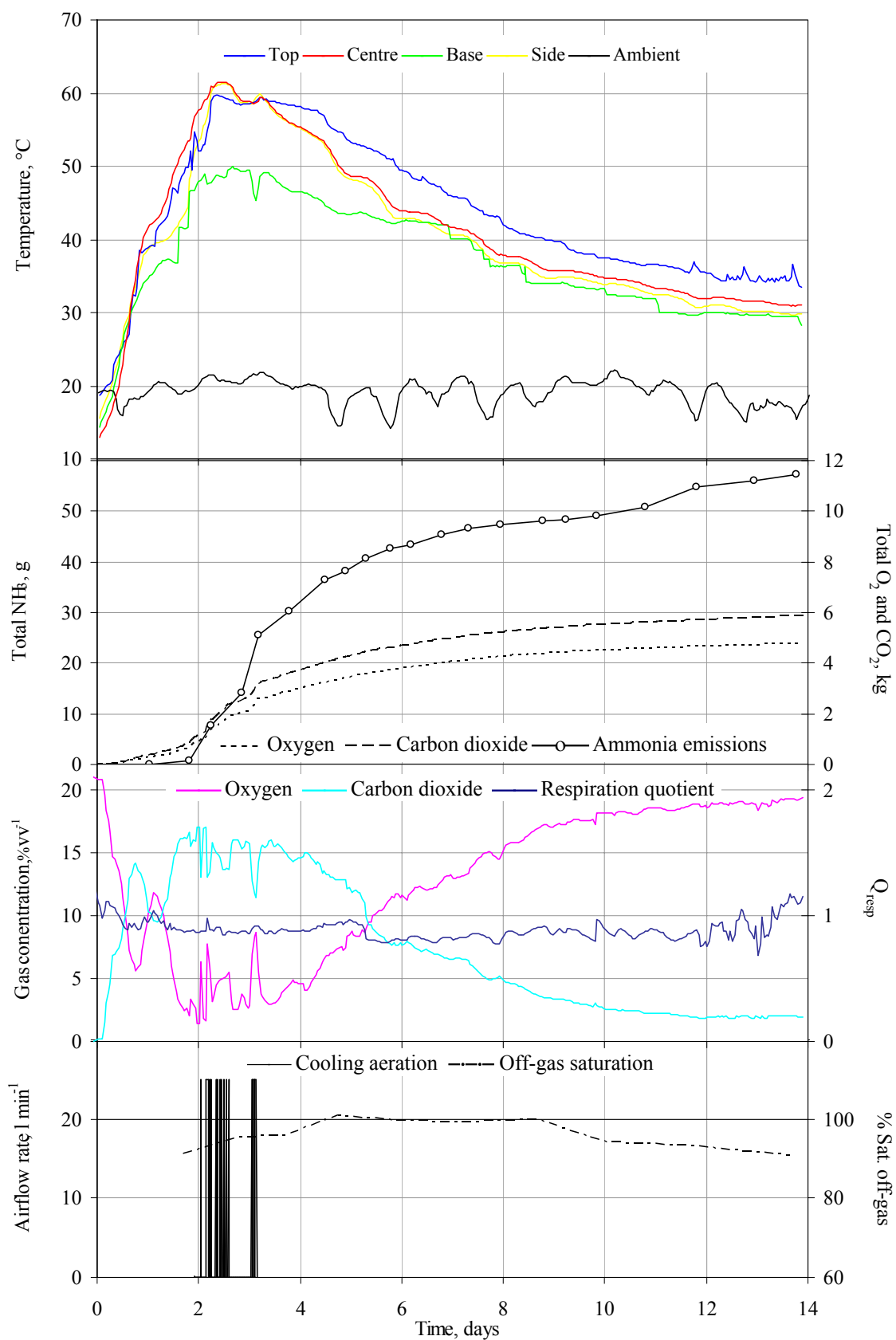


Figure A6.19. Profiles of process variables for experiment R3-7-15

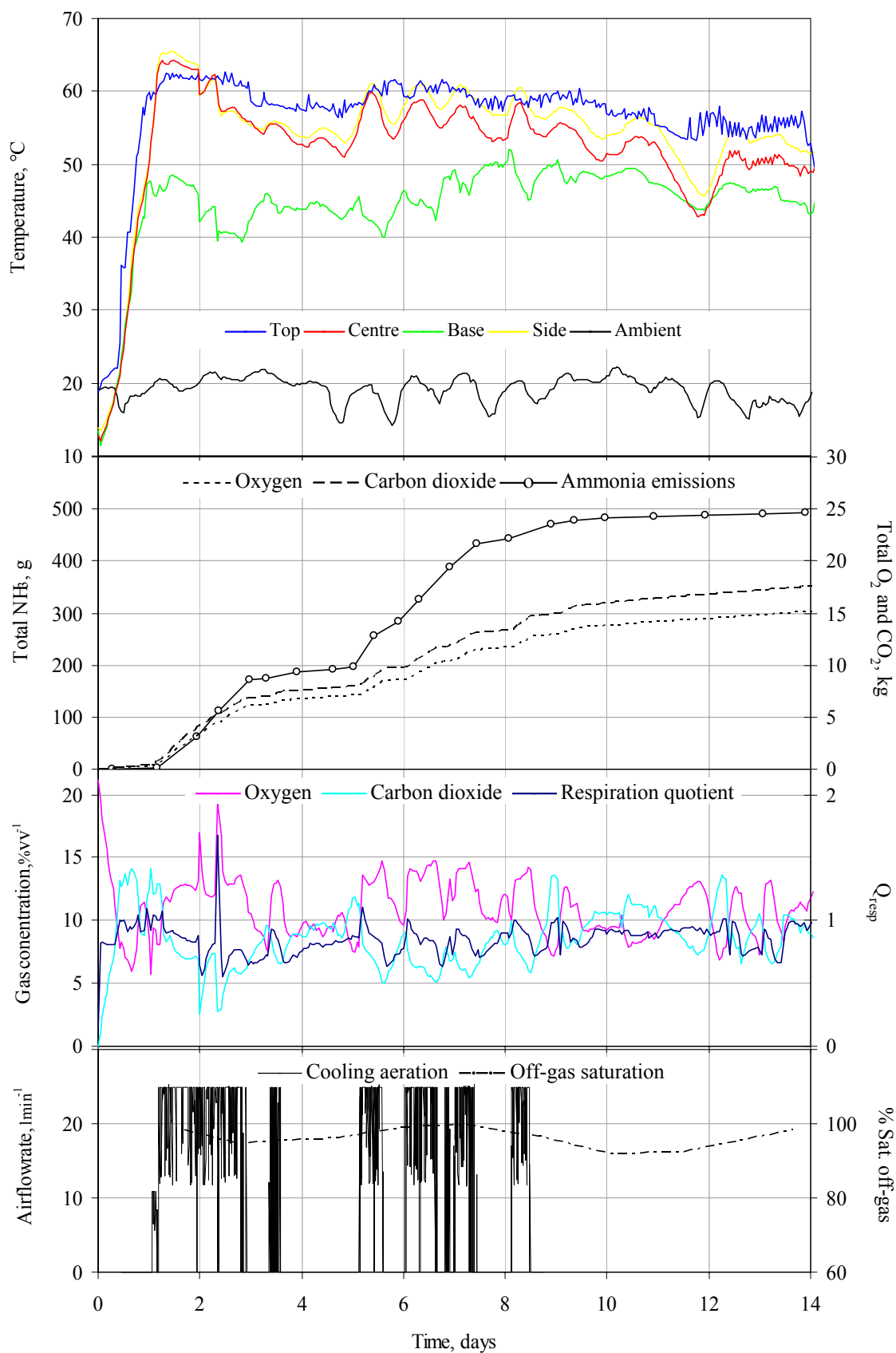


Figure A6.20. Profiles of process variables for experiment R2-8-15

Oxygen concentrations above $5\% \text{ v v}^{-1}$ do not limit microbial activity [Haug 1993]. Therefore, microbial activity was limited for 28 hours, 11 hours after the start in R1-6-15 and for almost 70 hours, 36 hours after the start in R3-7-15. The higher demand for cooling aeration in R2-8-15 maintained the oxygen concentration above $5\% \text{ v v}^{-1}$ in the organic material, which was most important when the temperature first reached 60°C and the oxygen concentration in the organic material was at a minimum. The increase in the oxygen concentration was obvious when the cooling aeration was active but in R1-6-15 and R3-7-15 it was not sustained for long enough to aerate the organic material sufficiently. In such a situation, an overriding response to oxygen concentration feedback operating in parallel with the temperature feedback would be useful.

As the off-gas concentration profiles suggest and the total oxygen and carbon dioxide profiles confirm, the oxygen demand was much higher in the organic material with an initial C:N ratio of 15 than with an initial C:N of 20 (Trial 1). For example, after 11 days, the mass of oxygen consumed in R2-8-15 was at least 5 times higher than that in the experiments of Trial 1.

The activation of the cooling aeration in R2-8-15 between day 5 and 9 when the centre temperature was below 60°C probably occurred because the organic material had slumped slightly and fallen away from the centre thermistor probe but had still maintained contact with the centre thermocouple on the cooling aeration control system. This situation was confirmed by the fact that the centre temperature was lower than the side temperature (Figure A6.20) such that the radial temperature difference across the organic material in R2-8-15 was $\leq 2^\circ\text{C}$ for the first 6 days but was between 2°C and 4°C thereafter. The radial temperature difference was $3 \pm 1^\circ\text{C}$ in R1-6-15 for 95 % of the 14 days but $\leq 2^\circ\text{C}$ in R3-7-15 for 12 of the 14 days. Again, due to the excessive cooling of the base section, the

vertical temperature difference in the organic material was greater than 10 °C in R2-8-15 when the cooling aeration was on between day 1 and 9. Otherwise, the vertical difference was within 10 °C for 73 % and 84 % of the time in R1-6-15 and R3-7-15, respectively.

The ammonia emissions from all three reactors were measurable within 2 days of the start. The low initial C:N ratio of the organic material appears to have overridden the delaying effect that the low initial pH may have on the ammonia emissions, which occurred in R2-6-15 of Trial 3. The total mass of ammonia emitted from R1-6-15 and R3-7-15 was 44 g and 57 g, respectively. About 10 times as much ammonia was estimated to have been lost from R2-8-15.

A6.1.6.2. Analysis of organic material

Tables A6.13 summarises the microbial, physical and chemical analysis of the organic material in each reactor before and after composting. The overall percentage losses in total, VS and water mass is given in Table A6.7.

Table A6.7. Mass changes in the organic material with a C:N ratio in Trial 6.

T6 C:N =15		Total mass, kg		TS mass, kg		VS mass, kg		Total loss %	TS loss %TS	Water loss %	VS loss %TS
Reactor	PH	Initial	Final	Initial	Final	Initial	Final				
R 1	6	46.3	38.5	16.2	14.7	14.1	12.5	17	9	21	11
R 3	7	47.1	42.0	16.4	15.6	14.3	13.4	11	5	14	6
R 2	8	47.0	34.4	16.3	14.5	14.2	12.2	26	11	35	14

The TS loss reflects the composting conditions in the reactors, with the highest reduction being in R2-8-15. The TS loss was relatively high in R1-6-15 considering that thermophilic conditions only lasted for about 6 days compared with the 13 days in R2-8-15.

The top layer of the composted organic material unloaded from R1-6-15 was wet and with a little white fungal growth on the top surface. The sides of the middle section were wet and the core was drier but still moist and with white growth. The base section was wet around

the sides and the core was moisture but there was no white fungal growth. The top layer and sides of the composted organic material unloaded from R3-7-15 were very wet. The middle section was also quite wet but becoming drier towards the base section, which was still moist. There was some white fungal growth throughout and a strong smell of ammonia. The top surface of the composted organic material unloaded from R2-8-15 was dry with white fungal growth (Figure A6.21). The organic material underneath was moister and showed some white fungal growth. The middle and base section was dry and sporiferous with white fungal growth at the core. The sides were wet. There was a strong smell of ammonia throughout the organic material.



Figure A6.21. The white fungal growth on the composted organic material in R3-7-15.

Microbial analysis of the composted organic material showed that inactivation of the pathogen markers was complete in R2-8-15 but that concentrations of about 6×10^5 CFU g⁻¹ TS and 2×10^5 CFU g⁻¹ TS were detected in the middle and base sections of R1-6-15. Although pathogen markers were detected in all sections of R3-7-15, the concentrations were below

1×10^3 CFU g⁻¹ TS. Inactivation of general microbial populations also occurred, perhaps because of high ammonia concentrations, with the population concentration decreasing by two orders in R1-6-15 and R2-8-15 and by an order in R3-7-15.

96 %, 78 % and 90 % of the initial TN was retained in the composted organic material from R1-6-15, R3-7-15 and R2-8-15, respectively. The fraction of the TN that was AN increased by about 30 % and 70 % in R1-6-15 and R3-7-15, respectively, and decreased by about 30 % in R2-8-15, which reflected the relative masses of ammonia emitted. However, although it was not surprising that the highest mass was emitted from R2-8-15, as the low initial C:N and relatively high initial pH of the organic material promoted ammonia emissions, the estimated 500 g of ammonia emissions contained 410 g of nitrogen, which was significantly higher than the 54 g decrease in the TN mass.

The COD of the organic material in R3-7-15 and R2-8-15 decreased by about 30 %. In R1-6-15, the COD was initially relatively low because the sample may have contained a relatively high portion of straw and so the COD appears to have increased. The COD of the composted organic material is comparable with that of R3-7-15 and R2-8-15 and, so, the stability of the organic material probably increased in R1-6-15.

A6.2. Summary of the organic material analysis

Table A6.8. Analysis of the initial and final (composted) organic material in Trial 1 (C:N 20)

Date	Reactor 1 (pH 8)				Reactor 2 (pH 7)				Reactor 3 (pH 6)			
01/10/01 to 10/11/01	Initial	Final			Initial	Final			Initial	Final		
		Top	Mid	Base		Top	Mid	Base		Top	Mid	Base
Microbial population counts \log_{10} CFU g ⁻¹ TS												
General	4.9	7.2	6.7	6.7	5.4	7.1	6.8	∞	3.7	∞	∞	∞
Coliform	3.1	clear	clear	Clear	5.0	6.5	clear	clear	5.4	6.6	6.1	clear
Physical analyses												
MC %	64	52	30	39	61	67	46	22	63	41	54	64
TS %	36	48	70	61	39	33	54	78	37	59	46	36
VS %TS	88	86	87	86	89	85	87	87	88	83	83	76
ASH %TS	12	14	13	14	11	15	13	13	12	17	17	23
TOC %TS	49	48	48	48	50	47	48	48	49	46	46	43
ρ_{bulk} kg m ⁻³	65	48	50	50	56	53	96	-	61	42	43	53
ω_{bulk} kg m ⁻³	177	105	79	82	145	158	179	-	172	72	93	146
FAS %	83	93	92	92	86	85	83	83	83	93	91	86
Mass kg	40.0	8.5	10.7	2.7	40.1	12.2	14.4	2.7	40.0	8.5	6.2	8.5
TS mass kg	14.6	4.0	7.5	1.7	15.5	4.1	7.7	2.1	14.7	5.0	2.9	3.1
VS mass kg	12.8	3.5	6.5	1.4	13.8	3.5	6.7	1.8	12.9	4.2	2.4	2.3
Chemical analyses												
TN %TS	2.3	2.0	2.0	2.0	2.6	2.1	2.4	2.5	2.7	3.0	3.4	3.1
AN %TS	0.5	1.0	0.7	0.8	0.5	0.5	0.9	1.1	0.6	2.2	1.7	1.2
ON %TS	1.7	1.0	1.3	1.2	2.1	1.6	1.5	1.4	2.1	0.7	1.7	1.9
C:N	22	24	25	25	19	23	20	19	19	16	14	14
COD %TS	43	25	25	25	25	25	44	39	16	18	38	12
pH wet	7.6		8.1		6.2	6.7	6.1	7.4	5.5	7.8	7.8	7.9
pH dry	7.1		7.8		4.8	7.1	7.0	7.7	4.4	6.9	7.7	7.5

Table A6.9. Analysis of the initial and final (composted) organic material in Trial 2 (C:N 25)

Date	Reactor 1 (pH 6)				Reactor 2 (pH 8)				Reactor 3 (pH 7)			
31/12/01 to 14/01/02	Initial	Final			Initial	Final			Initial	Final		
		Top	Mid	Base		Top	Mid	Base		Top	Mid	Base
Microbial population counts log ₁₀ CFU g ⁻¹ TS												
General	6.6	7.3	4.8	4.7	6.1	7.5	7.0	6.9	6.3	3.3	4.2	4.3
Coliform	6.3	clear	clear	Clear	6.0	clear	clear	clear	6.2	clear	clear	clear
Physical analyses												
MC %	63	66	68	57	65	47	71	47	63	66	66	20
TS %	37	34	32	43	35	53	29	53	37	34	34	80
VS %TS	87	86	86	82	88	86	83	87	87	87	85	88
ASH %TS	13	14	17	15	12	14	17	13	12	13	15	12
TOC %TS	49	48	46	47	49	48	46	48	49	48	47	49
ρ _{bulk} kg m ⁻³	49	48	51	53	49	47	49	45	49	51	47	39
ω _{bulk} kg m ⁻³	107	149	142	140	107	127	113	100	107	145	82	50
FAS %	95	96	95	95	95	96	95	96	95	95	96	96
Mass kg	37.4	11.9	9.0	8.3	37.3	10.3	10.0	4.9	37.3	13.1	8.6	5.4
TS mass kg	13.9	4.0	2.8	3.6	13.1	5.5	2.9	2.6	13.8	4.5	3.0	4.3
VS mass kg	12.2	3.5	2.3	3.0	11.5	4.7	2.5	2.2	12.1	3.9	2.5	3.8
Chemical analyses												
TN %TS	2.3	2.4	3.2	3.3	2.3	1.8	3.8	2.1	2.3	2.2	2.8	2.2
AN %TS	0.6	1.0	1.4	1.0	0.5	0.7	0.8	0.4	0.9	0.3	0.5	0.3
ON %TS	1.7	1.4	1.8	2.4	1.8	1.1	3.0	1.7	1.4	1.9	2.3	1.9
C:N	22	20	15	15	22	26	12	23	22	22	17	22
COD %TS	41	38	37	28	47	39	16	18	45	28	30	23
PH wet	6.9	7.9	7.4	7.0	7.0	8.2	8.3	7.9	6.6	8.3	8.3	7.2
PH dry	5.1	7.4	6.8	6.9	7.5	7.6	8.1	7.6	5.8	8.3	8.1	6.9

Table A6.10. Analysis of the initial and final (composted) organic material in Trial 3 (C:N 15)

Date	Reactor 1 (pH 7)				Reactor 2 (pH 6)				Reactor 3 (pH 8)			
18/02/02 to 06/03/02	Initial	Final			Initial	Final			Initial	Final		
		Top	Mid	Base		Top	Mid	Base		Top	Mid	Base
Microbial population counts \log_{10} CFU g ⁻¹ TS												
General	5.4	5.0	3.4	3.4	6.7	3.4	2.6	2.6	5.5	3.7	5.0	5.1
Coliform	6.9	clear	clear	clear	7.4	clear	clear	clear	5.2	clear	clear	clear
Physical analyses												
MC %	64	58	66	66	62	64	58	57	63	66	67	64
TS %	36	42	34	34	38	36	42	43	37	34	33	36
VS %TS	87	73	84	84	88	85	82	82	87	83	85	85
ASH %TS	13	27	16	15	12	15	18	22	13	17	15	15
TOC %TS	48	41	46	47	49	47	46	43	49	46	47	47
ρ_{bulk} kg m ⁻³	62	60	57	58	62	70	67	68	63	59	55	54
ω_{bulk} kg m ⁻³	173	132	138	175	165	197	163	170	171	139	145	161
FAS %	84	88	87	87	85	83	86	86	84	87	87	87
Mass kg	45.1	13.3	12.7	15.6	46.6	11.5	10.6	11.8	46.4	14.2	11.4	16.4
TS mass kg	16.2	5.6	4.3	5.3	17.5	4.2	4.5	5.0	17.0	4.8	3.7	5.9
VS mass kg	14.2	4.1	3.6	4.5	15.3	3.5	3.7	3.9	14.9	4.0	3.2	5.0
Chemical analyses												
TN %TS	3.9	4.5	4.5	4.5	3.3	3.8	3.7	3.6	3.7	4.0	4.1	4.3
AN %TS	0.7	1.5	1.9	2.0	1.0	1.3	1.2	1.3	1.0	1.7	1.8	1.5
ON %TS	3.2	3.0	2.6	2.5	2.3	2.5	2.5	2.3	2.7	2.3	2.2	2.8
C:N	13	9	10	11	15	12	12	13	13	11	11	11
COD %TS	71	43	51	51	68	55	40	40	84	55	68	72
pH wet	6.9	8.2	8.8	8.8	6.2	8.9	8.6	8.6	7.8	8.9	8.9	9.0
pH dry	6.8	9.0	9.5	9.6	3.5	9.3	9.2	9.3	7.0	9.4	9.4	9.3

Table A6.11. Analysis of the initial and final (composted) organic material in Trial 4 (C:N 20)

Date	Reactor 1 (pH 7)				Reactor 2 (pH 6)				Reactor 3 (pH 8)			
13/04/02 to 28/04/02	Initial	Final			Initial	Final			Initial	Final		
		Top	Mid	Base		Top	Mid	Base		Top	Mid	Base
Microbial population counts \log_{10} CFU g ⁻¹ TS												
General	5.2	4.3	5.3	5.3	5.7	-	5.2	5.3	5.5	4.7	4.4	4.5
Coliform	3.2	clear	4.1	clear	3.25	clear	clear	clear	3.4	clear	clear	clear
Physical analyses												
MC %	60	59	59	65	59	53	61	64	61	53	58	53
TS %	40	41	41	35	41	47	39	36	39	47	42	47
VS %TS	88	76	88	88	87	87	86	86	88	85	84	84
ASH %TS	12	24	12	15	13	13	14	14	12	15	16	16
TOC %TS	49	42	49	47	48	48	48	48	49	47	47	46
ρ_{bulk} kg m ⁻³	47	63	60	55	51	55	58	59	54	54	52	53
ω_{bulk} kgm ⁻³	117	153	138	160	124	117	149	163	138	114	124	112
FAS %	96	92	93	94	96	95	95	95	87	95	95	95
Mass kg	37.8	14.0	9.1	10.1	38.1	11.7	9.8	8.9	37.6	10.8	11.1	9.1
TS mass kg	15.2	5.7	3.8	3.5	15.6	5.5	3.8	3.2	14.6	5.1	3.8	3.8
VS mass kg	13.4	4.4	3.3	3.0	13.6	4.8	3.3	2.7	12.8	4.3	3.2	3.2
Chemical analyses												
TN %TS	2.8	3.9	3.2	3.1	2.8	2.7	2.9	2.8	2.9	3.5	3.1	3.0
AN %TS	0.6	1.3	1.5	1.3	0.5	1.2	1.2	1.1	0.6	1.4	1.4	1.3
ON %TS	2.2	2.7	1.7	1.8	2.3	1.5	1.7	1.7	2.3	2.1	1.7	1.7
C:N	18	11	16	16	17	18	17	17	17	13	15	15
COD %TS	69	64	62	61	63	54	65	65	70	43	43	42
pH wet	6.1	8.7	8.6	8.5	5.8	5.7	6.1	6.0	6.6	8.7	8.7	8.7
pH dry	5.2	8.6	8.4	8.5	5.2	4.1	5.6	6.0	5.3	8.0	8.3	8.1

Table A6.12. Analysis of the initial and final (composted) organic material in Trial 5 (C:N 25)

Date		Reactor 1 (pH 8)			Reactor 2 (pH 7)				Reactor 3 (pH 6)			
13/04/02 to 28/04/02	Initial	Final			Initial	Final			Initial	Final		
		Top	Mid	Base		Top	Mid	Base		Top	Mid	Base
Microbial population counts log ₁₀ CFU g ⁻¹ TS												
General	5.7	2.5	3.4	3.3	5.6	2.2	5.2	5.3	5.9	4.0	4.7	4.8
Coliform	6.7	clear	clear	clear	4.3	clear	clear	clear	3.8	clear	clear	clear
Physical analyses												
MC %	64	56	50	58	62	50	60	63	64	65	60	52
TS %	36	44	50	42	38	50	40	37	36	35	40	48
VS %TS	90	86	87	83	89	86	83	87	89	85	88	89
ASH %TS	10	14	13	17	11	14	17	13	11	15	12	11
TOC %TS	50	48	49	46	49	48	46	48	49	47	49	49
ρ _{bulk} kg m ⁻³	49	54	54	55	52	57	60	62	54	48	53	55
ω _{bulk} kg m ⁻³	135	120	153	131	137	138	172	168	150	103	111	115
FAS %	95	96	97	95	96	94	95	95	95	96	95	94
Mass kg	37.5	8.0	10.8	4.7	37.7	9.3	9.9	7.4	37.7	9.7	9.7	6.0
TS mass kg	13.6	3.6	5.4	2.0	14.2	4.6	4.0	2.8	13.5	3.4	3.9	2.9
VS mass kg	12.2	3.1	4.7	1.6	12.6	4.0	3.3	2.4	12.0	2.9	3.4	2.6
Chemical analyses												
TN %TS	2.2	2.7	2.2	2.3	2.3	2.7	3.7	3.8	2.4	2.3	3.1	3.1
AN %TS	0.6	0.4	0.6	0.5	0.6	0.5	1.0	1.0	0.6	1.2	0.8	0.7
ON %TS	1.6	2.3	1.6	1.8	1.7	2.2	2.7	2.8	1.8	1.1	2.3	2.4
C:N	23	18	22	22	22	18	12	12	21	21	16	16
COD %TS	32	31	36	37	53	37	44	43	41	36	47	46
pH wet	6.9	7.8	8.1	8.1	6.9	8.0	8.0	8.0	6.0	7.5	7.8	7.8
pH dry	7.2	7.7	7.8	7.8	6.2	7.7	7.4	7.4	5.9	7.1	7.6	7.5

Table A6.13. Analysis of the initial and final (composted) organic material Trial 6 (C:N 15)

Date	Reactor 1 (pH 6)				Reactor 2 (pH 8)				Reactor 3 (pH 7)			
27/08/02 to 10/09/02	Initial	Final			Initial	Final			Initial	Final		
		Top	Mid	Base		Top	Mid	Base		Top	Mid	Base
Microbial population counts \log_{10} CFU g ⁻¹ TS												
General	6.8	4.4	4.9	5.0	6.3	5.1	4.2	4.0	6.0	5.1	5.8	5.0
Coliform	6.6	2.7	5.8	6.2	4.6	clear	clear	clear	4.3	2.2	2.5	2.6
Physical analyses												
MC %	65	60	61	66	65	60	57	57	65	64	64	60
TS %	35	40	39	34	35	40	43	43	35	36	36	40
VS %TS	87	85	85	85	87	83	85	84	88	86	86	86
ASH %TS	13	15	15	15	13	17	15	16	12	14	14	14
TOC %TS	48	47	47	47	48	46	47	47	49	48	48	48
ρ_{bulk} kg m ⁻³	68	60	60	60	68	67	69	69	63	63	63	64
ω_{bulk} kg m ⁻³	196	173	158	178	181	158	188	160	195	206	203	165
FAS %	93	96	96	96	94	93	93	93	94	94	94	94
Mass kg	46.3	14.2	13.3	11.0	47.0	9.6	12.2	12.6	47.1	13.3	4.7	4.1
TS mass kg	16.2	5.7	5.2	3.6	16.3	3.8	5.3	5.4	16.4	4.7	5.2	5.7
VS mass kg	14.1	4.9	4.4	3.2	14.2	3.2	4.5	4.6	14.3	4.1	4.5	4.9
Chemical analyses												
TN %TS	3.6	3.5	4.2	4.0	3.3	3.2	3.4	3.3	3.6	2.9	3.0	3.0
AN %TS	1.6	1.8	2.8	2.0	1.3	1.0	0.8	1.0	1.1	2.0	2.0	2.1
ON %TS	2.0	1.7	1.4	2.0	2.0	2.2	2.6	2.3	2.5	0.9	1.0	0.9
C:N	13	14	11	11	15	14	14	14	13	16	16	16
COD %TS	58	47	59	71	73	65	57	49	68	51	46	47
pH wet	7.5	8.8	8.9	9.0	7.8	8.8	8.8	8.8	7.1	9.0	9.0	9.1
pH dry	8.4	-	-	-	8.9	-	-	-	8.2	-	-	-

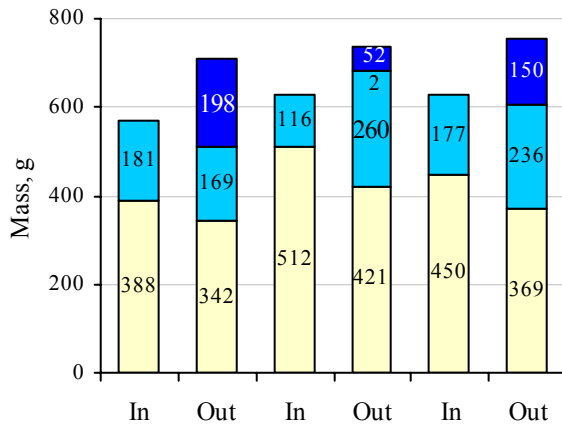
A6.3. Nitrogen dynamics

Table A6.14. Ammonia emissions and associated process variables

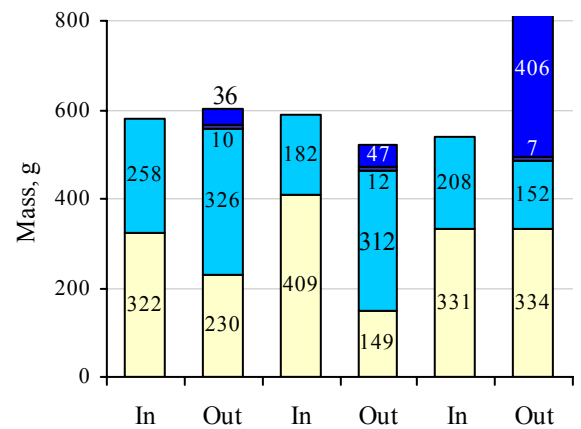
Trial	pH	Mass NH₃ g	Mass NH₃-N % Amm-N	Mass NH₃-N % Tot-N	Mean air flow rate l h⁻¹	Mean temperature (σ)¹ °C	Duration¹ Days	Emission rate² g day⁻¹
3	6	238	109	35	390	54.9 (2.9)	13.8	16.6
C:N = 15	7	63	45	8	100	40.6 (1.0)	13.5	4.3
M:S = 4:1	8	181	84	24	160	49.3 (1.8)	12.5	13.3
6	6	44	14	6	130	47.5 (2.0)	8.6	4.7
C:N = 15	7	57	26	6	135	42.3 (1.4)	11.6	4.5
M:S = 4:1	8	494	195	75	615	51.7 (3.1)	8.6	52.8
1	6	18	15	4	102	52.5 (1.1)	38.5	0.5
C:N = 20	7	6	6	1	137	53.0 (0.6)	32.1	0.2
M:S = 3:1	8	46	49	11	258	60.7 (1.9)	10.1	4.2
4	6	0	0	0	100	47.2 (1.1)	13.8	0.0
C:N = 20	7	22	20	4	101	38.2 (0.8)	13.0	1.5
M:S = 3:1	8	36	33	7	102	42.9 (0.8)	13.7	2.6
2	6	12	13	3	207	51.7 (1.6)	11.8	1.1
C:N = 25	7	54	37	14	760	55.6 (2.3)	10.9	4.7
M:S = 2:1	8	103	136	28	520	52.7 (3.2)	8.0	15.5
5	6	46	48	12	516	54.1 (2.2)	11.4	3.6
C:N = 25	7	129	116	33	303	51.2 (2.9)	8.4	14.8
M:S = 2:1	8	173	168	48	366	55.6 (1.5)	8.4	19.3

¹ standard deviation of temperature from the mean (spatially and temporally)

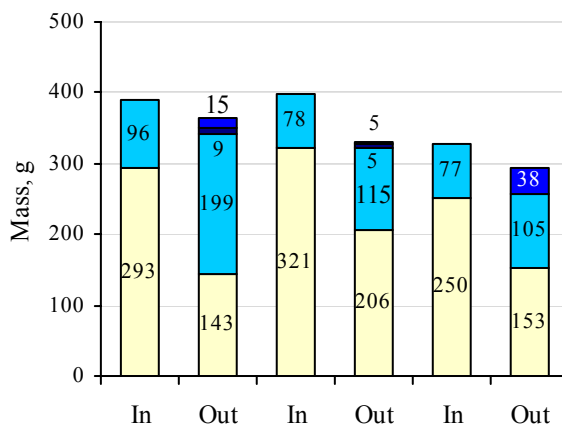
a) Trial 3



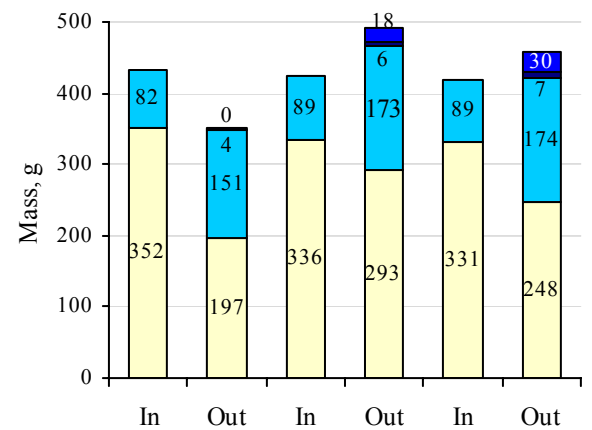
b) Trial 6



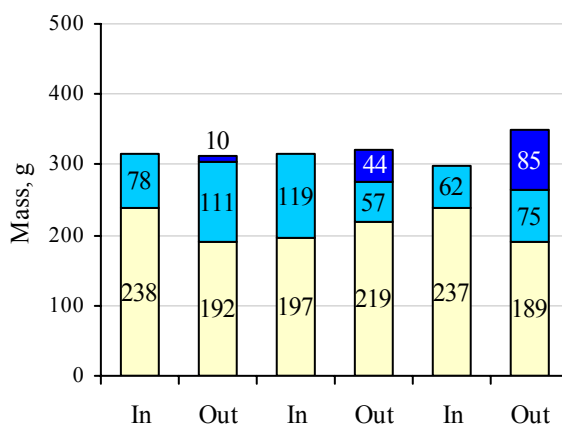
c) Trial 1



d) Trial 4



e) Trial 2



f) Trial 5

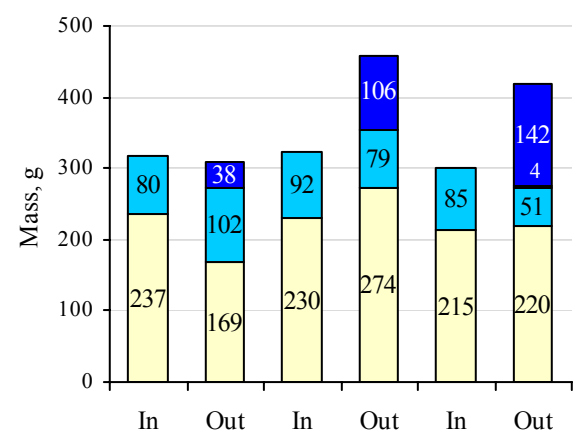


Figure A6.22. Nitrogen inputs and outputs

ON AN LN NH₃(g)

A6.4. *Genstat* (Version 6) statistical analysis

A6.4.1. Input data

Table A6.15. Input data for *Genstat* (Version 6) statistical analysis

C:N	pH	R	pH-meas. ¹	TS loss %kg	Airflow l h ⁻¹	T-NH ₃ °C	NH ₃ rate ² mg (g day) ⁻¹	T≥55 ³ days	Mean T ⁴ °C	Paths ⁵	Unit ⁶
15	6	2	6.2	22	389	54.9	26.1	14	54.2	0	7
15	7	1	6.9	7	100	40.6	7.6	0	39.6	0	8
15	8	3	7.8	15	160	49.3	22.4	4	49.0	0	9
15	6	1	7.5	9	131	47.5	8.6	3	40.9	0	16
15	7	3	7.1	4	135	42.3	8.2	12	40.7	1	17
15	8	2	7.8	11	358	51.7	44.7	5	51.8	1	18
20	6	3	5.5	25	102	52.5	1.2	8	51.9	1	1
20	7	2	6.2	10	137	53.0	0.4	10	51.3	1	2
20	8	1	7.6	10	258	60.7	11.8	7	53.1	0	3
20	6	2	5.8	20	100	47.2	0.0	12	47.8	0	10
20	7	1	6.1	15	101	38.2	3.5	5	38.0	1	11
20	8	3	6.6	13	102	42.9	6.4	8	41.6	0	12
25	6	1	6.0	25	214	51.6	3.1	14	46.3	0	4
25	7	3	6.6	15	474	52.7	14.9	15	50.5	0	5
25	8	2	7.5	16	387	55.6	40.9	10	53.0	0	6
25	6	3	6.6	24	516	55.6	12.6	11	55.2	0	13
25	7	2	6.9	21	303	51.1	45.5	12	52.5	0	14
25	8	1	7.2	20	366	54.1	63.5	11	54.2	0	15

¹ The measured pH of the organic material before composting

² The mean ammonia emission rate during the time leading up to 95 % of the total mass emitted. The Airflow and T-NH₃ values correspond to this period

³ The time for which the temperature was ≥55 °C

⁴ The mean temperature of the organic material over the composting period

⁵ Paths refers to the pathogen markers

⁶ The unit is the data that the statistical analyses make reference to

Figure A6.3 shows the main *Genstat* (Version 6) window in with the spreadsheet containing the eighteen sets (Row column) of experimental data (Table A6.15), which is in the view behind the ANOVA window. The ANOVA window is encoded to assess the significance of the individual and combined effects of the C:N ratio (CN) and pH on the percentage loss (dMTS%).

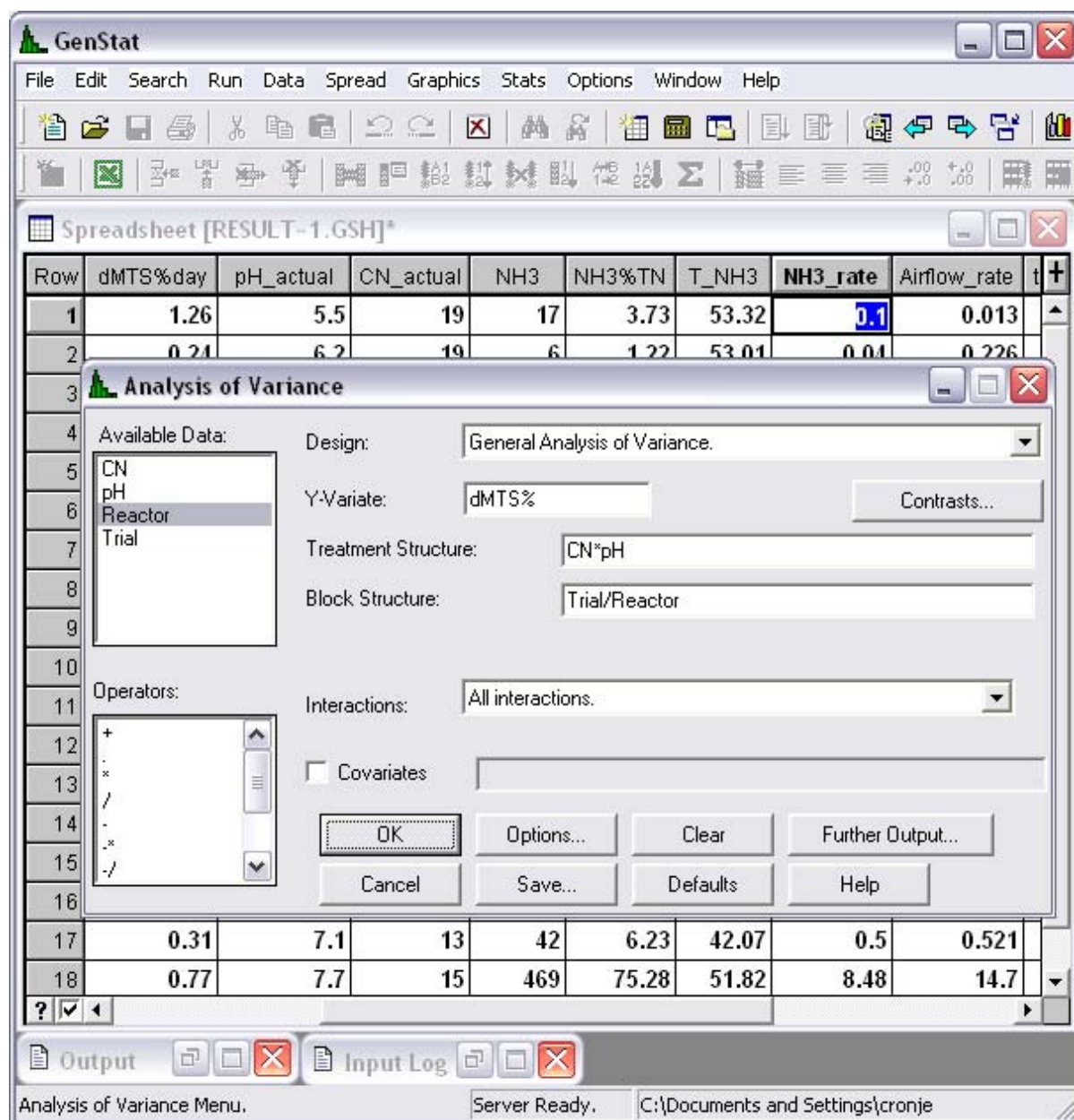


Figure A6.23. Main view and statistical analysis window in *Genstat* (Version 6).

A6.4.2. Output from statistical analysis

After running the statistical analysis, an Output window reports the details and results of the statistical test (Figure A6.24). The terms used in the *Genstat* (Version 6) Output are defined in Table A6.16.

Table A6.16. The meaning of the statistical terms used in the *Genstat* (versions 6) output

Abbreviation	Full term	Meaning
d.f	Degrees of freedom	The number of extra independent parameters included when a term is added into an analysis of variance, regression or generalised linear model.
s.s	Sum of squares	The sum of the squared values of a variable.
m.s.	Mean square	The variance attributed to the linear dependence on the fitted term. The ratio of the sum of squares and the degrees of freedom.
	Residual	The difference between the ‘true’ value of a variable and the value that was observed e.g. in an experiment. The difference is assumed to have arisen because of random variance.
v.r	Variance ratio	The ratio of the mean square for a term in an analysis of variance and the appropriate residual of the mean squares.
F pr.	Probability factor	The probability of the variance ratio value occurring by chance if there is no relationship between the variables, assuming that it has an F distribution (i.e. making the usual ANOVA assumption that the residuals are from independent of normal distributions with equal variances).
Vaf	Variance account for	A summary of how much of the variability of the set of response measurements can be attributed to the fitted model. The difference between the residual and total mean squares expressed as a percentage of the total mean squares.
s.e	Standard error of the mean	The error in the mean results from random variations in the data points. Based here on the residual mean square.
t(n)	t-statistic	Indicates the significance of the association between the variate and the fitted term for n degrees of freedom.
t pr.	t-probability	The probability of the t-statistic value occurring by chance if there is no relationship between the variables.
	Leverage	The influence of an observation. A large value indicates that the fit of the model strongly depends on the particular observation

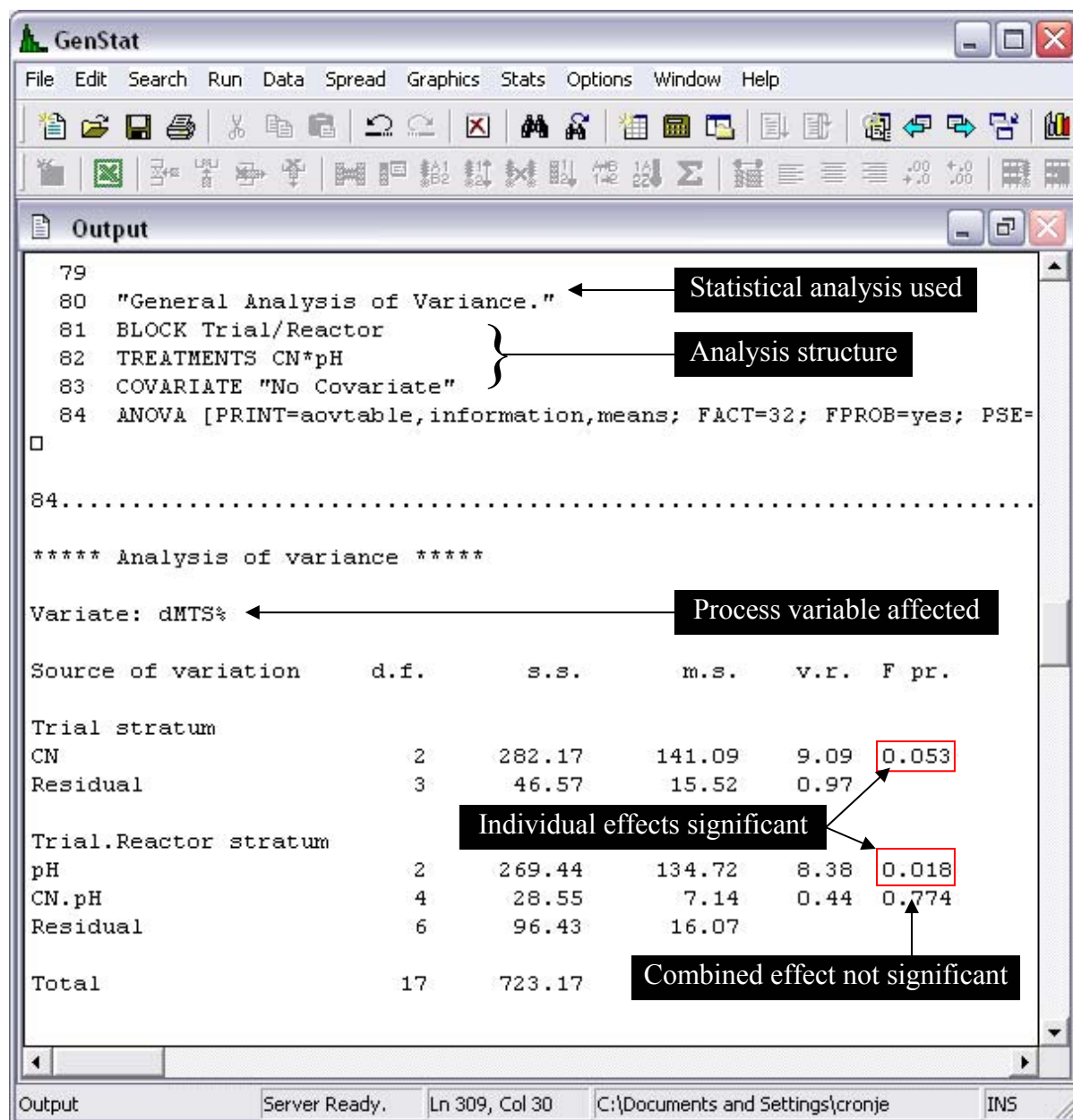


Figure A6.24. The Output view in *Genstat* (Version 6)

A6.4.2.1. Ammonia emissions

"General Analysis of Variance."

***** Analysis of variance *****

BLOCK Trial/Reactor

TREATMENTS CN*pH

ANOVA NH3rate

Variate: NH3rate

*** Summary of analysis ***

Source of variation	d. f.	s. s.	m. s.	v. r.	F pr.
Trial stratum					
CN	2	2078.51	1039.25	4.74	0.118
Residual	3	657.51	219.17	2.49	
Trial.Reactor stratum					
pH	2	1774.83	887.41	10.06	0.012
CN.pH	4	950.15	237.54	2.69	0.134
Residual	6	529.04	88.17		
Total	17	5990.04			

***** Tables of means *****

Grand mean 17.9

CN	15	20	25
	19.6	3.9	30.1
pH	6	7	8
	8.6	13.3	31.6

		pH	
CN	6	7	8
15	17.4	7.9	33.6
20	0.6	2.0	9.1
25	7.9	30.1	52.2

*** Standard errors of differences of means ***

Table	CN	pH	CN.pH
rep.	6	6	2
s. e. d.	8.55	5.42	11.48
d. f.	3	6	7.38

Except when comparing means with the same level (s) of
CN
d. f. 9. 39
6

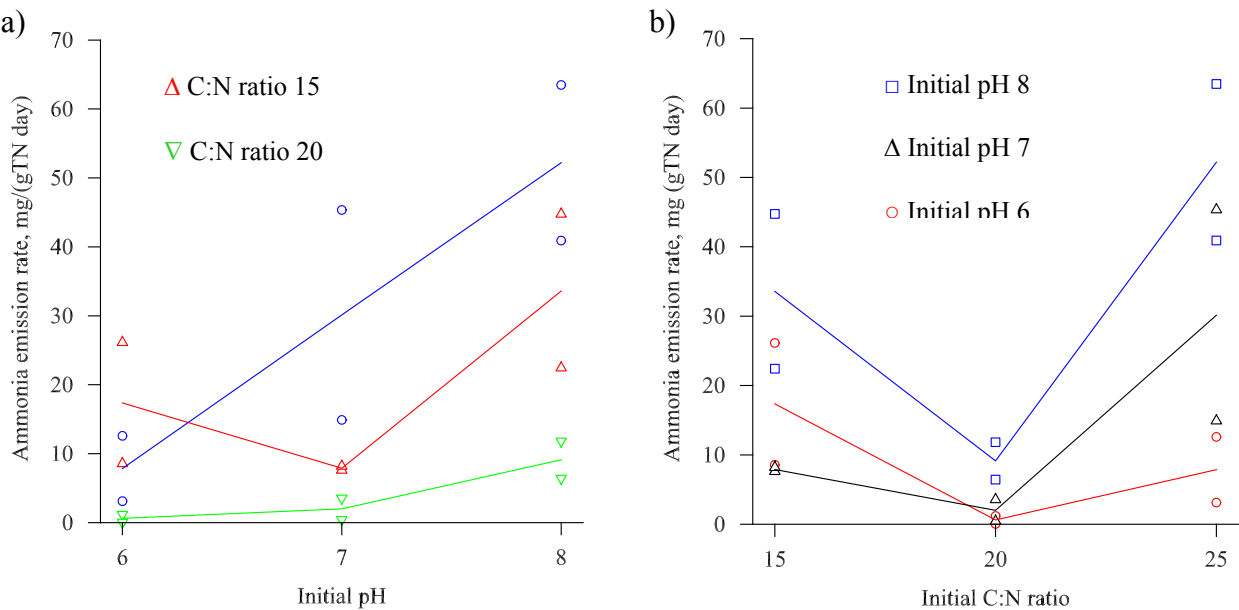


Figure A6.25. The mean values of the ammonia emissions for the initial pH (a) and C:N ratio (b) of the organic material groups.

***** Regression Analysis *****

"Simple Linear Regression"

MODEL NH3rate
TERMS pH-measured
FIT pH-measured

Response variate: NH3rate
Fitted terms: Constant, pH-measured

*** Summary of analysis ***

	d. f.	s. s.	m. s.	v. r.	F pr.
Regression	1	1802.	1802. 2	6. 89	0. 018
Resi dual	16	4188.	261. 7		
Total	17	5990.	352. 4		

Percentage variance accounted for 25.7

Standard error of observations is estimated to be 16.2

* MESSAGE: The following units have large standardized residuals:

Unit	Response	Residual
15	63.5	2.54

* MESSAGE: The following units have high leverage:

Unit	Response	Leverage
1	1.2	0.25

*** Estimates of parameters ***

	estimate	s.e.	t(16)	t pr.
Constant	-80.5	37.7	-2.14	0.048
pH-measured	14.53	5.54	2.62	0.018

.....

"Simple Linear Regression"

MODEL NH3rate

TERMS Airflow

FIT Airflow

Response variate: NH3rate

Fitted terms: Constant, Airflow

*** Summary of analysis ***

	d. f.	S. S.	m. S.	v. r.	F pr.
Regression	1	2054	2053.6	8.35	0.011
Residual	16	3936	246.0		
Total	17	5990	352.4		

Percentage variance accounted for 30.2

Standard error of observations is estimated to be 15.7

* MESSAGE: The following units have large standardized residuals:

Unit	Response	Residual
15	63.5	2.42

* MESSAGE: The following units have high leverage:

Unit	Response	Leverage
13	12.6	0.27

*** Estimates of parameters ***

	estimate	s. e.	t(16)	t pr.
Constant	-0.68	7.41	-0.09	0.928
Airflow	0.0770	0.0267	2.89	0.011

"Simple Linear Regression"

MODEL NH3rate

TERMS T-NH3

FIT T-NH3

Response variate: NH3rate

Fitted terms: Constant, T-NH3

*** Summary of analysis ***

	d. f.	s. s.	m. s.	v. r.	F pr.
Regression	1	660.	660.1	1.98	0.178
Residual	16	5330.	333.1		
Total	17	5990.	352.4		

Percentage variance accounted for 5.5

Standard error of observations is estimated to be 18.3

* MESSAGE: The following units have large standardized residuals:

Unit	Response	Residual
15	63.5	2.37

* MESSAGE: The following units have high leverage:

Unit	Response	Leverage
3	11.8	0.24
11	3.5	0.29

*** Estimates of parameters ***

	estimate	s. e.	t(16)	t pr.
Constant	-34.7	37.6	-0.92	0.370
T-NH3	1.049	0.745	1.41	0.178

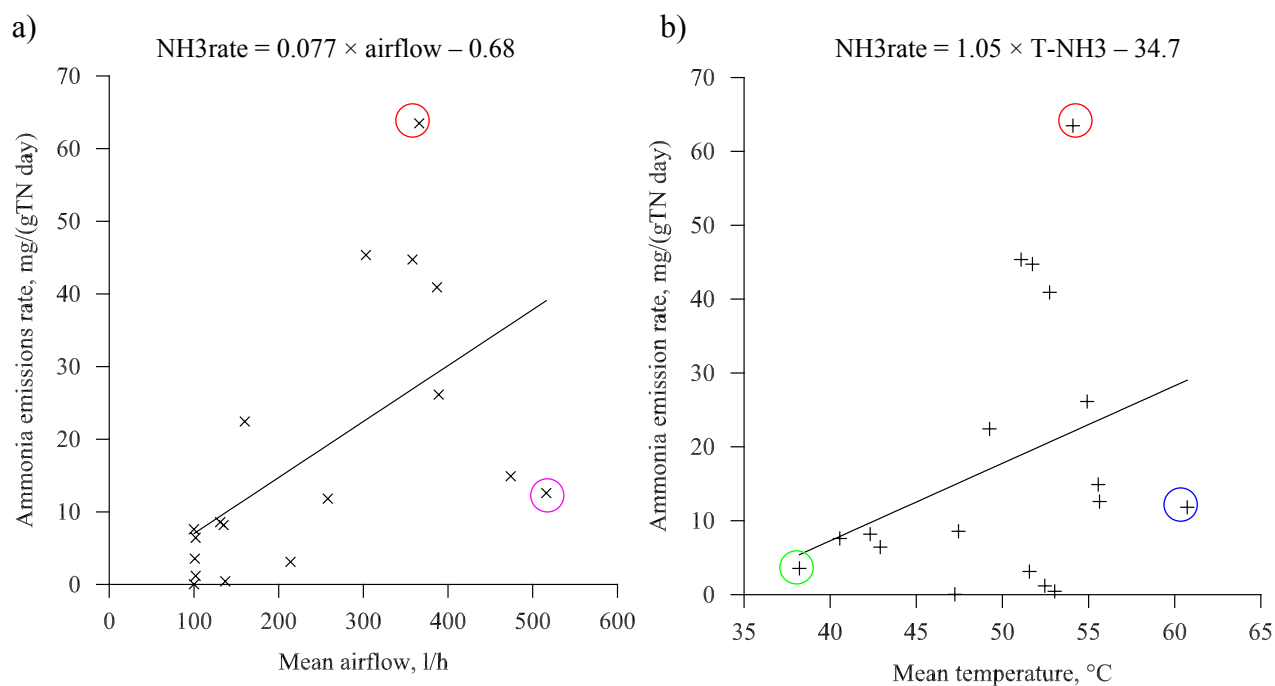


Figure A6.26. The relationship between the ammonia emission rate and the mean airflow and temperature.

"Simple Linear Regression with Groups"

MODEL NH3rate
TERMS Airflow*CN
FIT Airflow

Response variate: NH3rate
Fitted terms: Constant + Airflow

*** Summary of analysis ***

	d. f.	s. s.	m. s.	v. r.	F pr.
Regression	1	2054	2053.6	8.35	0.011
Residual	16	3936	246.0		
Total	17	5990	352.4		

Percentage variance accounted for 30.2

Standard error of observations is estimated to be 15.7

* MESSAGE: The following units have large standardized residuals:

Unit	Response	Residual
15	63.5	2.42

* MESSAGE: The following units have high leverage:

Unit	Response	Leverage
13	12.6	0.27

*** Estimates of parameters ***

	estimate	s.e.	t(16)	t pr.
Constant	-0.68	7.41	-0.09	0.928
Airflow	0.0770	0.0267	2.89	0.011

ADD_CN

Response variate: NH3rate

Fitted terms: Constant + Airflow + CN

*** Summary of analysis ***

	d. f.	s. s.	m. s.	v. r.	F pr.
Regression	3	2478	826.0	3.29	0.052
Residual	14	3512	250.9		
Total	17	5990	352.4		
Change	-2	-424	212.1	0.85	0.450

Percentage variance accounted for 28.8

Standard error of observations is estimated to be 15.8

* MESSAGE: The following units have large standardized residuals:

Unit	Response	Residual
15	63.5	2.35

*** Estimates of parameters ***

	estimate	s.e.	t(14)	t pr.
Constant	9.0	10.6	0.85	0.407
Airflow	0.0498	0.0395	1.26	0.228
CN 20	-11.77	9.66	-1.22	0.243
CN 25	2.3	11.2	0.20	0.843

Parameters for factors are differences compared with the reference level:

Factor	Reference level
CN	15

ADD CN. Airflow

Response variate: NH3rate

Fitted terms: Constant + Airflow + CN + Airflow.CN

*** Summary of analysis ***

	d. f.	s. s.	m. s.	v. r.	F pr.
Regression	5	2912.	582. 4	2. 27	0. 114
Residual	12	3078.	256. 5		
Total	17	5990.	352. 4		
Change	-2	-434.	217. 0	0. 85	0. 453

Percentage variance accounted for 27.2

Standard error of observations is estimated to be 16.0

* MESSAGE: The following units have large standardized residuals:

Unit	Response	Residual
4	3.1	-2.90
15	63.5	2.28

* MESSAGE: The following units have high leverage:

Unit	Response	Leverage
3	11.8	0.96

*** Estimates of parameters ***

	estimate	s. e.	t(12)	t pr.
Constant	-1.0	13.7	-0.07	0.944
Airflow	0.0970	0.0565	1.72	0.112
CN 20	-2.7	21.5	-0.13	0.902
CN 25	36.6	28.7	1.27	0.227
Airflow.CN 20	-0.040	0.127	-0.31	0.759
Airflow.CN 25	-0.1117	0.0860	-1.30	0.218

Parameters for factors are differences compared with the reference level:

Factor	Reference level
CN	15

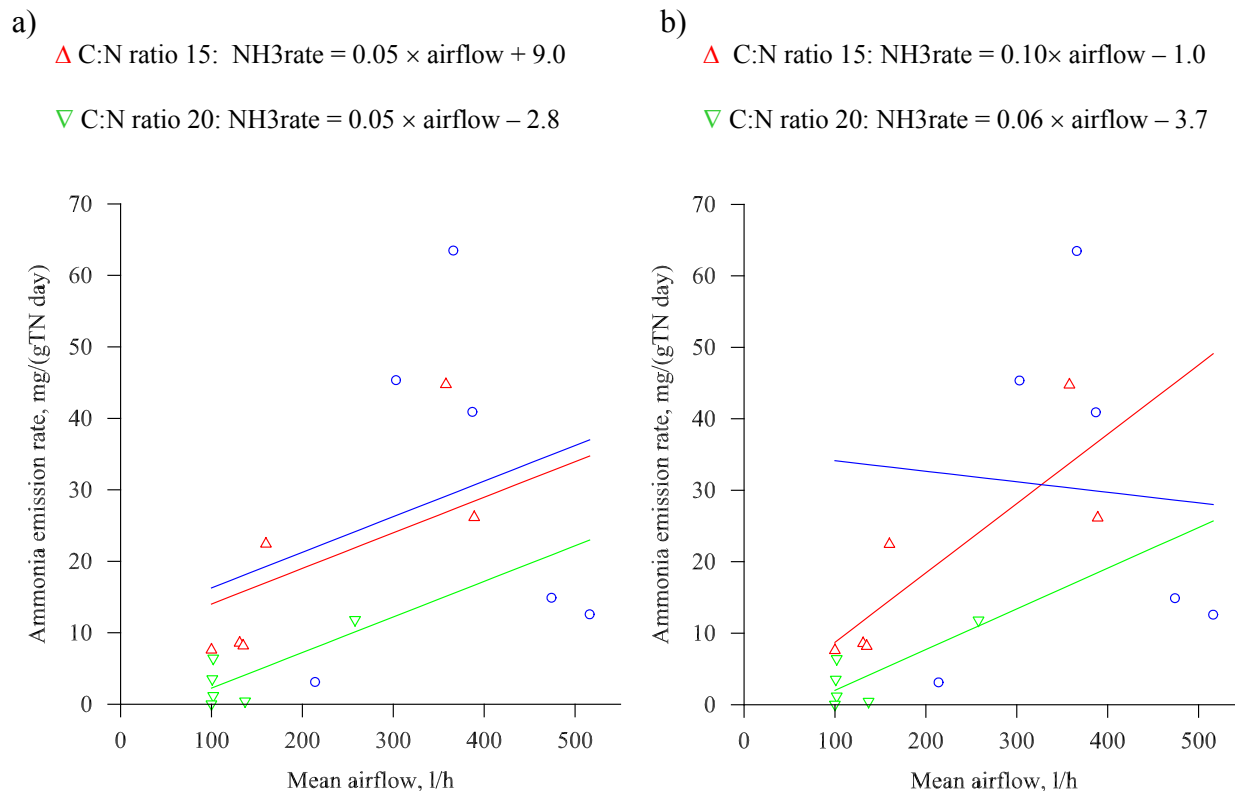


Figure A6.27. The relationship between the ammonia emission rate and the mean airflow in initial pH groups: a) parallel lines b) separate lines

"Simple Linear Regression with Groups"

MODEL NH3rate
 TERMS Airflow*pH
 FIT Airflow

Response variate: NH3rate
 Fitted terms: Constant + Airflow

*** Summary of analysis ***

	d. f.	s. s.	m. s.	v. r.	F pr.
Regression	1	2054	2053.6	8.35	0.011
Residual	16	3936	246.0		
Total	17	5990	352.4		

Percentage variance accounted for 30.2

Standard error of observations is estimated to be 15.7

* MESSAGE: The following units have large standardized residuals:

Unit	Response	Residual
15	63.5	2.42

* MESSAGE: The following units have high leverage:

Unit	Response	Leverage
13	12.6	0.27

*** Estimates of parameters ***

	estimate	s.e.	t(16)	t pr.
Constant	-0.68	7.41	-0.09	0.928
Airflow_rate	0.0770	0.0267	2.89	0.011

ADD pH

Response variate: NH3rate

Fitted terms: Constant + Airflow + pH

*** Summary of analysis ***

	d.f.	s.s.	m.s.	v.r.	F pr.
Regression	3	3398	1132.5	6.12	0.007
Residual	14	2593	185.2		
Total	17	5990	352.4		
Change	-2	-1344	672.0	3.63	0.054

Percentage variance accounted for 47.4

Standard error of observations is estimated to be 13.6

* MESSAGE: The following units have large standardized residuals:

Unit	Response	Residual
14	45.4	2.08
15	63.5	2.07

*** Estimates of parameters ***

	estimate	s.e.	t(14)	t pr.
Constant	-8.26	7.96	-1.04	0.317
Airflow	0.0697	0.0235	2.96	0.010
pH 7	7.08	7.90	0.90	0.385
pH 8	20.95	7.89	2.66	0.019

Parameters for factors are differences compared with the reference level:

Factor	Reference level
pH	6

ADD pH. Airflow

Response variate: NH3rate

Fitted terms: Constant + Airflow + pH + Airflow.pH

*** Summary of analysis ***

	d. f.	s. s.	m. s.	v. r.	F pr.
Regression	5	4020.	804.0	4.90	0.011
Residual	12	1970.	164.2		
Total	17	5990.	352.4		
Change	-2	-623.	311.3	1.90	0.192

Percentage variance accounted for 53.4

Standard error of observations is estimated to be 12.8

* MESSAGE: The following units have large standardized residuals:

Unit	Response	Residual
5	14.9	-2.30
14	45.4	2.40

* MESSAGE: The following units have high leverage:

Unit	Response	Leverage
5	14.9	0.79
13	12.6	0.67

*** Estimates of parameters ***

	estimate	s. e.	t(12)	t pr.
Constant	-1.23	9.57	-0.13	0.900
Airflow	0.0407	0.0331	1.23	0.243
pH 7	2.8	13.5	0.21	0.841
pH 8	-8.4	17.0	-0.49	0.632
Airflow.pH 7	0.0160	0.0505	0.32	0.757
Airflow.pH 8	0.1110	0.0584	1.90	0.082

Parameters for factors are differences compared with the reference level:

Factor Reference level
pH 6

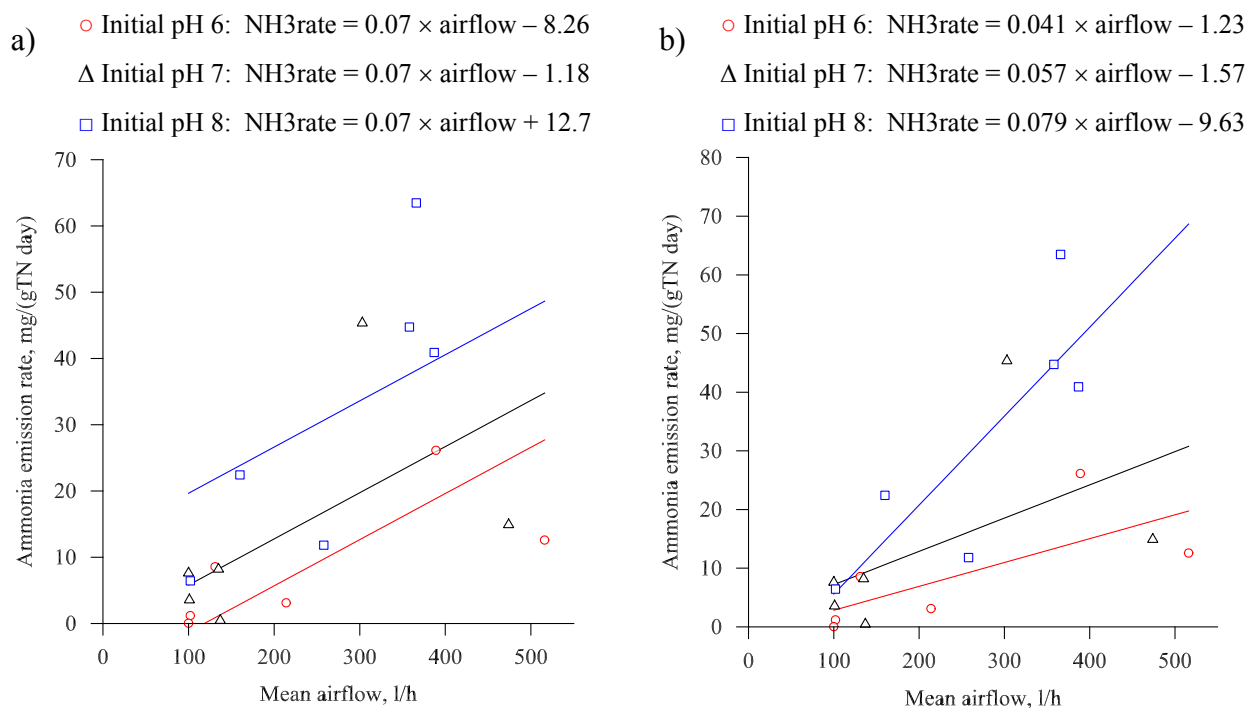


Figure A6.28. The relationship between the ammonia emissions and ammonia emission rate and the airflow rate within the initial pH groups

A6.4.2.2. Pathogen marker inactivation

"Modelling of binomial proportions. (e.g. by logit)."

***** Regression Analysis *****

Response variate: Paths

Binomial totals: 1

Distribution: Binomial

Link function: Logit

Fitted terms: Constant, $T \geq 55^\circ\text{C}$

MODEL Bugs; NBINOMIAL=1

*** Summary of analysis ***

	d. f.	deviance	mean deviance	deviance ratio	approx F pr.
Regression	1	0.33	0.332	0.24	0.634
Residual	16	22.58	1.411		
Total	17	22.91	1.348		

Dispersion parameter is estimated to be 1.25 from the residual deviance

* MESSAGE: The following units have high leverage:

Unit	Response	Leverage
1	1.00	0.36
2	1.00	0.29

*** Estimates of parameters ***

	estimate	s.e.	t(16)	t pr.	antilog of estimate
Constant	-1.12	1.09	-1.03	0.317	0.3253
T \geq 55°C	0.0446	0.0920	0.48	0.634	1.046

* MESSAGE: s.e.s are based on the residual deviance

.....

***** Regression Analysis *****

Response variate: Paths

Binomial totals: 1

Distribution: Binomial

Link function: Logit

Fitted terms: Constant, Mean-T

MODEL Bugs; NBINOMIAL=1

*** Summary of analysis ***

	d.f.	deviance	mean deviance	deviance ratio	approx F pr.
Regression	1	3.71	3.714	3.09	0.098
Residual	16	19.20	1.200		
Total	17	22.91	1.348		

Dispersion parameter is estimated to be 1.26 from the residual deviance

* MESSAGE: The following units have high leverage:

Unit	Response	Leverage
11	1.00	0.22

*** Estimates of parameters ***

	estimate	s.e.	t(16)	t pr.	antilog of estimate
Constant	7.90	5.23	1.51	0.150	2707.
Mean-T	-0.180	0.110	-1.64	0.121	0.8351

* MESSAGE: s.e.s are based on the residual deviance

.....

***** Regression Analysis *****

Response variate: Paths

Binomial totals: 1

Distribution: Binomial

Link function: Logit

Fitted terms: Constant, NH3rate

*** Summary of analysis ***

	d. f.	devi ance	mean devi ance	devi ance rati o	approx F pr.
Regressi on	1	7. 45	7. 4468	7. 70	0. 014
Resi dual	16	15. 47	0. 9667		
Total	17	22. 91	1. 3479		

Dispersion parameter is estimated to be 0.967 from the residual deviance

*** Estimates of parameters ***

	estimate	s. e.	t(16)	t pr.	anti log of estimate
Constant	1. 108	0. 988	1. 12	0. 278	3. 029
NH3rate	-0. 411	0. 266	-1. 55	0. 142	0. 6632

MESSAGE: s. e. s are based on the residual deviance

***** Regression Analysis *****

Response variate: Paths

Binomial totals: 1

Distribution: Binomial

Link function: Logit

Fitted terms: Constant, res-time

*** Summary of analysis ***

	d. f.	devi ance	mean devi ance	devi ance rati o	approx F pr.
Regressi on	1	4. 71	4. 711	4. 55	0. 049
Resi dual	16	16. 56	1. 035		
Total	17	21. 27	1. 251		

Dispersion parameter is estimated to be 1.03 from the residual deviance

* MESSAGE: The following units have high leverage:

Unit	Response	Leverage
1	1.00	0.46
2	1.00	0.46

*** Estimates of parameters ***

	estimate	s.e.	t(16)	t pr.	antilog of estimate
Constant	-3.81	1.94	-1.96	0.067	0.02220
Res-time	0.158	0.112	1.41	0.178	1.171

* MESSAGE: s.e.s are based on the residual deviance

A6.4.2.3. Total solids loss

"General Analysis of Variance."

***** Analysis of variance *****

BLOCK Trial/Reactor
TREATMENTS pH*CN
ANOVA dMTS%

Variate: dMTS%

*** Summary of analysis ***

Source of variation	d.f.	s.s.	m.s.	v.r.	F pr.
Trial stratum					
CN	2	233.66	116.83	4.58	0.122
Residual	3	76.49	25.50	2.03	
Trial.Reactor stratum					
pH	2	250.92	125.46	10.01	0.012
CN.pH	4	54.84	13.71	1.09	0.438
Residual	6	75.19	12.53		
Total	17	691.09			

***** Tables of means *****

Variate: dMTS%

Grand mean	15.66		
CN	15	20	25
	11.40	15.38	20.21
pH	6	7	8
	20.78	11.99	14.22
	pH		
CN	6	7	8
15	15.58	5.60	13.02
20	22.26	12.39	11.49
25	24.51	17.97	18.15

*** Standard errors of differences of means ***

Table	CN	pH	CN. pH
rep.	6	6	2
s. e. d.	2.915	2.044	4.105
d. f.	3	6	7.95

Except when comparing means with the same level(s) of
 CN 3.540
 d. f. 6

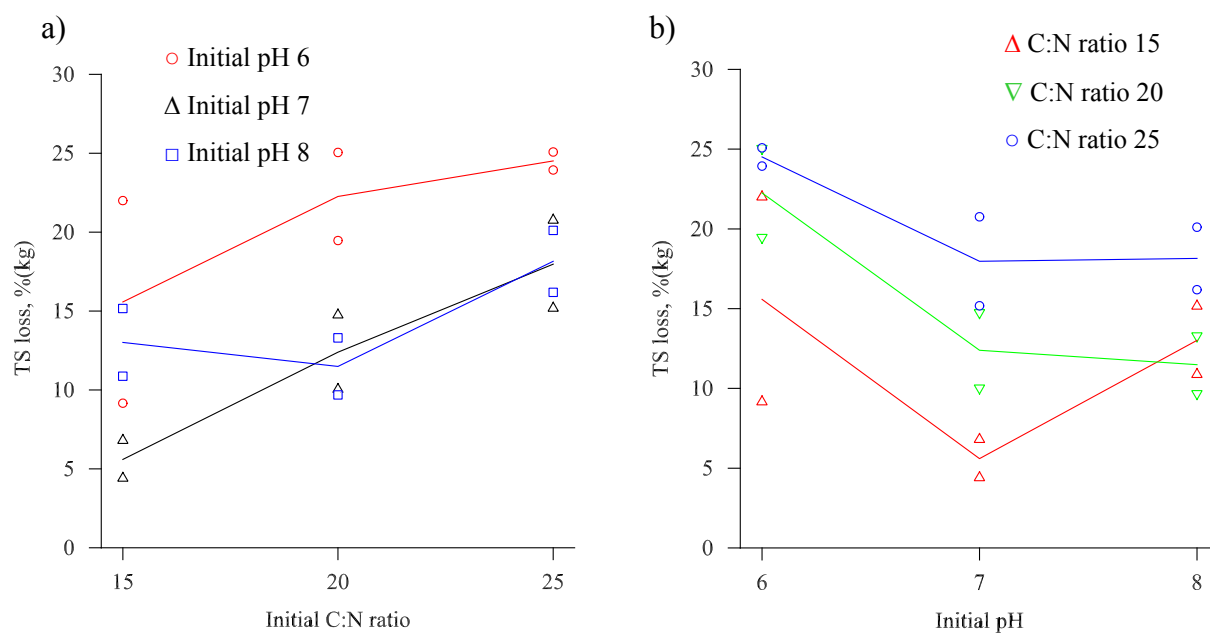


Figure A6.29. The ammonia emissions means for the initial pH (a) and C:N ratio (b) groups.

***** Regression Analysis *****

"Simple Linear Regression"

MODEL dMTS%

TERMS pH-measured

FIT pH-measured

Response variate: dMTS%

Fitted terms: Constant, pH-measured

*** Summary of analysis ***

	d. f.	s. s.	m. s.	v. r.	F pr.
Regression	1	193.6	193.63	6.23	0.024
Residual	16	497.5	31.09		
Total	17	691.1	40.65		

Percentage variance accounted for 23.5

Standard error of observations is estimated to be 5.58

* MESSAGE: The following units have high leverage:

Unit	Response	Leverage
1	25.05	0.25

*** Estimates of parameters ***

	estimate	s. e.	t(16)	t pr.
Constant	47.9	13.0	3.69	0.002
pH-measured	-4.76	1.91	-2.50	0.024

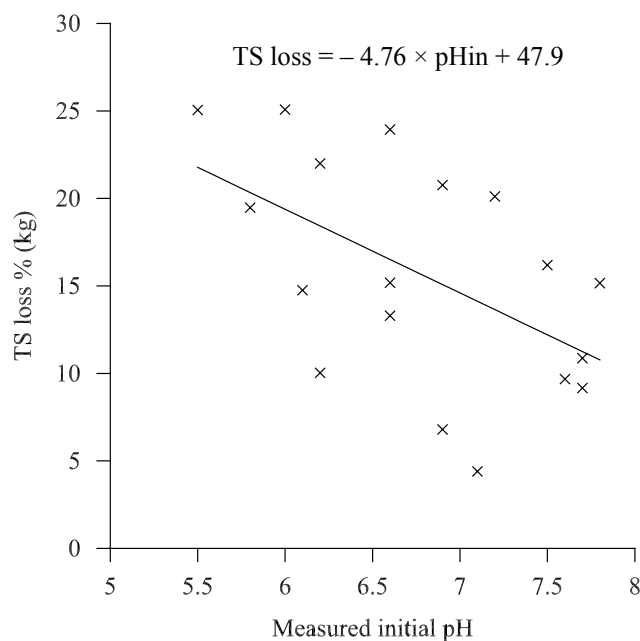


Figure A6.30. The relationship between the TS loss and the measured initial pH.

"Simple Linear Regression"

MODEL dMTS%

TERMS res-time

FIT res-time

Response variate: dMTS%

Fitted terms: Constant, res-time

*** Summary of analysis ***

	d. f.	s. s.	m. s.	v. r.	F pr.
Regression	1	5.9	5.94	0.14	0.714
Residual	16	685.1	42.82		
Total	17	691.1	40.65		

Residual variance exceeds variance of response variate

Standard error of observations is estimated to be 6.54

* MESSAGE: The following units have high leverage:

Unit	Response	Leverage
1	25.05	0.49
2	10.03	0.49

*** Estimates of parameters ***

	estimate	s. e.	t(16)	t pr.
Constant	14.43	3.64	3.97	0.001
Res-time	0.068	0.183	0.37	0.714

.....

"Simple Linear Regression"

MODEL dMTS%

TERMS Mean T

FIT Mean T

Response variate: dMTS%

Fitted terms: Constant, Mean T

*** Summary of analysis ***

	d. f.	s. s.	m. s.	v. r.	F pr.
Regression	1	194.7	194.66	6.27	0.023
Residual	16	496.4	31.03		
Total	17	691.1	40.65		

Percentage variance accounted for 23.7

Standard error of observations is estimated to be 5.57

* MESSAGE: The following units have high leverage:

Unit	Response	Leverage
11	14.75	0.25

*** Estimates of parameters ***

	estimate	s. e.	t(16)	t pr.
Constant	-12.8	11.5	-1.12	0.279
Mean T	0.589	0.235	2.50	0.023

.....

PUBLICATIONS

Proceedings of the 2002 International Symposium on Composting and Compost Utilization

Poster presentation abstract: Oxygen uptake rate of composting pig manure (May 2002).

Authors: Angela L. Cronjé^{1,2}, Claire Turner¹, Adrian G. Williams¹, Andrew J. Barker² and Stuart Guy².

Oral presentation manuscript: Ammonia emissions and pathogen inactivation during composting (May 2002).

Authors: Angela L. Cronjé^{1,2}, Claire Turner¹, Adrian G. Williams¹, Andrew J. Barker² and Stuart Guy².

Compost Science and Utilization

Paper: The respiration rate of composting pig manure (accepted Dec 2002).

Authors: Angela L. Cronjé^{1,2}, Claire Turner¹, Adrian G. Williams¹, Andrew J. Barker² and Stuart Guy².

Environmental Technology

Paper: Composting under controlled conditions (accepted Apr 2003).

Authors: Angela L. Cronjé^{1,2}, Claire Turner¹, Adrian G. Williams¹, Andrew J. Barker² and Stuart Guy².

¹ Silsoe Research Institute, Wrest Park, Silsoe, Bedfordshire, MK45 4HS, UK

² The University of Birmingham, Edgbaston, Birmingham B5 2TT, UK

Aerobic Activity in Pig Manure

A. CRONJÉ^{1*}, A. BARKER², S. GUY², C. TURNER¹ AND A. WILLIAMS¹

¹Silsoe Research Institute, Wrest Park, Silsoe, Bedfordshire, MK45 4HS, United Kingdom

²Chemical Engineering, University of Birmingham, Edgbaston, Birmingham, B5 7TT

The rate of oxygen consumption during composting is a measure of the aerobic microbial activity and is linked to the decomposition of volatile solids (VS) in the substrate. The rate of loss in mass is a function of the VS present and is related to oxygen up-take rates by the reaction rate coefficient, k . This work investigated the decomposition of pig manure and pig manure-straw mix in aerobic conditions using a constant pressure respirometer and a gas analyser respirometer, respectively. Experiments were carried out at constant temperatures at 5 °C intervals between 10 °C and 70 °C and the corresponding oxygen up-take rates were measured. The aim was to formulate an equation, which expressed k as a function of temperature for each substrate. The concentration of oxygen in the manure-straw mix was measured for about 4 days at each temperature and the initial specific oxygen up-take rate (SOUR) was used to calculate k . The maximum rate of activity occurred at 60°C which corresponded to a maximum value of $k = 0.24 \text{ day}^{-1}$. Activity increased exponentially as the temperature rose from 10 °C ($k = 0.01$) to 60 °C. At higher temperatures the activity slowed although significant oxygen up-take was still measured at 70 °C. The maximum rate of activity in the manure occurred between 50 °C and 55 °C with the corresponding k value of 0.02 day^{-1} . Above this temperature the activity decreased sharply and almost no oxygen up-take was measured at 70 °C. The addition of straw appeared to increase the microbial activity, and therefore the value of k , by an order of magnitude and to extend the temperature range over which aerobic activity took place. The value of k is temperature dependent. A single equation, which describes both the rise and fall in k as a function of temperature, may be used to improve a compost model that is based on substrate decomposition.

Oxygen Uptake Rate of Composting Pig Manure



Angela Cronjé^{1,2} • Dr A. J. Barker¹ • Dr S. Guy¹ • Dr C. Turner² • Dr A. G. Williams²

¹The University of Birmingham, Edgbaston, Birmingham, B5 7TT, United Kingdom.

²Silsoe Research Institute, Wrest Park, Silsoe Bedfordshire, MK45 4HS, United Kingdom



Composting of solid organic material is an autothermal, **aerobic** process. The pattern of oxygen consumption with time can be used to indicate the rate of substrate decomposition. **Oxygen uptake rate** is expressed by the coefficient, k , and is related to the rate of loss of the volatile solids mass, m , by:

$$\frac{dm}{dt} = k (m - m_e)$$

The equilibrium mass, m_e , is the residual mass of volatile solids.

Coefficient k varies with temperature, T , which, in composting, typically ranges between 0 and 70°C

Respirometry

The rate coefficient k is defined as:

$$k = \left[\frac{\text{Specific Oxygen Uptake Rate}}{\text{Chemical Oxygen Demand}} \right]$$

The **SOUR** is evaluated from the cumulative hourly oxygen uptake rates measured using **respirometry**.

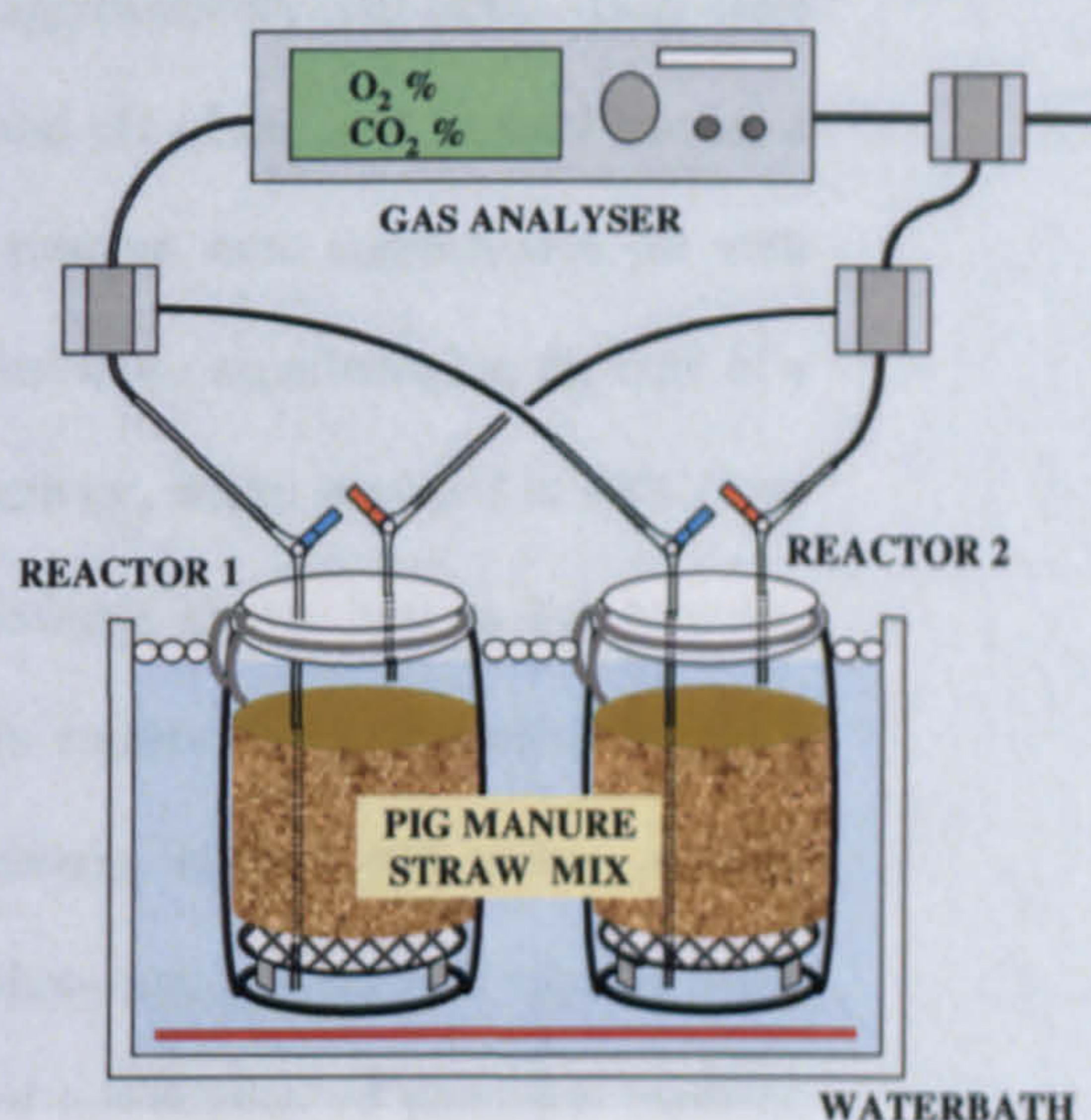
The initial oxygen uptake rate is rapid as the '**fast**' fraction of the substrate decomposes. The rate then decreases on the decomposition of the '**slow**' fraction.

A double power equation describes the temperature profile of k during each stage:

$$k_{T \text{ fast / slow}} = k_{T_1 \text{ fast / slow}} [C_1^{(T - T_1)} - C_2^{(T - T_2)}]$$

Constants C_1 and C_2 correspond to set temperatures T_1 and T_2

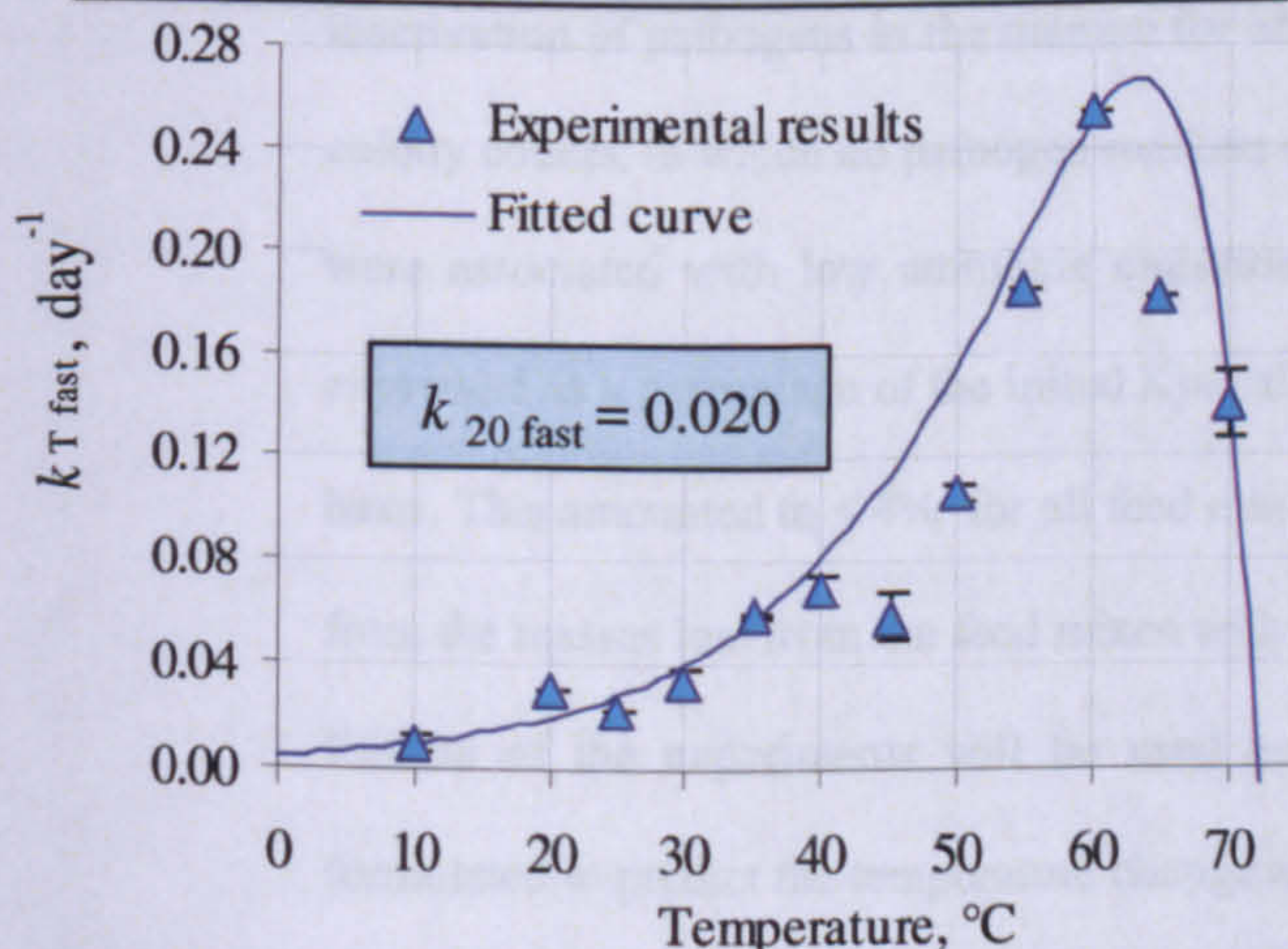
Continuous gas analysis respirometer



Experimental results and curve fitting

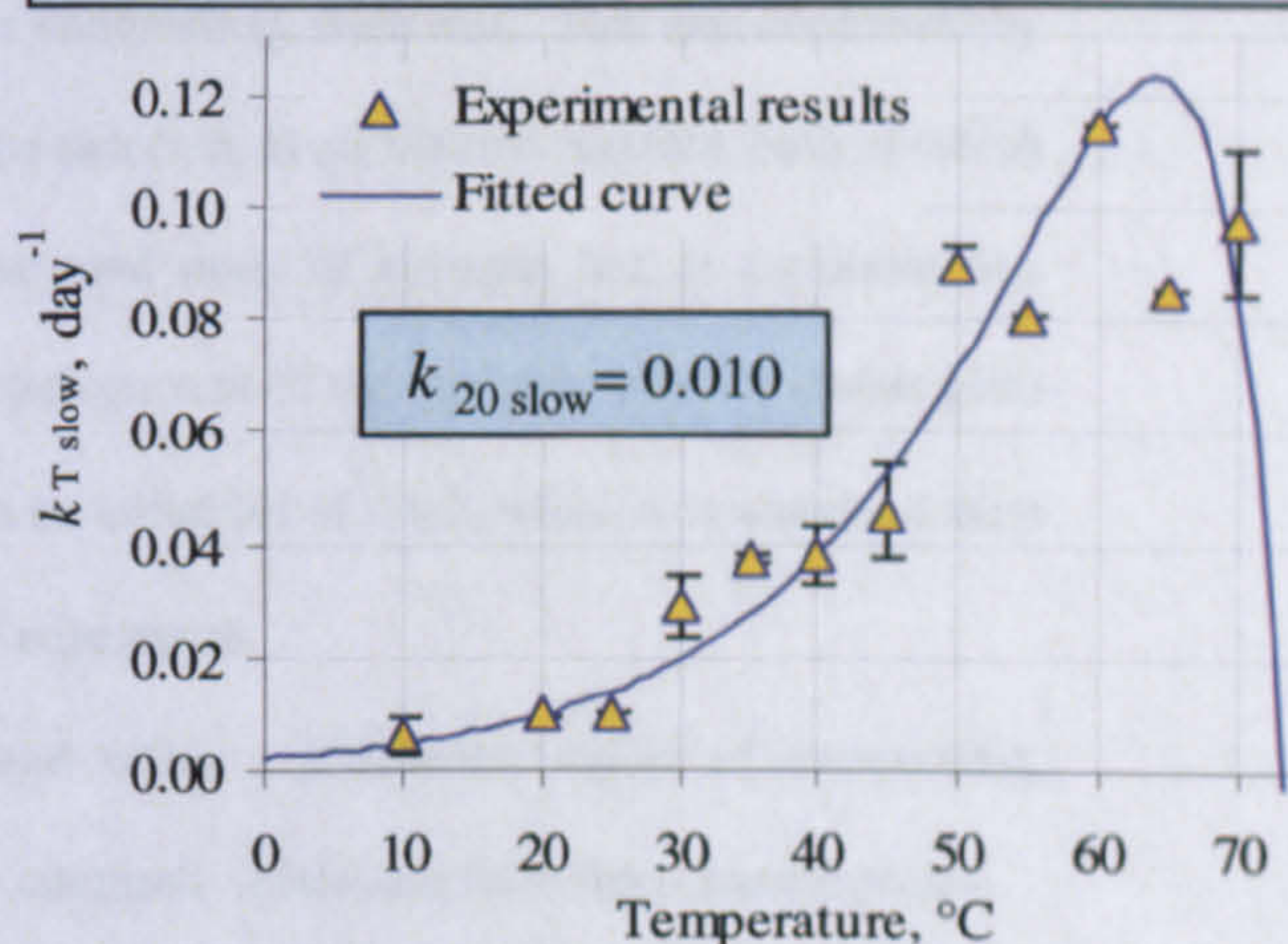
Fast stage

$$k_{T \text{ fast}} = k_{20 \text{ fast}} [1.075^{(T - 20)} - 1.185^{(T - 50)}]$$



Slow stage

$$k_{T \text{ slow}} = k_{20 \text{ slow}} [1.0725^{(T - 20)} - 1.174^{(T - 55)}]$$



- The maximum reaction rate occurs between 60 and 65°C on the fitted curve, as found experimentally
- The decomposition rate can be modelled by considering composting in two stages
- The model predicts that activity ceases at about 73°C

Sponsored by the Engineering and Physical Sciences Research Council and Silsoe Research Institute

Contact: Angela Cronjé • Tel: +44 (0)1525 860 000 • e-mail: angela.cronje@bbsrc.ac.uk

Ammonia Emissions and Pathogen Inactivation During Composting

Angela L. Cronjé^{1*}, Andrew J. Barker², Stuart Guy², Claire Turner¹ and

Adrian G. Williams¹

1. Silsoe Research Institute, Wrest Park, Silsoe, Bedfordshire, MK45 4HS, U. K.

2. Department of Chemical Engineering, University of Birmingham, B5 7TT, U. K.

The composting of pig manure and straw was investigated using three cylindrical reactors operated under controlled conditions, each with a working capacity of approximately 210 litres. They were used to investigate the effects of the carbon to nitrogen ratio and pH of the feed on total ammonia emissions and pathogen inactivation. Heat losses from the reactors were compensated for with external heat sources. The conditions inside, therefore, resembled those experienced at the core of a large composting heap. The period of maximum microbial activity, which occurred at 60°C, was prolonged using temperature feedback aeration control to dissipate excess heat in the material. Baseline aeration of a flow rate based on the initial total solids content of the feed mix, ensured a constant supply of oxygen for aerobic activity. The ammonia, oxygen and carbon dioxide concentrations in the off-gas were analysed. The total viable colony counts in the feed mix and in the composted substrate were compared to estimate the extent of inactivation of pathogen markers. Temperature profiles showed that the material in all reactors had been exposed to temperature of 55°C and above for at least seven days. Therefore the criteria, set out by the U. S. EPA for thermal inactivation of pathogens in the manure for container composting, were met. This was confirmed by colony counts, in which no pathogen markers could be detected, in all but two reactors, both of which were associated with low ammonia emissions. The total mass of nitrogen lost as ammonia was expressed as a percentage of the initial Kjeldahl nitrogen content of the feed mix on a dry matter (dm) basis. This amounted to < 4% for all feed mixes with an initial pH of ≤ 6.2 , which was a marked drop from the masses lost from the feed mixes with no pH adjustment. Results of the experiments will be used to test and refine a simulation model of composting, formulated to predict the temperature change and the ammonia volatilised from feed characteristics.

Introduction

In the UK, approximately 90 million tonnes of farmyard manure (FYM) are collected annually. Handling FYM incurs considerable costs for farmers. In most cases it is stored in field heaps, in which spontaneous but unpredictable composting takes place, before it is spread on land. Management of the heaps is limited, although turning is occasionally carried out to improve the process. Composting reduces the volume, mass (typically by 40%) and water content of FYM and produces a more stable organic material making subsequent land application more uniform and less costly (Gibbs *et al* 2000).

Agriculture is responsible for at least 80% of the total ammonia (NH₃) emissions (350 kt annually) in the UK. Storage and spreading of FYM has been identified as a significant source of NH₃ emissions contributing almost 40% to the annual total from agriculture (MAFF 1998). The release of NH₃ gas is of environmental concern because it contributes to soil acidification and is the principal cause of eutrophication when it is deposited on land and in watercourses. It also represents a loss of valuable ammonia-N (c.196 kt per annum) (Pain 2000) and is an inefficient use of manure as an organic fertiliser.

FYM contains significant levels of harmful faecal pathogens, and the possibility of crop contamination after land application has raised concerns (Maule 1998). Composting has long been used to destroy such pathogens (Haug 1993) and to render the manure safe for handling. However, after uncontrolled composting, faecal coliforms (eg. *E. coli* O157), streptococci and salmonellae are sometimes still detected (Farrell 1992). According to the U. S. EPA, to ensure complete pathogen inactivation in open heaps, the temperature must be held at 55°C or above for at least fifteen days and the heap turned five times during this period (Farrell 1992).

Composting is an effective method for treating FYM and has the potential to biologically convert the unpleasant substrate into a more stable, less heterogeneous material with minimum impact on air, land and water environments. The aim of this work was to investigate controlled composting of FYM in which the following hypothesis could be tested and the data used to verify a proposed model of the corresponding aspects of the process.

The ammonia emissions from composting farmyard manures can be reduced by adjusting the pH and the carbon to nitrogen (C:N) ratio of the feed, whilst still achieving conditions in which thermal inactivation of pathogens is complete.

A low C:N ratio, high moisture content and few or no air spaces are features of manure, which do not promote efficient composting. Conversely straw, the most widely used animal bedding in the UK, has a high C:N ratio, low moisture content and a high absorbency of liquid – over three times its dry mass. A mix with a C:N ratio between 25 and 30, and moisture content of 55-65% is considered ideal for composting (Bishop *et al* 1983, Imbeah 1998) as is a pH between 6 and 7.5 (McKinley *et al* 1986). Substrate pH is related to NH_3 emissions by assuming that the NH_3 emissions are proportional to the concentration of free NH_3 in the manure (Scotford and Williams 2001). Temperature also needs to be considered as it influences the equilibrium between ammonium ions and ammonia in the liquid and gas phases, and the desorption rate. The majority of descriptions of the complex processes involved in ammonia release from composting pig manure is qualitative and requires investigation and modelling to link ammonia emissions with process variables.

To investigate the composting of FYM on a field scale would be costly and time consuming and outdoor conditions are notoriously difficult to control, which essentially excludes quantification of some process variables (Finstain *et al* 1989). The factors that control the process may not be necessarily obvious and results highly empirical. Another

aspect to consider is the observed lack of homogeneity of microbial activity in outdoor composting (Viel *et al* 1987). Therefore, for this investigation composting was carried out indoors in vessels designed for the control of external factors and assessment of the process. A major problem encountered with experiments carried out on a smaller scale is the disproportionately large heat losses from the surface due to the large outer surface area-to-volume ratio (Finstain *et al* 1989). In order to simulate the process accurately, the heat losses needed to be reduced and an environment created that provided sufficient nutrients, moisture and aeration to optimise the growth rates of microbial populations (Das and Keener 1997).

US EPA states that to achieve pathogen inactivation in a contained composting system, the temperature of the material should be above 55°C for a minimum of just three consecutive days (Farrell 1992). High temperature is the most important factor of pathogen inactivation. However, the presence of NH₃ may also enhance pathogen inactivation but, as yet, this effect has not been quantified. Although sufficiently high temperatures are required for pathogen kill, excessively high temperatures need to be avoided, as it has a detrimental effect on the general microbial population. In manure, biological activity slows above 60°C and it is generally believed to stop altogether at 82°C (Miller 1993). Microbial activity is optimal between 50°C and 60°C and consequently decomposition of the substrate is optimised

The findings of the investigation and the potential of a working model could present the farming community with new and effective procedures for handling their FYM with the added benefit of knowing the product is safe to spread on the land.

Materials and Methods

Reactor and Rig

The design of the reactor vessel is illustrated in Figure 1. The three reactors (labelled as R1, R2 and R3) held approximately 210 l of substrate each and were operated in parallel. Each was supplied with a 4 l min^{-1} baseline upward flow of humidified air for 5 minutes every 10 minutes to support aerobic activity. The temperature of the substrate during composting was controlled with a cooling airflow of 20 l min^{-1} . This was activated when the k-type thermocouple (T_{60}) in the centre measured temperatures above 60°C - a temperature feedback aeration control strategy.

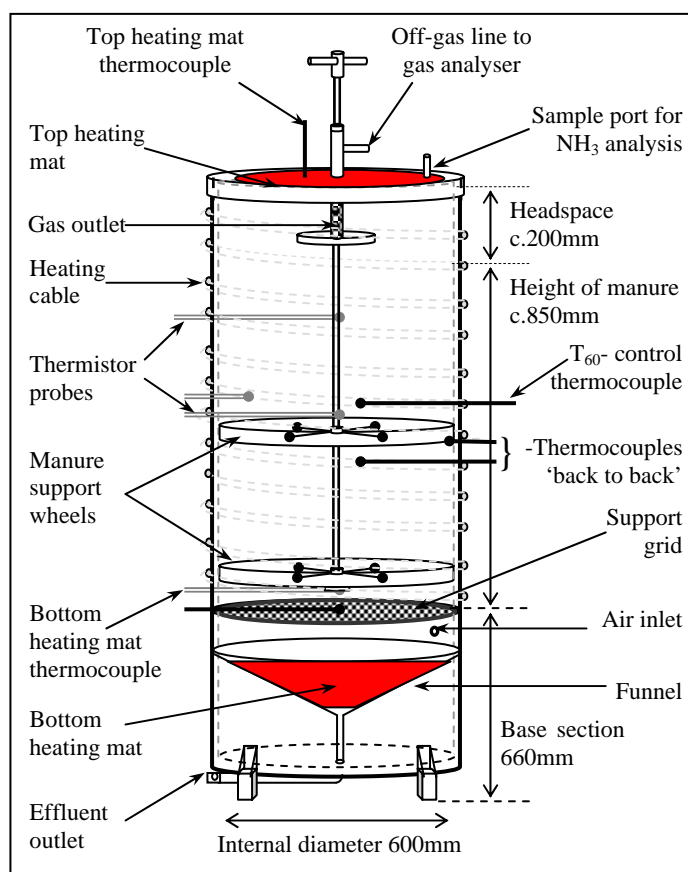


Figure 1. Schematic of the reactor design

The airflow rates were calculated from the total solids (TS) content of the feed using the factors of 0.28 and $1.4 \text{ l min}^{-1} \text{ kg TS}$ for the respective flow rates (Fraser and Lau 2000). Air

entered the vessel at the base between the funnel, which collected any effluent, and the supporting grid, and exited from the central outlet port in the lid.

The temperature was recorded by thermistor probes positioned in the centre, top, bottom and side of the substrate and was logged half-hourly. This was used as the primary means of monitoring the progress of the composting. Heat losses from the surface were compensated for with heat supplied from a heating cable, coiled around the reactor. The output from a pair of k-type thermocouples, configured 'back to back' to give a zero reading when recording the same temperature, controlled the cable so that the radial gradient across the reactor was minimised. The polypropylene reactor body was covered with foil to help distribute the heat supplied evenly over the surface. Heating mats on the base and top prevented condensation on the inner surfaces of the stainless steel funnel and aluminium lid and reduced the vertical gradient in the reactor.

The rig was equipped with facilities to analyse ammonia (NH_3), oxygen (O_2) and carbon dioxide (CO_2) in the incoming air and the off-gas. The NH_3 was collected from an independent gas line drawn from the reactor headspace or the inlet air line into acid traps containing 0.4 M sulphuric acid (H_2SO_4). Each trap unit consisted of a condensate collection tube, two acid-containing tubes and an integrating gas meter. Tubes were changed twice a day for the first ten days and daily thereafter. A combined gas analyser continuously measured the O_2 and CO_2 concentrations in the central off-gas stream. A PC-based logger successively recorded the measurements from each reactor, hourly for fifteen minutes, while controlling the solenoid valves on the gas lines through a digital interface. The gas sample lines leaving the reactors were heated to prevent condensation on the inside of the pipes.

Substrate Preparation

The substrates used in this investigation were pig manure (C:N = 10) and chopped winter wheat straw (C:N = 96). The manure was collected from the slatted floors of housed weaner pigs and stored in airtight containers at 2°C for at least three weeks. The manure pH at this stage was consistently about 5.8. If mixed with straw and left at ambient temperature for a day the pH was typically increased to between 7.8 and 8.1. Three levels of pH (6, 7 and 8) were investigated for C:N ratios 25 and 20, which equated to the respective mixing ratios of manure to straw (M:S) of 2 and 3 kg kg⁻¹ (Table 1). Hereinafter, the trial number, target initial pH and reactor identify each feed mix.

TABLE 1
The composition of the feed mixes

Feed substrates	Trial 1 (C:N = 20)			Trial 2 (C:N = 25)		
	T1-8-R1	T1-7-R2	T1-6-R3	T2-6-R1	T2-8-R2	T2-7-R3
Pig Manure, kg	27	27	27	20	20	20
Straw, kg	9	9	9	10	10	10
Solid Urea, g	28	28	28	0	0	0
Water, l	5.30	4.80	3.60	7.20	8.80	8.40
1 M H ₂ SO ₄ , l	0.00	0.50	1.77	1.66	0.00	0.47

After thoroughly mixing the manure with the straw, the mix was kept in sealed black bin liners in cold storage for a further week until the pH had gradually increased to about 8. Immediately prior to loading a reactor, the mix was wetted to adjust the pH and the moisture content (to 65%) with a solution of distilled water, urea and H₂SO₄ (Table 1). The feed was mixed again, then loaded and enclosed in the reactor. The volume of acid in the solution was determined from small-scale experiments using 0.1 M H₂SO₄ on representative manure mixes. The specific volume of acid to decrease the pH from 8 to 7 and from 8 to 6 was estimated to be 0.12 l and 0.43 l kg⁻¹, respectively.

Analysis

The feed and composted mixes were analysed to evaluate the changes in pH, nitrogen and carbon content and the degree of pathogen marker reduction. They were further characterised by water, total and volatile solids content, chemical oxygen demand (COD) and bulk density analysis to give an indication of the stability of the composted material compared with the feed. A sample of about 1 kg was taken from each feed just prior to loading and from the top, centre and bottom layer of the composted manure mix when unloading each reactor. These samples were used for chemical and physical analysis and were stored at 2°C in airtight containers until analysis was complete within a week of sampling. For microbial analysis, two samples per reactor of approximately 200 g were collected in sterile containers from the feed immediately on loading and from the composted material on opening the reactors at the end of the run from the top-middle and middle-bottom layers. The samples were also stored at 2°C for no longer than three days.

A mean 'dry' pH was determined from at least three direct measurements of the sample with a standard Ion Sensitive Field Effect Transistor (ISFET) probe with the Sentron 2001 pH system. The mean 'wet' pH of two 10 g samples was determined using standard methods (MAFF/ADAS 1986). The pH of the manure mix in the reactor was measured daily with the temperature-compensating pH probe inserted through ports in the reactor body. The Kjeldahl nitrogen (Kj-N) (ammoniacal and organic nitrogen) was determined by digestion and steam distillation analysis (APHA 1998, Persson 1996). Ammoniacal nitrogen (amm-N) content of the mix sample and the acid traps was analysed by steam distillation. The total organic carbon (TOC) content was estimated from the ash content (ASH) by the relationship:

$$\text{TOC}\% = (100 - \text{ASH}\%)/1.8 \quad (\text{Lo et al 1993})$$

Ash content was determined by combustion of the dried sample at 550°C for 5 hours. The TS content was calculated from the mass of a wet sample after drying at 105°C for 16 hours. The C:N ratio was calculated with the Kj-N and TOC content of the sample. The standard closed reflux titrimetric method was used to determine the COD (APHA 1998). The bulk density was determined according to a British standard method developed for soil and soil improvers (BS EN 13040:2000). The degree of pathogen inactivation was estimated from counts of colony forming units (CFU) plated onto McConkey's agar, a coliform-selective medium, and incubated for 24 hours at 37°C. General population colony counts were estimated from populations plated on a nutrient agar medium.

Results and Discussion

The principal changes in the substrate mix composition and the total mass of NH₃ emitted in Trial 1 and Trial 2 are summarised in Table 2. The decrease in dry matter was expressed as a percentage of that in the feed mix (dm_{in}). The greatest loss, about 25%, occurred in the manure mix with the lowest initial pH in both trials, namely T1-6-R3 and T2-6-R1. Contrary to C:N ratio theory and previous findings (Hansen *et al* 1989, Dewes 1999, Fraser and Lau 2000), the total mass of NH₃ emitted from the T2-8-R2 (205 g) was more than four times that emitted from T1-8-R1 (46 g); the feed with the lower C:N ratio. The combination of low NH₃ emissions from T1-6-R3 and T2-8-R1 and a relatively large decrease in dry matter resulted in a final C:N < 20, a value considered necessary for composted material (Fraser and Lau 2000). The outcome of T1-7-R2 and T2-7-R3 were remarkably different in terms of NH₃ emissions and, therefore, of NH₃-N loss. The results from T1-7-R2 were similar to T1-6-R3, whereas those of T2-7-R3 were more like T2-8-R3. It is not yet known that whether such dissimilarity can be attributed to the difference in the respective measured initial pH values of 6.2 and 6.6.

TABLE 2
Changes in the feed mix after composting

		Mass loss (% dm)	Kj-N loss (% dm)	NH ₃ -N loss (% Kj-N _{in}) ^a	pH		Final C:N
Trial 1					Initial	Final	
C:N = 20	T1-8-R1	10	22	11.5	7.6	7.9	24.5
M:S = 3	T1-7-R2	10	19	1.2	6.2	7.0	20.9
	T1-6-R3	25	12	3.7	5.5	7.6	14.7
Trial 2							
C:N = 25	T2-8-R2	16	12	56.3	7.5	8.0	21.8
M:S = 2	T2-7-R3	15	13	26.8	6.6	7.9	19.8
	T2-6-R1	25	4	1.8	6.0	7.2	17.0

^a the mass of nitrogen (N) lost as NH₃ based on mass of Kj-N in feed

TABLE 3
Populations of pathogen markers, log₁₀ (CFU g_{dm}⁻¹)

		Feed Samples	Composted Manure Samples		
			Bottom	Middle	Top
Trial 1 (C:N = 20)					
	T1-8-R1	3.0	- ^a	-	-
	T1-7-R2	3.0	-	-	6.7
	T1-6-R3	5.2	-	6.4	6.6
Trial 2 (C:N = 25)					
	T2-8-R2	6.4	-	-	-
	T2-7-R3	6.0	-	-	-
	T2-6-R1	6.4	-	-	-

^a. ‘-’ indicates a plate free of pathogen markers

Trial 1

The temperature of T1-8-R1, T1-7-R2 and T1-6-R3 rose to 60°C after day 1, 2 and 8, respectively (Figure 2). During this initial phase of aerobic activity, which was less intense in T1-6-R3, the O₂ concentration in the off-gas decreased to a minimum (Figure 3).

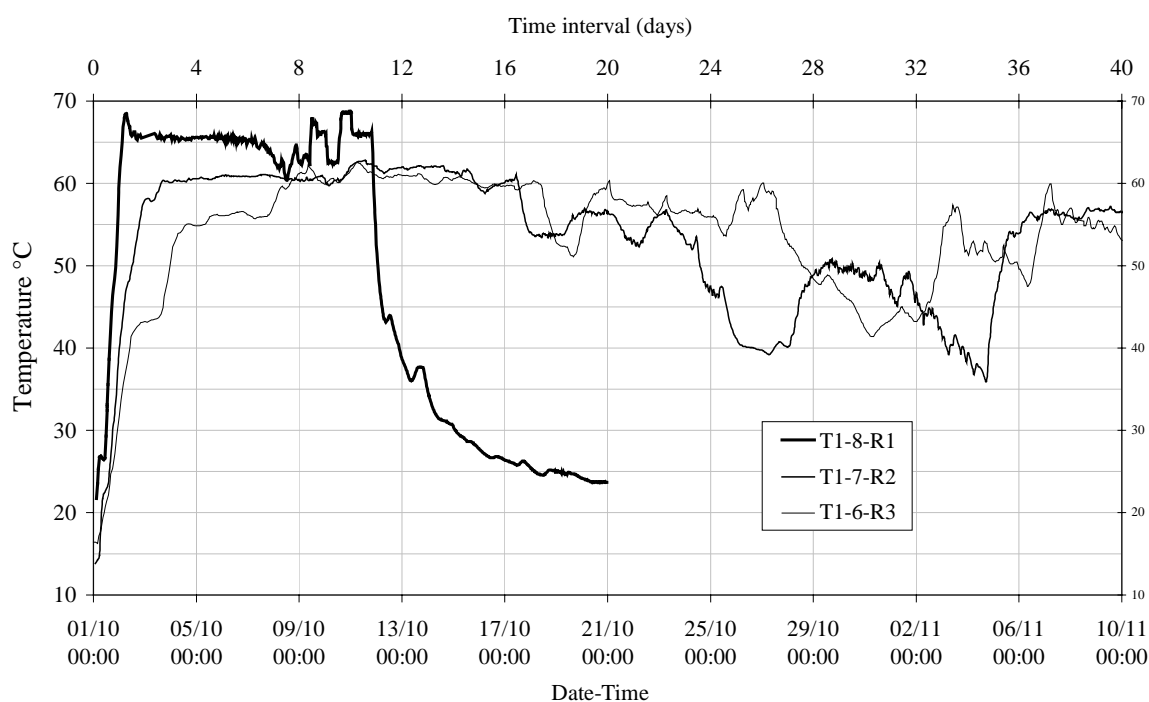


Figure 2: Trial 1 - temperature-time profiles of the centre temperature in the reactors

On reaching the upper temperature limit the cooling aeration was activated and the O₂ replenished. The measured gas concentration profiles (Figure 3) were characteristic of the temperature feedback aeration control strategy used (Fraser and Lau 2000). The most striking difference between the temperature-time profiles (Figure 2) was the relatively rapid cooling that occurred in T1-8-R1 after twelve days at 65°C compared with the gradual decrease and subsequent fluctuations in temperature that characterised the profiles of T1-7-R2 and T1-6-R3. It was clear from the demand placed on the cooling airflow by each reactor that the most intense microbial activity during the first 14 days took place in T1-8-R1. Temperatures above 55°C were achieved for 15 and 9 consecutive days in T1-7-R2 and T1-6-R3, respectively,

which should have been sufficient for pathogen inactivation. However, on inspection of plated samples of the composted, manure pathogen markers were found to still be present in the top layer in T1-7-R2 and top to middle in T1-6-R3. In fact, the number of colonies counted in the respective layers increased about tenfold from the number counted in the feed. No pathogen markers were detected in T1-8-R1 (Table 3).

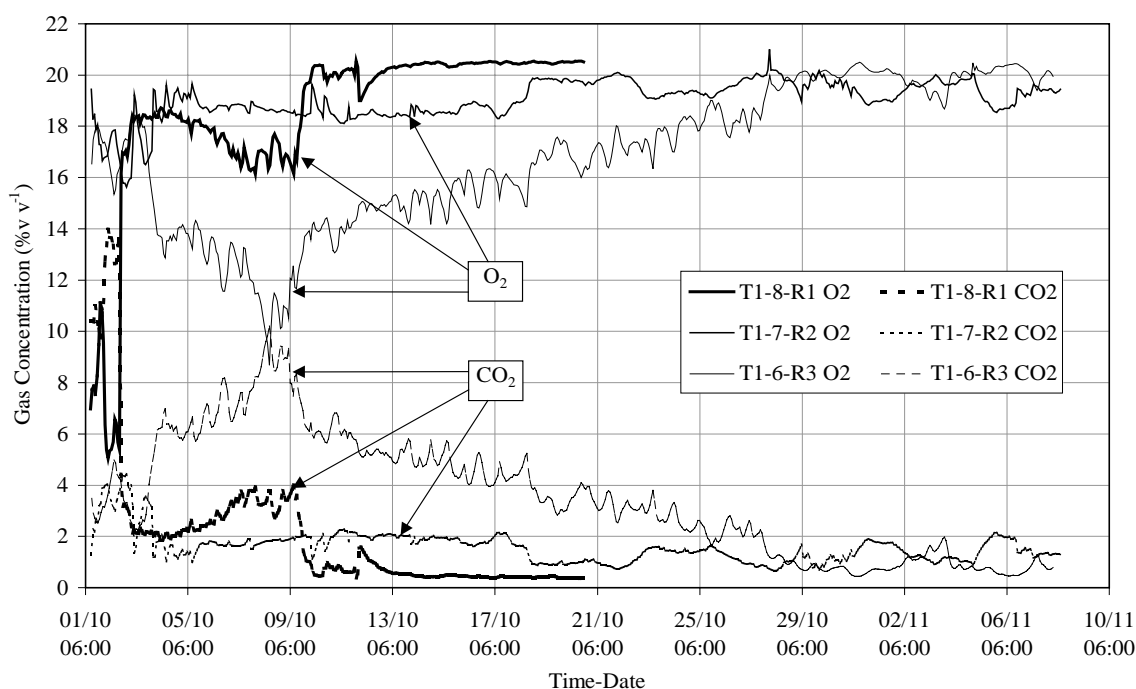


Figure 3: Trial 1 – O₂ (solid lines) and CO₂ (broken lines) concentrations in reactor off-gas.

The characteristic sharp increase in temperature in the initial stages of composting resulted in high NH₃ emissions from T1-8-R1, which peaked once the maximum temperature was reached and emissions reduced thereafter (Dewes 1999) (Figure 4). The total masses collected in the acid traps were 46g, 6g and 18g for T1-8-R1, T1-7-R2 and T1-6-R3, respectively. Ten days after loading, more than 95% of this total had been volatilised from T1-8-R1 but only 11% (2g) and 21% (1g) had been emitted from T1-7-R2 and T1-6-R3. Significant levels of NH₃ were detected from T1-8-R1 after a day, T1-7-R2 after day 12 and from T1-6-R3 after day 8. The mass of NH₃ volatilised, based on the decrease in dry matter

mass ($\Delta m = dm_{in} - dm_{out}$), equated to 32.4, 3.8 and 4.8 $g_{NH_3} kg_{\Delta m}^{-1}$ in order of decreasing pH

- as much as a tenfold decrease, possibly as a consequence of adding the acid.

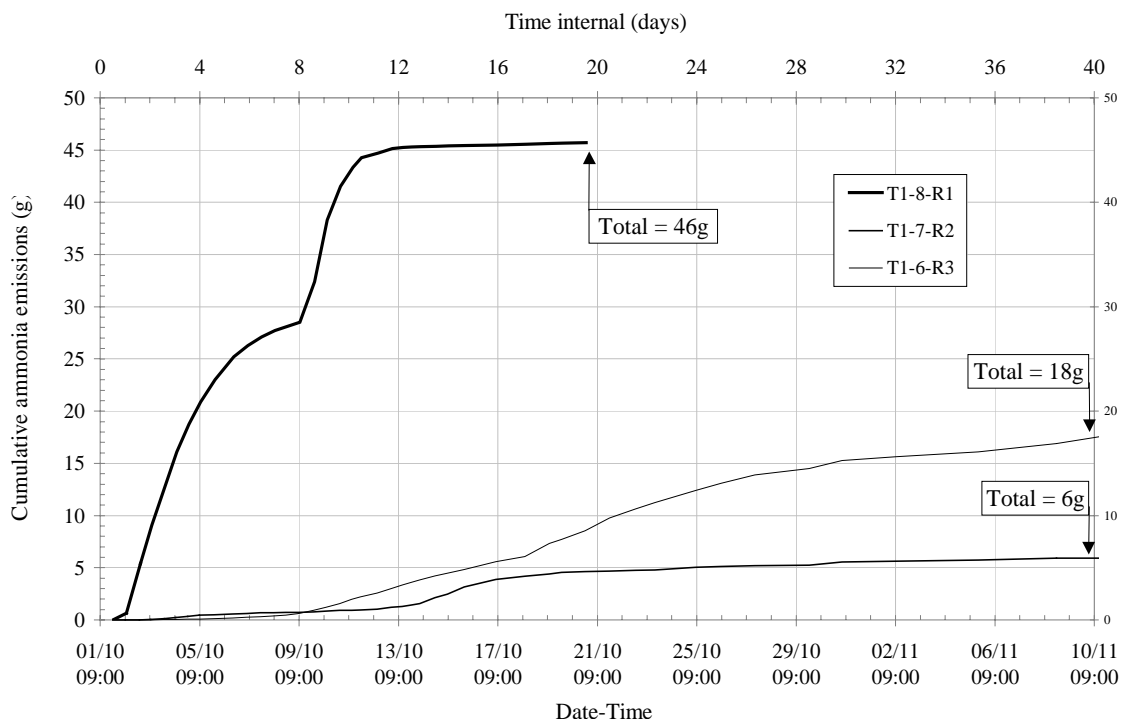


Figure 4. Trial 1 - NH_3 emissions from reactors with a C:N = 20

Trial 2

The temperature in T2-8-R2 and T2-7-R3 rose rapidly to 60°C as a result of intense microbial activity during the first 24 hours (Figure 5). Despite the equally rapid initial rise in temperature, T2-6-R1 took just over two days to reach 60°C as a result of a slow-down in activity around 45°C. This was also observed in T1-6-R3 and Figure 3 shows a drop in oxygen up-take at this stage. A change in microbial populations from mesophiles to thermophiles tends to take place at about 45°C (van Ginkel 1996) and the effect of the low pH may have exaggerated this change. Nevertheless, the temperature-time profiles (Figure 5) followed a similar temperature course for the first week. After day 7, T2-8-R2 gradually cooled to 50°C and subsequently fluctuated between 45 and 55°C up to day 16 whereas T2-7-

R3 and T2-6-R1 had already cooled to room temperature. The run was stopped at this stage because the NH_3 emissions from all three reactors had practically ceased. NH_3 emissions had all but concluded after a week with 95% of the total mass lost by day 6 in T2-8-R2 and by day 10 in T2-7-R3 and T2-6-R1.

Temperatures above 55°C lasted for 7, 10 and 8 consecutive days in T2-8-R2, T2-7-R3 and T2-6-R1, respectively. The results of the microbial analysis (Table 3) showed that no pathogen markers could be detected in any of the three composted manure mixes.

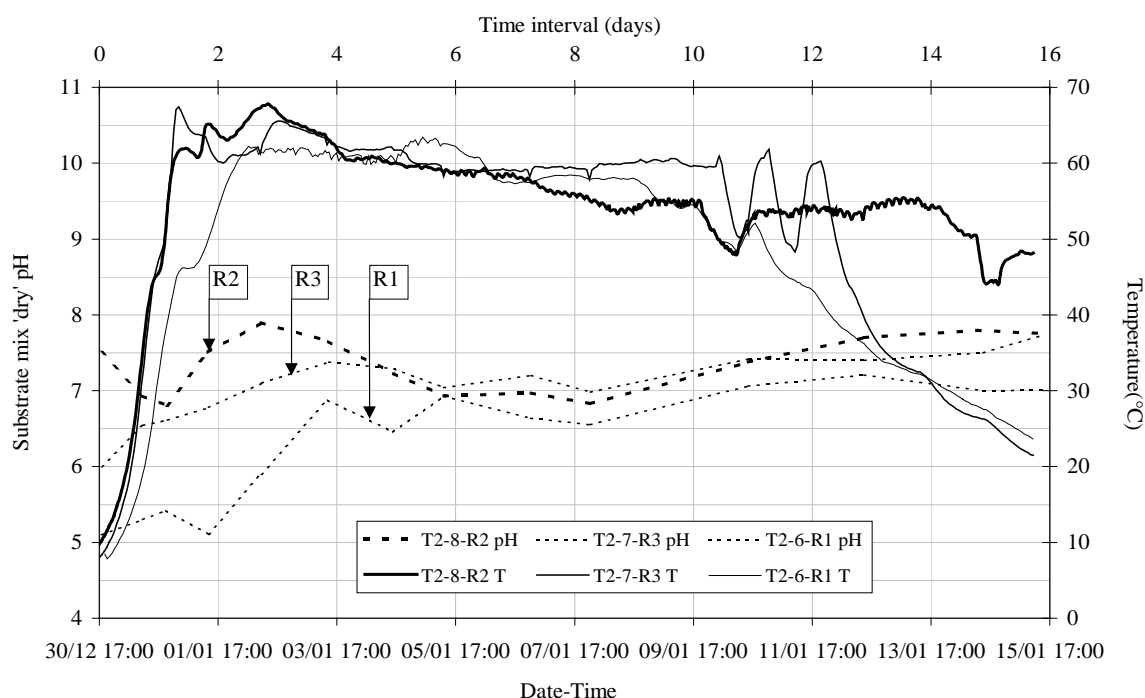


Figure 5: Trial 2 - Temperature-time and pH profiles at the centre of the reactors

Daily measurements of the substrate pH were taken at four points (top, bottom and two middle) in the reactors. An average of the values are plotted (Figure 5). pH readings as low as 5.2 were measured at points in the T2-6-R1 up to three days after loading. Thereafter, the average pH rose gradually only to exceed 7 after day 10, by which time just less than 95% of the total NH_3 volatilised had been emitted. A maximum average pH of about 7.4 and 8.0 was observed in T2-7-R3 and T2-8-R2, which coincided with the period of NH_3 volatilisation.

This was followed by a gradual decrease in T2-8-R2 pH to less than 7 on day 6 and a subsequent rise to 7.8 by the end of the trial.

Significant levels of NH_3 were emitted from T2-7-R3 although these only amounted to half the total lost from T2-8-R2. Comparatively little NH_3 was volatilised from T2-6-R1, totalling only 7g. When corrected for the decrease in dry matter mass, the total mass of NH_3 emitted from each substrate mix, in order of decreasing pH was: 78.2, 49.4 and $1.6\text{g}_{\text{NH}_3} \text{kg}_{\text{Adm}}^{-1}$.

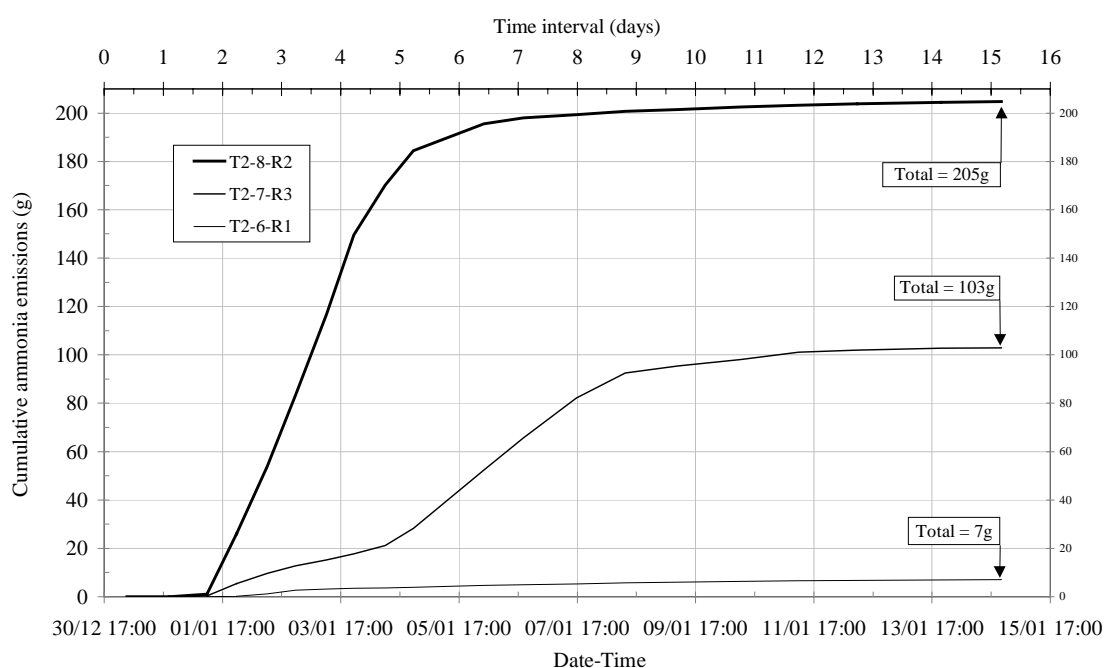


Figure 6. Trial 2 – Cumulative NH_3 emissions from reactors with a C:N = 25

Conclusion

- The temperature of the manure mix rose and stayed above 55°C for more than seven consecutive days in all cases. The criterion for thermal inactivation of pathogens for in-vessel composting was therefore satisfied. The colony counts in all but two reactors, both of which had low ammonia emissions, confirmed that no pathogen markers could be detected. Lower pathogen inactivation may therefore be a consequence of low ammonia emissions.

2. The ammonia emissions from feed mixes with an initial pH < 6.6 were substantially lower than those from feeds with a pH \geq 6.6 with 1.2 to 3.7% of feed nitrogen lost as ammonia in the former and 12 to 56% in the latter. The reduction in ammonia emissions reduced the loss in Kjeldahl nitrogen, so effectively increasing the fertiliser value of composted FYM.
3. The C:N ratio seems to have had little influence on the ammonia emissions from the mixes with the lowest pH. A comparison between the total mass of ammonia emitted from the manure mixes of the higher pH, showed that more than four times the amount was emitted for C:N = 25 than for C:N = 20. This outcome was not consistent with other findings and requires further investigation.
4. The addition of acid appears to enhance the decomposition of the substrate. The 25% loss of dry matter in the feed of pH 6 was approximately 15% and 10% more than the other substrates in Trial 1 and Trial 2, respectively.

From the results available at this stage in the investigation, a tentative conclusion can be drawn that: reducing the pH of the feed substrate seems to be a more effective means of reducing ammonia emissions than increasing the C:N ratio. This will be tested statistically once more results are available.

Acknowledgements

This research is principally funded by an ESPRC grant, with further support from the University of Birmingham, Silsoe Research Institute and BBSRC.

References

APHA, AWWA, WEF. 1998. Standard Methods for the Examination of Water and Wastewater, 20th edition. Public Health Association, Washington, D. C.

Bishop, P. L. and C. Godfrey. 1983. Nitrogen Transformation During Sludge Composting. *Biocycle: Journal of Waste Recycling*, 24:34-39.

British Standard BS EN 13040:2000. Soil Improvers and Growing Media Sample Preparation for Chemical and Physical Determination of Dry Matter Content, Moisture Content and Laboratory Compacted Bulk Density

Das, K. and H. M. Keener. (1997) Numerical Model for the Dynamic simulation of a Large Scale Composting System, *Transactions of the American Society of Agricultural Engineers*, 40(4):1179 - 1189

Dewes, T. 1999. Ammonia Emissions During the Initial Phase of Microbial degradation of Solid and Liquid Cattle Manure. *Bioresource Technology*, 70:245-248.

Elwell, D. L., H. M. Keener and R. C. Hansen. 1996. Controlled, High Rate Composting of Mixtures of Food Residuals, Yard Trimmings and Chicken Manure. *Compost Science and Utilization*, 4(1):6-15

Farrell, J. B. 1992. Fecal Pathogen Control During Composting. *Science and Engineering of Composting*, 282-300.

Finstein, M. S., J. A. Hogan and F. C. Miller. 1989. Physical Modelling of the Composting Ecosystem, *Applied and Environmental Microbiology*, 55:1082-1092.

Fraser, B. S. and A. K. Lau. 2000. The Effects of Process Control strategies on Composting Rate and Odour Emission. *Compost Science & Utilisation*, 8:274–292.

Gibbs, P., R. J. Parkinson, S. Burchett and T. Misselbrook. 2000. Effective Use of Animal Manures on Farm Through Compost Technology. *Microbiology of Composting and Other Biodegradation Processes Conference*, Innsbruck, Austria 17-20 October 2000.

Ginkel, J. T van. 1996. Physical and Biochemical Processes in Composting Material. Ph. D Thesis. Agricultural University Wageningen, The Netherlands.

- Hansen, R. C., H. M. Keener and H. A. J. Hoitink. 1989. Poultry Manure Composting: Design Guidelines for Ammonia. American Society of agricultural Engineers, Paper No.89-4075, St Joseph, MI, USA.
- Haug, R. T. 1993. The Practical Handbook of Composting Engineering. Lewis Publishers, Boca Raton, Florida, USA.
- Hogan, J. A., F. C. Miller and M. S. Finstein. 1989. Physical Modelling of the Composting Ecosystem. *Applied and Environmental Microbiology*, 1082-1092
- Imbeah, M. 1998. Composting Piggery Waste: A Review. *Bioresource Technology*, 63:197-203.
- Lo, K. V., A. K. Lau, P. H. Liao. 1993. Composting of Separated Solid Swine Wastes. *Journal of Agricultural Engineering Resources*, 54:307-317.
- MAFF. 1998. The Code of Good Agricultural Practice for the Protection of Air [Online]. Available: <http://www.defra.gov.uk/envirocogap/aircode.pdf>.
- MAFF/ADAS. 1986. The Analysis of Agricultural Materials. Ref. Book 427, 3rd ed.
- Maule A. 1998. Environmental Survival of E. coli 0157: Implications for Spread of Disease. International Food Hygiene Conference: E. coli 0157, Paris, October 1998
- McKinley, V. L., J. R. Vestal and A. E. Eralp. 1986. Microbial Activity in Composting. The Biocycle Guide to In-vessel Composting. The JG Press, Inc.
- Miller F. C. 1993. Composting as a Process Based on the Control of Ecologically Selective Factors. Soil Microbial Ecology. Applications in Agricultural and Environmental Management. F. Blaine Metting Jr.
- Pain, B. F., T. H. Misselbrook, S. C. Jarvis, B. J. Chambers, K. A. Smith, J. Webb, V. R. Philips and R. W. Sneath. 2000. Inventory of Ammonia Emissions from UK Agriculture 1998. Ministry of Agriculture, Fisheries and Food. Contract Report WA0630.

Persson, J. A. 1996. Handbook for Kjeldahl Digestion, 2nd edition. IS BN 91-630-3471-9

Scotford, I., M. and A. G. Williams. 2001. Practicalities, Costs and Effectiveness of Floating Plastic Cover to Reduce Ammonia Emissions from a Pig Slurry Lagoon. *Journal of Agricultural Engineering*, 80(3):273 – 281.

Viel M., D. Sayag, A. Peyre and L. André. 1987. Optimization of In-Vessel Co-Composting Through Heat Recovery. *Biological Wastes*, 20:167-185

The Respiration Rate of Composting Pig Manure

Angela L. Cronjé^{1,2*}, Claire Turner¹, Adrian G. Williams¹, Andrew J. Barker² and

Stuart Guy²

¹Silsoe Research Institute, Wrest Park, Silsoe, Bedford MK45 4HS, United Kingdom

²Chemical Engineering, University of Birmingham, Edgbaston, Birmingham B15 2TT, United Kingdom

The rate at which oxygen is consumed during composting is a measure of aerobic microbial activity and is linked to the rate of organic material decomposition. The rate of loss in mass is a function of the mass of the degradable organic fraction and is related to oxygen uptake rate by the reaction rate coefficient, k . The decomposition of a pig manure and straw mix was investigated at temperatures between 10°C and 70°C using respirometric techniques. The oxygen concentrations in the reactor were measured continuously for about 4 days and then converted to hourly oxygen uptake rates for each incubation temperature, T . The specific oxygen uptake rate was used to calculate the reaction rate coefficient at T , k_T , for the observed fast and slow stages of decomposition. The effect of the environmental factors were taken into account using a multiplicative approach and a relationship, which expressed k_T for each stage as a function of T , was formulated. The maximum measured rate of activity occurred during the fast stage at 60°C where $k_{T \text{ fast}} = 0.31 \text{ day}^{-1}$. Activity increased exponentially with the temperature in both stages up to about 60°C. At higher temperatures the activity slowed but most noticeably in the fast stage. The dependence of k_T on T during each stage was described by a double power expression, which predicted that activity would cease around 73°C. The relationships may be used to improve a compost model that is based on a first order reaction rate kinetics for the decomposition of organic material.

Introduction

Composting is an autothermal, aerobic process and is recognised as an effective method for treating organic waste, such as farmyard manure (FYM). It has the potential to convert the

waste biologically into a stable, less heterogeneous material that has a lower impact on air, land and water environments than if left untreated. A decrease in mass, volume and water content of the FYM makes it easier and less costly to handle. Greater consistency of the composted material and inactivation of pathogens of faecal origin are desirable consequences for FYM that is to be spread on land (Gibbs *et al* 2000). During composting, temperature rises as a result of microbial activity from ambient up to about 70°C. Temperature is the most important factor in pathogen inactivation. The United States Environmental Agency (US EPA) states that, to achieve pathogen inactivation in a contained composting system, the temperature of the material should be above 55°C for a minimum of just three consecutive days (Farrell 1992).

Pig manure has little free air space (FAS) due to its lack of structure and high moisture content, typically about 75% for separated solid manure (Lo *et al* 1993, Imbeah 1997, Petersen *et al* 1998, Gendesbien *et al* 2001). It also has a low carbon to nitrogen ratio (C:N) of about 10 (Petersen *et al* 1998, Cronjé *et al* 2002). These characteristics do not promote ideal composting conditions. Straw is used widely as bedding for farm animals and when mixed with the manure provides structure, absorbs moisture (more than three times its weight (Jeppson 1998)), and is a source of carbon. The reported optimum C:N ratio for composting ranges from 20:1 and 40:1 (Bishop *et al* 1983, Rynk 1992, Mohee 1998, Imbeah 1998, Eckini *et al* 2002), as it depends on the organic material and the process criteria. Likewise, the optimum moisture content for composting is not universally applicable as the physical structure and water holding capacity of organic materials vary (Jeris and Regan 1973 II, Finstein and Hogan 1992, Jeppsson 1998).

A moisture content of between 55 % and 65 % on a wet basis is generally recommended for composting (Bishop *et al* 1983, Imbeah 1998) but composting is feasible with higher moisture

contents if there is enough oxygen to maintain aerobic activity (Liao *et al* 1993). An undesirable consequence of composting, particularly with materials of a low C:N, is the loss of nitrogen, which occurs mainly through ammonia volatilisation. This not only lowers the agronomical value of the composted material but also impacts on the natural ecosystems where the ammonia is deposited (Gibbs *et al* 2000). Nitrogen retention has, therefore, become an important aspect of the process management. Although the open structure enhances the distribution of oxygen in the material and promotes aerobic conditions, pockets of anaerobic activity may remain. During unmanaged composting, anaerobicity can dominate resulting in an unstable, malodorous organic material in which pathogens have been detected (Farrell 1992) and this needs to be avoided.

Measuring the oxygen uptake rate of the composting material provides a clear indication of the aerobic activity and, therefore, the decomposition rate of the degradable organic fraction. The oxygen demand varies during stages of composting as the temperature and organic composition change (Hamelers 2002). The dependence of the rate on composition has received little attention (Hamelers 2002). The readily available organic fraction is used first during the 'fast' stage, and this is followed by the 'slow' stage, during which the decomposition of larger, more complex organic compounds, as well as the possible on-set of rate-limiting environmental conditions, occurs (Keener *et al* 1993). The distinction between the two stages of decomposition may not be obvious in larger scale composting operations (Haug 1993). The rate of decomposition of the material is a function of the mass of the degradable organic fraction and is related to oxygen uptake rate by the reaction rate coefficient, k (Mohee 1998). The value of k depends on a number of environmental factors, such as temperature, moisture content, biodegradability, FAS, pH and the C:N of the organic material (Haug 1993, Ekinici *et al* 2002, Keener *et al* 2002). Accurate measurement of the

effect of the factors in relation to biological activity in manures is difficult, as composting is a complex process. The aim of the investigation was to evaluate the dependence of the reaction rate coefficient on temperature. Expressing k as a function of temperature is useful for application in a dynamic model of composting on a macroscopic scale (Haug 1993).

Process kinetics

Keener (1993) proposed that the process rate, based on the unit amount of degradable organics, follows first order reaction kinetics and is expressed as:

$$\frac{dm}{dt} = -k(x_1, x_2, \dots, x_n)(m_t - m_e) \quad (1)$$

m_t is the mass of degradable organic matter, m , at time t and m_e is the mass remaining when no further loss in m occurs. This state of equilibrium is reached after about 6 months to 1 year. x_i represents the effect of an environmental factor on the process. If all these factors remain constant, the solution to expression (1) is a dimensionless variable known as the compost mass ratio R_m . The standard solution to a first order differential rate equation takes the form of an exponential time expression, such that:

$$R_m = \frac{m_t - m_e}{m_0 - m_e} = e^{-k(x_1, x_2, \dots, x_n)t} \quad (2)$$

R_m ranges from 1 at $t = 0$ to 0 at equilibrium. It is useful indicator of degree of decomposition and, therefore, the stability of the composted material (Hamelers 2002).

Reaction Rate Coefficient

The dependence of k on the numerous environmental factors (x_1 to x_n) is assumed to be multiplicative (Haug 1993, Richard 1997, Keener *et al* 2002) so that the exponent term can be written as:

$$k(x_1, x_2, \dots, x_n) = k^\ominus \cdot f_1(x_1) \cdot f_2(x_2) \cdot \dots \cdot f_n(x_n) \quad (3)$$

k^\ominus is the value of the reaction rate coefficient under standard conditions and f_i , the function of each factor's effect. When the process is carried out under standard conditions the functions all equal 1 and $k \rightarrow k^\ominus$. The value of k depends on the organic material to be composted (Hamelers 2002) and has usually required empirical evaluation. Hamelers (2001, 2002) questioned the use of the multiplicative approach as it assumes that the environmental factors act independently of each other and that the organic material is homogeneous. Hamelers (2001) proposed a theoretical (deductive) model, which considered the processes occurring during composting on a particular scale as opposed to this somewhat empirical (inductive) approach, which was predominantly derived from experimental data and considers the composting process on a macro-scale, to describe the effect of factors on the process kinetics. Although the deductive approach was able to account for the combined effects of environmental factors, parameter estimation is complicated and further simplification is required for practical applications. The first order rate expression was shown to be applicable over a short time period of approximately 3 days (Keener *et al* 1992) and the organic material is unlikely to show a loss of structure and therefore free airspace due to compaction. Furthermore, for bench scale experiments, a well-prepared organic material can be considered to be relatively homogenous with little variation of organic material within and between the samples.

There is no standardised laboratory method for determining reaction rate coefficient for composting solid organic material (Stentiford 1993). Here, the empirical value of k was calculated using the relationship between the specific oxygen uptake rate (SOUR) and the

chemical oxygen demand (COD) of the material to be composted and had the dimension $[T^{-1}]$ (Mohee 1998).

$$k = \frac{\text{SOUR}}{\text{COD}} \quad (4)$$

The SOUR was derived from the gradient of the line on a plot of the cumulative mass oxygen consumed against time. In this work, the factor investigated was temperature, T . The other environmental factors were optimised, where possible, and kept as constant as possible between the experiments so that variation in their effects was minimised. The reaction rate coefficient was therefore specified as k_T .

Factor Effect Functions

The principal factors other than temperature, which significantly affect the SOUR, and therefore k , are moisture content (MC), free airspace (FAS) and oxygen concentration in the airspaces of the organic material (OC) (Haug 1993). Another factor that has been investigated is the C:N ratio (Ekinici *et al* 2002).

A number of expressions have been proposed, which describe the effect of moisture content on the decomposition rate for specific organic material (Haug 1993, Mohee 1998, Keener *et al* 2002, Richard *et al* 2002). The S-shaped logistic curve proposed by Haug (1993), f_{MC} , was used to predict the effect for moisture contents below about 75% and is given as

$$f_{MC} = \frac{1}{e^{(-17.7 \cdot MC + 7.1)} + 1} \quad (5)$$

The experimental data, on which expression (5) was based, shows that microbial activity gradually falls at moisture contents above 75% (Haug 1993), which was also observed by Richard *et al* (2002). Considering the physical structure of straw, its relatively high water

holding capacity and the reported range of working moisture contents for composting pig manure amended with a bulking agent (Liao *et al* 1993, Imbeah 1997, Jeppsson 1998), expression (5) was judged to describe the effect on the rate coefficient best. It also concurs with the statement that: ‘values reported for optimum moisture content range from 25 to 80% wet basis, with most values in the 50 to 70% range’ (Richard *et al* 2002). At a moisture content of 50%, $f_{MC} > 0.86$ but it falls to 0.5 at 40% (Figure 1).

Haug (1993) proposed a similar S-shaped logistic curve to describe the effect of the FAS, f_{FAS} , on k and is given as:

$$f_{FAS} = \frac{1}{e^{(-23.7 \cdot FAS + 3.5)} + 1} \quad (6)$$

Expression (6) is a feasible representation of the FAS effect as the factor varies linearly with the moisture content (Richard *et al* 2002) and above 35% rate limiting effects are avoided (Keener *et al* 2002). Sufficient FAS does not, however, guarantee that the oxygen concentration in the air spaces is high enough not to limit the rate. The kinetics of oxygen transfer during composting are complex and depend on diffusion transport and particle size (Haug 1993, Hamelers 2001). The effect of the oxygen content on microbial activity is minimal at concentrations above 5% (Keener *et al* 2002), as was verified by experimental data (Schulze 1962). The function, f_{OC} , was developed from experimental data of Schulze (1962) and was generalised and simplified to a Monod-type expression (Haug 1993).

$$f_{OC} = \frac{O_2 \%}{O_2 \% + 2} \quad (7)$$

The effect of the C:N ratio on the reaction rate coefficient, $f_{C:N}$, was empirically evaluated from experiments with mixes of poultry litter and paper mill sludge (Ekinci *et al* 2002) and is given as:

$$f_{C:N} = e^{-0.5 \cdot \left(\frac{C:N + 35.9}{11.7}\right)^2} \quad (8)$$

The expressions (5) to (8) are graphically illustrated in Figure 1.

Figure 1

Respiration Quotient

The respiration quotient (Q_{resp}) is used in the study of biochemical systems (van Ginkel 1996). It is defined as the moles of carbon dioxide emitted with respect to the moles of oxygen consumed and is expected to be close to 1 for aerobic respiration based on carbohydrates.

$$Q_{\text{resp}} = \frac{\text{Volume of CO}_2 \text{ emitted}}{\text{Volume of O}_2 \text{ consumed}} = \frac{(\% \text{CO}_{2\text{out}} - \% \text{CO}_{2\text{in}})}{(\% \text{O}_{2\text{in}} - \% \text{O}_{2\text{out}})} \quad (9)$$

where $\% \text{CO}_2$ and $\% \text{O}_2$ are the respective measured percentage volume concentrations of the carbon dioxide and oxygen measured and subscript 'in' and 'out' correspond to the initial and final gas concentrations, respectively, of an incubation time interval in a microbial system.

The Q_{resp} of organic compounds do, however, vary and can range from 0.5 to 3.3 (van Ginkel 1996). In anaerobic conditions, carbon dioxide is produced without the consumption of oxygen and so the Q_{resp} becomes greater than 1. As temperature increases, the carbon dioxide-producing anaerobic activity decreases. Q_{resp} can, therefore, reveal the type of organic material decomposing and the relative importance of aerobic and anaerobic reactions (Van Ginkel 1996).

Materials and Methods

Apparatus

Figure 2

The two 3-litre sealed glass reactor vessels of the respirometer were held at a constant temperature in a thermostatically controlled water bath (Figure 2). The organic material was supported on stainless steel grids in the reactors. Gas entered and left each reactor through the

screw tap ports in the lid. The concentration of oxygen and carbon dioxide in the gas was continuously measured by a Servomex Series 4100 gas analyser and logged by a PC based program.

Procedure

Preparation and analysis of the organic material

Solid pig manure was collected from the slatted floor on which weaner pigs were kept at a local farm. The manure was mixed with dry chopped straw in the mass ratio of 2:1 respectively, which gave a C:N ratio of approximately 25 and a moisture content of 55%. To avoid moisture becoming a limiting factor for the microbial activity during the experiment, as a result of the material drying out, distilled water was added to the mix to give an initial moisture content of 80%. 700 g batches of the mix were frozen for at least 3 days. Two days before an experiment, a batch was thawed at 2°C. 250 g were used in each reactor vessel and the remainder was used for analysis. The standard closed reflux titrimetric method was used to determine the COD (APHA 1998). The total solids (TS) and volatile solids (VS) contents were calculated from the mass of a wet sample after drying at 105°C for 16 hours and combustion of the dried residue at 550°C for 5 hours, respectively. The total organic carbon (TOC) content was estimated from the VS using expression (10) (Lo *et al* 1993):

$$\text{TOC}\% = \frac{\text{VS}\%}{1.8} \quad (10)$$

The ammoniacal nitrogen (Amm-N) and Kjeldahl (Kj-N) nitrogen contents were analysed by steam distillation (APHA 1998). For Kj-N, the sample was digested prior to distillation (Persson 1996). Kj-N is the sum of the ammoniacal nitrogen and organic nitrogen (Org-N) contents and was assumed to represent the total nitrogen content of the sample. The C:N ratio was, therefore, calculated from the Kj-N and TOC contents. The pH of the sample was measured using a standard Ion Sensitive Field Effect Transistor (ISFET) probe with the

Sentron 2001 pH system, after dilution to 1:10 (mass basis) with deionised water (MAFF/ADAS 1986). The fractional FAS for a 2:1 mix was calculated from bulk density determined according to a British standard method developed for soil and soil improvers (BS EN 13040:2000), and the TS and VS contents (Haug 1993).

Incubation

The selected incubation temperatures were 10°C and between 20°C and 70°C in 5°C intervals. A freshly thawed sample of organic material was incubated at one of the stated temperatures and the series of experiments were carried out in a randomised temperature order. The reactors were incubated in the thermostatically controlled water bath for about 4 days. The water was kept at the same depth in the bath through out the incubation period of each experiment.

At the start of the experiment, whilst equilibrating, the apparatus was filled with nitrogen gas and run as a closed system to test for any gas leaks. If free of leaks, the apparatus was flushed and filled with air, which provided the oxygen. Each hour, the gas in one of the reactors was analysed. The oxygen and carbon dioxide concentrations were continuously measured for 45 minutes and the readings were logged every 5 minutes during this period. To ensure aerobic conditions, the reactor was flushed with fresh air for 15 minutes after the analysis. An hour lapsed between consecutive analyses of gas from each reactor. The gas was pumped through the system at approximately two l min⁻¹.

Oxygen uptake rate

The concentration of oxygen and carbon dioxide in the FAS was assumed to be the same as the content of the gas leaving the system. The oxygen and carbon dioxide concentrations were displayed as percentages of the total gas volume by the gas analyser. The total gas volume was taken as that which occupied all the respirometer tubing and corresponding

reactor vessel. The gas analyser was supplied with calibration gases (air, nitrogen and 8% CO₂ in nitrogen) every 6 hours. The logged readings of the respirometer gases were converted for any drift by assuming it was linear between calibrations and adjustments were made accordingly. The gas leaving the reactors passed through in a desiccation column and a gas filter, which removed water and any particles above 0.6µm in diameter. All gas entering the reaction chambers of the gas analyser was dry and close to room temperature. The volume of oxygen respired, ΔV_{O₂} ml, was converted to an hourly oxygen uptake rate (HOUR) in mg O₂ h⁻¹g_{TS}⁻¹ with expression (11). The gas was assumed to behave ideally and the effect of the difference in temperature of the gas in the reactor, T_{Reactor}, and in the tubes, T_{Tube}, was accounted for.

$$\text{HOUR} = \frac{\Delta V_{O_2}}{\Delta t} \cdot \frac{M_r}{22.4} \cdot \frac{273}{V_{\text{Total}}} \left[\frac{V_{\text{Reactor}}}{T_{\text{Bath}}} + \frac{V_{\text{Tube}}}{T_{\text{Amb}}} \right] \cdot \frac{1}{m_{\text{TS}}} \quad (11)$$

where: Δt = time interval between consecutive gas measurements (h)

M_r = relative molecular mass of oxygen (32 g)

22.4 = volume of gas occupied by 1 mg-mol of an ideal gas at 273 K (ml)

T_{Bath} = incubation temperature (K)

T_{Amb} = ambient temperature (K)

V_{Reactor} = volume of the reactor occupied by gas (ml)

V_{Tube} = volume of the tubing and the gas analyser occupied by gas (ml)

V_{Total} = Total volume of the respirometer occupied by gas (V_{Reactor} + V_{Tube}) (ml)

m_{TS} = the mass of total solids, TS, in the composting material (g).

Likewise, the hourly carbon dioxide emission rate (HCER), in mg CO₂ h⁻¹g_{TS}⁻¹, was calculated from the volume of carbon dioxide emitted ΔV_{CO₂} ml using expression (11) with the appropriate substitution for ΔV_{O₂} and M_r, which is 44 g for carbon dioxide.

Results and Discussion

The mean values with standard deviations (σ) from the analysis of the samples of the pig manure and straw mix for the 14 experiments are given in Table 1. The measured COD varied between some samples of the organic material, as indicated by the high standard deviation value. The average COD was used in expression (4) to calculate the k_T value for the corresponding SOUR.

Table 1

Specific Oxygen Uptake Rate

The cumulative oxygen uptake (COU), in $\text{mg O}_2 \text{ g}_{\text{TS}}^{-1}$, and cumulative carbon dioxide emitted (CCE), in $\text{mg CO}_2 \text{ g}_{\text{TS}}^{-1}$, determined from the sum of the mass of the oxygen gas consumed and carbon dioxide emitted between consecutive logged gas readings, was plotted against the incubation time. The gradient of the plots was equal to the SOUR and specific carbon dioxide emission rate (SCER), respectively. The rate of oxygen uptake varied during the incubation period, as was indicated by a change in gradient. Haug (1993) considered a 'fast' and 'slow' fraction of the organic material, which during decomposition corresponded to a 'fast' and 'slow' oxygen uptake rate. These periods were termed the fast and slow stages respectively (Figure 3). Figure 3 shows the cumulative mass profile for oxygen and carbon dioxide for the incubation temperature of 30°C and 50°C. The clusters of points represent the readings, which were logged every 5 minutes during the 45-minute period when the gas in the reactor was analysed.

Figure 3

The fast stage lasted for about the first 10 hours after the lag time and the slow stage corresponded to the time thereafter, which was evident by a marked decrease, by about half, in the gradient of the lines. The lines were fitted to the designated data (selected by eye)

using the least square method with a 95% confidence level. The regression line was fitted with *Microsoft Excel 97*.

The mean SOUR values of the two reactors are given in Table 2. The ‘*’ indicates SOUR values that are based on the reading of just one of the reactors as the other leaked. The rate measured at 70°C was still higher than those recorded at mesophilic temperatures (30°C to 45°C) and, although temperatures above 60°C occur during composting, the operating conditions are not optimal.

Table 2

Respiration Quotient

The respiration quotient, Q_{resp} , was determined using expression (9). Where possible, as with the average SOUR and SCER values in Table 2, the average Q_{resp} of the two reactors was calculated and plotted against the incubation temperature (Figure 4).

Figure 4

The Q_{resp} increased from 0.5 at 10°C to about 1 at 30°C and then decreased to between about 0.6 and 0.8 at the higher incubation temperatures. This confirmed that aerobic activity prevailed during the incubation period. Ammonification and nitrification of nitrogen-containing compounds takes place at the lower temperatures of the mesophilic stage of composting (around 30°C). The reactions have an average Q_{resp} of 1 and 0.9, respectively (van Ginkel 1996). This may have contributed to the rise in the average Q_{resp} values of about 1 between 20°C and 30°C but the overall effect would be small as nitrogen-containing compounds make up less than 5% of the total solid in the organic material. The Q_{resp} of glucose and its associated complex compounds, which were in abundance, is also 1 and the likely reason for the increase in the Q_{resp} . The half-lives of the carbonaceous compounds in soil are 3, 15 and 360 days for glucose, cellulose and lignin, respectively (Sylvia *et al* 1998).

It would be expected that, along with the readily degradable fraction of the pig manure, only the glucose and short-chain polysaccharides of the straw were used during the 4 days. The Q_{resp} for the fast and slow stages were similar, which suggests that types of reactions did not vary much. During the composting of synthetic garbage, the Q_{resp} varied between 0.8 and 0.9 over the thermophilic temperature range (45°C to 63°C) (Schulze 1960). The corresponding values for the composting pig manure and straw mix were lower and varied between 0.5 and 0.8. The difference may be due to the dissimilarity of the organic materials or that the excess of oxygen in the respirometer's reactors enabled reactions to take place that would have otherwise been suppressed if oxygen was not surplus.

Factor effect functions

The factors considered were the FAS, oxygen content (OC) and moisture content (MC). The effect of the C:N ratio, expression (8), was based on empirical data, for which the optimum C:N ratio was about 35. Mohee (1998), however, found that for a mix of chicken manure and bagasse, the oxygen uptake was highest for a C:N ratio of 25. The optimum C:N ratio depends on the organic material and as shown in Figure 1 it is clear that correcting for the C:N ratio, about 24 in this case, could give a deceptively low value for the factor. In the absence of a $f_{\text{C:N}}$ expression specific to mixes of pig manure and straw, the C:N ratio was assumed to be close to optimum and was not corrected for.

The FAS was above 40% in all the manure and straw mixes so that the value of f_{FAS} did not contribute an environmental effect to the reaction rate coefficient. The oxygen content in the organic material did not drop below 8 % v v⁻¹ ($f_{\text{OC}} = 0.800$) during any of the experiments and the mean values of f_{OC} were approximately 0.900 or above.

The mean moisture content factor, f_{MC} , was above 0.950 for all the experiments, although there was some drying of the organic material in the experiments at the higher temperatures nearing the end of the incubation period.

The mean multiplicative total environmental factor determine for each incubation temperature is given in Table 3 along with the calculated minimum and maximum values.

Table 3

The measured reaction rate coefficient, k_T , was corrected for the effect of the environmental factors, using to expression (12), to give the reaction rate coefficient possible under optimum conditions, $k_{T\text{ opt}}$

$$k_{T\text{ opt}} = \frac{k_T}{f_{\text{total}}} \quad (12)$$

The Reaction Rate Coefficient

For simplicity the $k_{T\text{ opt}}$ is represented as k_T from here on. The reaction rate coefficient of the pig manure and straw mix increased exponentially with incubation temperature up to a maximum around 60°C for both the fast (Figures 5) and slow (Figure 6) stages of decompositions. The k_T values of the slow stage were about half those of the corresponding values of the fast stage. The error bars represent the maximum and minimum values recorded at the particular incubation temperature.

The equations fitted to the data were based on expression (13), which was used to describe the dependence of k_T on temperature during aerobic digestion of liquid wastes (Andrews and Kambhu 1973, Haug 1993)

$$k_T = k_{TR1} (C_1^{T-TR1} - C_2^{T-TR2}) \quad (13)$$

where: k_{TR1} = reaction rate coefficient of reference temperature TR1, day⁻¹

C_1, C_2 = reference temperature constants

TR1, TR2 = reference temperatures, °C

T = substrate temperature, °C

Initial attempts to determine the values of the equation parameters with a statistical program, GenStat, failed due to the lack of data points at temperatures above 60°C. The next approach taken was to estimate the values of the parameters from literature and by application of basic mathematical techniques for curve fitting, such as differentiation of expression (13) to determine the temperature, which corresponds to the turning point of the curve, T_{\max} . Haug (1993) provided insight to the magnitude of the temperature constants and values of the reference temperatures. TR2 was taken to be about 10°C below T_{\max} and was designated as 50°C. The values of temperature constants were then iteratively adjusted with reference to 20°C for TR1 and, correspondingly, k_{20} . The best fit curve was determined by the highest 'percentage variance accounted for' value. This value does not necessarily give a goodness of fit criterion but is good for comparing the fit of different curves to the data points.

Figures 5 and 6

The temperature constants and reference temperatures, which describe the dependence of k_T on T for the fast and slow stages of composting pig manure and straw mix are given in Table 4.

Table 4

Analysis of the curve fitting shows the percentage variance accounted for by the expressions for the fast and slow stages were 78 % and 75 %, respectively. The curves fitted the data well for the rise in activity up to 60°C, which was reflected by the higher percentages of 89 % and 86 % for the respective stages. More measurements of activity at temperatures above 60°C are needed to verify the fit of the curve. The activity was predicted to cease around 73°C. This upper temperature limit is realistic. At temperatures above 60°C, the activity of enzymes, such as some cellulases, declines (Keener *et al* 1993) and temperatures between

70°C and 75°C are lethal to many micro-organisms (Van Ginkel 1998). Regarding pathogen inactivation in a pig manure and straw mix, the concept of 'the hotter the better' only applies to conditions where the temperature is below 65°C.

The effect of temperature on the rate of decomposition in biological systems can be expressed by a temperature coefficient Q_{10} , where an increase of 10°C typically causes the reaction rate to double over a limited temperature range (Haug 1993, Johnson 1999). It is therefore expressed as:

$$Q_{10} = \frac{k_T}{k_{T-10}} = 2 \quad (14)$$

During the fast and slow stages of the reaction up to 60°C, the mean Q_{10} was 2.00 ($\sigma = 0.19$) and 1.77 ($\sigma = 0.32$), respectively. The Q_{10} values were similar to the values found with composting garbage of about 1.7 (Wiley 1958) and 1.9 (Schulze 1960). A Q_{10} less than 2 is indicative of diffusion controlled reactions because diffusion coefficients vary less with temperature (Haug 1993). As this microbial system appeared to be aerobic through out the experiment, the diffusion of nutrients to the micro-organisms, after the exhaustion of the readily degradable organic material, may have been the controlling factor during the slow stage of the experiments, which resulted in a decrease in Q_{10} .

Mass Ratio

The degree of decomposition of the pig manure and straw mix after incubation, as given by the mass ratio, R_m , indicates the stability of the organic material and is therefore an assessment of the performance of the microbial system at the incubation temperature. A lower R_m corresponds to a more stable material. As given in expression (2) there are two methods of calculating the degree of decomposition. The first is by direct measurement of the total solids content of organic material before and after incubation, and the second uses the

reaction rate coefficient evaluated for incubation temperature under consideration. Due to a small difference in the actual incubation time of each experiment, the second method was used to estimate the degree of decomposition after a set time period so that a comparison of the performance of the microbial system could be made between the incubation temperatures. To verify this method, R_m was calculated by the first method and compared with values calculated by the second method for the actual duration of the experiment. The three sets of calculations are presented in Figure 7, where

- (i) Gives the standardised mass ratio value for a 3 days incubation period, R_m (3d), using a weighted k_T value to take into account the change from the fast to the slow stage of decomposition.
- (ii) Gives the mass ratio calculated with weighted k_T values for the total duration of incubation R_m (td).
- (iii) Gives the mass ratio calculated using initial and final dry masses of the material and an estimated equilibrium mass of the mix.

Figure 7

The results for (i) showed that the degree of decomposition, and therefore the stability, did increase with the temperature up to 60°C, a pattern, which reflected that shown by the reaction rate constant. The plots for cases (ii) and (iii) follow a similar pattern. The difference between the R_m values of the circled points less than 10%. The largest difference was found between R_m values at 38°C and 40°C, about 40% and 24%, respectively. The differences between the rest of the corresponding values were less than 20%. The pattern shown in case (i) therefore gives a reasonably accurate indication of the change in stability of the incubated organic material with temperature and 60°C does indeed seem to be the optimal working temperature for a mix of pig manure and straw.

Both methods are subject to analytical errors. With the first method errors arise in the determination of the total solids mass by sample drying. The second method requires the COD of the organic material to be determined, which can be a variable factor in heterogeneous solid organic material. This method also relies on the accurate determination of the k value and any errors are carried through to the R_m value, although to a lesser extent. The first method is independent of k and, therefore, a useful check of the results.

Conclusions

The rate of oxygen uptake provides a clear indication of aerobic microbial activity during composting. In the mix of pig manure and straw, the respiration quotient was rarely greater than 1. The majority of reactions during composting can therefore be expected to be aerobic when sufficient oxygen is available. The reactions, however, may become diffusion-controlled as the microbial activity did not double with the 10°C increase in temperature during the slow stage as it did in the fast stage. The oxygen uptake rate and, consequently, the reaction rate coefficient, increased exponentially with temperature up to a maximal rate, which was followed by a rapid decrease at higher temperatures because of the inactivation of micro-organisms. The activity at thermophilic temperatures up to 70°C was noticeably higher than at mesophilic temperatures. The highest rate of activity occurred around 60°C, which also corresponded to the composted material of greatest stability. This is, therefore, the temperature at which a unit composting a mix of pig manure and straw should aim to operate. Two distinct stages of the microbial activity were observed at all the temperatures investigated. The activity during fast stage was about twice that of the slow stage. A clear change from the readily degradable fraction of the pig manure and straw to the fraction more resistant to microbial degradation occurred. The reaction rate coefficient for each stage can

be described a function of temperature by a double power expression. The expressions account for about 75% of the data and predict that microbial activity in the pig manure and straw mix would cease at about 73°C. The expressions can be used to improve a dynamic model of composting that is based on the substrate decomposition.

This work has ultimately highlighted the importance of temperature control during the process in order to maintain a high rate of activity and good degree of decomposition usually synonymous with a more stable composted material. Further investigation of the effect of the C:N on the oxygen uptake rate in a pig manure and straw mix would be beneficial.

Acknowledgements

This research was funded by The Engineering and Physical Sciences Research Council (EPSRC) and Silsoe Research Institute (SRI) with further support from the University of Birmingham.

References

- Andrews, J. F., Kambhu, K. 1973. Thermophilic Aerobic Digestion of Organic Solid Wastes. EPA – 670/2-73-061, PB 222 396. NTIS, Springfield, VA, USA.
- Bishop, P. L. and C. Godfrey. 1983. Nitrogen transformation during sludge composting. *Biocycle: Journal of Waste Recycling*, 24: 34-39.
- British Standard BS EN 13040:2000. Soil improvers and growing media sample preparation for chemical and physical determination of dry matter content, moisture content and laboratory compacted bulk density.
- Cronjé, A. L., C. Turner, A. G. Williams, A. J. Barker, S. Guy. 2002. Ammonia emissions and pathogen inactivation during composting. In: JG Press (eds). *Proceedings of the 2002 International Symposium: Composting and Compost Utilization*, Columbus Ohio, USA.

- Ekinci, K., H. M. Keener and D. L. Elwell. 2002. Composting short paper fiber with broiler litter and additives II: Evaluation and optimization of decomposition rate versus mixing ratio. *Composting Science and Utilization*, 10(1): 16-28.
- Farrell, J. B. 1992. Fecal pathogen control during composting. *Science and Engineering of Composting*. Renaissance Publications, Ohio, USA. pp. 282-300.
- Finstein, M. S., F. C. Miller and P. F. Strom. 1986. Monitoring and evaluating composting process performance. *Journal of Water Pollution Control Federation*, 58: 272-278
- Gendebien, A. H., R. Ferguson, J. Brink, H. Horth, M. Sullivan, R. Davis, H. Brunet, F. Dalimier, B. Landrea, D. Krack, J. Perot, C. Orsi. 2001. Survey of wastes spread on land. European Commission-Directive-General for Environment. [Online]. Available at <http://europa.eu.int/comm/environment/waste/studies/compost/landspreading.pdf>
- Gibbs, P., R. J. Parkinson, S. Burchett and T. Misselbrook. 2000. Effective use of animal manures on farm through compost technology. In. (eds.) *Proceedings of the Microbiology of Composting and Other Biodegradation Processes Conference*, Innsbruck, Austria 17-20 October 2000.
- Hamelers, H. V. M. 2001. A mathematical model for composting kinetics. Ph. D Thesis. Agricultural University Wageningen, Wageningen, The Netherlands. 293p.
- Hamelers, H. V. M. 2002. Modelling composting kinetics: A deductive approach. In. JG Press (eds.) *Proceedings of the 2002 International Symposium: Composting and Compost Utilization*, Columbus, Ohio, USA.
- Haug, R. T. 1993. *The Practical Handbook of Compost Engineering*. Lewis Publishers, Boca Raton, Ann Arbor, London, Tokyo. 715p
- Haug, R. T. and W. F. Ellsworth. 1991. Measuring compost substrate degradability. *Biocycle*, January 1991: 56-62.
- Imbeah, M. 1997. Composting piggery waste: A review. *Bioresource Technology*, 63: 197-203.
- Jeppsson, K. H. 1998. Ammonia emissions from different deep litter materials for growing finishing pigs. *Swedish Journal of Agriculture*, 28: 197-206.

- Jeris, J. S. and R. W. Regan. 1973. Controlling environmental parameters for optimum composting I: experimental procedures and temperature. *Compost Science*, 14(1):10-15.
- Jeris, J. S. and R. W. Regan. 1973. Controlling environmental parameters for optimum composting II: moisture, free air space and recycle. *Compost Science*, 14(2): 8-15.
- Johnson, A. T. 1999. Biological process engineering. John Wiley and Sons, Inc., New York, USA. pp. 360-368.
- Keener, H. M., C. Marugg, R. C. Hansen and A. A. J. Hoitink. 1993. Optimizing the efficiency of the composting process. *Science and Engineering of Composting: Design, Environmental, Microbiological, and Utilization Aspects*. Renaissance Publications, Worthing, Ohio, USA. pp. 54-94.
- Keener, H. M., K. Ekinici, D. L. Elwell, F. C. Michel Jr. 2002. Principles of composting process optimization. In: JG Press (eds). *Proceedings of the 2002 International Symposium: Composting and Compost Utilization*, Columbus Ohio, USA.
- Lo, K. V., A. K. Lau, P. H. Liao. 1993. Composting of separated solid swine wastes. *Journal of Agricultural Engineering Resources*, 54: 307-317.
- Liao, P. H., A. T. Vizcarra, A. Chen and K. V. Lo. 1993. Composting separated solid swine manure. *Journal of Environmental Science and Health*, 9: 1889-1901.
- MAFF/ADAS. 1986. The Analysis of Agricultural Materials. Ref. Book 427, 3rd edition.
- Marugg, C., M. Grebus, R. C. Hansen, H. M. Keener and H. A. J. Hoitnik. 1993. A kinetic model of the yard waste composting process. *Compost Science and Utilization*, Premier issue: 38-51.
- Mohee, R. 1998. Composting potential of bagasse and broiler litter and process simulation using a dynamic model. A dissertation presented for the degree of doctor in philosophy, University of Mauritius.
- Persson, J. A. 1996. *Handbook for Kjeldahl Digestion*, 2nd edition. IS BN 91-630-3471-9
- Petersen, S. O., A. M. Lind, S. G. Sommer. 1998. Nitrogen and organic matter losses during storage of cattle and pig manure. *Journal of Agricultural Science*, 130: 69-79.

- Richard, T. L. 1997. The kinetics of solid-state aerobic biodegradation. Ph. D. Thesis. Cornell University. Ithaca, NY. 357 pp
- Schulze, K. L. 1960. Rate of oxygen consumption and respiratory quotients during the aerobic decomposition of a synthetic garbage. *Compost Science*, Spring, 1960: 36-40
- Schulze, K. L. 1962. Continuous thermophilic composting. *Compost Science*, Spring 1962: 22-34.
- Smits, J. P., A. Rinzema, J. Tramper, E. E. Schlosser, W. Knol. 1996. Accurate determination of process variables in a solid-state fermentation system. *Process Biochemistry*, 31(7): 669-678.
- Standard Methods for the Examination of Water and Wastewater 20th edition. 1998. Clesceri, S. C., A. E. Greenberg, and A. D. Eaton (eds.). APHA, AWWA, WPCF. New York, USA.
- Stentiford, E. 1993. Diversity of composting systems. *In. Science and Engineering of Composting*. Renaissance Publications, Ohio, USA. pp. 95-110
- Sylvia, D. M., J. J. Fuhrmann, P. G. Hartel and D. A. Ziberer. 1998. *Principles and Applications of Soil Microbiology*. Prentice Hall.
- Van Ginkel, J. T. 1996. Physical and biochemical processes in composting material. Ph. D Thesis. Agricultural University Wageningen, Wageningen, The Netherlands. 179p.
- Wiley, J. S. 1957. II Progress report on highrate composting studies. *In. Proceedings of the 12th Industrial Waste Conference*, Purdue University. pp 596-603.

Figures and Tables

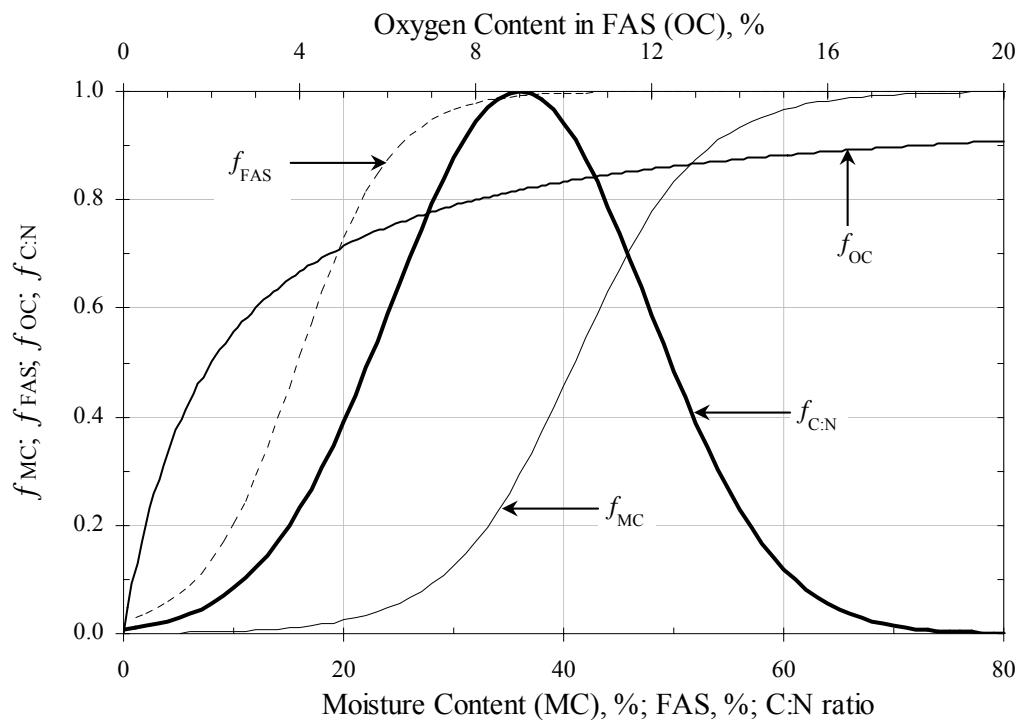


Figure 1: The relationships between the effect functions and corresponding factors.

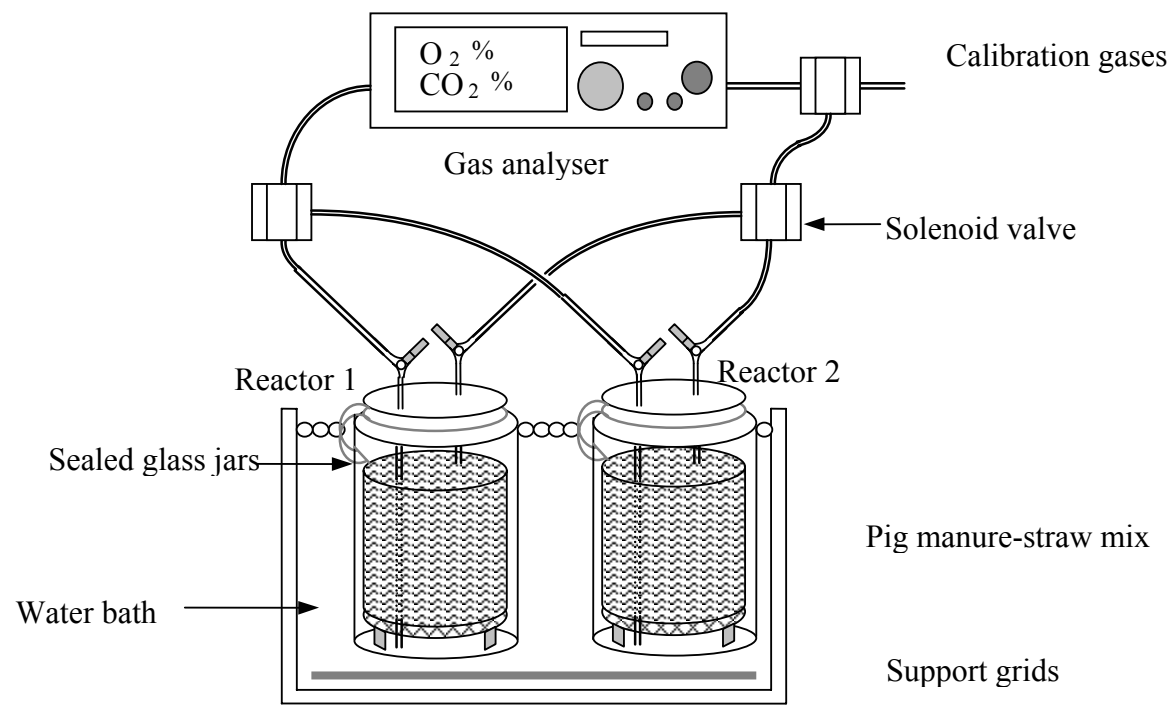


Figure 2: The respirometer

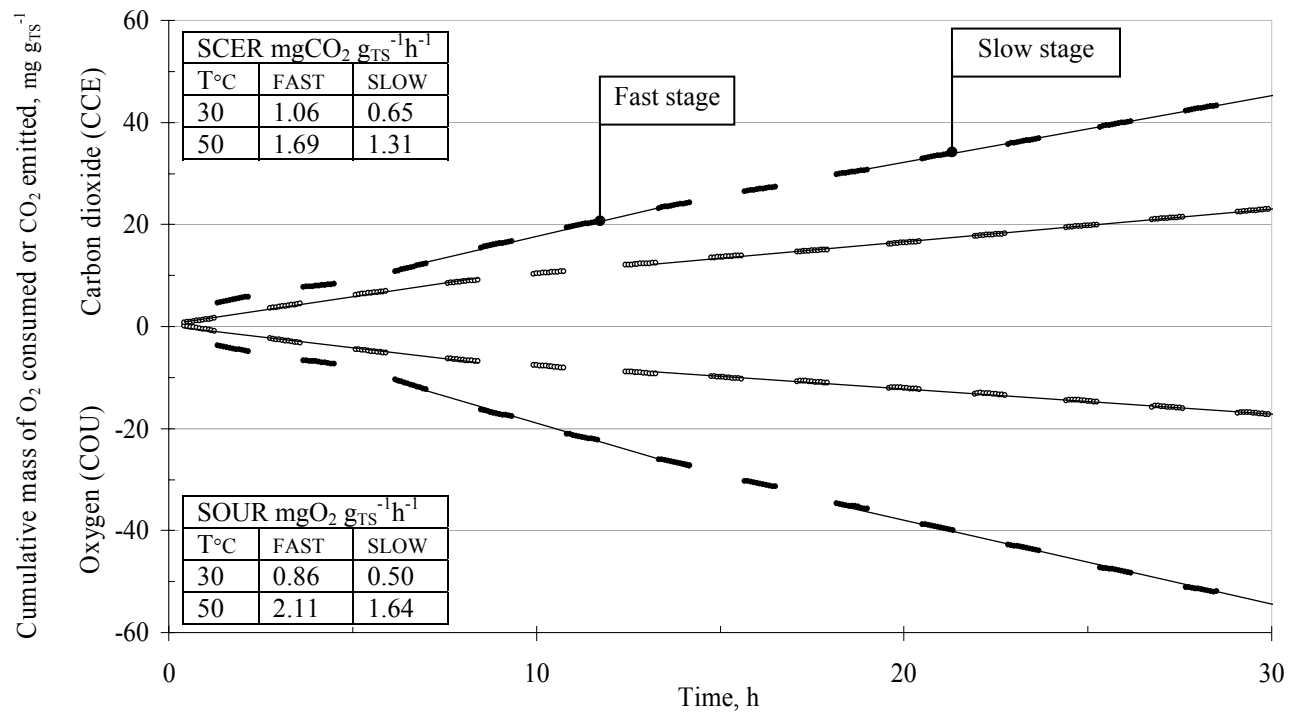


Figure 3: The time profile of the cumulative hourly emission rate of CO_2 (HCER) and uptake rate of O_2 (HOUR) for Reactor 1 incubated at 30°C (o) and 50°C (•).

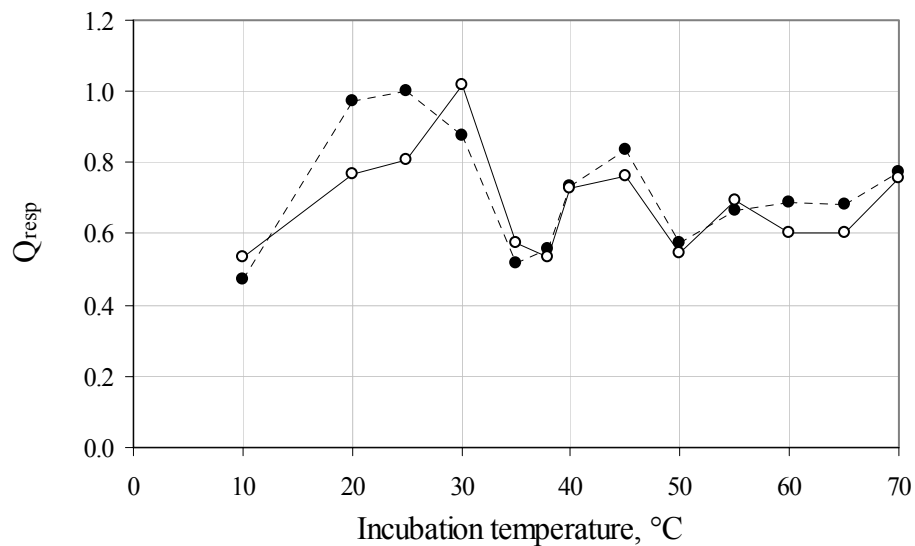
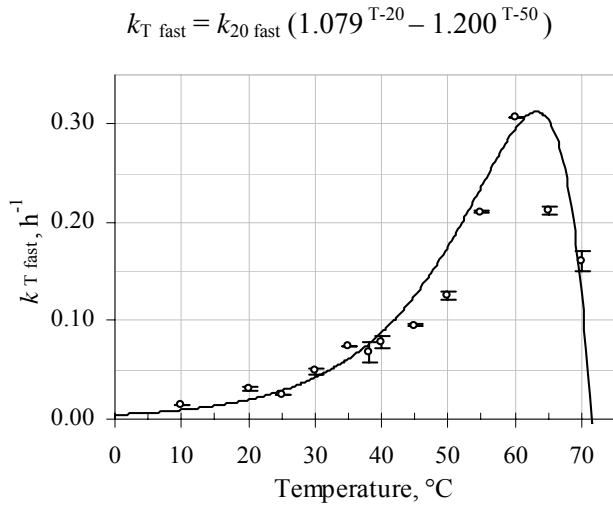
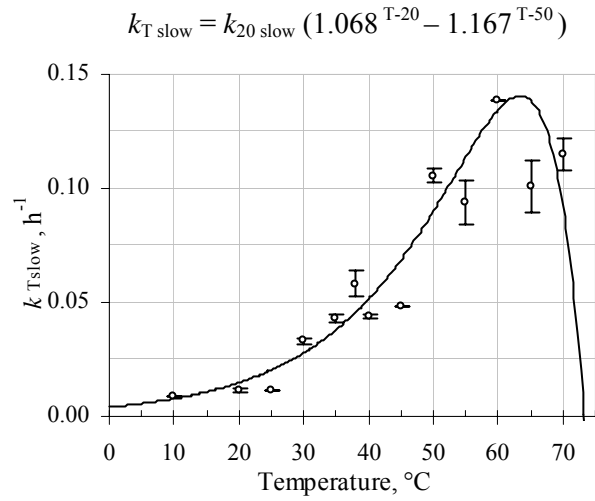


Figure 4: The change in average respiration quotients, Q_{resp} , with temperature for the fast (•) and slow (o) stages.

Figure 5: Fast stage kinetics of k_T

[(o) Experimental data, (—) Fitted Curve]

Figure 6: Slow stage kinetics of k_T

[(o) Experimental data, (—) Fitted Curve]

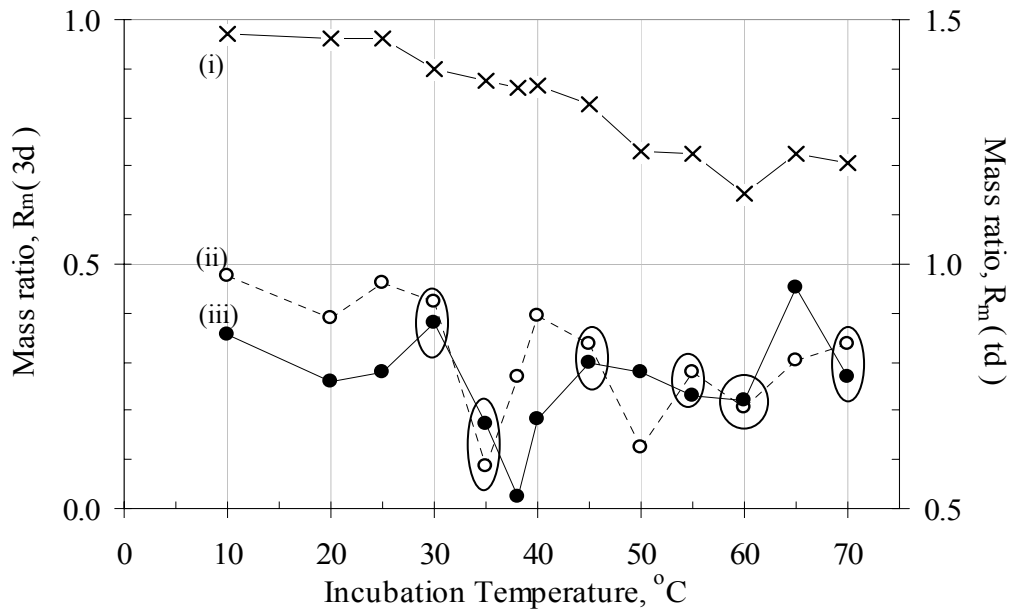
Figure 9: (i) $R_m(3d)$ (—×—): mass ratio after a 3 day incubation period.(ii) $R_m(td)$ (---- o ----): mass ratio after the total incubation period using k_T .(iii) $R_m(td)$ (—●—): mass ratio after the total incubation using the mass values.

Table 1: The mean values of the physical and chemical characteristics of the pig manure and straw mix samples before incubation

	TS %	TS g	VS % _{TS}	TOC % _{TS}	Amm-N % _{TS}	Org-N % _{TS}	C:N	COD mg O ₂ g _{TS} ⁻¹	pH	FAS
Mean	20.4	50.7	86.8	48.4	0.33	2.06	23.8	459	8.01	0.73
σ	1.4	3.4	1.8	0.5	0.06	0.27	2.8	102	0.17	0.01

Table 2: The SOUR and SCER between 10°C and 70°C for the fast and slow stages

Temperature, °C	10*	20	25*	30	35	38	40	45	50	55	60*	65	70
SOUR fast stage mg h ⁻¹ kg _{TS} ⁻¹	243	500 ± 53	412	807 ± 56	1231 ± 2	1523 ± 20	1268 ± 99	1106 ± 162	2011 ± 59	3425 ± 23	4776	3371 ± 61	2562 ± 179
SOUR slow stage mg h ⁻¹ kg _{TS} ⁻¹	119	189 ± 11	195	547 ± 21	708 ± 32	722 ± 4	768 ± 21	955 ± 95	1694 ± 51	1522 ± 153	2160	1600 ± 180	1836 ± 113
SCER fast stage mg h ⁻¹ kg _{TS} ⁻¹	143	562 ± 16	398	1027 ± 6	1055 ± 27	1007 ± 86	1200 ± 3	1448 ± 10	1635 ± 10	2905 ± 25	4007	2916 ± 25	2578 ± 105
SCER slow stage mg h ⁻¹ kg _{TS} ⁻¹	67	225 ± 7	243	674 ± 53	538 ± 90	797 ± 22	690 ± 97	825 ± 7	1368 ± 62	1437 ± 102	1673	1606 ± 143	1776 ± 117

Table 3. The mean, minimum and maximum values of the total environmental factor determined for each incubation temperature.

f_{total}	10	20	25	30	35	38	40	45	50	55	60	65	70
Mean	0.911	0.908	0.908	0.903	0.900	0.898	0.901	0.874	0.878	0.888	0.855	0.871	0.874
Min	0.909	0.903	0.905	0.895	0.876	0.874	0.890	0.814	0.795	0.750	0.399	0.752	0.697
Max	0.911	0.911	0.912	0.907	0.905	0.907	0.909	0.899	0.901	0.905	0.901	0.909	0.910

Table 4: Values of the constants that describe the dependence of k_T on T

	Fast stage	Slow stage
TR1	20	20
TR2	50	50
k_{TR1}	0.020	0.015
C1	1.079	1.068
C2	1.200	1.167

COMPOSTING UNDER CONTROLLED CONDITIONS

A. Cronjé^{*1}, C. Turner¹, A. Williams¹, A. Barker² and S. Guy²

^{*} angela.cronje@bbsrc.ac.uk

¹ Silsoe Research Institute, Wrest Park, Silsoe, Bedford, MK45 4HS, United Kingdom

² Chemical Engineering, University of Birmingham, Edgbaston, Birmingham, B5 7TT,
United Kingdom

Abstract

Three cylindrical reactors, each with a working capacity of approximately 200 litres, were used to investigate composting. The process was optimised and conditions were controlled so that composting on a laboratory-scale thermally resembled that occurring in the core of large open heaps. A baseline flow of humidified air aerated the reactors in five-minute bursts. The reactors operated as closed systems with facilities to analyse the composition of the off-gas for ammonia, oxygen and carbon dioxide.

Temperature was used to monitor the progress of the process. Heat loss from the reactor surface was compensated for with an external heat source. A basic model of radial conductive heat losses showed that 53 watts per square-metre would be the maximum heat flux needed to keep the temperature difference across the reactor to within a degree when running at 60 °C. A heating cable was used, which could supply 150 watts per square-metre, and the radial temperature difference was reduced to within a degree in more than 60 % of the recorded temperatures in the case studies presented. The temperature of the composting material was held at 60 °C using a high flow rate 'cooling' aeration with temperature feedback. This, however, led to a mean vertical temperature difference of at least 10 °C. The aeration strategy resulted in a well-aerated material, which favoured aerobic microbial activity

and the temperature increased as a result of the internally generated heat associated with composting. Three-quarters of the ammonia was emitted in the first week.

Keywords: Heat loss simulation, Temperature optimisation

INTRODUCTION

Composting is an aerobic process, in which a solid organic material is converted to a more stable, humified product. The process exploits the auto-thermal, self-selective activity of microbial populations of the organic material, which usually has a high porosity and, consequently, a relatively low thermal conductivity. The material is, therefore, self-insulating and tends to accumulate the heat generated by the microbes. The high temperatures reached contribute to the inactivation of potentially harmful pathogenic microbes [1]. A reduction in mass, bulk volume and water content of the organic material, and pathogen inactivation makes composting a particularly attractive method for managing large volumes of biological wastes, such as farmyard manures (FYM). Handling FYM also incurs considerable costs for farmers. It is usually stored in large, unmanaged outdoor heaps before it is spread on fields. Composting occurs spontaneously in the heaps but it is unpredictable and tends to be influenced largely by the ambient conditions. FYM can contain human and animal pathogens although some are more prevalent in different manures. After uncontrolled composting, pathogens, such as faecal coliforms (*e.g. E. coli O157*), streptococci and salmonellae, are sometimes still detected [2]. To be considered as a process to further reduce pathogens (PFRP), the United States Environment Protection Agency (USEPA) recommends that during composting the organic material experiences temperatures between 55 °C and 76 °C for at least 3 to 15 days depending on the compost system [3].

Composting in outdoor windrows can be carried out successfully in passively [4] and actively [5] aerated systems. However, to evaluate composting on this scale experimentally would be costly and time consuming and the factors controlling the process may not be obvious, as outdoor conditions are difficult to control [6]. There is also a lack of homogeneity of microbial activity in windrow composting [7]. To represent the process better, a laboratory-scale in-vessel compost unit is needed in which a degree of control of conditions can be achieved.

The major factor to consider when composting is the accumulation and distribution of heat in the material as this also influences the other process variables. Composting is most effective in an environment that provides an optimum temperature, has sufficient nutrients, moisture and oxygen, and a suitable pH to optimise the growth rates of microbial populations [8]. One documented means of controlling the temperature of the process is through deliberate removal of heat using forced aeration [9]. The flow of air through the reactor controls the spatial distribution of gases, moisture and temperature and consequently, the decomposition rate of the organic material, which is usually optimal between 50 °C and 60 °C [1]. Air is therefore supplied to provide the oxygen to support aerobic activity and hence generate heat. The flow of air will move heat through the material from which it will eventually be lost due to sensible heat loss and evaporation. The airflow rate is therefore crucial to the temperatures reached.

Experiments carried out on a laboratory scale tend to have disproportionately large heat losses due to the relatively large outer surface area-to-volume ratio [6]. In a commercial facility, evaporation accounts for about 76 % of heat lost whereas in a laboratory-scale unit most of the heat is lost to the surroundings through the reactor walls [8]. Viel [7] found that

three-quarters of the microbially generated heat dissipated from the walls of an insulated reactor.

A vertical temperature gradient is often established during composting as a result of the evaporation of water from the organic material and, to a lesser extent, the sensible heating of the air flowing through the material. The temperature difference was found to be greater than 10 °C between the lower and upper layers of material composting in a vessel one metre (m) deep [pers. com. 10]. Conductive heat losses and temperature gradients have been reduced by controlling the surrounding air temperature [6], continuous circulation of compost gases in a reactor insulated with double layer insulation [11], and integrally controlled jacket heaters [9]. Another problem encountered in closed systems is condensation on the inside surface of the reactor lid causing uncontrollable temperature fluctuations [10] and misleading concentrations of highly soluble off gases, such as ammonia. For the laboratory experiments to be reliable and representative of the composting process, heat losses from the system need to be addressed so that comparisons can be made with composting in larger field heaps.

The presence of ammonia in the off-gas from heaps needs to be controlled. The release of ammonia not only represents a loss of valuable ammoniacal nitrogen (c. 230 kilotons per annum in the United Kingdom) [12] and an inefficient use of manure as an organic fertiliser, but also is an environmental concern. When deposited on the land, ammonia contributes to acidification and eutrophication of unmanaged soils. This can occur locally or the gas can be carried considerable distances, crossing national boundaries [13]. Ammonia emissions are particularly noticeable when composting nitrogen-rich organic material, such as manure.

The aim of this work was to design a compost unit, in which thermal conditions represent those experienced at the core of a large compost heap, such as a commercial

windrow. The unit consisted of three reactors equipped with control and monitoring systems, which measured and recorded process variables such as the temperature and off-gas composition. The results from two case studies are presented to illustrate the effectiveness of the reactor's control system to optimise operating conditions. The two examples were taken from a series of 18 experiments carried out in the reactors, in which the effect of the initial carbon to nitrogen (C:N) ratio and pH of the organic material on aspects of the composting process and ammonia emission, in particular, was investigated. The organic material was a mix of separated solid pig manure (total solids, TS, *c.*18 %) and chopped wheat straw (TS *c.*90 %). The C:N ratio was determined by the mixing ratio of manure to straw (M:S), which was 2:1 and 4:1 on a wet mass basis, in Case 1 and 2, respectively. The results of the experiments were also used to test and verify a model of composting under controlled conditions, in which the temperature and off-gas composition were predicted from the initial properties of the organic material.

MATERIALS AND METHODS

Reactor Design

The reactor body was made from a 10 millimetre-thick polypropylene sheet, rolled into a cylindrical vessel with an internal diameter of 600 millimetres (mm), height of 1700 mm and total volume of 424 litres (l), about half of which could be occupied by the organic material (Figure 1). A stainless steel funnel for leachate collection, a perforated plenum and an aluminium lid were also included. Forced air entered between the funnel and plenum and exited through the main centre port in the lid. The impact plate (**IP**) on the gas

outlet enhanced mixing of the off-gas in the headspace. Some off-gas was also drawn from a smaller side port in the lid for analysis of the ammonia content. Two spoked wheels held 400 mm apart on a stainless steel rod, served as internal supports for the organic material in the vertical reactor. Without this initial support, compaction in the lower layers when loading the reactor would restricted airflow into the organic material and so lead to channelling up the sides of the reactor instead of aerating the organic material sufficiently to meet oxygen demands during the initial stages of intensive composting. The external surface of the reactor between the lid and the funnel was covered with aluminium foil, which helped to distribute the heat supplied by a heating cable evenly over the surface. The whole reactor was covered with rock wool insulation panels to further reduce heat losses.

Figure 1.

Modelling Radial Heat Loss

The conductive radial heat losses were simulated to estimate the temperature difference across the reactor for three cases: a) the reactor without insulation, b) the reactor insulated with rock wool panels, and c) the reactor insulated with rock wool panels and supplied with an external heat source, such as a heating cable. A horizontal section of the reactor, including the wall and insulation, of length, L , was considered (Figure 2). The organic material in the section was divided into nine elements of equal mass. The wall was one and the insulation was divided into two elements of equal mass. The radius of an element, r , corresponded to that of outer vertical surface and the temperature, T , was taken as that at the mean radius. The surroundings were nominated as 0, the outermost element, as 1 and the central element, as ' n ', where n was the number of elements in the section. ' S '

denoted the outside surface of the reactor. The centre was assumed to be hottest so that heat flowed radially through the material from n to 0.

Figure 2.

The mass in each element was assumed to be constant during a simulation. The heat balance across an element, j , was therefore given as:

$$\frac{dQ_j}{dt} = M_j \cdot C_{p_j} \frac{dT_j}{dt} = \frac{dQ_{\text{gen}}}{dt} + \frac{dQ_{\text{in}}}{dt} - \frac{dQ_{\text{out}}}{dt} \quad (\text{i})$$

where Q_j = heat content of element j , Joules (J)

M_j = mass of element j , kilograms (kg)

C_{p_j} = specific capacity of element j , $\text{J kg}^{-1} \text{K}^{-1}$

T_j = temperature of element j , K

Q_{gen} = heat generated by microbial activity in element j , J

Q_{in} = heat flowing radially into element j from element $j+1$, J

Q_{out} = heat flowing radially from element j to element $j-1$, J

Heat generation was determined from the heat released as a result of electron transfer per gram of oxygen consumed in aerobic respiration, $13.6 \text{ kJ g}^{-1} \text{O}_2$ [1]. The oxygen uptake rate (OUR) was based on the volatile solids (VS) at temperature, T , in degrees centigrade [14] and was expressed in $\text{gO}_2 (\text{kgVS h})^{-1}$.

$$\text{OUR} = 0.11 \times 1.066^T \quad (\text{ii})$$

The temperature of the outermost element ($n=1$) depended on the heat loss from the element to the ambient air. The process involved conduction of heat across the element and its subsequent loss from the reactor surface by convection and radiation, which operated in parallel. Conduction through element 1 was driven by the temperature difference between the element and the outside surface and therefore considered the log mean area of the element.

Convection and radiation were surface effects driven by the temperature difference between the reactor surface and the surrounding air and were therefore concerned with the outside surface area of the reactor. The respective heat flows by conduction, convection and radiation, q_{cond} , q_{conv} and q_{rad} were described by equations (iii) to (v), respectively.

$$q_{\text{cond}} = (T_1 - T_s) \cdot \frac{2 \cdot \pi \cdot L \cdot k_1}{\ln \frac{r_0}{r_1}} \quad (\text{iii})$$

k_1 was the thermal conductivity of the material of element 1 ($\text{W m}^{-1} \text{K}^{-1}$).

$$q_{\text{conv}} = A \cdot h_{\text{conv}} \cdot (T_s - T_0) \quad (\text{iv})$$

A was the outside surface area of the reactor (m^2) and h_{conv} was the convective heat transfer coefficient ($\text{W m}^{-2} \text{K}^{-1}$)

$$q_{\text{rad}} = A \cdot h_{\text{rad}} \cdot (T_s - T_0) \quad (\text{v})$$

h_{rad} was the radiative heat transfer coefficient ($\text{W m}^{-2} \text{K}^{-1}$).

The total heat loss from the reactor surface was the sum of the convective and radiative heat loss such that

$$q_{\text{conv+rad}} = (T_s - T_0) \cdot 2 \cdot \pi \cdot r_0 \cdot L \cdot h_c \quad (\text{vi})$$

h_c was the combined heat transfer coefficient of convection and radiation ($\text{W m}^{-2} \text{K}^{-1}$).

A combined coefficient was used because heat losses by convection and by radiation from the reactor surface occurred independently of each other and their effect on total heat loss was therefore additive. For surface temperatures around 40°C , convective and radiative heat transfer coefficients are both about $5 \text{ W m}^{-2} \text{K}^{-1}$, with the latter becoming relatively more important at higher temperatures. The value of h_{rad} depends on the temperature difference between the surface and the ambient temperature. A 5°C change in the temperature difference results in about a 2.5 % change in the value of h_{rad} . h_c was assumed to be a constant $10 \text{ W m}^{-2} \text{K}^{-1}$ for these simulations.

Convection and radiation operated in series with conduction. The heat loss was therefore dependent on the limiting mechanism, be it the transfer through the element or from the reactor surface. At steady state, the flow of heat by conduction equalled that by convection plus radiation. Substituting for the surface temperature, an unknown in equations (iii) and (iv), gave equation (v), which described the heat flow from the element 1 to the air (element 0).

$$\frac{dQ_{(1,0)}}{dt} = \frac{2\pi \cdot L \cdot [T_1 - T_0]}{\frac{1}{h_c \cdot r_0} + \frac{\log_e \frac{r_0}{r_1}}{k_1}} \quad (\text{vii})$$

The conductive transfer of heat between the elements n to 2 was described by equation (viii)

$$\frac{dQ_{(n,n-1)}}{dt} = \frac{2 \cdot \pi \cdot L \cdot k_n \cdot [T_n - T_{n-1}]}{\log_e \frac{r_{n-1}}{r_n}} \quad (\text{viii})$$

k_n was the thermal conductivity of element n, $\text{W}(\text{m K})^{-1}$

For case c, the heat supplied by the heating cable (Q_{cable}) to the wall ($n=3$), was included in equation (ix), which defined the wall temperature.

$$\frac{dT_3}{dt} = \frac{Q_4 - Q_3 + Q_{\text{cable}}}{M_3 \cdot C_{p3}} \quad (\text{ix})$$

A constant vertical airflow was included in the heat balance to remove excess heat from each element of organic material so that the centre temperature equilibrated at a final temperature equal to the initial temperature.

Values of the physical properties of the materials in the section of the reactor are given in Table 1. The specific heat capacity, thermal conductivity, bulk density of the organic material were experimentally determined for a mix of manure and straw with an M:S of 2:1. The thermal properties varied linearly with the moisture content, as given by the respective

equations in Table 1. They are also reported to vary with the ash content of the solids fraction, as the inorganic solids have a higher heat capacity than the organic solids [1]. However, the correlation is less pronounced than with the moisture content because, for example, the specific heat capacity of water is about four times greater than that of the solids [1]. Furthermore, for an M:S of 4:1, the ash content of the total solids is less than 2 % higher than that in the M:S of 2:1 and the corresponding increase in the specific heat capacity of the organic material is small. The physical properties of the polypropylene reactor wall were provided by the manufactures of the reactor body (Forbes Plastics Tanks and Environmental Technologies, Downham Market, UK).

Simulations of the radial heat loss were carried out for three initial temperatures of the organic material, 20 °C, 40 °C and 60 °C, and three moisture contents, 50 %, 65 % and 80 %. As with the mass of the organic material, the moisture content was assumed to be constant during a simulation. The ambient temperature was a constant 5 °C.

Table 1

Results of Heat Loss Simulations

One iteration lasted one second. Temperatures equilibrated after about 55 000 iterations and a simulation was therefore equivalent to 14 hours (h). For the organic material with a moisture content of 65 %, the final temperature reached in each unit was plotted against the reactor radius to give a temperature profile across the reactor for 20 °C, 40 °C and 60 °C (Figures 3, 4 and 5, respectively). The minimum and maximum error bars on the data points represent the equilibrium temperatures obtained for simulations with the organic material at a moisture content of 50 % and 80 %, respectively.

Figures 3, 4 and 5.

The error bars indicate that effect of the moisture content on radial heat losses was not linear between 50 % and 80 % and the difference between the equilibrium temperatures of these moisture contents in each unit was greater for the insulated than the uninsulated reactor. The insulation did reduce the temperature difference by about 35 % but there was still about a 50 % drop in temperature between the centre and side elements of the organic material. In order to keep the temperature difference in the section to within a degree, a maximum of approximately 11 W was required from the external heat source, which equates to a power flux of about 58 W m^{-2} . This value did not depend on the moisture content of the organic material. The heating cable supplied 15 W m^{-1} of length of cable, so that the power flux to the reactor was

$$= 15 \times \frac{\text{cable length } (\approx 20 \text{ m})}{\text{covered area of reactor } (\approx 2 \text{ m}^2)} = 150 \text{ W m}^{-2} \quad (\text{x})$$

and the power input to the section was 29 W. The power supply of the heating cable was nearly three times that required to compensate for the radial losses and the time for which it operated, therefore, needed to be controlled.

Temperature Monitoring and Control

The temperature of the organic material during composting was measured by thermistors sealed in stainless steel probes and logged hourly by data loggers (Squirrel Series 1200, Grant Instruments Ltd, Cambridge, UK). The probes were positioned at three points along the central axis of the reactor, top (1), centre (2) and base (3), 400 mm apart (Figure 1). A fourth thermistor (4) was embedded 40 mm from the side into the composting

material and was positioned vertically level with the thermistor at (2) so that the radial temperature gradient could be monitored.

Four control loops on each reactor operated to limit the upper temperature and to reduce the radial and vertical temperature gradients. The temperature controllers (Model 2208L, Eurotherm Controls Ltd, Worthing, UK) responded to input signals from K-type thermocouples encapsulated in stainless steel. An on/off mode was used to control the temperature of the material (**A**) (Figure 6). The controller actuated a solenoid valve to supply a high flow rate when the central temperature exceeded 60°C, in order to dissipate the surplus heat. The upper limit of 60 °C was decided on from respirometry work carried out on a similar material [16]. The controllers in the control loops dealing with the temperature gradients (**B**), (**C**) and (**D**) (Figure 6) operated in proportional, integral and differential (PID) mode and were self-tuning. The control loop (**B**) was set up to keep the temperature difference between the centre and side of the composting material to $\leq 1\text{ }^{\circ}\text{C}$

Figure 6.

The vertical temperature difference in the material develops as a consequence of evaporation, sensible heating of the air and heat losses from the top and base surfaces of the reactor. The silicon rubber heating mats (Holroyd Components Ltd, Saffron Walden, UK) were used to heat the funnel and lid. A PID controller (T_{Base}) regulated the base mat in response to the temperature measured by the thermocouple situated just above the plenum (**C**). The set-point temperature was manually adjusted to align it with that at the centre of the bed so that the cooling effect of the baseline airflow was reduced. Likewise, PID control was used to regulate the heat produced by the top mat (T_{Top}). It acted in response to the temperature reading in the headspace below the lid surface (**D**). The temperature set point

was also altered manually to keep the temperature about a degree above that at the centre of the bed in order to avoid condensation on the inside of the lid.

The pipes carrying gas for analysis to the acid trap bubblers and to the gas analyser were heated with self-adhesive silicon heating tape (Clayborn Precision Heating Tape, Truckee, CA, USA) to prevent condensation inside. An on/off analogue temperature controller regulated the heating about the set point temperature of $60^{\circ}\text{C} \pm 2^{\circ}\text{C}$.

Air Supply

A 2-stage aeration strategy was used. The baseline airflow aerated the material for 5 minutes every 10 minutes at 5 litres per minute (1 min^{-1}). An on/off asymmetric timer actuated a 2-way solenoid valve on the airline and the controller automatically recorded the time for which the valve was open. The flow rate was determined from the total solids content of the feed substrate using a factor of $0.28\text{ l min}^{-1}\text{ kg}^{-1}\text{ TS}$ [9]. When air is supplied in bursts, as opposed to a continuous low flow rate, channelling along paths of least resistance in the material is less pronounced and the air is forced into less accessible areas of the material. The airflow of the 'cooling' aeration was delivered at 25 l min^{-1} to dissipate the excess heat when the core temperature of the material was above 60°C . The flow rate was determined using a factor of $1.40\text{ l min}^{-1}\text{ kg}^{-1}\text{ TS}$ [9]. The time for which the three-way solenoid valve on the 'cooling' aeration airline (Figure 6) was open was recorded every 10 minutes by a PC-based logger and was expressed as a percentage of the time. For example, 100 % implied that the valve had been open for the whole 10 minutes and 250 litres of air had flowed into the reactor.

Considerably more air was supplied to remove the excess heat generated by microbial activity than was needed to replace the oxygen consumed and the material was well aerated. For example, about 9 times more dry air, in kg (kg TS h)^{-1} , was required to dissipate excess heat from the organic material than to meet the stoichiometric oxygen demand for aerobic respiration at 60 °C.

Moisture Control

Controlling the water content of the organic material was essential to maintain conditions favourable for high microbial activity. As the temperature rose, more water evaporated. The higher airflow rate also increased water evaporation. In an attempt to achieve a uniform moisture distribution throughout the organic material and to delay the onset of moisture limitation, the baseline air supply was humidified at 40 °C by bubbling the air through a closed water cylinder before passing into the reactor. A relative humidity probe (Hygroclip S3, Rotronic Instruments Ltd, Crawley, UK) continuously monitored the relative humidity and temperature of the air leaving the humidifier. The relative humidity was about 50 % and the mass of water in the humidified air (*c.* 24 g kg^{-1} dry air) was more than twice that in atmospheric air (*c.* 10 g kg^{-1} dry air). The baseline airflow therefore carried approximately 61 grams of water per day into the organic material.

Off-gas Analysis

Analysis of the gas composition from the reactors provided a valuable means of monitoring the process. Gas was analysed for oxygen, carbon dioxide and ammonia. A

sample of gas, drawn from the off-gas leaving through the central gas outlet (Figure 1), was passed through a condenser, which was a modified refrigeration unit, to remove the water vapour from the gas phase. The gas then passed through the dessicator column to further dry the gas before it entered the gas analyser. Silica gel was used as its change in colour from blue to pink gave a clear indication when the desiccant needed to be renewed. The oxygen and carbon dioxide concentrations in the dry gas was determined by a combined paramagnetic oxygen and infrared carbon dioxide gas analyser (Model 4102, Servomex Group Ltd, Crowborough, UK) with analogue outputs. A PC-based logger recorded the concentrations in the off-gas from each reactor, for 15 minutes every hour, by controlling the solenoid valves on the gas lines through a digital interface. Standard gases of nitrogen, air and $9 \pm 0.12\%$ carbon dioxide in nitrogen were used to calibrate the readings every 12 hours. The water collected in the condenser was used to determine the average water content of the off-gas over about 24 hours.

Ammonia in the gas drawn from the headspace of each reactor was collected using sulphuric acid traps [17]. A trap consisted of, two side-arm boiler tubes containing 0.4 molar (M) sulphuric acid (H_2SO_4), a side-arm boiler tubes to collect any condensate carried over and an integrating gas meter (Remus 4 G 1,6, Schlumberger Ltd) (Figure 7). Tubes were changed twice a day for the first 10 days and daily thereafter. The mass of ammonia collected was determined using steam distillation with back titration [16], which had a minimum detection limit of 50 mg l^{-1} .

Figure 7

Organic Material Analysis

The total solids (TS) content was determined from a wet sample dried at 105°C for 16 hours and the volatile solids (VS) content from the dried sample ashed at 550°C for 5 hours [18]. The ammoniacal nitrogen (Amm-N) and Kjeldahl nitrogen (Kj-N) contents were analysed by steam distillation [18]. For Kj-N, the sample was digested prior to distillation [19]. Kj-N is the sum of the Amm-N and organic nitrogen (Org-N). The Kj-N was assumed to represent the total nitrogen (TN) content of the organic material. Nitrates and nitrites were not considered because these compounds are generally not present in pig manure [22, 23, 24]. This was confirmed by initial analytical tests on the manure with Merckoquant test strips, which detected concentrations of nitrate and nitrites above 10 mg l⁻¹ and 2 mg l⁻¹, respectively. The carbon to nitrogen ratio (C:N) was calculated from the total organic carbon (TOC) content, estimated from the VS content [1], and the TN content.

The pH of the sample, diluted to 1:10 (mass basis) with dionised water [20], was measured using a standard Ion Sensitive Field Effect Transistor (ISFET) probe with the Sentron 2001 pH system. The COD was analysed by the standard closed reflux titrimetric method [18]. The bulk density (BULK) was determined according to a British standard method developed for soil and soil improvers [21]. The density of pathogen markers was estimated from counts of colony forming units (CFU) in sample extracts plated onto McConkey's agar, a coliform-selective medium, and incubated at 37°C for 24 hours.

RESULTS

To assess the effectiveness of the control systems to optimise composting conditions in the reactors, the temperature-time and spatial profiles for two case studies are presented (Figures 8 and 9). Measurement of the ammonia emissions was central to the series of experiments carried out in the reactors. The cumulative mass of ammonia emitted is therefore shown, using the same time axis as the temperature, along with the 'cooling' aeration profile, which indicates the average airflow rate over 10 minute intervals.

Analysis of the organic material before and after composting is given in Table 3. An increase in TS content was the result of the loss of water from the organic material in the off-gas. The moisture content was still in the 55-65% range that is considered ideal for composting [25, 26] and did not appear to have become limiting. The stability of the composted material can be gauged from the organic content as indicated by the VS content, COD and C:N ratio [1]. There was a decrease in all of these variables, which suggested that the organic material was more stable after two weeks of intense composting. The standard method used to determine the VS content, however, does not distinguish between the organic material readily available for metabolism and that, which is not normally metabolised during composting. Neither does the method distinguish between the volatile material of the manure and the bulking agent (straw). Approximately 23 %TS of straw is lignin, a carbonaceous compound that is measured as part of VS but which is relatively resistant to microbial attack. The amount broken down does depend on the composting conditions [26]. Straw contributed 64 %TS and 46 %TS to the respective mixes and for these reasons it was not surprising that the VS content was above 80 % before and after composting. The sensitivity of the VS test is poor because a high percentage of the TS are volatile [5]. The C:N ratios of the respective

mixes decreased as a result of a drop in TOC, by about 16 % and 27 %, and an increase in TN content by 13 % and 10 %. The COD was reduced by more than the 20 % suggested for a stable composted refuse mix [1]. The condition, however, is not definitive and is specific to type of organic material. The organic material in the case studies was more stable after the period of intense activity but it was not necessarily stable and needed more time to mature. The bulk density increased in Case 2 but decreased in Case 1. The reason for this was probably due to the larger quantity of bulking agent in the organic material of the lower mixing ratio, which resisted compaction during composting. The degree of compaction was also reduced by the internal spoked wheels, which supported the organic material and helped maintain the open structure.

Table 2.

No pathogen markers were detected in the samples of composted organic material in both the case studies. This confirmed the effectiveness of the composting conditions, especially the high temperatures reached, to ensure sufficient pathogen inactivation. The core temperature was above 55 °C for 9 consecutive days in Case 1 (Figure 8) and 13 consecutive days in Case 2 (Figure 9). The mean temperature in both mixes was 55.3°C during the 14 days (Table 3).

Table 3

The side temperatures closely followed those measured at the centre during the 14 days. The respective radial temperature differences for Case 1 and 2 were $<|1|$ °C for 61 % and 68 % and $<|2|$ °C for 95 % and 98 % of the temperatures recorded hourly. In Case 2, the greatest deviation occurred when a power cut on the 4th day stopped the heating cable and the forced aeration from operating for about 12 hours, shown by the dotted lines on Figure 9. The radial temperature difference increased as heat was lost from the reactor wall

and the centre, side and base temperatures rose rapidly with no airflow to remove the excess heat. When operating, the cooling aeration was effective in maintaining the optimal temperature for microbial activity at about 60 °C. The demand for the cooling aeration was noticeably lower after the 6th day than it was for the high demand period beforehand as a result of a drop in microbial activity and therefore heat generation rate, which is directly related to decomposition [5]. With a decrease in the intensity of cooling aeration, the base temperature rose and the vertical temperature difference between the centre and base more than halved from 19 °C before the power cut to about 9 °C after day 6, when the aeration was mainly baseline. In Case 1, the demand for cooling aeration was practically constant up the 7th day. However, the centre temperature was higher than 60 °C from the day 2 to day 5 as the heat generated by microbial activity was initially greater than could be dissipated by the high airflow. Demand for the 'cooling' aeration during the 14 days resulted in a relatively uniform vertical temperature gradient of about 10 °C. The distinct drop in temperature after day 12 was probably caused by exhaustion of the readily decomposable organic material. The mix in Case 1 contained half the amount of manure than the mix in Case 2 and the initial rapid rate of microbial activity could not be sustained.

Figures 8 and 9

The mass of ammonia collected in the acid traps was scaled up by considering the volume of gas that passed through the air traps (as measured by the integrating gas meter) with respect to the volume of gas that passed through the reactor during the same time period. The total mass of ammonia emitted was 103 g in Case 1 and 225 g in Case 2. The difference was likely to be due to the higher initial nitrogen content in the organic material with the higher manure content (M:S of 4:1). About three-quarters of the total ammonia was emitted during the first week. The combination of high temperatures and high airflow rates during the

initial intense stage of composting contributed to the rapid loss of ammoniacal nitrogen from the organic material as ammonia.

CONCLUSIONS

The reactor unit is a promising tool with which to study composting on a smaller, more manageable scale than the traditional large outdoor windrows. It allowed the process conditions to be controlled so that the change in process variables, which would be expected to occur at the core of the windrow, could be evaluated without ambient conditions affecting the outcome. One of the many aspects of composting that could be studied with this closed system is gaseous emissions, in particular highly soluble gases such as ammonia. The absence of pathogen markers in the composted material confirmed that high temperature treatment that can be achieved in well managed composting, is an effective method of dealing infected organic material.

The external heating cable proved to be an effective, compact and relatively cheap way to compensate for the heat losses from the reactor surface and so minimise the temperature gradients, which were predicted to occur even when insulated. Actual radial temperature differences were marginally greater than those predicted by the heat transfer simulation model.

Aeration played a vital role, not only for controlling the reaction rate but also as a means of monitoring the progress of the process. The aeration demand, as with temperature, provides rapid online tracking of the degree of decomposition without having to deal with sampling and the errors involved.

The feature of the system, which needs more attention, is moisture control. Recirculation of the off-gas back to the reactor could be considered in order to reduce both moisture loss and the vertical moisture and temperature gradient generated by the cooling air.

ACKNOWLEDGEMENTS

The research was funded by the Engineering and Physical Sciences Research Council (EPSRC) and Silsoe Research Institute (SRI) with further support from the University of Birmingham.

REFERENCES

1. Haug, R. T. *The Practical Handbook of Compost Engineering*. Lewis Publishers, Boca Raton, Florida, USA (1993).
2. Farrell, J. B. Faecal Pathogen Control During Composting. *Sci. Eng. Compost.*, 282-300 (1992).
3. Turner, C., The Thermal Inactivation of *E. coli* in Straw and Pig Manure. *Bioresource Technol.*, **84**, 57-61 (2002).
4. Fernandes, L., Zhan, W., Patni, N. K. and Jui, P. Y., Temperature Distribution and Variation in Passively Aerated Static Compost Piles. *Bioresource Technol.*, **48**, 257-263 (1994).
5. Finstein, M. S., Miller, F. C. and Strom, P. F., Monitoring and Evaluating Composting Process Performance. *J. Water Pollut. Control Fed.*, **58**, 272-278 (1986).

6. Finstein, M. S., Hogan, J. A. and Miller, F. C., Physical Modelling of the Composting Ecosystem. *Appl. Environ. Microb.*, **55**, 1082-1092 (1989).
7. Viel, M., Sayag, D., Peyre, A. and André, L., Optimization of In-Vessel Co-Composting Through Heat Recovery. *Biol. Waste*, **20**, 167–185 (1987).
8. Das, K. and Keener, H. M., Numerical Model for the Dynamic Simulation of a Large Scale Composting System. *T. Am. Soc. Agr. Eng.*, **40**, 1179-1189 (1997).
9. Fraser, B. S. and Lau, A. K., The Effects of Process Control Strategies on Composting Rate and Odor Emission. *Compost Sci. Util.*, **8**, 274-292 (2000).
10. Stocks, C., The Stabilisation of Brewery Waste by Composting. PhD Thesis. Sch. Chem. Eng., U. Birmingham, UK (2000).
11. Smårs, S., Beck-Friis, B., Jönsson, H. and Kirchmann, H., An Advanced Experimental Composting Reactor for Systematic Simulation Studies. *J. Agr. Eng. Resour.*, **78**, 415–422 (2001).
12. Pain, B. F., Misselbrook, T. H., Jarvis, S. C., Chambers, B. J, Smith, K. A., Webb, J., Philips, V. R. and Sneath, R. W., *Inventory of Ammonia Emissions from UK Agriculture 1998* (2000).
13. MAFF, Code of Good Agricultural Practice for the Protection of Air. London, MAFF, 80pp. (1998).
14. Schulze, K. L., Rate of Oxygen Consumption and Respiratory Quotients during the Aerobic Decomposition of a Synthetic Garbage. *Compost Sci.*, Spring, 36-40 (1960).
15. Perry, R. H. and Green, D. W., *Perry's Chemical Engineers' Handbook*, 6th edition. McGraw-Hill Book Company, New York, USA (1984).

16. Cronjé, A. L., Barker, A. J., Guy, S., Turner, C. and Williams, A. G., Oxygen Up-take Rate of Composing Pig Manure. In: *Proc. Int. Symp. Compost. Compost Util.*, May 2002, Columbus, Ohio, USA. JG Press Inc., Emmaus, USA. (2002).
17. Martinez, J., Jolivet, J., Guiziou, F., and Langeoire, G., Ammonia Emissions from Pig Slurries: Evaluation of Acidification and the Use of Additives in Reducing Losses. In: *Proc. of the Int. Symp. Ammonia and Odour Control from Animal Production Facilities*. Oct. 1997, Vinkeloord, The Netherlands. Voermans, J. A. M. and Monteny G. J. (eds.), Rosmalen, The Netherlands: NVTL, pp. 421-428 (1997).
18. APHA, AWWA, WEF, *Standard Methods for Water and Wastewater Examination*, 20th edition. Public Health Assoc., Washington, DC (1998).
19. Persson, J. A., *Handbook for Kjeldahl Digestion*, 2nd ed. IS BN 91-630-3471-9 (1996).
20. MAFF/ADAS, *Analysis of Agricultural Material*. Ref. Book 427, 3rd ed. (1986).
21. British Standard BS EN 13040:2000, Soil Improvers and Growing Media Sample Preparation for Chemical and Physical Determination of Dry Matter Content, Moisture Content and Laboratory Compacted Bulk Density. (2000).
22. Kirchmann, H. and Lundvall, A., Treatment of Solid Animal Manures: Identification of Low NH₃ Emission Practices. *Nutr. Cycl. Agroecosys.*, **51**, 65-71 (1998).
23. Sommer, S. G. and Dahl, P. Nutrient and Carbon Balance During the Composting of Deep Litter. *J. Agr. Eng. Resour.*, **74**, 145-153 (1999).
24. Petersen, S. O., Lind, A-M, Sommer, S. G., Nitrogen and Organic Matter Losses During Storage of Cattle and Pig Manure. *J. Agr. Sci. Cambridge*, **130**, 69-79 (1998).
25. Bishop, P. L. and Godfrey, C. Nitrogen Transformation During Sludge Composting. *Biocycle: J. Waste Rec.*, **24**, 34-39 (1983).

26. Imbeah, M. Composting Piggery Waste: A Review. *Bioresource Technol.*, **63**, 197-203 (1998).
27. Richard, T., Effect of Lignin on Biodegradability. www.cfe.cornell.edu/compost/calc/lignin.html. Updated Oct. 2000.
28. Barrington S., Choiniere, D., Trigui, M. and Knight, W., Effect of Carbon Source on Compost Nitrogen and Carbon Losses. *Bioresource Technol.*, **83**, 189-194 (2002).
29. Lo, K. V., Lau, A. K. and Liao, P. H., Composting of Separated Solid Swine Wastes. *J. Agr. Eng. Resour.*, **54**, 307-317 (1993).
30. Barrington S., Choiniere, D., Trigui, M. and Knight, W., Compost Convective Airflow Under Passive Aeration. *Bioresource Technol.*, **86**, 259-266 (2002).

FIGURE TITLES

- Figure 1. The design of the reactor
- Figure 2. The section of reactor across which the temperature difference is determined by simulating the radial conductive heat losses.
- Figure 3. Simulated heat losses at 20 °C (No insulation —●—, Insulation —o—, Heating cable supplying 2.95 W and insulation —Δ—)
- Figure 4. Simulated heat losses at 40 °C (No insulation —●—, Insulation —o—, Heating cable supplying 6.75 W and insulation —Δ—)
- Figure 5. Simulated heat losses at 60 °C (No insulation —●—, Insulation —o—, Heating cable supplying 10.6 W and insulation —Δ—)
- Figure 6. The configuration of the control system of each reactor.
- Figure 7. An ammonia acid trap.

Figure 8. Case 1: The temperature, ammonia emission (-o-) and cooling aeration profiles for the organic material with a mixing ratio of 2.

Figure 9. Case 2. The temperature, ammonia emission (-o-) and cooling aeration profiles for the organic material with a mixing ratio of 4.

TABLES

Table 1. The thermal and physical properties of the materials considered in the radial heat loss model.

Quantity	Symbol	Units		Rock wool (insulation)	Polypropylene (wall)	Organic material
Specific heat capacity	C _p	J (g K) ⁻¹		1090 [15]	1800	0.032 (1-TS) + 0.986
Thermal conductivity	k	W (m K) ⁻¹		0.052 [15]	0.330	0.005 (1-TS) - 0.165
Combined heat transfer coefficient	h _c	W (m ² K) ⁻¹		10 [15]	10 ¹	-
Heat generation	H _{gen}	W kg ⁻¹ VS	20°C	-	-	1.50
			40°C	-	-	5.37
			60°C	-	-	19.28
Mass (per element)	M	Kg		0.520	1.028	0.591
Section length	L	M		0.100	0.100	0.100
Outer radius	r	M		0.356	0.306	0.300
Density	ρ	kg m ⁻³	50 %	100 [15]	900	92
			65 %			165
			80 %			303
Total solids	TS	%		-	-	35
Volatile solids	VS	%TS		-	-	88

¹ for case a where the reactor element is not insulated

Table 2. Characteristics of the organic material before and after composting.

Time, days	TS %	VS %TS	Mass kg	Mass kg TS	Amm-N kg	Org-N kg	C:N	pH	COD gO ₂ kg ⁻¹ TS	BULK kg TS m ⁻³	Pathogens log ₁₀ CFU g ⁻¹ TS
Case 1											
0	37.1	87.8	37.3	13.8	0.12	0.20	21.3	6.6	450	49	6.2
14	43.3	86.7	27.0	11.7	0.06	0.22	19.8	7.9	270	46	None
% loss			27	15	53	-11					
Case 2											
0	37.5	87.4	46.6	17.5	0.18	0.39	15.0	6.2	680	62	7.4
14	40.3	81.2	33.9	13.7	0.17	0.34	12.4	8.7	400	70	None
% loss			27	22	7	12					

Table 3. Summary of the composting process.

	Mean air flow rate l min ⁻¹		Mean vertical temperature difference, °C		Mean temperature	Radial temperature difference, °C			
	0 - 6 days	6 - 14 days	0 - 6 days	6 - 14 days	°C	ΔT<1°C	ΔT<2°C	mean	σ
Case 1	19.1	7.0	10.0	10.5	55.3	61%	95%	0.68	0.84
Case 2	12.8	3.4	19.3	8.8	55.3	68%	98%	0.70	0.65

FIGURES

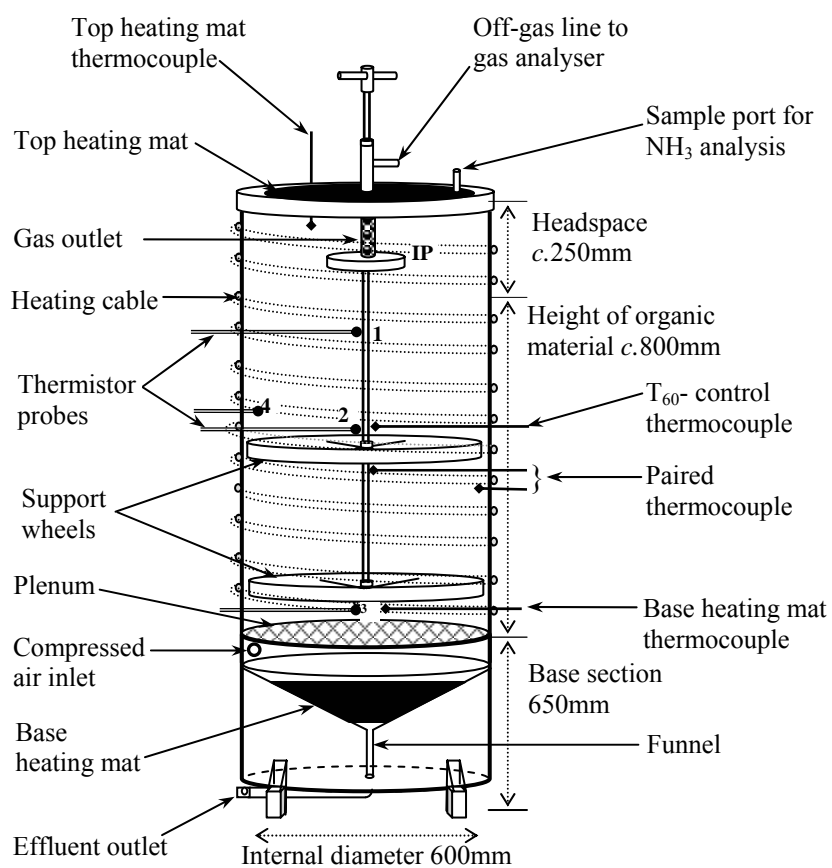


Figure 1.

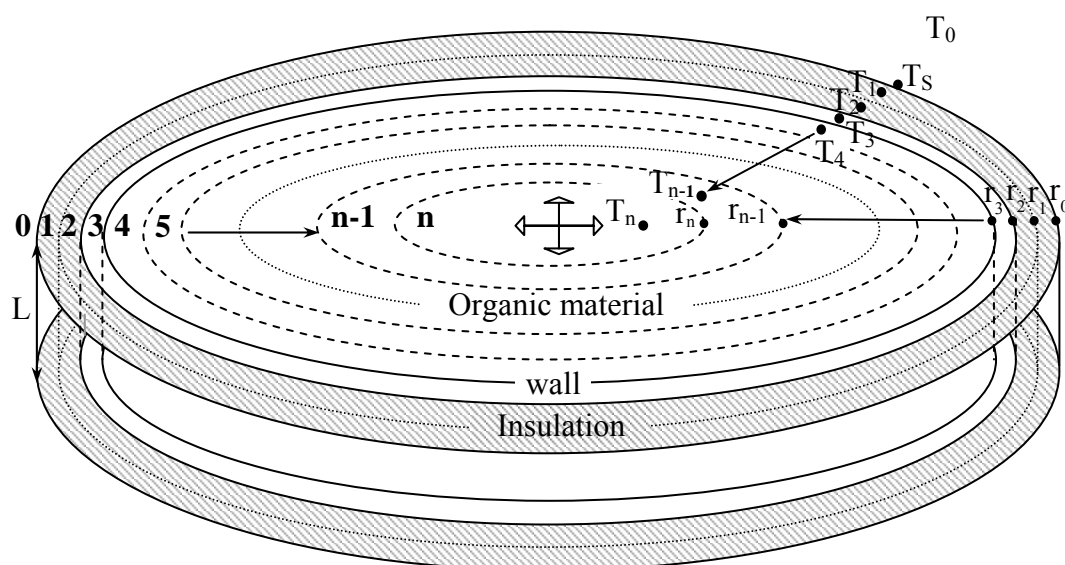


Figure 2.

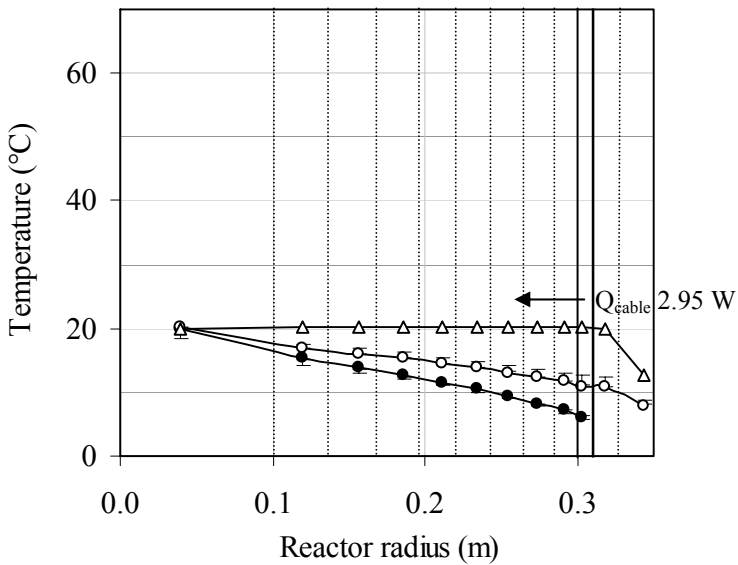


Figure 3.

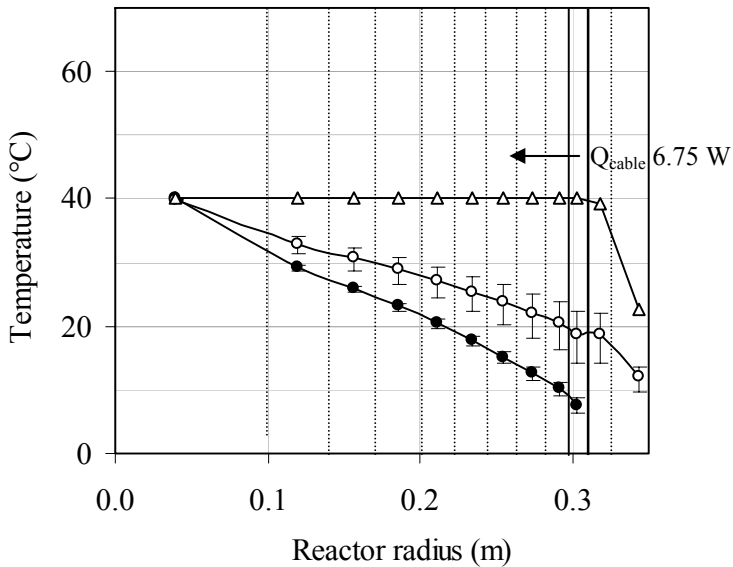


Figure 4

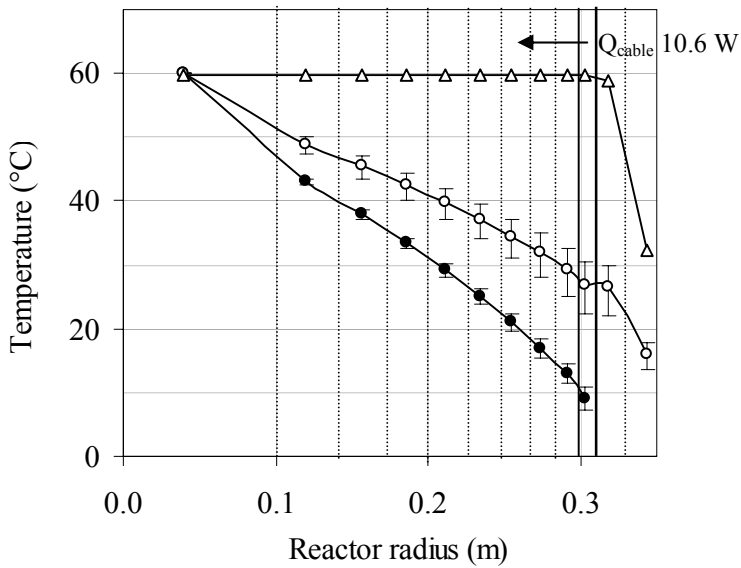


Figure 5.

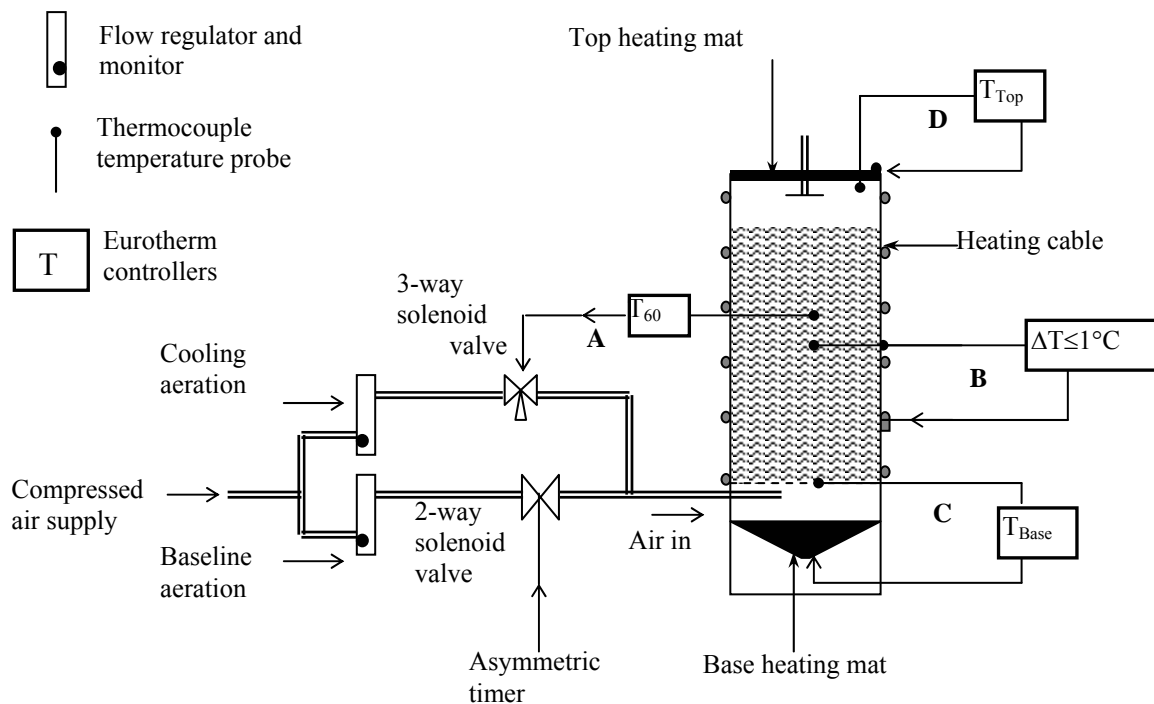


Figure 6.

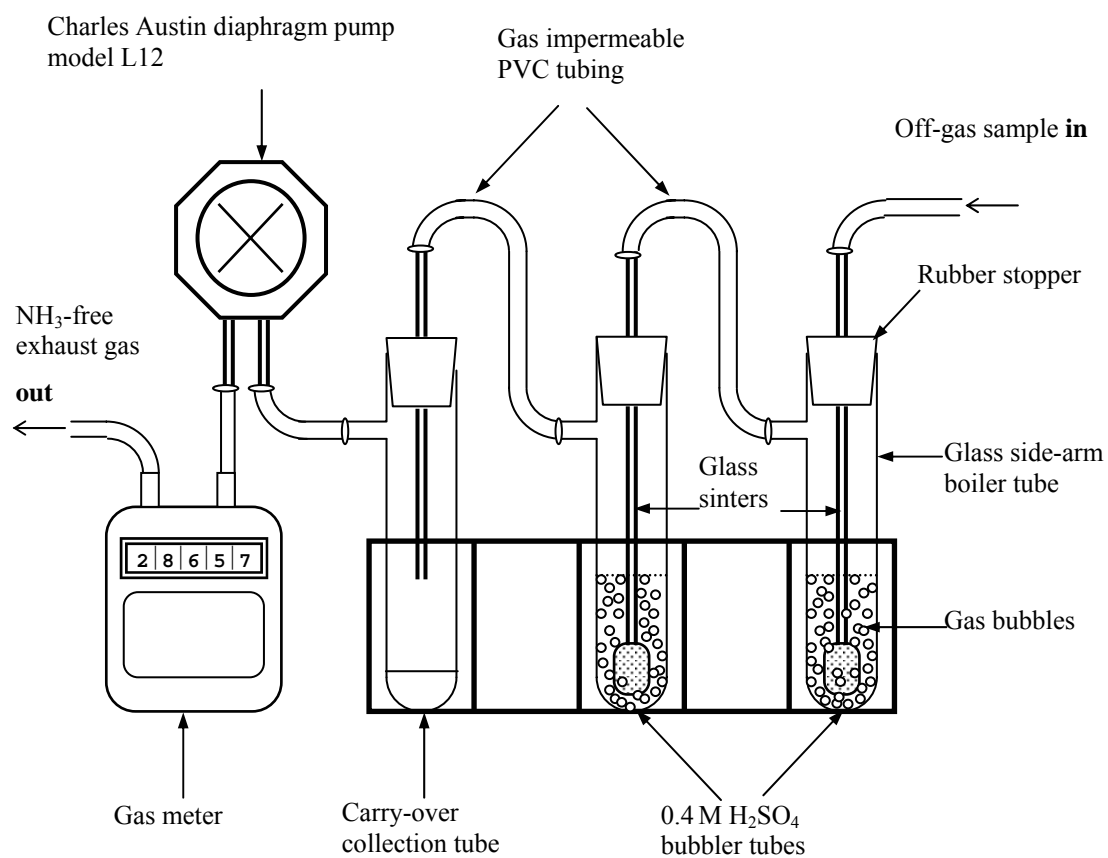


Figure 7.

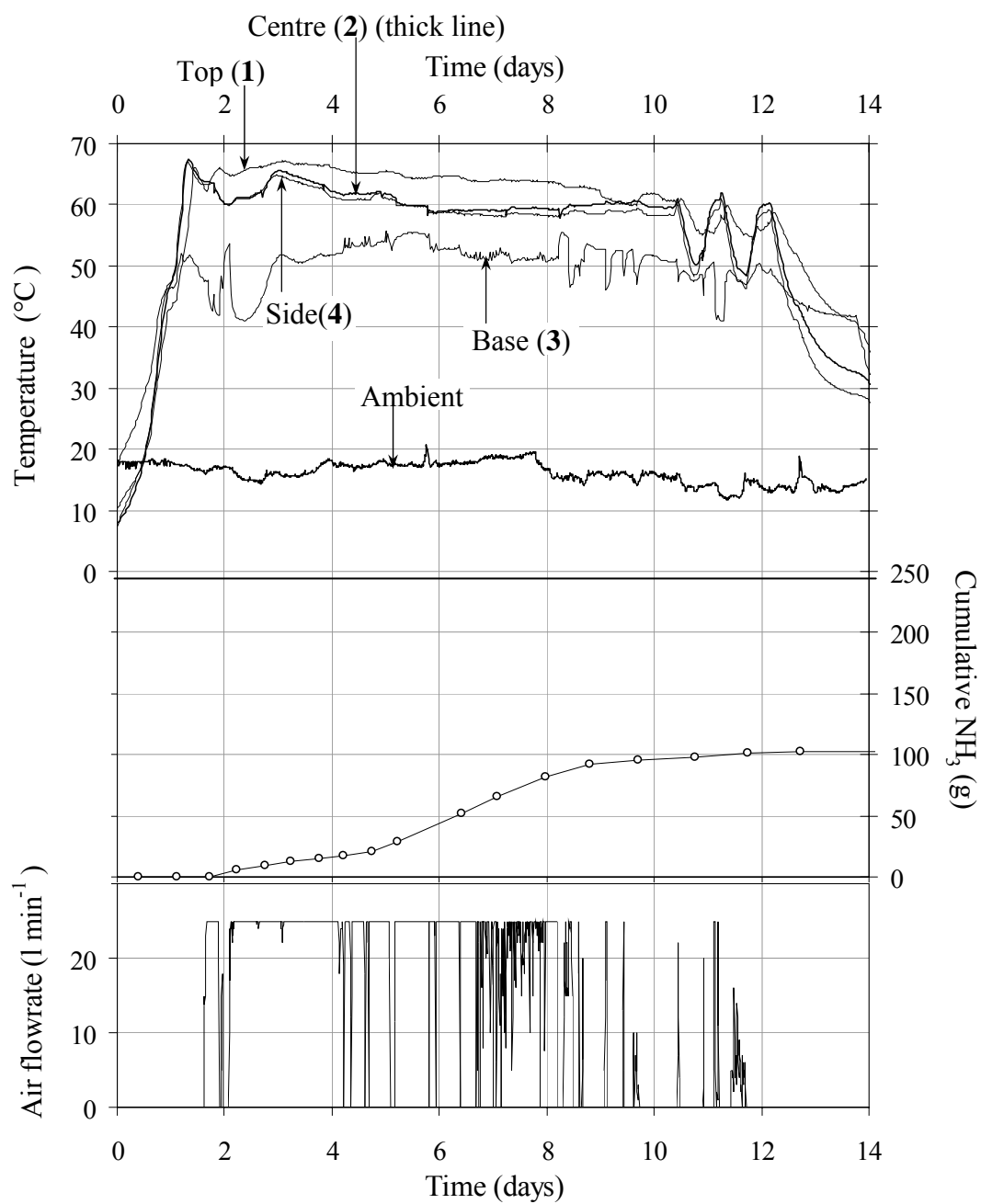


Figure 8.

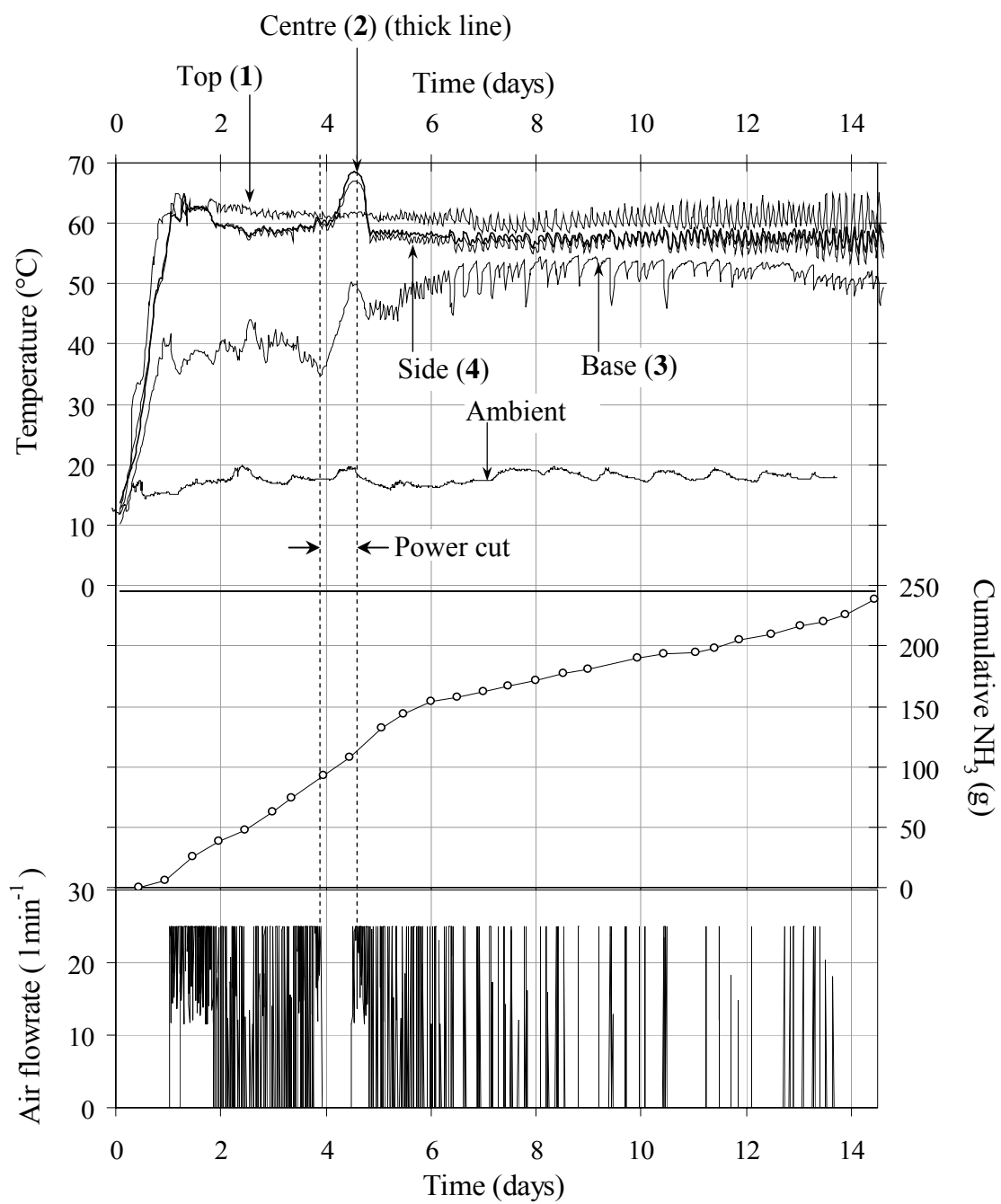


Figure 9.